CFTRI-MYSORE
8455
Chemical applica...

TLMS

TECHNIQUE OF ORGANIC CHEMISTRY

ARNOLD WEISSBERGER, *Editor*

Volume IX

CHEMICAL APPLICATIONS OF SPECTROSCOPY

Second completely revised
and augmented edition

Part I

TECHNIQUE OF ORGANIC CHEMISTRY

ARNOLD WEISSBERGER, *Editor*

Volume I:	Physical Methods of Organic Chemistry *Third Edition*, in Four Parts
Volume II:	Catalytic, Photochemical, and Electrolytic Reactions *Second Edition*
Volume III:	Part I. Separation and Purification Part II. Laboratory Engineering *Second Edition*
Volume IV:	Distillation *Second Edition*
Volume V:	Adsorption and Chromatography
Volume VI:	Micro and Semimicro Methods
Volume VII:	Organic Solvents *Second Edition*
Volume VIII:	Investigation of Rates and Mechanisms of Reactions In Two Parts *Second Edition*
Volume IX:	Chemical Applications of Spectroscopy In Several Parts *Second Edition*
Volume X:	Fundamentals of Chromatography
Volume XI:	Elucidation of Structures by Physical and Chemical Methods In Two Parts
Volume XII:	Thin-Layer Chromatography
Volume XIII:	Gas Chromatography

TECHNIQUE OF ORGANIC CHEMISTRY

Volume IX

CHEMICAL APPLICATIONS OF SPECTROSCOPY

Second Completely Revised and Augmented Edition

Editor

W. WEST

PART I

Authors of Part I

RALPH S. BECKER
A. B. F. DUNCAN
F. A. MATSEN
D. R. SCOTT
W. WEST

1968
INTERSCIENCE PUBLISHERS
a division of John Wiley & Sons, New York · London · Sydney · Toronto

E1, 5:f"n,1,N49
N48.9B

8455
28/2/69

CFTRI-MYSORE
8455
Chemical applica..

Copyright © 1968 by John Wiley & Sons, Inc.
First Edition copyright © 1956
by Interscience Publishers, Inc.

All rights reserved. No part of this book may
be reproduced by any means, nor transmitted,
nor translated into a machine language without the written consent of the publisher.

LIBRARY OF CONGRESS CATALOG CARD NUMBER 45-8533
SBN 470 93160X
Printed in the United States of America

INTRODUCTION TO THE SERIES

Organic chemistry, from its very beginning, has used specific tools and techniques for the synthesis, isolation, and purification of compounds, and physical methods for the determination of their properties. Much of the success of the organic chemist depends upon a wise selection and a skillful application of these methods, tools, and techniques, which, with the progress of the science, have become numerous and often intricate.

The present series is devoted to a comprehensive presentation of the techniques which are used in the organic laboratory and which are available for the investigation of organic compounds. The authors give the theoretical background for an understanding of the various methods and operations and describe the techniques and tools, their modifications, their merits and limitations, and their handling. It is hoped that the series will contribute to a better understanding and a more rational and effective application of the respective techniques. Reference is made to some investigations in the field of chemical engineering, so that the results may be of assistance in the laboratory and help the laboratory chemist to understand the problems which arise when his work is stepped up to a larger scale.

The field is broad and some of it is difficult to survey. Authors and editor hope that the volumes will be found useful and that many of the readers will let them have the benefit of their criticism and of suggestions for improvements.

A. W.

Research Laboratories
Eastman Kodak Company
Rochester, New York

TECHNIQUE OF ORGANIC CHEMISTRY

GENERAL PLAN OF THE SERIES

Volume I (Third Edition, in four parts). **Physical Methods of Organic Chemistry.** *Authors:* A. E. Alexander, D. H. Anderson, J. R. Anderson, J. C. Arthur, Jr., E. D. Bailey, N. Bauer, G. L. Beyer, E. R. Blout, L. O. Brockway, L. M. Corliss, A. H. Corwin, R. L. Custer, B. P. Dailey, G. Donnay, J. D. H. Donnay, K. Fajans, D. D. Fitts, G. K. Fraenkel, A. L. Geddes, H. S. Gutowsky, F. A. Hamm, W. D. Harkins, J. M. Hastings, W. Heller, E. E. Jelley, W. Klyne, C. G. Le Fevre, R. J. W. Le Fevre, S. Z. Lewin, W. N. Lipscomb, W. J. Mader, H. Mark, L. Meites, D. H. Moore, L. D. Moore, Jr., O. H. Muller, J. B. Nichols, W. C. Nixon, G. Oster, A. C. Parker, M. A. Peacock, R. B. Pontius, J. G. Powles, H. A. Scheraga, P. W. Selwood, T. Shedlowsky, R. Signer, D. R. Simonson, W. M. Siri, E. L. Skau, C. P. Smyth, M. Spiro, D. W. Stewart, J. M. Sturtevant, W. Swietoslawski, J. F. Swindells, C. Tanford, G. W. Thomson, B. M. Tolbert, R. Ullman, M. J. Vold, R. D. Vold, R. H. Wagner, H. Wakeham, C. E. Waring, S. Wawzonek, W. West, N. B. Woodall, and N. Wotherspoon

Volume II (Second Edition). **Catalytic Reactions.** V. I. Komarewsky, C. H. Riesz, and F. L. Morritz; **Photochemical Reactions.** C. R. Masson, V. Boekelheide, and W. A. Noyes, Jr.; **Electronic Reactions,** S. Swann, Jr.

Volume III (Second Edition). **Part I. Separation and Purification.** C. M. Ambler, G. Broughton, D. Craig, L. C. Craig, A. B. Cummins, F. B. Hutto, Jr., A. L. Jones, K. Kammermeyer, F. W. Keith, Jr., E. MacWilliam, E. G. Scheibel, R. E. Stauffer, and R. S. Tipson. **Part II. Laboratory Engineering.** J. W. Axelson, R. S. Egly, R. F. Eisenberg, M. P. Hofmann, R. R. Kraybill, G. H. Miller, J. H. Rushton, and W. C. Streib

Volume IV (Second Edition). **Distillation.** C. S. Carlson, C. H. Deal, J. C. Hecker, D. E. Orgen, E. S. Perry, A. Rose, E. Rose, R. S. Tipson, F. E. Williams, and T. J. Williams

Volume V. Adsorption and Chromatography. H. G. Cassidy

Volume VI. Micro and Semimicro Methods. N. D. Cheronis. With contributions by A. R. Ronzio and T. S. Ma

Volume VII. Organic Solvents. A. Weissberger and E. S. Proskauer. Second Edition by J. A. Riddick and E. E. Toops, Jr.

Volume VIII (Second Edition, in two parts). **Investigations of Rates and Mechanisms of Reactions.** *Editors:* S. L. Friess, E. S. Lewis, and A. Weissberger. *Authors:* J. C. Balaceanu, M. L. Bender, S. A. Bernhard, C. E. Boozer, J. F. Bunnett, G. M. Burnett, B. Chance, L. DeMaeyer, M. Eigen, S. L. Friess, E. M. Grunwald, J. Higgins, F. M. Huennekens, J. C. Jungers, M. Kreevoy, E. S. Lewis, R. Livingston, A. Maccoll, E. F. MacNichol, Jr., H. W. Melville, B. K. Morse, R. M. Noyes, G. Porter, F. J. W. Roughton, G. A. Russell, W. H. Saunders, Jr., H. Strehlow, and A. Weller

Volume IX. Chemical Applications of Spectroscopy (Second Edition, in several parts). *Editor:* W. West. *Authors:* R. S. Becker, A. B. F. Duncan, W. Gordy, F. A. Matsen, C. Sandorfy, and W. West

Volume X. Fundamentals of Chromatography. H. G. Cassidy

Volume XI (in two parts). **Elucidation of Structures by Physical and Chemical Methods.** *Editor:* K. W. Bentley. *Authors:* B. Belleau, K. W. Bentley, K. Biemann, J. C. D. Brand, A. R. H. Cole, J. K. N. Jones, J. F. King, E. Leete, P. de Mayo, S. McLean, F. J. McQuillin, K. H. Overton, M. B. Perry, N. Polgar, K. T. Potts, A. I. Scott, E. Y. Spencer, J. B. Stothers, G. A. Swan, Z. Valenta, and B. C. L. Weedon

Volume XII. Thin-Layer Chromatography. Justus G. Kirchner

Volume XIII. Gas Chromatography. O. E. Schupp

Volume IX
Part I

PREFACE TO THE SECOND EDITION

The Second Edition of Volume IX of the *Technique of Organic Chemistry* attempts to carry out the aim of its predecessor of twelve years ago—to offer a comprehensive account of the theory of spectra of organic compounds, as up to date as possible, over the spectral region extending from microwave to ultraviolet radiations, useful as an introduction for readers unfamiliar with the theory, and with coverage adequate to the needs of the organic chemist engaged in spectroscopic studies.

In offering a completely rewritten and updated presentation of the subject, it has seemed best to meet the interests of various groups of readers by issuing the work in separate parts, of which the present Volume constitutes Part I, devoted essentially to the electronic absorption and emission spectra of organic compounds. Part II, on Microwave Molecular Spectra, by Professor Walter Gordy and Dr. Robert L. Cook, will appear shortly, to be followed by further Parts treating Electron and Nuclear Resonance Phenomena and Infrared and Raman Spectroscopy.

In the present Part I, after an introductory sketch of molecular electronic spectra and their empirical application in indicating the structure of organic compounds, the general theory of molecular spectra is developed by Professor A. B. F. Duncan in a chapter which includes an introduction to the group theoretical methods that have been so useful in spectroscopic theory. The electronic spectra of important classes of specific organic compounds are treated by Professor F. A. Matsen, Professor R. S. Becker, and Dr. D. R. Scott, and the fluorescence and phosphorescence of organic compounds are described by Professor Becker. A certain amount of overlap and repetition of some of the theoretical topics in the various chapters may be found useful, according to the expository aims of the Volume, in the assimilation of the theory by readers who may meet it for the first time.

As for the First Edition, the editor wishes to record his appreciation of the unfailing assistance accorded him by the general editor of the series, Dr. A. Weissberger, and by the editorial staff of the publishers during the preparation of this volume.

W. West

June, 1968

TECHNIQUE OF ORGANIC CHEMISTRY

Volume IX
Part I

CHEMICAL APPLICATIONS OF SPECTROSCOPY

CONTENTS OF PART I

I. Introductory Survey of Molecular Spectra. By W. West . . . 1

II. General Theory of Electronic Spectra. By A. B. F. Duncan . . 105

III. Interpretation of Electronic Absorption Spectra. By F. A. Matsen, R. S. Becker, and D. R. Scott 199

IV. Fluorescence and Phosphorescence Spectroscopy. By Ralph S. Becker 337

Author Index 459

Subject Index 473

Important Constants

Velocity of light in vacuum	$c = 2.997925 \times 10^{10}$ cm/sec
Planck's constant	$h = 6.6256 \times 10^{-27}$ erg sec
Electronic charge	$e = 4.80298 \times 10^{-10}$ esu (cm$^{3/2}$ g$^{1/2}$/sec)
Electron rest mass	$m_e = 9.1091 \times 10^{-28}$ g
Ratio of charge to mass for electron	$e/m_e = 5.27274 \times 10^{17}$ cm$^{3/2}$/(g$^{1/2}$ sec)
Radius of first Bohr orbit of H atom	$a_0 = 5.29167 \times 10^{-9}$ cm
Bohr magneton	$\mu_B = 9.2732 \times 10^{-21}$ erg/gauss
Nuclear magneton	$\mu_N = 5.0505 \times 10^{-24}$ erg/gauss
Avogadro's number	$N = 6.02252 \times 10^{23}$ molecules/mole
Boltzmann constant	$k = 1.38054 \times 10^{-16}$ erg/(°K molecule)
Gas constant	$R = 8.31433 \times 10^{7}$ ergs/(°K mole)
	$= 1.98717$ cal/(°K mole)
Rydberg constant for infinite mass	$R_\infty = 109737.31$ cm^{-1}

Conversion Tables for Energy Units

1 cal/mole $= 6.9473 \times 10^{-17}$ erg/molecule
$= 4.3364 \times 10^{-5}$ eV
$= 0.34976$ cm^{-1}
1 erg/molecule $= 1.4394 \times 10^{16}$ cal/mole
$= 6.2397 \times 10^{11}$ eV
$= 5.0345 \times 10^{15}$ cm^{-1}
1 eV $= 23{,}060$ cal/mole
$= 1.6021 \times 10^{-12}$ erg/molecule
$= 8065.7$ cm^{-1}
1 cm^{-1} $= 2.8591$ cal/mole
$= 1.9863 \times 10^{-16}$ erg/molecule
$= 1.2398 \times 10^{-4}$ eV

CHAPTER I

INTRODUCTORY SURVEY OF MOLECULAR SPECTRA

W. West

Research Laboratories, Eastman Kodak Company, Rochester, New York

I. General Nature of Spectra . . . 2
II. Spectroscopic Units . . . 4
  A. Units Referring to Wave Properties of Radiation . . . 4
  B. Units Referring to Photon Energy of Radiation . . . 6
  C. Units Referring to Intensity of Absorption . . . 7
  D. Deviations from Beer's Law . . . 8
III. The Origin of Spectra . . . 9
  A. General Nature of Rotational, Vibrational, and Electronic Spectra . . . 9
  B. Pure Rotational Spectra . . . 13
  C. Vibration–Rotation Spectra . . . 15
  D. Electronic Spectra . . . 20
  E. Emission Spectra . . . 27
IV. Potential Energy Curves . . . 28
  A. The Ground State . . . 28
  B. Excited Electronic States and the Franck-Condon Principle . . . 28
  C. Morse's Equation for the Potential Energy Curve . . . 40
  D. Predissociation . . . 42
V. Intensities in Molecular Spectra . . . 44
  A. General . . . 44
  B. Classical Theory of Absorption and Emission . . . 46
  C. Quantum Theory of Absorption and Emission . . . 49
VI. Applications of Electronic Absorption Spectra to Structure Determination . . . 56
  A. The Concept of the Chromophore . . . 56
  B. Classification of Electrons and Orbitals in Organic Compounds . . . 57
  C. Electronic Spectra of the Various Chromophores . . . 59
    1. Saturated Hydrocarbons . . . 59
    2. Saturated Compounds Containing Atoms with Nonbonding Electrons . . . 60
    3. The Isolated Ethylenic Bond . . . 62
    4. Conjugated Ethylenic Bonds . . . 63
    5. Polyacetylenes . . . 69
    6. Aliphatic Carbonyl Compounds . . . 70
    7. Compounds Containing 1,2-Carbonyl Groups . . . 73
    8. α,β-Unsaturated Carbonyl Compounds and Polyene Aldehydes . . . 76
    9. Characterizing Derivatives of Carbonyl Compounds . . . 82
    10. Multiple-Bond Nitrogen Groups . . . 83
    11. Aromatic Compounds . . . 85
    12. Condensed-Ring Hydrocarbons . . . 91

13. Spatial Orientation of Electronic Transitions in Organic Molecules . 93
14. *N*-Heterocyclic Compounds 95
15. Steric Effects on Spectra 96
16. Solvents for Ultraviolet Absorption Spectroscopy 98
References 99

I. GENERAL NATURE OF SPECTRA

Spectroscopy is concerned with interactions between material substances and a form of energy, electromagnetic radiation, in which energy is abstracted from, added to, or scattered in the radiation field by the matter. The abstraction of energy from the field constitutes the phenomenon of absorption of radiation by matter. Matter may also emit radiation, when radiant energy appears at the expense of kinetic or potential energy of the matter. In scattering, radiation is deflected from its initial direction of propagation by the matter, the process sometimes occurring without a net change in the distribution of energy between the radiation field and the matter, or sometimes, as in the Raman effect, with some energy exchange, signaled by the fact that the wavelength of the scattered radiation is not identical with that of the incident radiation.

The propagation of radiation can be regarded as a wave phenomenon characterized by a *wavelength* which may vary from kilometers for radio waves to fractions of an angstrom unit (10^{-8} cm) for the γ-rays emitted in radioactive disintegrations, by a uniform *velocity* of propagation of all wavelengths in vacuum, c, by a *frequency* enumerating the undulatory disturbances, transverse to the direction of propagation, which occur at a given point in the radiation field in 1 sec, and by directional properties described as the state of polarization. Radiation can differ in quality as well as in quantity, and it is the quality that is determined by the wavelength λ and frequency $\tilde{\nu}$, related by the equation $c = \tilde{\nu}\lambda$. When the radiation is characterized by a single frequency and associated wavelength in vacuum, it is said to be *monochromatic*, although theory shows that the concept of monochromaticity is an idealized abstraction, any finite wave train necessarily showing a small range of frequencies. When radiation enters a transparent material, there is no loss of energy, but the velocity of propagation is reduced below the value in vacuum. The ratio of the velocity in vacuum to the velocity in the medium is the refractive index of the medium. The frequency is unaltered, and therefore the wavelength is diminished in the medium. In contrast to the passage of radiation through vacuum, the velocity in material media depends, in general, on the wavelength, i.e., the refractive index varies with wavelength. This variation is the origin of the phenomenon of dispersion, i.e., the separation of radiation into its constituent components by passage through a prism. The variation of velocity with wavelength over the whole range of wavelengths of electromagnetic radiation is very complicated, but, for restricted wavelength ranges in transparent media, the refractive index usually increases with increasing frequency.

The intensity of the various interactions between radiation and matter depends on the wavelength. Absorption is highly selective with respect to wavelength. No material is highly absorbent toward all wavelengths, and no material is without high absorptivity toward some group of wavelengths. A spectrum consists of a regular arrangement of the component parts of heterogeneous radiation according to their wavelengths; the sorting is usually accomplished by utilizing dispersion, in prism spectroscopy, or diffraction by means of gratings. The radiation of a self-luminous source so analyzed constitutes an emission spectrum, and if all wavelengths over a wide range are present, the spectrum is said to be continuous. For example, an incandescent solid, such as a lamp filament, yields a continuous spectrum of useful intensity over the wavelengths comprising all the *visible spectrum* (the wavelengths of which decrease regularly from red to violet), a considerable part of the *infrared spectrum*, of wavelengths longer than those of the red, and of the *near ultraviolet*, the wavelengths of which are smaller than those of the violet. A longer range within the ultraviolet is furnished by various types of electrical discharge through hydrogen. If now an absorbing medium is placed in the path of the radiation of such a source, either before it is resolved by a spectrometer or in the resolved beam, the resultant spectrum will be weakened in intensity for the particular wavelengths absorbed by the medium, and the modified spectrum constitutes the absorption spectrum of the medium. If the medium is visibly colored, the spectrum of the source, which in the absence of an absorbing medium is spread out over a continuously colored bright band from red to violet, will be crossed by one or more black bands corresponding to the wavelengths selectively absorbed, and similar gaps in the emission spectrum of the source will be found if the absorbing substance selectively absorbs infrared or ultraviolet light. In modern practice, the determination of the wavelengths absorbed is accompanied by quantitative measurements of the amount of energy absorbed, the combined operation being described as spectrophotometry. Various methods are used in measuring the energy abstracted from the spectrum of the source by the absorbing medium, for details of which the practical manuals (1) should be consulted.*

---

* For example, for visible and ultraviolet spectra, *Chemical Spectroscopy*, *Practical Spectroscopy*, *Absorption Spectrophotometry*, and *Analytical Absorption Spectroscopy* (1).

II. SPECTROSCOPIC UNITS

A. Units Referring to Wave Properties of Radiation

The wavelike behavior of radiation is described by the wavelength, frequency, and wave number of the oscillating electric and magnetic fields, vibrating perpendicularly to each other and to the direction of propagation, that constitute the radiation. In the propagation of monochromatic radiation there is, at a given instant, a sinusoidal variation of the magnitude of the electrical and magnetic fields with distance in the direction of propagation, and the wavelength of the radiation is the constant distance between neighboring points for which the phase is the same, such as adjacent crests or adjacent troughs.

The unit of wavelength commonly used for the visible and ultraviolet spectral region is the angstrom, equal to 10^{-10} m (or 10^{-8} cm), for which the symbol is Å. The recently adopted primary standard of wavelength is that of a very sharp orange-red line of an isotope of krypton, ^{86}Kr, excited by the passage of an electrical discharge through the gas; this standard has displaced the red line of cadmium formerly used. According to the recommendation of the 11th General Conference on Weights and Measures, Paris, 1960, the meter is equal to 1,650,763.73 wavelengths in vacuum of the ^{86}Kr line. The wavelength of the primary standard line in vacuum is therefore 1/1,650,763.73 m, equal to 6057.80210 Å.

The millimicron, mμ, equal to 10 Å, is frequently used in the chemical literature as a unit of wavelength in the visible and ultraviolet regions. According to the recommendation of the Commission on Symbols, Units and Nomenclature of the International Union of Pure and Applied Physics, the millimicron is redesignated the *nanon* (nanometer, equal to 10^{-9} m), for which the symbol *nm* is used.

In near infrared spectroscopy, the wavelength unit usually employed is the micron, $\mu = 10^{-6}$ m; 1 μ = 10,000 Å.

More fundamental than wavelength is the concept of *frequency of oscillation* of the radiation. This statement is true even in the description of radiation itself, for, as already pointed out, the frequency of a given train of monochromatic radiation is invariable (within the theoretical limitations already referred to), while the wavelength depends on the medium traversed. Of greater importance is the fact that the frequency of radiation can be directly related theoretically to energy differences in atoms and molecules, and to frequencies of vibration and rotation of molecules. The relation between the oscillation frequency of the radiation and the wavelength is given by the equation for the propagation of the wave train:

$$u = \tilde{\nu}\lambda$$

where u is the velocity, $\tilde{\nu}$ the frequency, and λ the wavelength of the radiation in the medium. If c is the velocity of light in vacuum, 2.997925×10^{10} cm/sec, and λ the wavelength in this medium, $\tilde{\nu} = c/\lambda$. The frequency is usually expressed in oscillations per second; for example, the frequency of radiation of wavelength 4000 Å in vacuum is 7.4944×10^{14} sec^{-1}. Oscillation frequencies themselves, however, are rarely used (except in the microradiowave region), although a unit, the *fresnel*, equal to 10^{12} sec^{-1} is sometimes used. Of greater practical convenience is the reciprocal of the wavelength, *the wavenumber*, which expresses the number of waves in one centimeter length of the wave train in vacuum. The symbol for wavenumber is ν, and the unit is the reciprocal centimeter, cm^{-1}. The symbol σ has recently been proposed for the wavenumber, but common practice in the chemical literature is still to use ν for the wavenumber. One reciprocal centimeter is sometimes termed one kayser, K, and wave numbers in the visible and ultraviolet regions are sometimes expressed in kilokaysers, kK, one kilokayser being equal to 1000 cm^{-1}. For example, the wavenumber for radiation of wavelength 4000 Å in vacuum is 25,000 cm^{-1} or 25.00 kK.

If the wavenumbers refer to wavelength in a medium of constant refractive index, they will be directly proportional to the frequencies, and can be used for most theoretical purposes in place of the frequencies. Since, however, except in the extreme ultraviolet, spectroscopic measurements of wavelength usually refer to the value in air and are based on standard wavelength determinations made in air, it is necessary, in the precise computation of wavenumbers, to reduce the observed wavelengths to their greater values in vacuum, before forming the reciprocal, by adding $(n - 1)\lambda_{\text{air}}$ where n is the refractive index of air at the wavelength in question.

A table of wavenumbers for wavelengths measured in air between 2000 and 10,000 Å reduced to their values in vacuum was compiled by Kayser as Tabelle der Schwingungszahlen (2). For high precision spectroscopy, Kayser's table has been superseded by tables calculated by Edlén from more recent measurements of the dispersion of standard air (3). A table of corrections to be applied to the wave numbers in Kayser's table is given in ref. 3. The greatest correction, at wavelength 2000 Å, amounts to 0.078 cm^{-1}. The effect on the wavenumber of reducing wavelengths measured in air to their values in vacuum is quite appreciable; for example, the wavenumber of a spectral line at 4000 Å as measured in air is 25,000 cm^{-1}, whereas if the wavelength is expressed as its value in vacuum, the wavenumber, according to Kayser's table, is 24,992.958 cm^{-1}, or, with Edlén's correction, 24,992.932 cm^{-1}, some 7 cm^{-1} less.

Electromagnetic radiation of wavelength in the millimeter and centimeter ranges comprises the *microwave* region, utilized in electron spin resonance and nuclear magnetic resonance spectroscopy. The spectral region in which wavelengths are in the meter and kilometer range is called the *radiowave* region, since these are the waves used in ordinary radio transmission. The quality of radiation in these regions is usually defined in terms of the frequency, expressed in cycles (per second). In the microwave region, the unit frequently employed is the kilomegacycle, kMc, 10^9 sec^{-1}. For example, the frequency of radiation of wavelength 1 mm in vacuum is 299.8 kMc. In the radio region frequencies are often expressed in kilocycles, kc, 10^3 sec^{-1}.

The state of polarization of radiation absorbed or emitted is sometimes characteristic of the absorption or emission process. In dealing with oriented structures, such as crystals, adsorbed layers, or nematic phases, it is usually necessary to specify the direction of vibration of the radiation with respect to some axis in the structure, while the Raman and fluorescent emission even from liquids and solutions may be polarized or depolarized when excited by polarized or unpolarized radiation.

B. Units Referring to Photon Energy of Radiation

The bridge between the quantum or photon aspect of radiation and the wavelike properties is formed by the equations

$$\begin{aligned} E &= h\tilde{\nu} \\ E &= hc/\lambda \end{aligned} \tag{1}$$

where E is the energy of the photon associated with frequency $\tilde{\nu}$ and wavelength λ in vacuum. The energy of a photon is directly proportional to the associated frequency or wavenumber and inversely proportional to the wavelength in vacuum. For example, substitution of the numerical values from Table I, p. 61, into Eqs. 1 shows that the energy of a photon of wavelength 4000 Å in vacuum is 4.9658×10^{-12} ergs, and the energy of a photon of wavelength 2000 Å is double that quantity.

The energy of a molecule that has absorbed a photon of frequency $\tilde{\nu}$ is increased by the energy of the photon, $h\tilde{\nu}_{\text{absorbed}}$, and similarly, the energy of a molecule that has emitted a photon is lowered by an amount $h\tilde{\nu}_{\text{emitted}}$. Energy exchanges between material substances and radiation are of interest in photochemical reactions and in other radiation-induced changes in matter, and since energy changes in matter are usually expressed for a mole of the material, it is convenient to introduce a unit for the energy of N photons, where N is Avogadro's number. This energy unit, the energy of a "mole" of photons, $E = Nh\tilde{\nu} = Nhc/\lambda$, is called the einstein. Substitution of the values of the constants in the equation along with the conversion factor 4.1840×10^{10} ergs/kcal gives the equation for the value of the einstein as a function of wavelength

$$\begin{gathered} E\,(\text{kcal/einstein}) = 2.8591 \times 10^5/\lambda\,(\text{Å}). \\ \lambda\,(\text{Å}) = 2.8591 \times 10^5/E\,(\text{kcal}). \end{gathered}$$

Energy may also be expressed in electron volts. One electron volt, the symbol for which is eV, is the kinetic energy of an electron which has dropped from rest through a potential difference of 1 V, or the equivalent energy in a molecule or photon. The magnitude of the electron volt is 1.60210×10^{-12} ergs per single electron, molecule, or photon, or 23.06 kcal/mole or einstein.

$$E\,(\text{kcal})/\text{mole} = 23.06\,E\,(\text{eV}).$$
$$E\,(\text{eV}) = E\,(\text{kcal/mole})/23.06.$$

The wavelength and wave number of the photon whose energy is 1.00 eV are 12,399 Å and 8066 cm^{-1}, respectively. Hence the conversion formulas for the energy in electron volts of quanta of wavelength λ in angstroms and wave number ν in reciprocal centimeters are

$$\begin{aligned} E\,(\text{eV}) &= 12{,}399/\lambda\,(\text{Å}) \\ &= (\text{cm}^{-1})/8066 \\ \lambda\,(\text{Å}) &= 12{,}399/E\,(\text{eV}) \\ \nu\,(\text{cm}^{-1}) &= 8066 \times E\,(\text{eV}) \end{aligned}$$

C. Units Referring to Intensity of Absorption

The absorption spectrum of a pure chemical substance has been compared to the fingerprint of an individual; no two substances have the same absorption pattern just as no two individuals have the same pattern of lines and whorls in their fingerprints. No less characteristic of a substance than the wavelengths of its absorption bands is the intensity of the bands, depending on the fraction of incident radiant energy absorbed by a given amount of the substance in the beam. Both wavelength and intensity of absorption depend on such conditions as temperature, concentration of the absorbing substance and the solvent; but in a given environment every substance has a unique spectrum. In attempting to identify a compound by comparing its absorption spectrum with that of a known compound, not only must the characteristic wavelengths match, but also the intensity of the absorption of the unknown must be consistent with that of the known.

While, strictly speaking, no two substances absorb identically in any spectral region, the difference in the spectra of closely related chemical compounds is not equally obvious in all regions. For example, the difference in the visible absorption spectra in solution of two dyes differing only in the substitution of a methyl for an ethyl group attached to a basic nitrogen may be quite small, but there will always be some region where great and obvious differences exist. The infrared region longer than about 5 μ is the "fingerprint region" par excellence.

The simplest situation with respect to the intensity of absorption is that in which the Lambert-Beer law is obeyed. In this case, if I_o is the intensity of a parallel beam of monochromatic radiation incident normally on a layer of absorbing medium of thickness l and molar concentration c, the intensity of the emergent beam is given by

$$I = I_o 10^{-\epsilon c l} \tag{2}$$

where ϵ is a quantity independent of c, but depending on wavelength, temperature, and solvent. This equation expresses the fact that each layer of given thickness in the medium absorbs the same fraction of the radiation incident on it, or, reduced to ultimate terms, that each molecule of the absorbing substance absorbs a constant fraction of the radiation incident upon it. According to the recommendation of the Committee of the Optical Society of America, ϵ is termed the molar absorptivity; formerly it was called the molar extinction coefficient and is still frequently so called. Equation 2 can be expressed as

$$\log_{10} I_o/I = D = \epsilon c l \tag{3}$$

in which D is often called the *optical density*; the term adopted by the Committee on Colorimetry of the Optical Society of America is the *absorbance*. This equation shows that the molar extinction coefficient is the absorbance of a layer of thickness 1 cm and concentration 1 mole/liter. The importance of the absorbance is that, so long as Beer's law is obeyed, the quantity is proportional to the concentration of the absorbing substance, other conditions remaining constant.

D. Deviations from Beer's Law

Deviations from Beer's law may be real or apparent. Since the molar extinction coefficient depends on wavelength, the law can be strictly true only for monochromatic light. The exit beam from any spectrophotometer, whose energy is measured or compared with some standard in the determination of extinction coefficients, always comprises a range of wavelength, determined by the resolving power and dispersion of the spectrometer and the slit widths used; and for the applicability of Beer's law it is necessary that there be no great variation of the extinction coefficient of the substance over this band of wavelengths. Otherwise apparent deviations from Beer's law will be found. In practice, the law is found to be obeyed by a great many substances over a considerable range of concentrations. True deviations can be expected when the concentration of the absorbing molecules is high enough for them to exert perturbing forces on each other. The effects of association and dissociation are particularly strong in causing deviations from Beer's law; for example, aqueous solutions of dyes, which are prone to dimerize and polymerize, rarely follow Beer's law over any extended concentration range

III. THE ORIGIN OF SPECTRA

A. General Nature of Rotational, Vibrational, and Electronic Spectra

It is well known that, while the kinetic energy of a free molecule can vary in a continuous manner, the energy associated with periodic motions of the molecule as a whole (rotations), and of the constituent atoms in the molecule relatively to one another (vibrations), and the internal electronic energy which holds the molecule together, can assume values only from a discrete set, the so-called *quantized energy levels* which characterize *stationary states*. On placing a molecule in an electromagnetic radiation field, a transfer of energy from the field to the molecule will occur if certain conditions are fulfilled, whereby the molecule passes from one quantized state to another with the gain of energy ΔE at the expense of radiation energy of a frequency $\tilde{\nu}$ such that

$$\Delta E = h\tilde{\nu} \tag{4}$$

In this equation, Bohr's frequency equation, h is the universal Planck constant, 6.626×10^{-27} erg sec. The molecule is said to absorb radiation of frequency $\tilde{\nu}$, and to become excited to the new state. Similarly, a molecule in an excited state may revert to the normal state, losing energy ΔE which appears as radiation of frequency $\tilde{\nu}$, and the molecule is said to emit radiation of this frequency. Whether, in any given case, the intramolecular energy change can actually be effected by interaction with the radiation field depends essentially on whether the energy change is or is not accompanied by a change in the electrical center of the molecule. If the transition is accompanied by a so-called dipole moment of transition (usually abbreviated to the term transition moment), electrical work can be done by the field on the molecule or vice versa, and absorption or emission of radiation will occur; otherwise, the intramolecular change cannot be effected by radiation. The rules governing the intensity of radiation absorbed or emitted in various types of energy transitions are summarized in *Selection Rules*, a knowledge of which is of great importance in connecting spectral features with molecular structure.

Transitions within the molecule which are possible according to the selection rules are said to be *allowed*, while transitions which cannot occur by interaction with radiation are called *forbidden transitions*. In the sequel we shall encounter examples of so-called forbidden transitions associated with a spectrum of relatively low, but not vanishing intensity. In spectroscopic parlance the term "forbidden transition" is often applied to one which is merely improbable, but not absolutely forbidden; the well-known absorption spectrum of benzene at about 2600 Å is an example.

In addition to the translational energy of the molecule as a whole, changes in which are not accompanied by absorption or emission of radiation, the molecular energy may be regarded, to a first approximation, as composed of quantized additive components associated with (*1*) the rotation of the molecule, (*2*) the vibrations of the constituent atoms, and (*3*) the intramolecular electronic motion. The reason for this separability of electronic, nuclear, and rotational motion lies in the different orders of magnitude of the respective frequencies—the frequency of the electronic motion ($\sim 10^{15}$ sec^{-1}) is normally great in comparison with that of the heavy nuclei ($\sim 10^{12}$ sec^{-1}), which may therefore, to a first approximation, be taken as fixed, and similarly, the molecular rotations, with a frequency of the order of 10^{10}/sec, are much slower than the vibrations. The speed of the electrons in the atom is of the order 10^7 or 10^8 cm/sec, and, since an electronic transition involves the motion of the electron over a distance of the order of 10^{-8} cm, the time required for the transition will be some 10^{-15} or 10^{-16} sec. In this time, the nuclei, vibrating with a frequency of some 10^{12} oscillations/sec, will have covered a distance of only one-thousandth or less of the amplitude, and can therefore be regarded practically as fixed. We shall find these considerations important in discussing such matters as the relative intensities of absorption bands and the Franck–Condon principle. When these relations do not hold, the separability of the total energy into additive components breaks down.

The energy levels for the rotation of the molecule are relatively close to each other, and, if a rotational transition is permitted, the frequency of the absorbed radiation is low, and the wavelength long. The pure rotational spectra, in fact, occur in the microwave region, at wavelengths of the order of 1 cm, and extend into the long infrared region. The separation of the vibrational levels is greater, and the corresponding spectra are of higher frequency and smaller wavelength, the most important vibrational spectra occurring as absorption in the near infrared from about 1 to 30 μ. Finally, electronic levels are mostly so far apart in energy that the radiation involved in transitions between these levels has the high frequencies associated with visible or ultraviolet light. In a general way one can therefore associate the microwaves and far infrared with molecular rotations, the nearer infrared with nuclear vibrations and the visible and ultraviolet regions with electronic transitions. But naturally there are no sharp dividing lines separating these various molecular processes. Pure rotational spectra involving transitions to highly excited rotational states occur in the near infrared, while purely electronic transitions can also occur in that region. In fact, one of the most remarkable examples of the universality of the fundamental Bohr frequency equation (4) is the recent observation in the radio spectrum from interstellar space of a sharp emission line of wavelength 21 cm originating in a purely electronic transition in the neutral hydrogen atom; the ground electronic state of this atom is a doublet level of exceedingly small energy separation, transitions between which can occur with the absorption or emission of radiation of wavelength 21 cm. In gases, vibrational transitions are in general accompanied by changes in the rotational state, so that the spectrum corresponding to a transition between two vibrational levels, instead of being a single line, contains a number of lines close together representing the rotational transitions superposed on the vibrational transition. Similarly, electronic spectra of gaseous molecules may assume a very complicated structure because of the superposition of vibrational and rotational changes on the electronic transition. The state of affairs is shown diagrammatically in Figure 1, which indicates the relative spacing of the rotational and vibrational energy levels associated with two electronic levels A and B of a diatomic molecule. The energy increases upward in the figure; the relative spacings of the rotational levels, indicated by the short horizontal lines, and the vibrational levels,

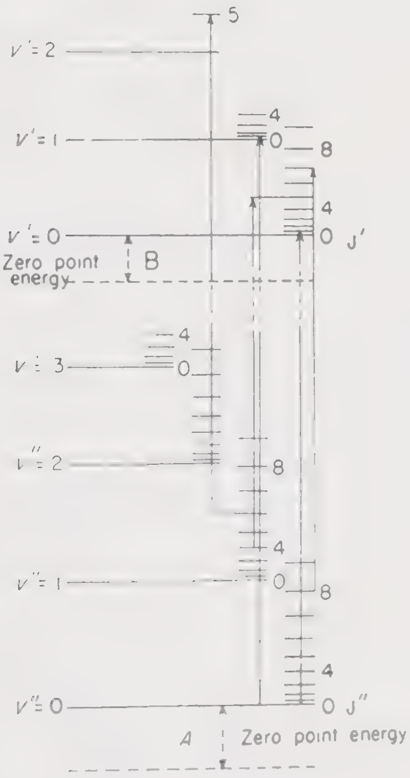

Fig. 1. Rotational and vibrational levels associated with electronic levels of a diatomic molecule, and some corresponding rotational and vibrational changes accompanying electronic excitation.

represented by the longer horizontal lines, are realistic, but, for economy of space, the electronic levels A and B have been drawn much closer than is correct for a visible or ultraviolet absorption spectrum, which is indicated by breaking the vertical lines representing a few of the spectral transitions possible in this system. To the rotational levels are assigned numbers 0, 1, 2, etc., which indicate the rotational quantum number J, and similarly the vibrational levels are characterized by a vibrational quantum number v. The rotational levels open up with increasing rotational energy, while the vibrational levels tend to converge. The dotted horizontal lines associated with the electronic levels A and B indicate the energy which the molecule would possess at the absolute zero of temperature if it were possible to suppress the vibratory motion of the nuclei which persists under these conditions; the energy interval between the dotted line and the lowest possible vibrational state, with $v = 0$ and $J = 0$, is the *residual energy* of the molecule at the absolute zero in virtue of the nuclear vibrations. This quantity is usually called the *zero-point* energy.

There are a great many permitted transitions between the vibrational and rotational levels of A and B, a few of which are indicated as absorption transitions by the vertical arrows, and it will be clear how complicated a pattern can arise in the absorption spectrum of the molecule associated with an electronic transition which in an atom would be represented by a single very narrow absorption line.

Observed at sufficiently high resolving power, the visible and ultraviolet absorption spectra of diatomic molecules and of some relatively simple polyatomic molecules are indeed found to consist of myriads of exceedingly fine lines constituting the rotational structure of the spectrum (4).* Various circumstances, however, arise in which this structure is not observed. In the first place, the lines may be so close together as to be unresolvable, as is true for the visible and ultraviolet spectra of most organic molecules examined even with instruments of high resolving power. Figure 1 shows that the spacing between vibrational levels is much greater than that between rotational levels, and the electronic spectrum even of a complicated molecule may show a relatively easily resolvable vibrational structure, consisting of absorption maxima representing specific vibrational transitions between the two electronic levels (see Fig. 4). Since in the gaseous state each of these maxima is associated with an overlapping series of rotational lines, the vibrational spectrum associated with an electronic transition consists of a series of more or less broad bands, usually with an asymmetric distribution of intensity determined by the concentration of unresolved rotational lines; the aggregate of the vibrational maxima gives rise to the well-known resemblance of the molecular spectrum to the shaded flutings of classical columns which, in the early days of spectroscopy, led to their description as fluted-band spectra.

---

* For references to polyatomic molecules and free radicals showing rotational structure in their electronic band spectra see Ramsay (4). Rotational structure has been observed in spectra of a molecule as large as azulene.

To illustrate, the ultraviolet absorption spectrum of benzene shown in Figure 4 is associated with a single electronic transition, and the wide spread of absorption in wavelength is caused by the changes in the motion of the atomic nuclei (vibrations and rotations) that accompany the electronic excitation. In particular, the band structure is determined by vibrational changes. The term electronic vibrational spectrum appropriate to such a system has been telescoped to *vibronic spectrum*.

The spectra of most organic substances are examined in solution. Only in liquids derived from molecules of the lowest molecular weights, such as H_2 or its isotopes, are quantized rotations observed (5,6).* Molecular collisions occur before a rotation can be completed, the levels of the individual molecules are perturbed to various degrees, and the concept of quantized rotations in the condensed state breaks down. In some cases, the spectrum of a liquid cannot even be regarded as formed from that of the gas by smudging the rotational fine structure, but shows essentially new features. However, the vibrational bands persist in many liquids and solutions, and a well-defined vibrational structure is seen in the spectra of a number of organic molecules.

Even in gases the rotational and sometimes the vibrational structure of an electronic spectrum may disappear. In large molecules, the spacing between consecutive rotational lines may be less than the width of the line imposed by the random thermal motion (the Doppler width). Moreover, recognizable structure in a spectrum requires the existence of discretely quantized states in both the initial and final electronic levels. If a molecule is stable, the ground electronic state will always be quantized, but on excitation, the molecule may dissociate. The dissociated state corresponds to a continuum of energy levels separated by arbitrarily small intervals representing infinitesimally small increases in the kinetic energy of the dissociated fragments, and transitions to such a state give rise to continuous spectra.

B. Pure Rotational Spectra

The frequency of any absorption spectral feature is determined by the Bohr condition:

$$h\tilde{\nu}\,(\text{sec}^{-1}) = E' - E''$$

where E' and E'' are the energies of the upper and lower levels between which the transition occurs. In quantum mechanics the rotational energy of a diatomic molecule regarded as a system of two particles separated by a fixed distance R_0, rotating about an axis through the center of gravity and perpendicular to the molecular axis, is given by the expression

---

* See refs. 5 and 6 for examples of rotational energy levels of hydrogen isotopes in a liquid environment.

$$E_J = [J(J + 1)h^2]/8\pi^2 I \tag{5}$$

in which J, which may possess one of the integral values 0, 1, 2, etc., is the rotational quantum number and I the moment of inertia of the molecule. The rotational energy is inversely proportional to the moment of inertia, and it is this quantity which mainly determines the position of the rotational spectrum, and, along with the selection rule for permitted changes in J, the closeness together of the lines corresponding to the various rotational transitions. In rotational motion, the moment of inertia plays the same role as the mass in rectilinear motion. Its value for the rigid diatomic rotator is

$$I = [m_1 m_2/(m_1 + m_2)]R_0^2 \tag{6}$$

The mass term can be gathered into the quantity μ

$$\mu = m_1 m_2/(m_1 + m_2) \tag{7}$$

called the *reduced mass* of the system, and

$$I = \mu R_0^2 \tag{8}$$

The permitted changes in J for the diatomic molecule undergoing purely rotational changes are $\Delta J = \pm 1$, so that the absorption line of longest wavelength in the rotational spectrum corresponds to the change in J from 0 to 1. From Eq. 5, $E_0 = 0$ and $E_1 = 2h^2/8\pi^2 I$ so that the frequency of the first pure rotational line is

$$\tilde{\nu}\,(\text{sec}^{-1}) = 2h/8\pi^2 I$$

and the corresponding wavenumber is

$$\begin{aligned}\tilde{\nu}\,(\text{cm}^{-1}) &= 2h/8\pi^2 Ic \\ &= 2B\end{aligned}$$

where

$$B = h/8\pi^2 Ic = 27.99 \times 10^{-40}/I\ \text{cm}^{-1} \tag{9}$$

Proceeding in this way for the other permitted rotational transitions $J = 1 \rightarrow J = 2$, $J = 2 \rightarrow J = 3$, etc., it is seen that the pure rotational spectrum for the diatomic molecule (always regarded as having a fixed internuclear separation) consists of a series of lines at wavenumbers $2B$, $4B$, $6B$, etc., i.e., with a constant wavenumber separation of $2B$. The spacing is inversely proportional to the moment of inertia, and the pure rotational spectrum therefore furnishes a means of measuring the moment of inertia and hence the internuclear separation of the diatomic molecule.

Applying this theory to CO, we find the reduced mass of the molecule to be

$$\begin{aligned}\mu &= [M_1M_2/(M_1 + M_2)] \times 1.66 \times 10^{-24}\ \text{g}\\ &= 11.38 \times 10^{-24}\ \text{g}\end{aligned}$$

where M_1 and M_2 are the atomic weights of the atoms in the molecule, carbon and oxygen in this case, and the constant is the mass of an atom of unit atomic weight. The internuclear separation at equilibrium is 1.13×10^{-8} cm (estimated, among other ways, from Eq. 9), and the moment of inertia is therefore $14.5 \times 10^{-40}\ \text{g cm}^2$, B is 1.93 cm^{-1}, and the longest line of the pure rotational spectrum is at somewhat under 4 cm^{-1}, followed by a series spaced at this value. The wavelength of the longest line is about 0.25 cm. The energies of the first four rotational levels of CO regarded as a rigid rotator are 0, 11.04, 33.1, and 66.2 cal/mole.

It is not surprising that diatomic molecules do not behave in detail as rigid rotators. As the rotational energy increases, the centrifugal force causes a stretching of the molecule, similar to the separation of the massive spheres of the governor of a steam engine; the moment of inertia increases and the separation of the lines of the rotational spectrum diminishes with increasing wavenumber. Qualitatively, the results for the rigid model are useful, the prime characteristic of the actual spectra being that the line separation is the greater the smaller the moment of inertia.

Only molecules with a permanent electric moment exhibit pure rotational spectra, since only then will there be a periodic variation of the electrical distribution along directions fixed in space. Diatomic elementary molecules, e.g., H_2, O_2, N_2, have therefore no pure rotational spectra in absorption nor have symmetrical polyatomic molecules like CH_4 or $H_2C{=}CH_2$ such a spectrum.

Polyatomic molecules, with the exception of a few linear molecules like $HC{\equiv}CH$ or HCN, have three moments of inertia about mutually perpendicular axes. Reference is made to Chapter II of this volume and to Part II for the discussion of the corresponding spectra.

C. Vibration–Rotation Spectra

The atoms in a molecule carry out periodic vibrations about equilibrium positions with amplitudes that are usually small compared with the internuclear separation. As the quantum mechanical theory shows, a certain amount of vibratory motion persists to the absolute zero of temperature, the so-called zero point energy. As the temperature is increased or, under certain conditions, on exposure to electromagnetic radiation, the vibrational energy increases in quantized steps. Consider a diatomic molecule, which has a single vibration along the line of centers. During the vibration the electrical distribution in the bond changes; if the two atoms are not identical the electrical center of the molecule will oscillate in synchronism with the nuclei, and the molecule will behave like an oscillating dipole. Under this condition, changes in the vibratory motion can be effected by the absorption or emission of radiation, sometimes specifically designated as dipolar radiation, and a vibrational spectrum arises. The vibrational quanta are of the order of one hundred times the rotational quanta, and the corresponding spectra occur in the near infrared between roughly 4000 and 100 cm^{-1}.

While the possession of a permanent dipole is essential for strong infrared absorption of diatomic molecules, symmetrical polyatomic molecules, such as CH_4, $H_3C—CH_3$, $H_2C{=}CH_2$, $H—C{\equiv}C—H$, do exhibit strong vibrational rotational absorption bands. In such molecules, the individual bonds have a dipole moment, and the nonpolarity of the molecule as a whole results from the mutual cancelling of the bond moments. In certain vibrational modes, however, the atoms do not move symmetrically, and the excitation of these vibrations causes a periodic motion of the electrical center of the molecule. Hence these vibrations can be excited radiationally, and concomitant rotational changes give rise to a vibration–rotation spectrum. On the other hand, these molecules do not exhibit a pure rotational spectrum.

If the molecule is in the gaseous state and therefore freely rotating, changes in the vibrational state may also be accompanied by changes in the rotational state. The vibrational quanta are so large that, at room temperature, most of the molecules are in the lowest vibrational state, $v = 0$ (v is the vibrational quantum number), and the chief vibrational transition effected by infrared light is to the state $v = 1$. At room temperature there is a distribution of molecules over a considerable number of rotational states, so that it is possible for the increase in vibrational energy induced by infrared light to be accompanied by a decrease, as well as by an increase in rotational energy. Instead, therefore, of a spectrum determined by pure vibrational changes, the near infrared spectra of gases consist of a spectrum whose position is fixed by the vibrational change, but which, by modulation with the rotational motion, exhibits a structure consisting of a series of lines at longer wavelength than that corresponding to the pure vibrational change and of a series at shorter wavelengths. The lines at longer wavelengths originate from molecules whose rotational energy decreases while the vibrational energy increases, and those at shorter wavelengths from molecules whose rotational energy increases simultaneously with the increase in vibrational energy. In fact, for most diatomic molecules in the gaseous state, the selection rule for the rotational change accompanying the vibrational change, $\Delta J = \pm 1$, prohibits absorption of the wavelength representing the pure vibrational change without rotational change; hence the typical vibration–rotation spectrum of a diatomic molecule

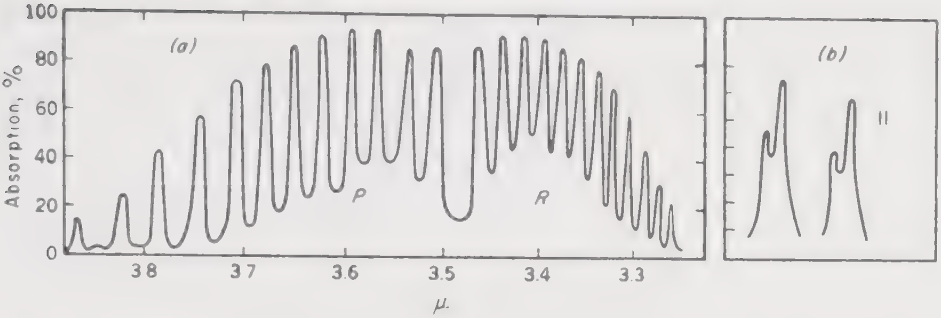

Fig. 2. Infrared absorption spectrum of HCl: (*a*) fundamental rotation–vibration band, showing *P* and *R* branches with *Q* branch absent; (*b*) two of the rotational lines in this spectrum, showing separate components of $H^{35}Cl$ and $H^{37}Cl$. (From *Physical Methods of Organic Chemistry*, Part III, 3rd ed., 1960, p. 161.)

consists of two branches, one toward longer wavelengths, the *P* or negative branch (ΔJ negative), the other toward shorter wavelengths, the *R* or positive branch (ΔJ positive) about a missing line. Figure 2 shows the rotation–vibration spectrum of gaseous hydrogen chloride, with the individual rotational lines in the two branches placed about a position of zero absorption, the small measured absorption at the missing line resulting from incomplete resolution of the lines in the *P* and *R* branches. At higher resolution, each of the rotational lines is resolved into two, the more intense of each pair belonging to $H^{35}Cl$, the other to $H^{37}Cl$.

If the vibrational motion of the molecule involves a component of the vibrating electric moment perpendicular to the line joining the atoms, $\Delta J = 0$ also becomes permitted, and there then appears between the *P* and *R* branches a zero or *Q* branch. This situation is rare among diatomic molecules, although it occurs in the odd-electron molecule NO, but is common among polyatomic molecules.

The separation of the lines of the rotational branches of vibrational bands is approximately the same as for the pure rotational lines; the observed convergence toward lower frequencies of the lines in the *P* branch and the increasing separation of the lines of the *R* branch toward higher frequencies are caused by the centrifugal stretching effect, but, since the molecular constants are not quite the same in the upper and lower vibrational states, the separation of the rotational lines is not exactly the same as for the pure rotational spectrum.

For quantitative treatment of the vibrational behavior of diatomic molecules the simplest model is the simple harmonic oscillator, the quantum mechanical analysis of which accounts for important aspects of the observed spectra, although there are important deviations of the actual molecule from the model. In this model, the atoms oscillate in unison about equilibrium positions, under the influence of a restoring force proportional to the displacement from their equilibrium positions. The frequency of oscillation is given by the equation

$$\tilde{\omega} = (1/2\pi)(k/\mu)^{1/2} \tag{10}$$

where k, the *force constant*, is the restoring force in dynes per centimeter displacement from the equilibrium position, and μ, the reduced mass. The quantum mechanical expression for the energy of the simple harmonic oscillator of frequency $\tilde{\omega}$ sec^{-1} is

$$E_v = (v + 1/2)h\tilde{\omega} \tag{11}$$

where the vibrational quantum number v can assume one of the values 0, 1, 2, ... The lowest vibrational state, $v = 0$, is associated with the zero-point energy $(1h/2)\tilde{\omega}$, and the higher states are arranged equidistant above the lowest state at a separation of $h\tilde{\omega}$ ergs. The theory shows that the selection rule for the absorption or emission of radiation by the simple harmonic oscillator is $\Delta v = \pm 1$; hence a molecule in the lowest vibrational state could gain only one quantum by absorption, and the absorption spectrum would consist of a single vibrational band, of frequency $\tilde{\nu}$ equal to the mechanical frequency of oscillation $\tilde{\omega}$.

Actual molecules do not conform in detail to the simple harmonic model. The actual molecule is an anharmonic oscillator. Classically, the effect of anharmonicity is to make the frequency no longer independent of the amplitude, while the quantum mechanical analog is that the vibrational energy levels crowd together with increasing value of the vibrational quantum number. Another consequence of anharmonicity shown by quantum mechanics is that jumps of more than one vibrational quantum are permitted. The vibrational absorption spectrum at room temperature, instead of being limited to the transition from $v = 0$ to $v = 1$, also contains the transitions $v = 0$ to $v = 2, 3$, etc., at approximately twice, three times, etc., the frequency of the longest wave band. In analogy with acoustical terminology, the $1 \leftarrow 0$ vibrational band* is often called the *fundamental* or first *harmonic*, and the bands at higher frequency, corresponding to the transitions $2 \leftarrow 0$, $3 \leftarrow 0$ the first and second *overtones*, or the second and third *harmonics*. The overtones also contain P and R rotational branches, with intervals between the lines nearly the same as in the fundamental, but, because of somewhat different interactions between the rotational and vibrational motion, not exactly the same.

---

* The recommended spectroscopic convention in writing a radiational transition is to place the symbol for the state of higher total energy on the left; thus the vibrational absorption transition from state $v = 0$ to $v = 1$ is written $1 \leftarrow 0$, called the zero–one transition, while the corresponding emission transition is written $1 \rightarrow 0$.

Although overtones are permitted for the anharmonic oscillator, their intensity rapidly decreases with the ordinal number. While a few centimeters of HCl gas at atmospheric pressure is adequate for the measurement of the fundamental, very long path lengths are necessary in observing the fourth overtone.

The theory of the anharmonic oscillator shows that the wave number corresponding to the pure vibrational transition from $v = 0$ to $v = 1$ (which, it will be remembered, appears in the rotation–vibrational absorption spectra of diatomic molecules as the missing line because of the forbidden nature of the rotational transition $\Delta J = 0$) differs from that for the corresponding harmonic oscillator by an amount determined by the anharmonic factor x. For the $1 \leftarrow 0$, $2 \leftarrow 0$, $3 \leftarrow 0$ transitions (the "fundamental" and the first and second "overtones"), the wavenumbers of the missing line are given by

$$\begin{aligned} \nu_{1\leftarrow 0} &= \omega_e - 2\omega_e x \\ \nu_{2\leftarrow 0} &= 2\omega_e - 6\omega_e x \\ \nu_{3\leftarrow 0} &= 3\omega_e - 12\omega_e x \end{aligned} \tag{12}$$

where ω_e is the mechanical frequency of the oscillator for very small displacements expressed as a wavenumber. It will be seen also that the overtones are not at exactly twice and three times the frequency of the fundamental, being displaced to lower frequencies than for the strict harmonic relationship. The constants ω_0 and x can be determined from observations of the resolved rotation–vibration spectra and solution of the simultaneous Eqs. 12.

The vibrational–rotational spectra of polyatomic molecules are complicated by the facts that, unless the molecules are linear, three moments of inertia are present (two equal in the symmetrical top), which complicates the rotational structure, and that more than one vibration occurs; $(3n - 6)$ vibrational modes occur in a nonlinear molecule containing n atoms. Besides overtone bands of the individual vibrations, *combination* frequencies are observed corresponding to the simultaneous excitation of more than one mode of vibration. The symmetry of the molecule and of the vibrational modes are important factors in determining the spectra of polyatomic molecules. These matters are discussed in detail in Chapter II of Part I, and in Parts II and III.

Although symmetrical diatomic molecules, such as H_2, O_2, N_2, have no permanent dipole moments, and therefore according to the selection rules for dipolar radiation should possess no rotation–vibration infrared spectra, these gases at high pressure have recently been shown to exhibit infrared absorption maxima at the frequencies known from Raman and ultraviolet spectra to represent their vibrational frequencies (7). The intensity of this absorption increases as the square of the pressure of the absorbing gas. Moreover, at a fixed pressure of the absorbing gas, e.g., H_2, high pressures of foreign gas transparent to the frequencies absorbed by H_2 (e.g., He, Ar, N_2) induce the infrared absorption with an intensity proportional to the pressure of the foreign gases. These relations show that the pressure-induced absorption is caused by molecules absorbing during the act of collision—the mutual distortion of the colliding partners produces a dipole moment which can interact with the radiation field (8). The selection rules for the radiation of such induced dipoles are different from that for the permanent moment ($\Delta J = 0, \pm 2$), and the observed contours of the absorption bands are consistent with this interpretation. Rotation and rotation–vibration spectra are further discussed in Chapter II, Sections II-D and II-E.

D. Electronic Spectra

Electronic levels in molecules are separated by much greater energy intervals than the vibrational levels, and the spectra originating in transitions from the ground to excited electronic levels occur mainly in the visible and ultraviolet regions.

The simplest electronic spectra are those of atoms in the vapor state. The atoms in sodium vapor, for example, exhibit an absorption spectrum consisting of close pairs of sharp lines; the pair of longest wavelength, at 5896 and 5890 Å, constitute the well-known *D* lines, the next pair is near wavelength 3302 Å, the third near 2853 Å, and the whole series converges on a limit near 2412 Å. If, for the moment, we disregard the pairing of the lines, the successive lines in the spectrum arise from electronic excitations from the lowest to the consecutive members of a particular type of excited level, the convergence limit corresponding to excitation to the ionized state Na^+ and a free electron. The doubling of the absorption lines is caused by the fact that each of the excited levels is split into a close doublet for reasons discussed in Chapter II.

Each electronic state in a molecule has its own pattern of vibrational and rotational levels, as illustrated diagrammatically in Figure 1 for two electronic states of a diatomic molecule. The electronic transition is in general accompanied by vibrational and rotational changes, and since in polyatomic molecules a great many possibilities may exist for these latter changes, the spectrum becomes a complicated assembly of lines spread over a considerable spectral region. Figure 3 shows diagrammatically the vibrational transitions accompanying the electronic excitation of a hypothetical diatomic molecule. The interval between the levels 1 and 0 in the lower state, expressed in reciprocal centimeters, is approximately the vibrational "frequency" (properly, the corresponding wave number) of the atoms in the lower state, and similarly the corresponding interval for the upper state, which has been drawn smaller than for the lower state, is approximately the frequency of the molecular vibration in the upper state. The molecular excitation, in this example,

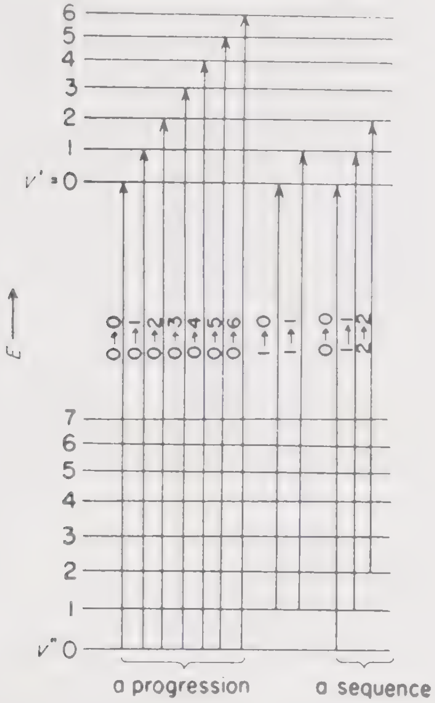

Fig. 3. Vibrational transitions accompanying electronic transitions of a diatomic molecule.

weakens the force constant somewhat, as is often observed in practice. The absorption spectrum consists of a series of vibrational sub-bands, representing the $0 \leftarrow 0$, $1 \leftarrow 0$, $2 \leftarrow 0$, etc., transitions, the numbers representing the value of v in the excited and ground states, respectively. The intensity distribution among the sub-bands is determined by the Franck-Condon principle, to be discussed in the next section. Such a series of bands associated with transitions from a common vibrational level in one electronic state to successive levels in another constitutes a band *progression*. Bands corresponding to transitions with a given value of Δv, as the $0 \leftarrow 0$, $1 \leftarrow 1$, $2 \leftarrow 2$, etc., bands are near each other and form a band *sequence*. Sequences are often prominent in the emission spectra of thermally or electrically excited vapors, containing a population of electronically excited molecules distributed over a number of vibrational states, but, since in normal absorption measurements, at room temperature, the initial state of most of the molecules is the level $v = 0$ of the ground electronic state, sequences are not usually pronounced in absorption spectra. If, however, the vibrational frequency of the molecule is low, that is, if the vibrating nuclei are of high atomic weight or the bond is very weak, the population of molecules in the first vibrationally excited state of the ground electronic state may be adequate for absorption from this level to be observed. The corresponding $0 \leftarrow 1$ band will be weaker and at longer wavelengths than the $0 \leftarrow 0$ band. If the absorbing material is in thermal equilibrium at temperature T K, the fraction of molecules in the ground electronic state possessing one quantum of vibrational excitation will be proportional to the Boltzmann factor $\exp\{-\Delta E_v/kT\}$ where ΔE_v is the energy difference between the first excited and the lowest vibrational levels in the ground electronic state. The intensity of the $0 \leftarrow 1$ vibrational band is therefore highly dependent on the temperature, and becomes vanishingly small at low temperatures.

Conversely, high temperatures broaden vibrational bands in electronic spectra and introduce new vibrational bands; for example, at 500°C the absorption spectrum of benzene vapor in the region covered in Figure 4 becomes a single broad band without vibrational structure (9).

For polyatomic molecules the situation is complicated by the existence of many vibrational modes each with its own set of vibrational quantum numbers. The intensity of the vibrational bands for this case can also be gauged from the Franck-Condon principle (10), which shows that the strongest vibrational transitions in electronic spectra involve vibrational modes which are totally symmetrical (i.e., modes for which the symmetry of the molecule is preserved when any symmetry operation appropriate to the molecular configuration is performed; Chapter II). In highly symmetrical molecules, few of the vibrational modes are totally symmetrical, with the result that the spectra, although complicated enough, are much simpler than if a great many of the total number of $3n$–6 vibrational modes were represented. Figure 4 shows the absorption spectrum of benzene vapor in the 2700–2400-Å region, as recorded by a Cary automatic spectrophotometer. The various maxima represent different vibrational bands, each of which is composed of unresolved rotational lines. The vibrational structure itself is not completely resolved; at the resolution of a concave grating of 3 m focal length several of the maxima are further resolved into distinct vibrational bands.

The spectrum consists of groups of bands, in which the short wavelength band in each group is the most intense. The vibrational analysis has been carried out by Sponer et al. (11) for benzene, and by Sponer (12) for C_6D_6. The strong bands A_0^0, A_1^0, etc. (in the terminology of Sponer et al.), are arranged in a pattern determined by the totally symmetrical "breathing vibration" of the ring in the upper electronic state, in which the carbon atoms oscillate radially in the same phase; the frequency interval of the progression is 923 cm^{-1}. The corresponding breathing frequency in the ground state is known from the Raman spectrum to be 992 cm^{-1}. The band A_0^0 is the $0 \leftarrow 0$ transition of this vibration, A_1^0 the $1 \leftarrow 0$ transition, and so on.

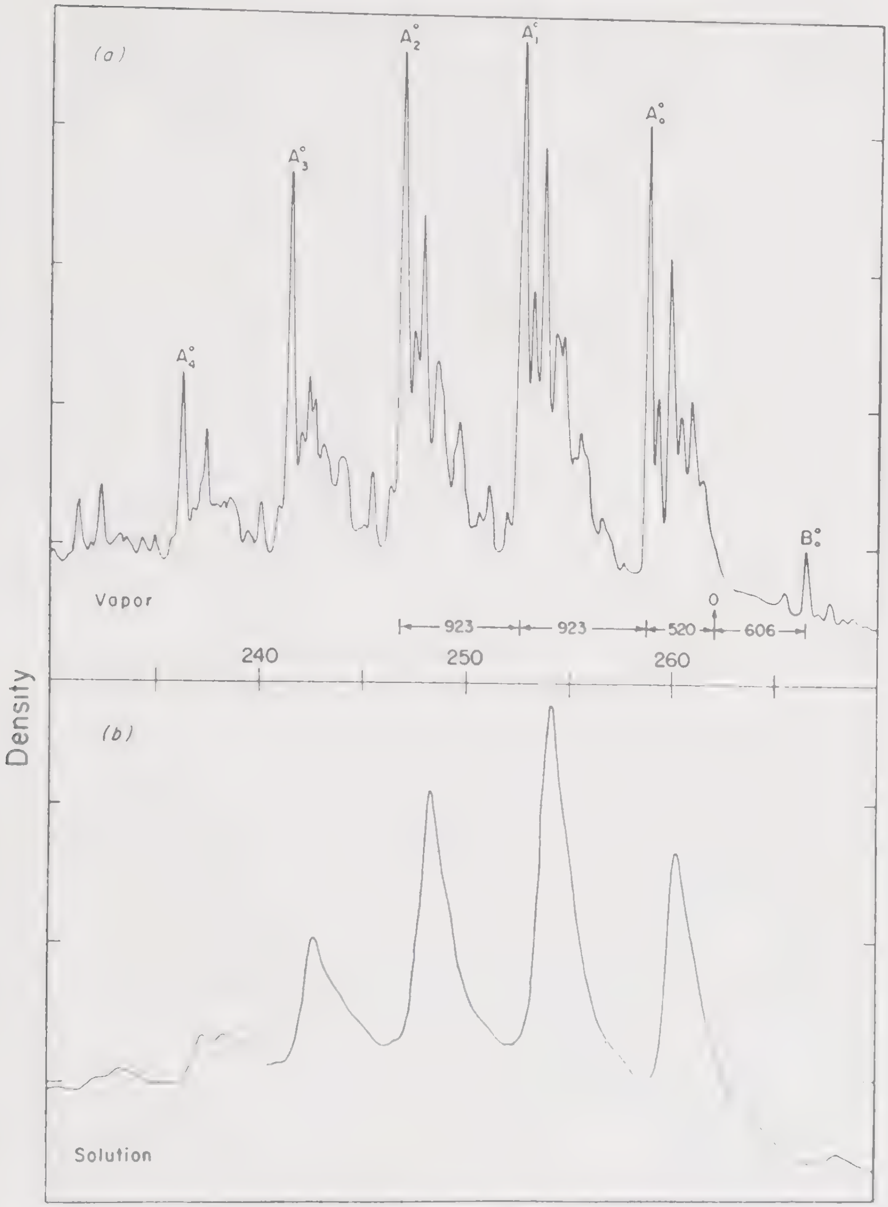

Fig. 4. Ultraviolet absorption spectrum of benzene: (*a*) vapor; (*b*) solution in ethanol.

The frequency of the A_0^0 band (corrected for zero-point energy) does not, however, represent the pure electronic transition associated with this spectrum. As will be discussed in detail in Chapter II, the electronic transition associated with this absorption spectrum of benzene is forbidden, but is rendered possible, but of relatively low probability, if accompanied by a change in the vibrational quantum number of a particular type of vibration (E_g^+). A vibration of this class has a frequency of 606 cm^{-1} in the ground state and 520 cm^{-1} in the excited electronic state, and the analysis shows that the electronic origin of this absorption spectrum is 520 cm^{-1} lower than the wave number of the $A_0{}^0$ band. The $A_0{}^0$ band therefore represents the transition from the vibrationless state of the ground level to the excited electronic state with one quantum of vibration of the 520 cm^{-1} frequency, and zero quanta of the 923 cm^{-1} vibration, the $A_1{}^0$ from the vibrationless ground state to the excited state with one quantum of the 520 cm^{-1} vibration and one quantum of the 923 cm^{-1} vibration, and so on. The feeble band at longer wavelength ($B_0{}^0$) is 606 cm^{-1} lower than the electronic origin of the spectrum, and, from its temperature dependence, represents the transition from the ground state with one quantum of the $E_g{}^+$ mode of vibration to the vibrationless upper electronic state. The other bands, in addition to the strong progression $A_0{}^0$, $A_0{}^1$, etc., represent other combinations of transitions of the $E_g{}^+$ vibrations with transitions of the breathing frequency and with other frequencies, including the totally symmetrical C—H vibration, in which the hydrogen atoms oscillate radially in phase with a frequency of 2565 cm^{-1}.

Figure 4 represents the benzene spectrum in dilute alcoholic solution as recorded by the same instrument using the same slit width. While the main pattern of the vibrational structure associated with the breathing frequency is still clearly evident, the detail with respect to the other bands in the gaseous spectrum has almost disappeared in solution. Solvent interactions of variable magnitude broaden the bands and the resulting overlap obscures the individual vibrational bands. In general, the observed absorption bands in solution can be expected to be the superposition of unresolved vibrational bands, and the position of the maximum or maxima is to some degree an accidental circumstance depending on the overlap of different spectral features. The spectra of aromatic hydrocarbons in solution, and of their derivatives containing substituents unconjugated with the rings, exhibit relatively well-resolved vibrational structure, although much less resolved than in the corresponding vapors, and the spectra of some cyclic dienes, such as ergosterol, of the diphenyl polyenes and of the carotenes also show well-defined vibrational structure. At room temperature, cyclohexadiene exhibits a broad band in about the same position as the benzene middle ultraviolet bands, which is partially resolved into separate vibrational bands in liquid propane solution at liquid nitrogen temperature (13). In general, it is found that the spectra of aromatic compounds show narrower absorption bands at low temperature, while those of aliphatic compounds remain diffuse.

The sharpness of vibrational bands in solution, even among the aromatic compounds, varies much with the structure of the compound itself, and with the solvent. The resolution is clearest in the spectra of the hydrocarbons, benzene, naphthalene, anthracene, etc.; the introduction of substituents, even of a single methyl group, somewhat lowers the resolution, and hydroxyl and amino groups cause a great loss in the resolution of vibrational structure in solution (see Chapter III, Fig. 27). The rigidity associated with closed rings is favorable to the appearance of resolved vibrational structure. Vibrational structure cannot be discerned in the ultraviolet spectrum of biphenyl or of the biphenylparaffins Ph$\cdot$(CH$_2$)$_n$$\cdot$Ph, although some ill-defined structure appears in *ortho*-substituted biphenyls in which no free rotation about the internuclear bond can occur, being replaced by a restricted torsional oscillation about a nonplanar equilibrium configuration of the nuclei (14). The diphenyl polyenes, which tend to retain a planar configuration because of the resonance in the chromophoric chain, exhibit vibrational structure in solution and, in cases like these, the introduction of crowding substituents which prevent the maintenance of the planar configuration obscures the vibrational structure. Whereas diphenyl methane, as has already been mentioned, exhibits no vibrational structure in its ultraviolet spectrum in solution, fluorene

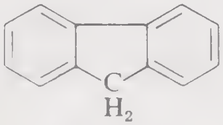

which is made planar and rigid by the linkage joining the carbon atoms of the two rings ortho to the CH$_2$ group, exhibits vibrational structure. When the molecular structure is loose, allowing low frequency motion of one part of the molecule relative to another, a number of corresponding vibrational bands will appear in the spectrum, hence the tendency toward overlapping and concealing the spectral structure is enhanced by this condition. This effect of lack of molecular rigidity in obscuring vibrational structure was recognized by Lewis and Calvin (15), who termed it the "loose bolt" effect.

The tendency of bulky groups to broaden the absorption bands even in spectra showing little or no resolved vibrational structure has been noticed among some azomethine dyes (16).

Solvent–solute interaction may also obscure vibrational structure, both by perturbing the electronic energy levels and by introducing low frequency vibrations. These effects are most pronounced in the polar solvents, and, conversely, the nonpolar solvents, such as hexane and cyclohexane, are most likely to preserve vibrational structure. For example, phenol in hexane solution shows some sign of vibrational structure, almost entirely lost in alcoholic solution (Fig. 5).

Vibrational structure is, of course, not the only way by which structure, or apparent structure, can appear in an absorption region in the visible or ultraviolet spectrum. The highest vibrational frequencies in organic molecules are those of the bond-stretching oscillations of C—H, N—H, and O—H

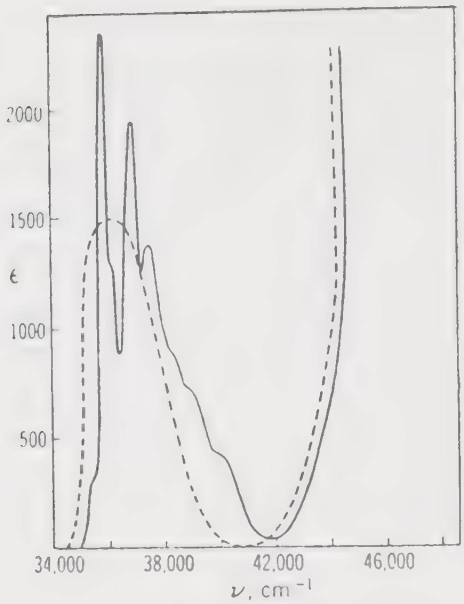

Fig. 5. Absorption spectrum of phenol, in hexane (solid line), and in alcohol (broken line). (From *Physical Methods of Organic Chemistry*, Part III, 3rd ed., A. Weissberger, Ed., 1960, p. 1805.)

groups, of magnitude about 3000 cm^{-1} in the ground electronic state and lower in excited electronic states; for example, in the first excited singlet state of benzene, the C—H frequency is about 2500 cm^{-1}. Intervals between absorption maxima or between shoulders in an electronic spectrum that are greater than 2500 cm^{-1} are therefore not likely to be ascribable to vibrational structure. Two separate electronic levels may permit independent electronic transitions in the same spectral region. For example, the spectrum of naphthalene in the near ultraviolet (Chapter III, Fig. 38) can be seen by inspection to consist of two series of absorption bands (^1L_a and ^1L_b in one spectral description, discussed in Chapter III) the long wavelength members of which are separated by an interval of about 2600 cm^{-1}. In this case, the differences in the appearance and intensity of the bands in the two regions suggest that they belong to independent electronic transitions, but if the separation interval had been somewhat smaller and the intensity difference less, more than a superficial inspection might have been necessary to decide if independent electronic transitions were involved.

The existence of an apparently pure substance as a mixture of isomers absorbing at slightly different wavelengths may introduce an apparent structure by the overlap of the spectra of the independent species. Mixtures of stereoisomers, such as those of *trans*- and *cis*-stilbene or the *trans* and *cis* forms of carotinoids can give spectra of this nature.

E. Emission Spectra

The emission of light represents the loss of energy by a molecule that has undergone a radiational transition from a higher to a lower state. Fluorescence and phosphorescence, discussed in detail in Chapter IV, involve the emission of radiation accompanying the return of an electronically excited atomic or molecular state to the ground electronic state, the initial excitation having been accomplished by the absorption of radiation. Electronically excited molecules and radicals may be produced by high temperatures, and the emission of radiation accompanying transitions to lower states is observed in the spectra of flames (17). Excitation may also be caused by high potential electrical discharges; disruption of molecules often results from this type of excitation, but some molecules, especially among the aromatic derivatives, can be excited without extensive decomposition by the high frequency Tesla discharge (18). Advances in the emission spectroscopy of electronically excited organic molecules have recently been made by introducing the complex molecule into the positive column of a discharge tube in which access of the vapor to the electrodes is prevented by cold traps, a carrier gas such as helium, neon, or argon being introduced to carry the current to the electrodes (19). At high ratio of the concentration of the inert gas to that of the organic substance, some aromatic molecules emit a spectrum that is the counterpart of the electronic absorption spectrum of longest wavelength; as the ratio is lowered, the spectra of free radicals and other fragments also appear.

The energy of chemical reactions at room temperature is sometimes sufficient to excite organic molecules to upper electronic states from which the ground level is reached by the emission of radiation. This process constitutes the phenemonon of chemiluminescence (19a). Long-known examples of chemiluminescent reactions are the oxidation of pyrogallol, of organomagnesium compounds, of lophine (α,β,μ-triphenylglyoxaline), and of 3-aminophthalhydrazide (luminal). Hydrogen peroxide is often the oxidizing agent in these reactions. It has recently been shown that the emission spectrum accompanying the oxidation of alkaline pyrogallol by hydrogen peroxide consists of a narrow band at about 630 mμ (20), identical with the chemiluminescent emission accompanying the reaction between hydrogen peroxide and hypochlorite in alkaline solution (21). These emission spectra have been shown to originate from an electronically excited form of molecular oxygen, $^1\Sigma_g^+$ modified by hydration, or from a collision complex or dimer of two diatomic oxygen molecules in the $^1\Delta_g$ state (22) (Chapter II, Fig. 1). It will be noticed from the relevant selection rules (Chapter II, Section II-D) that transitions from these states to the ground state of molecular oxygen, $^3\Sigma_g^-$, are strongly forbidden, and the excited singlet states of this molecule are therefore of relatively long life.

IV. POTENTIAL ENERGY CURVES

A. The Ground State

In considering such matters as the relative intensities of the various vibrational bands in an electronic system and other problems, much insight can frequently be gained by examining curves showing the variation of the potential energy of a molecule with the distance between the atoms. Such curves are simplest for diatomic molecules, when the potential energy is simply plotted as a function of the internuclear distance R in a two-dimensional diagram. For polyatomic molecules, the configuration can be specified only in polydimensional diagrams, and the relation between potential energy and configuration is then represented by a surface in polydimensional space. Qualitative insight, however, into the behavior of polyatomic molecules can often be derived from a two-dimensional diagram of the potential energy as a function of a generalized configuration coordinate represented on the axis of abscissas.

Figure 6*a* is a schematic drawing of the potential energy of a diatomic molecule as a function of the internuclear separation in its lowest electronic state. One of the nuclei is regarded as fixed, and the other vibrates about an equilibrium point on the line joining the nuclei, under the influence of restoring forces that hold the atoms together when their distance exceeds the equilibrium distance, and prevent their collapse into each other when the molecule is compressed. The total vibrational energy, kinetic plus potential, must have one of the quantized values appropriate to the vibrational motion. The description of the motion of the vibrating nuclei according to classical mechanics is much like the description of two vibrating masses joined by a spring, with a complete statement of the position and momentum of the oscillating particle at every point in its path. On the molecular scale, however, the motion is governed by quantum mechanics, which does not provide a detailed description of the path of the oscillating atoms in space and time, but is limited to statements regarding the distribution of the probability with which the moving atoms will be found at specified distances from each other. It will be necessary to discuss the quantum mechanical motion of an oscillator in connection with the Franck-Condon principle, but it will also be useful to visualize the classical motion. Although the two descriptions deviate markedly for the quantized vibrational states of low energy, the quantum mechanical motion approximates the classical for states of high vibrational quantum number.

B. Excited Electronic States and the Franck-Condon Principle

The forces holding the atoms together in a molecule depend on the electronic configuration, and the potential energy curves for the various

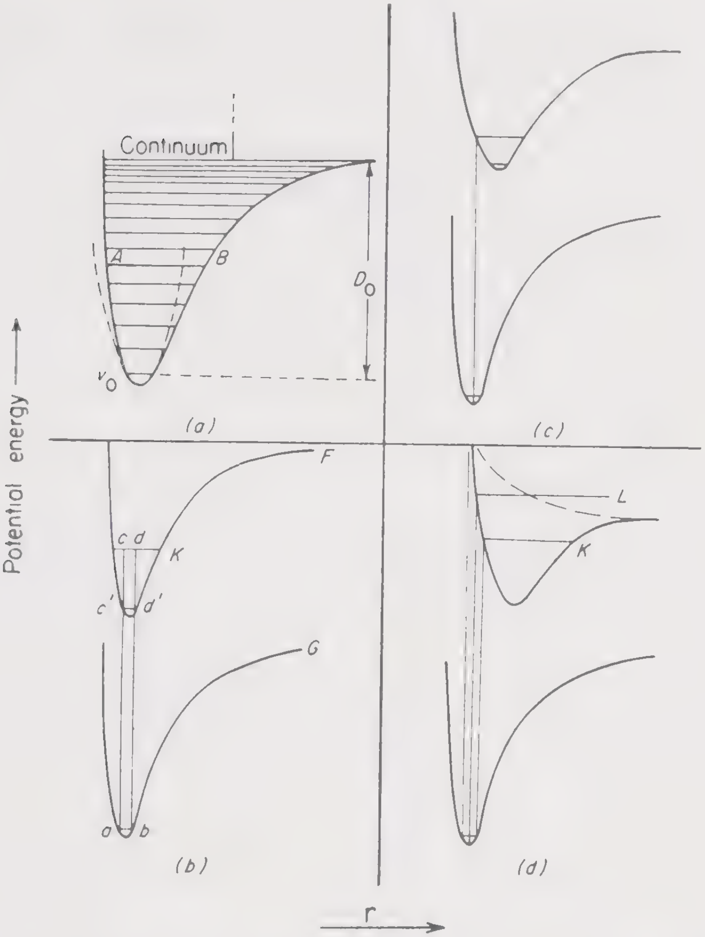

Fig. 6. Potential energy curves: (*a*) for the ground state, (*b*), (*c*), and (*d*) for the ground state and various excited states, illustrating the application of the Franck-Condon principle.

electronic states in which the molecule can exist are in general different from each other. In Figures 6*b*, *c*, and *d*, potential energy curves for the ground electronic state *G* and for an excited electronic state *F* are drawn. Franck (23) pointed out that when a photon is absorbed of sufficient energy to cause electronic excitation from state *G* to *F*, the change in the electronic configuration occurs in an interval of the order of 10^{-15} sec, in which time the relatively massive atoms have scarcely moved. The time required for a single vibration is of the order of 10^{-12} sec; hence in 10^{-15} sec, the atomic nuclei will have moved only about 1/1000 of the amplitude of the oscillation. After the electronic excitation, the molecule will therefore find itself with nearly the same nuclear configuration and vibrational kinetic energy and momentum which it possessed in the ground state at the moment of absorption. In Franck's treatment the motion of the oscillating atoms was described by classical mechanics (except for quantization of the vibrational energy), that is, the vibrating atoms behaved much like two macroscopic masses joined by a spring. An oscillator on the molecular scale does not behave in this way, but in the manner described by the wave equation of quantum mechanics, and Condon (24) showed how Franck's principle applied to vibronic transitions in molecules oscillating according to quantum mechanics. It will be convenient first to consider the application of the Franck-Condon principle to the quasiclassical model of the oscillator and then to the quantum mechanical model.

During a classical vibration, as the atoms are separated to greater than the equilibrium distance, a constantly increasing restoring force is exerted and the atoms are ultimately brought to rest and begin to move toward each other under an attractive force. As they approach each other at distances less than the equilibrium distance, increasing repulsive forces are brought into play, the atoms are again brought to rest, and begin to separate again. The motion of the atoms then consists of an oscillatory motion about an equilibrium distance of separation R_e, which is the distance at which the attractive and repulsive forces balance. Consider a vibration of amplitude AB, Figure 6*a*. The total energy, kinetic and potential, is constant, but the relative amounts of kinetic and potential energy change over the vibration. At the turning points A and B the kinetic energy is zero and all the energy is potential, while at the equilibrium distance the velocity of the atoms and the kinetic energy are a maximum and the potential energy is a minimum. The points on the continuous curve represent this variation of potential energy U with internuclear distance, while a horizontal line such as AB represents a state of constant total vibrational energy. Since the total vibrational energy is quantized, only discrete values of this total energy are possible, and these are indicated by the series of horizontal lines representing the different possible values of the vibrational energy, distinguished by vibrational quantum numbers 0, 1, 2, etc.

If the atomic oscillations were simple harmonic (restoring force proportional to the displacement from equilibrium), the potential energy distance curve would be a parabola symmetrical about the vertical line through the equilibrium point. Such a parabola is drawn in the dashed curve, and it is seen that the actual motion for small oscillations is approximately simple harmonic. A simple harmonic oscillator, however, would possess infinite stability and therefore does not correspond to any real molecule—the dissociable molecules of chemistry are subject to smaller and smaller restoring forces as the separation of the atoms from the equilibrium position is increased. The value of the restoring force is $-dU/dR$, where U is the potential energy, i.e., the restoring force at any internuclear separation R is given by the negative of the tangent to the potential energy curve at R, a positive slope indicating attraction, and a negative slope, repulsion. The true potential energy curve, corresponding to smaller attractive forces than for the harmonic oscillator at large values of R and to greater repulsive forces at small values of R, therefore deviates from a parabola in the manner shown in Figure 6*a*. Eventually, at sufficiently great internuclear separation the restoring force vanishes, the two atoms separate entirely, i.e., the molecule dissociates, and the potential energy curve becomes a horizontal line. The vertical distance D_0 between the lowest vibrational energy, corresponding to $v = 0$, and the horizontal portion of the potential energy curve is the dissociation energy of the molecule in the lowest electronic state. The lowest vibrational energy is above the minimum in the potential energy by an amount equal to the zero-point energy.

Another consequence of the anharmonic nature of the interatomic force in the molecule is that the separation of the vibrational levels becomes smaller with increasing vibrational quantum number. The levels converge on a value representing the dissociation energy. Above that level, a continuous sequence of energy values is available to the system, corresponding to dissociation of the molecule and separation of the fragments with arbitrary values of the kinetic energy.

In the case illustrated in Figure 6*b* the equilibrium separation between the atomic nuclei is about the same for the ground and the excited electronic states, i.e., the minimum of the potential energy curve for the excited state F is approximately vertically above the minimum for the ground state. This situation will usually imply that for the excited state the force constant for oscillations of small amplitude (Eq. 10), and therefore the vibration frequency and the shape of the potential energy curve near the minimum will be about the same as for the ground state. At room temperature most of the molecules will be in the lowest vibrational state of the ground electronic state, and, according to the Franck-Condon principle, an absorption transition to the excited state without change in the position and momentum of the atomic nuclei (a *vertical transition*) will find the molecule in the lowest vibrational state of the excited electronic state. The corresponding absorption band, the $0 \leftarrow 0$ band in the vibronic absorption spectrum, will be intense. Consider the probability of a transition from the state of thermal equilibrium to a high vibrational state K of the excited electronic state for the case illustrated in Figure 6*b*. According to the Franck-Condon principle the excited molecule will have a configuration defined by the position coordiates corresponding to points between c and d. These configurations, however, are associated with large amounts of kinetic energy, given by the vertical distances cc' and *dd'*, whereas the kinetic energy for this configuration in the ground state is zero at *a* and *b* and small at intermediate points. The transition to level *K* is therefore improbable, and the corresponding absorption band will be of very low intensity. Figure 7*a* shows schematically the shape of the absorption band associated with this type of relation between the potential energy curves for an assembly of molecules in solution, for which the vibrational bands are broadened by a variety of intermolecular interactions. The 0 ← 0 band, at the longest wavelength, is the most intense, the 1 ← 0 band appears as a shoulder at a shorter wavelength, and higher vibrational transitions are of very low intensity. Polymethine dyes in organic solvents frequently exhibit

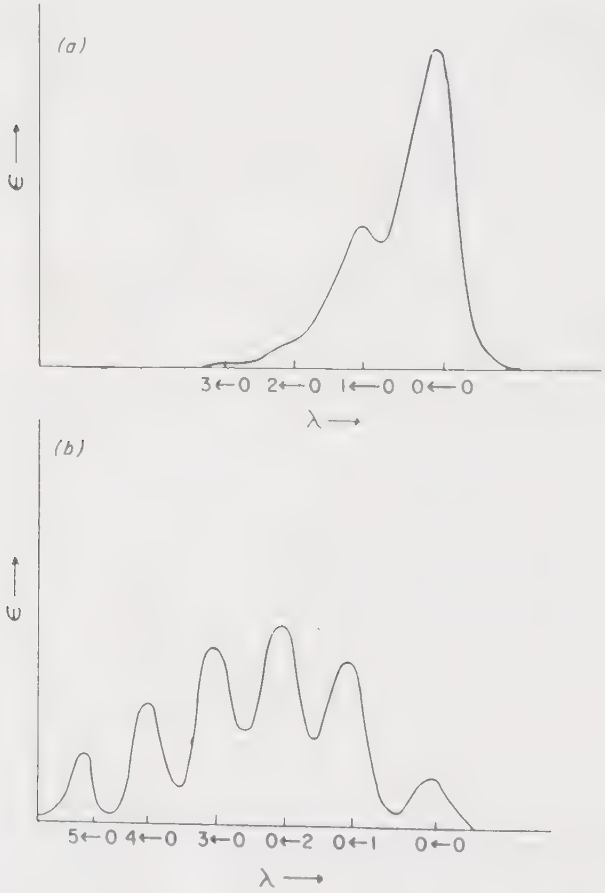

Fig. 7. Distribution of intensity among vibrational bands in an electronic spectrum as determined by the Franck-Condon principle: (*a*) little change in internuclear equilibrium distance in ground and excited electronic states; 0 ← 0 vibrational transition most intense; (*b*) increase in internuclear equilibrium distance on electronic excitation; 0 ← 0 vibrational transition less intense than those to higher vibrational quantum numbers in the excited state.

an absorption spectrum of this type, although the polymolecular nature of these substances may introduce complications not considered in this elementary treatment.

In Figure 6*c* the equilibrium separation between the atoms in the diatomic molecule is greater in the excited electronic state than in the normal; the shallower and broader minimum in the potential energy curve for the excited state indicates a loosening of the binding forces. The principle of constant internuclear separation now causes the most probable transition to be associated with a vibrationally excited upper electronic state, and the most intense vibrational band in the absorption spectrum is not the $0 \leftarrow 0$ band, but the $2 \leftarrow 0$ for the situation represented. Figure 7*b* shows the corresponding absorption spectrum for the substance in solution.

Figure 6*d* represents the case in which the potential energy curve for the excited electronic state is so much displaced to greater distances with respect to the curve for the ground state that, although transitions to states like K are possible in the part of the diagram corresponding to a stable discretely quantized molecule, so also are transitions to states like L, in the part of the diagram corresponding to a dissociated molecule with a continuum of energy values. The absorption spectrum in this case consists, therefore, of a discrete band series at longer wavelengths, converging on a continuum which extends to the shorter wavelengths. I_2 furnishes an example of this type of spectrum, while for Br_2 and Cl_2 the upper curve is so shallow and so far displaced toward the right that the most probable transitions are into the continuum, and the band spectrum at longer wavelengths is feebler than the continuum, for Cl_2, very feeble indeed. Figure 8 illustrates the type of spectrum associated with these cases.

The extreme case is that in which the upper curve has no minimum at all, as in the dotted curve of Figure 6*d*. Here there is no stable configuration of the excited molecule, and the upper state corresponds solely to a dissociative continuum of energy levels. The absorption spectrum is now wholly continuous. The spectra of the alkyl iodide vapors about 2600 Å appear to be of this class, although it is interesting that in this case a spectrum is found at shorter wavelengths, below 2000 Å, corresponding to excitation to a still higher electronic level, which exhibits discrete vibrational bands.

In practice, the Franck-Condon principle applied to the classical model of the oscillating molecule is useful in giving one a feel for the way in which the intensity of an absorption or emission vibronic spectrum is distributed among the vibrational bands. Since, however, the quantum mechanical version of a molecular oscillator is quite different from the classical description, it is important to see that, as Condon showed, the principle holds also in quantum mechanics, in fact, with greater precision than in the literal classical application. Such classical concepts as a precise turning point with accurately zero

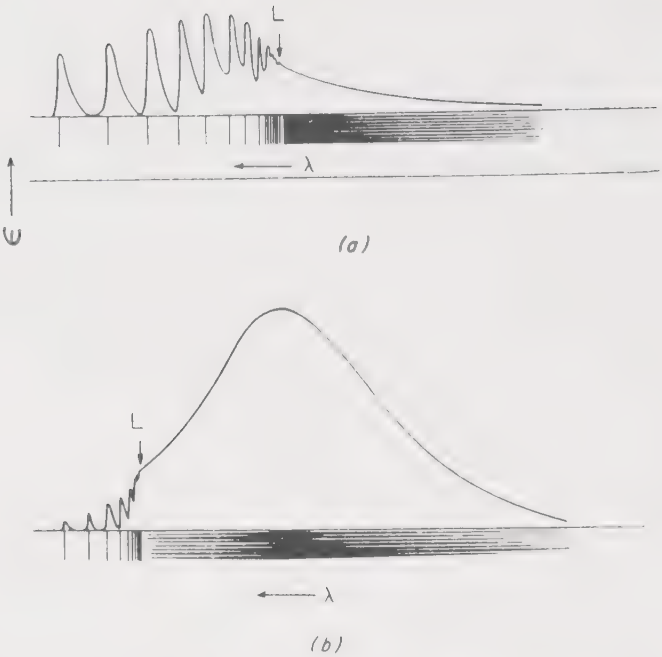

Fig. 8. Schematic diagram of electronic spectra with vibrational bands converging on dissociative continua: (*a*) roughly resembles the spectrum of iodine vapor, and (*b*) that of bromine vapor.

momentum can, according to Heisenberg's uncertainty principle, play no part in the description of the motion of an oscillator on the molecular scale. Instead, the motion of a vibrating atomic nucleus within a molecule in the intramolecular potential field $V(R)$ that causes the oscillation is determined by quantum mechanics.

In the quantum mechanics governing the behavior of a particle in an atomic or molecular system, a time-independent state (stationary state) of the motion in the potential field that determines the motion is associated with a function of the position coordinates of the particle $\psi(r)$, such that $\psi^2(r)$ is the probability that the particle is situated within the volume dr about any specified value of r, if $\psi(r)$ is real. If $\psi(r)$ is complex, $\psi^2(r)$ in the expression for the probability is replaced by the product of ψ and its complex conjugate ψ^*. $\psi(r)$ is often an undulatory function of the coordinates, similar to the functions that describe classical wave motion, and is on that account frequently called the wave function for the state; mathematically it is an *eigenfunction* of a differential equation. In the case under consideration, the oscillation of the atomic nuclei in a diatomic molecule, the motion can be represented as the oscillation of a particle of mass $\mu = m_1m_2/(m_1 + m_2)$, where m_1 and m_2 are the two nuclear masses, in the one-dimensional potential field $V(R)$

prevailing in the molecule. R is the internuclear distance and μ is the reduced mass of Eq. 8. In quantum mechanics the definite classical trajectory in which the position of the particle is explicitly stated in all phases of the motion is replaced by statements of the probability distribution of the particle over the space available to it.

The stationary state wave functions for the motion of a single particle of mass m moving in three dimensions in a potential energy field $V(x,y,z)$ are found by solving the Schroedinger equation

$$\left(\frac{\partial^2}{\partial x^2} + \frac{\partial^2}{\partial y^2} + \frac{\partial^2}{\partial z^2}\right)\psi(x,y,z) + \frac{8\pi^2 m}{h^2}\,[E - V(x,y,z)] = 0$$

subject to the auxiliary restrictions that $\psi(x,y,z)$ be single-valued, continuous, and finite over the space accessible to the particle. In this equation, E is a constant. Different physical systems, such as an electron in the field of an atomic nucleus, or the nuclei in a diatomic molecule vibrating under the influence of the attractive and repulsive potentials to which they are subjected, differ only in the mass of the particle and the form of the potential energy $V(x,y,z)$ that it possesses. Usually for a given system, a set of acceptable solutions of ψ can be found, each associated with a value of the constant E. E is found to represent the total energy of the system in its various stationary states.

For the vibrational motion of the nuclei in a diatomic molecule, the wave function can be written $\psi^v(R)$, where R is the internuclear distance. The Schroedinger equation is therefore

$$\frac{d^2\psi^v(R)}{dx^2} + \frac{8\pi^2\mu}{h^2}\,[E_v - V(R)]\psi = 0 \tag{13}$$

where E_v is the total energy of the vibrational state described by vibrational quantum number v, $\psi^v(R)$ is the corresponding vibrational wave function, and μ is the reduced mass for the oscillating atoms (Eq. 8). The possible values of v are $v = 0, 1, 2, \ldots$. If the motion is simple harmonic, $V(R) = kR^2$, where $k = 2\pi^2\mu\tilde{\omega}^2$ and $\tilde{\omega}$ is the frequency of the vibration (sec^{-1}). Solution of Eq. 13 for harmonic motion gives

$$E_v = (v + 1/2)h\tilde{\omega}$$

If the motion is anharmonic, a power series expansion can be used for V, $V(R) = kR^2 + k'R^3 + \cdots$, or some other function. In Figure 9 approximate shapes of $\psi^v(R)$ for different anharmonic vibrational states of two electronic states G and I are sketched about the horizontal lines that represent spatially the amplitude of the classical oscillation and energetically, the total vibrational energy (25). The functions are oscillatory and extend appreciably outside the classical turning points. For the lowest vibrational state, $v = 0$,

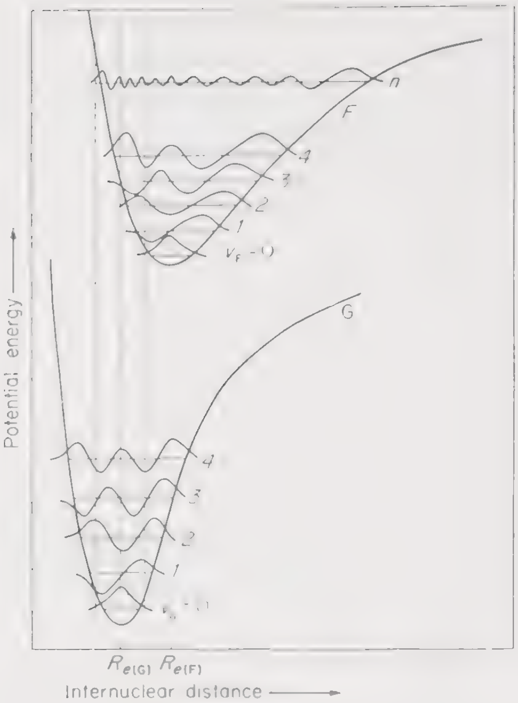

Fig. 9. Vibrational wave functions in two electronic states.

in which the vibrational energy is the "half quantum" of zero-point energy, the function is bell shaped. At high values of v, the motion approximates the classical motion in the sense that the probability distribution $(\psi^v)^2$ is greatest near the extremes, although always retaining an oscillatory character. The energy level for a high vibrational quantum number n in the upper electronic state has been drawn out of place in the diagram, but is introduced to show the rapid changes of the sign of the vibrational function characteristic of large values of the vibrational quantum number. The motion of the classical oscillator associated with the type of potential energy curve F depicted for the excited electronic state is highly anharmonic, and the anharmonicity is reflected in the greater distance between the maxima of ψ on the right compared with the left, corresponding to lower classical velocity and lower momentum in the right-hand part of the path of the oscillator. For the harmonic oscillator, ψ^v is symmetrical, for even values of v, about the central point, and antisymmetrical for odd values of v.

In considering how the intensities of the vibrational bands in a vibronic spectrum are affected by the form of the vibrational wave functions, it will be convenient to outline the theory of spectral intensities, discussed in detail in Chapter II.

In the classical theory of absorption, an electron in an atom or an atomic nucleus in a molecule was considered to have a natural frequency of oscillation determined by its mass and the restoring force holding it about its equilibrium position. In a radiational field of frequency near the natural electronic frequency, the oscillator, supposed initially at rest, was forced into synchronous vibration with an amplitude x in the x direction, and an electric dipole moment ex was induced by the radiation, where e is the electronic charge. Similar electric moments were induced classically by the interaction of radiation on charged atomic nuclei. The rate of energy absorption from the radiation field for electronic vibrations in the x direction was proportional to the square of the induced dipole moment $(ex)^2$, with similar expressions for vibrations in the y and z directions.

In quantum mechanics the synchronous vibration of the electron in step with the oscillating electric vector of the electromagnetic field is replaced by the concept of a transition between two stationary states induced by the radiation if its frequency is $\tilde{\nu} = (E_2 - E_1)/h$. The two states are designated 1 and 2, characterized by wave functions ψ_1 and ψ_2 and energies E_1 and E_2. The expression for the probability of the transition turns out to be analogous to the classical expression; it depends on the square of a *transition dipole moment*

$$\mathbf{m} = \int \psi_2 \mathbf{M} \psi_1 \, d\tau \tag{14}$$

where $\mathbf{M} = \sum_i er_i$, and r_i is the general symbol for the position coordinate of the ith electron. ψ_1, ψ_2 are the total wave functions for states 1 and 2 and $d\tau$ is the generalized differential of all the space coordinates involved, electronic and nuclear.

In the expression for the transition dipole moment, the electronic charge e can be placed outside the integral

$$\mathbf{m} = e \int \psi_2 \Big(\sum_i \mathbf{r}_i \Big) \psi_1 \, d\tau \tag{14a}$$

The integral in Eq. 14a is called the matrix element of the transition moment; it is the quantum mechanical counterpart of the position coordinate vector $\sum_i \mathbf{r}_i$ in the classical expression $e \sum_i \mathbf{r}_i$ for the radiation-induced dipole moment, where $\mathbf{r}_i$ is the displacement of electric charge caused by the absorption of radiation. The matrix element may be regarded as the effective length of the dipole induced by the transition (see p. 49). The square of the matrix element of the transition moment is called the *dipole strength* for the transition D and the probability of the transition (the intensity of absorption or emission) is proportional to D.

In the case of the oscillating diatomic molecule it will be assumed that the electronic and vibrational wave functions can be separated, and it can also be shown that the rotational motion can be ignored (26). The total wave function can then be expressed as the product of an electronic function ψ^e and a vibrational function ψ^v. The value of ψ^e depends on the electronic coordinates r, and also slowly changes with the internuclear separation, so that it depends on the nuclear coordinates R as a parameter; ψ^v depends only on the nuclear coordinates. If ψ is the total wave function

$$\psi = \psi^e(r,R)\psi^v(R)$$

and the transition dipole moment integral for an electronic transition from state 1 to state 2 with a simultaneous vibrational transition from quantum number m in the electronic state 1 to n in state 2 is

$$\mathbf{m}_{2,n\leftarrow 1,m} = \iint \psi_2{}^e(r,R)\psi^v_{2,n}(R)\mathbf{M}\psi^e_1(r,R)\psi^v_{1,m}(R)\,dr\,dR$$

where $\mathbf{M}$ depends only on the electronic coordinates.

The integration over the electronic coordinates can be carried out at fixed values of R to yield an electronic dipole transition moment

$$Q^e = \int \psi_2{}^e(r)\mathbf{M}\psi_1{}^e(r)\,dr$$

where Q^e depends on R parametrically. The transition dipole moment for the combined electronic and vibrational transition is therefore

$$\mathbf{m}_{2,n\leftarrow 1,m} = \int \psi^v_{2,n}(R)\mathbf{Q}^e\psi^v_{1,m}(R)\,dR$$

The value of $\mathbf{Q}^e$ does not change greatly as the nuclear coordinates change during an oscillation, and the term can be replaced by some average constant value $\overline{\mathbf{Q}}^e$. The transition dipole moment for the vibronic transition under consideration is

$$\mathbf{m}_{2,n\leftarrow 1,m} = \overline{\mathbf{Q}}^e \int \psi^v_{2,n}(R)\psi^v_{1,m}(R)\,dR \tag{15}$$

and the probability of the transition is proportional to $(\mathbf{m}_{2,n\leftarrow 1,m})^2$. The square of $\overline{\mathbf{Q}}^e$ determines roughly the intrinsic intensity of the electronic transition, which depends on the nature of the electronic states themselves, while the contribution to the absorption made by a particular $n \leftarrow m$ subband in the vibrational progression is determined by the square of the integral over the product $\psi_{1,m} \cdot \psi_{2,n}$ of the corresponding vibrational functions. This integral is often called the *overlap integral*.

To evaluate the integral for the $n \leftarrow 0$ band, the product is formed at a given value of the nuclear coordinates and integrated over the coordinates.

One condition for an appreciable value of the integral is that the vibrational function of the upper state possess nonzero values over the range of coordinates within which the lower function has appreciable values; i.e., the vibrational functions must overlap in the coordinate region appropriate to the initial vibrational state. Also, the upper function must not change sign rapidly in the region of overlap; otherwise, in the integration, the negative values of the product will more or less cancel the positive values and the value of the integral will be small.

Considering now the relative intensities of the subbands in the absorption vibronic spectrum associated with transitions between the G and F states of Figure 9, one sees that for the $0 \leftarrow 0$ band there is only a slight overlap of the extreme right portion of the curve $\psi^v_{G,0}$ on the extreme left portion of $\psi^v_{F,0}$; hence the intensity of this subband will be low. For the $1 \leftarrow 0$ band, the bell-shaped lower function overlaps somewhat on the left-hand minimum of the upper vibrational function, hence the product $\psi^v_{F,1} \cdot \psi^v_{G,0}$ and the integral are negative, but the square of the integral is positive and the $1 \leftarrow 0$ band will be stronger than the $0 \leftarrow 0$. The overlap increases with increasing values of v for the upper state up to about v_F equal to 4 or 5, for whose vibrational functions the left-hand maximum and minimum, respectively, occur at distance coordinates not very different from the maximum of $\psi^v_{G,0}$ and the corresponding absorption bands will be relatively intense.

Consider now the $n \leftarrow 0$ transition, where n is a large vibrational quantum number for the excited electronic state (represented energetically out of proportion with the lower vibrational levels in Figure 9). The function $\psi_{F,n}$ oscillates rapidly in the coordinate region away from the extremes (the quantum mechanical counterpart of the high momentum and velocity of the classically oscillating particle in this part of its path). Although the overlap of $\psi^v_{G,0}$ with $\psi^v_{F,n}$ is good, the rapid changes in the sign of the latter function render the value of the integral small and the corresponding absorption is weak.

The quantum mechanical requirement of a large value of the overlap integral for relatively strong absorption in a band in a vibronic progression leads then to essentially the same result as the arguments based on the classical motion of the oscillating nuclei, namely, that the highly probable transitions between two electronic states are those during which the atomic nuclei scarcely change their positions and momenta. The main difference between the quasiclassical and the quantum mechanical versions of the oscillating molecule is that the intensity differences between bands predicted by quantum mechanics are less abrupt than those predicted by the strict application of the Franck-Condon principle to the classical oscillator. For example, in the case illustrated in Figure 9, vertical transitions from the turning points of the classical path of the oscillator in the state $v_G = 0$ entirely miss the path in the state $v_F = 0$, and the $0 \leftarrow 0$ transition would be absent, while according to quantum mechanics, in this case, weak absorption in this transition is to be expected. The difficulty, too, that vertical transitions from the turning points of the classical oscillator in the lower electronic state may meet the potential energy curve for the upper state at points that are not associated with quantized vibrational states is also avoided in the quantum mechanical treatment.

C. Morse's Equation for the Potential Energy Curve

A very convenient expression for the potential energy of a vibrating diatomic molecule as a function of the internuclear distance that reproduces the essential characteristics of the curves in Figure 6 was proposed by Morse (27):

$$V(R - R_e) = D \exp\{-2a(R - R_e)\} - 2D \exp\{-a(R - R_e)\} \qquad (16)$$

The equation contains three constants, D, a, and R_e. The potential energy has a minimum value $-D$ when $R = R_e$, the equilibrium internuclear distance, and approaches zero asymptotically as R approaches infinity, corresponding to dissociation of the molecule. These aspects of Morse's function are in agreement with the curves of Figure 6. D is the energy difference between the minimum of the curve and the asymptote $V = 0$ at infinite internuclear separation, i.e., it is equal to the dissociation energy D_0 of the molecule in its lowest vibrational state plus the zero-point energy. The Morse function remains finite at $R = 0$, but the rate of change of V is very great as R approaches zero, and the deviation of the curve from the true potential energy curve in this region is of no great consequence.

If in the Schroedinger Eq. 13 Morse's expression is introduced for $V(R)$, the solution leads to values of the total energy of the oscillating molecule W_v that are, to a very close approximation, of the form

$$W_v = -D + h\omega_e[(v + \tfrac{1}{2}) - x(v + \tfrac{1}{2})^2] \qquad (17)$$

where $v = 0, 1, 2, \ldots$, ω_e is the frequency of oscillation in reciprocal centimeters for small displacements about the equilibrium point, the v's are the vibrational quantum numbers and the second term in the equation represents the quantized vibrational energies. The second coefficient of ω_e represents the effect of anharmonicity in the vibrational motion (cf. Eq. 12). Empirically, the vibrational energy of many diatomic molecules is well expressed by Eq. 17, although terms $y(v + \frac{1}{2})^3$ must sometimes be introduced (Chapter II, Section II-C).

To draw the potential energy curve of a diatomic molecule with the aid of Morse's function, one must know R_e, a, and D or $\omega_e x$ of Eq. 17. Morse's solution of the Schroedinger equation for the diatomic molecule oscillating in a potential field described by Eq. 16 shows that the frequency $c\omega_e$ of very small oscillations about the equilibrium distance of separation is given by

$$c\omega_e = \frac{a}{2\pi}(2D/\mu)^{1/2}\ \mathrm{sec}^{-1}$$

where c is the velocity of light and μ, the reduced mass of the molecule in grams (27). In this equation, D is in ergs. Hence

$$a = 2\pi c\omega_e(\mu/2D)^{1/2} \tag{18}$$

When the vibrational energy can be expressed by Eq. 17, the constant D (the dissociation energy plus zero-point vibrational energy) has the value (27,28)

$$D = (hc{\omega_e}^2/4\omega_e x)\ \mathrm{ergs} = ({\omega_e}^2/4\omega_e x)\ \mathrm{cm}^{-1} \tag{19}$$

Substitution for D in ergs in Eq. 18 gives

$$\begin{aligned} a &= (8\pi^2 c\mu\omega_e x/h)^{1/2}\ \mathrm{cm}^{-1} \\ &= 2.436 \times 10^7\ (M\omega_e x)^{1/2}\ \mathrm{cm}^{-1} \end{aligned}$$

where M is the reduced mass in atomic weight units, i.e.,

$$M = M_1 M_2/(M_1 + M_2)$$

M_1 and M_2 being the two atomic weights on the scale $0 = 16$; $\omega_0 x$ is in reciprocal centimeters. In using this value of a to draw the potential energy curve, one must express R and R_e in centimeters; if the distance coordinates are in angstrom units, the value to be used for a is

$$a = 0.2436(M\omega_e x)^{1/2}\ \mathrm{cm}^{-1}$$

The constants ω_e, $\omega_e x$, and D can be derived from an analysis of the vibrational spectrum (28). If D is known, either from the vibrational analysis or otherwise, $\omega_e x$ can be expressed from Eq. 19 in terms of D, to give

$$a = (2\pi^2 cM/Dh)^{1/2}\omega_e = 1.218 \times 10^7\ \omega_e(M/D)^{1/2}$$

In using this value of a, R and R_e are to be expressed in centimeters. The constant R_e can be evaluated accurately if rotational structure is known (Eqs. 6, 7, 8), but when this information is lacking, an empirical expression suggested by Morse (27)

$$\omega_e {R_e}^3 = 3000\ \mathrm{cm}^{-1} \quad (R_e \text{ in angstrom units})$$

is useful for drawing approximate potential energy curves for diatomic molecules. An improved variant of this formula is given by Clark (29).

D. Predissociation

Another phenomenon readily understood from a study of potential energy curves is *predissociation*. It is sometimes observed in the electronic spectrum of a gas that a well-defined structure originating in the superposition of vibrational and rotational transitions on the electronic transition exists down to a certain wavelength, but that at shorter wavelengths the rotational structure quite suddenly becomes blurred, and sometimes the vibrational subbands themselves become merged to a continuum. In some cases well-defined fine structure reestablishes itself at shorter wavelengths. Before the mechanism of this effect was clearly understood, V. Henri associated the disappearance of rotational structure with a highly strained but not yet completely dissociated molecule, and termed the region of ill-defined structure a *predissociation spectrum*. This is not quite the currently accepted explanation, but the terminology has persisted.

Predissociation in absorption involves, besides the ground electronic level, two excited electronic levels in one of which the molecule has a lower dissociation energy than the other. The absorption transition carries the molecule to the more stable of the excited levels, but for certain internuclear distances a radiationless transition to the less stable level occurs in a very short time after excitation, and the molecule dissociates.

Figure 10 illustrates two cases in which predissociation could occur. In *a* the curves for the two excited electronic states A and B cross as shown, state B being associated with a lower dissociation energy D_B than A. Direct transitions from the ground state to B by absorption may be forbidden or, if allowed, would, in the case illustrated, be at short wavelengths, but, if certain conditions are fulfilled, a radiationless transition from A to B may occur.

The absorption spectrum associated with the $A \leftarrow G$ transition will be normal until the wavelength corresponding to *ga* is reached, after the absorption of which the molecule has enough energy to cause excitation to the dissociated condition of the B electronic state. In the absence of state B, a molecule excited to the configuration *a* would begin to vibrate with an amplitude *aa′*, the potential energy traversing the course *aea′* during the oscillation. At the crossing point *c* the molecule is in a nuclear configuration appropriate to both states A and B and there is a certain probability that the molecule will proceed along the curve for B instead of that for A. If it does, the energy adsorbed from the radiation corresponding to the transition *ga* will carry the molecule to the horizontal part of the curve B, i.e., the molecule will dissociate. If this transition takes place in a very short time, the life of the molecule in state A is very short, shorter than a rotational period, and the rotational quantization breaks down. If the time of transition from A to B

is shorter than a vibrational period, vibrational quantization will also disappear, and the spectrum in the region starting at the wavelength corresponding to *ga* and continuing for some distance to shorter wavelengths will be continuous.

If the molecule traversing curve *A* possesses great kinetic energy at the crossing point *c*, it is less likely to switch to curve *B*. Hence, if transitions from *G* to configurations like *b* occur, the molecule is likely to remain on curve *A* and the normal quantized rotations and vibrations will reappear at some shorter wavelength.

In Figure 10*b*, we presuppose a repulsive state *B*, transitions to which from the ground state *G* are forbidden. *B* cuts the curve for the excited stationary state *A* in two places. According to the classical description of the motion, a molecule in the ground vibrational state of *G* would require excitation by the transition *gc′* in order to acquire sufficient energy to pass over to state *B*, and diffuseness in the spectrum would appear at the corresponding wavelength. However, in quantum mechanics, there is a certain probability of dissociation, by the "tunnel effect," of a molecule in the configuration corresponding to *d*, below the intersection, and in this case there is a gradual onset of diffuseness.

The tunnel effect can readily be understood from the spreading of the vibrational wave functions beyond the classical limits of the oscillating motion as illustrated in Figure 9. If, in Figure 10*b*, the configuration *d*

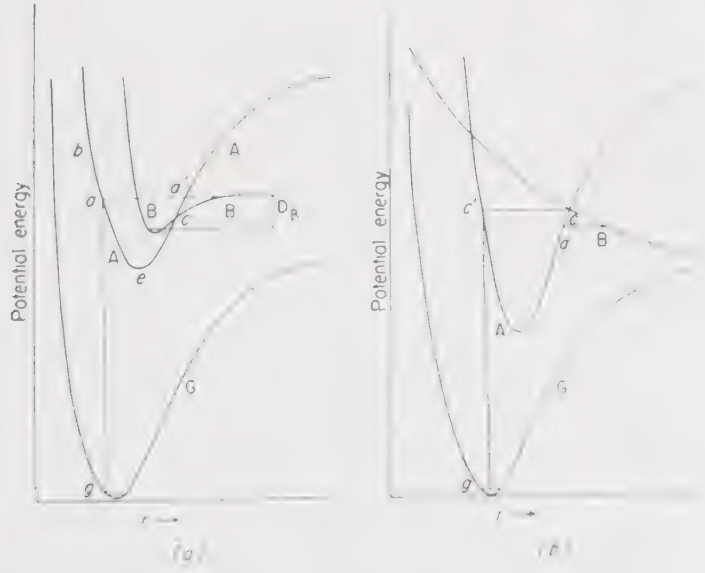

Fig. 10. Potential energy curves illustrating predissociation.

corresponds to a vibrational level of state *A*, the spread of the associated vibrational wave function to the right along the line through *d* indicates a finite probability that the particle will be found in this region. Similarly the dissociated atom in state *B* with the energy indicated by the horizontal line through *d* can be found on this line to the left of curve *B*. If the distance along this horizontal line joining the two curves is not too great, there is a finite probability that the vibrating particle in state *A*, of energy indicated by *d*, will appear as a dissociated particle of the same energy in state *B*, without the necessity of its surmounting the energy barrier represented by the energy difference of configurations *d* and *c*.

Predissociation is relatively common among polyatomic molecules, because of the large number of possible points of intersection of the potential energy surfaces consequent on the numerous degrees of freedom. The phenomenon is important in connection with the photochemical decomposition of complex molecules.

V. INTENSITIES IN MOLECULAR SPECTRA (30)

A. General

A knowledge of the strength or intensity of absorption in molecular spectra is important theoretically and in many practical applications. The intensity is no less characteristic of an absorption spectrum than the wavelength or frequency, and in the use of spectra for identification or diagnosis, as much weight must be placed on the intensity as on the position and shape of the absorption band. The frequency of the band depends on the energy difference between the upper and lower states between which a radiation-induced transition takes place, and the intensity depends on the probability of occurrence of the transition. We have already distinguished between "allowed transitions," which occur with high probability and therefore yield intense spectra, and "forbidden transitions," which sometimes are strictly forbidden and cannot be effected by absorption of radiation, but which often in practice, under the influence of external fields such as arise in the condensed state or of other perturbations, occur with low probability and yield feeble spectra.

The practical measure of the intensity of absorption at any frequency is the value of the molar extinction coefficient ϵ, also called the molar absorbance, at the frequency in question. This coefficient is defined by the relation

$$\epsilon_\nu = (1/cl)\log_{10}(I_0/I)_\nu$$

where c is the concentration of the absorbing substance in moles per liter, l the length of the absorption path, and I_0 and I are the intensities incident on and emerging from the absorbing layer. The units of ϵ are therefore

l mole^{-1} cm^{-1}. If Beer's law is followed, ϵ_ν is independent of the concentration of the absorbing medium. The most intense electronic absorption spectra, those of dyes in solution, have values of ϵ of the order of magnitude of 10^5 liter moles^{-1} cm^{-1} at the frequency of maximum absorption. Values of ϵ below about 1000 at the absorption maximum of electronic spectra correspond to improbable or quasiforbidden transitions. As an example of the orders of magnitude of the values of ϵ in permitted and forbidden transitions, the values for various electronic transitions in benzene may be cited; below 1850 Å, benzene in a solution of paraffins exhibits intense bands with ϵ of the order of 45,000 associated with a permitted electronic transition which appears to be the first member of a Rydberg series, other members of which are observed at shorter wavelengths (31); at about 2000 Å occurs the maximum of a band series with a value of the extinction coefficient about 6000 in paraffin solution (31), probably indicating a quasiforbidden transition; the well-known absorption bands of benzene at 2550 Å exhibit $\epsilon_{\max}$ equal to 215, indicating a forbidden transition, and the very feeble singlet → triplet electronic transition about 3400 Å has $\epsilon_{\max}$ much below unity.

One aspect of intensity in molecular electronic spectra has already been discussed; the distribution of intensity over the vibrational bands of a single electronic transition, governed by the Franck-Condon principle (Section IV-B). The present discussion is concerned with the probability of the electronic transition in itself, irrespective of the manner in which the absorption is distributed over the various vibrational transitions that may accompany the electronic excitation. The measure of the total probability of the electronic transition for a given vibronic band system is the integral of the molecular extinction coefficient over all wavenumbers covered by the band, $\int_{\nu_1}^{\nu_2} \epsilon \, d\nu$, where ν_1 and ν_2 are the wavenumber limits of the band system, including any continuum associated with the electronic transition. If ϵ is plotted against wavenumber on a linear scale, the area under the curve between the limits ν_1 and ν_2 gives the value of the integrated molar extinction coefficient. The area may be evaluated with the planimeter or by cutting out the area from the graph and weighing it, determining the area by comparison with the weight of a known area cut from the same sheet of paper. The data from modern automatic spectrophotometers can be presented on punched cards or magnetic tape in a form suitable for computation by a computor of the integrated molar extinction coefficient by interpolation formulas such as Simpson's rule or the trapezoidal rule for the determination of areas. A rough estimate of the integrated extinction coefficient may be made by multiplying the value of the molar extinction coefficient at the wavenumber of maximum absorption by the half-width of the band, i.e., by the interval between the two wavenumbers at which the value of the molar extinction coefficient is one-half the maximum value. Since the wavelength of the maximum absorption on a vibronic band spectrum of an organic molecule is usually an accidental feature determined by overlapping vibrational bands, no special theoretical significance can be attached to ϵ_{max}, and moreover the value of ϵ_{max} depends on the temperature, but, as will be shown, the value of the integrated molar extinction is related to theoretical quantities describing the intensity of the band system. Since the total probability of a given electronic transition is practically independent of temperature, the integrated molar extinction is expected to be independent of temperature, as is experimentally verified, for example, in the spectra of cyanine dyes, provided no change in the molecular state of the absorber occurs with change in temperature, such as dimerization or other aggregation effects at low temperature.

We shall outline the essential results of the classical and quantum theories of the intensity of the absorption of radiation. In both theories absorption of radiation by a molecule depends on the development of induced electric moments as a result of the displacement of electrons bound in the molecule by the electric field of the radiation when the frequency of the radiation is close to a characteristic frequency of an electron in the molecule, but the mode of calculation of the induced moments and the interpretation of the characteristic frequencies of the electrons are very different in the two theories.

B. Classical Theory of Absorption and Emission

In the classical theory an electron bound in a molecule is considered to oscillate in harmonic motion with respect to a fixed positive charge with a characteristic frequency determined by the electronic mass and the binding force. If at any moment the displacement of the electron from the positive charge is x, the electric moment is ex. In classical theory, the acceleration represented by the oscillating motion of the electron causes the emission of radiation at a rate proportional to $(ex_0)^2$, where x_0 is the amplitude of the oscillation. It is well known how this prediction by the classical theory of a steady loss of internal energy by the emission of radiation by electronic oscillators within atoms and molecules is inconsistent with atomic and molecular stability. Nevertheless we shall proceed with the classical discussion, since it leads to equations of the correct form.

If a molecule containing bound oscillating electrons is placed in an electromagnetic field of wavelength long compared with atomic dimensions, so that the electrical intensity over the molecule is practically constant, the electron is set into forced vibration with the same frequency as the radiation, but in general the motion of the forced vibration is not in phase with that of the radiation. The displacement of the electron caused by the field generates an induced electric moment that can be resolved into two components, one, ex_0 oscillating in phase with the light, where x_0 is the amplitude of the forced oscillation; the other, vibrating 90° out of phase with the light, with an amplitude $-\beta x_0$, giving an out-of-phase component of the electric moment $-\beta e x_0$, where β includes coefficients related to the dissipation of energy as heat and therefore associated with absorption of the radiant energy. Detailed analysis (32) shows that this second component of the forced oscillation is of appreciable magnitude only when the frequency of the radiation is very near the natural frequency of the electron. Under this condition, the rate of dissipation of the radiation is proportional to the square of the out-of-phase induced electric moment.

If the frequency of the radiation is not near the characteristic frequency of the electron in the molecule, the interaction between the radiation and the matter takes the form of scattering, without any absorption of radiant energy. The forced oscillation conferred on the electron by the electric field of the radiation causes it to emit a spherical wavelet as a Hertzian oscillator, but in an assembly of molecules, destructive interference renders the intensity of the scattered radiation in directions other than the forward and backward directions very small. Phase differences between the original beam and the forward scattered beam yield a resultant oscillation equivalent to the propagation of the radiation through the medium at a lower velocity than in vacuum, i.e., the medium exhibits a refractive index n greater than unity. Since the classical theory of the variation of the refractive index with the frequency of the radiation (dispersion) introduces a term, the *oscillator strength*, important with respect to the intensity of absorption bands, we shall sketch the manner in which the dispersion equations are obtained.

When the frequency of the radiation is not near the characteristic frequency of the electron, the forced displacement of the electron by the electric field of the radiation is

$$x = \frac{e}{4\pi^2 m}\left(\frac{1}{\tilde{\nu}_0{}^2 - \tilde{\nu}^2}\right)E \cos 2\pi\tilde{\nu}t$$

where $\tilde{\nu}_0$ is the characteristic frequency in reciprocal seconds of the electron, e and m are the electronic charge and mass, respectively, $\tilde{\nu}$ is the frequency of the radiation, and $E \cos 2\pi\tilde{\nu}t$ is the electrical intensity of the radiation field at the position of the electron. The effect of the magnetic intensity of the radiation is negligible. The corresponding induced electric moment is

$$ex = \frac{e^2}{4\pi^2 m}\left(\frac{1}{\tilde{\nu}_0{}^2 - \tilde{\nu}^2}\right)E \cos 2\pi\tilde{\nu}t$$

and the polarizability of the electronic oscillator, defined as the ratio of the induced electric moment to the inducing field strength, is

$$\alpha = \frac{e^2}{4\pi^2 m}\left(\frac{1}{\tilde{\nu}_0{}^2 - \tilde{\nu}^2}\right)$$

If the molecule contains a number of vibrating electrons, each with its own characteristic frequency, $\tilde{\nu}_i$

$$\alpha = \frac{e^2}{4\pi^2 m} \sum_i \left(\frac{1}{\tilde{\nu}_i^2 - \tilde{\nu}^2} \right) \tag{20}$$

where the summation is carried out over all the oscillators.

Experimentally, Eq. 20 describes the frequency dependence of the polarizability and of the related refractive index of gases, except that usually the contributions of the various characteristic frequencies are smaller than those calculated. Agreement with observation can be found by replacing the value 1 in the numerator of the summation in Eq. 20 by a number f, one for each characteristic frequency contributing to the polarizability, so that the equation becomes

$$\alpha = \frac{e^2}{4\pi^2 m} \sum_i \left(\frac{f_i}{\tilde{\nu}_i^2 - \tilde{\nu}^2} \right) \tag{21}$$

The quantities f_i are the *effective number of dispersion electrons* with the characteristic frequency ν_i; they are also called the *oscillator strengths* of the corresponding oscillators. For example, the various spectral lines emitted by an atom can be associated, in classical theory, with corresponding electronic oscillators, each with a particular value of f.

The polarizability is related to the refractive index of an assembly of molecules by the Lorentz-Lorenz relation

$$\frac{n^2 - 1}{n^2 + 2} = \frac{4\pi}{3} N'\alpha$$

where N' is the number of molecules per cubic centimeter. For gases, $n^2 + 2 \sim 3$ and the dispersion equation for gases is therefore

$$n^2 - 1 = \frac{N'e^2}{\pi m} \sum_i \left(\frac{f_i}{\tilde{\nu}_i^2 - \tilde{\nu}^2} \right) \tag{22}$$

The oscillator strength f_i is also related to the intensity of the corresponding absorption band determined classically by the electronic frequency ν_i. The rate of energy dissipation (absorption) is determined by the out-of-phase polarizability associated with the electronic oscillation in the radiation field, which involves f_i in the same way as the in-phase polarizability associated with dispersion. The final result is that the oscillator strength for an absorption band whose integrated molar extinction coefficient is $\int_\nu \epsilon \, d\nu$ is

$$f = \frac{2303mc^2}{\pi N e^2} \int_\nu \epsilon \, d\nu = 4.319 \times 10^{-9} \int_\nu \epsilon \, d\nu \tag{23}$$

N in this equation is Avogadro's number, c is the velocity of light, and ν is expressed in reciprocal centimeters. The factor 2303 involves the conversion from natural to decadic logarithms as well as the number of cubic centimeters in a liter required by the introduction of the molar extinction coefficient.

C. Quantum Theory of Absorption and Emission

In quantum mechanics the classical concept of an electron in the molecule vibrating with a characteristic frequency in a stationary state excited into a forced vibration when the molecule is placed in a radiation field of a frequency near the characteristic frequency is replaced by the concepts of nonradiating stationary states in which the electronic motion is described by a wavelike distribution of probability density, and of a radiation-induced perturbation forcing the electron from one stationary state to another if the frequency of the radiation equals the energy difference between the two states divided by h. Characteristic frequencies and induced dipole moments again appear in the theory of absorption, but the frequencies are now transition frequencies and the induced dipole moment is the effect of a displacement of electronic charge accompanying the transition.

The lower and the higher of the two molecular states may be called 1 and 2, respectively, characterized by wave functions ψ_1 and ψ_2. If, for simplicity, the oscillations of the electric field of the radiation are supposed to be parallel to the x direction, the probability of a radiation-induced transition is found to depend on the square of an induced dipole moment ex_{12}, the *transition moment*, where e is the electronic charge and x_{12} is the average displacement in the x direction, periodic in the time, induced by the transition. The x coordinate is measured from the center of gravity of the positive charge in the molecule, which charge center can be taken as fixed. Since the electronic displacement must be averaged over the probability distribution of the displacement, the wave functions necessarily enter into the expression for the average, which is $x_{12} = \int \psi_2{}^* x \psi_1 \, dx$, where $\psi_2{}^*$ is the complex conjugate of ψ_1. The transition moment is therefore

$$ex_{12} = e \int \psi_2{}^* x \psi_1 \, dx$$

The total collection of the quantities analogous to x_{12} for all possible stationary states and transitions between stationary states of the system can be arranged as the components or elements of a matrix, some of which, such as $x_{11} = \int \psi_1{}^* x \psi_1 \, dx$, etc., represent the average value of the x coordinate of the electron in the stationary states, and the others, such as $x_{12} = \int \psi_2{}^* x \psi_1 \, dx$, represent time-dependent average displacements of the electron accompanying a transition. The quantity x_{12} is therefore the matrix element of the electronic displacement for the transition $2 \leftarrow 1$, and represents the average displacement of the electron in the x direction, varying periodically with the time with a frequency which the theory shows to be equal to $(E_2 - E_1)/h$, induced by the absorption of this radiation polarized in the x direction. x_{12} is therefore effectively the induced dipole length. The square of the integral x_{12}, to which the probability of the transition is proportional, is called the *dipole strength*, D_{12} for the transition.

If q_i is the general symbol for the position coordinate of the ith electron in the system, the transition dipole moment for the absorption transition $2 \leftarrow 1$ is

$$\mathbf{M}_{12} = eq_{12} = e\int \psi_2^*\Big(\sum_i q_i\Big)\psi_1\, dv \tag{24}$$

the summation being carried out over all the electrons affected by the transition and the integration over all space available to the electrons. Equation 24, in its general form applicable to a radiational transition between any stationary states whatever, is the fundamental equation for all problems of intensity in quantum mechanics. A radiational transition is possible if the value of the integral is greater than zero and forbidden if the integral vanishes. One of the factors determining the nonvanishing or vanishing of the integral is the symmetry of the wave functions in the integrand, and a transition may be allowed or not because of symmetry. In such cases it is possible to determine if the integral is greater than zero without a knowledge of specific expressions for the wave functions, if their symmetry is known. For if, in Eq. 24, the quantity to be integrated changes its sign on the application of any symmetry operation applicable to the system, i.e., is antisymmetrical with respect to the symmetry operation, the integral will vanish by the cancelling of components of equal magnitude but of opposite sign. If the integral is not to vanish, the integrand must be symmetrical with respect to all symmetry operations applicable to the system. If therefore the behavior of ψ_1, ψ_2, and q_i with respect to the symmetry operations is known, the vanishing or nonvanishing of the integral can be readily ascertained and the selection rules that depend on symmetry for radiational transitions found. The subject is best pursued after an introduction to the symmetry of molecular systems and wave functions and to the methods of group theory in Chapter II, and examples of symmetry-based selection rules are discussed in Chapters II and III.

By comparison of the equations for the rate of absorption of energy according to classical and quantum theory, it is found that the oscillator strength f_{12} is related to the transition moment by the equation

$$f_{12} = \frac{8\pi^2 mc\nu \mathbf{M}_{12}{}^2}{3he^2} \tag{25}$$

$$= 4.704 \times 10^{29}\nu\mathbf{M}_{12}{}^2 \tag{25a}$$

where m and e are the charge and mass of the electron and ν is the wave number in reciprocal centimeters of the absorption band. **M** is in electrostatic units. If the value of f_{12} is obtained from Eq. 23, the transition moment can be calculated. The equation is

$$\mathbf{M} = \left(\frac{3he^2f}{8\pi^2mc\nu}\right)^{1/2} = 0.0958\left(\frac{\int_\nu \epsilon_\nu\, d\nu}{\nu}\right)^{1/2} \text{ debyes} \tag{26}$$

For example, the value of f_{12} from the integrated molar extinction coefficient of the visible absorption bands of dyes is approximately 1; if the band maximum is at 5000 Å, for which ν is 20,000 cm^{-1}, $\mathbf{M}_{12} = 10^{-17}$ esu or 10 debyes. If the transition is polarized in one direction and one electron is excited by the absorption, the effective dipole length for the transition is $\mathbf{M}/e = 2 \times 10^{-8}$ cm or 2 Å.

Before the advent of quantum mechanics, Einstein had considered the equilibrium between radiation and matter in terms of the notions of absorption and emission according to the Bohr theory, the Maxwell-Boltzmann relation for the equilibrium distribution of energy among the atoms, and Planck's equation for the equilibrium distribution of energy among the frequencies of the radiation.

Consider radiational transitions between a lower state 1 and a higher state 2 of an atom immersed in isotropic radiation of which the density at the frequency capable of inducing the transition $2 \leftarrow 1$ is $\rho(\tilde{\nu})$ ergs/cm^3 per unit interval of frequency unit (sec^{-1}). If N_1 is the number of atoms in state 1, the number of absorption acts per second will be $N_1B_{12}\rho(\tilde{\nu})$, where B_{12} is a constant characteristic of the atom, the Einstein absorption probability coefficient for the transition $2 \leftarrow 1$. The excited atoms in state 2 spontaneously revert to the lower state with the emission of radiation, and if N_2 is the number of atoms in state 2 the number of spontaneous emission acts per second will be N_2A_{21}, where A_{21} is the Einstein spontaneous emission probability coefficient for the transition $2 \rightarrow 1$. The state of equilibrium will be determined by equating the rate of emission to the rate of absorption; the ratio N_2/N_1 denoting the equilibrium concentrations of the atoms in the states 1 and 2 is given by the Maxwell-Boltzmann expression, $N_2/N_1 = e^{-h\tilde{\nu}/kT}$, where $\tilde{\nu}$ is the frequency of the radiation in reciprocal seconds that brings about the transition, and one can then find a value for the radiation density of frequency $\tilde{\nu}$. If it is assumed that the spontaneous emission process is the only emission process, the value obtained for the radiation density in this way is not that given by Planck's equation. To remedy this situation, Einstein was compelled to introduce, in addition to the spontaneous emission, an emission process, the probability of which was proportional to the radiation density within the enclosure of the frequency involved in the emission; hence the rate of this induced emission

6455
18/12/67

is $N_2B_{21}\rho(\tilde{\nu})$/sec, where B_{21} is the probability coefficient of induced emission. The equilibrium for the radiation is then determined by

$$N_1B_{12}\rho(\tilde{\nu}) = N_2[A_{21} + B_{21}\rho(\tilde{\nu})]$$

which, along with the Maxwell-Boltzmann expression for N_2/N_1, leads to Planck's equation for the radiation density if

$$\frac{A_{21}}{B_{12}} = \frac{8\pi h\tilde{\nu}^3}{c^3} \qquad \text{and} \qquad B_{21} = B_{12} \tag{27}$$

Nearly 40 years after its formulation by Einstein, the concept of stimulated emission came to fruition in the invention of radiation-amplifying devices, the maser and the laser, depending on this process.

There should be a relation between the Einstein coefficients A_{21}, B_{12} and the transition moments of the quantum mechanical description of emission and absorption. The rate of energy emission by an atom by the spontaneous process can be expressed both in terms of the quantum mechanical theory involving the square of the transition moment, and in terms of the Einstein formalism. By comparing these expressions it is found that

$$A_{21} = \frac{64\pi^4\tilde{\nu}^3}{3hc^3}\mathbf{M}_{21}{}^2 \tag{28a}$$

and, from Eq. 26

$$B_{12} = B_{21} = \frac{8\pi^3}{3h^2}\mathbf{M}_{12}{}^2 \tag{28b}$$

States 1 and 2 may be degenerate, that is, more than one state, each with its own wave function, may possess the energy E_1 or E_2. If G_1 is the number of states possessing the lower energy E_1 to which any one of the states possessing energy E_2 can revert radiationally, and similarly if G_2 is the number of states of energy E_2 to which any one state associated with the energy E_1 can undergo a transition, the equations for the Einstein coefficients include these factors. We shall also rewrite the equations in terms of the wave number ν of the transition, in which spectroscopic data are usually expressed, instead of the frequency. In the evaluation of B_{21} from the conditions for equilibrium between the radiation and the matter, as sketched above, the radiation density is now expressed as ergs per cubic centimeter per unit wavenumber range in reciprocal centimeters, and the value of B_{21} becomes $1/c$ times that in Eq. 28b. The Einstein coefficients are now related to the transition moment and to the oscillator strength, f, by the equations

$$A_{21} = \frac{64\pi^4\nu^3G_1\mathbf{M}_{21}{}^2}{3h} = \frac{8\pi^2e^2\nu^2G_1f_{21}}{mcG_2} \tag{29a}$$

$$B_{12} = \frac{8\pi^3G_2\mathbf{M}_{12}{}^2}{3h^2c} = \frac{\pi e^2}{mhc^2\nu}f_{12} \tag{29b}$$

Equations 27a and b and 28a and b are frequently written in terms of the dipole strength D. Since D equals the square of the matrix element of the electrical displacement, i.e.,

$$D = \left[\int \psi_2^*\left(\sum_i q_i\right)\psi_1 \, dv\right]^2 = Q^2$$

and the transition moment $\mathbf{M} = eQ$, hence

$$\mathbf{M}^2 = e^2Q^2 = e^2D$$

and e^2D can be substituted for $\mathbf{M}$ in these equations to obtain relations between the Einstein coefficients, the oscillator strengths, and the dipole strengths.

There is also an interesting relation between the intensity of absorption and the mean lifetime of the molecule in its excited state before it returns to the lower state with the emission of radiation. This lifetime may be called the radiative lifetime. The relation follows from the meaning of the Einstein spontaneous emission coefficient A_{21} as the number of times per second a molecule in the excited state reverts to the lower state with the emission of radiation. The mean lifetime in the excited state is therefore

$$\tau = 1/A_{21}$$

Using the relation in Eq. 29a between A_{21} and the oscillator strength f, and the relation in Eq. 23 between f and the integrated molar absorption coefficient, we find

$$\tau = \frac{mc}{8\pi^2e^2\nu^2f}\left(\frac{G_2}{G_1}\right) = \frac{1.50G_2}{\nu^2fG_1} \tag{30}$$

$$= \frac{N}{8\pi 2303\nu^2c\int_\nu \epsilon \, d\nu}\left(\frac{G_2}{G_1}\right) = \frac{3.47 \times 10^8}{\nu^2\int_\nu \epsilon \, d\nu}\left(\frac{G_2}{G_1}\right) \tag{31}$$

An intense absorption band is therefore associated with a relatively short preradiative mean life of the excited state, and a feeble band with a relatively long preradiative life. If the excited state is deactivated only by radiating, i.e., if the quantum yield of fluorescence is unity, the value of τ from Eqs. 30 and 31 is the actual, and maximum possible lifetime of the excited state. This may be called the intrinsic lifetime of the excited state. If the excited state loses its energy by other processes, such as collisional deactivation with the solvent, or by internal energy transfer, the actual mean life will be less than the intrinsic value calculated from the oscillator strength or integrated molar absorption coefficient. As an example of the orders of magnitude of the lifetimes of excited states, a dye molecule with an absorption maximum at

5000 Å, corresponding to 20,000 cm^{-1}, has an oscillator strength approaching unity. For strong absorption bands of most organic molecules, involving transitions between singlet states, G_2 and G_1 equal 1, and, from Eq. 30, $\tau = 3.8 \times 10^{-9}$ sec. In general, the intrinsic lifetime of organic molecules in excited states associated with very strong absorption bands is of the order of 10^{-8} to 10^{-9} sec. Conversely, knowing the radiative lifetime, we can calculate from Eq. 31 the value of the integrated molar absorption coefficient, and estimate the molar extinction coefficient at the maximum.

As will be shown in detail in subsequent chapters, organic molecules containing conjugated bond systems, possess, besides the short-lived excited states associated with the normal absorption spectra, excited states whose lifetimes may be many orders of magnitude greater than 10^{-9} sec, frequently of the order of milliseconds, and for some aromatic hydrocarbons, of the order of 10 sec. For reasons to be discussed in the later chapters, these metastable excited states are called triplet states. Such states may be reached by direct absorption from the ground state, but the long lifetime of the excited state requires that the intensity of this absorption band be very low.

In applying Eqs. 30 and 31 to absorption bands involving a transition from the ground state, 1 (singlet), to a triplet excited state, 2, one must consider the value of the ratio G_2/G_1. A recent analysis (33) shows that the value of G_2 to be used in applying Eq. 31 to calculate the intrinsic lifetime of the excited triplet from the integrated intensity of the triplet ← singlet absorption spectrum varies from 1 to higher values, but that the value best suited to most organic compounds at 77 K is $G_2 = 3$, with $G_1 = 1$ as usual for a singlet state. Using the value 3 for G_2/G_1 in Eq. 30, one finds that the oscillator strength for the triplet ← singlet absorption transition at 5000 Å of a hypothetical molecule, the lifetime of whose excited triplet state is 10^{-2} sec, is 1.13×10^{-5}, and from Eq. 31, $\int_\nu \epsilon_\nu \, d\nu = 2.4 \times 10^2$ liter mole^{-1} cm^{-2}. The integral is approximately the product of the maximum value of the molar extinction coefficient and the interval between the wavenumbers at which the molar extinction coefficient is half the maximum value, $\Delta\nu_{1/2}$.

$$\int_\nu \epsilon_\nu \, d\nu \sim \epsilon_{\max} \, \Delta\nu_{1/2} \tag{32}$$

For many vibronic band systems, $\Delta\nu_{1/2}$ is about 5000 cm^{-1}; in such a case the integrated molar absorption coefficient just calculated would correspond to $\epsilon_{\max}$ about 0.05 liter mole^{-1} cm^{-1}.

The relations in Eqs. 23–31 are derived for atomic gases exhibiting sharp absorption lines for which absorption and fluorescent emission coincide in wavelength, and their application to molecular spectra in the condensed phase can give only approximate results. Lewis and Kasha (34) introduced a correction n^2, into the denominator of Eqs. 30 and 31, where n is the refractive index of the solution, and Strickler and Berg (35) have derived a modified equation

$$\tau = \frac{3.47 \times 10^8}{n^2 \langle n_f{}^{-3} \rangle_{\mathrm{av}^{-1}} \int \epsilon_\nu \, d \ln \nu} \left(\frac{G_2}{G_1} \right) \tag{33}$$

applicable to strong transitions involving broad absorption bands in solution. The symbol $\langle n_f{}^{-3} \rangle_{\mathrm{av}^{-1}}$ indicates the reciprocal of the mean value of ν^{-3} in the fluorescence spectrum. The lifetimes of excited singlet fluorescent states of organic molecules in solution calculated from Eq. 33 were found usually to agree with experimental values.

All of the preceding discussion of the intensity of emission and absorption bands has been concerned with the interaction between radiation and oscillating electrical dipoles. An atom or molecule may contain two dipoles in orientation such that their moments cancel; the system nevertheless generates an electrostatic field. Such an arrangement of charges is called a quadrupole and can react with a radiation field so as to absorb or emit energy; the process is called *quadrupole emission* or *absorption.*

Two electrons on opposite sides of a positive charge may oscillate in directions perpendicular to the line joining them; the resultant dipole moment again is zero. The electronic motion is equivalent to a part of a circular coil in which an oscillating current flows. Such a coil generates a magnetic field as if an oscillating magnetic dipole were placed at the center of the coil with its axis perpendicular to the coil. An oscillating magnetic dipole can radiate or absorb radiation in the same way as an electric dipole, giving rise to *magnetic dipole radiation.*

The intensities of quadrupole and magnetic dipole radiation are usually much smaller than that of dipole radiation, but these radiations may be allowed when the dipolar radiation is forbidden. A component of quadrupole or magnetic dipole radiation may therefore yield observable intensity of emission or absorption when the dipole component is forbidden.

As a final remark regarding the topics of this section, attention may be drawn to the plea of Mulliken and Person (36) for more complete spectroscopic information than data on $\lambda_{\max}$ and $\epsilon_{\max}$, especially with respect to comparison of the spectroscopic behavior of series of related compounds such as molecular complexes. The oscillator strength and the transition moment **M** are of great theoretical importance. These quantities usually parallel $\epsilon_{\max}$ in a general way, but their dependence on the frequency and on the breadth of the band may result in some lack of parallelism with $\epsilon_{\max}$ in the comparison of spectra at different frequencies and with different band shapes. The relevant equations are Eqs. 23, 25, 26, and 32.

VI. APPLICATIONS OF ELECTRONIC ABSORPTION SPECTRA TO STRUCTURE DETERMINATION

A. The Concept of the Chromophore

The theory of molecular spectra outlined in Section III of this chapter, and developed in detail in the subsequent chapters of this Volume, permit in principle a description of the sizes, shapes, and bond structures of molecules in their ground and excited states. In practice, mathematical difficulties limit rigorous theoretical treatment to relatively few symmetrical molecules. The absorption of radiation, however, is a constitutive property, often associated with the presence of specific groups in the molecule, characterized by absorption bands in selective spectral regions, approximately independent of the rest of the molecule. In the infrared region, characteristic vibrational bands denote the presence of definite linkages in the molecule, such as C—H, C═O, C—O·NH$_2$, and Raman frequencies are similarly associated with structural units in the molecule. In the visible and ultraviolet spectral regions, the primary effect of the absorption of a quantum of radiation by a molecule is usually to excite one electron, the energy required and hence the wavelength of the effective radiation being determined by the binding energy of the excited electron and its energy in the excited state. These energies are determined by the nature of specific atoms and atomic groupings in the molecule, and are influenced to only a secondary degree by other atoms and groups for which the electronic binding is very different. Atomic groups in a molecule and their associated chemical bonds that determine an electronic absorption spectrum are called chromophores, an adaptation of the terminology for this concept introduced by Witt (37) many years ago in his theory of the color of dyes. In the visible and ultraviolet regions, the wavelength, intensity, and general appearance of the electronic band spectra along with the effect of environmental conditions, such as pH and solvent, are the most important factors for the characterization of compounds. For example, aldehydes and ketones containing the unconjugated carbonyl group show a characteristic absorption spectrum of relatively low molar extinction coefficient with a maximum about 280–290 mμ without well-marked vibrational structure in solution, the maximum being displaced to shorter wavelengths with increasing polarity of the solvent. An unknown compound exhibiting an absorption spectrum with all these characteristics would be judged to contain very probably an unconjugated aldehydic or ketonic carbonyl group, and closer examination of the spectrum could probably distinguish between these alternatives, while a deviation of the spectrum from any of the characteristics of this carbonyl chromophoric spectrum would throw serious doubt on this identification, unless some reasonable special circumstance could be adduced for the deviation.

Such spectrostructural identifications could be made purely empirically, by comparison of the spectra of unknown materials with those of known compounds, with due emphasis on the completeness of the correlation with respect to wavelength, intensity, shape, and environmental behavior. Some understanding, however, of the theory and terminology of electronic spectra of organic molecules will be useful in making structural deductions from spectral data. It might be natural to seek some analogy between the absorption spectra of organic molecules and the spectra of simple atoms such as sodium or mercury in the vapor state. The atomic absorption spectrum arises from electronic transitions from the ground state to successive excited states of regularly increasing energy and principal quantum number, the frequencies of successive absorption lines being arranged in a well-defined series called a Rydberg series. This series converges on a limiting frequency which determines the ionization potential of the atom.

Such spectra are indeed found for organic molecules, but only at very short wavelengths below 2000 Å within the vacuum ultraviolet region. Absorption of these energetic quanta yields highly excited electronic states in which the electron is far removed from all the atomic nuclei in the molecule and moves round a central positive charge much like an electron in the field of an atomic core. Successive electronic levels in these highly excited states form a Rydberg series, as for atoms, converging on a limit representing the ionization potential of the molecule. The vibrational structure associated with each member of the series is often simple, being concentrated in a single vibrational band, hence the series is readily recognized. Examples of Rydberg series in molecular spectra have been observed for a number of molecules, such as methyl halides, formaldehyde, acetylene, acetonitrile, and benzene (38). In a sense, these Rydberg series spectra for molecules constitute the simplest molecular spectra, but, although highly important for the determination of molecular ionization potentials, these spectra have not been much used in the structural analysis of large molecules.

B. Classification of Electrons and Orbitals in Organic Compounds

The spectra of organic compounds in the visible and ultraviolet regions are generated by valence electrons, which participate in holding the atoms in the molecule together, or by nonbonding electrons, localized on specific atoms such as nitrogen, oxygen, sulfur, or halogen atoms, for example, the "lone pair" on the nitrogen atom. The spectroscopic designation of a nonbonding electron, or of the associated orbital (i.e., the stationary state of that electron with respect to energy and probability distribution in space) is n. Since the valence electrons are associated with the bonding between atoms, they move in the field of at least two atomic centers, and their state is described by a molecular orbital about the two or more atomic nuclei, in contrast to the atomic orbital that describes the state of an electron localized about a single atomic nucleus. In saturated organic compounds containing only single bonds, the two electrons concerned in each bond are for the most part localized about the two bonded atomic nuclei, and are influenced to only a minor degree by atoms outside that bond. The molecular orbitals occupied by such localized bonding electrons are called σ orbitals; the electrons are σ electrons and the bond arising from the presence of two electrons shared between two atomic centers is a σ bond. The probability distribution of the σ electron is rotationally symmetrical about the bond. The absorption of radiation of appropriate frequency excites the σ electron to an orbital for which the probability distribution, still rotationally symmetrical about the bond, has a node at a point in the bond, that is, a point between the two atomic centers at which ψ^2 is zero (Chapter II, Section II-A, and Fig. 2). This state of the excited electron is therefore antibonding, denoted by σ^*; since, however, only one of the two originally bonding electrons is excited by the absorption, there is still some bonding power in the excited state, and excitation of the electron to the antibonding orbital does not imply dissociation. The σ electrons are the most tightly bound of the valence electrons, that is, they are of lowest energy, and the σ^* state is the highest excited state of the valence electrons, hence $\sigma^* \leftarrow \sigma$ absorption transitions require the absorption of high energy photons, of wavelength shorter than 2000 Å. The valence electrons of saturated hydrocarbons are all of the σ type, and their absorption is confined essentially to the short wavelength ultraviolet region accessible only by spectrographs that can be evacuated to eliminate the absorption of atmospheric oxygen.

In the simplest unsaturated stable molecule, ethylene, three of the valence electrons of each carbon atom occupy σ orbitals, two of them embracing the carbon atom and one of the attached hydrogen atoms, the third embracing the two carbon atoms. The three σ orbitals associated with each doubly bonded carbon atom are in the ground state coplanar and directed at an angle of 120° to each other. The remaining valence electron of each carbon atom occupies a molecular orbital of a different type, a π orbital, formed by the overlap of p atomic orbitals of each of the carbon atoms. The π orbital, like the p atomic orbital from which it is derived, has a node in the plane containing the carbon and hydrogen nuclei, and the maximum density of charge in this orbital therefore occupies two regions above and below the molecular plane. The binding of π electrons to the nuclei is weaker than that of σ electrons, and the nonbonding π^* state reached by absorption is lower than the σ^* state, hence the $\pi^* \leftarrow \pi$ transitions of ethylenic compounds are at longer wavelengths than the $\sigma^* \leftarrow \sigma$ transitions of saturated hydrocarbons. Nevertheless most of the absorption associated with the single (nonconjugated) ethylenic double bond is at wavelengths below 200 mμ.

A nonbonding electron on an atom linked to another may on excitation spend most of its time between the bonded atoms. If the molecule is saturated, the n electron after excitation occupies a σ^* orbital, and the transition is $\sigma^* \leftarrow n$. For example, in alkyl halides, a nonbonding electron on the halogen atom occupies after excitation a σ^* orbital about the halogen atom and the adjacent carbon atom. The n electrons are more loosely held to the atomic nucleus than the σ electrons, and an $\sigma^* \leftarrow n$ transition is therefore at longer wavelengths than the $\sigma^* \leftarrow \sigma$ transition, frequently at the shorter wavelengths in the ordinary ultraviolet. If the atom carrying n electrons is doubly bonded to another atom, excitation of the n electron will take it to a π^* orbital, and the $\pi^* \leftarrow n$ transition will be at still longer wavelengths.

The absorption bands corresponding to $\pi^* \leftarrow n$ transitions are characteristically shifted to shorter wavelengths as the polarity of the solvent is increased (39), while $\pi^* \leftarrow \pi$ bands are displaced to longer wavelengths with increasing refractive index, and, if the chromophore is associated with a permanent dipole moment, with increasing polarity of the solvent. The solvent displacement is a convenient diagnostic criterion for the $\pi^* \leftarrow n$ transition, as well as the relatively low intensity of the band.

C. Electronic Spectra of the Various Chromophores

1. SATURATED HYDROCARBONS

In saturated hydrocarbons the chromophores are valence electrons in σ bonds, and the absorption spectra, arising from $\sigma^* \leftarrow \sigma$ transitions, are in the vacuum ultraviolet region. Rydberg transitions also give rise to hydrocarbon absorption in this region. The longest wavelength band of methane is at 1220 Å. With increasing chain length and especially with increasing chain branching, the long wavelength thresholds of absorption of paraffins move to longer wavelengths, but no matter how long the chain, saturated hydrocarbons show no well-defined absorption maxima at wavelengths longer than 200 mμ; at most, the spectra of these compounds, as liquids, show inflections in a feeble absorption curve at wavelengths above 200 mμ. Purified saturated hydrocarbons, such as n-hexane, n-heptane, isopentane, 3-methylpentane, and methylcyclohexane, are therefore useful solvents for ultraviolet spectroscopy, which because of relatively small interaction with solutes, give the best resolved vibrational structure of the solute in the dissolved state (40,41). Isopentane, for example (40,41), shows useful transmission to 179 mμ in a layer of 1 cm, and retains its purity for some months if kept in a tightly stoppered bottle. The cycloparaffins absorb generally similarly to the uncyclized compounds, except that cyclopropane shows a weak band with a maximum at 195 mμ, longer than the bands of uncyclized paraffins or of cyclized paraffins containing more carbon atoms in the ring (42) (cf. cyclohexane, $\lambda_{\max}$ 150 mμ).

2. SATURATED COMPOUNDS CONTAINING ATOMS WITH NONBONDING ELECTRONS

Saturated alcohols, ethers, mercaptans, thioethers, amines, and alkyl halides show absorption bands at longer wavelengths than the hydrocarbons because of $\sigma^* \leftarrow n$ transitions.

The characteristic absorption band maxima of saturated alcohols are at wavelengths below 200 mμ (Table I), and the spectra show only "end absorption" at longer wavelengths. The transparency of alcohols makes them convenient polar solvents (Chapter III, Fig. 15). Saturated ethers likewise are transparent to near 200 mμ.

The electrons in the sulfur atom are more loosely bound than those in the oxygen atom, and corresponding spectra are displaced to longer wavelengths in sulfur compounds. Mercaptans show an absorption band about 227 mμ, thioethers in alcoholic solution show a maximum about 210 mμ, $\epsilon_{\max}$ about 1000 for the dimethyl compound, increasing with the size of the alkyl group. A weak shoulder appears at longer wavelengths in the spectrum of the lower alkyl members of the series, but disappears in thioethers containing branched alkyl groups.

Alkyl disulfides show a relatively weak band ($\epsilon_{\max}$ 400) at about 252 mμ.

The absorption spectrum of the saturated aliphatic amines (Table I) is characterized by a feeble $\sigma^* \leftarrow n$ band with maxima at wavelengths increasing with the number of alkyl groups from about 215 to 236 mμ in the vapor state, and by a stronger band with a maximum usually shorter than 200 mμ.

Of the saturated alkyl halides containing one halogen atom, the chlorides show a $\sigma^* \leftarrow n$ band with a maximum at wavelengths below 200 mμ; the bromides, at wavelengths just longer than 200 mμ; and the iodides show a well-marked band with a maximum about 257 mμ. The fluorides absorb similarly to the hydrocarbons. The shift to long wavelengths with increasing atomic number of the halogen is qualitatively parallel to decreasing ionization potential of the halogen atoms and of the alkyl halides, consistent with the interpretation of the absorption bands as $\sigma^* \leftarrow n$ bands. The $\sigma^* \leftarrow n$ nature of the transition is confirmed by the observation of a displacement to shorter wavelengths with increasing polarity of the solvent (52).

Compounds containing more than one halogen atom on the same carbon atom exhibit more complicated absorption spectra, containing several electronic transitions in the quartz ultraviolet region. The band of longest wavelength is at longer wavelength than the band for the simple halides, but bands also occur at shorter wavelengths (Table I). Orbital interactions between the halogen atoms, especially large in the iodo compounds, causes splitting of the ground and excited levels of the $\sigma^* \leftarrow n$ transitions.

TABLE I
Saturated Compounds Containing Nonbonding Electrons
($\sigma^* \leftarrow n$ Transitions)

Compound	Solvent	λ_{max} (mμ)	ϵ_{max} (l mole^{-1} cm^{-1})	Ref.
Methanol, CH_3OH	Vapor	184	150	43
Dimethylether, $(CH_3)_2O$	Vapor	184	2520	44
Methyl mercaptan, CH_3SH		227		45
Dimethylsulfide, $(CH_3)_2S$	Ethanol	210	1020	46
		229	140	
Diisoamyldisulfide	Ethanol	252	400	47
Methylamine, CH_3NH_2	Vapor	215	600	48
		175	2200	
Dimethylamine, $(CH_3)_2NH$	Vapor	220	100	48
		191	3300	
Trimethylamine, $(CH_3)_3N$	Vapor	227	900	48
		199	3950	
Piperidine, 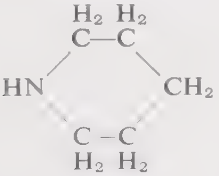	Vapor	236	180	49
		200	3600	
Piperazine, 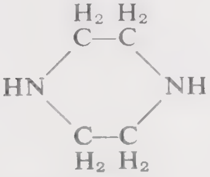	Vapor	?	?	
		195	4750	49
Methyl chloride, CH_3Cl	Vapor	173	200	50; 50a
Methyl bromide, CH_3Br	Vapor	204	200	51
Methyl iodide, CH_3I	Heptane	258	378	52
	Water	249		52
n-Butyl iodide, BuI	Heptane	257	486	52
	Water	250		
t-Butyl iodide, Me_3CI	Heptane	269	575	52
Dibromomethane, CH_2Br_2	Heptane	220		52
Bromoform, $CHBr_3$	Heptane	205		52
		224		
Diiodoethane, CH_2I_2	Heptane	212	1580	52
		240	600	
		290	1300	
Iodoform, CHI_3	Heptane	274	1300	52
		307	1860	
		349	2170	

3. THE ISOLATED ETHYLENIC BOND

The absorption spectrum of ethylene consists of a broad band beginning at about 2000 A and rising to an intense flat maximum about 162 mμ (53). This band is associated with a $\pi^* \leftarrow \pi$ transition, in which the ground state is planar and the excited state nonplanar. The diffuseness of the band is probably connected with the great change in molecular shape that accompanies the transition (54). Superposed on the $\pi^* \leftarrow \pi$ spectrum in olefins is a series of sharp vibrational bands which may be associated with a Rydberg transition in which coplanarity of the atoms is maintained (55).

Structural correlations are found among acyclic and cyclic olefins. The maximum of the $\pi^* \leftarrow \pi$ band shifts regularly to longer wavelengths with increasing number of alkyl substituents, and depends only to a secondary degree on the size of the substituents (56–59). At room temperature, a long wavelength shoulder is observed on the $\pi^* \leftarrow \pi$ band of olefins such as tetramethylethylene, cyclohexene, hexene-1, etc., which is greatly reduced in intensity at the temperature of liquid nitrogen (58). The shoulder results from molecules excited at room temperature in the ground state with respect to torsional vibrations, which make Franck-Condon transitions to excited states of lower energy than those to which the vibrationless ground state molecules make their transition. As the temperature is lowered, the concentration of vibrationally excited ground state molecules is diminished.

Structural correlations among the olefins are illustrated in Table II. The spectra in solution are displaced bathochromically from those of the vapor

TABLE II
Absorption of Monoolefinic Bond

Compound	Solvent	λ_{max} (mμ)	ϵ_{max}	Ref.
Ethylene	Vapor	162	~10,000	53
1-Hexene	Vapor	177	11,800	59
1-Hexene	Sat. hydrocarbon	179		58
cis-2-Butene	Vapor	174		59
trans-2-Butene	Vapor	178	13,000	59
2-Methylpropene	Vapor	188	11,300	59
2-Methyl-1-butene	Vapor	188	9,700	59
Tetramethylethylene	Vapor	187	15,600	59
Tetramethylethylene	Sat. hydrocarbon	192	10,000	58
Cyclohexene	Vapor	176	8,000	59
Cyclohexene	Sat. hydrocarbon	183	6,800	58
Allyl alcohol	Hexane	189	7,600	62
Vinyl chloride	Vapor	183		63
1,4-Pentadiene	Vapor	ca. 180	19,000	59
1,5-Hexadiene	Vapor	178	26,000	59

by as much as 10 mμ. The general bathochromic effect of increasing the number of alkyl substituents is clearly shown, and small but real differences exist between *cis* and *trans* isomers of disubstituted olefins. The spectrum of cyclohexene resembles that of the acyclic *cis*-2-alkenes, although the intensity appears to be lower. A double bond exocyclic to a five- or six-membered ring has a bathochromic effect with respect to the corresponding endocyclic bond (60).

Complex steroids and triterpenoids containing a single double bond show spectra in the short wavelength ultraviolet region that are useful in determining the nature of the ethylenic linkage (61). The spectrum of complex olefinic compounds, however, may be overlaid by absorption originating in the saturated carbon skeleton and depending on the number of quaternary carbon atoms in the molecule (61). This spectrum can be eliminated by subtraction of the absorption curve of the corresponding dihydrocompound, or of a saturated compound with essentially the same carbon skeleton, number of quaternary carbon atoms, and substituent groups. The corrected curves then show maxima which resemble in shape and wavelength those of simple olefins, which may be useful in determining the nature of the double bond in the complex compound.

If the molecule contains more than one isolated (nonconjugated) double bond, the chromophores absorb independently, and the intensity is additive in the number of double bonds. For example, the absorption maximum of 1,5-hexadiene, in which two 1-alkene linkages are separated by two methylene groups, is about 178 mμ, the characteristic region for 1-alkenes (Table II) and the maximum molar extinction coefficient is 26,000, twice that for the single 1-alkene linkage (59). Since band widths may change, the better comparison of intensities between related compounds is in terms of oscillator strengths. Spectral additivity of unconjugated chromophores is observed in general. A single methylene group between the two chromophores does not afford complete insulation. For example the absorption maximum of 1,4-pentadiene, in which the ethylene linkages are formally unconjugated but separated by a single methylene group, is very broad and displaced to longer wavelengths than for the typical position for 1-alkenes, to about 180 mμ, and the maximum molar extinction coefficient is only about 40% greater than that of the isolated ethylene bond (59). Some interaction occurs between the chromophores of this molecule.

4. CONJUGATED ETHYLENIC BONDS

The absorption spectrum of compounds containing conjugated ethylenic bonds is not merely an intensified version of the simple olefinic spectrum; a progressive displacement to longer wavelengths with increasing number of conjugated bonds is observed, with a concomitant increase of the intensity of the absorption. For example, the butenes, containing a single double bond, show an absorption maximum when dissolved in saturated hydrocarbons at about 178 mμ, and the unconjugated 1,4-pentadiene absorbs at about 185 mμ but butadiene has its maximum in solution at about 217 mμ. The absorption band of longest wavelength of conjugated polyenes is bathochromically displaced steadily through the ultraviolet region with increasing number of conjugated bonds, and ultimately enters the visible spectral region. In Table III are listed the spectra of the vinylogous series of compounds $H(CH{=}CH)_nH$

TABLE III
Absorption of Conjugated Polyenes

Compound $H(CH{=}CH)_nH$	Solvent	λ_0 (mμ)	ϵ_{max}	Ref.
$n = 2$; 1,3-Butadiene	Gas	210		64
	Hexane	217	20,900	64a
$n = 3$; 1,3,5-Hexatriene	Isooctane	268	42,700	65
$n = 4$; 1,3,5,7-Octatetraene	Cyclohexane	304		65
$n = 5$; 1,3,5,7,9-Decapentaene	Isooctane	334	121,000	65
$n = 6$; 1,3,5,7,9,11-Dodecahexaene	Isooctane	364	138,000	65
$n = 7$; 1,3,5,7,9,11,13-Tetradecaheptaene	Isooctane	390		65
$n = 8$; 1,3,5,7,9,11,13,15-Hexadecaoctaene	Isooctane	410		65
$n = 10$; 1,3,5,7,9,11,13,15,17,19-Eicosadecaene	Isooctane	447		65
All-*trans*-β-carotene ($n = 11$)	Hexane	480	139,000	66

from $n = 2$ to $n = 10$ (65) (with the exception of $n = 9$). The spectra of compounds for which $n > 2$ show well-defined vibrational structure, with an interval of approximately 1500 cm^{-1} for the lower members and a somewhat smaller interval for the higher members, about that to be expected in a progression mainly determined by the value of the conjugated C=C oscillation frequency in the upper electronic state. Table III gives the wavelength of the subband of longest wavelength and the molar extinction coefficient of the strongest vibrational band. Some of the compounds in Table III have not been obtained in a state of purity, and for these the value of the molar extinction coefficient cannot be given. At $n = 8$, the absorption of the series enters the visible. The carotenes, e.g., *trans*-β-carotene, $n = 11$

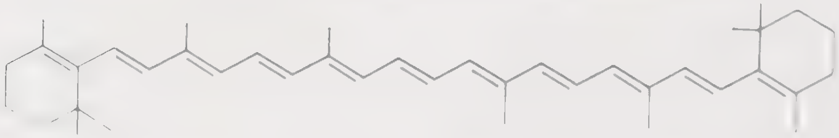

in which methyl groups are indicated by the strokes, are alkylated members of the series of polyenes with a strong visible color. The spectra of the vinylogous series $CH_3(CH{=}CH)_nCH_3$ has also been described (67), as have those of polyenes terminating in aldehydic (68,69) and carboxylic groups (70), α,ω-diphenyl polyenes (71), and polyene azines (69).

The wavelength shift caused by one additional vinyl group in the conjugated polyenes and in similar series decreases regularly with increasing chain length. Lewis and Calvin proposed the equation $\lambda_{\max}^2 = A + Bn$, where A and B are constants, for the wavelength of the absorption band of longest wavelength of conjugated polyenes as a function of the number n of the double bonds (72). But empirical equations, such as $\lambda_{\max}^2 = A - BC^n$, where A, B, and C are constants, give better agreement with observation for a number of polyene and *p*-polyphenyl series (73).

The ultraviolet and visible spectra of compounds containing conjugated chains arise from the excitation of an electron in the π system which occupies delocalized orbitals extending over all the conjugated atoms in the chain; the transition is $\pi^* \leftarrow \pi$. The intense $\pi^* \leftarrow \pi$ absorption bands of conjugated polyenes are shifted to longer wavelengths with increasing refractive index of the solvent (74); the shifts are relatively small. The dielectric constant of the solvent has only a minor effect on the position of the absorption band.

The data in Table III refer to the absorption of the compounds as the isomer in which the conjugated chain is in the fully extended all-*trans* configuration. When n is greater than 3, *cis* isomers also exist, spectrally distinguishable from the all *trans* isomer. Among the carotenes the absorption of *cis* isomers usually occurs at somewhat shorter wavelengths than for the all *trans* isomer, the molar extinction coefficient at the maximum is lower, and the second electronic transition, at shorter wavelengths than the first, representing excitation to a higher π^* level, is stronger for the *cis* configuration—a "*cis* band" appears. These characteristics of *cis* isomers are discussed in greater detail in Chapter III, Section IV-D.

In the spectra of the conjugated dienes, the effect of the *cis* vs. *trans* configuration is shown by the comparison of cyclic compounds containing the two double bonds in a single ring with compounds containing one of the double bonds in a ring structure and the other exocyclic. For example, 3-methylene cyclohexene, **1**, with a *trans* configuration of the conjugated chain

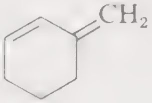

1

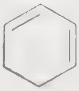

2

has its absorption maximum at 230 mμ, while cyclohexadiene, **2**, has its maximum at 256 mμ.

The attachment of alkyl substituents to the conjugated dienes and polyenes have well-defined spectral effects which have been of great value in the elucidation of the structure of those steroid and terpenoid compounds, the molecules of which contain diene systems. The effects are summarized in rules given by Woodward (75), Evans and Gillam (76), and Fieser and co-workers (77,78). See also refs. 79–81.

In applying the rules to steroid and terpenoid compounds, a distinction must be made between the type of molecule in which the conjugated bonds are in the same ring, homoannular compounds, and that in which the conjugated bonds are in different rings, heteroannular compounds. Woodward's rule for the effect of substituents in uncyclized dienes (75), which also applies to the effect of including the conjugated diene bonds in a heteroannular structure, is as follows. Butadiene, whose absorption band in hexane solution is at 217 mμ, is taken as the basic diene. For each alkyl substituent add 5 mμ to the wavelength; if a double bond in the diene structure is exocyclic to a six-membered ring, add an additional 5 mμ for each such exocyclic bond. The bathochromic effect of exocyclization probably is the result of bond strain whereby the ground level is raised with respect to the excited level. Table IV illustrates Woodward's rule for this type of conjugated diene. Since the spectra of hydrocarbons are not highly solvent sensitive, it is not necessary, within the accuracy with which the rule applies, to specify the solvent.

Fieser and Fieser suggest wavelength 214 mμ for the basic diene in calculating the wavelength of conjugated dienes based on *trans*-butadiene, with the same effects of alkyl substituents and exocyclic bonds as in Woodward's rule.

Homoannular dienes absorb at essentially longer wavelengths than similarly substituted heteroannular compounds, probably as a consequence of the *cis*, in contrast to the *trans* arrangement of the double bonds. Fieser and Fieser's rule for the wavelength of maximum absorption of homoannular dienes and polyenes is as follows (78): basic diene wavelength 253 mμ; add 5 mμ for every alkyl substituent or ring residue; add 5 mμ for every exocyclic double bond; add 30 mμ for every bond that extends the conjugated chain beyond two double bonds. If the molecule contains both heteroannular and homoannular double bonds, the calculation of the absorption maximum is based on the homoannular part. For example, the predicted absorption maximum for ergostatriene

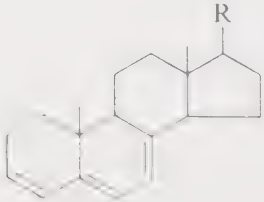

TABLE IV
Woodward's Rule for Conjugated Dienes

Compound	λ_{max}		ϵ_{max}	Solvent	Ref.
	Calculated	Observed			
Butadiene 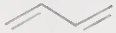		217	20,900	Hexane	64a
Piperylene 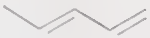	217 + 1(5) = 222	223.5	23,000	Ethanol	79
Isoprene 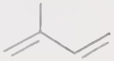	217 + 1(5) = 222	220	23,900	Hexane	64a
β,γ-diMe butadiene 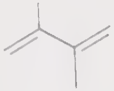	217 + 2(5) = 227	226		Hexane	82
$\Delta^{2,4}$-Hexadiene 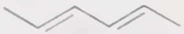	217 + 2(5) = 227	227	25,000	Hexane	79
3-Methylene-cyclohexene 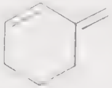	217 + 2(5) + 1(5) = 232	231	21,000	Cyclohexane	83
Allylidene cyclohexane 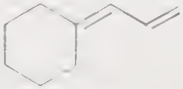	217 + 2(5) + 1(5) = 232	236.5		Ethanol	64a
β-Phelandiene 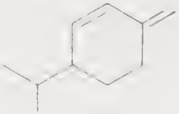	217 + 2(5) + 1(5) = 232	232	9,100		64a
$\Delta^{3,5}$-Cholestadiene 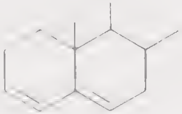	217 + 3(5) + 1(5) = 237	235			84

is 253 + 4 × 5 (for substituents on carbon atoms of the homoannular chromophore) + 30 (for one additional conjugated double bond) + 2 × 5 (for two exocyclic double bonds) = 313 mμ; the observed value is 316 mμ.

Substitution of an amino group in the ω position of an acyclic conjugated chain causes a marked shift of the absorption to long wavelengths; for example, the absorption maximum of 4-diethylaminobutadiene is at 281 mμ, ϵ_{max}, 23,500 (85), in contrast to the absorption of butadiene at 217 mμ. The shift to long wavelengths caused by the introduction of the amino group is connected with the participation of the "lone pair" of electrons of the nitrogen atom in the π system of the conjugated chain. This circumstance defines the behavior of the amino group as an auxochrome to the conjugated chain. In the language of the resonance theory, the uncharged structure *a* of the molecule resonates with the dipolar structure *b*.

$$\underset{(a)}{CH_2{=}CH{-}CH{=}CH\cdot N(C_2H_5)_2} \leftrightarrow \underset{-}{\ddot{C}}H_2{-}CH{=}CH{-}\underset{(b)}{CH}{=}\underset{+}{N}(C_2H_5)_2$$

The auxochromic effect of the dialkylamino group is still more pronounced in the spectra of the singly charged ions of the α,ω-bisdimethylaminopolyenes, the members of which series from $n = 0$ to $n = 6$ have been prepared (86). These compounds are acyclic versions of the cyanine dye ions, in which latter compounds the basic nitrogen atoms are contained in heterocyclic nuclei such as pyridine or benzothiazole, linked by a polyene chain, and the members of the dimethylaminopolyene series from $n = 2$ on are visibly colored. The long wavelength absorption maxima and ϵ_{max} for these compounds are listed in Table V.

TABLE V

Absorption of α,ω-Bisdimethylaminopolyene ions $(CH_3)_2\overset{+}{N}{=}CH(CH{=}CH)_n\cdot N(CH_3)_2ClO_4^-$, in CH_2Cl_2

n	λ_{max} (mμ)	ϵ_{max}	n	λ_{max} (mμ)	ϵ_{max}
0	224	14,500	4	625	295,000
1	313	64,500	5	734	353,000
2	416	119,500	6	848	(220,000)[a]
3	519	207,000			

[a] Compound probably impure.

Unlike the various uncharged polyene series, the bisdimethylaminopolyene ions show an approximately constant displacement of their absorption maxima of 100 mμ to longer wavelengths for each additional vinyl group in the conjugated chain, in this respect resembling cyanine dyes that contain identical heterocyclic nuclei (87,88). There is also a difference in the type of vibrational structure of the electronic spectra of the uncharged polyenes and singly charged ions of the symmetrical polyenes with terminal basic groups. In the latter molecules, the bond order in the conjugated chain is to a first approximation the same for all the bonds in the chain in both the ground and excited states, while in the uncharged polyenes, alternation between double and single bonds takes place to different degrees in the two states. In the ions, therefore, no great change in bond length occurs on electronic excitation, and, according to the Franck-Condon principle, the 0 ← 0 vibrational band is much the strongest in the vibrational progression. A greater change in internuclear distances occurs on excitation of the uncharged polyenes, with the result that more vibrational bands are represented in the vibrational progression of the electronic spectra, the 0 ← 0 band is not always the strongest, and in any case several subbands are shown in the spectra of intensity comparable to that of the 0 ← 0, if that band is the strongest. These facts are illustrated in the spectra of carotenes and cyanine dyes, respectively (Figs. 65 and 58 of Chapter III).

5. POLYACETYLENES

The strong absorption of acetylene is in the vacuum ultraviolet, although weak bands are observed between 210 and 250 mμ (see Chapter III, Section III-B-5). Polyacetylenes, $R\cdot(C{\equiv}C)_n\cdot R$, with $R = CH_3$ (89,90), *tert*-butyl (89), or phenyl (91), show electronic spectra with well-marked vibrational structure, the absorption region being displaced to longer wavelengths with increasing values on n. These compounds show a very strong band system at short wavelengths and a weaker system at longer wavelengths, both systems increasing in wavelength with increasing number of conjugated acetylenic bonds, as is illustrated in Table VI for the dimethylpolyacetylenes.

TABLE VI

Absorption of Dimethylpolyacetylenes $\mathrm{Me(C{\equiv}C)_nMe}$ in Ethanol

n	Strong bands, mμ (10^{-4} ε in brackets)					Weaker bands, mμ (ε in brackets)				Ref.
2						218.5 (300)	226.5 (360)	236 (330)	250 (160)	92
3				207 (13.5)	239 (105)	253 (130)	268 (200)	268 (200)	306 (120)	93
4	205 (2.43)	215 (9.15)	226 (19.8)	234 (28.1)		286 (140)	306 (180)	328 (180)	354 (105)	93
5	224 (2.90)	233 (9.50)	247 (24.3)	260 (35.2)		324.5 (230)	347.5 (210)	373.5 (150)	394 (120)	90
6	242 (4.7)	255 (12.8)	268.5 (31.7)	284 (44.5)						90

6. ALIPHATIC CARBONYL COMPOUNDS

Aldehydes and ketones containing an unconjugated carbonyl group show a characteristic absorption maximum within the range 270–300 mμ, of low molar extinction coefficient, often between 10 and 20 l mole^{-1} cm^{-1} (Chapter III, Fig. 17), and a stronger absorption band system about 180 mμ, with still stronger systems at shorter wavelengths. The band near 300 mμ has the characteristics of a $\pi^* \leftarrow n$ band, i.e., its intensity is low and it is shifted to shorter wavelengths in solvents capable of forming hydrogen bonds, the band at about 180 mμ appears most likely to be a $\sigma^* \leftarrow n$, and those at shorter wavelengths represent $\pi^* \leftarrow \pi$ and Rydberg transitions (94–97). In addition, a very feeble absorption system has been observed for formaldehyde on the long wavelength side of the band at 300 mμ, representing a transition of one of the n electrons to a triplet level of the π system.

The $\pi^* \leftarrow n$ band of formaldehyde vapor is at about 304 mμ and at longer wavelengths in hydrocarbon solution (Table VII). Vibrational structure appears in the spectrum both of the vapor and of the solution; the interval corresponds to the C—O stretching frequency, 1180 cm^{-1}, in the excited state (100).

Substitution of a hydrogen atom in formaldehyde by alkyl groups shifts the absorption to shorter wavelengths, for example to 289 mμ, in the spectrum of acetaldehyde, and to still shorter wavelengths in the ketones (275 mμ for acetone in hexane). As is illustrated in Table VII, the absorption of the carbonyl group in cyclic aliphatic ketones is displaced to longer wavelengths than for comparable acyclic compounds. The presence of a halogen atom on the carbon atom adjacent to the CO group in cyclohexanones affects the absorption spectrum differently according as the halogen atom is oriented axially or equatorially, and the ultraviolet spectra can be used to distinguish between these orientations and to determine the isomeric composition of mixtures (115). For example, the equatorially substituted 2-chloro-4-*tert*-butylcyclohexanone has its absorption maximum at a wavelength slightly shorter than the maximum of the parent ketone, while the isomer containing the chlorine in axial orientation absorbs at considerably longer wavelengths and with greater intensity (107) (Table VII).

Solvents influence the position of the characteristic absorption band in the near ultraviolet of aldehydes and ketones in the way typical for $\pi^* \leftarrow n$ bands polar solvents shift the absorption to shorter wavelengths (116). Table VIII (117) shows that hydroxylic solvents cause a greater hypsochromic shift than aprotic polar solvents of comparable dielectric constant. The large shifts caused by hydroxylic solvents are probably associated with hydrogen bonding, which acts on the lone pair electrons more than on the π^* electrons, lowering the ground state with respect to the excited state (118–120). The

TABLE VII
Absorption of Carbonyl Compounds

Compound	Solvent	λ_{max} (mμ)	ϵ_{max}	Ref.
Aldehydes:				
Formaldehyde, $H_2C{=}O$	Vapor	304	18	98
	Vapor	175	18,000	99
	Isopentane	310	5	100
Acetaldehyde, $MeHC{=}O$	Vapor	289	12.5	98
	Vapor	182	10,000	101
	Hexane	293	12	102
Propionaldehyde, $EtHC{=}O$	Vapor	290	15	98
	Hexane	290	18	102
Ketones:				
Acetone, $Me_2C{=}O$	Vapor	274	13.6	103
	Cyclohexane	275	22	104
Methylpropylketone, $MePrC{=}O$	Hexane	278	14.5	105
Cyclopentanone	Isooctane	300	18	106
Cyclohexanone	Isooctane	291	15	106
2-Chloro-4-*tert*-butylcyclohexanone,				
equatorial	Isooctane	286	17	107
axial	Isooctane	306	49	107
Camphor	Hexane	295	14	108
Fenchone	Hexane	293	20	108
Acetylacetone, $Me \cdot CO \cdot CH_2 \cdot CO \cdot Me$	Ethanol	272	110	109
				109a
Acetyl chloride, $MeCO \cdot Cl$	Heptane	240	34	110
				110a
Acetyl bromide, $MeCO \cdot Br$	Heptane	250	93	111
				110a
Ethyl acetate, $MeCO \cdot OEt$	Vapor	211	47.5	112
	Water	204	60	105
Acetamide, $MeCO \cdot NH_2$	Water	ca. 214	ca. 100	110
Acetic anhydride, $(MeCO)_2O$	Vapor	220	73	112
Acetic acid, $MeCO \cdot OH$	Vapor	203	depends on pressure	113
	Ethanol	204	41	110
Succinic acid, $CO \cdot OH(CH_2)_2CO \cdot OH$	Water	204	100	110

shift is also partly a result of the Franck-Condon effect (118,120). Immediately after the vertical transition (Section IV-B of this chapter) the excited molecule in a hydroxylic environment is in the nuclear configuration and in the configuration of solvent atmosphere appropriate to equilibrium in the ground state, which however represents a strained configuration of the excited state, hence the absorption transition is of higher energy than if the large Franck-Condon factor were absent.

TABLE VIII

Effect of Solvents on $\pi^* \leftarrow n$ Band of Acetone (117)

Effect of hydroxyl solvents		Effect of aprotic solvents	
Solvent	λ_{max} (mμ)	Solvent	λ_{max} (mμ)
Heptane	277	Acetonitrile	274
tert-Butanol	273	Ether	277
i-Propanol	272	Chloroform	275
Ethanol	270		
Methanol	269.5		
Water	265		

Two nonconjugated carbonyl groups cause absorption in the normal carbonyl region. Acetylacetone, for example, has an absorption maximum in alcoholic solution close to that of acetone (Table VI), although the intensity appears to be greater than that of two independent carbonyl chromophores. In alkaline solution the enol form of this compound is formed. The absorption band of the enol is about 270 mμ, close to that of the keto form, but the molar absorption coefficient of the enol, 12,000, is very much greater. The enol content of a solution can be simply determined from a measurement of the molar extinction coefficient at the 270 mμ maximum (109a).

The introduction of atoms with nonbonding electrons, such as Cl, NH_2, O-alkyl, or OH groups, on the carbon atom of the carbonyl group causes a large shift of the absorption spectrum to shorter wavelengths, while the molar extinction coefficient remains relatively low (see Table VII) (acid chlorides, amides, esters, acid anhydrides, and carboxylic acids). The chlorine atom and especially the nitrogen atom of the amides and the oxygen atom of the hydroxy group can conjugate with the carbonyl group, donating electrons to the carbonyl carbon atom, and raising the energy of the π^* orbital with reference to the orbital occupied by the n electrons in the ground state. The $\pi^* \leftarrow n$ transition energy is therefore raised and the absorption shifted to shorter wavelengths. The absorption band of acetyl chloride is about 240 mμ, that of acetamide is an indistinct shoulder at about 214 mμ, and acetic acid shows a maximum at about 203 mμ. Two nonconjugated modified carbonyl groups in the same molecule cause absorption in the same region as for the single chromophore; for example, succinic acid absorbs in the same region as acetic acid, with about double the intensity (Table VII).

The carboxylate anion shows no definite absorption maximum at wavelengths greater than 200 mμ; only a gradual increase in absorption takes place from the long wavelength side ("end absorption").

Ketene, $H_2C{=}C{=}O$, in hexane solution, has an absorption maximum at 325 mμ, $\epsilon_{max} = 20$ (121).

Aliphatic thioketones show an absorption band in the visible spectral region, of low molar extinction coefficient, comparable to that of the $\pi^* \leftarrow n$ band of the ketones. The transition appears to be $\pi^* \leftarrow n$, displaced to long wavelengths from the corresponding carbonyl transition because of the looser binding of the valence electrons in the sulfur atom than in the oxygen atom. The band for cyclohexanethione as at wavelength 504 mμ (114). The molar extinction coefficient, which seems to be below 10, is uncertain because of the chemical instability of the compound.

7. COMPOUNDS CONTAINING 1,2-CARBONYL GROUPS

In the 1,2-dialdehydes and diketones, such as glyoxal, $H\cdot CO\cdot CO\cdot H$, or biacetyl, $CH_3\cdot CO\cdot CO\cdot CH_3$, there is a lone pair nonbonding orbital and a π^* orbital on each oxygen atom. As a result of a small interaction, the energies of the two n orbitals are slightly different, and similarly, two π^* orbitals are present, with a greater energetic separation. Apart from selection rules, therefore, four $\pi^* \leftarrow n$ transitions might occur, but two are forbidden by molecular symmetry and only two $\pi^* \leftarrow n$ bands are observed (95b,123). One of these is at a wavelength near the normal carbonyl band about 290 mμ, and the other is at longer wavelengths, sometimes entering the visible spectrum. Glyoxal, for example, shows a structured band with a maximum about 450 mμ and another band about 270 mμ (95b); biacetyl has a maximum about 422 mμ, $\epsilon_{\max} = 22.7$ in heptane (110a,124) and a band of comparable intensity at about 282 mμ (110a,125), beside a strong band in the short wavelength ultraviolet. The hypsochromic effect of substituting methyl for hydrogen that causes simple ketones to absorb at shorter wavelengths than comparable aldehydes appears to operate also in the 1,2-dicarbonyl compounds.

The open-chain 1,2-dialdehydes and ketones occur mostly in the planar *trans* form, in which the interaction between the π^* electrons is expected to be less than for the planar *cis* isomer, because of the greater overlap of the wave functions in the latter orientation. The planar *cis*-1,2-dicarbonyl compounds might therefore be expected to show their absorption band at longer wavelengths than the planar *trans*. This conclusion seems to be verified with respect to the $\pi^* \leftarrow n$ absorption band of the longer wavelength in alicyclic diketones (126). In compounds of formula **1** the carbonyl groups are forced

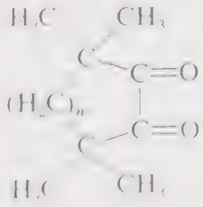

1

into the *cis* configuration when the ring is small, $n = 1$, but as the ring size is increased, the adjacent carbonyl groups are forced from coplanarity and assume a mutual orientation depending on the size (126). From models of the molecules containing different ring sizes, Leonard and Mader (126) estimated the most probable range of angles between the carbonyl groups in these alicyclic diketones. The wavelengths of the $\pi^* \leftarrow n$ absorption bands and the angle between the carbonyl groups are shown in Table IX. The wavelength of the longer of the two $\pi^* \leftarrow n$ transitions of the carbonyl groups is markedly sensitive to the angle of twist about the intercarbonyl bond. In camphor quinone, chosen as the model compound for $n = 1$, the carbonyl groups must be nearly coplanar and in the *cis* orientation ($\theta = 0^\circ$), and its long wavelength absorption band, at 466 mμ (Table IX), is at a longer wavelength than that of any other of the compounds tabulated. The wavelength for camphor quinone is substantially greater than that for the coplanar *trans*-biacetyl, at 422 mμ. As the size of the ring increases, the carbonyls cease to be coplanar, and when the ring is very large, $n = 14$, giving an eighteen-member ring, the flexibility is great enough for the repulsion of the oxygen atoms to tend to induce the *trans* configuration. With increasing nonplanarity, the first $\pi^* \leftarrow n$ band is steadily shifted to shorter wavelengths, reaches a minimum value when θ is about 90°, and, as θ continues to increase and the chromophores tend to become *trans* to one another, the wavelength increases again. The second $\pi^* \leftarrow n$ band is much less affected by the mutual orientation of the carbonyl groups: there seems to be some tendency for the wavelength to increase with increasing values of θ up to 90°, and to retreat as the configuration tends toward the *trans* type.

The conjunction of three adjacent carbonyl groups in the acyclic compound 1,2,3-triketopentane does not displace the long wavelength absorption band much beyond that of biacetyl, probably because one of the end carbonyls is not coplanar with the other two (127). The alicyclic compound 4,4,5,5-tetramethyl-1,2,3-cyclopentanetrione, however, absorbs in the red spectral region (128), indicating a strong bathochromic effect of a third carbonyl chromophore in coplanar *cis* orientation with respect to an adjacent pair in similar orientation (126).

Oxalyl chloride $(CO \cdot Cl)_2$, shows similar indications of interaction between the adjacent carbonyl chromophores, modified by the presence of the chlorine atom. In heptane solution this compound shows a broad structured band extending from about 380 to about 280 mμ, with a molar extinction coefficient of 24 at the maximum, 318 mμ. This value of the absorption maximum can be compared with that for acetyl chloride, 240 mμ. At wavelengths below 280 mμ, the absorption increases rapidly without showing definite maxima to about 200 mμ, where the molar extinction coefficient is about 1600 (110a).

TABLE IX
$\pi^* \leftarrow n$ Absorption of 1,2-Dicarbonyl Compounds

Compound	θ (deg)	Solvent	$\lambda_{\max}$ (mμ)	$\epsilon_{\max}$	$\lambda_{\max}$ (mμ)	$\epsilon_{\max}$	Ref.
Glyoxal, $(HCO)_2$	180	Hexane	450^a		280		95b
Biacetyl, $(H_3C\cdot CO)_2$	180	Heptane	422^a	22.7	270	18	110a
Camphor quinone,							125
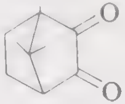	0–10	95% ethanol	466	30	271	21	126
Compound **1**, $n = 2$	0–60	95% ethanol	380	10	298	28	126
Compound **1**, $n = 3$	90–110	95% ethanol	337	33	299	33	126
Compound **1**, $n = 4$	100–140	95% ethanol	343^b	21	$296^{a,b}$	43	126
Compound **1**, $n = 14$	100–180	95% ethanol	384	21	287^a	59	126
Bipivaloyl, $(CH_3)_3C$ 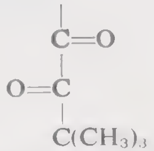 $(CH_3)_3C-C(=O)-C(=O)-C(CH_3)_3$	90–180	95% ethanol	365	21	270^a	52	126
Oxalyl chloride, $(COCl)_2$	180	Heptane	318^a	24			110a
Oxalic acid, $(CO\cdot OH)_2$	180	Water	250	50			

---

[a] Band shows vibrational structure.

[b] Compound impure.

Similarly, the weak carboxyl band at about 205 mμ for saturated monocarboxylic acids and for dicarboxylic acids containing two or more CH_2 groups is displaced to about 250 mμ and intensified in oxalic acid.

8. α,β-UNSATURATED CARBONYL COMPOUNDS AND POLYENE ALDEHYDES

Aldehydes and ketones in which the carbonyl group is conjugated to a C=C double bond (α,β-unsaturated compounds), or to a conjugated system of such bands, show two characteristic absorption regions at wavelengths above 200 mμ, a relatively feeble band at wavelengths longer than that of the 280 mμ band of the unconjugated carbonyl group, and an intense band at shorter wavelengths (Chapter III, Fig. 17). The low intensity of the long wavelength band and its hypsochromic displacement in hydroxylic solvents suggest that the transition is $\pi^* \leftarrow n$, analogous to the transition associated with the band about 280 mμ of the unconjugated aldehydes and ketones. But while the π^* orbital of the latter compounds is localized about the carbon–oxygen linkage, the long wavelength displacement of the band in the conjugated compounds suggests that the excited π^* orbital is nonlocalized, extending over the atoms contained in the conjugated chain. The energy of the orbital is then reduced and the $\pi^* \leftarrow n$ absorption occurs at longer wavelengths. As the number of double bonds conjugated with the carbonyl group increases, as in the polyene aldehydes, the $\pi^* \leftarrow n$ band is progressively shifted to longer wavelengths. The intense band at shorter wavelengths appears to be the analog of the $\pi^* \leftarrow \pi$ band in the conjugated dienes (95b); it occurs at a shorter wavelength than that of the diene band. For example, the $\pi^* \leftarrow \pi$ band of acrolein, $CH_2{=}CH{-}CH{=}O$, is at 208 mμ in alcoholic solution (Table X), while that of butadiene, $CH_2{=}CH{-}CH{=}CH_2$, is at 217 mμ (Table IV).

The effect of solvents on the positions of the characteristic bands of the α,β-unsaturated carbonyl compounds illustrates the difference in the nature of the transitions –the $\pi^* \leftarrow n$ band shows the characteristic displacement to shorter wavelengths in increasingly polar solvents, especially hydroxylic solvents, while the $\pi^* \leftarrow \pi$ band is affected in the opposite direction. These effects are illustrated for mesityl oxide, $(CH_3)_2C{=}CH{-}CO{-}CH_3$ (136), in Table XI.

From Table X it can be seen also that alkyl substitution displaces the maximum of the $\pi^* \leftarrow \pi$ and $\pi^* \leftarrow n$ bands in opposite directions, the $\pi^* \leftarrow \pi$ band to longer wavelengths, and the $\pi^* \leftarrow n$ to shorter. The effect of alkylation on the position of the intense $\pi^* \leftarrow \pi$ band can be summarized in empirical rules, determined from the observed spectra of a large number of compounds, similar to those already discussed for the conjugated dienes, and, like the rules for the dienes, first stated by Woodward (137). The rules for

TABLE X

Absorption of α,β-Unsaturated Aldehydes and Ketones and of Polyene Aldehydes

Compound	Solvent	λ_{max} (mμ)	ϵ_{max}	λ_{max} (mμ)	ϵ_{max}	Ref.
Acrolein, $H_2C{=}CH{-}CH{=}O$	Hexane	197				95b,133
	Ethanol	208[a]		328	13	129
		(208)[a]				
Crotonaldehyde, $CH_3{\cdot}CH{=}CH{-}CH{=}O$	Hexane	217	16,500	333		95b
	Ethanol	220	15,000	322	28	69
		(220)				
Tiglicaldehyde, $CH_3{\cdot}CH{=}C{\cdot}CH_3{-}CH{=}O$	Ethanol	228	> 5000	290	11	130
		(230)				
Citral, $(CH_3)_2C{=}CH{\cdot}(CH_2)_2{\cdot}C(CH_3){=}CH{-}CH{=}O$	Ethanol	238	13,500	324	65	131
		(230)				
2,4-Hexadienal, $CH_3{\cdot}(CH{=}CH)_2{-}CH{=}O$	Ethanol	271	25,000	ca. 366[b]	ca. 30	132
2,4,6-Octatrienal, $CH_3{\cdot}(CH{=}CH)_3{-}CH{=}O$	Ethanol	315	37,000	ca. 380[b]	?	132
2,4,6,8-Decatetraenal, $CH_3(CH{=}CH)_4{-}CH{=}O$	Ethanol	353	41,000	ca. 380[b]	?	132
2,4,6,8,10-Dodecapentaenal, $CH_3(CH{=}CH)_5{-}CH{=}O$	Ethanol	377	51,000	?	?	132
Methyl vinyl ketone, $CH_2{=}CH{-}C(CH_3){=}O$	Ethanol	219	3600	324	24	133
	Isooctane	(225)		331	25.1	134
Ethylideneacetone, $CH_3{\cdot}CH{=}CH{-}C(CH_3){=}O$	Ethanol	224	9750	314	38	133
		(225)				
Mesityl oxide, $(CH_3)_2C{=}CH{-}C(CH_3){=}O$	Ethanol	235	14,000	314	60	133
		(235)				
3,4-Dimethylpent-3-ene-2-one, $(CH_3)_2C{=}C(CH_3){-}C(CH_3){=}O$	Ethanol	249	> 4000			133
		(247)				

---

[a] The numbers in brackets give the wavelength of the absorption maximum calculated from Woodward's rules.

[b] Shoulders.

(continued)

TABLE X (*continued*)

Absorption of α,β-Unsaturated Aldehydes and Ketones and of Polyene Aldehydes

Compound		Solvent	λ_{max} (mμ)	ϵ_{max}	λ_{max} (mμ)	ϵ_{max}	Ref.
2-Cyclohexylidenecyclohexane-1-one,	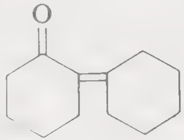	Ethanol	258 (257)	>800			133
2-Cyclopentenone,	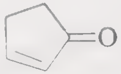	Cyclohexane (ethanol)	210 (214)	15,500	330^c	37	135
cf. 3-Cyclopentenone (nonconjugated),	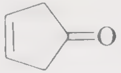	Cyclohexane	190	4000	290^c	10	135
3-Methyl-2-cyclopentenone,	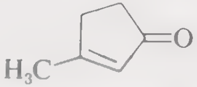	Ethanol	235 (235)	12,950	310	48	133

---

[c] Band shows vibrational structure.

TABLE XI

Solvent Effect on $\pi^* \leftarrow \pi$ and $\pi^* \leftarrow n$ Bands of α,β-Unsaturated Ketones; Mesityl Oxide (136)

	$\pi^* \leftarrow \pi$ Band		$\pi^* \leftarrow n$ Band	
Solvent	$\lambda_{\max}$ (mμ)	$\epsilon_{\max}$	$\lambda_{\max}$ (mμ)	$\epsilon_{\max}$
n-Hexane	229.5	12,600	327.0	40
Ether	230.0	12,600	326.0	40
Ethanol	237.0	12,600	325.0	90
Methanol	238.0	10,700	312.0	55
Water	244.5	10,000	305.0	60

TABLE XII

Woodward's Rules for the Effect of Alkyl Substitution on the Wavelength of the $\pi^* \leftarrow \pi$ Absorption Band of α,β-Unsaturated Ketones (137)

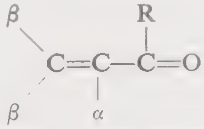

Substituent		Most probable wavelength in ethanol[a] (mμ)
None		215
α, or β	No exocyclic C=C bond	225
α,β or β,β	(1) No exocyclic C=C bond	235
	(2) One exocyclic C=C bond	240
α,β,β	(1) No exocyclic C=C bond	247
	(2) One exocyclic C=C bond	252
	(3) Two exocyclic C=C bonds (133)	257

[a] Solvent corrections. To obtain the position of the $\pi^* \leftarrow \pi$ band in ethanol from its observed position in: methanol, subtract 1 mμ; chloroform, ± 0; ether, add 6 mμ; *n*-hexane, add 7 mμ.

α,β-unsaturated ketones are given in Table XII. As for the dienes, residues of a six-membered ring produce the same spectral effect as alkyl groups, with the same effect as in the dienes of an additional shift of +5 mμ for each exocyclic double bond. The position of the short wavelength band of the compounds in Table X as given by the empirical rules is indicated in brackets in the table. Compounds containing a C=O group conjugated with a double bond in a five-member ring (2-cyclopentenones) show a spectral maximum at shorter wavelengths than those predicted by Woodward's rules (138). For example, the observed $\pi^* \leftarrow \pi$ maximum for 2-cyclopentenone is at 210 mμ in cyclohexane; in ethanol, it would be about 217 mμ. According to the normal Woodward rule, the maximum in alcohol of an α,β-unsaturated ketone with one alkyl substituent on the carbon atom (in this case the residue of the five-member ring) should be at 225 mμ. The deviation is outside the normal experimental deviations from the predicted values for acyclic unsaturated ketones and for those in which the C=O group is conjugated with a double bond in a six-member ring. The empirical rules found to apply to 2-cyclopentenones are given in Table XIII (139) and for α,β-unsaturated aldehydes in Table XIV (133). The effect of conjugation of the C=O group with an ethylenic double bond is nicely shown by the comparison of the spectra of 2- and 3-cyclopentenones (Table X).

TABLE XIII
Effect of Alkyl Substitution on $\pi^* \leftarrow \pi$ Band of 2-Cyclopentenones (139)

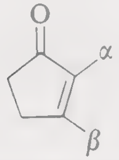

Substituent	mμ
None	214
α or β	224
α and β	236

TABLE XIV
Effect of Alkyl Substitution on the $\pi^* \leftarrow \pi$ Band of α,β-Unsaturated Aldehydes (133)

Substituent	Most probable wavelength in ethanol (mμ)
Parent	208
α or β	220
α,β or β,β	230
α,β,β	242

The spectra of unsaturated carbonyl compounds are much more influenced by the nature of the solvent than those of the dienes, and in the tables, the solvent is assumed to be ethanol. If the spectrum is measured in another solvent, the solvent correction in Table XII should be made in applying the rules.

As an example of the application of Woodward's rules, the spectrum of mesityl oxide may be computed (Table X). The substituents are β,β, hence the expected wavelength is 235 mμ, in agreement with the observed value. For 2-cyclohexylidene-cyclohexane-1-one (Table X) the substituents are α (the cyclohexane residue), β,β (the residues of the second ring), and the C=C double bond is exocyclic to two rings. The expected wavelength is 257 mμ and the observed is 258 mμ (133).

Table X shows the positions of the $\pi^* \leftarrow \pi$ and of the $\pi^* \leftarrow n$ bands of the series of polyene aldehydes. As the length of the conjugated chain increases, the wavelength and intensity of the $\pi^* \leftarrow \pi$ band steadily increase, until, in the compound with five olefinic bonds, the tail of the absorption enters the visible spectral region. The relatively feeble $\pi^* \leftarrow n$ band appears only as a shoulder on the overlapping tail of the stronger band and becomes difficult to identify when the chain length becomes long.

Cyclohexane derivatives containing 1,4-olefinic and carbonyl bonds across from each other in the boat form of the ring

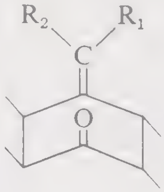

although not conjugated in the usual sense, show spectra with some of the characteristics of those of α,β-unsaturated ketones. In addition to a strong band ($\epsilon \sim 10{,}000$) at about 190 mμ, these compounds show a moderately intense band in the region 210–240 mμ, the region of the characteristic $\pi^* \leftarrow \pi$ absorption of the conjugated unsaturated ketones. The $\pi^* \leftarrow n$ band, however, of these 1,4-compounds is not very different in wavelength and intensity from the band in nonconjugated compounds (140). A theoretical discussion of the coupling between olefinic and carbonyl groups is given in ref. 141.

The α,β-unsaturated acids and acrylic and crotonic acids show intense absorption about 210 mμ and at shorter wavelengths, without a well-defined maximum, which is probably a portion of the $\pi^* \leftarrow \pi$ band, and, at 250-260 mμ, a shoulder, $\epsilon \sim 100$, which is probably the $\pi^* \leftarrow n$ band of the carbonyl group as modified by the adjacent OH group and the conjugated olefinic bond (142). Rules for the effect of alkylation on the band of short wavelength of α,β-unsaturated acids, analogous to those for the corresponding aldehydes and ketones, have been given by Nielsen (143). Substitution of the α-carbon atom gives a maximum about 208 mμ; the maximum for disubstitution in the α,β or β,β positions is about 217 mμ, and at 225 mμ for α,β,β trisubstituted compounds. In the two latter cases, 5 mμ are to be added for an exocyclic double bond or for an endocyclic double bond in cyclic compounds containing five or seven members.

9. CHARACTERIZING DERIVATIVES OF CARBONYL COMPOUNDS

Some of the condensation products of aldehydes and ketones useful in the identification of these compounds show much more intense absorption spectra in the middle ultraviolet region than the parent carbonyl compounds. These spectra therefore afford a more sensitive test for small amounts than do those of the parents and in any case constitute useful confirmatory tests. The semicarbazones, thiosemicarbazones, and phenyl hydrazones show high absorption. The oximes of unconjugated aldehydes and ketones show only end absorption at wavelengths above 200 mμ, while the absorption of the oximes of α,β-unsaturated carbonyl compounds is near the $\pi^* \leftarrow \pi$ band of the parents and is of similar intensity. Data are collected in Table XV, derived from extensive tables in ref. 144.

TABLE XV

Absorption of Characterizing Derivatives of Aldehydes and Ketones (144)

	In unconjugated C=O compound		In α,β-unsaturated compound	
Derivative	$\lambda_{\max}$ (mμ)	$\epsilon_{\max}$	$\lambda_{\max}$ (mμ)	$\epsilon_{\max}$
Oxime,				
$>C{=}NOH$	<200		230–240	13,000–23,000
Semicarbazone,				
$>C{=}N{-}NH\cdot CO\cdot NH_2$	225–230	11,000–13,000	264–274	20,000–33,000
Thiosemicarbazones,				
$>C{=}N{-}NH\cdot CS{-}NH_2$	271–272	20,400–24,400	300–302	25,000–37,000
2,4-Dinitrophenylhydrazones,				
$>C{=}N{-}NH\cdot C_6H_3(NO_2)_2$	362–367[a]	17,500–25,000	366–395	25,000–31,500

[a] The phenylhydrazones of aldehydes absorb about 5 mμ to shorter wavelengths.

10. MULTIPLE-BOND NITROGEN GROUPS

The nitro, nitroso, azo, and diazo groups contain multiple-bonded N and O atoms, each of which may carry nonbonding electrons. π orbitals will therefore participate in the bond, and one or more $\pi^* \leftarrow n$ transitions are to be expected besides $\pi^* \leftarrow \pi$ transitions. Absorption data in the spectral region longer than 200 mμ are summarized in Table XVI.

In the unconjugated *nitro group*, 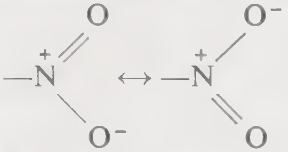 , each O atom has a nonbonding orbital in the plane of the group; by interaction, they give rise to two nonbonding orbitals for the group, of different energy. The absorption band of the nitro group of longest wavelength represents an $\pi^* \leftarrow n$ transition of a lone pair oxygen electron to the antibonding π^* orbital about one of the N—O linkages, and is therefore analogous to the carbonyl absorption near 280 mμ, which it resembles in position and intensity. Near 200 mμ is a stronger band, attributable to a $\pi^* \leftarrow \pi$ transition.

If the NO_2 group is conjugated with an olefinic bond, as in α,β-nitro-olefins, the $\pi^* \leftarrow \pi$ absorption is displaced to 230–240 mμ ($\epsilon \sim$ 3,000–10,000), by an effect similar to the conjugative effect in the corresponding carbonyl compounds, but apparently the displaced $\pi^* \leftarrow n$ band to be expected is hidden in the long wavelength tail of the stronger band.

The *alkyl nitrates*, RO—NO_2, which may be regarded as alkoxy-nitro compounds, absorb somewhat similarly to the nitroparaffins; a weak band at about 260 mμ appears as a shoulder on the long wavelength edge of a stronger band rising steadily in intensity towards 200 mμ.

The blue color of the alkyl nitroso compounds, R—N=O, originates in a weak band, probably representing an $\pi^* \leftarrow n$ excitation of a nonbonding electron on the nitrogen atom, at about 670 mμ. A second relatively weak band at about 260–300 mμ may represent a similar transition of a nonbonding electron more tightly held by the oxygen atom into the π orbital system.

The *alkyl nitrites*, RO—N=O, show a band with well-marked vibrational structure about 340–380 mμ ($\epsilon \sim$ 80), and a stronger maximum about 220 mμ ($\epsilon \sim$ 1000).

The *alkyl azo compounds*, R—N=N—R, show a well-marked maximum of low intensity about 340 mμ, probably an $\pi^* \leftarrow n$ band, and a region of stronger absorption at shorter wavelengths rising steadily in intensity toward 200 mμ. A feeble shoulder at about 240 mμ may represent a second $\pi^* \leftarrow n$ transition.

The *alkyl diazo compounds*, $R{=}\overset{+}{N}{=}\overset{-}{N}$, owe their yellow color to a weak absorption band about 410 mμ, displaced to about 378 mμ in diazoacetic

TABLE XVI

Absorption of Multiple Bonded N—O and N—N Groups

Compound	Solvent	λ_{max} (mμ)	ϵ_{max}	λ_{max} (mμ)	ϵ_{max}	Ref.
—NO_2 in nitromethane	Gas	270	9, 20	198	ca. 3500	145,146
	Ethanol	260	39.1	201		147
—O—NO_2 in methyl nitrate	Gas	260 (sh)	ca. 9	End Absorption	ca. 2500 at 200 mμ	145
—NO in nitroso-2-methyl propane	Gas	670[a]	14	260	6	145
O—NO in *tert*-butyl nitrite	Gas	380[a]	75	220	1800	148
—N=N— in azoethane	Gas	355	10	End Absorption	ca. 700 at 200 mμ	149
Azomethane	Water	342	15.8			150
=N=N in diazomethane	Gas	410	ca. 3			150,151
	Diethyl ether	417	6.9			150
Ethyl diazoacetate	Ethanol	378	16	149	10,000	152,153
—N=N=N in ethylazide	Ethanol	287	20	222	150	152,153

[a] Vibrational structure.

ester: a much stronger band appears at shorter wavelengths. The *alkyl azides*, $R{-}N{=}\overset{+}{N}{=}\overset{-}{N}$, show a weak band about 290 mμ and a somewhat stronger one about 220 mμ.

11. AROMATIC COMPOUNDS

The absorption spectra of aromatic compounds and the effect of substituents are discussed in detail in Chapter III, and here only a qualitative survey will be made of the spectra of some important compounds. The spectrum of benzene shows three well-defined electronic systems at wavelengths above 180 mμ, all representing $\pi^* \leftarrow \pi$ transitions (Chapter III, Fig. 26). A strong band appears with a maximum about 184 mμ, $\epsilon \sim 60{,}000$, without vibrational structure in solution. A system of moderate intensity, $\epsilon \sim 10{,}000$, showing poorly resolved vibrational structure, appears at about 204 mμ, and a system of low intensity, $\epsilon \sim 250$, with well-marked vibrational structure, has a maximum at about 254 mμ. The two latter systems are symmetry-forbidden with respect to the electronic configurations of the ground and excited states, but, as is discussed in Chapter III, the symmetry conditions necessarily for a radiational transition are induced if the electronic excitation is accompanied by simultaneous excitation of a vibration of appropriate symmetry.

In Table XVII the spectra of a number of benzene derivatives are summarized. The data have been compiled from standard collections, including *International Critical Tables*, Vol. 5, *Landolt-Börnstein Zahlenwerte und Funktionen*, 6th ed., Vol. 1, Part 3, *DMS UV Atlas of Organic Compounds*, Gillam and Stern, *Electronic Absorption Spectroscopy* (144), and Friedel and Orchin, *Ultraviolet Spectra of Aromatic Compounds* (154).

Alkylation causes only minor changes in position and intensity of the various benzene spectral systems, and except when the number of substituents is large, vibrational structure is retained. In the table, $\lambda_{\max}$ refers to the vibrational subband of highest intensity if structure is present, otherwise, to the maximum of the unresolved envelope. Halogen, cyano, hydroxyl, carboxyl, and sulfonic groups likewise do not markedly change the position of the benzene bands although they cause some increase in intensity of the characteristic long wavelength system.

Marked spectral changes are caused by amino, aldehydic, and ketonic groups and nitro and nitroso groups. The nonbonding electrons of these groups can conjugate with the π system of the ring, causing the appearance of a $\pi^* \leftarrow n$ band on the long wavelength side of the characteristic benzenoid absorption. Since the excited electron in the n,π^* state (i.e., the state in which one of the original lone pair electrons remains in its n orbital and the other is excited into the π system of the molecule) is nonlocalized, the wavelength of the $\pi^* \leftarrow n$ band is longer than that of the corresponding band of the

TABLE XVII
Absorption of Some Benzene Derivatives

Compound	Solvent	$\lambda_{\max}$ (mμ)	$\epsilon_{\max}$	$\lambda_{\max}$ (mμ)	$\epsilon_{\max}$	$\lambda_{\max}$ (mμ)	$\epsilon_{\max}$	$\lambda_{\max}$ (mμ)	$\epsilon_{\max}$
Benzene	Hydrocarbon			254	250	204	8,800	184	68,000
Toluene	Hydrocarbon			262	260	208	7,900	189	55,000
Hexamethylbenzene	Hydrocarbon			271	230	221 (sh)	10,000	202	51,000
Chlorobenzene	Hydrocarbon			267	200	210	7,400		
Iodobenzene	Hydrocarbon	285 (sh)	180	258	660	207	7,000		
Benzonitrile	Methanol			267	830				
Phenol	Hydrocarbon			271	1260	213			
Phenolate ion	Dil. NaOH			286	2400	235	9,400		
Benzoic acid	Ethanol			272	855	226	9,800		
Aniline	Methanol			280	1320	230	7,000		
Anilinium ion	Dil. acid			254	160	203	7,500		
Benzylamine	Hydrocarbon			260	100				
Benzaldehyde	Ethanol	328	20	280	1660	240	16,000		
Acetophenone	Hexane	320	40	276	800	238	13,000		
Phenylacetone	Ethanol	280	180	250	400	210	12,000		
Benzophenone	Ethanol	330	160	252	20,000				
p-Benzoquinone	Hexane	435	10	285	500	245	20,000		
Nitrobenzene	Hexane	330 (sh)	140	280 (sh)	1000	252	10,000		

o-Nitrobenzaldehyde	Hexane	330	300	290	1300	248	5,300	221	45,200
m-Nitrobenzaldehyde	Hexane	360	86	289	1000	260 (sh)	5,000	226	26,000
		330	140						
p-Nitrobenzaldehyde	Hexane	340	230	296	1950	258	16,000		
o-Nitrodimethylaniline	Ethanol	430	2200	295 (sh)	1500	247	10,000		
m-Nitrodimethylaniline	Ethanol	405	1070	Concealed		250	30,000		
p-Nitrodimethylaniline	Ethanol	389	30,000	310 (sh)	1000	Increasing to shorter wavelengths			
Nitrosobenzene	Vapor	755	53	280	9000				
Styrene	Hexane			282	740	248	15,000		
trans-Cinnamic acid	Hexane			283	56,000	215	35,000	204	36,000
cis-Cinnamic acid	Hexane			280	25,000	215	17,000	200	31,000
trans-Stilbene	Heptane			294	28,000	228	16,000	202	24,000
cis-Stilbene	Ethanol			274	10,000	225	24,000		
trans-Azobenzene	Ethanol	442	500	314	22,700	228	14,400		
cis-Azobenzene	Ethanol	438	1500	283	5000	245	11,000		
Biphenyl	Hydrocarbon			Concealed		248	17,000	202	44,000
2-Methylbiphenyl	Hydrocarbon			270 (sh)	900	236	10,250	200	43,000
2,2′-Dimethylbiphenyl	Hydrocarbon			264	800	228 (sh)	6,000	198	43,000
2,6,2′,6′-Tetramethylbiphenyl	Hydrocarbon			263	490	218 (sh)	23,000	< 200	> 63,000
Fluorene	Ethanol			301	10,000	261	17,000	208	36,000

unconjugated $C{=}O$, NO_2, etc., chromophore. For example, phenylacetone, $C_6H_5CH_2\cdot CO\cdot CH_3$, shows a band at 280 mμ, near the position of the unconjugated ketonic carbonyl $\pi^* \leftarrow n$ band, the characteristic benzenoid absorption at about 250 mμ, and strong absorption near the benzenoid band about 200 mμ. The intensities of the carbonyl and long wavelength benzenoid band are somewhat exalted over their normal values in this ketone, possibly because a single separating CH_2 group in general does not completely prevent interaction between two chromophores; but the spectrum of phenylacetone to a first approximation is essentially the sum of the spectra of the partial chromophores present in the molecule. In acetophenone, in which the carbonyl group is directly attached to the ring, a relatively weak band appears at 319 mμ, probably the $\pi^* \leftarrow n$ band of the carbonyl displaced by conjugation with the π electrons of the ring, and correspondingly, a band at about 280 mμ, $\epsilon \sim 1100$, probably represents the benzenoid band, shifted and considerably increased in intensity as a result of conjugation of the ring π electrons with the π electrons of the carbonyl group. In the spectra of aromatic compounds containing nonbonding electron pairs, such as amino, nitro, and carbonyl groups, an intense band appears in the region 230–250 mμ which has been attributed by some authors to a charge transfer transition involving the flow of electrons from donor substituents to the ring, e.g., from the amino group to the ring, or from the ring to acceptor substituents like the nitro group (155–157).

In the spectrum of *aniline*, the band at 280 mμ is probably the benzenoid band, shifted and intensified as the result of charge flow from the amino group to the ring. In the language of the resonance theory, structures such as 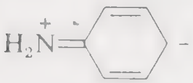 contribute to the molecular state, to a greater extent in the excited state. Similarly, in the phenolate ion, resonance structures participate,

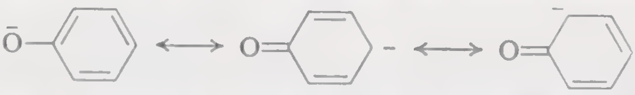

and the spectrum of this ion is similar to that of aniline. In the anilinium ion, 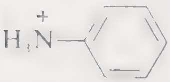, the nonbonding electron pair that in aniline can conjugate with the π electrons of the ring is absent, and the spectrum of this ion is similar to that of benzene (Table XVII).

When both electron-donating and electron-accepting substituents are present and well conjugated with the benzene ring, the dominant feature in the spectrum is an intense band at relatively long wavelengths that can be associated with a $\pi^* \leftarrow \pi$ transition in a chromophore extending through the benzene ring from the donor to the acceptor atom. For example, the strongest band in the spectrum of *p-nitrodimethylaniline* has a maximum at about 390 mμ, $\epsilon = 30{,}000$, connected with a transition involving the passage of an electron from the amino to the nitro group. The conjugation can be represented by the structure

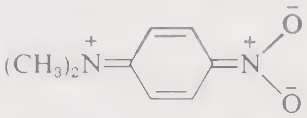

In the spectrum of the *meta* compound, the strongest band is at about 247 mμ, $\epsilon \sim 30{,}000$, in the region corresponding to the passage of charge between substituents and the ring. At 430 mμ, somewhat longer than for the strong band of the *para* compound, a relatively feeble band appears, $\epsilon \sim 2200$, suggesting a weak transition involving transfer of an electron between the amino and nitro groups. Since, apart from steric interference, the electronic behavior of the ortho compound is expected to resemble that of the para, similar spectra might be expected for these isomers; in fact, the spectrum of the *ortho* compound resembles that of the *meta*. For both, the strongest band is about 250 mμ, and the band of the *ortho* compound of longest wavelength, at 430 mμ, is less than one-tenth as intense as that of the *para* compound. The steric relations between the dimethylamino group and the *o*-nitro group are apparently not favorable for conjugation between the π electrons of these two groups through the benzene nucleus. Even when the amino and nitro groups are in the 1,4 positions, their conjugation can be disturbed by the presence of bulky substituents *ortho* to the nitro group. For example, in the spectrum of 3,5-di-*tert*-butyl-4-nitroaniline, only a feeble band appears about 380 mμ, $\epsilon = 540$, and the spectrum is similar to that of the corresponding un-nitrated di-*tert*-butylaniline. The bulky substituents on the carbon atom adjacent to that bearing the nitro group force the plane of the latter group at right angles to the plane of the ring, causing minimum overlap of the π orbitals of this group with those of the ring, hence minimum conjugation between the nitro group and the ring and, through the ring, with the amino group (158).

Spectral relations similar to those observed for the *o*-, *m*-, and *p*-nitrodimethylanilines are found among *o*-, *m*-, and *p*-nitro derivatives of phenols, carboxylic acids, and other compounds (159,160).

In the spectrum of *styrene*, the band at about 280 mμ, $\epsilon = 740$, represents the benzenoid absorption as displaced to longer wavelength and intensified by conjugation with the ethylenic double bond. In the *cinnamic acids* a very intense band about 280 mμ is presumably the effect of further conjugation of the carboxylic acid carbonyl group within the chromophore. The intensity of this band for the *cis* compound is only about half of that for the *trans*, indicating the effect of the shorter chromophoric length imposed by the *cis*, as compared with the *trans* configuration. In *stilbene*, delocalized π orbitals comprehend all of the carbon atoms in the two benzene rings and the interconnecting ethylenic double bond. For the trans compound, the most intense band is that at longest wavelength, which can be associated with a transition in which the main component of the transition dipole moment is along the long axis of the molecule. In the spectrum of *cis*-stilbene, the corresponding band is at somewhat shorter wavelengths and shows less than half the intensity of the band for the *trans* compound, and the most intense band is at 225 mμ, which may correspond to a transition polarized perpendicularly to the long molecular axis. This kind of spectral relation between *cis* and *trans* compounds is of frequent occurrence.

The spectrum of *azobenzene* is similar to that of stilbene, with, in addition to the strong $\pi^* \leftarrow \pi$ bands in the ultraviolet, a relatively weak $\pi^* \leftarrow n$ band in the visible. ϵ equals several hundreds. The effect of the conjugation on the $\pi^* \leftarrow n$ band in azobenzene can be seen by comparing its position and intensity with that of azomethane, $\lambda \sim 350$ mμ, $\epsilon \sim 10$. As for stilbene, the $\pi^* \leftarrow \pi$ band of longest wavelength of the *trans* configuration of azobenzene is at longer wavelength and more intense than for the *cis* compound. The $\pi^* \leftarrow n$ band of *cis*-azobenzene is, however, more intense than the corresponding band of the *trans* compound, consistent with the greater overlap of the nonbonding electrons on the nitrogen atoms in the *cis* configuration.

Biphenyl and its *ortho*-substituted derivatives show spectrally interesting effects of interaction between adjacent benzene chromophores (161–163). The spectrum of biphenyl consists of a broad band with a maximum about 250 mμ, $\epsilon = 17{,}000$, with, in 4,4′-dimethyl- and in 4,4′-dichlorobiphenyl, a feeble shoulder at about 295 mμ, $\epsilon \sim 500$. Although the strong band is at about the position of the longest wavelength benzenoid band, its great intensity suggests that it may represent the benzene band at 204 mμ, as shifted by conjugation of the two rings. The rings in biphenyl are about 23° out of coplanarity, but there is sufficient overlap of the π orbitals to allow some conjugation. The shoulder at about 295 mμ may similarly represent the effect of conjugation on the feeble benzene band at 254 mμ. In the spectrum of 2-methylbiphenyl, the benzenoid shoulder at 270 mμ is more prominent, and the strong band of the conjugated chromophore is reduced in intensity and shifted hypsochromically to 236 mμ. The *ortho* substituent causes the angle between the planes of the benzene rings to be increased, with consequent decreases in the overlap of the π electrons and of the conjugation. As additional *ortho* substituents are added, these effects are increased, until the spectrum of 2,2′,6,6′-tetramethylbiphenyl resembles that of two independent alkylated benzene molecules, with the characteristic structured benzenoid band at about 264 mμ, an intense shoulder at about 210 mμ equivalent to the benzene band at 204 mμ and indications of a stronger band below 200 mμ, all at an intensity roughly twice that of the benzene spectrum. On the other hand, biphenyls alkylated in the 3,3′,4, and 4′-positions show spectra resembling that of unsubstituted biphenyl. In fluorene

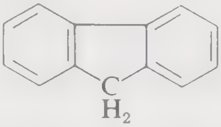

the single methylene group acting as an *ortho,ortho′*-alkyl substituent keeps the two rings more nearly coplanar, and the conjugation is enhanced over that in biphenyl. The strong structured band in the spectrum of fluorene at 301 mμ, $\epsilon = 10{,}000$, probably represents the benzenoid absorption at 254 mμ, shifted and greatly intensified by the conjugation, the band at 261 mμ corresponds to the biphenyl band at 248 mμ, itself corresponding to the benzene band at 204 mμ, and the fluorene band at 208 mμ and the biphenyl band about 202 mμ correspond to the benzene band near 180 mμ.

12. CONDENSED-RING HYDROCARBONS

The theory and nomenclature applicable to $\pi^* \leftarrow \pi$ transitions in aromatic hydrocarbons are discussed in later chapters. Here, an outline of the spectral relations in these compounds is given in terms, for descriptive purposes, of the systematics introduced by Clar (164). The condensed ring hydrocarbons are first classified into *cata*-condensed and *peri*-condensed compounds. In the *cata*-condensed group, no carbon atom belongs to more than two rings, while *peri*-condensed compounds contain carbon atoms common to more than two rings. The *cata*-condensed aromatic hydrocarbons are further divided into the linear series benzene, naphthalene, anthracene, naphthacene, etc., and into bent or angular ring systems, such as those in phenanthrene, **1**, triphenylene, **2**, 1,2-benzanthracene, **3**, or 1,2,3,4-benzanthracene, **4**. Pyrene, **5**, and coronene, **6**, are examples of *peri*-condensed compounds.

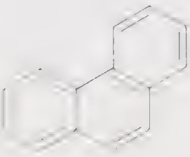
1

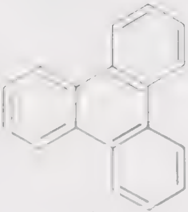
2

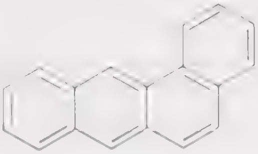
3

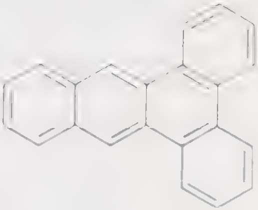
4

The ultraviolet absorption spectra of the *cata*-condensed hydrocarbons resemble that of benzene, with a steady displacement of the band systems to longer wavelengths with increasing number of rings in the structure. Three readily recognized band systems appear in the spectra of a number of these compounds and probably are always present, although one of the systems may be concealed (Table XVIII). The spectrum of naphthalene is essentially a displaced benzene spectrum. A strong structureless band appears with a maximum about 220 mμ, ϵ = 100,000 and then a band of intermediate intensity with poorly resolved vibrational structure with a maximum at 275 mμ, ϵ = 5200, analogous to the benzene system about 204 mμ, and a

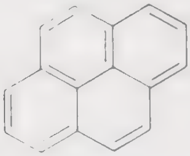
5

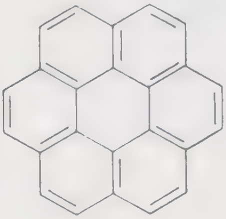
6

TABLE XVIII

Condensed-Ring Aromatic Hydrocarbons

Linear *cata*-condensed compounds

	α		p		β	
	Onset (mμ)	ϵ_{max}	Onset (mμ)	ϵ_{max}	λ_{max} (mμ)	ϵ_{max}
Benzene	263	250	208	8800	184	68,000
Naphthalene	312	280	289	9300	220	100,000
Anthracene	—	—	379	9000	256	180,000
Naphthacene	—	—	476	9600	272	180,000
Pentacene	428	690	582	5800	303	160,000
Hexacene (unstable)	—	—	693	—	—	—
Angular *cata*-condensed compounds						
Phenanthrene	345	330	293	20,000	251	60,000
Triphenylene	340	290	284	18,200	257	150,000
1,2-Benzanthracene	385	1100	359	7900	290	126,000
1,2,3,4-Benzanthracene	374	430	349	7800	286	135,000

Peri-condensed compounds

	α		p		β_1		β_2	
	Onset (mμ)	ϵ_{max}	Onset (mμ)	ϵ_{max}	Onset (mμ)	ϵ_{max}	Onset (mμ)	ϵ_{max}
Pyrene	372	660	335	51,000	272	47,000	241	80,000
Coronene	428	560	342	71,000	305	316,000	—	—

weak system showing fairly well-resolved vibrational structure at 318 mμ, $\epsilon = 280$, the analog of the benzene system at 254 mμ (Chapter III, Fig. 35). In Clar's nomenclature the intense band at short wavelength is designated β, that at intermediate wavelength the intensity is *p* (*para*), and the weak band system is α. In the linear series, all these systems move to longer wavelengths with increasing number of rings, but the *p* band moves more rapidly than the α-band, with the result that in the spectrum of anthracene and naphthacene the α band is concealed in the more intense *p* band and in that of pentacene, the α band appears between the *p* and the β bands (Table XVIII).

The various bands of the angular *cata*-condensed aromatic compounds are at shorter wavelengths than those in the linear compounds containing the same number of rings, and the α band is usually recognizable as the system of lowest intensity and longest wavelength.

In the spectrum of the *peri*-condensed compound pyrene, four structured spectral systems appear at wavelengths greater than 200 mμ, of which that of longest wavelength is of lowest intensity and appears analogous to the α band of the *cata* condensed compounds.

To illustrate the use of the ultraviolet spectra of condensed ring hydrocarbons in structural identification, the recognition of a dihydromethylcholanthrene as the 6,7-dihydro derivative **7** may be cited because of the resemblance of its spectrum to that of 2-phenylnaphthalene, **8** (165). The isomer of **7**, reduced at the *a* and *b* positions, would have given a spectrum resembling that of phenanthrene.

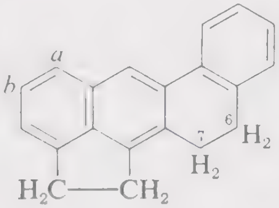

7

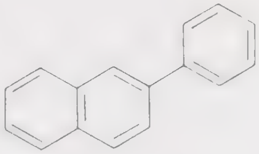

8

Further examples of the very considerable detail that can be achieved in the spectroscopic differentiation of quite similar polynuclear hydrocarbons can be found in the work of Jones (166).

13. SPATIAL ORIENTATION OF ELECTRONIC TRANSITIONS IN ORGANIC MOLECULES

The vibrating electronic moment associated with an optical transition is a vector and is oriented in a definite direction within the molecule. If the transition associated with a well-conjugated bond system is of the $\pi^* \leftarrow \pi$ type it must lie in the molecular plane, but, for example, in naphthalene, transition moments are to be expected parallel to the long axis and to the short axis of the molecule, respectively. Lewis and Calvin (167) introduced the terms x and y bands for absorption bands associated with transition moments vibrating parallel to the short and long molecular axes, respectively. To determine these directions, measurements may be carried out with polarized light under conditions in which the molecule is forced to assume a known orientation. The absorption is most intense when the electric vector of the light vibrates parallel to the direction of the transition moment. Such experiments have been carried out on crystals of organic compounds (168), but complications may then arise from the effect of the crystalline field on the electronic levels and from interactions between cooperative electronic states in the crystal and vibrational states (169). McClure has tried to avoid these difficulties by examining the polarization relations of the molecule in dilute solution in another crystalline compound into whose lattice the molecule under study can enter substitutionally. The host is chosen so that it is not likely to alter the electronic levels of the guest molecule very much; for example durene (1,2,4,5-tetramethylbenzene) proved to be a satisfactory matrix for naphthalene (170). The polarized absorption spectra of naphthalene in the matrix indicate that the electronic transition corresponding to the long wavelength α absorption band of naphthalene is polarized parallel to the long axis of the molecule, and that the adjacent more intense transition corresponding to the p system is parallel to the short axis. Similar observations on anthracene and naphthacene in solid solution in single crystals of naphthalene and phenanthrene indicate that the transition of longest wavelength in these molecules is polarized parallel to the short axis (171).

The direction of polarization of the electronic transitions of condensed ring hydrocarbons has been determined by Jones from observations on the effects of substituents that can conjugate with the rings (172). For example, in 1-naphthylamine, the conjugation of the amino group with the ring might be expected to lengthen the chromophore associated with the transition polarized parallel to the short axis of the naphthalene residue, while in 2-naphthylamine the lengthened chromophore will be associated with a moment polarized with a large component parallel to the long axis. It is found that the introduction of the amino group in the 2-position causes a strong bathochromic effect on the α system and greatly increases the intensity, but has little effect on the adjacent p system at shorter wavelengths, while the 1-amino group shifts the p system to longer wavelengths. The inference from these observations is that the long wavelength α system of naphthalene is polarized parallel to the long molecular axis, that is, is a y band in Lewis and Calvin's nomenclature, while the p system is polarized parallel to the short axis, in agreement with McClure's conclusions from polarization observations on naphthalene in solid solution. The effect of amino substitution in various positions in anthracene is consistent with the band system of longest wavelength being polarized parallel to the short molecular axis, again in agreement with direct observations of polarization on solid solutions.

14. *N*-HETEROCYCLIC COMPOUNDS

Azaaromatic compounds, in which $\diagdown\underset{\cdot\cdot}{\mathrm{N}}{/\!\!/}$ is substituted for $\diagdown\mathrm{CH}{/\!\!/}$ in the aromatic ring, are isoelectronic with respect to the π system to the corresponding homocyclic compounds and their absorption bands are similar. Quinoline, for example, shows three well-defined absorption bands at wavelengths greater than 200 $\mathrm{m}\mu$ that may be the analogs of the β, p, and α bands of naphthalene. In the quinoline spectrum a strong system about 230 $\mathrm{m}\mu$, $\epsilon \sim 34{,}000$ seems analogous to the β band of naphthalene at 220 $\mathrm{m}\mu$, $\epsilon \sim 100{,}000$, a system of moderate intensity at about 270 $\mathrm{m}\mu$, $\epsilon \sim 3400$ may correspond to the p band of naphthalene at 275 $\mathrm{m}\mu$, $\epsilon \sim 9{,}300$, and a structured system at 314 $\mathrm{m}\mu$, $\epsilon \sim 2{,}800$ resembles the structured system of naphthalene at 312 $\mathrm{m}\mu$, $\epsilon \sim 280$. Similarly the spectra of acridine (10-azaanthracene) and phenazine (9,10-diazaanthracene) are quite similar to that of anthracene. The $\pi^* \leftarrow \pi$ band of longest wavelength in the spectrum of pyridine shows a maximum about 251 $\mathrm{m}\mu$ ($\epsilon \sim 2000$), analogous to the α band of benzene at 254 $\mathrm{m}\mu$ ($\epsilon = 250$). The deviation from hexagonal symmetry in the pyridine molecule intensifies the transition of longest wavelength over that of benzene, and, for the same reason, the vibrational structure in the pyridine spectrum is less well resolved than that of benzene.

In addition to the $\pi^* \leftarrow \pi$ absorption systems, the spectra of azaaromatic compounds contain $\pi^* \leftarrow n$ bands on the long wavelength side of the $\pi^* \leftarrow \pi$ systems, associated with the transition of one of the lone pair electrons on the nitrogen atom to an antibonding orbital of the π system (173). In the case of pyridine the $\pi^* \leftarrow n$ band is observed only as a feeble shoulder in the long wavelength tail of the α band in nonpolar solvents. In hydroxylated solvents the shoulder disappears; the band becomes submerged in the adjacent $\pi^* \leftarrow \pi$ band, consistent with the general rule of hypsochromic displacement of $\pi^* \leftarrow n$ bands in hydroxylated solvents. In the pyridium salts the nonbonding electrons of the nitrogen atom in the base now participate in a valence bond, and it is consistent with the interpretation of the shoulder in the spectrum of the base as a $\pi^* \leftarrow n$ band that it disappears in the spectrum of the salts.

With increasing number of aza substituents, the $\pi^* \leftarrow n$ band becomes further removed from the long wavelength $\pi^* \leftarrow \pi$ band and often shows well-marked vibrational structure (174–176). In the spectrum of 1,2,4,5-tetrazine the $\pi^* \leftarrow n$ absorption band enters the visible spectral region. The relations between the $\pi^* \leftarrow n$ band and the $\pi^* \leftarrow \pi$ band of longest wavelength are shown in Table XIX (177) for azabenzenes.

TABLE XIX
Spectra of Azabenzenes in Cyclohexane Solution (177)

Compound	$\pi^* \leftarrow n$ band		$\pi^* \leftarrow \pi$ band	
	λ_{max} (mμ)	ϵ_{max}	λ_{max} (mμ)	ϵ_{max}
Pyridine	270		251	2000
Pyridazine, 1,2-diazabenzene	340	315	246	1300
Pyrimidine, 1,3-diazabenzene	298	326	243	2030
Pyrazine, 1,4-diazabenzene	328	1040	260	5600
3,5,6-Trimethyl-1,2,4-triazine	384	520	264	5100
sym-Tetrazine, 1,2,4,5-tetrazine	542	829	252	2150

N-alkylpyridinium salts, such as the perchlorate, absorb similarly to pyridine in acid solution, with some displacement of the maximum to longer wavelengths. The iodide, however, shows in addition, two bands at longer wavelength, at 295 and 380 mμ, respectively, in chloroform solution (178,179). These bands are attributed to a charge-transfer transition in a complex between the pyridinium cation and the iodide ion in which an electron passes from the anion to the cation (Chapter III, Section IV-A-1). Substituents affect the long wavelength absorption of pyridine much as they affect the α band of benzene, with the complication that three nonequivalent positions are available for monosubstituents. Usually a 4-substituent causes the smallest bathochromic shift, a 3- the greatest, and a 2-substituent has an intermediate effect. If the substituent is of acidic nature, like OH or COOH, the molecule may exist in a neutral, cationic, anionic, or zwitterionic form, depending on the acidity of the solution; the wavelength of the α band increases in the sequence neutral molecule, cation, anion, zwitterion (180).

Five-member rings containing two double bonds and a heteroatom such as nitrogen or oxygen absorb at short wavelengths in the general region of the corresponding cyclopentadiene. Pyrrole, for example, shows a band at about 211 mμ and furane absorbs at still shorter wavelengths. Compounds containing sulfur as the hetero atom absorb at longer wavelengths, thiophene, for example at about 231 mμ, $\epsilon = 4500$ in hexane.

15. STERIC EFFECTS ON SPECTRA

In many organic molecules, a π chromophore is conjugated with another to form a resultant chromophore of greater effective length, absorbing at longer wavelengths than either partial chromophore and with greater intensity. The conjugative interaction will be greatest when the $p\pi$ orbitals of the individual atoms are directed parallel to one another and when lone pair orbitals that are involved in the conjugation are parallel to the atomic p-

orbitals. This will often involve coplanarity of all of the atoms of the conjugated chain. Deviation from coplanarity of these atoms will decrease the interaction, with a consequent displacement of the absorption to shorter wavelengths and decrease in intensity. The spectra of the biphenyls have been discussed earlier in this chapter, and it will suffice to mention that, although in unsubstituted biphenyl the two rings are not coplanar, the overlap of the atomic $p\pi$ orbitals is sufficient to cause appreciable conjugation of the two rings. An intense absorption band which includes a long wavelength component derived from the α band of benzene and a shorter wavelength component possibly derived from the benzene p band is observed in the spectrum of biphenyl. Introduction of methyl groups in the ortho positions causes crowding, relieved by further twisting of the rings about the interlinking bond. As the crowding is increased by steady addition of methyl groups in the *ortho* positions, the long wavelength edge of the absorption band steadily retreats to shorter wavelengths, the general intensity of absorption falls, the characteristic vibrational structure of the benzene α band begins to appear near the position of that band in benzene, until finally, when all four ortho positions are occupied by methyl groups, the spectrum of the biphenyl resembles that of two independent alkyl benzene molecules. At wavelength 260 mμ, the molar extinction coefficient of the tetramethylbiphenyl is only about 5% that of the unsubstituted compound.

In the case of the 4-nitroanilines the condition for maximum conjugative interaction is coplanarity of the nitro group with the ring and parallelism of the lone pair orbital on the amino nitrogen atom with the $p\pi$ orbitals of the ring carbon atoms. This conjugation is associated with the appearance of an intense band at about 376 mμ, $\epsilon_{\max} = 15{,}500$; aniline, nitrobenzene, and benzene show no absorption of intensity greater than $\epsilon_{\max} = 100$ in this region. The introduction of bulky alkyl groups in the 3- and 5-positions forces the NO_2 group from coplanarity with the ring. The band at about 376 mμ almost disappears ($\epsilon = 540$) and the spectrum of 3,5-di-*tert*-butyl-4-nitroaniline resembles that of 3,5-di-*tert*-butylaniline. The deviation from coplanarity practically isolates the nitro group from conjugation with the ring and the amino group (158).

Nitrobenzene itself shows a strong band of diagnostic value at about 250–260 mμ, but this band is almost absent from the spectrum of *o*-nitro-*tert*-butylbenzene and *o*-nitrocumene, because of steric hindrance between the *ortho* substituent and the nitro group. The corresponding *para* compounds show the band with characteristic intensity (181).

Crowding effects are well illustrated in the spectra of dyes (182,183). Crowding always lowers the intensity of absorption in comparison with that of an uncrowded related dye. In symmetrical cyanine dyes, deviation from coplanarity of the atoms in the chromophoric chain causes a shift to longer wavelengths, while, if two different heterocyclic nuclei are present, the effect of crowding is to cause a shift of the absorption to shorter wavelengths. The uncrowded cyanine dye **1** shows maximum absorption at 604 mμ with ϵ_{max} 185,000, while the related dye **2**, in which the crowding introduced by the methyl groups in the 3- and 3′-positions forces the quinoline nuclei from coplanarity, absorbs at 640 mμ with about half the intensity.

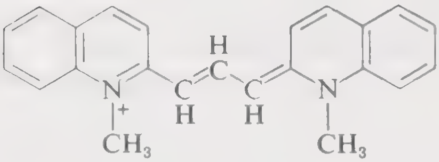

1

λ_{max} 604mμ, ε_{max} 185,000

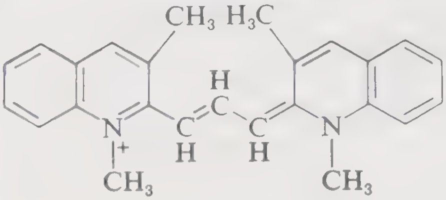

2

λ_{max} 640mμ, ε_{max} 97,000

16. SOLVENTS FOR ULTRAVIOLET ABSORPTION SPECTROSCOPY

Table XX, compiled from spectral curves in ref. 184, gives the approximate transmission limits for the solvents most frequently used in ultraviolet

TABLE XX
Transmission Limits of Some Solvents (184)

Solvent	n_D	DC	Approximate wavelengths at which transmission is 50% (mμ) 0.1 cm	1.0 cm
n-Hexane	1.37486^{20}	1.890^{20}	<200	210
Cyclohexane	$1.4266^{19.5}$	2.023^{20}	<200	220
2,2,4-Trimethylpentane (isooctane)	1.3915^{20}	1.940^{20}	<200	210
n-Heptane	1.38764^{20}	1.9^{25}	<200	210
Methanol	1.3288^{20}	32.63^{25}	199	216
Ethanol	1.3611^{20}	24.30^{25}	199	215
*Iso*propanol	1.3776^{20}	18.3^{25}		215
Diethylether	1.3526^{20}	4.335^{20}	203	245
1,4-Dioxane	1.4224^{20}	2.909^{25}	210	230
Tetrahydrofurane	1.4076^{21}			250
Acetonitrile	1.3441^{20}	37.0^{25}	210	215
Dimethylformamide	1.4269^{25}			270
Dimethylsulfoxide	1.4787^{21}	48.9^{25}		280
Dichloromethane	1.3348^{15}	9.08^{20}		235
Chloroform	1.4433^{25}	4.806^{20}		250
Carbon tetrachloride	1.4464^{20}	2.238^{20}		270
Benzene	1.5011^{20}	2.284^{20}		280
Acetone	1.3588^{20}	20.7^{25}		310

absorption spectroscopy along with their dielectric constants and refractive indices for the sodium *D* lines at room temperature. Purified saturated hydrocarbons are the most transparent solvents, and show any vibrational structure to best advantage. The aliphatic alcohols are highly transparent hydroxylic solvents, which may show special effects on the spectra of solutes because of hydrogen bonding with the solute. Acetonitrile is a transparent aprotic polar solvent. Diethyl ether and the cyclic ethers dioxane and tetrahydrofuran are solvents of relatively low dielectric constant; they cannot be used at 1 cm thickness in the short wavelength ultraviolet. The aprotic solvent dimethylformamide can sometimes be usefully compared in its spectral effect with the hydrogen bonding formamide. Carbon tetrachloride is usually spectroscopically inert, although it can form charge transfer complexes with electron-accepting solutes, for example, benzene. Benzene and acetone can be used only in the long wavelength ultraviolet because of their characteristic absorption bands in the middle ultraviolet. Solvent effects are discussed in detail in Chapter III.

References

1. W. R. Brode, *Chemical Spectroscopy*, 2nd ed., Wiley, New York, 1943; G. R. Harrison, R. C. Lord, and J. L. Loufbourow, *Practical Spectroscopy*, Prentice Hall, New York, 1948; G. E. Lothian, *Absorption Spectrophotometry*, Adam Hilger, London, 1944; M. G. Mellon, *Analytical Absorption Spectroscopy*, Wiley, New York, 1944.
2. H. Kayser, *Tabelle der Schwingungszahlen*, S. Hirzel, Leipzig, 1925; Corrections, *Phys. Rev.*, **48**, 98 (1935).
3. B. Edlén, *J. Opt. Soc. Am.*, **43**, 339 (1953).
4. D. A. Ramsay, *J. Chem. Phys.*, **43**, S18 (1965).
5. G. E. Ewing and S. Trajmar, *J. Chem. Phys.*, **41**, 814 (1964).
6. G. W. Holleman and G. E. Ewing, *J. Chem. Phys.*, **44**, 3121 (1966).
7. M. F. Crawford, H. L. Welsh, and J. L. Locke, *Phys. Rev.*, **75**, 1607 (1949); H. L. Welsh, M. F. Crawford, J. C. F. MacDonald, and D. A. Chisholm, *Phys. Rev.*, **83**, 1264 (1951).
8. J. van Kranendonk and R. B. Bird, *Phys. Rev.*, **82**, 964 (1951).
9. S. H. Bauer and C. F. Aten, *J. Chem. Phys.*, **39**, 1253 (1963).
10. H. Sponer and E. Teller, *Rev. Modern Phys.*, **13**, 76 (1941).
11. H. Sponer, G. Nordheim, A. L. Sklar, and E. Teller, *J. Chem. Phys.*, **7**, 207 (1939).
12. H. Sponer, *J. Chem. Phys.*, **8**, 705 (1940).
13. L. B. Arnold, Jr. and G. B. Kistiakowski, *J. Am. Chem. Soc.*, **54**, 1713 (1932).
14. L. W. Pickett, G. F. Walter, and H. Frame, *J. Am. Chem. Soc.*, **58**, 2296 (1936).
15. G. N. Lewis and M. Calvin, *Chem. Rev.*, **25**, 273 (1939).
16. G. H. Brown, B. Graham, P. W. Vittum, and A. Weissberger, *J. Am. Chem. Soc.*, **73**, 919 (1951).
17. A. G. Gaydon, *The Spectroscopy of Flames*, Wiley, New York, 1957.
18. W. H. McVicker, J. K. Marsh, and A. W. Stewart, *J. Chem. Soc.*, **123**, 642, 817 (1923).
19. H. Schuler, *Spectrochim. Acta*, **4**, 85 (1950); H. Schüler and L. Reinebeck, *ibid.*, **6**, 288 (1954); S. Leach, *J. Chim. Phys.*, **51**, 556 (1954).

19a. F. McCapra, *Quart. Rev.*, **1966**, 485 (a comprehensive review).
20. E. J. Bowen and R. A. Lloyd, *Proc. Chem. Soc.*, **1963**, 305; *Proc. Roy. Soc. (London)*, **A275**, 465 (1963); E. J. Bowen, *Nature*, **201**, 180 (1964).
21. H. H. Seliger, *Anal. Biochem.*, **1**, 60 (1960).
22. A. V. Kahn and M. Kasha, *J. Chem. Phys.*, **39**, 2105 (1963); **40**, 605 (1964); *Nature*, **204**, 241 (1964).
23. J. Franck, *Trans. Faraday Soc.*, **21**, 536 (1925).
24. E. U. Condon, *Phys. Rev.*, **28**, 1182 (1926).
25. L. Pauling and E. B. Wilson, *Introduction to Quantum Mechanics*, McGraw-Hill, New York, 1935, p. 73.
26. G. Herzberg, *Spectra of Diatomic Molecules*, 2nd ed., Van Nostrand, New York, 1950, p. 203.
27. P. M. Morse, *Phys. Rev.*, **34**, 57 (1929).
28. R. T. Birge and H. Sponer, *Phys. Rev.*, **28**, 259 (1926).
29. C. H. D. Clark, *Phys. Rev.*, **47**, 238 (1935).
30. R. S. Mulliken, *J. Chem. Phys.*, **7**, 14 (1939); R. S. Mulliken and C. A. Rieke, *Rept. Progr. Phys.*, **8**, 231 (1941).
31. W. J. Potts, Jr., *J. Chem. Phys.*, **23**, 73 (1955).
32. W. Kauzmann, *Quantum Chemistry*, Academic Press, New York, 1957, Chapters 15 and 16.
33. T. Azumi, C. M. O'Donnell, and S. P. McGlynn, *J. Chem. Phys.*, **45**, 2735 (1966).
34. G. N. Lewis and M. Kasha, *J. Am. Chem. Soc.*, **67**, 994 (1945).
35. S. J. Strickler and R. A. Berg, *J. Chem. Phys.*, **37**, 814 (1962).
36. R. S. Mulliken and W. B. Person, *Ann. Rev. Phys. Chem.*, **13**, 107 (1962).
37. O. N. Witt, *Ber. Deutsch. Chem. Ges.*, **9**, 522 (1876).
38. W. C. Price, *J. Chem. Phys.*, **4**, 539, 547 (1936).
39. M. Kasha, *Discussions Faraday Soc.*, **9**, 14 (1950).
40. H. B. Klevens and J. R. Platt, *J. Am. Chem. Soc.*, **69**, 3055 (1947).
41. W. J. Potts, *J. Chem. Phys.*, **20**, 809 (1952).
42. A. Pullman and B. Pullman, *Discussions Faraday Soc.*, **9**, 46 (1950).
43. A. J. Harrison, B. J. Cederholm, and M. A. Terwilliger, *J. Chem. Phys.*, **30**, 355 (1959).
44. A. J. Harrison and D. R. W. Price, *J. Chem. Phys.*, **30**, 357 (1959).
45. H. Ley and B. Arends, *Z. Physik. Chem.*, **B17**, 177 (1932).
46. E. A. Fehnel and M. Carmack, *J. Am. Chem. Soc.*, **71**, 84 (1949).
47. H. P. Koch, *J. Chem. Soc.*, **1950**, 2892.
48. E. Tannenbaum, E. M. Coffin, A. J. Harrison, *J. Chem. Phys.*, **21**, 311 (1953).
49. L. W. Pickett, M. E. Corning, G. M. Wieder, D. A. Semenow, and S. W. Buckley, *J. Am. Chem. Soc.*, **75**, 1618 (1953).
50. G. Herzberg and G. Scheibe, *Z. Physik. Chem.*, **B7**, 390 (1930).
50a. C. R. Zobel and A. B. F. Duncan, *J. Am. Chem. Soc.*, **77**, 2611 (1955).
51. D. Porret and C. F. Goodeve, *Proc. Royal Soc. (London)*, **165A**, 31 (1938).
52. K. Kimura and S. Nagakura, *Spectrochim. Acta*, **7**, 166 (1961).
53. P. G. Wilkinson and R. S. Mulliken, *J. Chem. Phys.*, **23**, 1895 (1955).
54. R. S. Mulliken, *Rev. Mod. Phys.*, **14**, 265 (1942).
55. E. P. Carr and H. Stücklen, *J. Chem. Phys.*, **4**, 760 (1936); **7**, 631 (1939).
56. J. T. Gary and L. W. Pickett, *J. Chem. Phys.*, **22**, 599, 1266 (1954).
57. D. Semenow, A. J. Harrison and E. P. Carr, *J. Chem. Phys.*, **22**, 638 (1954).
58. W. J. Potts, Jr., *J. Chem. Phys.*, **23**, 65 (1955).
59. L. C. Jones, Jr. and L. W. Taylor, *Anal. Chem.*, **27**, 228 (1955).
60. P. S. Ellington and G. D. Meakins, *J. Chem. Soc.*, **1960**, 697.

61. D. W. Turner, *J. Chem. Soc.*, **1959**, 30.
62. A. Lüthy, *Z. Physik. Chem.*, **107**, 285 (1923).
63. A. D. Walsh, *Trans. Faraday Soc.*, **41**, 35 (1945).
64. W. C. Price and A. D. Walsh, *Proc. Roy. Soc.* (*London*), **174A**, 220 (1940).
64a. A. Smakula, *Angew. Chem.*, **47**, 777 (1934).
65. F. Sondheimer, D. A. Ben-Efraim and R. Wolovsky, *J. Am. Chem. Soc.*, **83**, 1675 (1961).
66. L. Zechmeister and A. Polgár, *J. Am. Chem. Soc.*, **65**, 1522 (1943).
67. F. Bohlmann and H. Mannhardt, *Ber. Deutsch. Chem. Ges.*, **89**, 1307 (1956).
68. K. W. Hausser, R. Kuhn, A. Smakula and M. Hoffer, *Z. Physik. Chem.*, **B29**, 371 (1935).
69. E. R. Blout and M. Fields, *J. Am. Chem. Soc.*, **70**, 189 (1948).
70. K. W. Hausser, R. Kuhn, A. Smakula, and A. Deutsch, *Z. Physik. Chem.*, **B29**, 371 (1935).
71. K. W. Hausser, R. Kuhn, and A. Smakula, *Z. Physik. Chem.*, **B29**, 384 (1935).
72. G. N. Lewis and M. Calvin, *Chem. Rev.*, **25**, 273 (1939).
73. K. Hirayama, *J. Am. Chem. Soc.*, **77**, 373 (1955).
74. K. Hirayama, *J. Am. Chem. Soc.*, **77**, 379 (1955).
75. R. B. Woodward, *J. Am. Chem. Soc.*, **64**, 72 (1942).
76. L. K. Evans and A. E. Gillam, *J. Chem. Soc.*, **1941**, 851; **1943**, 565; **1945**, 432.
77. L. F. Fieser, M. Fieser, and S. Rajogopolan, *J. Org. Chem.*, **13**, 800 (1948).
78. L. F. Fieser and M. Fieser, *Steroids*, Reinhold, New York, 1959.
79. H. Booker, L. K. Evans, and A. E. Gillam, *J. Chem. Soc.*, **1940**, 1453.
80. H. Dannenberg, *Abhandl. Preuss. Akad. Wiss.*, **21**, 3 (1939).
81. L. Dorfman, *Chem. Rev.*, **53**, 47 (1953).
82. G. Scheibe, *Ber. Deutsch. Chem. Ges.*, **59**, 1333 (1926).
83. W. J. Bailey and J. C. Goosens, *J. Am. Chem. Soc.*, **78**, 2804 (1956).
84. J. B. Aldersley, G. V. Burkhard, A. E. Gillam, and N. C. Hindley, *J. Chem. Soc.*, **1940**, 10.
85. K. Bowden and E. A. Braude, *J. Chem. Soc.*, **1952**, 1068.
86. S. S. Malhotra and M. C. Whiting, *J. Chem. Soc.*, **1960**, 3812.
87. M. I. Fisher and F. M. Hamer, *Proc. Roy. Soc.* (*London*), **154A**, 703 (1936).
88. I. G. S. Brooker, *Rev. Mod. Phys.*, **14**, 275 (1942).
89. F. Bohlmann, *Ber. Deutsch. Chem. Ges.*, **86**, 63, 657 (1953).
90. C. L. Cook, E. R. H. Jones, and M. C. Whiting, *J. Chem. Soc.*, **1952**, 2883.
91. F. Bohlmann, *Ber. Deutsch. Chem. Ges.*, **84**, 545, 785 (1951).
92. J. B. Armitage, C. L. Cook, N. Entwhistle, E. R. H. Jones, and M. C. Whiting, *J. Chem. Soc.*, **1952**, 1998.
93. J. B. Armitage, C. L. Cook, E. R. H. Jones, and M. C. Whiting, *J. Chem. Soc.*, **1952**, 2010.
94. R. S. Mulliken, *J. Chem. Phys.*, **3**, 564 (1935).
95a. H. L. McMurry, *J. Chem. Phys.*, **9**, 231 (1941).
95b. H. L. McMurry, *J. Chem. Phys.*, **9**, 241 (1941).
96. A. D. Walsh, *Trans. Faraday Soc.*, **42**, 66 (1946).
97. J. A. Popple and J. W. Sidman, *J. Chem. Phys.*, **27**, 1270 (1957).
98. J. G. Calvert and J. N. Pitts, Jr., *Photochemistry*, Wiley, 1966, p. 368.
99. G. Fleming, M.M. Anderson, A. J. Harrison, and L. W. Pickett, *J. Chem. Phys.*, **30**, 351 (1959).
100. A. D. Cohen and C. Reid, *J. Chem. Phys.*, **24**, 85 (1956).
101. J. S. Lake and A. J. Harrison, *J. Chem. Phys.*, **30**, 361 (1959).

102. W. Herold and K. L. Wolf, *Z. Physik. Chem.*, **B21**, 165 (1931).
103. Ref. 98, p. 377.
104. K. Stich, G. Rotzler, and T. Reichstein, *Helv. Chim. Acta*, **42**, 1480 (1959).
105. K. L. Wolf, *Z. Physik. Chem.*, **B2**, 39 (1929).
106. E. M. Kosower and G. S. Wu, *J. Am. Chem. Soc.*, **83**, 3144 (1961).
107. N. L. Allinger, J. Allinger, L. A. Freiberg, R. F. Czaja, and N. A. LeBel, *J. Am. Chem. Soc.*, **82**, 5876 (1960).
108. H. L. Donle and G. Volkert, *Z. Physik. Chem.*, **B8**, 60, 68 (1930).
109. J. Bielecki and V. Henri, *Ber. Deutsch. Chem. Ges.*, **47**, 1690 (1914).
109a. P. Grossmann, *Z. Physik. Chem.*, **109**, 305 (1924).
110. H. Ley and B. Arends, *Z. Physik. Chem.*, **B17**, 177 (1932).
110a. B. D. Saksena and R. E. Kagarise, *J. Chem. Phys.*, **19**, 994, 999 (1951).
111. W. Herold, *Z. Physik. Chem.*, **B18**, 265 (1932).
112. Ref. 98, p. 439.
113. Ref. 98, p. 428.
114. M. J. Janssen, *Rec. Trav. Chim.*, **79**, 461 (1960).
115. R. C. Cookson and S. H. Dandegaonker, *J. Chem. Soc.*, **1955**, 352, 1651.
116. M. Kasha, *Discussions Faraday Soc.*, **9**, 14 (1950).
117. A. Balasobramanian and C. N. R. Rao, *Spectrochim. Acta*, **18**, 1337 (1962).
118. H. McConnell, *J. Chem. Phys.*, **20**, 700 (1952).
119. G. J. Brealey and M. Kasha, *J. Am. Chem. Soc.*, **77**, 4462 (1955).
120. G. C. Pimentel, *J. Am. Chem. Soc.*, **79**, 3323 (1957).
121. G. Forster, R. Skrabal, and J. Wagner, *Z. Elektrochem.*, **43**, 290 (1937).
122. K. Knox, R. G. W. Norrish, and G. Porter, *J. Chem. Soc.*, **1952**, 1477.
123. S. F. Mason, *Quart. Rev.*, **15**, 312 (1961).
124. L. S. Forster, *J. Am. Chem. Soc.*, **77**, 1417 (1955).
125. R. T. Holman, W. O. Lundberg, and G. O. Burr, *J. Am. Chem. Soc.*, **67**, 1669 (1945).
126. N. J. Leonard and P. M. Mader, *J. Am. Chem. Soc.*, **72**, 5388 (1950).
127. M. Calvin and F. L. Wood, *J. Am. Chem. Soc.*, **62**, 3152 (1940).
128. C. W. Shoppee, *J. Chem. Soc.*, **1936**, 269.
129. A. Lüthy, *Z. Physik. Chem.*, **107**, 285 (1923).
130. L. K. Evans and A. E. Gillam, *J. Chem. Soc.*, **1943**, 565.
131. A. Burawoy, *J. Chem. Soc.*, **1941**, 20.
132. K. W. Hausser, R. Kuhn, A. Smakula, and M. Hoffer, *Z. Physik. Chem.*, **29B**, 371 (1935).
133. L. K. Evans and A. E. Gillam, *J. Chem. Soc.*, **1941**, 815.
134. R. P. Mariella and R. R. Raube, *J. Am. Chem. Soc.*, **74**, 518 (1952).
135. L. D. Hess and J. N. Pitts, Jr., *J. Am. Chem. Soc.*, **89**, 1973 (1967).
136. G. Scheibe, G. Rössler, and F. Backenköhler, *Ber. Deutsch. Chem. Ges.*, **58**, 586 (1925).
137. R. B. Woodward, *J. Am. Chem. Soc.*, **63**, 1123 (1941); **64**, 72, 76 (1942).
138. A. E. Gillam and T. F. West, *J. Chem. Soc.*, **1942**, 486.
139. R. L. Franck, R. Armstrong, J. Kwiatek, and H. A. Price, *J. Am. Chem. Soc.*, **70**, 379 (1948).
140. S. Winstein, L. deVries, and R. Orloski, *J. Am. Chem. Soc.*, **83**, 2020 (1961).
141. H. Labhart and G. Wagnière, *Helv. Chim. Acta*, **42**, 2219 (1959).
142. *International Critical Tables*, Vol. 5, McGraw-Hill, New York, 1929, p. 377, Fig. 84.
143. A. T. Nielsen, *J. Org. Chem.*, **22**, 1539 (1957).
144. A. E. Gillam and E. S. Stern, *Introduction to Electronic Absorption Spectroscopy of Organic Molecules*, 2nd ed., Arnold Ltd., London, 1957.

145. Ref. 98, p. 454.
146. S. Nagakura, *Mol. Phys.*, **3**, 152 (1960).
147. T. Urbanski, *Tetrahedron*, **6**, 1 (1959).
148. Ref. 98, p. 455.
149. Ref. 98, p. 453.
150. G. Kortüm, *Z. Physik. Chem.*, **B50**, 361 (1941).
151. R. K. Brinton and D. H. Volman, *J. Chem. Phys.*, **19**, 1394 (1951).
152. K. L. Wolf, *Z. Physik. Chem.*, **B17**, 46 (1932).
153. Y. N. Sheinker, *Dokl. Akad. Nauk SSSR*, **77**, 1043 (1951).
154. R. A. Friedel and M. Orchin, *Ultraviolet Spectra of Aromatic Compounds*, revised ed., Wiley, New York, 1958.
155. S. Nagakura and J. Tanaka, *J. Chem. Phys.*, **22**, 236 (1954).
156. J. Tanaka, S. Nagakura, and M. Kobayshi, *J. Chem. Phys.*, **24**, 311 (1936).
157. J. N.Murrell, *J. Chem. Soc.*, **1956**, 3779.
158. B.M. Wepster, *Steric Effects in Conjugated Systems*, G. W. Gray, Ed., Butterworths, London, 1958, p. 82.
159. R. Grinter, E. Heilbronner, M. Godfrey, and J. N.Murrell, *Tetrahedron Letters*, **21**, 711 (1961).
160. R. Grinter and E. Heilbronner, *Helv. Chim. Acta*, **45**, 2496 (1962).
161. L. W. Pickett, G. Walter, and H. Frame, *J. Am. Chem. Soc.*, **58**, 2796 (1936).
162. M. T. O'Shaughnessy and W. H. Rodebush, *J. Am. Chem. Soc.*, **62**, 2906 (1940).
163. G. H. Beaven, ref. 158, p. 22.
164. E. P. Clar, *Polycyclic Hydrocarbons*, Academic Press, London, 1964.
165. L. F. Fieser and E. B. Hershberg, *J. Am. Chem. Soc.*, **60**, 940 (1938).
166. R. N. Jones, *J. Am. Chem. Soc.*, **63**, 151, 313 (1941).
167. G. N. Lewis and M. Calvin, *Chem. Rev.*, **25**, 273 (1939).
168. D. P. Craig and L. E. Lyons, *J. Chem. Phys.*, **20**, 1499 (1952).
169. H. Winston, *J. Chem. Phys.*, **19**, 156 (1951).
170. D. S. McClure, *J. Chem. Phys.*, **22**, 1668 (1954).
171. J. W. Sidman, *J. Chem. Phys.*, **25**, 115, 122 (1956).
172. R.N. Jones, *J. Am. Chem. Soc.*, **67**, 2127 (1945); *Chem. Rev.*, **41**, 353 (1947).
173. M. Kasha, *Discussions Faraday Soc.*, **9**, 14 (1950).
174. F. Halverson and R. C. Hirt, *J. Chem. Phys.*, **19**, 711 (1951).
175. R. C. Hirt, *Spectrochim. Acta*, **12**, 114 (1958).
176. M. Ito, R. Shimada, T. Kuraishi, and W. Mizushima, *J. Chem. Phys.*, **26**, 1508 (1957).
177. S. F. Mason, *J. Chem. Soc.*, **1959**, 1247.
178. E. M. Kosower, *J. Am. Chem. Soc.*, **80**, 3253 (1958).
179. E. M. Kosower, J. A. Scorez, W. M. Schwarz, Jr., and J. W. Paton, *J. Am. Chem. Soc.*, **82**, 2188 (1960).
180. S. F. Mason, *J. Chem. Soc.*, **1959**, 1253; **1960**, 209.
181. W. G. Brown and H. Reagan, *J. Am. Chem. Soc.*, **69**, 1033 (1947).
182. K. L. Brunings and A. W. Corwin, *J. Am. Chem. Soc.*, **64**, 593 (1942).
183. L. G. S. Brooker, F. C. White, R. H. Sprague, S. G. Dent, Jr., and G. Van Zandt, *Chem. Rev.*, **41**, 325 (1947).
184. *DMS UV Atlas of Organic Compounds*, Vol. 1, Plenum Press, New York, 1966.

CHAPTER II

GENERAL THEORY OF ELECTRONIC SPECTRA

A. B. F. DUNCAN
Department of Chemistry
University of Rochester, Rochester, New York

I. Principles of Atomic Spectra . . . 105
  A. Introduction . . . 105
  B. Quantum Mechanical Theory of the Hydrogen Atom . . . 108
  C. Quantum Mechanics of Many-Electron Atoms . . . 110
  D. Vector Coupling of Angular Momentum in Atoms . . . 117
  E. Intensities and Selection Rules in Atomic Spectra . . . 121
  F. Analysis of Atomic Spectra . . . 124
II. Theory of Diatomic Molecules . . . 124
  A. Molecular States of Diatomic Molecules . . . 124
  B. Relation of Diatomic Molecular Terms to Atomic Terms . . . 130
  C. Vibrational and Rotational Energy of Diatomic Molecules . . . 132
  D. Symmetry Properties and Selection Rules for Diatomic Molecules . . . 135
  E. Dissociation Energy of Diatomic Molecules . . . 137
  F. Analysis of Spectra of Diatomic Molecules . . . 138
III. Theory of Polyatomic Molecules . . . 139
  A. Classification of Electronic States by Molecular Symmetry . . . 139
IV. Application of Group Theory to Molecular Symmetry and Selection Rules . 140
  A. Concept of a Group . . . 140
  B. Representations and Character Sets . . . 142
  C. Classification of Eigenfunctions According to Group Theory . . . 144
  D. Selection Rules for Infrared and Raman Transitions . . . 146
  E. Enumeration of Normal Vibrations belonging to a Representation . . 149
  F. Application to *Trans*- and *Cis*-Dichloroethylene . . . 153
  G. The Benzene Molecule . . . 155
  H. Overtone and Combination Frequencies . . . 160
  I. Symmetry of Vibronic States . . . 163
V. Calculation of Electronic Eigenfunctions . . . 169
VI. Intensities of Electronic Transitions . . . 189
  References . . . 196

I. PRINCIPLES OF ATOMIC SPECTRA

A. Introduction

The first theoretical explanation of atomic spectra was given by N. Bohr in 1913. His explanation required two fundamental assumptions, which are stated as follows: the existence of nonradiative (stationary) energy states was assumed; these were quantized with respect to angular momentum; radiation was emitted or absorbed only in transitions between the stationary states. The mechanical model of Rutherford of a planetary system of electrons and nucleus was adopted by Bohr.

If it is assumed that an electron rotates about the nucleus in a circular orbit, with a linear velocity, v, the acceleration in such an orbit is v^2/r, where r is the radius of the orbit. The resulting force on the nucleus is mv^2/r, which is balanced by the electrical force of attraction, Ze^2/r^2. Ze is the charge on the nucleus and m is the mass of the electron. Equality of forces leads to

$$Ze^2/r^2 = mv^2/r$$

The angular momentum mvr is supposed to be quantized by a quantum number n, in units of $(h/2\pi)$; h is Planck's constant.

$$mvr = n(h/2\pi)$$

These simple equations are sufficient for elimination of v and calculation of r.

$$r = n^2(h^2/4\pi^2 mZe^2)$$

For the hydrogen atom, $Z = 1$, and for $n = 1$, $r = a_0 = 0.5292$ angstrom units.* The classical energy of the system of nucleus and one electron is the sum of potential and kinetic energies

$$E = -Ze^2/r + 1/2\, mv^2 = -Ze^2/2r$$

since $mv^2 = Ze^2/r$. From the value of r given above

$$E(n) = -2\pi^2 me^4 Z^2/h^2 n^2$$

The ionization energy of the electron in the H atom is

$$E(\infty) - E(1) = 2\pi^2 me^4/h^2 = e^2/2a_0$$

The quantity $(e^2/2a_0)$ is frequently taken as the unit of energy (Rydberg) in atomic units. More commonly $e^2/a_0 = 27.210$ eV is taken as the unit of energy in atomic units. More properly the electron rotates about the center of mass of the system, and the reduced mass of the system, μ, should be used. $\mu = mM/(m + M)$, where m is the mass of the electron and M is the mass of the nucleus. The lightest nucleus is hydrogen, with $M = 1840m$, and so the reduced mass is practically equal to the mass of the electron. μ becomes more nearly equal to m as M is increased.

---

* This value for the radius of the smallest Bohr orbit in the hydrogen atom is taken as the unit of length in "atomic units" and is designated as a_0.

According to the Bohr theory, the energy of any state of the hydrogen atom is a function of a single quantum number n. The assumption that radiation be emitted only between stationary energy states requires that the frequency $\tilde{\nu}$ (in reciprocal seconds) emitted is

$$\tilde{\nu} = [E(n_j) - E(n_i)]/h$$

where $n_j > n_i$, and both are integers. The same energy difference is related to the wave number, ν, of the spectroscopic transition by

$$\nu = [E(n_j) - E(n_i)]/hc = 1/\lambda \tag{1}$$

where λ is the wavelength in centimeters and c is the velocity of light. When the Bohr expression for the energy of the hydrogen states, $E(n) = -2\pi^2 me^4/h^2n^2$, is substituted into Eq. 1

$$\nu = 1/\lambda = (2\pi^2 me^4/h^3c)[(1/n_i^2) - (1/n_j^2)] \tag{2}$$

It has been known for a long time (Balmer, 1885) that a series of lines in the spectrum of the hydrogen atom fits a formula which may be written as

$$1/\lambda = \text{const }[(1/n_i^2) - (1/n_j^2)]$$

where $n_i = 2$ and $n_j = 3, 4, 5, \ldots$. The constant, which we now call the Rydberg constant for hydrogen, R_{H} should be given by the Bohr theory accurately as

$$R_{\mathrm{H}} = 2\pi^2 \mu e^4/h^3c$$

where we have used the reduced mass, μ, instead of m. The exact agreement of the experimental value of R_{H} with the theoretical value constituted one of the initial triumphs of the Bohr theory.

Other series in the hydrogen atom spectrum are well known, corresponding to $n_i = 1$ (Lyman series), 3, 4, 5, with n_j always greater than n_i. The complete spectrum of the hydrogen atom is accounted for by differences of *terms* of the form $T = R_{\mathrm{H}}/n^2$. On this basis, the lowest term is R, and the value of T decreases as $R/4$, $R/9$, $R/16, \ldots$ and becomes zero at the ionization potential. The lowest term corresponds to a wave number, $-Rhc$. The wavenumbers of the higher terms become progressively less negative, and become zero at the ionization potential. The terms are thus the negatives of the energies divided by hc.

The concept of atomic terms is important in the general discussion of atomic spectra. The terms are given more generally by $T = R/(n + a)^2$. The parameter a, the "quantum defect," may have different values for different types of electrons in the same atom.

B. Quantum Mechanical Theory of the Hydrogen Atom

The Schroedinger equation for the mechanical motion of this system may be solved exactly. The time-independent operator* form of this equation is

$$H\psi = E\psi \tag{3}$$

In Eq. 3, ψ is a function only of the space coordinates of the electron and is known as an amplitude wave function, or eigenfunction. Equation 3 and the second-order differential equation to which it is equivalent belong to the mathematical class of eigenvalue equations, which have solutions only for particular values of some parameter. In the present case, the solutions are the ψ and the parameters are the values of E. The solutions satisfy the mathematical requirements of continuity and single valuedness. In addition, ψ must vanish at the boundaries $\pm\infty$. But it is not required that ψ be real, and in general the solutions will be complex. However, the product $(\psi\psi^*)$ is real, where ψ^* is the complex conjugate of ψ. The time-independent functions are sufficient for treatment of the stationary energy states, but inadequate for detailed treatment of transition probabilities and intensities of spectroscopic transitions.

The following simplified and consistent notation will be used throughout this chapter. ψ alone will indicate a *general* and complete eigenfunction. The functional dependence of ψ is indicated, when necessary, by one or more general symbols in parentheses. For example, in $\psi(q)$, q indicates a general set of space coordinates of electrons, in particular the sets x, y, z, or r, θ, ϕ. Electrons, and their space coordinates are distinguished by numerical subscripts attached to the q. For example, $\psi(q_1)$, $\psi(q_2)$, or more generally $\psi(q_i)$, $\psi(q_j)$ all indicate one-electron functions of the electrons indicated by the subscripts. It will usually be possible to omit the q and write: $\psi(1)$, $\psi(2)$, $\psi(i)$, $\psi(j)$. Spin coordinates as designates by (s). Thus, $\psi(q,s)$ is an electronic eigenfunction of space and spin functions. One-electron functions of this type are known as spin orbitals and are designated as $\phi(1)$, $\phi(2)$, an abbreviation for $\psi(q_1,s_1)$, $\psi(q_2,s_2)$. An atomic orbital is a one-electron atomic function

---

* It is well known that functions may be multiplied, differentiated, integrated, and subjected to other operations which result in other functions. An operator is a rule for the operation and particular operators are defined most conveniently by equations which show the result of the operation. For example, the differential operators d/dx, d^2/dx^2 are defined by the equations

$$df(x)/dx = f'(x), \qquad d^2f(x)/dx^2 = f''(x) = df'(x)/dx$$

and the Laplace operator ∇^2 may be defined for a function $u(x,y,z)$ as

$$\nabla^2 u = \partial^2 u/\partial x^2 + \partial^2 u/\partial y^2 + \partial^2 u/\partial z^2$$

A clear and fundamental discussion of the operators of quantum mechanics is given in ref. 1, Section 3c.

of space coordinates and is designated by the letter u. Atomic spin orbitals and molecular spin orbitals are both designated by ϕ. (R) indicates a collective set of coordinates which define the relative positions of the nuclei. Thus, $\psi(q,R)$ is a function dependent on both electron and nuclear space coordinates. Time-dependent eigenfunctions, $\psi(q,t)$, are required only infrequently. Specific electronic and vibrational eigenfunctions are ψ^e, ψ^v. Other notations are defined at appropriate places in the text.

Returning to Eq. 3, H is the Hamiltonian operator. In the particular case of the hydrogen atom, H is a sum of kinetic and potential energy operators for the single electron. In atomic units the kinetic energy operator is $(-\nabla^2/2)$ and the potential energy operator† is $(-Z/r)$. Then we may write Eq. 3 as

$$(-\nabla^2/2 - Z/r)\psi = E\psi \tag{4}$$

If we multiply Eq. 4 by ψ^* and integrate over the coordinates of the electron, we obtain, since E is not a function of coordinates

$$\int \psi^*(-\nabla^2/2 - Z/r)\psi \, d\tau = E \int \psi\psi^* \, d\tau \tag{5}$$

where τ is a volume element of coordinate space.

The significance of the integral on the right side of Eq. 5 is as follows. The value of ψ at any point in space is determined by values of coordinates at that point. From the view of probability theory, $|\psi|^2 = (\psi\psi^*)$ gives the probability that the electron will be found at that point. However, the probability that the electron will be found somewhere in space is found by integration over all possible values of the spatial variables, and the result must be unity. When $\int \psi\psi^* \, d\tau = 1$, the function is said to be normalized. Exact solutions ψ_i which correspond to distinct (nondegenerate) values of E are orthogonal, indicated by $\int \psi_i\psi_j \, d\tau = 0$.

The mathematical details of solutions of Eq. 4 will not be repeated here since they are found in most textbooks on quantum mechanics. The final result is that the energy values are identical with those given by the Bohr theory, and are determined solely by the principal quantum number n. However, an extremely important point would be lost if we failed to describe some of the general features of the solutions, because the results show that the stationary energy states are described actually by additional quantum numbers, l and m. In the case of the hydrogen atom, apart from relativity corrections, states with different values of l for the same value of n have the same energy and are said to be degenerate. In the absence of an external field, which has a definite direction in space, energy states are also degenerate with respect to m.

---

† r is the distance of the electron from an origin at the center of the nucleus, provided that the reduced mass, is used for the mass of the electron. ∇^2 is the Laplace operator.

The Schroedinger equation for the hydrogen atom is separable in spherical polar coordinates r, θ, ϕ. The solutions may be written in the form: $\psi_{nlm} = R_{nl}(r)\cdot\Theta_{lm}(\theta)\cdot\Phi_m(\phi)$. R_{nl} is the radical part of the function. Θ_{lm} and Φ_m are angular parts which describe the directions of ψ in space. The number l takes values 0, 1, 2, . . ., $(n - 1)$. Mathematically, l is the number of nodes in the angular parts of the function, that is, the number of times the function becomes zero at the origin. The number of nodes in $R_{nl}(r)$, or the number of times the radial part of the function becomes zero between $r = 0$ and $r = \infty$, is $(n - l - 1)$.

The physical meaning of l is as follows: l quantizes states of an atom which differ by angular rotation and therefore by angular momentum. The angular momentum is in fact $[l(l + 1)]^{1/2}h/2\pi$. The quantum number m quantizes the component of angular momentum in a definite direction in space and has integral values from $+l$ to $-l$ or a total of $(2l + 1)$ values. It is apparent that in the absence of a definite direction in space, as would be provided by an external field, each state characterized by a fixed l, will be $(2l + 1)$ fold degenerate with respect to m. The degeneracy can be removed by the external field.

The numbers n and l are important in spectroscopic notation and in general discussion of spectra. Functions with $l = 0, 1, 2, 3, 4$ are s,p,d,f,g functions. The principal quantum number n is written before the l symbol to characterize a single electron function. Since $l \leqq (n - 1)$, we have: $1s$; $2s,2p$; $3s,3p,3d$; $4s,4p,4d,4f$. Real, unnormalized forms of the $2p$ functions are

$$\left.\begin{matrix} 2p_z \\ 2p_x \\ 2p_y \end{matrix}\right\} = R_{21}\left\{\begin{matrix} \cos\theta & \quad m = 0 \\ \left.\begin{matrix}\sin\theta\cos\phi \\ \sin\theta\sin\phi\end{matrix}\right\} & m = \pm 1 \end{matrix}\right.$$

In the absence of an external field, the z direction is, of course, not unique; the three functions are entirely equivalent with respect to rotation of axes and the significance of m disappears. The electron distribution with respect to the angle θ may be visualized easily from these forms (2). For example, $2p_z$ is zero in the xy plane, positive in the $+z$ direction ($\theta < 90°$), negative in the $-z$ direction ($\theta > 90°$). $2p_x$ and $2p_y$ have nodes similarly in the yx and xz planes.

C. Quantum Mechanics of Many-Electron Atoms

There are several difficulties which arise in treatment of atoms with more than one electron. First, there is the mutual electrostatic repulsions of pairs of electrons. This fact makes it impossible to obtain an exact solution of the Schroedinger equation of the problem by separation of variables. Next there is the question of electron spin, which is of no importance in discussion of the hydrogen atom, but becomes of critical importance in the many electron case. A third difficulty, perhaps not so fundamentally important, concerns the fact that various electrons are not subject to the same nuclear charge, even in the same atom, but to effective charges $(Z - s)$, where s measures a reduction in actual nuclear charge because of screening of the nuclear charge by other electrons.

The first difficulty usually is met by the assumption that each electron moves independently in the field of the nucleus and in an average field of the other electrons. The multiparticle Hamiltonian operator is thus replaced by a sum of simpler Hamiltonians—one for each electron—and the problem is reduced to the solution of one-electron Schroedinger equations. The one-electron functions so obtained are atomic orbitals and the corresponding eigenvalues, or one-electron energies, are orbital energies. The atomic orbitals are functions of space coordinates of single electrons and are approximate in the sense that they are not functions of relative interelectronic distances. In this approximation, the total eigenfunction for the atom is a product of atomic orbital functions and the total energy is a sum of orbital energies. The complete Hamiltonian operator H in atomic units for i electrons is

$$H = -\sum_i (\nabla_i^2/2 + Z/r_i) + \sum_{j>i} 1/r_{ij} \tag{6}$$

The first summation is made over the one-electron kinetic energy and potential energy operators of the i electrons. The second summation is made over pairs of electrons i and j so that each pair is counted once. The pair operator $(1/r_{ij})$ requires some discussion, but a prior discussion of electron spin, symmetry, and antisymmetry of eigenfunctions is necessary.

The presence of electron spin requires that each atomic function be a function of spin coordinates as well as the usual space coordinates. Atomic functions of this nature are spin orbitals (ϕ) and any one of them may be represented by a product form: $\phi = u(q)\alpha(s)$, where u is the space part and α is the spin part. There are only two possible spin functions, $\alpha(s)$ and $\beta(s)$, but either may be associated with a specific u. The total eigenfunction is then a product of spin orbitals of the individual electrons. It is necessary now to inquire into the nature of this product function.

As an example, we can consider the product function of a system consisting of two electrons and a nucleus. Let the two electrons have the same orbital function, u_i. We may associate either spin function with this orbital and obtain two spin orbitals: $(u_i)(\alpha) = \phi_i^\alpha$; $(u_i)(\beta) = \phi_i^\beta$. From these spin orbitals we may construct two independent two-electron eigenfunctions which are

$$\psi_1 = [\phi_i^\alpha(1)\phi_i^\beta(2) + \phi_i^\beta(1)\phi_i^\alpha(2)]/\sqrt{2} \tag{7a}$$

$$\psi_2 = [\phi_i^\alpha(1)\phi_i^\beta(2) - \phi_i^\beta(1)\phi_i^\alpha(2)]/\sqrt{2} \tag{7b}$$

where the normalizing factor is $1/\sqrt{2}$. In the above equations, (1) and (2) refer to the totality of coordinates, space and spin, of the two electrons. Now if the coordinates of electrons 1 and 2 are exchanged, which is equivalent to exchanging (1) and (2) in Eqs. 7a and 7b, it is seen that ψ_2 changes sign and is said to be antisymmetric while ψ_1 is unchanged and is symmetric. The situation may be generalized to show that all such eigenfunctions are symmetric or antisymmetric (3).

Quantum mechanics provides no basis of choice between symmetric and antisymmetric functions, but nature appears to prefer antisymmetric functions for electrons and other charged particles. Photons, on the other hand, are described by symmetric functions. The question is concerned closely with general quantum statistics of elementary particles, which we cannot discuss here. The requirement of antisymmetric eigenfunctions for electrons may be taken as a statement of the Pauli principle.

The Pauli principle more usually is stated as follows: a complete set of quantum numbers which is necessary for the identification of one electron cannot be identical with a complete set used for the description of another electron in the same system. In other words, two electrons in any system must differ in at least one of the quantum numbers, which are necessary for the description of the electrons. If the complete sets were identical, then the energy states of the two electrons would be identical, and this identity of states is what we are denying by writing an antisymmetric function for the two electrons and by stating the Pauli principle.

The equivalence of the two expressions of the Pauli principle, in terms of antisymmetry of eigenfunctions and nonidentity of sets of quantum numbers, follows from the following arguments. First, the eigenfunctions are themselves characterized by quantum numbers. If the set of quantum numbers is complete, there can be no remaining degeneracy in the energy of a state specified by the quantum numbers nor in the eigenfunction corresponding to the state. Now let us consider again the antisymmetric eigenfunction, Eq. 7b, and write it in the form of a determinant.

$$\psi_2 = \frac{1}{\sqrt{2}} \begin{vmatrix} \phi_i^{\alpha}(1) & \phi_i^{\beta}(1) \\ \phi_i^{\alpha}(2) & \phi_i^{\beta}(2) \end{vmatrix} \tag{7b}$$

The antisymmetry is seen easily in this form, since the exchange of electron coordinates is made by interchange of rows of the determinant, which changes the sign of the determinant and thus the sign of ψ_2. Now suppose that the two electrons have identical sets of quantum numbers. There is then no difference between ϕ_i^{α} and ϕ_i^{β}, and if they are equal, it is seen that the determinant vanishes. ψ_2 is then zero and is therefore unacceptable in the description of a physical situation. This argument does not prove anything relative to the choice of eigenfunctions, but does show the equivalence of the two statements of the Pauli principle in terms of antisymmetry of eigenfunction and nonidentity of sets of quantum numbers. This result suggests that eigenfunctions should be formulated as nonvanishing determinants so that they will have the proper antisymmetry to satisfy the Pauli principle. For example, for a case of n independent spin orbitals, with electrons numbered 1, 2, 3, . . .

$$\psi = \frac{1}{(n!)^{1/2}} \begin{vmatrix} \phi_1^{\alpha}(1) & \phi_2^{\beta}(1) & \phi_3^{\alpha}(1) & \cdots & \phi_n(1) \\ \phi_1^{\alpha}(2) & \phi_2^{\beta}(2) & \phi_3^{\alpha}(2) & \cdots & \phi_n(2) \\ \phi_1^{\alpha}(3) & \phi_2^{\beta}(3) & \phi_3^{\alpha}(3) & \cdots & \phi_n(3) \\ \vdots & \vdots & \vdots & & \vdots \\ \phi_1^{\alpha}(n) & \phi_2^{\beta}(n) & \phi_3^{\alpha}(n) & \cdots & \phi_n(n) \end{vmatrix} \tag{8}$$

The energy of the normal state of the He atom may now be obtained by evaluation of the integral $\iint \psi_2 H \psi_2 \, d\tau_1 \, d\tau_2$, where the volume elements $d\tau_1$ and $d\tau_2$ include the spin coordinates, and H is given by Eq. 6. Since H does not operate on the spin coordinates, we may integrate over these independently. The spin functions are normalized and are orthogonal and therefore any particular integral in the sum will vanish unless the spin functions are identical. The final result is

$$E = 2T_i + 2V_i + J_{ii} \tag{9}$$

where

$$T_i = \int u_i(-\nabla^2/2)u_i \, d\tau_1$$

$$V_i = \int u_i(-Z/r_i)u_i \, d\tau_1$$

$$J_{ii} = \iint u_i(1)u_i(1)r_{12}^{-1}u_i(2)u_i(2) \, d\tau_1 \, d\tau_2$$

The integral J_{ii} measures the electrostatic repulsion of two electron distributions $(u_i)^2(1)$ and $(u_i)^2(2)$, separated by an average distance r_{12}. T_i measures the kinetic energy of either electron (which, of course, have equal kinetic energy). V_i measures the potential energy of an electron in the field of the nucleus.

The first two integrals on the right of Eq. 9 come from the first summation on the right of Eq. 6. This will be shown in detail. It will be convenient to denote the first sum in Eq. 6 as H^c, where

$$H^c = -\nabla_1^2/2 - Z/r_1 - \nabla_2^2/2 - Z/r_2$$

and the subscripts 1 and 2 refer to the two electrons. Equation 7b is written out as

$$\psi_2 = (1/\sqrt{2})\{u(1)\alpha(1)u(2)\beta(2) - u(1)\beta(1)u(2)\alpha(2)\}$$

The subscript i is unnecessary and will be dropped temporarily, but is reintroduced in the final result, Eq. 9, for comparison later with results in Eq. 10, where the two electrons may have different orbital functions. We form the product $(\psi_2 H^c \psi_2)$ and obtain the integral

$$\begin{aligned}\int \psi_2 H^c \psi_2 \, dq_1 \, dq_2 \, ds_1 \, ds_2 \\ = \frac{1}{2}\Big\{\int [u(1)\alpha(1)u(2)\beta(2)] H^c [u(1)\alpha(1)u(2)\beta(2)] \, dq_1 \, dq_2 \, ds_1 \, ds_2 \\ + \int [u(1)\beta(1)u(2)\alpha(2)] H^c [u(1)\beta(1)u(2)\alpha(2)] \, dq_1 \, dq_2 \, ds_1 \, ds_2 \\ - 2\int [u(1)\alpha(1)u(2)\beta(2)] H^c [u(1)\beta(1)u(2)\alpha(2)] \, dq_1 \, dq_2 \, ds_1 \, ds_2\Big\}\end{aligned}$$

If we now integrate over the spin functions only, the last of the three integrals on the right is zero because the spin functions are orthogonal. This is seen clearly by writing the third integral as

$$\int [u(1)u(2)] H^c [u(1)u(2)] \, d\tau_1 \, d\tau_2 \int \alpha(1)\beta(1) \, ds_1 \int \alpha(2)\beta(2) \, ds_2$$

The first integral on the right may be written in a similar form and since the spin functions are normalized

$$\begin{aligned}\int [u(1)u(2)] H^c [u(1)u(2)] \, dq_1{}^1 \, dq_2{}^2 \int \alpha(1)\alpha(1) \, ds_1 \int \beta(2)\beta(2) \, ds_2 \\ = \int [u(1)u(2)] H^c [u(1)u(2)] \, dq_1 \, dq_2\end{aligned}$$

The second integral is easily seen to equal the first. We obtain thus

$$\int \psi_2 H^c \psi_2 \, dq_1 \, dq_2 \, ds_1 \, ds_2 = \int [u(1)u(2)] H^c [u(1)u(2)] \, dq_1 \, dq_2$$

If the specific form of H^c is inserted, the reader may show that the result is $2T + 2V$, with T and V defined above.

We now consider the other part of the Hamiltonian (Eq. 6), which involves the sum of the reciprocal interelectronic distances. In the present case there is only one such distance. We wish now to evaluate

$$\int \psi_2 (r_{12}{}^{-1}) \psi_2 \, dq_1 \, dq_2 \, ds_1 \, ds_2 = I(r_{12}{}^{-1})$$

which we may write out as follows:

$$\begin{aligned}I(r_{12}{}^{-1}) = \frac{1}{2}\int [u(1)u(2)] r_{12}{}^{-1} [u(1)u(2)] \, dq_1 \, dq_2 \\ \times \Big\{\int \alpha(1)\alpha(1)\beta(2)\beta(2) \, ds_1 \, ds_2 + \int \beta(1)\beta(1)\alpha(2)\alpha(2) \, ds_1 \, ds_2 \\ - 2\int \alpha(1)\beta(1)\alpha(2)\beta(2) \, ds_1 \, ds_2\Big\}\end{aligned}$$

We integrate over the spin functions, as before, and since they are orthonormal

$$\begin{aligned} I(r_{12}^{-1}) &= \int [u(1)u(2)]r_{12}^{-1}[u(1)u(2)]\, dq_1\, dq_2 \\ &= \int u(1)u(1)r_{12}^{-1}u(2)u(2)\, dq_1\, dq_2 \\ &= J = J_{ii} \end{aligned}$$

The two-electron integral is treated as follows: We may integrate first over the coordinates of electron (1) and r_{12}. When we do this, we obtain the average potential energy of the charge distribution $[u(1)u(1)]$ of electron (1) in the field of the second electron with charge distribution $[u(2)u(2)]$. If then we integrate this result over the coordinates of electron (2), we obtain the (repulsive) potential energy of the two charge distributions when the electrons are separated by an average distance r_{12}. The final result would be just the classical electrostatic energy between two point charges separated by r_{12}, if the two electrons were represented as points, rather than by the distributions above. This electrostatic energy is the coulomb energy, and the integral J is called a coulomb integral. The actual evaluation of the integral requires that we assume forms for the u functions.

A quantum mechanical description of the most general case, where the orbital functions are not identical, would lead too far from the purpose of this text. The expression for the energy (Eq. 9) is certainly not general. It may be instructive, however, to see what happens when the orbital functions in Eq. 7b are *not* identical. Now let the two orbital functions in a two-electron case be different, $u_i \neq u_j$. This situation will occur in the excited states of the helium atom. First, since the orbital functions are not the same, some quantum number must be different for the two electrons. This fact in itself satisfies the Pauli principle and therefore the spin functions for the two electrons may be the same or be different. As will become clear later, identical spin functions for the two electrons leads to a triplet state, while different spin functions lead to a singlet state. We will treat here only the second possibility and derive the expression for the energy of a singlet state.

The eigenfunction (Eq. 7a) is not appropriate to this situation because we have now two orbital functions and two spin functions, and thus four spin orbitals. However, it is necessary only that the *total* eigenfunction be antisymmetric to exchange of space (orbital) coordinates and spin coordinates. The spin function do not by themselves have exchange properties of symmetry and antisymmetry but combinations of α and β will have this property. Therefore, let us construct a two-electron orbital function which will be symmetrical and multiply it by a product spin function which will be antisymmetrical; the complete function will then be antisymmetrical. An appropriate symmetrical orbital function is $[u_i(1)u_j(2) + u_j(1)u_i(2)]/\sqrt{2}$, and an appropriate spin function is $[\alpha(1)\beta(2) - \beta(1)\alpha(2)]/\sqrt{2}$. On multiplying these together

$$\psi = \tfrac{1}{2}[\phi_i^{\alpha}(1)\phi_j^{\beta}(2) + \phi_j^{\alpha}(1)\phi_i^{\beta}(2) - \phi_i^{\beta}(1)\phi_j^{\alpha}(2) - \phi_j^{\beta}(1)\phi_i^{\alpha}(2)]$$

We evaluate the energy, as before, from $\iint \psi H \psi \, d\tau_1 \, d\tau_2$, and find after integration over the spin functions

$$E = T_i + V_i + T_j + V_j + J_{ij} + K_{ij} \tag{10}$$

The T and V terms are defined as in Eq. 9 and in fact Eq. 10 reduces to Eq. 9 when $u_i = u_j$, except for the new term K_{ij}.

$$J_{ij} = \int u_i(1)u_i(1)r_{12}^{-1}u_j(2)u_j(2) \, d\tau_1 \, d\tau_2$$

$$K_{ij} = \int u_i(1)u_j(1)r_{12}^{-1}u_i(2)u_j(2) \, d\tau_1 \, d\tau_2$$

The integrals J_{ij} and K_{ij} are coulomb and exchange integrals. Both measure the electrostatic repulsion between distributions of two electrons (1) and (2) at an average interelectronic distance r_{12}. There is nothing unusual in the distributions $(u_i)^2$ and $(u_j)^2$. Indeed, if the two electrons were located at fixed points in space, J_{ij} would be just the classical electrostatic energy of repulsion. However, a distribution $(u_i u_j)$ for an electron has no classical analog. The integral K_{ij} has no physical meaning—only a mathematical significance which is a consequence of the use of one-electron functions.

A quantitative description of atomic structure requires that we know the *forms* of the atomic orbitals. The orbitals evidently must satisfy the Schroedinger equation of any given problem and there are two general approaches which may be made to meet this requirement. The first approach is based on the idea that the energy of a definite state must be a minimum for an exact eigenfunction and so the best ψ corresponds to a minimum E in Eq. 3. A less exact function, such as one built up from atomic orbitals, will correspond to a higher (less negative) energy. In a simple, unsystematic way, we could try forms of ψ until we found one which corresponded to the lowest energy. A systematic development of this idea consists in assuming a sufficiently flexible form of ψ with several parameters which are to be determined so that E is a minimum with respect to each of the parameters. This is the principle of the variation method. Our test for merit of any trial eigenfunction will be a comparison of the energy calculated from it with experimental values of the energy.

A good trial eigenfunction is actually very complicated and unless the basis functions from which the complete function is built are chosen carefully, the variational procedure may not converge to the minimum energy or may do so only very slowly. The most generally useful forms of the radial parts of the basis functions will be exponential forms which have the correct behavior at atomic centers and approach zero at large distances. For these radial functions, forms like $r_i^{c_i} \exp(-k_i r_i)$ and linear sums of these are appropriate. These radial forms are multiplied by functions of the angular variables. The antisymmetrical products of the orbital trial functions are constructed and if this is insufficient, linear combinations of the determinantal forms are used. We have thus the parameters c_i and k_i in each basic exponential form and the coefficients in the various linear combinations as parameters to vary.

A second general approach is the method of the self-consistent field, or SCF method, developed by Hartree (4) and others which is essentially a method of numerical integration of differential forms of the Schroedinger equation. The basic principle of the method may be understood easily. We select one electron in an n-electron problem and assume an eigenfunction for it. Then the field of charge densities of the $(n - 1)$ electrons is calculated. This field is spherical or is made so by averaging over the angular distributions of charge density. This information is sufficient for a point to point solution of the Schroedinger equation for the electron which was selected, from which an improved value of the eigenfunction is obtained. The process is carried out for each of the electrons in turn and an improved set of orbitals is obtained. The field that is recalculated for these improved orbitals is usually not the same as that calculated initially. The whole process is repeated with the improved orbitals until no further improvement is obtained. This iterative process is shown to converge and in practice it is possible to obtain orbitals which are identical with an established accuracy to those in the preceding stage of iteration. Since the final orbitals result from a previously calculated field and these final orbitals reproduce the field with the established accuracy, the field is self-consistent in this sense. The SCF process may appear excessively laborious as we have described it; actually the process is made tractable by systematic methods developed by Hartree.

D. Vector Coupling of Angular Momentum in Atoms

Many features of atomic structures which depend on vector properties of angular momenta may be understood without additional quantum mechanical theory. The orbital motion of a single electron is quantized by a number l and angular momentum associated with this motion is characterized by a vector l, whose magnitude is $[l(l + 1)]^{1/2}h/2\pi$. Similarly the angular momentum associated with spin is characterized by a vector s with magnitude $[s(s + 1)]^{1/2}h/2\pi$. The total angular momentum of a single electron is described by a vector magnitude $[j(j + 1)]^{1/2}h/2\pi$. We discuss first the possibility of coupling the l and s vectors in a many electron atom in the absence of an external field. There will be two limiting cases of coupling: (*1*) The l vectors for the individual electrons add to form a vector L and the s vectors for the individual electrons add to form a vector S for the atom as a whole. The L and S vectors are coupled to form J, which is the total angular momentum vector of all the electrons of the atom. This limiting case is known as Russell-Saunders coupling (or L,S coupling) and is the most common case, especially for atoms with relatively few electrons. (*2*) In the other limit, l and s couple to form j for individual electrons. Then J is a vector sum of the j. This case is known as (j,j) coupling and occurs only in heavy atoms with many electrons. These limiting cases appear rarely in pure forms, especially (j,j) coupling.

In (L,S) coupling, the states of an atom are described by Roman capitals, S, P, D, F, . . ., corresponding to $L = 0, 1, 2, 3, \ldots$ The value of S is indicated in the quantity $(2S + 1)$, which is defined as the multiplicity and is attached as a left superscript to the L value. The value of J is indicated as a right subscript. For example, an atomic state symbol, or atomic term, $^2\mathrm{P}_{3/2}$, means that $L = 1$, $S = 1/2$, $J = 3/2$. The value $J = 3/2$ means that the L and S vectors lie in the same direction; if they were in opposite directions, then a different term, $^2\mathrm{P}_{1/2}$, results. The terms $^2\mathrm{P}_{1/2}$ and $^2\mathrm{P}_{3/2}$ are said to form a multiplet. The number of components in a multiplet is $(2S + 1)$, the multiplicity. Values of $(2S + 1) = 1, 2, 3, \ldots$ define singlet, doublet, and triplet states. The multiplicity, however, gives the actual number of components only if $L \geqq S$. For example, the lowest term in the H atom comes from a single $(1s)$ electron, for which $l = 0$, $L = 0$, $s = 1/2$, $S = 1/2$, and the term is $^2\mathrm{S}_{1/2}$. But here $L < S$ and the doublet term does not actually consist of two components. It may be added that the notation just described is frequently used even in cases where (j,j) coupling is known to be appreciable.

Coupling in a magnetic field will now be considered in relation to angular momentum. For individual electrons, we need to consider quantum numbers l and s and their associated angular momentum vectors as well as values of these vectors in the direction of the field. If the coupling of the l and s vectors is stronger than the interaction of either separately with the field, which will be the case if the external field is relatively weak, then it is the projection of j in the field direction which is significant. The value of $j \cos \theta$ is quantized by the number m_j, which takes integral values between $+j$ and $-j$, or a total of $(2j + 1)$ values. For any definite value of l, there are two values of j which are $(l + s)$ and $(l - s)$. Therefore, an energy state with a given value of l will be split into $2(2l + 1)$ sublevels in a weak magnetic field.

When the field becomes sufficiently strong, the l and s vectors become uncoupled and interact separately with the field. The projection of l in the field direction is quantized by a number m_l, which takes values from $+l$ to $-l$; there are thus $(2l + 1)$ values of m_l. The projection of s in the field direction is quantized by the number m_s, which has two values corresponding to $\pm 1/2$. An energy level with a definite value of l, therefore, will be split by a strong magnetic field also into $2(2l + 1)$ sublevels. While the *number* of sublevels is thus the same, whatever the field strength, the spacing or energy difference between sublevels is a function of field strength, increasing with field strength. If the field strength is reduced to zero, the energies of the sublevels become the same, with degeneracy $2(2l + 1)$. The *number* of sublevels persists to zero field strength, or we may say that the space quantization is independent of the field strength.

The number of sublevels is extremely important, in combination with the Pauli principle, to atomic structure and to the periodic system of the elements. Suppose first that we take the quantum numbers n, l, m_l, m_s as necessary for the description of any electron. By the Pauli principle, if two electrons have identical sets of these quantum numbers, it would be impossible to write an antisymmetric eigenfunction for their description. We have seen this in the case of the normal state of helium. Both electrons have $n = 1$ and $l = 0$; thus, m_l must be zero, and the two electrons cannot have the same value of m_s. Furthermore, we see that two s electrons with the same value of n must have different spin quantum numbers whatever the value of n. A "closed" shell of s electrons can contain a maximum of two electrons.

Before the concept of "closed" shells is properly defined, let us ask what is the maximum number of different sets of quantum numbers (l, s, m) for a fixed value of n and of l? The answer is that the number is just equal to the number of sublevels into which a level characterized by a definite n and l will be split in a magnetic field. This number of sublevels is $2(2l + 1)$. We see that for s electrons, with $l = 0$, the maximum number is 2; for p electrons, $l = 1$, the maximum number is six; for d electrons the number is ten. We define a closed shell of electrons, with fixed n and l values, as one which has $2(2l + 1)$ electrons in it.

We ask now how many electrons with a fixed value of n can have completely different sets of quantum numbers. The answer is found by summing the quantity $2(2l + 1)$ from $l = 0$ to $l = (n - 1)$, which gives $2n^2$. Thus, there can be two electrons with principal quantum number 1; eight with $n = 2$; 18 with $n = 3$; and 32 with $n = 4$. These numbers are recognized as numbers of elements in rows of the periodic table of elements. An electron shell could be defined as closed with respect to n when it contains $2n^2$ electrons, but such a concept is not particularly useful in atomic structure. A shell which does not contain the maximum number of electrons is by definition an open shell. A listing of shells, with their occupancy, constitutes an *electron configuration*. The concept of configurations is of fundamental importance because stationary energy states of atomic and molecular systems are derived on the basis of configurations.

We approach the questions of configuration and energies of states (or terms) by a series of examples of increasing complexity. The lowest state of the hydrogen atom is based on the configuration ($1s$). The only possible term which can be derived from this configuration is $^2S_{1/2}$ ($l = 0$, $L = 0$, $s = 1/2$, $S = 1/2$). Other configurations ($2s$), ($2p$), etc. correspond to excited terms. Since the helium atom in its ground state contains two ($1s$) electrons, the normal term for He is based on the configuration $(1s)^2$, which is a closed-shell configuration. Here $l_1 = l_2 = 0$; $L = 0$. The spin quantum numbers therefore must be taken as $s_1 = 1/2$, $s_2 = -1/2$, and $S = 0$. The only possible term is thus $^1S_0$. A closed-shell configuration always results in a single term, $^1S_0$. A configuration such as $(1s)(2s)$ corresponds to excited terms of helium. Since n is now different for the two electrons, S may be either 0, or 1, and the terms are $^1S_0$ and $^3S_1$. A calculation would show that both terms have an energy higher than $^1S_0$ from $(1s)^2$, but that $^3S_1$ is somewhat lower than the excited $^1S_0$ term. In boron, with five electrons, a configuration $(1s)^2(2s)^2(2p)$ may be assumed for calculation of the lowest term. If there is a question that this configuration, rather than $(1s)^2(2s)(2p)^2$ or even $(1s)(2s)^2(2p)^2$ will give terms of lower energy, the question must be settled by calculation. However, one may feel intuitively that shells of $1s$, $2s$, and $2p$, electrons are filled in the order given and this assumption is supported by detailed calculation. The lowest term then comes from $(1s)^2(2s)^2(2p)$, and because the $1s$ and $2s$ shells are filled, the term will be determined by the single ($2p$) electron. For it, $l = 1$, $s = 1/2$, $L = 1$, $S = 1/2$, and $J = 3/2$ or $1/2$. Calculation shows that $^2P_{1/2}$ is lower than $^2P_{3/2}$. For carbon, the configuration from which the lowest term is derived is $(1s)^2(2s)^2(2p)^2$ and the terms depend on the two $2p$ electrons. Here $l_1 = 1$, $l_2 = 1$ and $L = 0, 1, 2$; $S = 0, 1$. However, we may not combine all L values with both S values because of the Pauli principle. For example, $L = 2$ means that l for both electrons is taken in the same direction; therefore, they must have different values of s. So $L = 2$ can be used only with $S = 0$, and we obtain only ^1D and not ^3D. It is not so obvious why we obtain only ^3P and ^1S from the remaining possibilities, and not ^1P and ^3S as well, and the reason for this appears only after detailed analysis (5). Of the three terms obtained, ^1D, ^1S, and ^3P, the last is the lowest, and in particular the J level $^3P_0$ is lower than $^3P_1$, $^3P_2$. Tables of terms which result from all reasonable configurations of partly filled shells of electrons are found readily (6). Separate tables are given for equivalent and nonequivalent electrons. Equivalent electrons have the same (n,l) values. A pair of nonequivalent electrons belong to different (n,l) shells. For example, a configuration $(2p)(3p)$ consists of nonequivalent electrons and the terms are ^1D, ^1S, ^1P, ^3D, ^3S, ^3P. Terms of more than two nonequivalent electrons are too complicated for discussion here.

General rules for the lowest terms which result from a given configuration of equivalent electrons have been given by Hund (7). The lowest terms are those with the largest multiplicity. Of these, if there is more than one with the same multiplicity, the term with the largest value of L is lowest. In addition, if the lowest term has a multiplet structure, we wish to know which component (J value) is lowest. If the shell which determines the configuration is less than half filled, the lowest term has lowest J value and the energy of the multiplet sublevels increases with J. In this case, the multiplet terms are said to be normal. If the shell is more than half filled, the order of sublevels is inverted and the lowest term has the highest J value. In practice, if the shell is half filled, the lowest term turns out to be an S term and no ambiguity arises. Another useful rule states that a configuration of q equivalent electrons gives the same terms as a configuration of $(t - q)$ electrons, where t is the maximum number of equivalent electrons in the closed shell. For example, $(np)^q = (np)^{t-q}$, and since $t = 6$ for p electrons, $(np) = (np)^5$. Similarly, $(nd)^3 = (nd)^7$. These relations simplify the derivation of terms of equivalent electrons.

E. Intensities and Selection Rules in Atomic Spectra

Calculation of intensities of transitions between the stationary states is an important but difficult theoretical problem. The problem is treated formally by quantum mechanical perturbation theory. We assume that the system is in an initial energy state, described by a time-dependent eigenfunction $\psi(q_i,t)$. The system is brought to the final state, $\psi(q_j,t)$. During the transition between the states, the system is subjected to the perturbation of a radiation field. In one dimension (x), the perturbation is $E_x \sum_k e_k x_k$, where E_x is the component of the electric vector of the light wave in the x direction and e_k is the charge, x_k the x coordinate of the kth electron of the system. Thus, $\sum e_k x_k$ is the component of the total dipole moment in the x direction, which we write as M_x. E_x contains time factors which finally cancel the time factors in the eigenfunctions, with the result that the intensity of the transition can be obtained in terms of integrals over time-independent eigenfunctions. The intensity of a transition, for light polarized in the x direction is found to be proportional to $|X_{i,j}|^2$, where

$$X_{i,j} = \int \psi_i M_x \psi_j \, dV \tag{11}$$

and the ψ are the total time-independent eigenfunctions for the two states concerned in the transition. The total intensity is found by evaluation of $|X_{i,j}^2 + Y_{i,j}^2 + Z_{i,j}^2|$. We may compute integrals with the three components of the dipole moment separately, add the squares, and obtain a quantity which is proportional to the total intensity.

A selection rule is concerned simply with the question of whether the above integral is zero or not zero and not with the magnitude of the integral. The decision on the vanishing of the integral can be made usually without detailed information about the form of the eigenfunctions and actually without any calculations at all. We must accept first some basic mathematical results on oddness and evenness of integrands in definite integrals and the effect of this property on the integral.

The integrand, which is a product of functions of the variables of integration, must itself be odd or even because of the nature of the functions. For example, a function of x will be odd if $f(-x) = -f(x)$, and even if $f(-x) = f(x)$, which is obvious if we consider $f(x) = x^n$ ($n = 0, 1, 2, 3, \ldots$). Oddness and evenness of trigonometric functions may be seen most easily after they are expressed as functions of an argument $\cos\theta = x$, whereby the functions are transformed into various powers of x. Now if the integrand is even, its contribution to the integral in both negative and positive regions of integration will add, but if the integrand is odd, the contribution from the negative region will cancel that from the positive region and the integral will have the value zero. Therefore, it is required that the integrand in a definite integral be even, otherwise the integral vanishes. In the dipole-moment integral (Eq. 11), which determines the intensity, the component of M is necessarily odd, since it is a coordinate. It follows that if X_{ij} in Eq. 11 is not to vanish, the product of the eigenfunctions must also be odd (since the product of two odd functions is even) and this means that one of the eigenfunctions must be even and the other, odd. Quantities which differ in oddness and evenness are said to differ in *parity*.

Atomic eigenfunctions $\psi(r,\theta,\phi)$ are odd or even functions because the angular parts are odd or even trigonometric functions. Consider two atomic functions: $\psi_a = f_1(r)\cdot Y(\theta,\phi)$ and $\psi_b = f_2(r)\cdot Y(\theta',\phi')$, in an integral of the type in Eq. 11. The angular Y functions are odd or even, as we have stated. On the other hand, the product $f_1(r)\cdot f_2(r)$ is always positive and does not need to be considered in the oddness or evenness of the complete integrand. We need in fact to consider only an integrand $[Y(\theta,\phi)M_q Y(\theta',\phi')]$ and we may associate quantum numbers l,m with $Y(\theta,\phi)$ and l',m' with $Y(\theta',\phi')$. The general coordinate M_q may be expressed as a function of (θ,ϕ) by a transformation to spherical polar coordinates:

$$M_x = r\sin\theta\cos\phi$$
$$M_y = r\sin\theta\sin\phi$$
$$M_z = r\cos\theta$$

All components of M_q are odd functions of θ, and M_x, M_y are odd functions of ϕ, but M_z is an even function of ϕ. We may consider first the behavior of $[Y_{m,l}(\theta,\phi)M_q\ Y_{m',l'}(\theta',\phi')]$ with respect to m only. For a transition polarized in the z direction ($M_q + M_z$), m is even for M_z, so for a nonvanishing integral in Eq. 11, m must be even (or odd) for both ϕ and ϕ'. It follows that $m = m'$, or $\Delta m = 0$ for light polarized in the z direction. For M_x, M_y, m is odd and so m must differ by one unit in $Y_{m,l}$ and $Y_{m',l'}$, with the result that $\Delta m = \pm 1$ for light polarized in the x or y directions. The behavior of the integrand with respect to θ is more simple, since M_q is odd for all components. $Y_{m,l}$ and $Y_{m',l'}$ must differ in one unit in l, which leads to the result $l' = l \pm 1$ or $\Delta l = \pm 1$. The rules for Δm are applicable only in cases where there is a preferred direction in space, such as the direction of an external magnetic field in the Zeeman effect. The selection rule for l allows single electron transitions $s \leftrightarrow p$, $p \leftrightarrow d$, $d \leftrightarrow f$. Excitation of more than one electron simultaneously is not prohibited, but is a less common case.

Since the spin coordinates in two atomic states are independent of space coordinates, we may consider an integrand of spin functions separately and derive selection rules for multiplicity. The independence of spin and space coordinates is true and consequently the selection rule is exact only when (j,j) coupling is negligible. If pure (L,S) coupling is assumed, then because of the orthogonality of spin functions, the integral over these functions is zero unless the functions are the same. This result implies that the spin quantum numbers for the two states must be identical, and consequently the multiplicities of the two states must be the same, or $\Delta S = 0$. As is clear, the multiplicity rule is rigid only for pure (L,S) coupling; in the mercury atom, where apparently there is significant (j,j) coupling, singlet–triplet transitions are almost as intense as singlet–singlet transitions. In the helium atom, singlet–triplet transitions do not appear with appreciable intensity.

The selection rules for atomic terms are more difficult to justify. It is more simple to state what is *not* allowed than to state what is allowed. A configuration is odd when the sum of the l values for all the electrons is an odd number, even otherwise. All terms which are derived from a given configuration are therefore either all even or all odd and are said to have the same parity. An immediate consequence is that there will be no transitions possible between terms derived from the same configuration with dipole radiation. For example, the configuration $(1s)^2(2s)^2(2p)^2$ of the carbon atom is evidently even. The resulting terms, ^{3}P, ^{1}D, ^{1}S, do not combine in optical transitions. For the same reason we can see that if one electron is excited from an even configuration and its l value changes by ± 1, an odd number, then the configuration after excitation must be odd. As a result, S $\leftrightarrow$ P, P $\leftrightarrow$ D, D $\leftrightarrow$ F for one-electron transitions.

The final configuration may not be reached directly from the initial one, but, nevertheless, the two configurations may yield terms with the same L value. It is possible in such cases to have $\Delta L = 0$ provided that the rule $\Delta l = \pm 1$ is satisfied. Consider the configuration $(1s)^2(2p)^2$, which gives a ^{3}P (even) term and a configuration $(1s)^2(2s)(2p)$ which gives also a ^{3}P term.

But the latter term is odd. There is nothing to prevent a transition between these terms ($^3P \leftrightarrow {}^3P$), and $\Delta L = 0$. The single-electron transition is $(2p \leftrightarrow 2s)$ and $\Delta l = \pm 1$ is satisfied.

There are no selection rules for the principal quantum number, n, provided the angular factors in the eigenfunctions allow the transition. The selection rules for J follow from the rules for L and S. They are $\Delta J = 0, \pm 1$. The particular transition $J = 0$ to $J' = 0$ is forbidden.

F. Analysis of Atomic Spectra

Discussion of this important topic must be restricted to a few general remarks. Any analysis, by which we mean interpretation, starts with accurate values of energy differences observed in transitions between atomic levels and when available, intensities associated with the transitions. Regularities in these energy intervals are looked for in some systematic way. A very simple type of regularity is shown in energy levels which converge to an ionization potential. More frequently, the regularities are apparent in repeated multiplet patterns. From selection rules and intervals between the components in the repeated multiplet patterns, conclusions about the J values in the two atomic states responsible for the multiplet may be reached. Further confirmatory evidence may be obtained from the patterns which result from splitting of levels in a magnetic field.

Another helpful factor, when it is known, is the nuclear spin of the atomic nucleus. The presence of nuclear spin causes a hyperfine structure and this hyperfine splitting of levels can be seen in spectra obtained with very high resolving power. For any definite isotopic species, the nuclear spin is a constant and interacts as a spin vector with J to describe the total angular momentum, which is quantized. The hyperfine structure can be predicted if the nuclear spin is known. Conversely, the nuclear spin may be deduced accurately from measurement and analysis of the hyperfine structure.

II. THEORY OF DIATOMIC MOLECULES

A. Molecular States of Diatomic Molecules

A molecule differs from an atom essentially in the fact that the molecular eigenfunction must depend on coordinates of the nuclei as well as coordinates of the electrons. In the diatomic molecule there is one nuclear coordinate, R, the interatomic distance. The first question which arises is the possibility of separating the energies of electronic and nuclear motion, which corresponds to the possibility of writing the total eigenfunction as the product of an electronic part and a nuclear part of the form $\psi = \psi(q,R) \cdot \psi(R)$. In this product, $\psi(q,R)$ is a solution of the Schroedinger equation of all electrons obtained under the condition that the nuclei are fixed in positions in space, while $\psi(R)$ describes the nuclear motion of rotation and vibration. The total energy is then the sum of electronic energies and the energies of nuclear motion.

This fundamental problem was investigated theoretically by Born and Oppenheimer, who reached the conclusion that an approximate separation is indeed possible, essentially because of the small ratio of the mass of an electron to the mass of a nucleus. The approximation appears to be justified experimentally by the fact that intervals between electronic energy levels (at least, for the lower electronic levels) are usually very much greater than the intervals between vibrational and rotational levels.

The electronic energy, as defined above, is a function of the nuclear coordinates, or of the internuclear distance in a diatomic molecule. A plot of electronic energy (E_e) against R has a typical form shown in Figure 1, which shows curves for two states of the oxygen molecule. The energy decreases sharply as R is increased from very small values, reaches a minimum at some equilibrium separation of atoms, R_e, and then rises to an asymptotic value which is the energy of the separated atoms. A minimum is not always present, but instead E_e may decrease continuously to the asymptotic value. This behavior means physically that the molecular state is not stable and the atoms repel each other at all values of R.

The form of the potential curve (Fig. 1) shows that energy changes continuously from $R = 0$ to $R = \infty$, and this fact suggests that the electronic

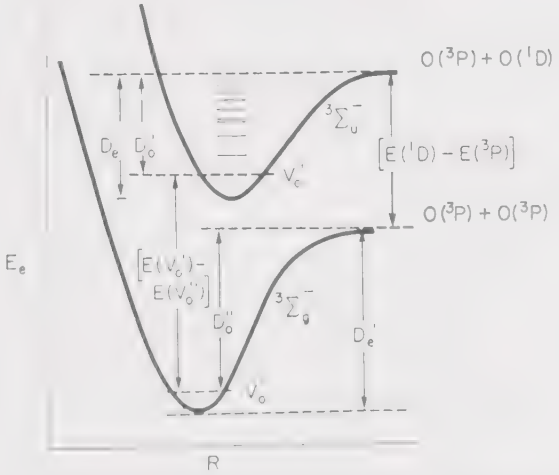

Fig. 1. Electronic energy as a function of internuclear distance for two states of the O_2 molecule.

eigenfunctions change continuously also. At $R = 0$, the two atoms are superimposed and we describe the system as an "united atom." In the most simple case of H_2^+, the united atom is He^+ (apart from a difference in mass) and the eigenfunctions are approximately hydrogenic. The eigenfunctions may be described in terms of angular momenta of atomic systems: *ns*, *np*, *nd*,. . . . If now we separate the nuclei slightly, the system behaves as if it were in an external field in the direction of the line of nuclei and quantum numbers for components of angular momentum in the field direction are appropriate. In the atomic case, the numbers would be the values of m_l, but in the molecular case we use the number λ, which takes values $\lambda = 0, 1, 2, \ldots$ The states of single electrons are designated as σ, π, δ, corresponding to $\lambda = 0, 1, 2$. States with $\lambda > 0$ are doubly degenerate. The one-electron eigenfunctions of the system are called molecular orbitals and are described for small values of R by writing the one-electron atomic description followed by the λ value, as $1s\sigma$, $2s\sigma$, $2p\sigma$, $2p\pi$, $3s\sigma$, $3p\sigma$, $3p\pi$, $3d\sigma$, $3d\pi$, $3d\delta$. This is the united atom notation for molecular orbitals.

At $R = \infty$, the atoms are separated and we have for the lowest state of H_2^+ the description $(1s_a, 1s_b)$. The electron is in the field of nucleus *a* or *b* and the separated system may be considered as $\{H^+(a), H(b)\}$ or $\{H^+(b), H(a)\}$. At $R = \infty$, the atomic orbitals $1s_a$ and $1s_b$ have equal energies, but as R decreases, we can imagine that the $1s$ level of the separated atoms splits into two levels because of the molecular field, corresponding to molecular orbitals of the form:

$$\sigma_g 1s = (1s_a + 1s_b)$$
$$\sigma_u 1s = (1s_a - 1s_b)$$

$\sigma_g 1s$ is lower in energy than $1s$ and $\sigma_u 1s$ is higher in energy than $1s$. As R decreases continuously to zero, $\sigma_g 1s$ goes over into the $1s\sigma_g$ level of the united atom. But $\sigma_u 1s$ must be correlated with the lowest odd term $2p\sigma_u$ of the united atom. $\sigma_g 1s$ remains lower than any other molecular orbital in this system at all values of R.

The molecular orbital forms $\sigma_g 1s$ and $\sigma_u 1s$ are most easily visualized from plots of electron density of $(\sigma_g 1s)^2$ and $(\sigma_u 1s)^2$ along the internuclear axis, which is taken as the z axis in a coordinate system centered at the midpoint of line of centers of the nuclei. The nuclei, *a* and *b*, are located symmetrically at the points $z_a = -R/2$ and $z_b = +R/2$. Typical plots of electron density in the two orbitals are shown in Figure 2, for an arbitrary separation of nuclei R. The detailed shapes of the curves will depend on the analytical forms assumed for $1s_a$ and $1s_b$. The *shapes* of the curves will not change greatly in the region of molecule formation as R is changed. The figures are symmetrical, of course, about the z axis.

It is apparent that the electron density is highest at the nuclei for both

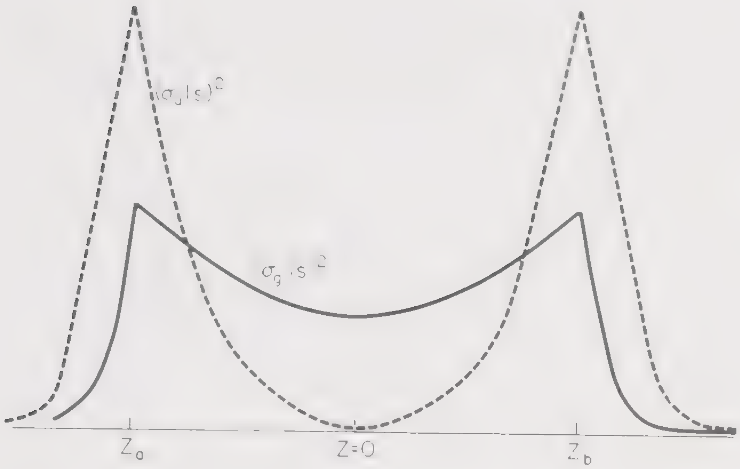

Fig. 2. Variation of electron density along the internuclear axis for a bonding molecular orbital (full line) and for a nonbonding molecular orbital of $H_2{}^+$.

$\sigma_g 1s$ and $\sigma_u 1s$, and the absolute density at the nuclei is considerably higher for $\sigma_u 1s$, but drops to zero at the midpoint. We say that $\sigma_u 1s$ has a node in the xy plane. It is this plane which is associated with the (u,g) (odd, even) behavior of the molecular eigenfunction (see p. 122). As R is decreased to zero, the node in $\sigma_u 1s$ persists and is retained in the united atom, which may be described as $2p_z$. On the other hand, the electron density in $\sigma_g 1s$ never becomes zero at the midpoint and in the case shown drops at the midpoint to about one-half of its maximum value.

There is a further point of interest which comes from a comparison of the two curves. It is seen that the charge density in the region between the nuclei is relatively greater for $\sigma_g 1s$ than for $\sigma_u 1s$. This indicates qualitatively that the electron has a greater probability of being found in the region of chemical binding between the nuclei for $\sigma_g 1s$ than for $\sigma_u 1s$, and we conclude that the former is more bonding than the latter. A better qualitative measure of bonding would come from a comparison of the charge densities of the molecular orbitals with the charge densities of the separate atoms evaluated in the region between the nuclei. The essential difference between the charge density in a molecular orbital and the sum of charge densities of separate atomic functions from which the molecular orbital is constructed lies in what may be called the overlap charge density. Let us write the charge density of $(\sigma_g 1s)$ as

$$(\sigma_g 1s)^2 = N_g{}^2\{(1s_a)^2 + (1s_b)^2 + 2(1s_a)(1s_b)\}$$

where the last term on the right is the overlap charge density and N_g is a normalizing factor. Let us take simple exponential forms for $1s_a$, $1s_b$: $1s_a = \exp(-r_a)$, $1s_b = \exp(-r_b)$. At the midpoint $r_a = r_b = r$, and $(\sigma_g 1s)^2 = N_g^2[4\exp(-2r)]$, whereas the total atomic charge density has one-half this value. On the other hand,

$$(\sigma_u 1s)^2 = N_u^2\{(1s_a)^2 + (1s_b)^2 - 2(1s_a)(1s_b)\}$$

and after the same substitution, $(\sigma_u 1s)^2 = 0$ at the midpoint.

However, $\sigma_u 1s$ is not the next to lowest orbital for all values of R, but is so only at large values of R. $2s$ of the united atom, at small R, goes into $2s\sigma_g$, which correlates with $\sigma_g 2s$ at large R. Therefore, $\sigma_g 2s$ must cross $\sigma_u 1s$ at some intermediate value of R, since it correlates with $2p_z$ of the united atom but $\sigma_g 2s$ and $\sigma_g 1s$ can never cross. An important requirement in the correlation of states of the (almost) united atom and of the (almost) separated atoms is that the odd, even (u,g) property of the molecular orbital, as well as its λ value, be unchanged from $R = 0$ to $R = \infty$. In heteronuclear diatomic molecules, with unlike atoms, there is, of course, no (u,g) property, and only the λ value must be unchanged. This means that curves of energy of two orbitals plotted against R cannot cross if the λ values of the two orbitals are the same. Correlation diagrams (8), which show approximate orbital energies over the complete range of R, are essential to the interpretation of electronic structure of diatomic molecules. We show a portion of a diagram for like atoms in Figure 3.

The states of many diatomic molecules may be described by writing the orbital angular momentum of the entire electron system in the direction of the internuclear axis as Λ. The states are classified by their Λ values as $\Sigma, \Pi, \Delta, \ldots$, correspond to $\Lambda = 0, 1, 2, \ldots$. The relation of Λ to the λ values of the individual electrons depends on the type of coupling. If the resultant orbital angular momentum Λ is coupled to the internuclear axis and if at the same time we can add the λ values of the electrons in Russell-Saunders coupling, then $\Lambda = \sum_i \lambda_i \cdot \Lambda$ can always be defined for very small internuclear distances as $\Lambda = |M_L|$, where M_l is component of L for the united atom in the direction of the axis. At $R = \infty$, $\Lambda = |M_{L_a} + M_{L_b}|$. In some coupling cases, Λ cannot be defined and thus has no significance as a quantum number.

The resultant electronic spin for a diatomic molecule is defined as a sum of spin values for the separate electrons, $S = \sum_i s_i$, or as a sum of the total spin values for the constituent separated atoms. In the latter case, the total electronic spin of the molecule is quantized by a number Σ, which takes values $\Sigma = S, (S - 1), (S - 2), \ldots, -S$, or $(2S + 1)$ values, but Σ is not defined when $\Lambda = 0$. The multiplicity $(2S + 1)$ is defined, as for atoms, but gives the actual number of components of the multiplet only when $\Lambda > 0$. Note that Λ takes only positive values but Σ takes positive as well as negative

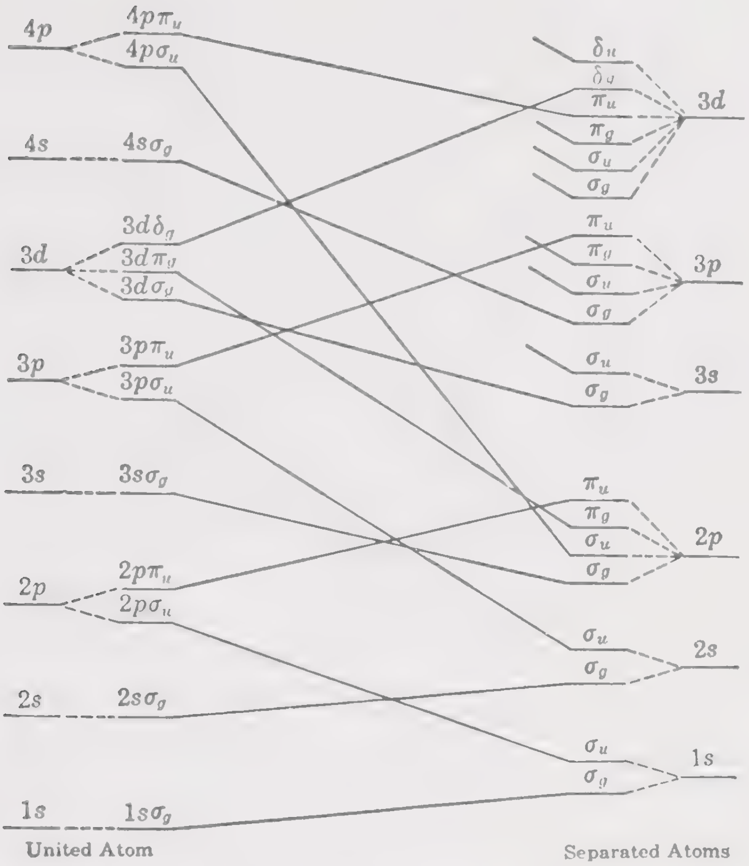
4p
4pπ_u
4pσ_u
4s
4sσ_g
3d
3dδ_g
3dπ_g
3dσ_g
3p
3pπ_u
3pσ_u
3s
3sσ_g
2p
2pπ_u
2pσ_u
2s
2sσ_g
1s
1sσ_g
United Atom
δ_u
δ_g
π_u
π_g
σ_u
σ_g
3d
π_u
π_g
σ_u
σ_g
3p
σ_u
σ_g
3s
π_u
π_g
σ_u
σ_g
2p
σ_u
σ_g
2s
σ_u
σ_g
1s
Separated Atoms

Fig. 3. Correlation diagram for homonuclear diatomic molecules. From H. Eyring, J. Walter and G. E. Kimball, *Quantum Chemistry*, Wiley, New York, 1944, p. 207.

values. The total angular momentum in the direction of the axis may be quantized by $\Omega = |\Lambda + \Sigma|$, when $|\Lambda + \Sigma|$ is defined.

These molecular quantum numbers are useful in the derivation of *possible* molecular terms from the terms of constituent atoms. They are also useful for the designation of molecular terms. A molecular term is designated by writing the Λ value, the multiplicity $(2S + 1)$ as a left superscript and the numerical value of $|\Lambda + \Sigma| = \Omega$ as a right-hand subscript. Thus ${}^3\Pi_1$ means that $\Lambda = 1$, $\Sigma = 0$, $S = 1$, $\Omega = 1$; ${}^3\Pi_0$ corresponds to $\Sigma = -1$. The $|\Lambda + \Sigma|$ value is usually omitted unless a particular component of a multiplet is being discussed.

The molecular term symbol is completed by designation of symmetry properties. If the two atoms are identical, the molecule has a center of symmetry at the midpoint of the line of centers. If an origin of coordinates is taken at this point, a molecular eigenfunction is designated (u) if it changes sign when the signs of coordinates of electrons and nuclei are changed. The molecular state which corresponds to the eigenfunction is designated by a subscript u (ungerade, or odd). If the molecular eigenfunction does not change sign on this operation, described as inversion, the molecular state is g (gerade, or even). Thus we write Σ_g, Σ_u, Π_g, Π_u of any multiplicity. A second symmetry operation is a reflection of the electrons in a plane which contains the molecular axis. If this operation causes the molecular eigenfunction to change sign, the molecular state symbol is designated by a minus sign as a right superscript. If the sign is not changed, the state is designated +. This symmetry operation is possible only for Σ states. States with $\Lambda > 0$ are doubly degenerate and the eigenfunction may be written as a linear sum of terms, which are transformed by the symmetry operation into other combinations which possess both plus and minus properties. There is, therefore, no difference between Π^+ and Π^- terms. If the diatomic molecule consists of identical atoms, we may thus have $\Sigma_g{}^+$, $\Sigma_g{}^-$, $\Sigma_u{}^+$, $\Sigma_g{}^-$ states of any multiplicity. If the atoms are not identical, the (u,g) property is lost, but Σ^+ and Σ^- remain.

B. Relation of Diatomic Molecular Terms to Atomic Terms

We may derive in a formal way a list of all molecular terms, or states, which can result from specified states of the constituent atoms. The form of potential energy curves suggests that we can start either at $R = 0$ and split the united atom, or at $R = \infty$ and bring the two atoms together. The totality of molecular terms must be necessarily the same when they are derived in either way. However, the energies of the molecular terms near the two limits are far from the same. A few examples of derivation of molecular terms will be given here and the general references may be consulted for tables of such terms.

Suppose that a molecule dissociates into two atoms, each in a P state. The multiplicities of the states will be ignored for the moment. If the atoms are labeled a and b, $L_a = L_b = 1$; $M_{L_a} = M_{L_b} = -1, 0, +1$; and

$$\Lambda = |M_{L_a} + M_{L_b}| = 0, 1, 2$$

Alternatively, at R near zero, we have $\lambda_a = \lambda_b = 1$ and $\Lambda = \sum_i \lambda_i = 0, 1, 2$. Thus, we obtain Σ, Π, Δ states. If the multiplicities are included, we obtain in the same way from (^{1}P,^{1}P) only singlet molecular states; from (^{1}P,^{3}P) only triplet states; from (^{2}P,^{2}P) singlet and triplet states; from (^{3}P,^{3}P) singlet, triplet, and quintet states. In all cases we have derived the multiplicity of the molecular states from $S = (S_a + S_b), (S_a + S_b - 1)\cdots(S_a - S_b)$.

Derivation of molecular states in this way gives a very large number of possible states, but the actual states which occur are restricted by the Pauli principle. This restriction will be understood more clearly if we derive states from molecular electron configurations or configurations of molecular orbitals. We are assuming when we do this that the electrons do not belong to either nucleus, but belong to the molecule as a whole. We must first see how such configurations are written. We begin with the concept of λ shells.

At small internuclear distances, the quantum numbers n, l, and m of the individual electrons are well defined and consequently m_l, the value of m in the direction of the internuclear axis. By definition, m_l becomes the λ of a molecular orbital as the nuclei are separated slightly. Just as in an atom, $m_s = \pm\frac{1}{2}$. When $\lambda = 0$, there will be just two electrons with sets of completely different quantum numbers, which will be the sets: $m_l = 0, m_s = +\frac{1}{2}$ and $m_l = 0$, $m_s = -\frac{1}{2}$. A λ shell with $\lambda = 0$ (or a σ shell), therefore, can contain only two electrons. If $\Lambda > 0$, we have to consider the two values $\pm m_l$ which correspond to a definite value of λ. We then obtain a maximum of four electrons in π, $\delta, \ldots$ shells, whose sets of quantum numbers satisfy the Pauli principle. In a $2p\pi$ shell, the four complete sets correspond to the quantum numbers, in order n, λ, m_l, m_s: $2,1,1,1/2$; $2,1,1,-1/2$; $2,1,-1,1/2$; $2,1,-1,-1/2$. We write molecular orbital configurations in a notation of λ shells with the probable energy decreasing from left to right. It is instructive to write a few examples of simple cases.

In the hydrogen molecule we have two electrons, both with $n = 1$, $l = 0$, $\lambda = 0$. We have found that the lowest energy molecular orbital is $\sigma_g 1s$, and we can have two electrons in this orbital provided the spins of the electrons are different. The lowest state will be a singlet state and is derived from the configuration $(\sigma_g 1s)^2$. The state symbol can be written from the rules given above. Since both orbitals are σ_g the state is g; the state must be ${}^1\Sigma_g$ since $\lambda = 0$ for both electrons. The $\pm$ symmetry of the state cannot be so simply determined. According to Wigner and Witmer, Σ^+ is obtained when $(L_a + L_b + \sum_i l_{ia} + \sum_i l_{ib})$ is even and Σ^- when the sum is odd. Evidently, the sum is even here and the state symbol is ${}^1\Sigma_g{}^+$.

If one electron is in the orbital $(\sigma_g 1s)$ and the other in $(\sigma_u 1s)$, the configuration is written $(\sigma_g 1s)(\sigma_u 1s)$ and the two electrons may have the same or different spins. There are two resulting states, ${}^1\Sigma_u{}^+$ and ${}^3\Sigma_u{}^+$. The ${}^3\Sigma_u{}^+$ state has no minimum in its potential energy curve and is the lower state of the continuous emission spectrum of the hydrogen molecule. The configuration $(\sigma_u 1s)^2$ gives another ${}^1\Sigma_g{}^+$ state of high energy. All states which arise from the above three configurations have the same value of the energy at $R = \infty$ and dissociate there into the same products, two H atoms in their normal states. These are, moreover, the only configurations and the only states possible with a basic set of $1s$ electrons.

As a further example, consider the configuration and lowest states of the diatomic B_2 molecule. The configuration from which the lowest state is derived is $(1s_a)^2(1s_b)^2(\sigma_g 2s)^2(\sigma_u 2s)^2(\pi_u 2p)^2$. In writing this configuration, we have filled λ shells in order of decreasing energy up to $(\pi_u 2p)^2$; the last shell is not closed since it can contain four electrons. In deriving the possible molecular terms, we need to consider only the unfilled shell or a configuration of two π electrons. In general such a configuration will give ${}^{1,3}\Sigma_g{}^+$, ${}^{1,3}\Sigma_g{}^-$, ${}^{1,3}\Delta_g$ terms, but when the atoms are identical, as in this case, the Pauli principle restricts the possibilities to ${}^3\Sigma_g{}^-$, ${}^1\Delta_g$, ${}^1\Sigma_g{}^+$. The state of greatest multiplicity is expected to be the lowest in energy and actually ${}^3\Sigma_g{}^-$ is the lowest state.

Examination of correlation diagrams shows that some molecular orbitals decrease in energy as the separated atoms come together and the decrease continues until small values of R are reached. For example, $\sigma_g 1s$ goes into $1s\sigma_g$, $\sigma_g 2s$ goes into $2s\sigma_g$, and the energy is lower at $R = 0$ than at $R = \infty$. On the other hand, the energies of some orbitals such as $\sigma_u 1s$ and $\pi_g 2p$ increase as R is increased. Orbitals which decrease in energy as R decreases are bonding orbitals. Those which increase in energy as R decreases are said to be antibonding. Some orbitals undergo little change in energy with R and these are nonbonding. Inner-shell electrons such as $1s$ electrons in O_2 and N_2 are nonbonding. We might expect that the total bonding in a molecule might be associated very approximately with the bonding nature of orbital pairs. It must be realized that such an approximation is very crude, since bonding nature of any pair of electrons would be altered by electronic interaction.

As an example, we consider the molecular orbital configuration of N_2 from which the ground state is derived:

$$\begin{array}{cccccc} (1s_a)^2 & (1s_b)^2 & (\sigma_g 2s)^2 & (\sigma_u 2s)^2 & (\pi_u 2p)^4 & (\sigma_g 2p)^2 \\ \text{NB} & \text{NB} & \text{B} & \text{AB} & \text{B} & \text{B} \end{array}$$

The letters below the orbitals, NB, B, AB, indicate nonbonding, bonding, and antibonding character. It is apparent that there are four bonding *pairs* [two from $(\pi_u 2p)^4$] and one antibonding pair, resulting in strong net bonding of three pairs of electrons. The concept of bonding and antibonding electrons loses most of its meaning and utility when the nuclear charges on the two atoms are different. However, if the charges are not too different, as in CO, the concept remains useful.

C. Vibrational and Rotational Energy of Diatomic Molecules

The classification of electronic levels has been considered in the approximation that the total eigenfunction is separable into an electronic part and a part which depends only on the nuclear coordinates. We now consider briefly the latter part by which vibrational and rotational motion are described. It is simplest to consider the normal or lowest electronic state of a diatomic molecule and to consider the transitions between the vibrational and rotational levels of this particular state, without simultaneous change in the energy of the electrons. These considerations lead to a brief discussion of infrared spectra.

To a good approximation, the rotational and vibrational energy in a diatomic molecule can be separated and can be discussed in terms of simple classical models, modified by quantum restrictions. We shall give here merely the principal results, without quantum mechanical discussion or proof. The vibrational energy, E_v, of a harmonic oscillator is given by

$$E_v = (h/2\pi)(k/\mu)^{1/2}(v + 1/2) = h\omega(v + 1/2)$$

In this formula, μ is the reduced mass, v is the vibrational quantum number with integral values 0, 1, 2, . . ., and k is the force constant in the potential of vibrational motion, $V = kx^2/2$. Note that the energy is not zero in the lowest vibrational energy state, but is $h\omega/2$, which is termed the zero point energy. In the harmonic oscillator approximation, changes of v by ± 1 only are allowed. This selection rule is relaxed if anharmonic terms are added to potential V; then there is no formal restriction on v. In practice, however, there cannot be large changes in v unless the anharmonic terms are large and this is possible only when there is a large change in internuclear distance. There is no way to have this large change so long as there is no electronic excitation. If the equilibrium distances in two electronic states were quite different, we might expect the possibility of change of v by many quanta. We find this frequently in the vibrational structure associated with electronic transitions, but not usually in the infrared. A series of vibrational transitions, which correspond to successive changes in the vibrational quantum number, is known as a progression. The presence of a long progression usually is an indication that the equilibrium distances in two electronic states is quite different. On the other hand, if the potential curves for two electronic states were directly above one another, then the principal transitions are sequences in which the vibrational quantum number has the same numerical value in the two states.

The vibrational term is defined as $E_v/hc = G(v)$ (in reciprocal centimeters).

$$G(v) = \omega_e(v + 1/2) - \omega_e x_e(v + 1/2)^2 + \omega_e y_e(v + 1/2)^3 \cdots \qquad (12)$$

ω_e is the frequency (in reciprocal centimeters) of the harmonic oscillator. x_e and y_e are anharmonic constants. The subscript e here refers to values at the equilibrium internuclear distance.

The rotational energy is discussed on the basis of the model of a rigid rotator. The rotational energy is quantized by a number J, and has the form

$$E_{rot} = (h^2/8\pi^2 I)J(J + 1) \qquad \text{and} \qquad I = \mu R^2$$

where I is the moment of inertia at the rotator. The rotational terms, $E_{rot}/hc = F(J)$ are given by the simple formula

$$F(J) = (h/8\pi^2 cI)J(J + 1) = BJ(J + 1) \tag{13}$$

If the normal electronic state is Σ ($\Lambda = 0$), as is true for most stable diatomic molecules, the selection rule for J requires that it change by $+1$ in absorption or -1 in emission. This rule applied to Eq. 13 leads to a very simple pure rotational spectrum. The rotational levels are at 0, $2B$, $6B$, $12B$, $20B$, . . . and the spacing between adjacent levels, or the transition energies, are $2B$, $4B$, $6B$, ... Such spectra have been observed in the far-infrared region for molecules like HCl and HF, which have a permanent dipole moment. There is no possibility of inducing a dipole moment by rotation. If the rotational energy is large, higher terms result from centrifugal stretching of the molecule. The effect of this is to add a term to $F(J)$ of the form $DJ^2(J + 1)^2$.

If simultaneous rotation and vibration is considered, $F(J) = B_v J(J + 1)$, with B_v defined as B, above in Eq. 13. B_v is taken to be a function of the vibrational quantum number of the form

$$B_v = B_e - \alpha_e(v + 1/2) + \cdots$$

where $B_e = B_v(R/R_e)^2$; R_e is the equilibrium internuclear distance for the lowest electronic state, while R is the effective internuclear distance in the vibration. The constant B_e can be determined from experimental data on rotational transitions in several consecutive vibrational levels. The internuclear distance R_e may thus be found with considerable accuracy. Since we expect B_v to be slightly different for each vibrational state, we write for two such states:

$$\begin{aligned} F(J) &= B_v' J(J + 1) \quad \text{for an upper state} \\ F(J) &= B_v'' J(J + 1) \quad \text{for a lower state} \end{aligned}$$

Transitions between the two vibrational states will occur with a rotational selection rule $\Delta J = \pm 1$ in absorption and in emission. The origin of the transition may be defined as the frequency (missing in this particular case) of the transition between the lowest rotational levels of the two vibrational states. Lines which appear in the spectrum for $\Delta J = +1$ will extend from the origin toward higher frequencies; those for $\Delta J = -1$ will appear on the lower-frequency side of the origin. The higher-frequency lines are said to form a R branch and the lower-frequency lines form a P branch. Since in general B_v' and B_v'' are different, the spacing between consecutive lines in the P and R branches will be somewhat different. If $B_v'' > B_v'$, the lines in the R branch will draw together more closely, and if $B_v'' < B_v'$, lines in the P branch become more close as J is increased. In vibrational transitions which accompany electronic transitions the difference between the B_v values may be so large that the density of lines in one of the branches becomes very large at some value of J and we say that a "head" is formed. At relatively low resolution this is one of the most prominent features observed in these transitions. On the other hand, B_v does not vary greatly in any one electronic state and so heads are not observed usually in infrared spectra.

If $\Lambda \neq 0$, then the selection rules allow $\Delta J = 0, \pm 1$, with the particular transition $J' = 0$ to $J'' = 0$ excluded. The remaining transitions with $\Delta J = 0$ constitute a Q branch. NO, which has a Π ground state, shows a Q branch in its infrared spectrum.

D. Symmetry Properties and Selection Rules for Diatomic Molecules

Selection rules for electronic transitions may be derived simply and elegantly from symmetry properties in a systematic way by group theory. For the diatomic molecule this is not necessary, since the principal results may be derived from our previous discussion of oddness and evenness of eigenfunctions and use of Eq. 11. If the two atoms are identical, there is a center of symmetry and electronic eigenfunctions must be symmetric (g) or antisymmetric (u) to inversion at this center. Consideration of Eq. 11 shows that g states cannot combine (in dipole radiation) with g states, but a g state can combine optically only with a u state. That is, we can have only transitions such as $\Sigma_g \leftrightarrow \Sigma_u$, $\Pi_g \leftrightarrow \Pi_u$. Similarly, electronic eigenfunctions for states with $\Lambda = 0$ are distinguished as Σ^+ and Σ^-, which are symmetric or antisymmetric to reflection in a plane of the nuclei. The selection rule here is $\Sigma^+ \leftrightarrow \Sigma^+$, $\Sigma^- \leftrightarrow \Sigma^-$, $\Sigma^+ \not\leftrightarrow \Sigma^-$. The selection rule for Λ is $\Delta\Lambda = 0, \pm 1$, and for the multiplicity, $\Delta S = 0$, as for an atom. The last rule is strict only for Russell-Saunders coupling.

The total eigenfunction has been regarded approximately as a product of electronic, vibrational, and rotational eigenfunctions. In a diatomic molecule, the vibrational eigenfunction is completely symmetrical to any symmetry operation and it may be disregarded in any discussion of symmetry properties. We discuss now symmetry properties of the rotational eigenfunctions, ψ_{rot}, which we assume depend only on J. The discussion will be limited and simplified by disregard of coupling of rotational and electronic motion.

With these approximations, ψ_{rot} is even when J is even, and odd otherwise. We designate the even levels $J = 0,2,4$ as $+$ for Σ^+ states and the even numbered levels as $-$ for Σ^- states. In addition, if the nuclei are identical, the rotational levels are classified as symmetric (s) and antisymmetric (a) because the operation of inversion will exchange or not exchange the coordinates of the two nuclei. We may thus have four situations for even values of $J = 0, 2, 4, \ldots$: $\Sigma_g{}^+, +, s$; $\Sigma_u{}^+, +, a$; $\Sigma_g{}^-, -, a$; $\Sigma_u{}^-, -, s$. The odd numbered levels show just the reverse ($+, -$) and (s, a) character. The selection rules for transitions between rotational levels are: $(+) \leftrightarrow (-)$ and $(s) \leftrightarrow (s)$, $(a) \leftrightarrow (a)$. The restriction $(s) \not\leftrightarrow (a)$ is extremely rigid, so long as the identical nuclei have zero nuclear spin. The $(+) \leftrightarrow (-)$ rule leads to the selection rule $\Delta J = \pm 1$ in the approximate model assumed. The selection rules $(s) \leftrightarrow (s)$ and $(a) \leftrightarrow (a)$ lead to the following interesting result. In an O_2 molecule composed of single isotopic species ^{16}O, which has zero nuclear spin, suppose that at some time all the molecules were in either symmetric or in antisymmetric rotational states. There is nothing in nature which would change this situation and the molecules would behave as if one set of rotational levels were entirely missing. If we examine the rotational transitions associated with a fixed electronic, vibrational transition, we find that alternate lines in the P and R branches are missing. This is because, of course, consecutive lines represent transitions where J changes by ± 1 and such transitions would be between symmetric and antisymmetric levels.

If the nuclear spins are not zero, then an interchange of coordinates of the nuclei does not lead to a completely identical state, since the orientations of the nuclear spin vectors may differ. In this case transitions will occur also between (s) and (a) levels and as a result there will be an alternation in intensity of consecutive rotational lines in the P and R branches. The relative intensities can be predicted by simple statistical considerations.

The nuclear spin vectors of the identical atoms, $[I(I + 1)]^{1/2}$, form a resultant vector $[T(T + 1)]^{1/2}$. In the case of H_2, $I = 1/2$ for each atom, and T takes values $T = 1, 0$ which means that the nuclear spins point in the same or opposite directions. The normal state of H_2 is $^1\Sigma_g{}^+$ and all the symmetric rotational levels correspond to $T = 0$ and antisymmetric levels to $T = 1$. The statistical weight of any rotational levels is $(2T + 1)$; for $T = 1$ this is 3 and for $T = 0$ it is 1. Thus, the relative populations of the symmetric to the antisymmetric levels are 1:3. This ratio is the intensity ratio of consecutive rotational lines in the spectrum. Conversely, the nuclear spin may be determined precisely from careful experimental measurement of relative intensities of the lines. In the D_2 molecule, we have a different situation because the nuclear spin of the deuterium atom is one and $T = 2, 1, 0$. The ground state of D_2 is also $^1\Sigma_g{}^+$ and the symmetrical rotational levels correspond to the even values of $T = 0, 2$, while the antisymmetrical levels correspond to $T = 1$. But the statistical weight of each symmetrical level is now 6 and for the odd levels is 3. Therefore, the intensity ratio of consecutive lines is 2:1. In general, for larger values of I, there are more even and more odd values of T and in consequence the intensity ratio approaches unity. No alternation in intensity can be observed, for example, in the spectrum of the iodine molecule, where $I = 2.5$ for the ^{127}I atom.

A further interesting result of nuclear spin should be mentioned. In the normal state of H_2 ($^1\Sigma_g{}^+$), the lowest rotational level is symmetric, while the next level, $J = 1$, is antisymmetric. The statistical distribution at room temperature between these levels is $s{:}a = 1{:}3$. However, the distribution at very low temperatures should be quite different so that most of the H_2 molecules would be symmetric. If H_2 is maintained at low temperatures in the presence of a catalyst, it is converted largely to the symmetrical form. If the H_2 is now removed rapidly from the catalyst, it will remain in the symmetrical form at room temperature in the absence of a catalyst. The same situation exists for D_2, but here the predominant form at room temperature is already the symmetric form and the low temperature treatment leads only to some further enrichment with respect to the symmetric form.

It is customary to define the term *ortho* as the modification which is present in larger statistical weight at *high* temperature and *para* as the modification with smaller statistical weight. For H_2, the symmetric form is *para*, while for D_2 it is *ortho*. A molecule such as ${}^{16}O^{16}O$ with zero nuclear spin will not, of course, exhibit *ortho* and *para* forms.

E. Dissociation Energy of Diatomic Molecules

The dissociation energy, D_e, of a diatomic molecule is defined as the difference in energy between the separated atoms and the energy of the molecule when the nuclei are at their equilibrium positions. In Figure 1, this is the distance from the minimum in the potential energy curve to the asymptote. The distance D_0 is measured from the zero vibrational energy level to the asymptote. Evidently, $(D_e - D_0)$ is the zero point energy. From Eq. 12, $G(0) = (\omega_e/2) - (\omega_e x_e/4) + (\omega_e y_e/8)$. In principle, if we knew the positions of all vibrational levels up to the asymptote, we could obtain D_0 directly from infrared spectra. Unfortunately, this information is not available for any case because of extreme experimental difficulties in locating vibrational transitions to states of high vibrational quantum number in the normal state.

The situation is somewhat more fortunate in electronic spectra where frequently long progressions are found because of the change of R_e in the electronic excitation. We may use the data on the excited state progression provided we know the dissociation products at the asymptotes for both normal and excited states and provided the progression actually extends sufficiently close to the dissociation limit so that extrapolation by Eq. 12 is certain. We can assume that the energy difference between the asymptotes is known accurately from data on atomic spectra.

In the favorable example of O_2, the vibrational levels (v') in an upper $({}^3\Sigma_u^-)$ state reached by absorption from the lowest vibrational level $(v'' = 0)$ of the $({}^3\Sigma_g^-)$ normal state, are known from $v' = 0$ effectively to $v' = \infty$. At $v' = \infty$, the molecule dissociates into O $({}^3P)$ + O $({}^1D)$. We know also that the lower state dissociates into O (^{3}P) + O (^{3}P). Therefore, the difference between the dissociation energies of the two states is $E\,(^1\mathrm{D}) - E\,(^3\mathrm{P}) =$ 1.96 eV. Now the dissociation energy of the lower state (D_0'') is found from the difference of energy from the lowest level of the lower state ($v'' = 0$) to the asymptote of the upper state ($v' = \infty$), minus the energy difference between the asymptotes of upper and lower states.

$$[E\,(v' = \infty) - E\,(v'' = 0)] - [E\,(^1\mathrm{D}) - E\,(^3\mathrm{P})] = D_0''$$

or

$$7.05 \qquad - \qquad 1.96 \qquad = D_0'' = 5.09 \text{ eV}$$

The dissociation energy D_0' of the upper state is given by

$$[E\,(v' = \infty) - E\,(v'' = 0)] - [E\,(v' = 0) - E\,(v'' = 0)]$$

or

$$7.05 \qquad - \qquad 6.10 \qquad = D_0' = 0.95 \text{ eV}$$

There are few molecules for which such extensive data are available. In other cases, the dissociation energies are obtained by extrapolation methods and are less exact.

F. Analysis of Spectra of Diatomic Molecules

Discussion of this topic must be restricted to a few general remarks. An analysis starts with a completely resolved spectrum which is not beyond the capabilities of the best modern instruments. We have thus the positions of the rotational levels known with high accuracy. The numbering of the J values for lines in the branches can be established from differences which fit formulas for the rotational terms. The spacing between adjacent levels is a function of moments of inertia of the system. If the identity of the species responsible for the spectrum is known, the spacing can be predicted, particularly when isotopic substitutions in the species are studied. Conversely, rotational structure is frequently helpful in establishment of identity of the species, if it is not known with certainty.

The prediction of spacing is based on mechanical models. The most simple model, which we have discussed, is the simple rotator, in which energy depends on a single quantum number J. In this model, any rotation about the internuclear axis is neglected. Such rotation is associated entirely with electronic motion and can be neglected so long as electronic-rotational coupling is neglected. If a rotation about the axis is included, the model becomes a symmetrical top and the energy depends on a quantum number K, as well as J. This model is essential in discussion of details of coupling of rotational and electronic motion. Reference must be made to specialized texts on spectroscopy for these complex details.

III. THEORY OF POLYATOMIC MOLECULES

A. Classification of Electronic States by Molecular Symmetry

Electronic states of polyatomic molecules may be classified by their multiplicities, just as states of atoms and diatomic molecules are classified. When the nuclear configuration of the electronic state is linear, as in the normal electronic states of CO_2 and C_2H_2, such states may be classified according to the component of orbital angular momentum in the direction of the line of centers as Σ, Π, $\Delta, \ldots$, just as in diatomic molecules. In nonlinear states, orbital angular momentum has little significance because of lack of a unique axis and other systems of classification are necessary. One basis is found in molecular symmetry.

Molecular symmetry has been used to some extent in classification of states of diatomic molecules. Σ states were classified as Σ^+ and Σ^- according to the behavior of the molecular eigenfunction on reflection in a plane of the nuclei and further as (u,g), (odd, even), if a center of symmetry existed. In a polyatomic molecule there may be a larger variety in elements of symmetry, such as axes of various orders and sets of symmetry planes through these axes. The presence of symmetry elements simplifies the description of molecular structure and spectra, essentially because it limits the number of acceptable eigenfunctions and allows a classification of the eigenfunctions according to their behavior with respect to the various rotations about axes and reflections in planes. The classification of eigenfunctions is evidently also a basis of classification of molecular states. The classification also forms a basis for selection rules, not only for electronic transitions, but for vibrational and rotational transitions. Classification of vibrational eigenfunctions by symmetry is of particular importance to the interpretation of electronic transitions, since the vibrational transitions associated with an electronic transition or the vibrational pattern can be resolved in many cases where the resolution of rotational structure is impossible. The vibrational structure or pattern is subject to selection rules for the individual vibrations, with the result that only selected vibrations may appear with particular electronic excitations. In this way, the interpretations of electronic states concerned in optical transitions are facilitated.

Molecular symmetry can be used only if it is discussed in a systematic way. Systematic treatment is made possible by group theory which today is basic to the understanding of crystal structures, molecular structure, and molecular spectra. It is, therefore, essential to give some discussion of group theory as it is applied to molecular spectra. The discussion will be made as simple as possible, with a possible loss of rigor. In many places it will be sufficient to give only results without proof. A more complete treatment of applications will be found in a number of standard texts. We shall be interested principally in the use of group theory to obtain optical selection rules. At the risk of repetition, some of the former specific discussion will be repeated in more general terms and for treatment of the vibrational transition problem application to vibrations of the normal state will be used. While the latter results will apply specifically to infrared and Raman spectra, these spectra really cannot be ignored in treatment of electronic spectra. The results can be transferred readily to problems of simultaneous electronic and vibrational excitation.

IV. APPLICATION OF GROUP THEORY TO MOLECULAR SYMMETRY AND SELECTION RULES

The selection rules for polyatomic molecular spectra are obtained completely from the behavior of the wave functions and the components of a general operator **P** under symmetry operations which are applied to a given molecule. For example, for dipole transitions, **P** is the dipole moment of the molecule, **M**. The wave functions will transform in various ways under these symmetry operations, as will the components of **P**, but the integrand $(\psi_i \mathbf{P} \psi_j)$ must be invariant or remain totally symmetrical under all symmetry operations. The only effect of a symmetry operation, which exchanges the coordinates of identical particles, is to change the order of integration, which has no effect on the value of the integral. On the other hand, if the functions ψ_i, ψ_j, or **P** are of such a nature that the integrand changes sign after a symmetry operation, then the integral must have a value of zero. This statement requires one qualification; if the integrand is transformed into a sum of terms by a symmetry operation, then *one* of these terms must be totally symmetrical or invariant. It is seen that optical transitions are permitted or denied by the transformation properties of wave functions under symmetry operations.

A. Concept of a Group

The concept of a group will be developed by means of a specific example. In Figure 4 configuration (E) shows four points, which may be atoms or groups, lying in the plane of the paper. Points *1* and *4* are identical and points *2* and *3* are identical, but the latter need not be identical with *1* and *4*. The distances *2–1* and *3–4* are equal, as are the angles *123* and *432*. The origin of coordinates (O) is taken at the midpoint of the line which joins *2* and *3*. The x axis is taken along the line *2–3*, and the z axis projects upward from the plane of the figure. Configuration (E) is called the initial figure and is the configuration before any symmetry operation is performed.

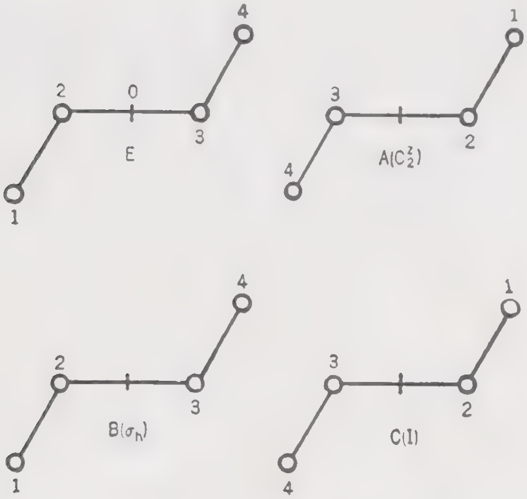

Fig. 4. Configuration of four points.

The figure possesses three elements of symmetry about which symmetry operations may be performed. The result of any symmetry operation is to produce a figure identical with the initial figure. The symmetry elements and the possible symmetry operations are:

(*1*) The identity operation, E, which is no operation and leaves the figure unchanged.

(*2*) The plane of the molecule, in which a reflection σ_h may be made, producing the configuration B from a configuration E. There is no permutation of identical points in this operation, but the z coordinate of every point is changed into its negative by the operation, which distinguishes it from E.

(*3*) A center of symmetry (*O*) through which an operation of inversion I may be performed. This operation consists in reversing the signs of coordinates of all points, so that *1* goes to *4* and *4* to *1*, *2* goes to *3* and *3* to *2*. The result is the configuration C.

(*4*) The twofold axis C_2^z in the z direction around which a rotation by 180° may be made, which transforms the configuration E into the configuration A. The operation is also called C_2^z. In general, an n-fold axis C_n is one about which rotation by 360°/n will produce identical configurations.

These symmetry elements are not all independent; it is seen that the presence of the plane σ_h and the symmetry axis perpendicular to this plane requires the presence of the center of inversion (*O*), and a similar correspondence exists between the operations.

These operations (or these configurations) are said to form a group. The product of any two operations, obtained by following one operation by another, must be equal to another operation of the group. If the configurations E, A, B, C are identified with the operations used to produce them from the initial configuration E, then any product, e.g., BA, must be equal to another configuration. For example, the operation C_2^z followed by I is the same as the operation σ_h, so we may write $I \times C_2^z = \sigma$ or CA = B. Similarly, C_2^z followed by C_2^z is equivalent to E, or AA = E. In this way a multiplication table of elements of the group may be constructed, which shows the results of combined operations. Such a multiplication table is shown in Table I, using the letters E, A, B, and C for the operations E, C_2^z, σ_h, and I. The first operation in a combined operation is looked for in the top row and the following operation in the first left-hand column outside the table. The result is found at the intersection of this row and column. For example, AB (B followed by A) = C; CA = B. The latter result may be verified from the corresponding symmetry operations which have been discussed.

TABLE I
A Group Multiplication Table

	E	A	B	C
E	E	A	B	C
A	A	E	C	B
B	B	C	E	A
C	C	B	A	E

In a sequence of three operations the associative law of multiplication holds: (CB)A = C(BA), as may be verified from Table I. The commutative law AB = BA is not obeyed generally for groups, although it happens to be obeyed for this particular group under discussion. The total number of symmetry operations is equal to the order (h) of the group. For the present group, the order is 4. The particular group under consideration is known as C_{2h}. It is a rotation group C_2 to which is added a reflection plane σ_h.

B. Representations and Character Sets

Any set of elements, which may be numbers or matrices, is said to form a *representation* (Γ_i) of a group, provided that the elements conform to the multiplication table of the group. One representation may be obtained immediately by assigning the number +1 to each element, so that A = B = C = E = +1. It is evident that this set of numbers satisfies the requirements for a representation. This representation (Γ_1) may appear trivial, but it occurs for every group and is known as the totally symmetrical representation. Other representations may be obtained easily from combinations of +1 and

-1. If we assign $+1$ to E and A, and -1 to B and C, then this set forms a representation (Γ_2). In a similar way we obtain the four representations shown in Table II.

TABLE II
Some Representations of the Group C_{2h}

	E	$A(C_2^z)$	$B(\sigma_h)$	C(I)
$\Gamma_1(A_g)$	1	1	1	1
$\Gamma_2(A_u)$	1	1	-1	-1
$\Gamma_3(B_g)$	1	-1	-1	1
$\Gamma_4(B_u)$	1	-1	1	-1

It can easily be shown that Γ_2, Γ_3, and Γ_4 satisfy the requirements for representations. For example, we show that Γ_3 is a representation, with $E = 1$, $A = -1$, $B = -1$, and $C = 1$. If E multiplied in turn by E, A, B, C is written as E(E, A, B, C), then $E(E, A, B, C) = 1(1, -1, -1, 1) = E, A, B, C$, which agrees with the first column of Table I. Similarly, $A(E, A, B, C) = -1(1, -1, -1, 1) = -1, 1, 1, -1 = A, E, C, B$, which agrees with the second column. The remainder of the proof is left to the reader. In a similar way it can be shown that $E, A, B, C = 1, -1, -1, -1$ is *not* a representation, nor is any other combination of ± 1 other than the combinations given in Table II. The four representations given in Table II are not, of course, all the representations which are possible. Further representations may be obtained by attaching vectors x_i, y_i, and z_i to each point i, and writing out the matrices which correspond to transformation of the vectors by the operations. These will be 12 row-12 column matrices, which will not be given here. However, it is possible to reduce these matrices by further *orthogonal* transformations. After the reductions have been carried as far as possible, there are left just the representations $\Gamma_1 \cdots \Gamma_4$. These representations are called *irreducible* representations, and it can be proved that $\Gamma_1 \cdots \Gamma_4$ are the only irreducible representations of this group.

The irreducible representations of the group C_{2h} are extremely simple; for many other groups the irreducible representations are sets of matrices and these are inconvenient to use. However, the sum of diagonal elements of a matrix, called the character (χ), is sufficient for most physical applications, and for all applications which are made here. Each irreducible representation will have a different set of characters. The characters of the representations of the group C_{2h} are identical with the representations themselves.

A product of sets of characters corresponding to two given representations will give the character set of another representation of the group. This may not, however, be an irreducible representation, but may be a reducible representation. The reducible representation can be reduced by orthogonal transformations, and the character set of a reducible representation is a sum of the character sets of irreducible representations. In the present group C_{2h}, the direct product of character sets always gives the character set of another irreducible representation. This is because all of the irreducible representations here are nondegenerate. The degeneracy of such a representation is indicated by the character of the identity operation E. If this is 2 or 3, the irreducible representation is said to be doubly or triply degenerate. Only groups which have an n-fold axis, with $n > 2$, among their symmetry elements, will have degenerate representations.

C. Classification of Eigenfunctions According to Group Theory

We will now show that the eigenfunctions of a molecular system may be classified, and that they are said to belong to definite representations of the symmetry group to which the molecule belongs. By the latter phrase, we mean that the molecule has a natural set of symmetry elements and symmetry operations which are the same as the point operations of a group. The eigenfunctions of molecule ψ_i must satisfy the Schroedinger equation

$$H\psi_i = E_i\psi_i$$

where H is the Hamiltonian operator for the system and the E_i are the eigenvalues of H. We assume that E_i is a nondegenerate energy value, so that no two ψ_i correspond to the same E_i. Then if any symmetry operation R is performed on ψ_i

$$RH\psi_i = RE_i\psi_i$$

However, the total energy operator H is invariant for any symmetry operation which permutes identical particles, and $RH = HR$; furthermore, since E_i is constant, we have

$$H(R\psi_i) = E_i(R\psi_i)$$

This means that $R\psi_i$ also satisfies the wave equation. However, the only functions which satisfy the wave equations—since we suppose that E_i is nondegenerate—are constant multiples of ψ_i; consequently, $R\psi_i = c\psi_i$ and the constant c must be equal to ± 1 in order that $R\psi_i$ shall be normalized. Thus

$$R\psi_i = \pm\psi_i$$

and the functions ψ_i may be classified by a set of operations R, some of which leave ψ_i unchanged, and others which change ψ_i into its negative. The set of coefficients of ψ_i for a given set of operations will be identical with the set of characters of one of the representations of the group. It may be shown in a similar way (9), that if E_i is k-fold degenerate, so that k different ψ_i belong to a given E_i, then a linear combination

$$\psi_{il} = \sum_{j=1}^{k} a_{jl}\psi_{ij} \qquad \left(\sum_{j=1}^{k} a_{jl}{}^2 = 1\right) \tag{14}$$

satisfies the Schroedinger equation, and $R\psi_{il}$ also satisfies the equation. Therefore, eigenfunctions which belong to degenerate eigenvalues E_i may be classified by representations of the group. These functions belong, of course, to representations with the same degree of degeneracy as the corresponding E_i to which the functions belong.

Reference to Table II shows that functions ψ_1 belonging to the representation Γ_1 are totally symmetric to all operations of the group. All other functions are antisymmetrical to two operations. With respect to the operation of inversion, which is of fundamental importance, the functions ψ_1 and ψ_3 (which belongs to Γ_3) are symmetrical, as shown by the transformations

$$I\psi_3 = +\psi_3 \qquad I\psi_1 = +\psi_1$$

The functions ψ_2 and ψ_4 belonging to Γ_2 and Γ_4 are antisymmetrical to this operation, with

$$I\psi_2 = -\psi_2 \qquad I\psi_4 = -\psi_4$$

The functions which are symmetric to I are labeled g, and those which are antisymmetric are labeled u [from *gerade* (even), *ungerade* (odd)]. The two types of g functions ψ_1 and ψ_3 are, respectively, symmetrical and antisymmetrical with respect to rotations by 180° about the symmetry axis $C_2{}^z$ and the corresponding representations are distinguished by the letters A and B, so that $\Gamma_1 = A_g$, $\Gamma_3 = B_g$. The functions ψ_2 and ψ_4 and the representations to which they belong are distinguished in the same way, so that $\Gamma_2 = A_u$ and $\Gamma_4 = B_u$. Furthermore, since ψ_i is associated with a definite E_i, which defines a definite state of the system, the energy states themselves may be classified A_g, A_u, B_g, and B_u for a molecule which belongs to the symmetry group C_{2h}. For molecules which belong to other groups, other distinguishing symbols are used for the representations, types of wave functions, and energy states; these symbols are similar in principle to the above in that they indicate specific behavior with respect to symmetry elements. A complete discussion of symbolism used to describe states of polyatomic molecules is given by Herzberg (10). Symbols for representations in other groups will be given subsequently in the present volume, but limitations of space will not allow a systematic and complete discussion. Whatever symbol is used, it refers to a specific representation and a specific type of wave function of a molecule belonging to a particular group.

D. Selection Rules for Infrared and Raman Transitions

The problem of selection rules will now be discussed. It is required that a product integrand $(\psi_i \mathbf{P} \psi_j)$ be totally symmetrical. We have shown that ψ_i and ψ_j belong to representations of a group. The components of **P** will also belong to and transform like representations of the group. We now replace ψ_i, **P**, and ψ_j by the sets of characters of the representations to which they belong, and obtain $(\chi_i \chi_P \chi_j)$, where χ_i and χ_j are the sets of characters of the representations to which ψ_i and ψ_j belong. χ_P is the set of characters of *one* of the components of **P**. With regard to the latter, if $\mathbf{P} = \mathbf{M}$, as in the calculation of absorption intensities, then we must know to what representations the vector components x, y, z belong. If $\mathbf{P} = \Delta\alpha$, as in the calculation of Raman intensities, then, we must know to what representations the components of polarizability $\Delta\alpha_{xx}$, $\Delta\alpha_{xy}$, $\Delta\alpha_{xz}$, $\Delta\alpha_{zz}$, etc., belong. This information may be obtained directly from the transformation properties of the vector or tensor components, and will be discussed in detail shortly. Now if $(\chi_i \chi_P \chi_j)$, when multiplied out, is directly equal to χ_1, the set of characters of the totally symmetrical representation, then the integral $\mathbf{P}^{ij} = \int \psi_i \mathbf{P} \psi_j \, dv$ will not be zero and a transition will be allowed between the states to which the functions ψ_i and ψ_j belong. The same will be true if the product $(\chi_i \chi_P \chi_j)$ gives a sum of terms, one of which is the set of characters of the totally symmetrical representation. On the other hand, if the product does not give the set of characters of the totally symmetrical representation, or contains this set as one term in a sum of terms, then the integral $\mathbf{P}^{ij} = \int \psi_i \mathbf{P} \psi_j \, dv$ is zero, and the transition is forbidden between states corresponding to ψ_i and ψ_j, at least for one component of **P**. It is evident that all components of **P** must be tried, for the integral may vanish for some components and not for others.

Before giving a detailed illustration of the application of the foregoing principles, we shall give a set of rules by which the components of **P** may be found. We suppose first that $\mathbf{P} = \mathbf{M}$, and that we wish to find the transformation properties of x, y, z for the group C_{2h}. These will be just the transformation properties of vectors pointing in the x, y, and z directions. The x vector will be reversed for the operations C_2^z and I but will remain unchanged in direction for σ_h and E. Hence x transforms with the set of characters $+1, -1, +1, -1$ for E, C_2^z, σ_h, and I, which are the characters for B_u. In the same way it is found that y transforms like B_u. The z vector is unchanged in direction by E and C_2^z but is changed in direction by σ_h and I, and transforms with the characters, $1, 1, -1, -1$ or like A_u. We are now in a position to give the selection rules for infrared and electronic spectra.

Suppose that ψ_i belongs to A_g which may be a definite vibrational (or electronic) state of the molecule. We ask to what possible final states the molecule can go with the absorption or emission of dipole radiation. Suppose that the light is polarized in the z direction. Then we try all possibilities for $(\chi_i z \chi_j)$ which are the products

$$\begin{aligned} A_gA_uA_g &= A_u \\ A_gA_uA_u &= A_g \\ A_gA_uB_g &= B_u \\ A_gA_uB_u &= B_g \end{aligned}$$

This may be verified by direct multiplication of the character sets in Table II. Evidently only $(A_gA_uA_u)$ is totally symmetrical, and the only possibility of transition from an A_g state with light polarized in the z direction will be to A_u states. In the same way it is found that with light polarized in the x direction, the only final states connected with an A_g initial state are of type B_u. The same result is obtained with light polarized in the y direction. This procedure may be simplified by noting that in the triple product $(\chi_i \chi_k \chi_j)$ $(\chi_k \chi_j)$ must be the same as χ_i, for only $(\chi_i \chi_i)$ will give χ_1, the set of characters of the totally symmetrical representation. If the set χ_i belongs to A_g then $(\chi_k \chi_j)$ must give A_g, and the only possibility for this is that $\chi_k = \chi_j$. This means that the final states in transitions from an initial state A_g will be limited to states which have the same sets of characters as the character sets for the components of **P**, or the sets for x, y, or z. In most stable molecules the ground state is totally symmetrical; consequently, the only excited states to which transitions are permitted are those which have the same transformation properties as the components of the dipole moment ($e\mathbf{r}$), that is, states whose eigenfunctions transform like x, y, or z.

This gives the selection rules for infrared absorption spectra, where the transitions usually occur between the lowest (nonvibrating) state of the molecule to a state where one quantum of vibration is excited. The normal vibrations are classified by the irreducible representations to which their wave functions belong. Consequently, it is customary to label the normal vibrations of a molecule by the same symbols as the representations to which the vibrational wave functions belong. It is, of course, possible that there will be no normal vibrations which belong to some representations, and that several may belong to other representations of a group. For example, a molecule with four atoms which conform to the group C_{2h} would have three normal vibrations of type A_g and none of type B_g. The allotment of normal vibrations to the various representations of a group is easily made by group theory. We shall defer this problem for the present.

The selection rules for the Raman effect follow in a similar way, but here $\mathbf{P} = \Delta\alpha$, where α is the polarizability, and the transformation properties of the components of the components $\Delta\alpha_{mn}$ have to be determined. A Raman line will appear if any of the products $(\chi_i \chi_{\Delta\alpha_{mn}} \chi_j)$ are not equal to zero, but will be forbidden if all such products are zero. The permitted Raman lines will correspond to fundamentals of the normal vibrations for which χ_j and $\Delta\alpha_{mn}$ belong to the same representation, since the initial state, which is the ground state, will be assumed to be totally symmetrical, or of the species A_g for the group C_{2h}.

The transformation properties of the components of $\Delta\alpha$ will be somewhat complicated in the general case. If the representations are all nondegenerate (as in the group C_{2h}), then the components of $\Delta\alpha$ will transform like products of coordinates. In the group C_{2h}, $\Delta\alpha_{xx}$ will transform like x times x or like B_u times $B_u = A_g$. $\Delta\alpha_{yy}$ and $\Delta\alpha_{zz}$ will also transform like A_g. $\Delta\alpha_{xy}$ also transforms like x times y or like B_u times $B_u = A_g$. But $\Delta\alpha_{xz}$ transforms like B_u times $A_u = B_g$ and $\Delta\alpha_{yz}$ transforms like B_g. The result is that $\Delta\alpha_{xx}$, $\Delta\alpha_{yy}$, $\Delta\alpha_{zz}$, and $\Delta\alpha_{xy}$ belong to A_g, while $\Delta\alpha_{xz}$ and $\Delta\alpha_{yz}$ belong to B_g.

In the infrared spectra, where the components of $\mathbf{r}$ (instead of $\Delta\alpha$) determine the allowed transitions from a ground state A_g, it was found that the only possible fundamentals were of normal vibrations of the species A_u and B_u. The only fundamentals which can appear in the Raman effect must have the same transformation properties as the components of $\Delta\alpha$ and it has just been found that these are of the species A_g and B_g. As a consequence, no fundamental vibration frequency for a molecule which conforms to the C_{2h} symmetry group can appear in both the Raman effect *and* in the infrared. This result is seen to follow from the presence of a center of symmetry, and the consequent division of the normal vibrations into the types *g* and *u*. An identical result occurs for every molecule with a center of symmetry. The only normal vibrations which are permitted in the infrared must belong to the representations of the components of the dipole moment (coordinates x, y, z) and the latter always belong to *u* representations; accordingly, the infrared fundamentals are all of the *u* type. The converse is true for the permitted Raman frequencies, which must belong to the representations of the components of $\Delta\alpha$. Since, in the present case at least, these transform like products of coordinates, they must of necessity be *g* types. Therefore, all Raman active fundamentals must be of a *g* type. This information is of considerable assistance in structure determinations. It is evident that a center of symmetry can be detected immediately through a comparison of the infrared and Raman spectrum of a compound.

It can also be seen that the use of selection rules has very great general utility for determining the structures of molecules which have some elements of symmetry. Inversion at a center of symmetry provides, perhaps, the greatest number of restrictions on the number of allowed transitions, but other symmetry elements and operations also offer restrictions. Consequently, a first step in determining geometric structure is to require complete data on the Raman and infrared spectra of the molecule. The depolarization ratios of the Raman lines are of further assistance. Then selection rules are developed for groups which correspond to possible symmetrical arrangements of the nuclei in the molecule, from which the allowed transitions are predicted and compared with observed spectra. In some cases of relatively high symmetry, selection rules for both types of spectra may forbid a fundamental. This does not happen in the group C_{2h} but occurs with other groups. Such predictions are also of value.

E. Enumeration of Normal Vibrations Belonging to a Representation

We shall now describe a method of finding the number of normal vibrations which belong to a given representation of a group. All the wave functions for all the normal vibrations must belong to the reducible representation of a group, and so the problem becomes one of finding the number of times (a_i) a given representation Γ_i is contained in the reducible representation Γ_r. If $\chi_r(R)$ is the character for the operation R in the reducible representation and $\chi_i(R)$ is the character for the same operation R in the ith irreducible representation of the group, then group theory gives the result (11)

$$a_i = \frac{1}{h}\sum_R \chi_r(R)\chi_i(R) \tag{15}$$

where h is the order of the group. The characters $\chi_i(R)$ are found in tables of characters; for the group C_{2h}, they are given in Table I. In order to use Eq. 15, it is necessary to find the characters $\chi_r(R)$. In the method given for finding these characters, use is made of the fact that terms will appear on diagonals of the transformation matrices for coordinates only for atoms (or points) which are unshifted or unpermuted in an operation R. Hence, we only have to obtain the transformation matrices for unshifted atoms; the character, which is the sum of diagonal terms, will be zero for all points or atoms which are permuted by R. Consider now a molecule with four identical atoms, which conforms to the symmetry group C_{2h}. Figure 4 will illustrate this case, if the points 1, 2, 3, 4 are identical. It is seen easily that the operations C_2^z and I shift all atoms, and hence, $\chi_r(C_2^z)$ and $\chi_r(\mathrm{I})$ are zero. The operation E leaves four atoms unshifted. For each atom, i, $x_i = x_i'$, $y_i = y_i'$, and $z_i = z_i'$ ($i = 1 \cdots 4$), so that the transformation matrix will have 12 rows and 12 columns. The diagonal elements will all be $+1$, and the off-diagonal elements will all be zero. The character $\chi_r(\mathrm{E})$ is therefore 12. The same result is obtained by considering each atom separately. For each the transformation matrix is

$$\begin{vmatrix} 1 & 0 & 0 \\ 0 & 1 & 0 \\ 0 & 0 & 1 \end{vmatrix}$$

and the total character is obtained by multiplying the character for one atom ($\chi = 3$) by the number of unshifted atoms (4), giving $\chi_r(\mathrm{E}) = 12$, as before. For σ_h, there are again four unshifted atoms. However, if vectors x, y, z are attached to each of the four unshifted atoms and reflection in the xy plane is made, z goes to $-z$, while x goes to x and y to y. The transformation matrix is now

$$\begin{vmatrix} 1 & 0 & 0 \\ 0 & 1 & 0 \\ 0 & 0 & -1 \end{vmatrix}$$

for which the character is $+1$ for each atom, giving $\chi_r(\sigma_h) = 4$ for the four atoms. The set of characters for χ_r are therefore 12 0 4 0 for the operations E, C_2^z, σ_h, and I. We may now apply Eq. 15 to the characters of each of the representations in turn, and we obtain, since the order of this group is 4

$$\begin{aligned} a(\mathrm{A}_g) &= (1/4)(12 + 0 + 4 + 0) = 4 \\ a(\mathrm{A}_u) &= (1/4)(12 + 0 - 4 + 0) = 2 \\ a(\mathrm{B}_g) &= (1/4)(12 + 0 - 4 + 0) = 2 \\ a(\mathrm{B}_u) &= (1/4)(12 + 0 + 4 + 0) = 4 \end{aligned}$$

It is seen that the representations A_g and B_u are each contained four times in the reducible representation, while the representations A_u and B_g are each contained twice. These numbers a_i do not give us the number of normal vibrations which belong to each representation, but they give us the distribution of the $3N$ (N = number of atoms) mechanical modes of motion of the molecule. The number of normal vibrations which belong to each representation will be found by subtracting from each a_i, the number of translations (T) and rotations (R) which belong to this representation.

The characters T_x, T_y, T_z for translation of the molecule as a whole in the x, y, z directions will be identical with those which have already been found for the components x, y, z of the vector **r**. It follows that in the group C_{2h}, T_z transforms like A_u and T_x and T_y belong to B_u.

The characters for the rotations R_x, R_y, R_z of the molecular system as a whole about fixed axes x, y, z are found from the following considerations. For convenience we use the geometry of Figure 4, and take the fixed axes to be identical with the molecular axes. We now imagine that each axis has attached to it a small perpendicular plane, in which a vector is rotating. The behavior of the rotations of the vectors about the axes when a symmetry operation is applied will be the same as the behavior of the components of angular momentum M_x, M_y, M_z about the respective axes. If p_x, p_y, p_z

are the components of linear momentum in the x, y, z directions, then

$$\begin{array}{ll} M_x = yp_z - zp_y & \text{transforms like } R_x \\ M_y = zp_x - xp_z & \text{transforms like } R_y \\ M_z = xp_y - yp_x & \text{transforms like } R_z \end{array} \tag{16}$$

If now a rotation by any angle φ is made about an axis C in the z direction, a vector such as the angular momentum with components M_x, M_y, M_z will be transformed according to the equation

$$\mathrm{C}^z(\varphi) \begin{vmatrix} M_x \\ M_y \\ M_z \end{vmatrix} = \begin{vmatrix} \cos\varphi & \sin\varphi & 0 \\ -\sin\varphi & \cos\varphi & 0 \\ 0 & 0 & 1 \end{vmatrix} \begin{vmatrix} M_x \\ M_y \\ M_z \end{vmatrix}$$

In our present case, the rotation is made by the angle 180°, and identifying M_x with R_x, etc., since they transform in the same way (Eq. 16), we have

$$\mathrm{C}_2{}^z \begin{vmatrix} R_x \\ R_y \\ R_z \end{vmatrix} = \begin{vmatrix} -1 & 0 & 0 \\ 0 & -1 & 0 \\ 0 & 0 & 1 \end{vmatrix} \begin{vmatrix} R_x \\ R_y \\ R_z \end{vmatrix} \tag{17}$$

Similarly, for the operation E, the angle φ is zero and

$$\mathrm{E} \begin{vmatrix} R_x \\ R_y \\ R_z \end{vmatrix} = \begin{vmatrix} 1 & 0 & 0 \\ 0 & 1 & 0 \\ 0 & 0 & 1 \end{vmatrix} \begin{vmatrix} R_x \\ R_y \\ R_z \end{vmatrix} \tag{18}$$

The operation of reflection σ_h is made in the xy plane, and it is instructive to note the behavior of the coordinates and linear momenta in Eq. 16 under this operation. It is easily seen that z and p_z are converted into their negatives; all other coordinates and linear momenta are unchanged. Direct substitution of $-z$ for z, $-p_z$ for p_z, in Eq. 16 shows that M_x goes to $-M_x$, M_y goes to $-M_y$, M_z goes to $+M_z$, and this transformation is the same as for R_x, R_y, and R_z for the operation σ_h. Accordingly

$$\sigma_h \begin{vmatrix} R_x \\ R_y \\ R_z \end{vmatrix} = \begin{vmatrix} -1 & 0 & 0 \\ 0 & -1 & 0 \\ 0 & 0 & 1 \end{vmatrix} \begin{vmatrix} R_x \\ R_y \\ R_z \end{vmatrix} \tag{19}$$

Finally, the transformation of R_x, R_y, and R_z under the operation I is obtained from the product of the transformation matrices in Eqs. 17 and 19, since C_2^z followed by σ_h is equivalent to I. Therefore, $\sigma_h \times C_2^z = I$, and

$$\mathrm{I}\begin{vmatrix} R_x \\ R_y \\ R_z \end{vmatrix} = \begin{vmatrix} -1 & 0 & 0 \\ 0 & -1 & 0 \\ 0 & 0 & 1 \end{vmatrix}\begin{vmatrix} -1 & 0 & 0 \\ 0 & -1 & 0 \\ 0 & 0 & 1 \end{vmatrix}\begin{vmatrix} R_x \\ R_y \\ R_z \end{vmatrix} = \begin{vmatrix} 1 & 0 & 0 \\ 0 & 1 & 0 \\ 0 & 0 & 1 \end{vmatrix}\begin{vmatrix} R_x \\ R_y \\ R_z \end{vmatrix} \tag{20}$$

The characters for R_x, R_y, and R_z for the operations of the group may now be read from Eqs. 17, 18, 19, and 20. From these matrix equations we have

$$\begin{array}{lll} \mathrm{E}\ \ R_x = R_x & \mathrm{E}\ \ R_y = R_y & \mathrm{E}\ \ R_z = R_z \\ C_2^z\ R_x = -R_x & C_2^z\ R_y = -R_y & C_2^z\ R_z = R_z \\ \sigma_h\ \ R_x = -R_x & \sigma_h\ \ R_y = -R_y & \sigma_h\ \ R_z = R_z \\ \mathrm{I}\ \ R_x = R_x & \mathrm{I}\ \ R_y = R_y & \mathrm{I}\ \ R_z = R_z \end{array}$$

from which it is seen that R_x transforms like the character set 1, −1, −1, 1 which is the set for B_g (Table II). R_y also transforms like B_g, while R_z transforms like A_g.

In Table III we repeat the characters of the representations from Table II. In addition the characters of the reducible representation for the system of four identical points are given in the bottom row. In the first column to the right of the characters, the values of a_i from Eq. 15 are given, and in the next three columns the number of translations, rotations (a_R), and normal vibrations (a_v) which belong to the various representations are given. Finally, in the last column, the predicted activity of the normal vibrations is given; IR means that the fundamental is allowed in the infrared spectrum, and Ram. that it is allowed in the Raman effect. It has been pointed out that no fundamentals may appear in both types of spectra for this case.

TABLE III

Symmetry Properties of a Four-Atom Molecule Belonging to C_{2h}

	E	C_2^z	σ_h	I	a_i	a_T	a_R	a_v	Activity
A_g	1	1	1	1	4		R_z	3	Ram.
A_u	1	1	−1	−1	2	T_z		1	IR
B_g	1	−1	−1	1	2		R_z, R_y	0	
B_u	1	−1	1	−1	4	T_x, T_y		2	IR
χ_r	12	0	4	0					

F. Application to *Trans*- and *Cis*-Dichloroethylene

No molecule with four atoms is known which conforms to the symmetry group C_{2h}, but symmetrical *trans* compounds of the type

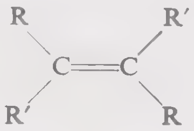

will have this symmetry group. The six-atom molecule *trans*-dichloroethylene is the simplest example. The character table and results for a_t, a_T (number of translations), a_R (rotations), and a_v (number of vibrations), with Raman or infrared activity, are given in Table IV. It is to be noted that the characters of the irreducible representations are, of course, the same as in Table III for the four-atom molecule. The characters of the reducible representation are different, owing to the fact that we have six, rather than four, atoms. The sum of the a_t $(= 3N)$ is accordingly different as is the number of fundamental normal vibrations. The distribution and number of translations and rotations are the same as for the four-atom case. Table IV shows that the 12 normal vibrations are distributed 5, 2, 1, and 4 to the representations A_g, A_u, B_g, and B_u, respectively. In the Raman effect there should appear six lines, five of which (belonging to A_g) should show low depolarization ratios, while the sixth (B_g) line should be depolarized to the limit. Six fundamental frequencies should appear in the infrared spectrum, all of which are different from those allowed in the Raman effect, so that there are no coincidences. This is what is observed experimentally (12).

TABLE IV

Symmetry Properties of a Six-Atom Molecule Belonging to the Group C_{2h}

	E	C_2^z	a_h	I	a_t	a_T	a_R	a_v	Activity
A_g	1	1	1	1	6		R_z	5	Ram.
A_u	1	1	−1	−1	3	T_z		2	IR
B_g	1	−1	−1	1	3		R_x, R_y	1	Ram.
B_u	1	−1	1	−1	6	T_x, T_y		4	IR
χ_r	18	0	6	0					

It is of interest to contrast the results predicted for the *cis* isomer. *cis*-Dichloroethylene belongs to the symmetry group C_{2v}, and its geometry is shown in Figure 5. The twofold symmetry axis C_2^z lies in the plane of the paper, which is the *xz* plane. The *y* axis projects upward from the plane of the paper from the midpoint of the line joining the two carbons. This point is

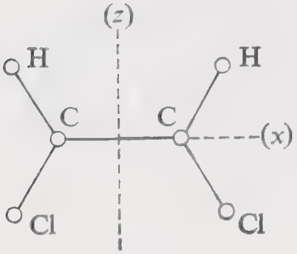

Fig. 5. Model of *cis*-dichloroethylene.

the origin of coordinates, but it is no longer a center of symmetry. In addition to the axis C_2^z, coincident with the z axis, and the plane of the molecule $\sigma_v(xz)$, there is a symmetry plane $\sigma_v(yz)$ through the C_2^z axis and perpendicular to the plane of the molecule. It is not proper to designate either plane σ_h, because there is no symmetry axis perpendicular to either plane.

The representations, character sets, and number of translations, rotations, and normal vibrations which belong to each symmetry class are given in Table V, just as for *trans*-dichloroethylene in Table IV. There are several

TABLE V

Symmetry Properties of a Six-Atom Molecule Belonging to the Group C_{2v}

	E	C_2^z	$\sigma_v(xz)$	$\sigma_v(yz)$	a_t	a_T	a_R	a_v	Activity
A_1	1	1	1	1	6	T_z		5	Ram., IR
A_2	1	1	−1	−1	3		R_z	2	Ram.
B_1	1	−1	1	−1	6	T_x	R_y	4	Ram., IR
B_2	1	−1	−1	1	3	T_y	R_x	1	Ram., IR
χ_r	18	0	6	0					

important differences which should be pointed out. Although there is a one-to-one correspondence between the sets of characters of the representations for C_{2h} and C_{2v}, A_1 and A_2 of C_{2v} do not correspond to A_g and A_u of C_{2h}; wave functions belonging to these representations differ by their behavior on reflection in the plane σ_v (yz) and in σ_v (xz). A and B are distinguished by their behavior with respect to rotation about the symmetry axis C_2^z. The number and distributions of normal vibrations are seen to correspond in the two dichloroethylenes, but the selection rules are profoundly modified. From Table V, it is seen that fundamental vibrations of species A_1, B_1, and B_2 of the *cis* form will be allowed in the infrared, accounting for ten fundamentals (compare with six allowed for the *trans* form). Furthermore, *all* of the fundamentals will be allowed in the Raman effect by one or more of the components of $\Delta\alpha$. It is easily found that the polarizability components transform like the product of coordinates; from Table V it is seen that $\Delta\alpha_{xx}$, $\Delta\alpha_{yy}$, and $\Delta\alpha_{zz}$ transform like A_1, $\Delta\alpha_{xy}$ like A_2, $\Delta\alpha_{xz}$ like B_1, and $\Delta\alpha_{yz}$ like B_2. The five lines of species A_1 will be partly depolarized, while the other seven will be depolarized to the limit. The observed Raman and infrared spectra of *cis*-dichloroethylene agree in all details with these predictions. Although we are not interested primarily in applications to chemical analysis, it might be pointed out that a mere count of the number of Raman lines would serve to distinguish one pure form from the other, or to detect small quantities of the *cis* form in supposedly pure *trans* form. Of more importance is the possibility of utilizing the relative intensities as a basis of quantitative analysis.

G. The Benzene Molecule

As a more complicated example of the use of infrared and Raman spectra in structure determinations, we shall consider the benzene molecule, which is well known to have the shape of a regular plane hexagon, and belongs to the symmetry group D_{6h}. We shall pretend that these facts are not well established, but shall consider that this structure is a possibility which is to be confirmed by spectroscopic evidence. This case has been treated extensively, both theoretically and experimentally, by Ingold and his co-workers (13). The pertinent geometric facts are shown in Figure 6, and the symmetry elements and operations are set out as follows: Symmetry elements, Group D_{6h}: one sixfold axis at center O; three twofold axes T, U, V, passing through opposite C and H atoms; three twofold axes P, Q, R bisecting angles TOU, UOV, and VOT; center of inversion at O; plane of molecule σ_h; three planes σ_v'' through T, U, $V \perp \sigma_h$; three plane σ_v' through P, Q, $R \perp \sigma_h$.

Not all of these elements are independent. The operations follow:

Operations about the sixfold axis. Two (C_6) rotations by $\pm 2\pi/6$, in one

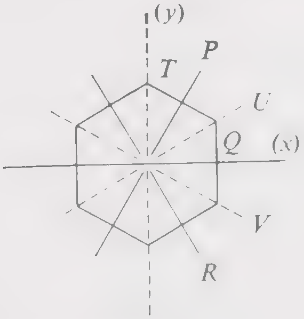

Fig 6. Axes in benzene.

symmetry class. Two (C_3) rotations by $\pm 2\pi/3$, in one symmetry class. One (C_2) rotation by $2\pi/2$, in a separate class.

Operations about the axes *TUV*. Three rotations (C_2'') by π, one about each axis. All these rotations are in the same symmetry class.

Operations about the axes *PQR*. Three rotations (C_2') by π, in one class. One rotation about each of the axes *P*, *Q*, *R*.

Operation I. Inversion at the center *O*, one class.

Operation E. One class.

The *other operations* may best be considered as combined operations, and will be the rotations followed by inversion at *O*. They are

$I \times C_2 = \sigma_h$, reflection in the plane of the molecule, one class.
$I \times 2C_3 = 2S_6$, two rotary reflections, rotations by $\pm 2\pi/3$ followed by I, one class.
$I \times 2C_6 = 2S_3$, two rotary reflections, rotations by $\pm 2\pi/6$ followed by I, one class.
$I \times 3C_2' = 3\sigma_v''$, reflections in the three planes perpendicular to σ_h through the axes *T*, *U*, *V*, all in one class.
$I \times 3C_2'' = 3\sigma_v'$, reflections in the three planes perpendicular to σ_h through the axes *P*, *Q*, *R*, in one class.

It should be noted in the foregoing that there are 24 operations, but only 12 symmetry classes. All symmetry operations which are in the same class have the same transformation matrix and the *same character*. The number of operations in a given class is given by the coefficient before the symbol for the operation. The order of the group, h, is the total number of *symmetry operations* (not the number of classes) and is 24 for the group D_{6h}. The number of irreducible representations is equal to the number of symmetry *classes*, or 12. In the groups C_{2h}, and C_{2v} which have been discussed, each symmetry operation formed a separate class and the idea of a symmetry class was not previously introduced. It may be said that the symbol for the group D_{6h} carries this meaning: if a twofold axis is added perpendicular to an *n*-fold axis, then an additional number of twofold axes are required equal to $(n - 1)$. The *n*-fold axis and the set of *n* twofold axes form a dihedral group D_n. In this case $n = 6$, which is the order of the principal axis. If, in addition, a plane of symmetry exists perpendicular to the *n*-fold axis, then for even *n*, a center of symmetry is required. The addition of the subscript h (for the plane σ_h) completes the symbol D_{6h}.

The character sets are given in Table VI, where the representations are shown, as usual, in the left-hand column. The last row gives the characters of the reducible representation for a molecule with 12 atoms, C_6H_6 or C_6D_6. The columns to the right of the characters show the number of times (a_i)

TABLE VI

Symmetry Properties of a Twelve-Atom Molecule Belonging to D_6h

							(IC_2)	$(2IC_3)$	$(2IC_6)$	$(3IC_2)''$	$(3IC_2')$						
	E	C_2	$2C_3$	$2C_6$	$3C_2''$	$3C_2'$	I	σ_h	$2S_6$	$2S_3$	$3\sigma_v'$	$3\sigma_v''$	a_t	a_T	a_R	$\Delta\alpha$	a_v	Activity
A_{1g}	1	1	1	1	1	1	1	1	1	1	1	1	2			$\alpha_{xx}^2 + \alpha_{yy}^2 \cdot \alpha_{zz}$	2	Ram.
A_{2g}	1	1	1	1	−1	−1	1	1	1	1	−1	−1	2		R_2		1	Ina.
B_{1g}	1	−1	1	−1	1	−1	1	−1	1	−1	1	−1	0				0	
B_{2g}	1	−1	1	−1	−1	1	1	−1	1	−1	−1	1	2				2	Ina.
E_{1g}	2	−2	−1	1	0	0	2	−2	−1	1	0	0	2 (2)		R_x, R_y	α_{xy}, α_{yz}	1 (2)	Ram.
E_{2g}	2	2	−1	−1	0	0	2	2	−1	−1	0	0	4 (2)			$\alpha_{xx}^2 - \alpha_{yy}^2, \alpha_{xy}$	4 (2)	Ram.
A_{1u}	1	1	1	1	1	1	−1	−1	−1	−1	−1	−1	0				0	
A_{2u}	1	1	1	1	−1	−1	−1	−1	−1	−1	1	1	2	T_z			1	IR.
B_{1u}	1	−1	1	−1	1	−1	−1	1	−1	1	−1	1	2				2	Ina.
B_{2u}	1	−1	1	−1	−1	1	−1	1	−1	1	1	−1	2				2	Ina.
E_{1u}	2	−2	−1	1	0	0	−2	2	1	−1	0	0	4 (2)	T_x, T_y			3 (2)	IR
E_{2u}	2	2	−1	−1	0	0	−2	−2	1	1	0	0	2 (2)				2 (2)	Ina.
χ_r	36	0	0	0	−4	0	0	12	0	0	0	4						

that each irreducible representation is contained in the reducible representation, the transformation properties of the translations and rotations, the number, a_v, of normal vibrations belonging to each representation, the transformation properties of the components of $\Delta\alpha$ which determine the Raman activity, and finally the activity of the normal vibrations in the Raman effect (Ram.) and in the infrared (IR). It is to be noted that a number of vibrations are not allowed in either spectrum; these are marked Ina. (inactive).

There are several features of Table VI which require additional comment. The representations are divided into u and g because of the center of inversion. A, B are nondegenerate representations and are distinguished by their behavior under rotation by π and $\pi/3$ about the sixfold axis. They are subdivided further into A_1, A_2, B_1, B_2 by their behavior on rotation about the T, U, V and P, Q, R axes. There are two twofold degenerate representations of the g type and two of the u type. E_1 and E_2 differ by their behavior under rotations about the sixfold axis. This degeneracy, which arises because of the set of twofold axes perpendicular to the sixfold axis, causes several complications. The rotations R_x, R_y about axes x and y (which lie in the plane of the molecule) are equivalent, and transform like a degenerate pair. The same is true for the translations T_x, T_y. When these translations and rotations are subtracted from the a_v, a degenerate pair should be counted as *one*. In Table VI, it should be remembered that the total number of normal vibrations will be 20, not $30 = (3N - 6)$, for 10 of the 20 normal vibrations are doubly degenerate. These are marked (2) in Table VI.

Table VI shows another interesting feature. It has been divided by lines into four parts. The upper left quarter, disregarding the symbol g, shows just the sets of characters for the representations and symmetry operations for the group D_6. The bottom left and top right quarters are merely duplicates of the top left. This is because I and products of I with other operations do not appear above the lower left section, and there is no difference between u and g. In the top right section I and its products do not change the characters of g representations. But there is a complete reversal of sign for every character in the lower right section. The complete set of characters may be written out easily from the characters of D_6, and the added operation of inversion, in the manner just indicated.

The characters for the reducible representation are obtained as follows. Rotations about the sixfold axis shift all atoms and the characters for the corresponding operations are zero. So $\chi_r(C_6) = \chi_r(C_3) = \chi_r(C_2) = 0$. The same is true for $\chi_r(C_2')$ and $\chi_r(I)$, $\chi_r(S_6)$, $\chi_r(S_3)$, $\chi_r(\sigma_v')$, since all atoms are shifted by these operations. The only operations which leave atoms unshifted are E, C_2'', σ_h, and σ_v''. For E, no atoms are shifted and $\chi_r(E) = 3N = 36$. In σ_h no atoms are shifted by reflection in the plane of the molecule. However, the z coordinate of each of the twelve atoms changes sign, while the x and y coordinates are unchanged, giving the transformation matrix

$$\begin{vmatrix} 1 & 0 & 0 \\ 0 & 1 & 0 \\ 0 & 0 & -1 \end{vmatrix}$$

for each atom, or a character of $+1$ per atom. Hence, $\chi_r(\sigma_h) = 12$.

The same result is obtained, of course, from the 36 by 36 transformation matrix resulting from 12 sets of simultaneous equations $x_i' = x_i$, $y_i' = y_i$, $z_i' = -z$ $(i = 1 \cdots 12)$. For each operation C_2'', four atoms (two C and two H) are unshifted. With C_2 about T, lying in the y direction

$$\begin{aligned} x_i' &= -x_i \\ y_i' &= y_i \quad (i = 1 \cdots 4) \\ z_i' &= -z_i \end{aligned}$$

This gives $\chi_r(C_2'', T) = -4$. The same result is obtained for rotation about the axes U and V. Similarly, on reflection in a plane σ_v'' through T, there are four unshifted atoms, for which $x_i' = -x_i$, $y_i' = -x_i$, $y_i' = y_i$, $z_i' = z_i$, and $\chi_r(\sigma_v'') = 4$. In this way the character set χ_r in the lowest row of Table VI is obtained.

The quantities a_i are easily computed by the equation

$$a_i = (1/h) \sum_R \chi_r(R)\chi_i(R) \tag{15}$$

from the characters $\chi_r(R)$ just deduced, and the characters or the representations i. In doing this care must be taken to sum over *operations*, and to multiply the characters for a symmetry class by the coefficient which precedes it, and which gives the number of operations (R) in a class. We give two examples $a(B_{1g})$ and $a(E_{2g})$. The reader may easily verify the other values of a_i in Table VI.

$$a(B_{1g}) = 1/24(36 - 0 + 0 - 0 - 12 - 0 + 0 - 12 + 0 - 0 + 0 - 12) = 0$$
$$a(E_{2g}) = 1/24(72 + 0 - 0 - 0 - 0 + 0 + 0 + 24 - 0 - 0 + 0 + 0) = 4$$

We shall not give the details of how the transformation properties of the translations and rotations are obtained. The translations offer no difficulties, but the rotations, which belong to the degenerate representation, are more difficult. The transformation properties of the components of $\Delta\alpha$ are complicated by the degeneracy; only $\Delta\alpha_{zz}$ transforms in a simple way.

The last column of Table VI, showing the activity in the Raman effect and in infrared spectra of the fundamentals of the normal vibrations, is of interest. Of the 20 fundamentals, seven are allowed in the Raman effect, and two of these should have low depolarization ratios. The others should be depolarized to the limit. Four fundamentals are allowed in the infrared, of which one is allowed for light polarized perpendicular to the plane of the benzene ring, and three for light polarized in the plane of the ring. Because of the plane of symmetry, fundamentals which are allowed in the Raman effect are forbidden in the infrared, and the converse is true. Nine fundamentals of symmetry species A_{2g}, B_{2g}, B_{1u}, B_{2u}, and E_{2u} are not allowed to appear in either spectra.

The agreement of the experiments with these theoretical predictions, as shown by Ingold and his co-workers (13), can be regarded as a major triumph of theory in the interpretation of spectra, and gives confidence in the theory as a whole. The D_{6h} structure is strongly supported by similar studies on benzene derivatives. It is interesting, however, to compare the predictions made on the basis of other symmetrical models of benzene, some of which were formerly thought to be highly probable, or even correct. A single Kekulé structure corresponds to a group D_{3h}, which has no center of symmetry. We may also consider a puckered ring (14), with alternate carbon atoms equidistant above and below a plane, which corresponds to a model with a group D_{3d}. Finally, we consider a model (group C_{6h}) in which the H atoms are in a separate plane parallel to the C atoms. A summary of expectations from these models are shown in Table VII, which is self-explanatory. It is clear that none of the other structures can account for the observed Raman and infrared spectrum of benzene.

TABLE VII
Possible Symmetry Models of Benzene

Group	D_{6h}	D_{3h}	D_{3d}	C_{6v}	No. of observed fundamentals
No. of Raman fundamentals	7	14	9	13	7
No. of above with low ρ	2	4	4	3	2
No. of infrared fundamentals	4	10	8	7	4
No. of inactive fundamentals	9	3	3	7	—
Center of symmetry	Yes	No	Yes	No	
Coincidences (fundamentals observed in both spectra)	0	7	0	7	0

H. Overtone and Combination Frequencies

It is relatively simple to obtain the selection rules, or the conditions for zero or nonzero intensity, for more complicated vibrational transitions by the method of group theory. The wave functions which represent the two vibrational levels connected by the absorption of overtone and combination frequencies will transform like products of the wave functions for the fundamental levels. For example, if we consider the nth level of the lth normal vibration [the $(n-1)$th overtone], then the wave function $\psi_j(nv_l)$ will transform like $[\psi_j(v_l)]^n$. But the latter will transform like the character set of the irreducible representation to which $\psi_j(v_1)$ belongs, raised to the nth power, or like $(\chi_l)^n$. A simple extension of this treatment to a combination frequency $n\nu_l \pm m\nu_m$ shows that the corresponding wave function $\psi_j\ (nv_l \pm mv_m)$ will transform like $(\chi_l)^n(\chi_m)^m$. The generalization to a more complicated combination frequency is made easily.

If the transition occurs from the normal (nonvibrating) state of the molecule, as is assumed in absorption, then the wave function for the initial state in the transition will usually transform like (χ_1), the set of characters for the totally symmetrical representation. If the excited vibrations are nondegenerate, then the product $(\chi_l)^n(\chi_m)^m$ is always the character set of an irreducible representation. Furthermore, for overtones

$$(\chi_l)^{(2p+1)} = (\chi_l) \qquad \text{and} \qquad (\chi_l)^{2p} = (\chi_1)$$

which means that an even overtone $(2p)\nu_l$ of a nondegenerate vibration will be totally symmetrical, while an odd overtone will transform like the fundamental of the same species.

If one or more of the vibrations are degenerate, then the product of characters corresponds to a reducible representation of the group, which frequently has a high dimension. The resulting state of a molecule with many such vibrations excited simultaneously will have a degeneracy which is equal to the dimension of this reducible representation. But this degenerate state will be split, in general, by the anharmonic forces into a number of states of lower degeneracy. This splitting corresponds to a reduction of the reducible representation of all the multiply excited vibrations into the irreducible representations to which the single vibrations belong. The problem is thus to find the number of times (a_i) which an irreducible representation with a character set χ_i is contained in the reducible representation of all the vibrations (with a character set χ_r). This information may be obtained by application of the familiar formula of Eq. 15.

As an illustration, we consider in detail the vibrational state of benzene which arises when one quantum each of the vibrations $\nu_3(A_{2g})$, $\nu_{12}(E_{1u})$, $\nu_{13}(E_{2u})$, and $\nu_{14}(E_{1u})$ is excited. The wave function for this excited vibrational state will transform like the product of characters of the representations

$$A_{2g} \times E_{1u} \times E_{1u} \times E_{1u} = A_{2g} \times (E_{1u})^3$$

It is found, from Table VI, that this product is the set of characters

$$\chi_r(A_{2g} \times (E_{1u})^3 = 8, -8, -1, 1, 0, 0 \mid -8, 8, 1, -1, 0, 0$$

The excited state is thus eightfold degenerate. The character set is divided by a vertical line to correspond to the lines of Table VI. In the application of Eq. 15 we note that the characters (χ_r) to the right of the line are the negatives of those to the left. We need not then try for (χ_i) any of the sets of the g representations in Table VI, since these sets are the same on both sides of the line and the corresponding sums, $\sum_R \chi_r(R)\chi_i(R)$, must be zero. Therefore, none of the states which result from the splitting of the eightfold degenerate state will be g type. Trials for the u states leads to:

$$\begin{aligned}
a(\mathrm{A}_{1u}) &= (8 - 8 - 2 + 2 + 0 + 0 + 8 - 8 - 2 + 2 + 0 + 0)/24 = 0\\
a(\mathrm{A}_{2u}) &= (8 - 8 - 2 + 2 + 0 + 0 + 8 - 8 - 2 + 2 + 0 + 0)/24 = 0\\
a(\mathrm{B}_{1u}) &= (8 + 8 - 2 - 2 + 0 + 0 + 8 + 8 - 2 - 2 + 0 + 0)/24 = 1\\
a(\mathrm{B}_{2u}) &= (8 + 8 - 2 - 2 + 0 + 0 + 8 + 8 - 2 - 2 + 0 + 0)/24 = 1\\
a(\mathrm{E}_{1u}) &= (16 + 16 + 2 + 2 + 0 + 0 + 16 + 16 + 2 + 2 + 0 + 0)/24 = 3\\
a(\mathrm{E}_{2u}) &= (16 - 16 + 2 - 2 + 0 + 0 + 16 - 16 + 2 - 2 + 0 + 0)/24 = 0
\end{aligned}$$

The eightfold degenerate state which results from the excitation of one frequency of species A_{2g} and three frequencies of type E_{1u} therefore splits into one B_{1u} state, one B_{2u} state, and three E_{1u} states. Transition to the E_{1u} state and hence to the combination level of the degenerate state will be allowed from the normal state with the electric moment in the plane of the molecule, since from Table VI T_xT_y transforms like E_{1u}.

In the same way it may be shown that a transition to the overtone level $3\nu_{12}(\mathrm{E}_{1u})$ results in the same degeneracy, which will be split in the same way, since Table VI shows that $(\mathrm{E}_{1u})^3$ transforms like $(\mathrm{A}_{2g}) \times (\mathrm{E}_{1u})^3$. For an overtone $2\nu_{12}$, which transforms like $(\mathrm{E}_{1u})^2$, the situation is different. This transformation is given by the character set

$$\chi_r(\mathrm{E}_{1w})^2 = 4, 4, 1, 1, 0, 0 \mid 4, 4, 1, 1, 0, 0$$

It is easily seen that this set must be a sum of character sets of irreducible g representations, and, in fact, is the sum $(\mathrm{A}_{1g} + \mathrm{A}_{2g} + \mathrm{E}_{2g})$. It is evident that this overtone will not be allowed in the infrared spectrum.

This result for overtones is general for molecules with a center of symmetry. Even overtones will be forbidden and odd overtones will be allowed in the infrared absorption spectrum. The opposite is true for the Raman effect: even overtones are allowed and odd overtones are forbidden for molecules with a center of symmetry. Matters are not simplified to this extent for molecules which lack this symmetry element, but the most general case may be treated by forming the set of characters which are the products of sets corresponding to the irreducible representations to which the individual vibrations belong, and reducing the resulting reducible character set by means of Eq. 15.

I. Symmetry of Vibronic States

The discussion above on pure vibrational symmetry may be applied with little modification to pure electronic transitions, unaccompanied by vibration and rotation. It is only necessary to identify ψ_i and ψ_j in Eq. 11 with electronic eigenfunctions. For an electronic transition from state (i) to state (j), we take the nuclear coordinates as fixed and equal to the set of distances and angles for the atoms in their equilibrium positions in the normal state (i). According to the Franck-Condon principle, the nuclear positions do not change during the electronic transition. However, the equilibrium nuclear positions of the final state may not correspond to those of the initial state. If the final positions are changed in such a way that the molecule belongs to a different symmetry group, perhaps through the loss of a symmetry axis or plane, then the result is complicated and treatment of such cases will be deferred. We assume here that both states and their eigenfunctions belong to the same symmetry group.

If the electronic and vibrational motion can be separated in the Born-Oppenheimer approximation and rotational motion is ignored, then $\psi = \psi^e(r,R)\cdot\psi^v(R)$, where we have labeled the electronic and vibrational functions specifically. A product function of this type is designated by the term "vibronic" and a vibrational–electronic state is a vibronic state. The intensity for a vibronic transition in dipole radiation is then proportional to the square of the integral

$$\iint \psi_i{}^e(r,R)\psi^v_{i,n}(R)\mathbf{M}\psi_j{}^e(r,R)\psi^v_{j,m}(R)\,dr\,dR \tag{21}$$

where r refers to all the electronic coordinates collectively and R to the nuclear coordinates. The second member of the double subscript on the vibrational eigenfunction indicates the quantum number of the vibrational level associated with the electronic state described by the first member. Since we consider one vibration at a time, it is not necessary to characterize the particular type of vibration further. For $n = m = 0$, the ψ^v are to be omitted and the integral will measure the intensity of the pure electronic transition, or the (0,0) transition. For nonzero values of (n,m) we may integrate over the electronic coordinates at fixed values of R, corresponding to the equilibrium positions of the nuclei in the state (i) and obtain

$$\int \mathbf{Q}^e\psi^v_{i,n}\psi^v_{j,m}\,dR \tag{22}$$

where $\mathbf{Q}^e = \int \psi_i{}^e\mathbf{M}\psi_j{}^e\,dr$, and $\mathbf{Q}^e$ is some function of R.

Evaluation of Eq. 22 requires some assumption about the dependence of $\mathbf{Q}^e$ on R. If it is assumed tentatively that $\mathbf{Q}^e$ is independent of R, which is justified when $\mathbf{Q}^e$ is large, then it may be removed from the integral and we are to investigate $\int \psi^v_{i,n}\psi^v_{i,m}\,dR$ for possible vibrational changes. We may now use the customary symmetry arguments to show that the integrand $(\psi^v_{i,n}\psi^v_{j,m})$ must transform like the totally symmetric representation of the molecular symmetry group. This is possible only if the direct product of the character sets corresponding to the two vibrations is the character set χ_1, or contains χ_1 if either vibration is degenerate. If the character set for $\psi^v_{j,o}$ is χ_j, then the set for $\psi^v_{j,m}$ is $(\chi_j)^m$. If the vibration is totally symmetrical, $(\chi_j)^m = (\chi_1)^m = (\chi_1)$ for all values of m. However, if the vibration is not totally symmetrical, $(\chi_j)^m = (\chi_1)$ for even values of m, but $(\chi_j)^m = (\chi_j)$ for odd values of m. Now if the transition occurs from a nonvibrating initial state or from an initial state in which only totally symmetrical vibrations are excited, then we can expect excitation of totally symmetrical vibrations with any number of quanta in the final state. But unsymmetrical vibrations by the same argument can be excited only with even quantum numbers.

A further conclusion may be drawn (15) from the requirement that $(\psi^v_{i,n}\psi^v_{j,m})$ must be totally symmetrical. If the same type of unsymmetrical vibration in both upper and lower states is considered, the equilibrium position for the vibration in both states must be the same and the potential minimum for the vibration in the upper state lies directly above that for the lower state. Consequently, the vibrational quantum number should not change for unsymmetrical vibrations. While the formal selection rules allow changes (0,0), (0,2), (0,4), . . . ,(1,1), (1,3), (1,5), . . . for such vibrations, in practice only (0,0), (1,1), . . . will be expected with appreciable intensity. This restriction can be regarded as a consequence of the Franck-Condon principle. In summary, we expect totally symmetrical vibrations to appear principally with electronic excitation and unsymmetrical vibrations to be excited with only a few quanta at most.

The situation is different when the electronic transition is forbidden by symmetry. In this case, we must reconsider the original integral (Eq. 21) and recall that the direct product of character sets of the five factors of the integrand must be χ_1, or χ_1 must be contained in the result. The order in which the factors are multiplied is not important. Consider first the product $(\psi_i^e\mathbf{M}\psi_j^e)$, which must be unsymmetrical if the electronic transition is not allowed. This conclusion is not modified if we assume that the molecule is not vibrating in the initial state or is vibrating in a symmetrical mode. Then if the product

$$(\psi_i^e\psi^v_{i,n}\mathbf{M}\psi_j^e) \times (\psi^v_{j,m})$$

is to be totally symmetrical, it is required that the two factors belong to the same unsymmetrical representation. In other words, a transition which is forbidden by electronic selection rules may be allowed, if at the same time an unsymmetrical vibration of appropriate symmetry is excited in the upper state.

A similar argument can be used to show that if excitation occurs to the nonvibrating level of the excited state (j), then an unsymmetrical vibration must be excited in the lower state (i). The (0,0) transition will not appear, but the (0,1) and/or (1,0) transitions of an unsymmetrical vibration of proper symmetry may appear. The foregoing symmetry arguments are sufficient to account for the observation of forbidden electronic transitions which are allowed by excitation of an unsymmetrical vibration, but do not afford an explanation for the mechanism of a forbidden transition of this nature.

We may assume that it is really the ψ_j^e function which is responsible for the forbiddenness, if for some other final state, with ψ_k^e, the transition is allowed by electronic selection rules. We may then take ψ_k^e, $\psi_{k'}^e$, and other functions of symmetry which allow the transition as unperturbed functions in a perturbation problem and expand ψ_j^e in a series of these unperturbed functions. The perturbing potential is furnished by the nuclear displacements of the one unsymmetrical normal vibration. For the perturbation to be effective, it is necessary that $E(\psi_j^e) - E(\psi_k^e)$ be fairly small, since the intensity will depend on the reciprocal of the square of this energy difference. Furthermore, the electronic states represented by ψ_i^e and ψ_k^e must be connected by an allowed optical transition. This means that there must be an allowed electronic transition in the spectral neighborhood of the forbidden transition, whose eigenfunction ψ_k^e is mixed with ψ_j^e by an unsymmetrical vibrational eigenfunction of proper symmetry. Since the transition is allowed only by a perturbation of this nature, the absolute intensity of a forbidden transition can never be very high.

The most studied example (16) of a forbidden electronic transition occurs in the spectrum of benzene, at approximately 2600 Å. Theoretical considerations (17) show that the normal state function belongs to the representation A_{1g} of the group D_{6h}, and that the lowest excited singlet state transforms like B_{2u}; the components of the dipole moment transform: $M_{x,y}$ (in the plane of the ring) like E_{1u}; M_z (perpendicular to the ring) like A_{2u}. Therefore the integrand of the electronic transition integral $(\psi_i^e \mathbf{M} \psi_j^e)$ transforms like

$$(A_{1g} \times E_{1u} \times B_{2u}) = E_{2g}$$

or like

$$(A_{1g} \times A_{2u} \times B_{2u}) = B_{1g}$$

where the representation symbols are used for the corresponding sets of characters. It is clear that the electronic transition is forbidden for both components of the dipole moment.

If now a vibration is to be excited in the upper state, which will allow the transition, it must belong to a representation which has a character set, $\chi_{j,m}$, so that

$$(\mathrm{A}_{1g} \times \mathrm{E}_{1u} \times \mathrm{B}_{2u} \times \chi_{j,m}) = \mathrm{A}_{1g}$$

or

$$(\mathrm{A}_{1g} \times \mathrm{A}_{2u} \times \mathrm{B}_{2u} \times \chi_{j,m'}) = \mathrm{A}_{1g}$$

From the table of characters (Table VI) it is found that $\chi_{j,m}$ must be the character set of the representation E_{2g}, while $\chi_{j,m'}$ is the set of the representation B_{1g}. There are no vibrations in benzene of type B_{1g} and the transition cannot occur with light polarized perpendicular to the benzene ring. There are four vibrations of type E_{2g} which will allow a transition with light polarized parallel to the ring. A similar argument shows that the transition will be allowed if one quantum of an E_{2g} vibration is excited in the lower state.

Now the condition $(\mathrm{A}_{1g} \times \mathrm{E}_{1u} \times \mathrm{B}_{2u} \times \mathrm{E}_{2g}) = \mathrm{A}_{1g}$, is not modified by multiplying both sides of the equality by the character set $[\chi(\mathrm{A}_{1g})]^n$ and this means that any number of quanta of a totally symmetrical frequency can be added to one quantum of the necessary E_{2g} frequency. Long progressions of the symmetrical frequency are prominently observed features of this transition in benzene. This result may be generalized further by stating that combinations and overtones of any vibrations may be allowed, provided that the product of their character sets, raised to appropriate powers, is equal to or contains the character set of A_{1g} (see Table VI). Further details of the observed spectrum may be explained completely by this generalization.

The rotational structure of the vibrational transitions is not resolved completely. However, the partly resolved structure of certain transitions allows the conclusion that the carbon–carbon distance increases slightly in this excited state, but the symmetry of the equilibrium configuration of nuclei remains that of a regular hexagon. Confirmation of many of the details of the spectrum is provided by studies of the analogous transition in deuterobenzenes and in halogen-substituted benzenes. The (0,0) transition, which is forbidden in benzene, may appear with unsymmetrical substitution. This transition appears also in the spectrum of solid benzene, because of the perturbation of lattice forces.

The detailed application of group theoretical principles is less interesting in smaller and less symmetrical molecules, essentially because selection rules will usually permit many more transitions and frequently all transitions. Thus, no complex vibrational pattern will appear which requires more than an elementary explanation. Interpretation of cases where the geometrical dimensions change radically provide further cases of interest.

It has been assumed, in all the foregoing discussion of molecular symmetry, that the initial and final states in an electronic transition conform to the same symmetry group. In the $^1\mathrm{B}_{2u}$ state of benzene just discussed, the carbon–carbon equilibrium bond distances changed, but in a symmetrical way, so that the excited state belonged to the group D_{6h}. In other cases, and in fact in some of the higher states of benzene, the equilibrium bond distances change in such an unsymmetrical way that the molecule conforms to a different group, usually of lower symmetry. If two of the carbon–carbon distances were different from the other four, the sixfold axis becomes a twofold axis and the group is D_{2h}. Or a molecule which in its normal state is triangular and belongs to the group C_{2v} may become linear ($C_{\infty v}$ or $D_{\infty h}$) in one or more of its excited states, or the reverse may occur. In such cases the selection rules may be deduced from group theory, but only on the basis of such symmetry elements as are common to the two groups concerned in the transition.

A large change in symmetry in the above sense is associated usually with excitation of unsymmetrical vibrations. The excitation may occur in the upper or in the lower state, or in both. Many transitions of this nature have been studied recently and evidence for change in symmetry has come from analysis of resolved rotational structure. The first example (18) studied in detail was the longest wavelength transition in acetylene, in the spectral region 1970–2470 Å. The lower state is characterized by a linear configuration of nuclei and belongs to the group $D_{\infty h}$; the upper state probably belongs to the representation A_u of the group C_{2h}. The vibrational structure shows that a doubly degenerate vibration is excited in the ground state. The ground state of HCN is also linear, but several of the excited states are bent (19). On the other hand, the radicals NH_2 and ND_2 are bent (20) in their normal states (group C_{2v}), but become linear in their lowest excited states. Ethylene and formaldehyde are planar in their normal states, but become nonplanar in certain excited states. The second (21), and perhaps all of the excited states of ammonia are planar, while the normal state conforms to the shape of a regular pyramid.

There is a further consequence of excitation to degenerate electronic states when the nuclear configurations in such states are nonlinear. The effect of excitation of unsymmetrical vibrations in these cases is of fundamental interest and was investigated first by Jahn and Teller (22).

The ground states of most stable polyatomic molecules are nondegenerate and the minimum of energy corresponds to some definite symmetrical arrangement of the atoms. In the excited state the same symmetrical arrangement may correspond also to a minimum energy of that state, with symmetrically altered bond distances and angles. This is usually the case for nondegenerate excited states. However, degenerate excited electronic states may be split by vibrational motion of the nuclei into states of lower symmetry, which may have lower energy than the degenerate state. It is easy to see that excitation of an unsymmetrical vibration will be required for this splitting. Jahn and Teller showed that when the symmetrical configuration of a doubly degenerate state was nonlinear, for example, in a plane square molecule, the potential energy curves of the pair of levels which resulted from the splitting could cross in the neighborhood of the symmetrical configuration and so had minima below the crossing point. These authors showed that the situation was different when the symmetrical configuration was linear. Although splitting of a doubly degenerate level occurs also in this case, the two potential curves do not cross, but have their minima at the linear configuration, which is therefore stable. They stated that in a nonlinear molecule, no electronic degeneracy was to be expected in the stable nuclear configuration.

The electronic spectra of tetrahedral and octahedral molecules result from allowed transitions from a nondegenerate ground state to excited states which are triply degenerate. The excited states are unstable with respect to these symmetrical configurations and may be split by unsymmetrical vibrations. The resulting split states will have stable minima below the symmetrical configuration, resulting in the excitation of unsymmetrical vibrations with many quanta or may have no minima at all, which results in a truly continuous spectrum. Actual observations (23a–c) of the electronic spectra of CH_4, CF_4, and SF_6 show only continuous absorption at the resolving power used. Whether the spectra are continuous, or consist of complicated unresolved vibrational structure probably cannot be answered with equipment available at the present time. It may be said that observation of such continua do not *require* the Jahn-Teller theorem for explanation since we cannot be sure that there are not neighboring electronic states which may perturb the states in question, leading also to a continuum.

Application of the Jahn-Teller theorem to a specific molecular case has not been made in detail. It is clear that the theory itself must be valid and the theory has been refined (24) so that we know what details should be examined for evidence of explanation by this theorem in a large number of specific cases. The lack of quantitative applications is apparently because the effects predicted are small, on the whole, and so there may be alternative explanations. In general, unexpected long progressions of unsymmetrical vibrations, particularly when they show unusually high intensities relative to symmetrical vibrations, are best explained by the Jahn-Teller theorem. Some of the vibrational structure associated with high energy transitions in benzene (25) have been explained in this way.

If the normal state of a molecule is electronically degenerate, the degeneracy may be removed and states of lower energy and lower symmetry may result from a Jahn-Teller mechanism. The mechanism would be reflected in observation of details of unsymmetrical vibrations in the infrared and Raman spectra. Such observations have been made recently (26) in the infrared spectra of RuF_6 and RhF_6. An authoritative review of the status of the Jahn-Teller theorem has been published recently (27).

When the degenerate excited state of a molecule has a linear configuration, the Jahn-Teller theorem does not predict instability with respect to less symmetrical configurations, at least in the lower approximations. However, there are effects, discussed first by Renner, which are expected to appear. The expected splitting in this case is so small that it is of the order of magnitude of the neglected terms in the Born-Oppenheimer approximation and the usual separation of electronic and vibrational motion cannot be made. The theory of the Renner effect has been treated in detail recently (28). An example of the Renner effect (20) appears in the lowest excited state of NH_2 (and ND_2) which is linear, although the ground state is bent. Conclusive evidence for the Renner effect is based on features of rotational structure observed at very high resolution which are not explained otherwise.

V. CALCULATION OF ELECTRONIC EIGENFUNCTIONS

The preceding discussion has explored the use of molecular symmetry in the interpretation of spectra of polyatomic molecules. The eigenfunctions themselves have not been discussed in any detail (only their behavior with respect to symmetry operations). We have discussed essentially only the possibility of electronic transitions and have obtained no information on the positions of electronic levels in an energy scale. Questions of absolute intensities of electronic transitions have been discussed only in a very general way. We have found that the total absolute intensity of an electronic transition approaches zero as a limit if the transition is forbidden by symmetry and remains small if the observable intensity is obtained by perturbations. Reference has been made to some examples of the general nature of such perturbations. All of this information has been obtained with little or no mathematical computation. Further aspects of interpretation require calculations based on use of approximate molecular eigenfunctions.

First, the molecular functions themselves must be calculated. By this we mean that some definite functional *form* of ψ, as a function of electronic coordinates, is determined by calculation. The calculation is made so as to assure that some physical molecular property has an extreme value. A variational method, or an equivalent Hartree-Fock method, is employed, as has been described for the analogous atomic problem. In the variational method, the energy is varied with respect to parameters in a trial eigenfunction. The parameters become determined when the minimum is reached, and serve to fix the functional form of the eigenfunction. The resulting form may be an analytic function of the electronic coordinates, or in the Hartree-Fock method may consist of tables of numerical values of the function at selected values of the coordinates. The form will change when the nuclear coordinates change, so that the calculation has to be repeated for every fixed set of nuclear coordinates. Most calculations have been made for the set of experimental nuclear coordinates for the electronic state in question, as found experimentally from spectra or (for the normal state) from electron diffraction.

It is possible to choose another molecular property, for example the dipole moment, and require that the eigenfunction reproduce the experimental dipole moment. This would be of interest only for the normal state eigenfunction since experimental data on dipole moments are not generally available for excited states. This criterion should be extremely useful because the dipole moment is much more directly related to the distribution of electron density than is the energy. However, the dipole moment does not have a fundamental maximum or minimum property as does the energy. We know that the energy calculated from an eigenfunction, for some definite state, can never be lower than the experimental energy, but the experimental energy should be approached as the eigenfunction is improved. Thus, the criterion of minimum energy is the most useful in practice at the present time.

There are various degrees of approximation which are used in discussion of molecular eigenfunctions and we wish to make it clear what they are and the nature of the approximations. Provisionally, we take only the approximation inherent in an orbital description. Accordingly, we assume only that the Schroedinger equation for a molecular system can be solved with eigenfunctions which are determinants of one-electron spin orbitals, or molecular orbitals, or with eigenfunctions which are linear sums of such determinants. The relative distances between electrons are omitted as coordinates in this approximation. Further approximations are concerned with the forms of molecular orbitals which are obtained as expansions into atomic orbitals whose coordinates are referred to the atomic nuclei of the problem. The latter approximations are in addition to the molecular orbital approximation itself. A molecular orbital which is expanded into atomic orbitals is referred to as a LCAO (linear combination of atomic orbitals) form. There are still further classes of approximations which are concerned with numerical solutions of the variational equations which result from use of trial eigenfunctions. Finally, there are approximations which are concerned with the actual evaluation of the numerous and difficult integrals which enter into any numerical calculation as separate parts of the energy, as integrals for the kinetic energy of electrons, potential energy of single electrons in the field of the nuclei, and electrostatic energy of pairs of electrons. It is without meaning to state that theoretical results are derived from "an approximate molecular orbital calculation," without making it clear just what are the approximations.

A central question which must be emphasized, but frequently is not, concerns the value of molecular orbital calculations. What are we trying to do and what are we trying to prove by these calculations? We should be trying specifically to find sets of ψ functions connected with definite energy states of molecules which satisfy the conditions

$$H\psi = E\psi$$

and

$$\int \psi H \psi^* \, d\tau = E \int \psi\psi^* \, d\tau$$

ψ is the determinantal function of *all* the electrons and H is the Hamiltonian operator for all the electrons. We hope that if we can find the ψ by calculation, we can use them to verify and perhaps to predict molecular properties. Among these properties are ionization energies, transition energies between molecular states, dipole and higher moments, intensities of optical transitions, geometries of excited states. Most of these properties are of direct interest to spectroscopy. But we should not forget that we are calculating what are essentially mechanical properties of a system and we are trying to understand interactions in mechanical systems. If we lose sight of the elementary concepts of mechanics in a calculation, then the calculation may become an unrewarding display of formalism. It is not always true that a calculation leads to better understanding of a problem, particularly when the calculation is oversimplified in order to make it tractable.

With this digression, we return to the calculation of the ψ, or what is the same, of the ϕ from which a definite ψ is constructed. We may regard the ϕ as molecular orbitals, each multiplied by a spin function. In principle, the forms of the ϕ are found by variation of the energy with respect to certain parameters contained in the trial forms, such as effective nuclear charges and effective principal quantum numbers. E finally must be stationary at a minimum value for all of the parameters. There are systematic ways of carrying through the variation, which will be described. So far, we have introduced only the orbital approximation; the exact Hamiltonian appropriate to the problem has been retained.

It is customary and in fact necessary at the present time to introduce the approximation that each ϕ may be represented by a LCAO form. The coefficients in the linear combinations are treated as variational parameters, when they are not determined uniquely by conditions of orthogonality of molecular orbitals, normalization, and by symmetry of the molecular structure. The expansion of each ϕ should be made into a *complete* set of atomic functions which may or may not be mutually orthogonal. Actually, it is necessary in practical computations to limit the set to a definite number of terms and use only atomic orbitals which are normally occupied in the molecular state which is being calculated, or in addition, in some neighboring atomic energy states. Then there remains the forms of the basic atomic orbitals which are chosen as for atoms with exponential or gaussian forms for the radial parts. Parameters descriptive of the effective nuclear charges and powers of the radial distances are included in the form of the atomic orbital. These parameters as well as the expansion coefficients are all to be determined by variation of the energy. In many calculations the parameters of the atomic orbitals are not varied, but values obtained from solution of atomic problems are adopted. In many cases, further flexibility is obtained by the use of several exponential or gaussian forms of each atomic orbital which introduces additional parameters. The use of Hartree-Fock atomic functions has been explored and their use appears to lead to increased accuracy.

Calculation of energies of excited states introduce further problems, among which are the choice of interatomic distances and angles, which are usually unknown for these states. If they are not known, these geometrical quantities may be introduced as additional parameters and the total energy varied with respect to them. Although the general methods of calculation of eigenfunctions for excited states are straightforward, actual direct calculation has not been attempted for polyatomic molecules.

Details of molecular orbital calculations have been treated so extensively at various levels of approximation in standard texts (29a,b), reviews, and journal literature that it will be necessary only to give essentials of the methods used, with a limited discussion of specific examples. We begin with discussion of methods in which the least number of approximations are made.

The basis of calculation in the Hartree-Fock self-consistent field (SCF) method has been discussed for atoms. This method is formally equivalent to the variational method. The application to molecules has been systematized and described clearly by Roothaan (30). As an illustration of the general procedure, let us assume that we are calculating the minimum energy of the normal state of a molecule with n electrons, with nuclei fixed in an equilibrium configuration. The electrons are in a configuration of closed shells and the state is, therefore, singlet and is represented by a single determinantal function. If the molecular orbitals are all nondegenerate, there are $(n/2)$ separate shells, each occupied by two electrons which have different spin functions. We require that the molecular orbitals be orthogonal and that the matrix of orbital energies, or one-electron energies, be diagonal. If the orbitals were not orthogonal, they can be made so and if the matrix of orbital energies were not diagonal, an orthogonal transformation can always be found which will accomplish this and the transformed functions remain molecular orbitals. In fact, the requirement of such a diagonal matrix is usually part of the definition of molecular orbitals. Furthermore, we require that the molecular orbitals belong to definite symmetry representations of the group to which the molecule belongs. This requirement simplifies the calculation because matrix elements of the complete Hamiltonian operator between orbitals of different symmetry are zero.

Next let the orbitals be expanded into linear combinations of the atomic orbitals of the problem. This approximation must be made, because at the present time it is not possible to obtain molecular forms directly by the SCF method, except perhaps for simple molecules, such as H_2. As stated above, the set of atomic orbitals is limited for practical computation. The atomic orbitals in any LCAO molecular orbital must transform as the symmetry representation of that molecular orbital. This fact restricts the LCAO form. If individual atomic orbitals do not have the proper transformation properties, it is necessary to take linear combinations of such orbitals which do have this property. Such linear combinations are symmetry orbitals.

The last point may be illustrated with the water molecule as an example. The ground state of this molecule has a triangular form and belongs to the symmetry group C_{2v}. The origin of coordinates is taken at the oxygen atom so that the z axis bisects the H_1–O–H_2 angle. The molecular plane is (y,z). The $(1s)$ orbitals of H_1 and H_2 do not transform separately like any representation of the group, but the linear combination $\sigma_1 = (1s)_1 + (1s)_2$ transforms like A_1 and the combination $\sigma_2 = (1s)_1 - (1s)_2$ transforms like B_2, since it is antisymmetrical both to rotation about z and to reflection in the plane (x,z). In addition, there are five atomic functions of the oxygen atom (which may be regarded also as symmetry orbitals) which are seen to transform: $1s$, $2s$, $2p_z$, as A_1; $2p_x$ as B_1; $2p_y$ as B_2. Thus, there will be four linearly independent molecular orbitals which are linear combinations of σ_1, $1s$, $2s$, $2p_z$, with symmetry A_1. There will be two molecular orbitals with symmetry B_2 constructed from σ_2 and $2p_y$. The remaining molecular orbital of symmetry B_1 will consist of $2p_x$ alone. The ten electrons of the molecule may be accommodated in five molecular orbitals and there are thus two orbitals unoccupied in the normal state of the molecule. It is found on subsequent calculation that one A_1 and one B_2 orbital are unoccupied. However, solution of the SCF problem determines all seven molecular orbitals and their corresponding orbital energies.

The solution proceeds as follows. The atomic orbitals of the problem are regarded as known, or explicit forms are adopted for them and no variation is made of parameters contained in the orbital forms. The molecular orbitals are of the form: $\phi_i = \sum_p a_{ip}u_p$, where the u_p are the atomic orbitals and the $a_{\cdot\cdot i}$ are regarded as unknowns to be determined by variation of the energy. A typical orbital will be

$$\phi_1(A_1) = a_{11}[(1s)_{H_1} + (1s)_{H_2}] + a_{12}(1s) + a_{13}(2s) + a_{14}(2p_z)$$

Variation of the energy with respect to these coefficients yields a set of linear equations which may be expressed in matrix form as

$$(\mathbf{H}^c + \mathbf{G})a_i = \epsilon_i \mathbf{S} a_i \tag{23}$$

$\mathbf{H}^c$, $\mathbf{G}$, and $\mathbf{S}$ are 7×7 matrices which factor by symmetry into one 4×4 matrix for the A_1 orbitals, one 2×2 for the B_1 orbitals and one 1×1 matrix for the single B_2 orbital. The a_i are column matrices (vectors) of the expansion coefficients $a_{i,p}$. $\mathbf{S}$ is the overlap matrix with elements

$$\mathbf{S}_{p,q} = \int u_p u_q \, d\tau$$

$\mathbf{H}^c$ is a matrix with elements

$$\mathbf{H}^c_{p,q} = \int u_p(-\nabla^2/2 - 1/r_{\mathrm{H}_1} - 1/r_{\mathrm{H}_2} - 8/r_{\mathrm{O}})u_q \, d\tau$$

where r_{H_1}, r_{H_2}, and r_{O} are distances of the electron to the atomic centers H_1, H_2 and oxygen. The nuclear charges on the hydrogens are unity and 8 on oxygen.

The elements of the $\mathbf{G}$ matrix are two electron integrals of the pair operator $(r_{12})^{-1}$. Reduction of these integrals give a large number of integrals classified as coulomb, exchange, hybrid, with orbitals on one, two, or three centers. Each of these integrals is multiplied by one of the squares or products of the original expansion coefficients. It becomes evident immediately that to compute the $\mathbf{G}$ matrix, we must assume trial values of the $a_{i,p}$. We do this, compute the $\mathbf{H}^c$ and $\mathbf{S}$ matrices, and proceed to solve the matrix equation (Eq. 16). Since the $a_{i,p}$ are not all zero, we solve the determinantal equation

$$|(\mathbf{H}^c + \mathbf{G}) - \epsilon_i \, \mathbf{S}| = 0$$

for the ϵ_i and then the linear equations (Eq. 23) for the a_i vectors. We thus obtain a set of $a_{i,p}$ which will not in general be identical with the set assumed for calculation of the $\mathbf{G}$ matrix. We use the new set to recompute the $\mathbf{G}$ matrix. This iterative process is continued until the $a_{i,p}$ agree with those of the preceding trial. With modern methods of high speed computing, the initial calculation of the necessary integrals, construction of the matrices, solution by the iterative process can be programmed in a systematic way to proceed continuously until the calculation is terminated by some predetermined criterion of accuracy in the $a_{i,p}$. Since we are varying the energy with respect to these coefficients, the energy becomes stationary when the coefficients no longer change. As a result we obtain the lowest energy consistent with the particular choice of atomic orbitals and we have found the best molecular orbitals of LCAO form which can be constructed with this choice of atomic orbitals. The total energy is found by adding the nuclear repulsion.

$$\sum_{\alpha \neq \beta} Z_\alpha Z_\beta / R_{\alpha\beta}$$

where the Z are the nuclear charges and the R are the distances between atoms α and β. The dissociation energy is the difference between the energies of the separated atoms, which should be computed with the same atomic functions used in the molecular calculation and the calculated molecular energy. Since the quantities between which this difference is taken are both large in comparison with the dissociation energy, the computed value of the dissociation energy is not expected to be very reliable. Nevertheless, the values of both the total energy and the dissociation energy agree closely with experimental values in the most careful and accurate calculations which have been made. The calculation of dipole moments with SCF functions are disappointing in most cases and it is evident that the dipole moment is much more sensitive to details of the eigenfunctions than is the energy. Perhaps the most fundamental reason for failure to obtain better values of the dipole moment lies in the inherent lack of electron correlation in a single configuration eigenfunction. If other configurations of electrons are considered and eigenfunctions derived from them are allowed to interact, it has been found (in the few cases investigated) that the energy is lower than obtainable from a single determinantal function, but the dipole moment is more substantially improved. We shall discuss the problem of electron correlation in a subsequent section.

The orbital energies found in solution of the problem approximate closely the ionization potentials of the molecule. The excitation energies are calculated from the difference between orbital energies and certain interaction integrals between excited state and normal state orbitals. The results for excitation energies usually are not very satisfactory. In the first place, the excited state orbitals are obtained in the SCF method as extra solutions from variation of the energy of the ground state. The excited orbitals in LCAO approximation must, therefore, contain the same atomic orbitals as were used for the ground state function, with the same orbital parameters, and can differ from the ground state molecular orbitals only in the coefficients of the linear combinations. This situation may be realized in the lower excited states of benzene, which will be discussed subsequently; at least, agreement of theoretical and experimental transition energies appears to be good there. However, in small molecules, the actual excited states are described poorly by the extra SCF functions. We expect in many cases that the atomic orbitals adopted for the description of the ground state will undergo changes in the principal quantum number or at least will change their effective nuclear charges and probably additional orbitals must be added to the linear combinations for better description of excited states.

It must be emphasized that the calculation described above has been made for a fixed configuration of the nuclei. If we wish to find the minimum at some other configuration in which a bond distance or angle is changed, all of the basic integrals which depend on such changes must be recomputed and the entire iterative SCF procedure must be repeated. Also the whole process must be repeated for even small changes in the effective nuclear charges of the atomic orbitals. Of even more importance is the fact that the eigenfunction so obtained lacks a fundamental property which is electron correlation.

The question of electron correlation is important in the theory of electron structure of any system with more than one electron. It is perhaps obvious that a lower value of the energy of a system with two or more electrons can be reached, if the electrons can be kept apart in their motion in space. The separation should result in a lower electrostatic repulsion which should be reflected in a lower potential energy of the system as a whole. An accurate eigenfunction should take this into account and should have some factor in it which will serve to force two electrons to move in different regions in space. Actually the only requirement which has been set on the eigenfunction, beside its mathematical properties, is that it conform to the Pauli principle. If the two electrons have the same spin, they must necessarily be in different orbitals, and this situation correlates the motion to some extent for the triplet states. But if the two electrons have opposed spins, there is no correlation provided by the Pauli principle. There is nothing to prevent two electrons spending most of their time, on an average, in the neighborhood of some nucleus, which will lead to a large average repulsive energy.

Correlation can be introduced directly into the total eigenfunction if the function is made to depend directly on the relative coordinates r_{12}, the distances between electron (1) and electron (2). It is easily seen, when ψ depends on r_{12}, that $|\psi|^2$ will be large when r_{12} is large, but small for small values of r_{12}. The effect will be accentuated if ψ depends on higher powers of the relative distance. The most accurate calculations (31) of the hydrogen molecule have introduced correlation in this way. Systems with more than two electrons and, therefore with more than one $r_{i,j}$ coordinate would be difficult to treat in this direct way and other ways of introducing correlation are considered. Another way is the method of configurational interaction, which can be used within the orbital approximation. This method will now be considered.

A closed-shell electron configuration, represented by a single determinantal function, corresponds to a definite state with a definite symmetry. States of the same symmetry will result, however, from other electron configurations and all states of the same symmetry representation of a molecule can interact, with a lowering of the total energy. If linear combinations of the determinantal functions of the same symmetry are formed with coefficients to be determined by further variation of the energy, then a lower energy is expected. A cumbersome way of doing this would be to apply the SCF procedure to each determinantal function separately and find the best single configuration functions. Then a linear combination of these best functions could be treated in a variational problem to yield a better set of functions, by reminimizing the total energy with respect to the coefficients. An alternate way, which may be more simple, is to examine the basis functions from which the determinants are constructed.

If we were to start with any complete set of basis functions and were to write all possible configurations of electrons to which these elementary functions could be assigned, write the corresponding determinant for each configuration, and vary coefficients in linear combinations of these determinantal functions, there would be obtained an eigenfunction which would be an exact solution of the Schroedinger equation. The solution will be inexact if basis functions are limited to incomplete sets and if the number of configurations is limited. However, we should expect some improvement in the eigenfunction and lowering of the energy even with a limited number of configurations. Some systematic basis has to be found for the choice of configurations so that the energy converges to a miminum value rapidly as configurations are added. The physical nature of the correlation which we are trying to introduce provides some basis of choice of the configurations.

In a two-electron case, we wish to have one electron, on the average, farther from the nuclei than the other. This can be done by choice of basis functions with low and high principal quantum numbers and with very different effective nuclear charges. If there exists a center of symmetry, a proper proportion of basis functions can be chosen which have *u* and *g* properties, usually an equal number of basis functions of the two types. This selection will tend to keep the two electrons on opposite sides of the center. With axial symmetry, we wish to correlate the motion with respect to the axis, so that the electrons are kept on opposite sides of a plane through the axis. Basis functions with proper angular factors, such as *p* functions, are required. This basis of choice can be extended in principle to systems with more than two electrons, by consideration of all possible pairs of electrons. In favorable cases, limited at present largely to the normal state of hydrogen, it is found in practice that a few configurations, perhaps five or six, will lower the energy substantially, but for close approach to the lowest energy and best eigenfunction 30-50 configurations are required. Even with a large number of configurations, the problem appears to be more tractable at the present time than use of relative electron coordinates, although the question is far from being settled.

It is encouraging to note that relatively good values for the electronic energy have been obtained, even without the use of electron correlation, for small polyatomic molecules, such as H_2O, CO_2, NH_3, CH_4, and CH_2CO. The majority of calculations on these molecules (29) have been made with single determinantal functions constructed from Slater forms for the atomic orbitals. Usually screening constants in the exponential forms of the orbitals were obtained from formulas proposed by Slater. In some calculations, atomic functions calculated and tabulated by Hartree were used with superior results. For example, the results of Kaplan on NH_3 with Hartree functions are somewhat better than results obtained by the present writer with Slater forms.

The calculations to which reference has just been made may be termed "nonempirical" or *ab initio* calculations. *All* electrons including the inner-shell electrons were included in the calculations and in most cases all necessary integrals were evaluated by standard mathematical methods. But even with high speed computing, a calculation on a molecule, such as formaldehyde (32) with 16 electrons, is a formidable problem. Somewhat more than 1100 integrals were required in this particular problem and many of the three and four center integrals are very difficult to compute. It is, therefore, necessary to examine some of the more empirical methods for the calculation of approximate eigenfunctions, particularly for large molecules.

Some of the earliest calculations concerned benzene (33) and more generally conjugated organic molecules. In these early calculations an approximation of electron separability was made which we call now the "π electron" approximation. It is well known that conjugated systems of single and double carbon–carbon bonds tend to enforce rigid nuclear configurations which are planar in conjugated rings or linear in conjugated chains. The $2p$ functions of carbon may be classified $2p\sigma$ and $2p\pi$ with respect to their behavior on reflection in a plane, which in benzene is the molecular plane. The $2p\sigma$, or σ functions, are symmetrical to this operation, but the $2p\pi$ (or π) functions have a node at this plane and are antisymmetrical to the reflection. The π electrons were considered to be much less tightly bound to the molecule and it was believed that transitions between the normal and lower excited states were associated primarily with these electrons. The σ electrons were thus ignored and the π electrons were treated separately with a Hamiltonian operator from which (σ, π) interaction terms were removed. All subsequent calculations have been based on this approximation, although calculations which include the σ electrons are stated to be in progress (34). The effect of the approximation is not easy to assess.

In order to clarify the nature and meaning of the special approximations used for large molecules, we consider again the case of benzene. This case has been treated very thoroughly, at different levels of approximation, but up to date always within the basic π approximation. We cannot give here a historical account of the many calculations and will begin instead with discussion of a significant molecular orbital calculation made by Goeppert-Mayer and Sklar (17), which has served as a model for subsequent calculations on benzene and related molecules.

In this treatment only the six electrons in $2p\pi$ functions were considered; the other electrons with the six-carbon nuclei were supposed to constitute a smoothed-out potential field of six C^+ ions in the sp^2 valence state. The hydrogen atoms were ignored. Six linear combinations of the π functions were taken to form complex MO's. The relative energies of the MO's were found first by the neglect of electronic interaction, so that the orbital transitions became known and it was thus possible to write configurations for the excited levels in terms of MO's. The resulting states were found from the symmetry properties of benzene by group theory. The antisymmetrized functions for the normal and excited states could thus be written out and the energies of the states found by direct integration of $\int \psi_i H \psi_i \, dv = E_i$, after the normalized MO's had been expanded in their LCAO forms. The excitation energies were obtained directly as differences between the E_i. The computed excitation energies agreed very well with experimental values from spectra, but this agreement was later shown to be partly accidental, due to cancellation of errors. This work neglected a large number of integrals representing nonneighbor interactions and also neglected the effect of configurational interactions. The neglect of the latter apparently operated in a direction opposite to the neglect of the integrals. The values obtained in this work are shown in the first column of Table VIII. The calculations were repeated by Roothaan and Parr (35), with results in the second column of Table VIII.

TABLE VIII

Computed Excitation Energies in Benzene (in eV)

State	GMS (17)	RP (35)	PCR (37)	MB (38)	MB (38)	Experimental values (39)
$^1A_{1g}$	0	0	0	0	0	0
$^1B_{2u}$	5.0	5.8	4.4	3.09	3.58	4.89
$^1B_{1u}$	5.8	7.2	9.0	8.92	8.77	6.14
$^1E_{1u}$	8.0	9.7	9.9	9.74	9.69	6.75
$^3B_{1u}$	1.5	3.0	4.1	2.51	2.56	3.66
$^3E_{1u}$	2.2	4.3	4.7	3.81	3.82	4.69
$^3B_{2u}$	3.0	5.6	8.2	8.17	7.95	5.76

The next important contribution to the problem was made by Craig (36), who pointed out the importance of configurational interaction. The excited state configurations considered by Goeppert-Mayer and Sklar gave three excited singlet and three excited triplet states, none with the symmetry of the ground state. If other configurations are considered, other states are obtained, and some of these will have the same symmetry as the states found by Goeppert-Mayer and Sklar. States which belong to the same symmetry representation will interact, with a consequent lowering of the energy, as much as 4 eV in some of the cases found by Craig. It was found that configurations obtained by excitation of two electrons gave states which were lower in some cases than states resulting from single-electron excitation.

The six MO's of the π electrons of benzene are ϕ_0, $\phi_{\pm 1}$, $\phi_{\pm 2}$, ϕ_3, in order of increasing energy; the orbital energies of ϕ_{+1}, and ϕ_{-1} are equal, and the energies of ϕ_{+2} and ϕ_{-2} are equal. The closed-shell configuration of the ground state may be written

$$(\phi_0)^2(\phi_{+1})^2(\phi_{-1})^2,\ {}^1\mathrm{A}_{1g}$$

The symmetry description of the state follows the configuration. The superscripts in the configuration indicate that two electrons are in the orbitals distinguished by the subscripts. Other configurations and low-lying excited states considered by Goeppert-Mayer and Sklar are

$$\left.\begin{matrix}(\phi_0)^2(\phi_{+1})^2(\phi_{-1})(\phi_{+2})\\(\phi_0)^2(\phi_{+1})^2(\phi_{-1})(\phi_{-2})\\(\phi_0)^2(\phi_{+1})(\phi_{-1})^2(\phi_{+2})\\(\phi_0)^2(\phi_{+1})(\phi_{-1})^2(\phi_{-2})\end{matrix}\right\},\ \begin{matrix}{}^1\mathrm{B}_{1u},\ {}^1\mathrm{B}_{2u},\ {}^1\mathrm{E}_{1u}\\{}^3\mathrm{B}_{1u},\ {}^3\mathrm{B}_{2u},\ {}^3\mathrm{E}_{1u}\end{matrix}$$

The states resulting from these configurations cannot interact with the ground (${}^1\mathrm{A}_{1g}$) state, nor with each other. States which belong to different symmetry representations cannot interact, since the Hamiltonian operator H is totally symmetric, and states of the same symmetry but different multiplicity do not interact because H is spin independent, in the usual approximation.

But it is possible to write other configurations which have the same symmetries as these states. For example

$$(\phi_2)^2(\phi_{+1})^2(\phi_{+2})^2,\ {}^1\mathrm{A}_{1g}$$

gives another ${}^1\mathrm{A}_{1g}$ state, which has an energy about 8.9 eV above the ground ${}^1\mathrm{A}_{1g}$ state. These two states will interact, and this furnishes an example of *configurational interaction*. The interaction energy is found by a perturbation calculation and is about -4.5 eV. The effect of this interaction is to lower the energy of the ground state by about 1.8 eV. Actually there are two other low-lying ${}^1\mathrm{A}_{1g}$ states below 10 eV which must also be considered, and the ground state energy is lowered still more. Since excitation energies are measured relative to the ground state, it is evident that configurational interaction will have a profound effect on excitation energies.

The necessity of configurational interaction is an expression of the fact that better wave functions are obtained when linear combinations of approximate functions (of proper symmetry) are used as trial functions for the variational calculation of state energies. The best wave function for each state will be found by inclusion of *all* functions of the same symmetry, which result from *all* possible configurations. When the energy of each linear combination is made an absolute minimum by a variational procedure, the solutions of the resulting secular equations—one for each symmetry species—will give more correct values of the energies of the individual states.

More recent computations on the π electron states of benzene were made by Parr, Craig, and Ross (37) and included all three- and four-centered integrals and configurational interaction between all states arising from excitation of one and two electrons, and a few corresponding to three-electron excitation. The results are shown in Table VIII, third column.

The most recent and definitive treatment (38) of benzene in the π electron approximation has included a much larger number of configurations than have been used previously. The multicenter integrals were computed exactly. Several different approximations of the core were considered. The fourth column of Table VIII is a repetition of column three with a much larger number of configurations. The multicenter integrals were approximated as by Parr, Craig, and Ross. The fifth column shows the result of use of accurate multicenter integrals with the same number of configurations as in column four. The effect of use of the accurate integral values is not large. The numerical values in each column are excitation energies, referred to the ground state as zero.

The energy of the ground state was computed with the various core approximations for different numbers of configurations. It is thus possible to see, by adding the ground state values (38) to the appropriate columns, that the energy of each state is decreased as the number of configurations is increased and thus the eigenfunctions are improved. But at the same time the agreement with experimental values in the last column becomes worse as the eigenfunctions are improved. It has been suggested that the σ–π interaction may be of greater importance than has been realized and conclusions must await a full treatment of the problem which includes both σ and π electrons.

Experiments show that there are three well-established transitions at about 2600, 2000, and 1835 Å. The corresponding upper states were assigned as B_{2u}, B_{1u}, and E_{1u} on the basis of all computations without configurational interaction. The transition at 1835 Å is strong and it must be assigned to the E_{1u} allowed transition. All evidence, including configurational interaction and the vibrational analysis, which was discussed earlier, is in favor of the assignment B_{2u} for the upper state of the transition at 2600 Å. The transition at 2000 Å, cannot, however, be regarded as settled (40).

The preceding computations on benzene have been made with considerable refinement and probably are the best which can be made within the π electron approximation. The majority of computations on organic compounds have been made at lower levels of approximations and we refer to them here as semiempirical computations. The present discussion will be confined to calculations of spectroscopic interest and the very numerous molecular orbital computations with application to resonance energies and stabilization. Bond orders, orienting effects, and chemical reactivity will not be discussed here. These applications are treated elsewhere in many standard textbooks. Nor is it desirable to give here a historical account of the semiempirical computations of spectroscopic interest. It also appears best to limit the discussion to cases in which conjugation is important and the spectra which are to be interpreted are associated with the states of the π electrons.

The general problem of conjugation was treated in the early papers of Hückel (41), who has given an excellent review of earlier work. Important early contributions were made by Lennard-Jones (42) and by Lennard-Jones and Coulson (43), and by Pauling (44) and his coworkers. A general theory of conjugated systems has been given by Coulson and Longuet-Higgins (45) and a general treatment of electron density in such systems was given by Coulson and Rushbrooke (46). In all the above papers computations of orbital energies were considered as only one aspect of the broad problem of the structure and chemical stability of conjugated systems.

The principal approximations which distinguish the semiempirical computations from the nonempirical computations are as follows:

(*1*) The matrix elements of the Hamiltonian are not obtained numerically by direct integration, but are evaluated from empirical data. In this approximation, the detailed form of the Hamiltonian does not have to be specified and no details of the electronic interaction have to be known.

(*2*) Matrix elements of the type $H_{pq} = \int u_p H u_q \, d\tau = \beta_{pq} (p \neq q)$ are neglected when the AO's u_p and u_q are referred to centers p and q which are not neighbors. Furthermore, all β_{pq} are set equal for all neighbors in many, although not all, computations.

(*3*) Overlap integrals $S_{pq} = \int u_p u_q \, d\tau$ are frequently neglected entirely, even when p and q are neighboring centers. The complete neglect of overlap, or the equivalent assumption that all AO's are orthogonal, is not usually made in the more recent papers. However, the dependence of S_{pq} on distance is frequently neglected and a constant average value of S_{pq} is used.

In computations on large molecules with many π electrons, some of these approximations are not as bad as might appear, particularly when absolute values of the excitation energies are not desired, but only excitation energies relative to some standard molecule (such as benzene). In such cases the relative contribution of the electronic interaction is about constant for large enough molecules. At the same time the C—C bond distances tend to become constant, which justifies the use of constant values for H_{pq} and S_{pq}. The neglect of nonneighbor interactions depends considerably on the shape of the molecule. In conjugated systems with long chains, the neglect is evidently less serious than in compact ring systems.

With the above approximations, the MO energies are obtained from solutions of the secular equation having the form

$$\det |H_{pq} - \epsilon S_{pq}| = 0$$

and remain expressed in terms of the elements $H_{pp} = \alpha_p$ and $H_{pq} = \beta_{pq}$ which are termed, respectively, "coulomb" and "exchange" integrals. In π electron systems the excitation energies can usually be expressed in terms of the single parameter β, which is further assumed to have a value largely independent of the detailed molecular structure, at least for compounds which are not too different. If an evaluation of β is necessary, this is usually done through resonance energy data based on thermochemical information, or the value of β is taken from computations on molecules, such as benzene or butadiene for which nonempirical computations have been made. An added refinement is to assume that β is proportional to S_{pq} and to use the extensive tables of overlap integrals (47). In this way some correction is introduced for the variations in internuclear distances.

The neglect of detailed electronic interactions often obscures the finer details of excited electronic levels and excitation energies. Frequently, the upper electronic states of symmetrical molecules are derived from a configuration which is degenerate and a computation which neglects electronic interactions will reveal only the average position or the center of gravity of a number of excited levels. Only an average excitation energy is obtained. This average value, however, may be compared with a corresponding average of the experimental electronic transitions. The resolution of a singlet and its corresponding triplet state can be obtained only in a computation which explicitly includes electronic interaction and then only if properly antisymmetrized molecular state functions are used. It must be stated, however, that even the nonempirical calculations do not give very good results for these singlet-triplet separations and that even with accurate computations it is usually better to compare computed singlet-triplet averages with corresponding experimental averages.

As an example of a typical semiempirical computation, we refer to calculations on benzene (and borazole) by Roothaan and Mulliken (48). Only the six $2p\pi$ AO's of benzene were considered, and nonneighbor interactions were neglected. The energies of the MO's were obtained by a solution of the determinantal equation

$$\begin{vmatrix} A & 2 & 0 & 0 & 0 & 0 \\ 2 & A & 0 & 0 & 0 & 0 \\ 0 & 0 & A & 1 & 0 & 0 \\ 0 & 0 & 1 & A & 0 & 0 \\ 0 & 0 & 0 & 0 & A & 1 \\ 0 & 0 & 0 & 0 & 1 & A \end{vmatrix} = 0 \qquad \begin{aligned} &\text{with} \\ &A = (\alpha - E)/(\gamma - SE) \\ &\alpha = \int u_i H u_i \, d\tau \\ &\gamma = \int u_i H u_j \, d\tau \\ &S = \int u_i u_i \, d\tau \end{aligned}$$

Subscripts i and j refer to neighboring carbon atoms on which the $2p\pi$ AO's

u_i and u_j are centered. The roots of this equation are $A = \pm 2, \pm 1$, the latter double root being repeated twice. The MO's of lowest energy correspond to $A = -2, -1, -1$, and these three MO's are occupied in the normal state of the molecule, each by two electrons. The longest wavelength transition occurs when an electron is excited from $A = -1$ to $A = +1$, and, since both levels are doubly degenerate, there is a possibility of four singlet and four triplet upper states, all unresolved in this approximation. Actually there are three excited singlet and three triplet states since the doubly degenerate E_{1u} states are not split even by electronic interaction. The excitation energy to the group of six states will be equal to the difference between $A = -1$ and $A = +1$. Making the substitutions $\alpha - E = -x$, $\gamma - sE = \beta$, there is obtained $x_2 - x_1 = -2\beta/(1 - S^2)$, and with $S = 0.25$, the excitation energy is -2.13β. If the experimental average excitation energy (5.5 eV) is introduced, then $\beta = -2.6$ eV. This is compared with $\beta = -3.1$ eV from resonance energy data (49).

As another, but more complex, example of the above method may be cited the computations on porphin and tetrahydroporphin by Longuet-Higgins, Rector, and Platt (50), who made use of "molecular orbital theory in its most simple form." Overlap of the AO's was neglected, as was non-neighbor interactions of AO's on centers other than r and s. Secular equations of the form

$$(\alpha_r - E)c_r + \sum_s \beta c_s = 0$$

were obtained, where

$$\alpha_r = \int u_r H u_r \, d\tau \qquad \beta = \int u_s H u_r \, d\tau$$

and c_r and c_s are the coefficients of AO's on centers r and s which are bonded together. The summation is over β values for all s atoms which are bonded to r. The approximation was made that α_r for the nitrogen atoms was the same as for the carbon atoms. Molecular symmetry was used to factor the secular equation and the coefficients c_r were found. The wave functions so obtained were used to obtain the electron densities in the two molecules. It was found that the lowest densities occurred at atoms 3, 8, 13, and 18 and it was expected that these positions should be the initial points of attack by nucleophilic reagents. The MO energies were obtained after correcting the E values from the secular equation for some of the approximations made. The difference between α_r for carbon and nitrogen was allowed for, and a correction was made for previous neglect of overlap. β was taken to be -2.85 eV. The observed energy levels were tentatively assigned to the computed levels.

Simplified MO computations on naphthalene, anthracene, and similar molecules were made by Coulson (51) and by Mann, Platt, and Klevens on azulene (52).

A simplified MO method has been applied to a wide variety of conjugated molecules by Platt (53). Using a constant overlap integral $S = 0.25$ and $\beta = -32{,}000\ \text{cm}^{-1}$ for short-chain polyenes and $\beta = -23{,}000\ \text{cm}^{-1}$ for ring systems, Platt was able to predict the first two to five lowest transitions in sixteen conjugated molecules to within $10{,}000\ \text{cm}^{-1}$ in all cases. An interesting generalization which emerged from this work was the classification of these spectra into "long field" and "round field" types. In spectra of the first type, the electronic interaction splits the lower excited states by a relatively small amount ($30{,}000\ \text{cm}^{-1}$ in benzene), and configurational interaction between states of the same symmetry has a profound effect on the absolute energies of the states. Molecules which show this type of spectra are benzene, triphenylene, coronene, and porphin. In the limiting case of "long field" spectra, the states are already split widely and electronic and configurational interactions would have only a small effect on the positions of the electronic energy levels. This limiting situation does not appear to be approached closely in practice, because the electronic interaction always remains large.

Matsen and co-workers (54) computed the wavelength shifts, relative to benzene, of a number of substituted benzenes by a semiempirical MO method, with good argeement with experiment. It is possible to derive the magnitudes of the interaction of the benzene ring π electrons with electrons of the same type in the attached group. The effect of these interactions on the intensities of transitions is marked, as will be discussed later. Approximate computations on polymethine dyes have been made by Herzfeld and Sklar 55).

Further significant contributions to the semiempirical formulation of the π-electron problem have been made by Pariser and Parr (56). Justification for many approximations is made, at least on physical grounds and many applications to other conjugated molecules are quoted. The emphasis in their work is placed on obtaining results which show satisfactory agreement with experiment. The calculation of two-electron integrals is the most laborious part of problems of this nature and when this is done by standard mathematical methods, the results appear to be physically unrealistic. These authors set out to simplify the problem of integrals in a systematic way. First, the general two-electron integral, which measures the electrostatic repulsion between two electrons, is reduced to a sum of coulomb integrals by an assumption of "zero differential overlap." Some of the resulting integrals which show unreasonable values when evaluated with Slater atomic orbitals and conventional screening constants are modified and treated as empirical quantities. Very accurate values of excitation energies in a variety of organic molecules were found after these approximations were made. The theoretical basis of the π electron approximation, especially the conditions of separability of σ and π electrons was examined thoroughly and critically by Lykos and Parr (57).

Another useful method for the treatment of π electron systems and their energy levels is based on a free-electron model. It was realized early by Hückel (41) that the π electrons were free, in a sense, to move around the perimeters of ring systems and that this motion could be quantized by "orbital ring quantum numbers." The idea is similar to the motion of electrons in metals, and has been developed for the treatment of conjugated systems in general by Pauling, Lonsdale, Schmitt, Bayliss, Kuhn, Simpson, and Platt. The computations of both wavelengths of absorption and intensities of transitions are made rather easily by this method and the results are capable of describing, at least qualitatively, a large number of observed spectra. The method is particularly valuable for molecules which are too difficult to treat by the approximate MO methods which have just been described.

The simplest approximation of this nature treats the π electrons as a one-dimensional gas, which is constrained to move in a rectangle of length X in a polyene, for example, or in the closed loop of length l of a *cata*-condensed ring system. The energy levels of the electrons (in cm^{-1}) are those of the quantum mechanical particle in a box of length X, and are

$$E_n = hn^2/8mcX^2 \tag{24a}$$

where $n = 1, 2, 3, \ldots$. Or, if the model is a closed loop, the energy levels are those of the plane rotator

$$E_q = h^2q^2/2ml^2 \tag{24b}$$

where $q = 0, 1, 2, \ldots$. The free-electron orbitals of the open chain each contain two electrons. The lowest orbital of the closed loop ($q = 0$) contains two electrons; the higher orbitals ($q > 0$) are doubly degenerate and contain four electrons. The longest wavelength transition will occur when an electron is excited from the highest orbital filled in the ground state to the lowest empty orbital. The excitation energies for the open chain are

$$\Delta E_n\,(\mathrm{cm}^{-1}) = h(2N + 1)/8mcX^2 \tag{25}$$

where N is the value of n for the highest level filled in the normal state. In the loop case, as applied to *cata*-condensed hydrocarbons (Chapter I, Section VI-E-12)

$$\Delta E_g = h^2(2q_l + 1)/2ml^2 \tag{26}$$

where q_l is the quantum number of the highest filled shell and is equal to [(number of π electrons -2)/4] for these hydrocarbons. In benzene, for example, $q_l = 1$ and ΔE_g in wave numbers is 51,000 cm^{-1}, which may be compared with the experimental center of gravity of levels at about 44,000 cm^{-1}. For naphthalene and anthracene, with $q_l = 2, 3$, agreement with computations by the LCAO–MO method (51) is very good.

Platt and Klevens (58,59) have made a comprehensive classification of the spectra of *cata*-condensed hydrocarbons (those in which no carbon atom belongs to more than two rings) based largely on the comparison of observed excitation energies with energies obtained by simplified MO and free-electron computations. They show that in all such compounds the longest wavelength electronic excitation is between a doubly degenerate filled orbital and a doubly degenerate empty orbital. If the excitation comes from the highest filled orbital, four excited states result, which these authors call L_b, L_a, B_b, and B_a in order of increasing energy. These states correspond to the benzene states B_{2u}, B_{1u}, and E_{1u} mentioned earlier, and to the lowest excited B_{1u}, B_{2u}, B_{1u}, and B_{2u} states of naphthalene. Other transitions from levels below the highest filled level are observed in larger hydrocarbons and are labeled C, K, and J states (or bands). Platt and Klevens identified a number of these states in two-, three-, four-, and five-ring hydrocarbons, and found regularities of wavelength shift and appearance of vibrational structure, particularly among the L and B transitions, The polarization, or direction of the dipole moment in the transition, was predicted in each case by the free-electron model, and agreed with the available experimental information. Relative intensities for this class of compounds are predicted well by the free-electron model. Suggestions were made for extension of this classification to other types of conjugated systems such as polyene chains, ring-chain systems, and the *peri*-condensed hydrocarbons (in which some carbon atoms belong to at least three rings). Identification in such cases is much less certain, due partly to the scarcity of experimental data. Refinements in the free-electron model would have to be made for computations on these systems.

Computations by the free-electron method have been made for porphin and tetrahydroporphin by Simpson (60) who neglected the effect of the nitrogens and of two double bonds. Simpson allowed for the splitting of degenerate levels by electronic interaction and obtained results which were similar to the MO computations of Longuet-Higgins, Rector, and Platt, although to a lower order of approximation.

Earlier qualitative computations were made by Simpson (61) on excitation energies and intensities of transition in three dyes of the type

$$\mathrm{Me_2\overset{+}{N}{=}CH{-}(CH{=}CH)_n{-}\bar{N}Me_2}$$

where $n = 1, 2, 3$. Simpson used the VB method, a modification of the Lewis and Calvin (62) method, the free-electron method, and molecular orbital methods, and compared his results obtained by these methods. The results were in qualitative agreement with experiment. Simpson pointed out recently (63) the importance of internal dispersion forces in the polyenes. Inclusion in the calculations of interaction energy terms arising from these forces gives results which are comparable to the inclusion of configurational interaction in MO computations. Simpson has given a treatment of merocyanine dyes by the VB method and by solution of the Schroedinger equation by the method of finite differences.

The simple assumption of a constant potential in the free-electron method has been discussed critically by Kuhn (64). This assumption appears to be relatively safe in the case of symmetrical polymethines and the symmetrical cases treated by Platt and by Simpson. In the case of unsymmetrical polymethine dyes, this assumption is bad, and Kuhn finds it necessary to assume a periodic potential, which adds a term $V_0(1 - 1/N)$ to the energy, where N is the number of π electrons and V_0 is the amplitude of the sine wave used to approximate the variation of the potential energy along the chain. V_0 is thus a measure of the asymmetry of the polymethine dye. Comparison of experimental spectra with calculations which included this refinement showed that V_0 was not itself quite constant over the entire chain length; with $V_0 =$ 2.00 eV, however, agreement was good.

In general, it appears that both the semiempirical MO methods and the free-electron methods are useful where qualitative information is sufficient, especially for the correlation of spectra. The free-electron method in the simple form described here requires little or no mathematics. The MO methods are somewhat more elastic in that refinements are more easily added, and are useful in many cases of nonconjugated molecules which have not been discussed. Both methods become difficult in application to unsymmetrical cases, the free-electron method because of the more complicated potential and the MO methods because of the more complicated secular equations to be solved. It is evident that the two methods will become completely equivalent when sufficient refinements are added.

The foundations of the free-electron method have been discussed recently by Ham and Ruedenberg (65). An authoritative series of six papers by Ruedenburg (66) present effectively the present status of the π-electron problem and discusses the validity of approximations in a critical way.

The present discussion of molecular orbital calculation has been very incomplete. Many important illustrations have been omitted, as have many references to past and current work on the subject. We have chosen the illustrations not because of their interest to current research, but as illustrations of basic principles. We have omitted discussion of valency and chemical binding because these important topics have been covered adequately elsewhere (67). Furthermore, we have chosen to omit entirely any discussion of the valence-bond or electron-pair method of calculation of molecular properties by quantum mechanical methods. We have concentrated on molecular orbital methods because spectroscopic transitions, in which we are primarily interested, are more simply and naturally treated in molecular orbital formulation, where the excited electron is not localized, but is assigned to the molecule as a whole.

VI. INTENSITIES OF ELECTRONIC TRANSITIONS

Electronic selection rules are based on the properties of the dipole moment integrals

$$\int \psi_i^e M_q \psi_j^e \, d\tau$$

For the selection rules it is only necessary to know whether or not the integral has a value of zero. This information may be obtained without computation by the use of group theory, which has been discussed. The above integral, or rather the square of its absolute value, is a measure of the intensity of the transition between the states whose functions appear in the integrand. If the wave functions are known, which implies that the states connected by the transition are known, the intensity may be computed with an accuracy limited only by the accuracy of the wave function. This theoretical result may be compared with an experimental value of the intensity derived from absorption coefficients measured over the complete width of the corresponding absorption band. The theoretical results vary greatly with the states of a single definite molecule, because the wave functions for the various states are very different. Consequently, a decision between two upper states reached by absorption from the normal state may be made in some cases by comparison of observed intensities with intensities computed from assumed wave functions. Along with the results of energy level computations and other evidence, computations of transition probabilities or intensities are of great assistance in the analysis of spectra.

In the following discussion, the treatment of Mulliken (68) will be followed largely and it will be convenient to use a similar notation. The quantities M_q used in previous discussions are components of the dipole moment vector $\sum_i e\mathbf{r}_i$, where $\mathbf{r}_i$ is the vector distance of the ith electron to the origin of a coordinate system fixed in the molecule and e is the electronic charge. A vector **Q** will now be defined by

$$\mathbf{Q} = \int \psi_k \sum_i \mathbf{r}_i \psi_l \, d\tau \tag{27}$$

which differs from the dipole moment by a factor e. In this expression ψ_k is the orbital wave function for the ground state and ψ_l is the function for the excited state to which a transition may occur. The integration is to be made over the volume elements of all the electrons in the molecule. The vector **Q** will have components Q_x, Q_y, and Q_z in a cartesian coordinate system so that

$$Q_x = \int \psi_k \sum_i x_i \psi_l \, d\tau \text{ etc.}$$

The vector components x, y, and z will usually be measured in angstrom units so that **Q** will be expressed in the same units. It is convenient to compute Q_x, Q_y, and Q_z separately, and $Q^2 = Q_x{}^2 + Q_k{}^2 + Q_z{}^2$. A further quantity, $D = G'Q^2$, is defined as the *dipole strength* of an electronic transition, and D will be expressed in square angstroms. G' is the orbital degeneracy of the upper state and is numerically equal to the number of independent wave functions which belong to the upper state, normally not greater than three. The dipole strength (or intensity) is independent of degeneracy in the lower state in absorption, because the presence of degeneracy in the normal state merely affects the distribution of molecules among the sublevels of the electronic state, and does not affect the absorbing power per molecule.

The **Q** vector is defined in terms of electronic wave functions, which correspond to a fixed set of internuclear distances, usually the equilibrium distances in the normal state. Actually, there will be a large number of vibrational and rotational levels associated with each electronic level. However, for any given initial state l, D will measure the sum of dipole strengths of all possible transitions to levels connected with the upper state function ψ_k, including vibrational, rotational, spin, and continuous levels. It is necessary, therefore, to compare D with an experimental value summed over all the initial levels and including all transitions connected with the upper level. The total strength D is the same for each initial level and the total D per molecule will be independent of the distribution of molecules over the sublevels of the lower state. As a consequence, D should be independent of temperature.

The total strength of an electronic transition may be measured experimentally as a sum of strengths of all possible transitions arising from a single definite rotational–vibrational level divided by the population of this particular initial level. The sum should be the same for any particular initial level chosen. This experimental method can be used only for completely resolved spectra whose structure has been analyzed, and thus has very limited application. In another method, the sum of dipole strengths from all initial rotational–vibrational levels of the normal electronic state to all levels of the upper state is obtained and this sum is divided by the total number of molecules. This method requires a continuous absorption spectrum and is particularly well adapted for measurements in solution. The method may be applied to gases, when the structure can be broadened into a continuum by the use of high pressures, either by the gas under investigation or by a foreign inert gas. Care must be taken that the structure is actually broadened. The absorption coefficients should be measured in the presence of foreign gases at a series of high pressures of foreign gas and the measurements extrapolated to zero partial pressure of foreign gas.

Actually, the electronic functions vary with internuclear distances because of molecular vibrations, and **Q** depends to some extent on vibrations. The magnitude of the dependence may be obtained by expanding **Q** in terms of coordinates of nuclear displacements (q_n) about the equilibrium values of the nuclear coordinates. This expansion leads to an expression of the form

$$\mathbf{Q} = \mathbf{Q}_0 + \sum_i \frac{\partial \mathbf{Q}}{\partial q_i} q_i + \frac{1}{2} \sum_{i,j} \frac{\partial^2 \mathbf{Q}}{\partial q_i \, \partial q_l} q_i q_j + \cdots \tag{28}$$

where $\mathbf{Q}_0$ is independent of the nuclear vibrations. The higher terms are usually very small in comparison with $\mathbf{Q}_0$, but these terms become important when $\mathbf{Q}_0$ is small or is zero, when the transition is forbidden by the electronic selection rules. Even when $\mathbf{Q}_0 = 0$, **Q** may have a small value, but it must be computed from the vibrational wave functions. This leads to a situation where **Q** will have a temperature dependence when the transition is forbidden by the electronic selection rules, but is allowed by excitation of a vibration of the proper symmetry.

If the absorption coefficients are measured in solution, a correction should, in principle, be made for the influence of the solvent (69). Actually, there is some question about the magnitude of the corrections to be made, since experimental comparisons between measurements on the same substance as a pure vapor and in solution have shown little difference (70,71). It appears that the experimental errors, especially in the vapor measurements, may be as large as the theoretical corrections, and accordingly, the solution values should not be corrected at present.

The experimental intensity is expressed most conveniently in terms of the f number or oscillator strength

$$f = (mc^2/\pi e^2 N) \int \alpha_\nu \, d\nu = 4.20 \times 10^{-8} \int \alpha_\nu \, d\nu \tag{29}$$

where α_ν is the absorption coefficient defined by

$$I_\nu / I_\nu^0 = \exp(-\alpha_\nu l)$$

I_ν^0 is the incident intensity of monochromatic light at a wavenumber ν and I_ν is the intensity after passage through a column of gas l cm long at 0 C and 76 cm Hg pressure. The integration is extended over the complete absorption band. The f number for a transition at a single wavenumber ν may be expressed in terms of the theoretical D by the relation

$$f = 1.085 \times 10^{11}\, \nu D = (8\pi^2 mc/3h)\nu D \tag{30}$$

It is customary to compare an f computed from Eq. 30 with an experimental f obtained by the use of Eq. 29, using an approximate experimental value of the wave number at which the absorption is at a maximum for ν in Eq. 30. As can be seen, the quantity actually computed theoretically is $D = G'Q^2$ from the wave functions. We shall illustrate the computation of $\mathbf{Q}$ for the simple case of particular transitions in the hydrogen molecule. The method of Mulliken (72) will be followed closely.

In the MO approximation, the configuration of the normal state of the hydrogen molecule is $(\sigma_g)^2$, corresponding to a ground state ${}^1\Sigma_g{}^+$. We consider an excited state ${}^1\Sigma_u{}^+$ from a configuration $(\sigma_g)(\sigma_u)$. The LCAO forms for these MO's are

$$\sigma_g = (1s_a + 1s_b)[2(1 + S)]^{1/2}$$
$$\sigma_u = (1s_a - 1s_b)[2(1 - S)]^{1/2}$$
$$S = \int 1s_a 1s_b \, d\tau$$

Accordingly, the orbital functions for the two states are

$$\psi_l = \sigma_g(1)\sigma_g(2)$$
$$\psi_k = [\sigma_g(1)\sigma_u(2) + \sigma_g(2)\sigma_u(1)]/\sqrt{2}$$

Spin functions are omitted, since they will disappear on subsequent integrations. If the z axis is taken to be coincident with the internuclear axis of the molecule, then $Q_x = Q_y = 0$ and $\mathbf{Q} = Q_z$. Then

$$\mathbf{Q} = \int \psi_l(z_1 + z_2)\psi_k \, d\tau_1 \, d\tau_2$$

where the integration is over the volume elements of the two electrons. $\mathbf{Q}$ may be reduced to a one-electron integral by introducing the MO forms of ψ_l and ψ_k and performing the required integrations. Since σ_g and σ_u are orthogonal

$$\begin{aligned}\mathbf{Q} &= \left[\int \sigma_g(2)\sigma_u(2)z_2 \, d\tau_2 + \int \sigma_g(1)\sigma_u(1)z_1 \, d\tau_1\right]\Big/\sqrt{2} \\ &= \sqrt{2}\int \sigma_u(z)\sigma_g \, d\tau\end{aligned}$$

If now the LCAO forms of σ_g and σ_u are introduced, the result after integration is

$$\mathbf{Q} = \left[\int (1s_a)(z)(1s_a)\, d\tau - \int (1s_b)(z)(1s_b)\, d\tau\right][2(1 - S^2)]^{1/2}$$

An integral $\int (1s_a)(z)(1s_a)\, d\tau$ is just the average value of the coordinate z for the function $(1s_a)$, so $\bar{z}_a$ is the average distance of the electron measured from a and $\bar{z}_b$ has a similar meaning. Hence

$$\mathbf{Q} = (\bar{z}_a - \bar{z}_b)/[2(1 - S^2)]^{1/2} = R_{ab}/[2(1 - S^2)]^{1/2}$$

since $(\bar{z}_a - \bar{z}_b)$ is equal to the internuclear separation. Mulliken found that $\mathbf{Q} = 0.80$ Å, using $R_{ab} = 0.74$ Å and $S = 0.75$, and with $\nu = \nu_{\max} = 99{,}000\ \text{cm}^{-1}$ in Eq. 30, then $f = 0.68$.

Transition between the same two states was also treated by the VB method, for which the state functions are

$$\psi_l = [1s_a(1)1s_b(2) + 1s_a(2)1s_b(1)]/[2(1 + S^2)]^{1/2}$$
$$\psi_k = [1s_a(1)1s_a(2) - 1s_b(1)1s_b(2)]/[2(1 - S^2)]^{1/2}$$

from which $\mathbf{Q} = SR_{ab}/(1 - S^4)^{1/2}$ and $f = 0.49$. Mulliken suggests that the correct value for f probably lies between these two values, since the true wave functions are expected to lie between the MO and the VB functions. Mulliken compares these f numbers with $f = 0.98$ for the sum of the two very strong sodium D lines and concludes that the transition in hydrogen has a very strong probability. Computations with MO and VB functions are made with equal ease in this case. In more complex molecules, the computations with VB functions are usually more difficult than with MO functions.

It is noticed that in the VB function

$$\psi_k = [1s_a(1)1s_a(2) - 1s_b(1)1s_b(2)]/[2(1 - S^2)]^{1/2}$$

both electrons are on atom a in the first term and both are on atom b in the second term. The ${}^1\Sigma_u{}^+$ state represented by this function is a mixture of the ionic forms H^+H^- and H^-H^+, and from the VB viewpoint there is a transfer of charge from one atom to the other, with each electron spending one-half of its time on each atom. The lower state to which ψ_l belongs is, of course, nonionic. Spectra of this type are called "charge transfer" spectra by Mulliken (72).

Mulliken predicted earlier (73,74) that transitions of the type just treated in detail should have high intensities. In diatomic molecules the electric moment changes along the internuclear axis. These transitions occur without a change in the principal quantum number of the electron and are classified as valence shell transitions in contrast to Rydberg transitions, in which a change in principal quantum number occurs. These valence shell transitions are called N (normal) → V transitions by Mulliken. The transitions occur between bonding and antibonding functions. It is to be noted that the computation of $\mathbf{Q}$ for N → V transitions does not require that the *forms* of the AO's be known, since $\mathbf{Q}$ is obtained as some function of the internuclear distances, as illustrated for the hydrogen case above.

The class of N → V transitions is extensive, and one or more may occur for every molecule. Mulliken has made computations for a large number of cases (68). Numerical values will not be quoted here, but the original references should be consulted for calculations on particular molecules. Because of the lack of uniformity in accuracy of experimental values, it would be misleading to present tables of comparisons of experimental with theoretical results. It may be stated, however, that the *average* of MO and VB computed values is close to the experimental values in most cases, at least within an order of magnitude, with the MO values too high, in general, and the VB values too low.

Another important class of valence shell transitions is found in the N → Q transitions (75). In this case an electron is transferred from a nonbonding orbital which is usually of a π type, to an antibonding or bonding orbital of a σ type. In a diatomic molecule the N → Q transition is a perpendicular type, since the nonbonding π electron function has its node along the internuclear axis, while the σ bonding or antibonding function has its node normal to the axis. As an example, the normal state configuration of HCl may be described in an MO treatment by: $(\sigma)^2(\pi_{\text{Cl}})^4$, ${}^1\Sigma^+$, with $\sigma = \alpha(3p\sigma_{\text{Cl}}) + \beta(1s_{\text{H}})$ and $\pi_{\text{Cl}} = 3p\pi_{\text{Cl}}$. The excited singlet Q state has the configuration $(\sigma)^2(\pi_{\text{Cl}})^3(\sigma^*)$, with $\sigma^* = \alpha^*(1s_{\text{H}}) - \beta^*(3p\sigma_{\text{Cl}})$. The orbital σ^* is evidently antibonding. The computation of the transition moment vector **Q** is considerably more difficult in this case than in the N → V case, for the detailed forms of the AOs must be assumed in addition to a ratio of the coefficients α/β. (The absolute values of α, β, α^*, and β^* can be found from α/β by orthogonality and normalization.) For the results of calculations on HCl, reference must be made to the original paper (76). Another example of the N → Q type of transition is found in the well-known absorption of ketones and aldehydes near 1900 Å. Computations on formaldehyde have been made by McMurry (77) and acetone and other ketones have been treated experimentally and theoretically by the present writer and his students (78). The N → Q transitions are found to be weaker as a class than the N → V transitions.

Another type of "perpendicular" transition is N → π, where excitation occurs from a nonbonding orbital to a π excited orbital. An example of this type is found in the longest wavelength transition in formaldehyde and other aldehydes and ketones. In C_{2v} symmetry, this type of transition is forbidden by electronic selection rules and the intensity cannot be calculated directly. The intensity of the transition in formaldehyde has been calculated by perturbation theory (79). This type of transition is often written $n \rightarrow \pi$.

In many-electron molecules the computations are more complicated, but one simplification can usually be made. For excitation from a single configuration all electrons which remain in closed shells during the transition may be ignored. If the electron comes from a nondegenerate closed shell, leaving one electron behind, **Q** will be a two-electron integral which may be reduced to a one-electron integral as was the case in the hydrogen transition described earlier. If the shell from which the electron comes is degenerate—containing four or six electrons—then the four- or six-electron integral can be reduced in a similar way.

We return to details of N → V transitions for selected types of molecules. A series of computations has been made by Mulliken (80) for transitions in conjugated systems. In butadiene there are four π electron MO's, $\phi_1 \cdots \phi_4$ in order of increasing energy. The excited states result when an electron in ϕ_1 or ϕ_2 is transferred into ϕ_3 or ϕ_4. The electron configurations for normal and excited states are (with state symbols and symmetry symbols for *trans* and *cis* forms)

$(\phi_1)^2(\phi_2)^2$	N [A_g (*trans*) or A_1 (*cis*)]
$(\phi_1)^2(\phi_2)(\phi_3)$	V_1 (B_u or B_2)
$(\phi_1)^2(\phi_2)(\phi_4)$	V_2 (A_g or A_1)
$(\phi_1)(\phi_2)^2(\phi_3)$	V_3 (A_g or A_1)
$(\phi_1)(\phi_2)^2(\phi_4)$	V_4 (B_u or B_2)

For the *trans* form, only transitions to V_1 and V_4 are allowed; all transitions are allowed for the *cis* form. Mulliken has made computations on the *trans* form, and on the *cis* form with three assumed (C=C—C) angles (90, 110, and 120°). Butadiene exists mainly in the *trans* form and the experimental f number is 0.53 for the longest wavelength band, compared to an "empirically corrected" theoretical value of $f = 0.52$ for N → V_1. The transition N → V_4 lies at much shorter wavelengths and no measurements are available.

The number of excited V states increases as the square of the number of double bonds in a polyene chain. If the polyenes higher than butadiene also have essentially a *trans* structure, then it is predicted that the excitation energy of the N → V_1 transition should decrease regularly, and at the same time the total intensity of transitions to all the V states should become more concentrated in the N → V_1 transition, which should also increase in absolute intensity as the number of double bonds is increased. All of these predictions appear to be realized, at least qualitatively. For example, the *trans* form of octatetraene (8 π electrons, 16 V states) has a total f number equal to 1.55, with 90% of the total intensity concentrated in the N → V_1 transition (81), while β-carotene with 11 double bonds has a still greater concentration of intensity in N → V_1 and $f = 7$. As the polyene chain becomes longer, the value of the excitation energy of N → V_1 appears to approach a limiting value, as does the f value. According to Mulliken, the limiting value of the excitation energy is connected with the decreasing importance of electronic interaction between electrons in MOs far removed along the chain. Polyene chains containing an odd number of carbon atoms (free radicals or ions in the case of conjugated systems) have also been treated by Mulliken. Computed results are similar to those obtained for even-numbered chains, provided that *trans* forms are assumed.

Mulliken has also made computations on *cis* forms of the polyenes with various assumed angles. In general, the total intensity of transitions to all the V states is less than with the *trans* forms of the same molecule, and the intensity is not as concentrated in the first N → V_1 transition. Cyclic dienes have N → V transitions of still lower intensity (82), as might be expected from comparison of *cis* and *trans* forms of chain polyenes. For example, the single allowed N → V transition in benzene with six π electrons has about the same intensity as the N → V transition in ethylene with two π electrons. In less symmetrical conjugated cyclic molecules than benzene, there will be more N → V transitions, but the higher transitions may be more intense than the lowest transition of the same type. This appears to be the case with fulvene. Computations made by Mulliken for *cis* and *trans* forms of some diphenyl polyenes $C_6H_5—(CH{=}CH)_n—C_6H_5$, with $n = 1, 2, 4$, agree very well with the available experimental measurements.

References

1. H. Eyring, J. Walter, and G. E. Kimball, *Quantum Chemistry*, Wiley, New York, 1944, Appendix III, p. 363.
2. L. Pauling and E. B. Wilson, Jr., *Introduction to Quantum Mechanics*, McGraw-Hill, New York, 1935, p. 148.
3. H. Margenau and G. M. Murphy, *The Mathematics of Physics and Chemistry*, 2nd ed., Van Nostrand, Princeton, 1956, p. 415.
4. D. R. Hartree, *The Calculation of Atomic Structures*, Wiley, New York, 1957.
5. G. Herzberg, *Atomic Spectra and Atomic Structure*, Dover, New York, 1944, p. 133.
6. Ref. 5, p. 132.
7. Ref. 5, p. 135.
8. G. Herzberg, *Spectra of Diatomic Molecules*, Van Nostrand, Princeton, 1950, p. 328.
9. Ref. 1, p. 185.
10. G. Herzberg, *Infrared and Raman Spectra of Polyatomic Molecules*, Van Nostrand, Princeton, 1945, p. 1.
11. Ref. 1, p. 184.
12. Ref. 10, p. 330.
13. W. R. Angus, C. R. Bailey, J. B. Hale, C. K. Ingold, A. H. Leckie, C. G. Raisin, J. W. Thomson, and C. L. Wilson, *J. Chem. Soc.*, **1936**, 971.
14. K. Rumpf and R. Mecke, *Z. Physik. Chem.*, **B44**, 299 (1939); ref. 10, p. 366, footnote 285.
15. H. Sponer and E. Teller, *Rev. Mod. Phys.*, **13**, 75 (1941).
16. H. Sponer, G. Nordheim, A. L. Sklar, and E. Teller, *J. Chem. Phys.*, **7**, 207 (1939).
17. M. Goeppert-Mayer and A. L. Sklar, *J. Chem. Phys.*, **6**, 645 (1938).

18. K. K. Innes, *J. Chem. Phys.*, **22**, 863 (1954); C. K. Ingold and G. W. King, *J. Chem. Soc.*, **1953**, 2702.
19. G. Herzberg and K. K. Innes, *Can. J. Phys.*, **35**, 842 (1957).
20. K. Dressler and D. A. Ramsay, *Phil. Trans. Roy. Soc. London*, **A251**, 553 (1959).
21. A. E. Douglas and J. M. Hollas, *Can. J. Phys.*, **39**, 479 (1961).
22. H. A. Jahn and E. Teller, *Proc. Roy. Soc.* (*London*), **A161**, 220 (1937); H. A. Jahn, *ibid.*, **A164**, 117 (1938).
23a. G. Moe and A. B. F. Duncan, *J. Am. Chem. Soc.*, **74**, 3140 (1952); H. Sun and G. L. Weissler, *J. Chem. Phys.*, **23**, 1160 (1955).
23b. C. R. Zobel and A. B. F. Duncan, *J. Am. Chem. Soc.*, **77**, 2611 (1955).
23c. T. K. Liu, G. Moe, and A. B. F. Duncan, *J. Chem. Phys.*, **19**, 71 (1951).
24. W. E. Moffitt and A. D. Liehr, *Phys. Rev.*, **106**, 1195 (1957); H. C. Longuet-Higgins, V. Öpik, M. H. L. Pryce, and R. A. Sack, *Proc. Roy. Soc.* (*London*), **A244**, 1 (1958).
25. A. D. Liehr and W. E. Moffitt, *J. Chem. Phys.*, **25**, 1074 (1956).
26. B. Weinstock, H. H. Claassen, and C. L. Chernick, *J. Chem. Phys.*, **38**, 1470 (1963).
27. H. C. Longuet-Higgins, *Advances in Spectroscopy*, Vol. II, H. W. Thompson, Ed., Interscience, New York, 1961, p. 429.
28. J. A. Pople and H. C. Longuet-Higgins, *Mol. Phys.*, **1**, 372 (1958).
29a. J. C. Slater, *Quantum Theory of Molecules and Solids*, Vol. 1, McGraw-Hill, New York, 1963, p. 401.
29b. L. C. Allen and A. M. Karo, *Rev. Mod. Phys.*, **32**, 275 (1960).
30. C. C. J. Roothaan, *Rev. Mod. Phys.*, **23**, 69 (1951).
31. H. M. James and A. S. Coolidge, *J. Chem. Phys.*, **1**, 825 (1933).
32. P. L. Goodfriend, F. W. Birss, and A. B. F. Duncan, *Rev. Mod. Phys.*, **32**, 307 (1960).
33. E. Hückel, *Z. Physik. Chem.*, **60**, 423 (1930); **70**, 204 (1931); **72**, 310 (1931); **76**, 626 (1932).
34. Ref. 29a, p. 233.
35. C. C. J. Roothaan and R. G. Parr, *J. Chem. Phys.*, **17**, 1001 (1949).
36. D. P. Craig, *J. Chem. Phys.*, **17**, 1358 (1949); *Proc. Roy. Soc.* (*London*), **A200**, 474 (1950).
37. R. G. Parr, D. P. Craig, and I. G. Ross, *J. Chem. Phys.*, **18**, 1561 (1950).
38. J. W. Moskowitz and M. P. Barnett, *J. Chem. Phys.*, **39**, 1557 (1963).
39. D. R. Kearns, *J. Chem. Phys.*, **36**, 1608 (1962).
40. T. M. Dunn and C. K. Ingold, *Nature*, **176**, 65 (1955).
41. E. Hückel, *Z. Elektrochem.*, **43**, 752 (1937).
42. J. E. Lennard-Jones, *Proc. Roy. Soc.* (*London*), **A158**, 280 (1937).
43. J. E. Lennard-Jones and C. A. Coulson, *Trans. Faraday Soc.*, **35**, 811 (1939).
44. L. Pauling and G. W. Wheland, *J. Chem. Phys.*, **1**, 362 (1933); L. Pauling and J. Sherman, *ibid.*, **1**, 679 (1933).
45. C. A. Coulson and H. C. Longuet-Higgins, *Proc. Roy. Soc.* (*London*), **A191**, 39 (1947).
46. C. A. Coulson andG. S. Rushbrooke, *Proc. Cambridge Phil. Soc.*, **36**, 193 (1940).
47. R. S. Mulliken, C. A. Rieke, D. Orloff, and H. Orloff, *J. Chem. Phys.*, **17**, 1248 (1949).
48. C. C. J. Roothaan and R. S. Mulliken, *J. Chem. Phys.*, **16**, 118 (1948).
49. R. S. Mulliken and C. A. Rieke, *Rev. Mod. Phys.*, **14**, 259 (1942).
50. H. C. Longuet-Higgins, C. W. Rector, and J. R. Platt, *J. Chem. Phys.*, **18**, 1174 (1950).
51. C. A. Coulson, *Proc. Phys. Soc.* (*London*), **A60**, 257 (1948).

52. D. E. Mann, J. R. Platt and H. B. Klevens, *J. Chem. Phys.*, **17**, 481 (1949).
53. J. R. Platt, *J. Chem. Phys.*, **18**, 1168 (1950).
54. W. W. Robertson, J. F. Music, and F. A. Matsen, *J. Am. Chem. Soc.*, **72**, 5260 (1950).
55. K. F. Herzfeld and A. L. Sklar, *Rev. Mod. Phys.*, **14**, 294 (1942).
56. R. Pariser and R. G. Parr, *J. Chem. Phys.*, **21**, 466, 568, 767 (1953).
57. P. G. Lykos and R. G. Parr, *J. Chem. Phys.*, **24**, 1166 (1956).
58. J. R. Platt, *J. Chem. Phys.*, **17**, 484 (1949).
59. H. B. Klevens and J. R. Platt, *J. Chem. Phys.*, **17**, 470 (1949).
60. W. T. Simpson, *J. Chem. Phys.*, **17**, 1218 (1949).
61. W. T. Simpson, *J. Chem. Phys.*, **16**, 1124 (1948).
62. G. N. Lewis and M. Calvin, *Chem. Rev.*, **25**, 273 (1939).
63. W. T. Simpson, *J. Am. Chem. Soc.*, **73**, 5363 (1951).
64. H. Kuhn, *J. Chem. Phys.*, **17**, 1198 (1949).
65. N. S. Ham and K. Ruedenberg, *J. Chem. Phys.*, **25**, 1, 13 (1956); *Errata*, **26**, 237 (1958).
66. K. Ruedenberg, *J. Chem. Phys.*, **34**, 1861, 1878, 1884, 1892, 1907, 1987 (with E.M. Layton, Jr.) (1961).
67. C. A. Coulson, *Valence*, Oxford University Press, London, 1952; L. Pauling, *The Nature of the Chemical Bond*, 3rd ed., Cornell University Press, Ithaca, 1960; B. Pullman and A. Pullman, *Les Theories Electroniques de la Chimie Organique*, Masson et Cie, Paris, 1952.
68. R. S. Mulliken and C. A. Rieke, *Rept. Progr. Phys.*, **8**, 231 (1941).
69. N. Q. Chako, *J. Chem. Phys.*, **2**, 644 (1934).
70. V. Henri and L. W. Pickett, *J. Chem. Phys.*, **7**, 439 (1939); L. W. Pickett, E. Paddock, and E. Sackter, *J. Am. Chem. Soc.*, **63**, 1073 (1941).
71. L. E. Jacobs and J. R. Platt, *J. Chem. Phys.*, **16**, 1137 (1948).
72. R. S. Mulliken, *J. Chem. Phys.*, **7**, 20 (1939).
73. R. S. Mulliken, *Phys. Rev.*, **50**, 1017, 1028 (1936).
74. R. S. Mulliken, *Phys. Rev.*, **51**, 315 (1937).
75. R. S. Mulliken, *J. Chem. Phys.*, **8**, 234 (1940).
76. R. S. Mulliken, *J. Chem. Phys.*, **8**, 382 (1940).
77. H. L. McMurry, *J. Chem. Phys.*, **9**, 231 (1941).
78. R. S. Holdsworth and A. B. F. Duncan, *Chem. Rev.*, **41**, 311 (1947).
79. J. A. Pople and J. W. Sidman, *J. Chem. Phys.*, **27**, 1270 (1957).
80. R. S. Mulliken, *J. Chem. Phys.*, **7**, 121 (1939).
81. R. S. Mulliken, *J. Chem. Phys.*, **7**, 364 (1939).
82. R. S. Mulliken, *J. Chem. Phys.*, **7**, 339, 353 (1939).

CHAPTER III

INTERPRETATION OF ELECTRONIC ABSORPTION SPECTRA

F. A. MATSEN
Department of Chemistry and Department of Physics, University of Texas, Austin, Texas

R. S. BECKER
Department of Chemistry, University of Houston, Houston, Texas

D. R. SCOTT*
Department of Chemistry, University of Texas, Austin, Texas

I. Introduction 200
II. Theory 201
  A. Introductory Survey 201
  B. Simple Orbital Theory 202
  C. The Orbital Theory of Atoms 203
  D. Molecular Orbital Theory 208
  E. The Homopolar Diatomic Molecule 211
  F. An Introduction to Group Theory 213
  G. The Heteropolar Diatomic Molecule: Perturbation Theory 219
  H. Linear Conjugated Polyatomic Systems 221
    1. Linear Combination of Atomic Orbitals-Molecular Orbital (LCAO–MO) 221
    2. Free-Electron Molecular Orbital Theory (FEMO) 224
  I. Other Transitions and Symbols 226
III. The Chromophores 227
  A. The Single Bond 227
    1. Molecular Hydrogen 227
    2. Paraffins 228
  B. The Multiple Bond 229
    1. Ethylene 230
    2. The Effect of Basic Substitution 231
    3. Alkyl Substitution: Hyperconjugation 235
    4. Diolefins 238
    5. Acetylene 240
  C. The Basic Group 241
  D. The Multiple-Bonded Basic Group 245
    1. The Carbonyl Group 246
    2. The Thiocarbonyl and Sulfoxide Groups 251
    3. Nitroso and Nitro Compounds 252
    4. Azo Compounds 256

---

* Present address: Materials Science Laboratory, Lockheed-Georgia Co., Marietta, Georgia.

E. The Benzene Chromophore . . . 257
  1. Benzene . . . 257
  2. Monosubstituted Benzenes . . . 262
  3. Alkyl Substitution . . . 266
  4. Chloroalkyl Substitution . . . 267
  5. The Substitution of Unsaturated Groups . . . 267
  6. Polysubstituted Benzenes . . . 268
  7. The Effect of Substitution on the 2000-Å Band of Benzene . . . 272
  8. Parabenzoquinone . . . 274
F. Condensed-Ring Aromatic Hydrocarbons . . . 277
  1. Naphthalene . . . 281
  2. Anthracene . . . 282
  3. Naphthacene and Higher Acenes . . . 287
  4. Phenanthrene and Other Phenes . . . 287
  5. Ionization Energies and Electron Affinities . . . 287
  6. Azulene . . . 289
G. The Heterocyclics . . . 291
  1. Saturated Heterocyclics . . . 291
  2. Unsaturated Five-Membered Heterocyclics . . . 292
  3. Aza Aromatic Heterocyclics . . . 295
IV. Special Topics . . . 298
A. Complexes . . . 298
  1. Charge Transfer Complexes . . . 298
  2. Organometallic Complexes . . . 301
B. Hydrocarbon Ions and Radicals . . . 302
  1. Simple Carbonium Ions . . . 302
  2. Aromatic Ions and Radicals . . . 303
C. Dyes and Other Extended Conjugated Systems . . . 306
D. Porphyrins, Chlorophylls, and Other Natural Pigments . . . 315
E. The Effect of Environment . . . 320
  1. Solvent Effects . . . 322
  2. The Classification of Transitions by Solvent Effects . . . 326
  3. The Effects of Temperature and Pressure . . . 327
List of Symbols . . . 329
General References . . . 330
Collections of Spectra and Spectral Data . . . 330
References . . . 330

I. INTRODUCTION

The three fundamental structural components of organic molecules giving rise to electronic absorption spectra are the single bond, the multiple bond, and the basic group*. Compounds containing only single bonds absorb below 1800 Å, the simplest multiple bond compounds below 2400 Å, and the simplest basic compounds below 3500 Å. The absorption by the multiple bond, the basic group, and various combinations of these fundamental components make up the great bulk of organic electronic absorption spectra. When the absorption by a particular component or group of components is under study, that group is called a *chromophore*.

---

* The modern definition of a base is a compound, radical, or ion which can donate a pair of electrons to an acid. While it is not this property which is of primary interest here, the phrase "basic group" does indicate a group containing an atom with an unshared pair of electrons and will be so used.

Interpretation of absorption spectra is greatly facilitated by studying the effect of substitution on the chromophore; the interpretation of the spectrum of the substituted chromophore is, of course, an end in itself. In some cases a group of substituents can be chosen so as to give an almost continuous change in the perturbation of the chromophore. Other useful information concerning the nature of the electronic transitions in the chromophore may result from a study of the effects of different solvents and/or pressure upon the spectrum.

II. THEORY

A. Introductory Survey

In principle all the properties of molecules are predictable *ab initio* by the methods of quantum mechanics. In practice such predictions have been made for only a few simple molecules (1). The calculations employ the variation principle, large sets of basis functions (many configurations), exact evaluation of integrals, and large electronic computers. There is some upper limit of molecular complexity beyond which one will not be able or will not wish to go because of the time and expense involved. At present this upper limit appears to be so low as to exclude most of the molecules of chemical interest. Even in those few cases for which precise computation and prediction are possible, there appears to exist a need to "understand" a molecule, i.e., a need to think about a molecule in simple terms and in relation to similar molecules. Such a model need not have a rigorous basis nor be completely consistent. The principal requirement of such a model is that it provide a language with which one can compare, and sometimes predict, the properties of similar molecules. For the electronic spectra of organic molecules, orbital theories provide such a model.

In this chapter we will use molecular orbital theory within the simple Hückel framework. A more recent development has been the semiempirical self-consistent field theories of which the Pariser-Parr-Pople treatments (4,6) are an outstanding example. Whereas the Hückel treatment is carried out with an undefined Hamiltonian and does not explicitly include electron interactions, the Pariser-Parr-Pople calculations employ a well-defined Hamiltonian and provide for electron interactions. There is, of course, partial equivalence between the Hückel and Pariser-Parr-Pople theories (2).

B. Simple Orbital Theory

An *orbital* is a wave function for a single electron. It is denoted by ϕ_a ($a = 1, 2, \ldots$). To each orbital is assigned by experiment and/or theory an *orbital energy* which is denoted by ϵ_a. These energies are not to be regarded as absolute numbers but as numbers to be used to correlate results for related molecules. The orbital energy is made up of two parts: one which represents the energy of the single electron in the absence of all other electrons, and a second which represents an approximation to the interaction with the remaining electrons. In simple orbital theory a *state* of a molecule is represented by a *configuration*, an assignment of the electrons to the several orbitals with no more than two electrons to an orbital (Pauli exclusion principle). The number of electrons assigned to the *a*th orbital in the *i*th configuration is denoted by ν_{ia}. The configuration wave functions are written as

$$\Phi_i = (\phi_1)^{\nu_{i1}}(\phi_2)^{\nu_{i2}}\cdots$$

In simple orbital theory the energy of the i^{th} configuration is

$$E_i = \sum_a \nu_{i_a}\epsilon_a$$

An important characteristic of orbitals is their behavior under a transformation of coordinates. Consider, for example, the operation of inversion i through the origin (Chapter II, pp. 142–148).

$$i\phi_a(x,y,z) \equiv \phi_a(-x,-y,-z)$$

If

$$i\phi_a = +\phi_a$$

ϕ_a is called a *gerade* orbital. If

$$i\phi_a = -\phi_a$$

ϕ_a is called an *ungerade* orbital.

In the simple orbital theory, electromagnetic radiation can cause a transition from an orbital of lower energy to one of higher energy, say $\phi_a \rightarrow \phi_b$. Such a transition can take place only if the transition moment

$$\mathbf{T}_{ab} \equiv \int \phi_a \mathbf{R} \phi_b \, d\tau$$

is not zero (Chapter II, p. 121). Here **R** is the electron position vector directed from the origin. Under inversion

$$i\mathbf{R} = -\mathbf{R}$$

It should be noted that the transition moment is a vector which is independent of the choice of coordinate system. If ϕ_a and ϕ_b are both gerade, the transition moment integral under an inversion of coordinates is

$$i(\mathbf{T}_{ab}) = \int \phi_a(-\mathbf{R})\phi_b \, d\tau = -\int \phi_a \mathbf{R} \phi_b \, d\tau$$

Since $\mathbf{T}_{ab}$ is independent of the coordinate system,

$$i(\mathbf{T}_{ab}) = \mathbf{T}_{ab}$$

or

$$-\int \phi_a \mathbf{R} \phi_b \, d\tau = \int \phi_a \mathbf{R} \phi_b \, d\tau = 0$$

The only vector which is the negative of itself is zero. If ϕ_a and ϕ_b are both ungerade,

$$i(\mathbf{T}_{ab}) = \int (-\phi_a)(-\mathbf{R})(-\phi_b) \, d\tau = -\int \phi_a \mathbf{R} \phi_b \, d\tau$$

$$i(\mathbf{T}_{ab}) = \mathbf{T}_{ab} = -\int \phi_a \mathbf{R} \phi_b \, d\tau = \int \phi_a \mathbf{R} \phi_b \, d\tau = 0$$

However, if one of the orbitals is gerade and the other ungerade, the transition moment is not necessarily zero. As a consequence we have the following selection rules:

gerade ↔ gerade:	forbidden
ungerade ↔ ungerade:	forbidden
gerade ↔ ungerade:	allowed

C. The Orbital Theory of Atoms

As an example of simple orbital theory we consider the orbital theory of atoms. The problem of one electron on a nucleus with charge Z has been solved exactly. The solutions are (Chapter II, p. 109 *et seq.*)

$$\phi_a = \phi_{nlm}$$

where n, l, and m are the principal, azimuthal, and magnetic quantum numbers, respectively. For $l = 0, 1, 2, \ldots$, these atomic orbitals are called $s, p, d, \ldots$. These orbitals are solutions to the Schroedinger equation for the hydrogen atom

$$H\phi_{nlm} = E_n\phi_{nlm}$$

where

$$H = -(h^2/8\pi^2 m)\nabla^2 - Ze^2/r$$

is the Hamiltonian operator for the one-electron atom and m is the mass of the electron. The orbital energies are

$$E_n = \int \phi^*_{nlm} H \phi_{nlm} \, d\tau$$
$$= -13.6 Z^2/n^2 \text{ eV}$$

Under inversion the atomic orbitals transform according to

$$i\phi_{nlm} = (-1)^l \phi_{nlm}$$

that is s, d, . . ., orbitals are gerade and p, f, . . ., orbitals are ungerade. Consequently, we have the following selection rules for transitions

$ns \leftrightarrow n's$: forbidden
$ns \leftrightarrow n'p$: allowed etc.

For more than one electron the Hamiltonian is

$$H = \sum_i^n H_i + \sum_{i>j} e^2/r_{ij}$$

Here H_i is the Hamiltonian for a single electron, and r_{ij} is the distance between the ith and jth electron. The polyelectronic problem cannot be solved exactly because of the terms in e^2/r_{ij}. However, products of the one-electron orbitals may be used as a basis for a discussion of the polyelectronic problem. For example, a wave function which gives a good description of the ground state of helium is (3)

$$\Phi_1 = \lambda_1(1s)^2 + \lambda_2(2s)^2 + \lambda_3(2p)^2 + \lambda_4(3s)^2 + \cdots$$

where the λ_i are determined by the variation principle. (Chapter II, p. 21 *et seq.*) As the number of terms in the wave function is increased, the accuracy of the wave function also increases. One cannot say that the electrons are assigned to specific orbitals so that *simple orbital theory does not rigorously hold in polyelectronic systems.* However, $\lambda_1 > \lambda_2, \lambda_3, \lambda_4$, so to a fair approximation the ground state wave function for helium is

$$\Phi_1 = (1s)^2 = 1s(1)1s(2)$$

Here (1) and (2) refer to the coordinates of electrons one and two. The energy of the ground state of helium is then given approximately by*

$$E(1s^2) = \int \Phi_1 H \Phi_1 \, d\tau$$
$$= E^0(1s^2) + J(1s^2)$$

---

* A superscript 0 denotes the configuration energy calculated without electron repulsion.

Here

$$\begin{aligned} E^0(1s^2) &= \int 1s(1)H_1 1s(1)\,d\tau_1 \int 1s(2)1s(2)\,d\tau_2 \\ &\quad + \int 1s(1)1s(1)\,d\tau_1 \int 1s(2)H_2 1s(2)\,d\tau_2 \\ &= 2E_1(1s) \\ &= -108.8 \text{ eV} \end{aligned}$$

and

$$\begin{aligned} J(1s^2) &\equiv \int 1s(1)1s(2)(e^2/r_{12})1s(1)1s(2)\,d\tau \\ &= 34.0 \text{ eV} \end{aligned}$$

$J(1s^2)$ is called a coulomb integral (Chapter II, p. 115) and has an experimental value of 29.8 eV. Then

$$E_1(1s^2) = -108.8 + 34.0 = -74.8 \text{ eV}$$

The experimental value is -79.0 eV. The discrepancy between theory and experiment can be reduced by a better choice of orbitals, e.g., by the use of self-consistent field orbitals (4) (Chapter II, p. 117).

By simple orbital theory and with the experimental value of the energy, the $1s$ orbital energy, ϵ_{1s}, is determined from

$$E(1s^2) \equiv 2\epsilon_{1s} = -79.0 \text{ eV}$$

to be

$$\epsilon_{1s} = -39.5 \text{ eV}$$

We turn now to a discussion of excited states. An excited state configuration for helium is

$$\Phi_2 = (1s)^1(2s)^1$$

The energy of this configuration, neglecting electron repulsion, is

$$E^0(1s2s) = E_1(1s) + E_2(2s) = -13.6Z^2(1/1^2 + 1/2^2) = -68.0 \text{ eV}$$

The theoretical electron repulsion is

$$J(1s2s) = \int 1s(1)2s(2)(e^2/r_{12})1s(1)2s(2)\,d\tau = 11.4 \text{ eV}$$

The experimental value is 9.6 eV. Using the experimental value

$$\begin{aligned} E(1s2s) &= E_1(1s) + E_2(2s) + J(1s2s) = -68.0 + 9.6 = -58.4 \text{ eV} \\ &\equiv \epsilon_{1s} + \epsilon_{2s} \end{aligned}$$

so with $\epsilon_{1s} = -39.5$ eV

$$\begin{aligned}\epsilon_{2s} &= E(1s2s) - \epsilon_{1s}\\ &= -18.9 \text{ eV}\end{aligned}$$

Note that $|\epsilon_{1s}| > |\epsilon_{2s}|$.

This is not, however, the whole story. If we distinguish mathematically between electrons, there are in fact two wave functions for $\Phi_2 = (1s)^1(2s)^1$

$$\Phi_{2a} = 1s(1)2s(2)$$

and

$$\Phi_{2b} = 1s(2)2s(1)$$

For both functions

$$E_{2a}{}^0 = E_{2b}{}^0 = E^0 = -68.0 \text{ eV}$$

When one writes wave functions which differ only in the labeling of electrons, one implies that the electrons are distinguishable. But by the uncertainty principle two electrons which occupy the same region of space are not distinguishable. Heisenberg resolved this difficulty by writing two new independent wave functions. They are

$$\begin{aligned}\Phi_{S2} &= 1/\sqrt{2}[1s(1)2s(2) + 1s(2)2s(1)]\\ \Phi_{T2} &= 1/\sqrt{2}[1s(1)2s(2) - 1s(2)2s(1)]\end{aligned}$$

where the energies corresponding to Φ_{S2} and to Φ_{T2} are, respectively

$$\begin{aligned}E(S2) &= E^0(1s2s) + J(1s2s) + K(1s2s)\\ E(T2) &= E^0(1s2s) + J(1s2s) - K(1s2s)\end{aligned}$$

Note that

$$E_{S2}{}^0 = E_{T2}{}^0 = E^0(1s2s) = -68.0 \text{ eV}$$

Here the so-called exchange integral

$$K(1s2s) = \int 1s(2)2s(1)(e^2/r_{12})1s(1)2s(2)\, d\tau$$

has a theoretical value of 1.2 eV. The experimental value is 0.4 eV. Using the experimental value

$$\begin{aligned}E(S2) &= E(1s2s) + 0.4 \text{ eV}\\ E(T2) &= E(1s2s) - 0.4 \text{ eV}\end{aligned}$$

This splitting is observed experimentally as

$$E(S2) - E(T2) = 0.80 \text{ eV}$$

Note that the splitting depends only upon the coulombic interactions of the electrons.

The simple orbital theory does not predict this splitting. It provides only the mean energy of the singlet and triplet states, that is,

$$E(1s2s) = [E(S2) + E(T2)]/2$$

The designations T and S refer to triplet and singlet states, respectively. These names arise from the fact that in a magnetic field the triplet state splits into three states, but the singlet state does not split. This effect, called the Zeeman effect, is due to the interaction of the spin magnetic moment with the magnetic field.

For certain applications it is convenient to obtain orbital energies, ϵ_i', defined in terms of ionization energies. For example,

$$\begin{aligned}\epsilon'_{1s} &= -I(1s^2) = -[E_1(1s) - E(1s^2)] = -E_1(1s) + 2E_1(1s) + J(1s^2)\\ &= E_1(1s) + J(1s^2) = [-54.4 + 29.8] = -24.6 \text{ eV}\end{aligned}$$

The experimental value -24.6 eV is to be compared with the theoretical ionization energy of -20.4 eV. The orbital energy, ϵ'_{1s}, is the negative of the energy required to remove a single electron from the $1s$ orbital. Note that

$$\begin{aligned}\epsilon_{1s} &= E(1s^2)/2 = 2E_1(1s)/2 + J(1s^2)/2 = E_1(1s) + J(1s^2)/2\\ &= -39.5 \text{ eV}\end{aligned}$$

and that the difference between ϵ'_{1s} and ϵ_{1s} is one-half the experimental electron repulsion, $J(1s^2)$. Likewise, for the energy required to remove a $2s$ electron from the $1s^1 2s^1$ configuration, an orbital energy, ϵ'_{2s}, may be defined as

$$\begin{aligned}\epsilon'_{2s} &\equiv -I(1s2s) = -[E_1(1s) - E(1s2s)]\\ &= -E_1(1s) + E_1(1s) + E_2(2s) + J(1s2s)\\ &= E_2(2s) + J(1s2s) = [-13.6 + 9.6] = -4.0 \text{ eV}\end{aligned}$$

Since

$$\begin{aligned}\epsilon_{2s} &= E(1s2s) - \epsilon_{1s} = E_1(1s) + E_2(2s) + J(1s2s) - [E_1(1s) + J(1s^2)/2]\\ \epsilon_{2s} &= E_2(2s) + J(1s2s) - J(1s^2)/2 = -18.9 \text{ eV}\end{aligned}$$

the difference between ϵ'_{2s} and ϵ_{2s} is also one-half the electron repulsion, $J(1s^2)$.

In simple orbital theory, the excitation energy, ΔE, for $1s^2 \rightarrow 1s^1 2s^1$ is given by

$$E(1s2s) - E(1s^2) = \epsilon_{2s} + \epsilon_{1s} - 2\epsilon_{1s} = \epsilon_{2s} - \epsilon_{1s} = 20.6 \text{ eV}$$

Note that replacing ϵ by ϵ' yields

$$E(1s2s) - E(1s^2) = \epsilon'_{2s} - \epsilon'_{1s} = -4.0 + 24.6 = 20.6 \text{ eV}$$

Therefore, the use of ϵ_i' values in place of ϵ_i values does not affect the excitation energy.

Finally we treat the problem of transition probabilities in two electron systems. The position vector for a two-electron system is

$$\mathbf{R} = \mathbf{r}_1 + \mathbf{r}_2$$

We consider first the transition between two singlet states

$$\Phi_{Sab} = 1/\sqrt{2}\,[\phi_a(1)\phi_b(2) + \phi_a(2)\phi_b(1)]$$

and

$$\Phi_{S'cd} = 1/\sqrt{2}\,[\phi_c(1)\phi_d(2) + \phi_c(2)\phi_d(1)]$$

Then

$$\mathbf{T}_{SS'} = \int \Phi_{Sab}\mathbf{R}\Phi_{S'cd}\,d\tau = [S_{bd}\mathbf{T}_{ac} + S_{bc}\mathbf{T}_{ad} + S_{ad}\mathbf{T}_{bc} + S_{ac}\mathbf{T}_{bd}]$$

where $\mathbf{T}_{ij} = \int \phi_i\mathbf{r}\phi_j\,d\tau$ and $S_{ij} = \int \phi_i\phi_j\,d\tau$. Thus, a singlet–singlet transition is allowed provided the orbital transition moments, $\mathbf{T}_{ij}$, are not zero. Consider next the transition probability between the singlet state, Φ_{Sab}, and the triplet state

$$\Phi_{Tcd} = 1/\sqrt{2}\,[\phi_c(1)\phi_d(2) - \phi_c(2)\phi_d(1)]$$

$$\begin{aligned}\mathbf{T}_{ST} = \int \Phi_{Sab}\mathbf{R}\Phi_{Tcd}\,d\tau &= \tfrac{1}{2}[S_{bd}\mathbf{T}_{ac} - S_{bc}\mathbf{T}_{ad} + S_{ad}\mathbf{T}_{bc} - S_{ac}\mathbf{T}_{bd} \\ &\quad + S_{ac}\mathbf{T}_{bd} - S_{ad}\mathbf{T}_{bc} + S_{bc}\mathbf{T}_{ad} - S_{bd}\mathbf{T}_{ac}] \\ &= 0\end{aligned}$$

We see that the transition probability between a singlet and a triplet state is zero irrespective of the orbital transition moments. This selection rule breaks down for atoms of high atomic number due to spin–orbit interaction.

D. Molecular Orbital Theory (5,6)

In molecules one may again assign electrons to orbitals. Some of the electrons are assigned to orbitals which extend over more than one atom and which are appropriately called *molecular orbitals*. For example, the lowest or ground state configuration of HF may be written $1s^22s^2x^2y^2\sigma^2$,* where σ is a molecular orbital extending over both hydrogen and fluorine.

It should be remembered that the wave functions $2s$, $2p$, etc., have been taken over from the hydrogen atom problem, and are not solutions to the molecular problem at all. It is not surprising that the hydrogen atom wave functions must be modified to secure a reasonably satisfactory description of the molecule. In certain situations the electrons are not assigned to specific s and p orbitals but to new atomic orbitals which are linear combinations of the old. These linear combinations are taken in such a way as to obtain stronger bonding in specific directions. The use of linear combinations of hydrogenic orbitals rather than the hydrogenic orbitals themselves is called *hybridization.* The electron configuration of HF was given above as $1s^2 2s^2 x^2 y^2 \sigma^2$. Without hybridization*

---

* z is a p orbital pointing along the bond axis. y lies perpendicular to the bond axis and in the plane of the molecule. x lies perpendicular to the bond axis and perpendicular to the plane of the molecule.

$$\sigma = 1s_{\mathrm{H}} + \lambda z_{\mathrm{F}}$$

Hybridization of the s and p orbitals on fluorine yields two new atomic orbitals:

$$\begin{aligned} di_{1\mathrm{F}} &= 2s_{\mathrm{F}} + \lambda z_{\mathrm{F}} \\ di_{2\mathrm{F}} &= \mu 2s_{\mathrm{F}} - z_{\mathrm{F}} \end{aligned}$$

where λ and μ are coefficients. The former of these is an orbital which projects farther toward the hydrogen atom than does the p orbital by itself. The second is nonbonding and projects out on the side of fluorine opposite to the bond. A new molecular orbital can now be written:

$$\sigma_1 = 1s_{\mathrm{H}} + \omega\, di_{1\mathrm{F}}$$

The electron configuration of HF is then $1s^2 x^2 y^2\, di_{2\mathrm{F}}{}^2 \sigma_1{}^2$.

The electron configuration of the ground state of carbon is $1s^2 2s^2 xy$. On bonding, enough energy is gained to promote the carbon atom to its valence state, $1s^2 2sxyz$. In this state the carbon atom can hybridize in three ways:

(*1*) *Tetrahedrally as in methane:*

$$\begin{aligned} te_1 &= 2s + x + y + z \\ te_2 &= 2s + x - y - z \\ te_3 &= 2s - x + y - z \\ te_4 &= 2s - x - y + z \end{aligned}$$

(*2*) *Trigonally as in ethylene:*

$$\begin{aligned} tr_1 &= 2s + \sqrt{2}\, z \\ tr_2 &= (2s) - z/\sqrt{2} + (\sqrt{3}/\sqrt{2})y \\ tr_3 &= (2s) - z/\sqrt{2} - (\sqrt{3}/\sqrt{2})y \end{aligned}$$

x unhybridized

---

* Normalization factors will be neglected throughout.

(3) *Digonally as in acetylene:*

$$\begin{aligned} di_1 &= 2s + z \\ di_2 &= 2s - z \end{aligned}$$

x and y unhybridized

The procedure of simple molecular orbital theory is as follows: (*1*) Assign to each atom in the molecule one or more orbitals, ϕ_a ($a = 1$–n). (*2*) Construct a matrix representation of a one electron Hamiltonian with elements

$$H_{ab} \equiv \int \phi_a H \phi_b \, d\tau$$

where $a,b = 1$ to n. The orbitals are assumed to be orthogonal and normalized, i.e.,

$$S_{ab} \int \phi_a \phi_b \, d\tau = \delta_{ab}$$

The exact form of the Hamiltonian is unimportant, but it must reflect the symmetry of the molecule. The matrix elements are not evaluated theoretically but are retained as parameters to be fitted from experimental data. However, H_{aa} may be regarded as the energy required to remove an electron from atom a, and H_{ab} may be regarded as an interaction energy between atoms a and b. (*3*) Diagonalize the matrix representation of the Hamiltonian determining its eigenvalues and eigenvectors. The eigenvalues are taken to be molecular orbital energies, and the eigenvectors to be the molecular orbitals.

To diagonalize the representation of the Hamiltonian the determinental equation

$$|H_{ab} - E\delta_{ab}| = 0$$

must be solved. This equation has n roots labeled $\epsilon_1, \epsilon_i \ldots \epsilon_n$. The eigenvectors are

$$\Psi_i = \sum_a c_{ia} \phi_a$$

where the c_{ia} are determined from the equation

$$\sum_a (H_{ba} - \delta_{ab} E_i) c_{ia} = 0$$

and

$$\sum_a |c_{ia}|^2 = 1$$

E. The Homopolar Diatomic Molecule

The simplest molecular system is the homopolar diatomic molecule. With the two atoms labeled A and B, the determinantal equation is

$$\begin{vmatrix} H_{AA} - E & H_{AB} \\ H_{AB} & H_{BB} - E \end{vmatrix} = 0$$

Since the molecule is homopolar, $H_{AA} = H_{BB}$. The two roots of the equation will be seen to be

$$E_1 = H_{AA} + H_{AB}$$
$$E_2 = H_{AA} - H_{AB}$$

Since H_{AB} is normally negative, $E_1 < E_2$ (see Fig. 1).

The equation for the coefficients becomes

$$(H_{AA} - E_i)c_{iA} + H_{AB}c_{iB} = 0$$

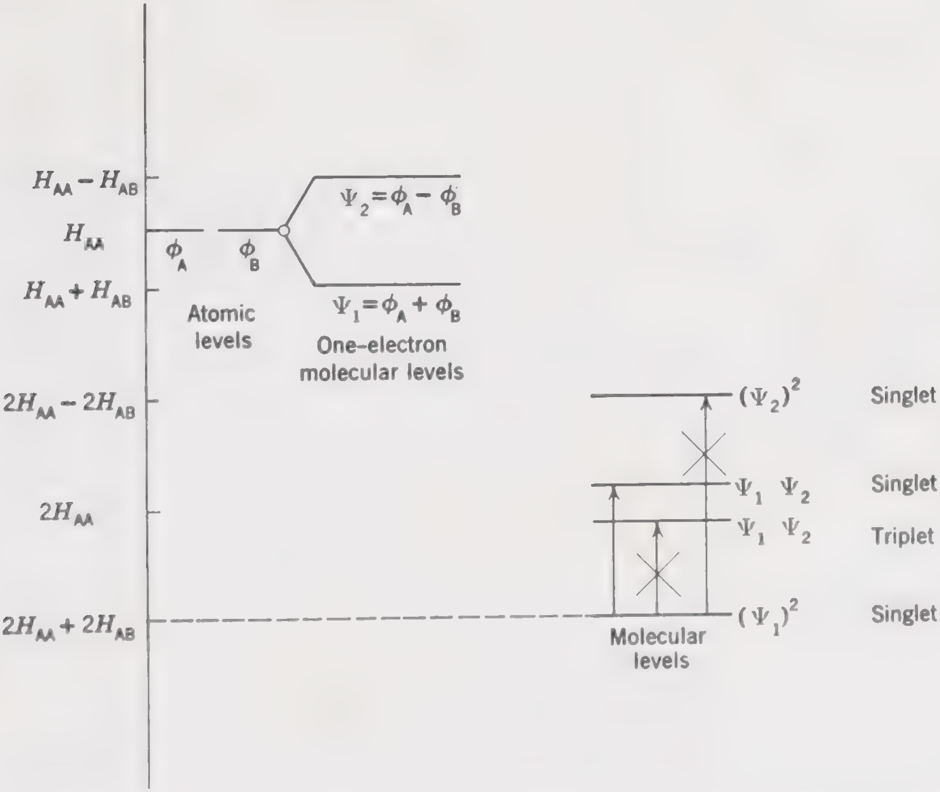
$H_{AA} - H_{AB}$
H_{AA}
$H_{AA} + H_{AB}$
ϕ_A
ϕ_B
Atomic levels
$\Psi_2 = \phi_A - \phi_B$
$\Psi_1 = \phi_A + \phi_B$
One-electron molecular levels
$2H_{AA} - 2H_{AB}$
$2H_{AA}$
$2H_{AA} + 2H_{AB}$
$(\Psi_2)^2$
Singlet
$\Psi_1 \ \Psi_2$
Singlet
$\Psi_1 \ \Psi_2$
Triplet
$(\Psi_1)^2$
Singlet
Molecular levels

Fig. 1. Molecular orbital representation of a two-electron homopolar diatomic molecule. Transitions marked × are forbidden.

Substitution of E_1 gives

$$[H_{AA} - (H_{AA} + H_{AB})]c_{1A} + H_{AB}c_{1B} = 0$$

and

$$c_{1A} = c_{1B}$$

Thus

$$\Psi_1 = c_{1A}(\phi_A + \phi_B)$$

Since only the form of the molecular orbital is important in this discussion, it will usually be written in the form*

$$\Psi_1 = \phi_A + \phi_B$$

By similar argument the second molecular orbital is associated with E_2 and becomes

$$\Psi_2 = \phi_A - \phi_B$$

The energy E_1 less is than E_2 since H_{AB} is commonly a negative quantity. Consequently, one may speak of Ψ_1 as lying lower than Ψ_2, that is, the molecule is more stable with an electron in Ψ_1 than in Ψ_2. Because of this stability, Ψ_1 may be spoken of as a bonding orbital and Ψ_2 as an antibonding orbital. It is often convenient to star antibonding orbitals (see the list of symbols).

To illustrate the formation of electron configurations, let us consider a diatomic molecule containing two electrons. Before electrons are added to the system, it carries a double positive charge. The addition of an electron to the lowest orbital gives the configuration $(\Psi_1)^1$. This corresponds to the hydrogen molecule ion which is described in Section III-A-1. The addition of the second electron to the lowest orbital gives the configuration of the ground state of the molecule $(\Psi_1)^2$. From these two orbitals we can also obtain configurations $(\Psi_1)^1$, $(\Psi_2)^1$, and $(\Psi_2)^2$. The energies of the three configurations, neglecting electron repulsion, are

$$\begin{aligned} E_{11} &= 2(H_{AA} + H_{AB}) = 2H_{AA} + 2H_{AB} \\ E_{12} &= H_{AA} + H_{AB} + H_{AA} - H_{AB} = 2H_{AA} \\ E_{22} &= 2(H_{AA} - H_{AB}) = 2H_{AA} - 2H_{AB} \end{aligned}$$

A molecule in the $(\Psi_1)^2$ configuration is normally a stable molecule with

$$\text{Binding energy} = 2H_{AA} - 2(H_{AA} + H_{AB}) = -2H_{AB}$$

i.e., the difference between the energy of the two separate atoms and the energy of the molecule in this configuration. The configurations $(\Psi_1)^2$ and $(\Psi_2)^2$ can occur only as singlet states, while $(\Psi_1)^1(\Psi_2)^1$ can occur both as a singlet and as a triplet state. The configuration energy E_{12} is the mean of the singlet and triplet energies.

---

* Normalization factors will be neglected.

We consider now the transition probabilities between the two molecular orbitals, Ψ_1 and Ψ_2. Both ϕ_A and ϕ_B are assumed to be symmetrical about the internuclear axis. Then only the component of **R** along the internuclear axis, **Z**, makes a contribution to the transition moment.

$$\begin{aligned}\mathbf{T}_{12} &= \int \Psi_1 \mathbf{Z} \Psi_2 \, d\tau \\ &= \int \phi_A \mathbf{Z} \phi_A \, d\tau - \int \phi_A \mathbf{Z} \phi_B \, d\tau + \int \phi_B \mathbf{Z} \phi_A \, d\tau - \int \phi_B \mathbf{Z} \phi_B \, d\tau\end{aligned}$$

Now

$$\int \phi_A \mathbf{Z} \phi_B \, d\tau, \qquad \int \phi_B \mathbf{Z} \phi_A \, d\tau \approx 0$$

and

$$\int \phi_A \mathbf{Z} \phi_A \, d\tau = \mathbf{Z}_A$$

a vector from the origin to the atom A, and

$$\int \phi_B \mathbf{Z} \phi_B \, d\tau = \mathbf{Z}_B = -\mathbf{Z}_A$$

so

$$\mathbf{T}_{12} = 2\mathbf{Z}_A \neq 0$$

and the transition is allowed.

Transitions between singlet and triplet states are forbidden (cf. Section II-C and Chapter II, p. 123). It should be pointed out that the selection rules are not absolute and that perturbation of the molecular states by certain vibrations, by collision, and by fields associated with substituted atoms tend to relax these rules. However, even in the presence of such perturbations, "forbidden" transitions are usually weaker than the allowed ones.

Since the singlet → triplet transitions are forbidden, the bands corresponding to these transitions are difficult to detect experimentally. As a result the theoretical excitation energy, which should be correlated with the mean of the corresponding singlet → singlet and singlet → triplet experimental energies, is normally correlated with the more intense singlet → singlet band only.

F. An Introduction to Group Theory

In Section E we labeled the two nuclei of a homopolar diatomic molecule A and B. Clearly this labeling is arbitrary, for the nuclei could equally well be labeled B and A. Equally clearly any physical property of the molecule such as the energy or the transition probability must be independent of such labeling. More formally we say that the Hamiltonian of a homopolar diatomic molecule commutes with the group $G = \{I,\sigma\}$. Here I is the identity operator, and σ is an operator which interchanges the nuclei A and B (see Note 2, Chapter II). Thus

$$\begin{aligned} I\phi_A &= \phi_A \\ I\phi_B &= \phi_B \\ \sigma\phi_A &= \phi_B \\ \sigma\phi_B &= \phi_A \end{aligned}$$

Note also that

$$\begin{aligned} I^2\phi_A &= I(I\phi_A) = I\phi_A = \phi_A \\ I\sigma\phi_A &= I\phi_B = \phi_B \\ \sigma I\phi_A &= \sigma\phi_A = \phi_B \\ \sigma^2\phi_A &= \sigma(\sigma\phi_A) = \sigma\phi_B = \phi_A = I\phi_A \end{aligned}$$

Thus, as operators

$$\begin{aligned} I^2 &= \sigma^2 = I \\ I\sigma &= \sigma I = \sigma \end{aligned}$$

These relations may be expressed in the form of a multiplication table

$$\begin{array}{c|cc} & I & \sigma \\ \hline I & I & \sigma \\ \sigma & \sigma & I \end{array}$$

The group $\{I,\sigma\}$ can be represented by the set of matrices $\Gamma = \{|I|, |\sigma|\}$, where

$$|I| = \begin{vmatrix} 1 & 0 \\ 0 & 1 \end{vmatrix} \quad \text{and} \quad |\sigma| = \begin{vmatrix} 0 & 1 \\ 1 & 0 \end{vmatrix}$$

These matrices are such as to form a representation of G. The matrices have the same rules of multiplication as do the operators they represent.* Thus

$$|I|\,|I| = \begin{vmatrix} 1 & 0 \\ 0 & 1 \end{vmatrix} \begin{vmatrix} 1 & 0 \\ 0 & 1 \end{vmatrix} = \begin{vmatrix} 1 & 0 \\ 0 & 1 \end{vmatrix} = |I|$$

$$|I|\,|\sigma| = \begin{vmatrix} 1 & 0 \\ 0 & 1 \end{vmatrix} \begin{vmatrix} 0 & 1 \\ 1 & 0 \end{vmatrix} = \begin{vmatrix} 0 & 1 \\ 1 & 0 \end{vmatrix} = |\sigma|$$

$$|\sigma|\,|I| = \begin{vmatrix} 0 & 1 \\ 1 & 0 \end{vmatrix} \begin{vmatrix} 1 & 0 \\ 0 & 1 \end{vmatrix} = \begin{vmatrix} 0 & 1 \\ 1 & 0 \end{vmatrix} = |\sigma|$$

$$|\sigma|\,|\sigma| = \begin{vmatrix} 0 & 1 \\ 1 & 0 \end{vmatrix} \begin{vmatrix} 0 & 1 \\ 1 & 0 \end{vmatrix} = \begin{vmatrix} 1 & 0 \\ 0 & 1 \end{vmatrix} = |I|$$

---

* For rules of matrix multiplication, see, for example, H. Margenau and G. M. Murphy, *The Mathematics of Physics and Chemistry*, Van Nostrand, New York, 1943, p. 290.

Because the matrices have two rows and two columns, the representation is said to be of dimension two. Certain representations called the irreducible representations are of particular importance.

The representation Γ can be transformed into a second representation $\Gamma_r = \{|I|_r, |\sigma|_r\}$ of the same dimension by a similarity transformation, i.e.,

$$|\Gamma_a|_r = |S|\,|\Gamma_a|\,|S^{-1}|$$

where

$$|S| = |S^{-1}| = \begin{vmatrix} 1/\sqrt{2} & 1/\sqrt{2} \\ 1/\sqrt{2} & -1/\sqrt{2} \end{vmatrix}$$

then

$$|I|_r = \begin{vmatrix} 1 & 0 \\ 0 & 1 \end{vmatrix}$$

and

$$|\sigma|_r = \begin{vmatrix} 1 & 0 \\ 0 & -1 \end{vmatrix}$$

We note that $|I|_r$ and $|\sigma|_r$ also satisfy the multiplication table. We note further that both $|I|_r$ and $|\sigma|_r$ are "factored" into two matrices of dimension one which also satisfy the multiplication. They therefore constitute representations of the group. We label these representations

$$\Gamma^1 = \{|1|, |1|\}$$
$$\Gamma^2 = \{|1|, |-1|\}$$

Γ_r is called a reduced representation. Γ^1 and Γ^2 are called irreducible representations because there exists no similarity transformation which will "factor" them into representations of smaller dimension.

The eigenfunctions of a Hamiltonian that commutes with a group transform according to the irreducible representation of the group. Thus, since for the homopolar diatomic molecule, $\Psi_1 = \phi_A + \phi_B$, $I\Psi_1 = \Psi_1$, and $\sigma\Psi_1 = \Psi_1$. Further, since $\Psi_2 = \phi_A - \phi_B$, $I\Psi_2 = \Psi_2$ and $\sigma\Psi_2 = -\Psi_2$. Therefore, Ψ_1 belongs to Γ^1 and Ψ_2 belongs to Γ^2.

Group theory provides a powerful scheme for identifying forbidden transitions. For the homopolar diatomic molecule the transformation σ transforms $\mathbf{Z} \to -\mathbf{Z}$. The value of a transition moment does not change when an operation which relables identical atoms is performed upon it. Thus

$$\int \Psi_i \mathbf{Z} \Psi_j \, d\tau = \int \sigma(\Psi_i \mathbf{Z} \Psi_j)\, d\tau = \int (\sigma\Psi_i)(-\mathbf{Z})(\sigma\Psi_j)\, d\tau$$

Then if Ψ_i and Ψ_j belong to the same irreducible representation, Γ^1, for example,

$$\mathbf{T}_{ij} = -\int \Psi_i \mathbf{Z} \Psi_j \, d\tau = \int \Psi_i \mathbf{Z} \Psi_j \, d\tau = 0$$

Thus, transitions between functions belonging to the same one-dimensional irreducible representations are forbidden. If Ψ_i and Ψ_j belong to different irreducible representations, Γ^1 and Γ^2, $\mathbf{T}_{ij}$ is not necessarily zero. The selection rules for the homopolar molecule are

$\Gamma^1 \leftrightarrow \Gamma^1$, $\Gamma^2 \leftrightarrow \Gamma^2$: forbidden
$\Gamma^1 \leftrightarrow \Gamma^2$: allowed

Group theory may be used to determine zero matrix elements of any operator. For example consider the matrix elements of the Hamiltonian, $\int \Psi_i H \Psi_j \, d\tau$. H is invariant under the transformation σ; therefore

$$\int \Psi_i H \Psi_j \, d\tau = \int (\sigma\Psi_i)(H)(\sigma\Psi_j) \, d\tau$$

If Ψ_i and Ψ_j belong to the same irreducible representation,

$$\int (\sigma\Psi_i) H (\sigma\Psi_j) \, d\tau = \int \Psi_i H \Psi_j \, d\tau$$

which is not necessarily zero. However, if Ψ_i and Ψ_j belong to different irreducible representations

$$\int (\sigma\Psi_i) H (\sigma\Psi_j) \, d\tau = -\int \Psi_i H \Psi_j \, d\tau = \int \Psi_i H \Psi_j \, d\tau = 0$$

since the integral is invariant to the transformation σ. Thus, Hamiltonian matrix elements over functions which do not belong to the same irreducible representations are zero.

We have used the operator σ to provide a simple introduction into the theory of groups. For the homopolar diatomic molecule one normally uses the inversion operator i.

$$i\Psi(x,y,z) \equiv \Psi(-x,-y,-z)$$

where x, y, and z are the coordinates of the electron. For a molecule, the inversion is performed through the center of the molecule. If ϕ_A and ϕ_B are s functions

$$i\phi_A = \phi_B$$
$$i\phi_B = \phi_A$$

If ϕ_A and ϕ_B are *p* functions

$$i\phi_A = -\phi_B$$
$$i\phi_B = -\phi_A$$

This is a consequence of the fact that *p* orbitals have positive and negative lobes.

The group $\{I,i\}$ is labeled C_i. It has the same multiplication table and the same irreducible representations as $\{I,\sigma\}$. In C_i the irreducible representations Γ^1 and Γ^2 are labeled A_g and A_u, respectively. Here *g* and *u* are the first letters in the German words *gerade* and *ungerade*.

If for the homopolar diatomic molecule the atomic orbitals ϕ_A and ϕ_B are *s* functions, the molecular orbital Ψ_1 is gerade and Ψ_2 is ungerade. If ϕ_A and ϕ_B are *p* functions, Ψ_1 is ungerade and Ψ_2 is gerade. The selection rules are

gerade ↔ gerade: forbidden
ungerade ↔ ungerade: forbidden
gerade ↔ ungerade: allowed

The homopolar diatomic Hamiltonian also commutes with the operators C_ϕ and C_ϕ^{-1} which are a rotation by an angle ϕ and $2\pi - \phi$, respectively, about the internuclear axis. The Hamiltonian also commutes with the rotation $C_{180} = C_{360/2} = C_2$ about an axis perpendicular to the internuclear axis. The group of all operators that commute with the Hamiltonian of a homopolar diatomic molecule is called

$$D_{\infty h} = \{I, C_\phi, C_\phi^{-1}, C_2, i, iC_\phi, iC_\phi^{-1}, iC_2\}$$

The irreducible representations are labeled

$$\Sigma_g^+, \Sigma_u^+, \Sigma_g^-, \Sigma_u^-, \Pi_g, \Pi_u, \Delta_g, \Delta_u, \text{etc.}$$

All the irreducible representations other than Σ are doubly degenerate representations, that is, there are two independent functions for each irreducible representation which yield the same energy, and each is transformed into a linear combination of the two under the operators in the group.

For a heteropolar diatomic molecule, the point group is $C_{\infty v} = \{I, C_\phi, C_\phi^{-1}, \sigma\}$, and the irreducible representations are Σ^+, Σ^-, Π, Δ, etc. Note that these are the same as for $D_{\infty h}$ except that the gerade–ungerade designation does not apply here. Orbitals involved in bond formation are often designated by the irreducible representations of $C_{\infty v}$. If we take the bond axis to be both the symmetry axis and the *z* axis, we may write

$$\sigma_A = s_A + \lambda z_A$$
$$\pi_A = x_A, y_A$$

Molecular orbitals may also be characterized according to $C_{\infty v}$ symmetry

$$\sigma_{MO} = \sigma_A \pm \sigma_B$$
$$\pi_{MO} = \pi_A \pm \pi_B$$

If the molecule possesses considerable symmetry, it is often useful to consider the total molecular symmetry. Methane belongs to the symmetry group T_d with irreducible representations A_1, A_2, E, T_1, and T_2. Here A_1 and A_2 are nondegenerate, E is doubly degenerate, and T_1 and T_2 are triply degenerate. We construct molecular symmetry orbitals as follows: We first hybridize the carbon orbitals so that they are directed toward the four hydrogen atoms to obtain the tetrahedral orbitals

$$\begin{aligned} te_1 &= 2s + x + y + z \\ te_2 &= 2s + x - y - z \\ te_3 &= 2s - x + y - z \\ te_4 &= 2s - x - y + z \end{aligned}$$

We then form bond orbitals with the four hydrogen orbitals which we label h_1, h_2, h_3, and h_4. Thus

$$\begin{aligned} \sigma_1 &= te_1 + \lambda h_1 & \sigma_1^* &= te_1 - \lambda^* h_1 \\ \sigma_2 &= te_2 + \lambda h_2 & \sigma_2^* &= te_2 - \lambda^* h_2 \\ \sigma_3 &= te_3 + \lambda h_3 & \sigma_3^* &= te_3 - \lambda^* h_3 \\ \sigma_4 &= te_4 + \lambda h_4 & \sigma_4^* &= te_4 - \lambda^* h_4 \end{aligned}$$

A bond orbital description of methane is then

$$(\sigma_1)^2(\sigma_2)^2(\sigma_3)^2(\sigma_4)^2$$

To obtain a symmetry orbital description, we construct symmetry orbitals from the bond orbitals

$$\begin{aligned} \Psi(A_1) &= \sigma_1 + \sigma_2 + \sigma_3 + \sigma_4 & \Psi^*(A_1) &= \sigma_1^* + \sigma_2^* + \sigma_3^* + \sigma_4^* \\ \Psi_1(T_2) &= 3\sigma_1 - \sigma_2 - \sigma_3 - \sigma_4 & \Psi_1^*(T_2) &= 3\sigma_1^* - \sigma_2^* - \sigma_3^* - \sigma_4^* \\ \Psi_2(T_2) &= 2\sigma_2 - \sigma_3 - \sigma_4 & \Psi_2^*(T_2) &= 2\sigma_2^* - \sigma_3^* - \sigma_4^* \\ \Psi_3(T_2) &= \sigma_3 - \sigma_4 & \Psi_3^*(T_2) &= \sigma_3^* - \sigma_4^* \end{aligned}$$

$\Psi^*(A_1)$ resembles the $3s$ orbital. The ground state configuration for the valence electrons is

$$[\Psi(A_1)]^2[\Psi(T_2)]^6$$

The orbitals designated $\Psi_i(T_2)$, where $i = 1,2,3$, are degenerate. The first excited state of methane is represented by

$$[\Psi(A_1)]^2[\Psi(T_2)]^5[\Psi^*(A_1)]^1$$

$[\Psi^*(A_1)] \sim 3s$ and may be considered to be the first member of a Rydberg series.

Benzene belongs to the point group D_{6h} with irreducible representations A_{1g}, A_{1u}, A_{2g}, A_{2u}, B_{1g}, B_{1u}, B_{2g}, B_{2u}, E_{1g}, E_{1u}, E_{2g}, and E_{2u}. The A and B representations are nondegenerate, and the E representations are doubly degenerate. The electronic spectrum is attributed to the six π electrons which are not localized into specific bonds so that we do not form bond orbitals. The six π orbitals form six symmetry orbitals of the type

$$\begin{array}{ll}
\Psi_1 = \Psi(A_{1u}) = x_A + x_B + x_C + x_D + x_E + x_F, & E_1 = \alpha + 2\beta \\
\Psi_2 = \Psi(E_{1g}) = 2x_A + x_B - x_C - 2x_D - x_E + x_F, & E_2 = \alpha + \beta \\
\Psi_3 = \Psi(E_{1g}) = x_B + x_C - x_E - x_F, & E_3 = \alpha + \beta \\
\Psi_4 = \Psi(E_{2u}) = 2x_A - x_B - x_C + 2x_D - x_E - x_F, & E_4 = \alpha - \beta \\
\Psi_5 = \Psi(E_{2u}) = x_B - x_C + x_E - x_F, & E_5 = \alpha - \beta \\
\Psi_6 = \Psi(B_{2g}) = x_A - x_B + x_C - x_D + x_E - x_F, & E_6 = \alpha - 2\beta
\end{array}$$

G. The Heteropolar Diatomic Molecule: Perturbation Theory

When atom A is not identical with atom B, $H_{AA} \neq H_{BB}$. The solutions to the secular equations in Section III–D are

$$\begin{array}{ll}
E_1 = \frac{1}{2}\{H_{AA} + H_{BB} + [(H_{AA} - H_{BB})^2 + 4H_{AB}^2]^{1/2}\}, & \Psi_1 = \lambda\phi_A + \phi_B \\
E_2 = \frac{1}{2}\{H_{AA} + H_{BB} - [(H_{AA} - H_{BB})^2 + 4H_{AB}^2]^{1/2}\}, & \Psi_2 = \phi_A - \eta\phi_B
\end{array}$$

The coefficient λ is given by $-H_{AB}/(H_{AA} - E_2)$ and η by $(H_{AA} - E_1)/H_{AB}$.* The expressions reduce to the homopolar expressions when H_{AA} is set equal to H_{BB}.

A very useful form of the equations may be obtained by rewriting them as

$$E = \frac{1}{2}\left\{H_{AA} + H_{BB} \pm (H_{AA} - H_{BB})\left[1 + \frac{4H_{AB}^2}{(H_{AA} - H_{BB})^2}\right]^{1/2}\right\}$$

Then for the case $|H_{AA} - H_{BB}| \gg H_{AB}$, the radical may be expanded so that

$$E \cong \frac{1}{2}\left[H_{AA} + H_{BB} \pm (H_{AA} - H_{BB})\left(1 + \frac{2H_{AB}^2}{(H_{AA} - H_{BB})^2} + \cdots\right)\right]$$

There are finally obtained

$$E_1 \cong H_{AA} + \frac{H_{AB}^2}{H_{AA} - H_{BB}}$$

and

$$E_2 \cong H_{BB} - \frac{H_{AB}^2}{H_{AA} - H_{BB}}$$

---

* Since Ψ_1 and Ψ_2 are orthogonal, that is, $\int \Psi_1\Psi_2 \, d\tau = 0$, it follows that $\lambda = (\eta - S_{AB})/(1 - \eta S_{AB})$. If the overlap integral is S_{AB} set equal to 0, $\lambda = \eta$.

The interpretation of the equations is straightforward. Let H_{AA} and H_{BB} be the energies of two independent states. E_1 and E_2 are the energies of the two states after they have interacted or have perturbed each other. It will be seen that two interacting levels always repel one another, and that the repelling effect is proportional to the square of the interaction energy and inversely proportional to the difference in energy between the two (see Fig. 2). This latter conclusion means that, other factors being equal, levels which are far apart will have a smaller influence on each other than levels which are close together. When more than two levels interact, the effects are additive, in this approximation. The expression for each energy will contain a term for every level with which there is interaction. These results are usually derived more elegantly under the heading of *perturbation theory.*

The utility of this approximation theory arises from the fact that a chromophore can be represented by one set of energy levels, and a substituent or auxochrome can often be represented by another level or levels. Their mutual

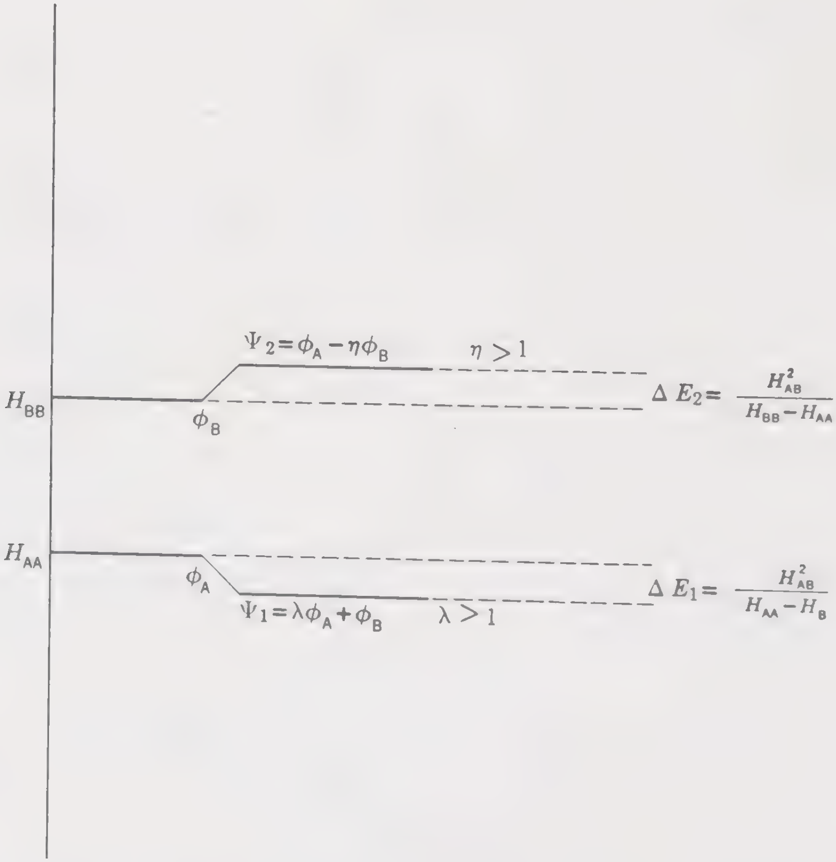
$\Psi_2=\phi_A-\eta\phi_B$
$\eta>1$
H_{BB}
ϕ_B
$\Delta E_2=\frac{H_{AB}^2}{H_{BB}-H_{AA}}$
H_{AA}
ϕ_A
$\Delta E_1=\frac{H_{AB}^2}{H_{AA}-H_B}$
$\Psi_1=\lambda\phi_A+\phi_B$
$\lambda>1$

Fig. 2. Energy levels and molecular orbitals for a heteropolar diatomic molecule.

interaction, which can be estimated by perturbation theory, determines the effect of the substituent on the spectrum of the chromophore.

As for the homopolar molecule, there are three molecular states or configurations for the heteropolar diatomic molecule: the ground state $(\Psi_1)^2$ and two excited states $\Psi_1\Psi_2$ and $(\Psi_2)^2$. In contrast to the homopolar molecule, the electron densities on the two atoms are different; the ratio, in the ground state, of electron density on atom A to that on atom B is λ^2. For $|H_{AA}|$ greater than $|H_{BB}|$, $\lambda > 1$, and atom A has the greater density. This movement of charge in a bond is called the inductive effect, and the attracting atom is said to be the more electronegative atom. The atomic electronegativity is a rough concept and is approximately measured by the ionization energy, so that a large H_{AA} is, in general, associated with a large ionization energy.

As for the homopolar molecule, there are two transitions from the ground state: $(\Psi_1)^2 \rightarrow \Psi_1\Psi_2$ and $(\Psi_1)^2 \rightarrow (\Psi_2)^2$. The second transition is forbidden in the one-electron approximation. Singlet–triplet transitions are again forbidden.

In the molecular orbital theory the first excited state is less polar than the ground state, since if $\lambda > 1$, then $\eta > 1$. Some arguments suggest that in the low-lying excited state the molecule should be in an essentially ionic state A^-B^+. It is a weakness of molecular orbital theory that it cannot describe such a process simply. It would be necessary to allow configuration interaction between all three configurations to describe excitation to an ionic state. Most heteropolar molecules also carry an unshared pair of electrons on the electronegative atom. These electrons usually participate in the excitation process associated with the long wavelength absorption (see Section III-C).

H. Linear Conjugated Polyatomic Systems

1. LINEAR COMBINATION OF ATOMIC ORBITALS–MOLECULAR ORBITALS (LCAO–MO)

For a linear system* of N identical carbon atoms, each contributing one atomic x orbital (7)

$$E_m = \alpha + 2\beta \cos (m\pi/(N + 1))$$

where m takes values one to N. Here $\alpha = \int x_i H x_i d\tau$ and $\beta = \int x_i H x_j r d\tau$. The levels for two, three, and six atoms are diagrammed in Figure 3. Each added atom moves the one-electron levels closer together. The molecular levels are then also compressed so that the absorption occurs at longer wavelengths. This is the qualitative description of the red shift of the

---

* A linear system is here defined as any acyclic nonbranched chain of atoms.

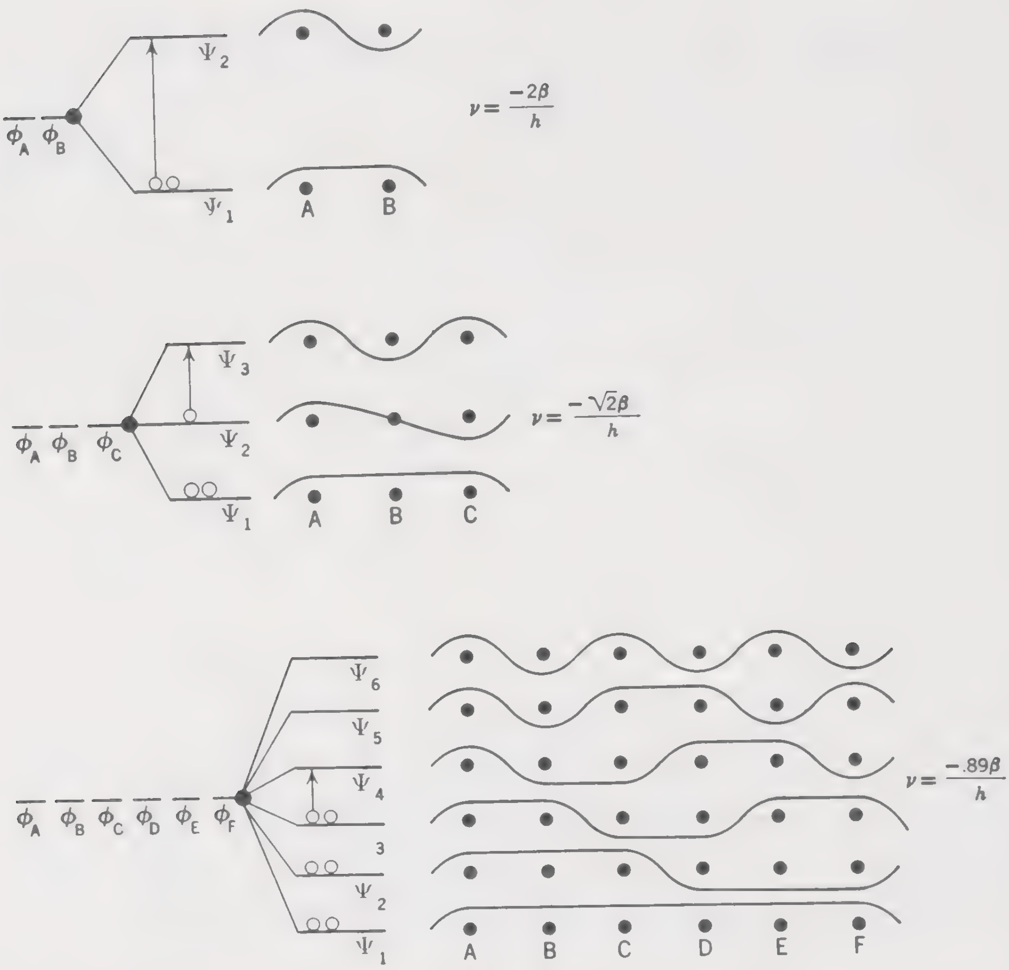

Fig. 3. Molecular orbital representation of a linear two-, three-, and six-atom system. The curved lines show the form of the molecular orbital.

long-wavelength absorption band which accompanies an increase in the length of a conjugated system.

Associated with each of these one-electron levels is a molecular orbital. These orbitals, just as for the diatomic system, are linear combinations of atomic orbitals. They are closely analogous to standing waves in a vibrating string. A molecular orbital for which the wave functions on adjacent atoms are of opposite sign is said to have a *node* between those two atoms. A molecular orbital for which the coefficient of the wave function on a given atom is zero and for which the wave functions on adjacent atoms have opposite sign is said to have a nodal plane through that atom. An example is $\Psi_2 = \phi_A - \phi_C$ in the linear three-atom system (see Fig. 3). Every molecular orbital will have a distinct number and/or arrangement of nodes. The analogy to a vibrating string may be carried further by noting that the greater the number of nodes in a molecular orbital or in a mode of vibration of a string, the greater is its excitation. An alternate representation to that given in Figure 3 is to locate the nodal planes with dotted lines.

It is inconvenient and often unnecessary to draw out the molecular levels in detail. A good deal of information can be obtained by filling in the one-electron levels to correspond to the ground state. The transitions to excited states can then be indicated by arrows which indicate which electrons are promoted to which levels. Thus, the excitation $(\Psi_1)^2 \rightarrow \Psi_1\Psi_2$ can be written $\Psi_1 \rightarrow \Psi_2$. In simple molecular orbital theory, the energy of the molecular state is the sum of the energies of the electrons in the one-electron levels.* Consequently, the excitation energy is the same whether calculated from the one-electron energies or the molecular states.

For a polyene with an even number of contributing atomic x orbitals and the same number of electrons, m equals $N/2$ for the highest filled orbital and equals $N/2 + 1$ for the lowest unfilled orbital. The excitation energy for the first or long wavelength transition, assuming all β's equal, is then

$$\begin{aligned}\Delta E &= 2\beta\left\{\cos\left[\frac{\pi}{2}\left(\frac{N+2}{N+1}\right)\right] - \cos\left[\frac{\pi}{2}\left(\frac{N}{N+1}\right)\right]\right\} \\ &= -4\beta \sin\,[\pi/2(N+1)]\end{aligned}$$

For large N

$$\Delta E \cong -4\beta\pi/2(N+1)$$

The wavelength is then given by

$$\lambda = hc/\Delta E \cong -hc(N+1)/2\beta\pi$$

and has a linear dependence on the chain length N for large values of N. The transition moment (and the intensity of the absorption band) for the long wavelength transition is predicted by theory to increase with the length of the chain in qualitative agreement with experiment. Experimentally it is found that for values of N to approximately 12, the predicted trend in λ is correct. However, for larger N, λ becomes nearly constant. If it is assumed that different β's are required for the classical singly and doubly bonded atoms, then the agreement between experiment and theory is markedly improved (see Fig. 4). This, in essence, signifies that there is bond alternation in the classical structure.

---

* In the more exact theory, in which electron repulsion is explicitly taken into account, this is no longer true.

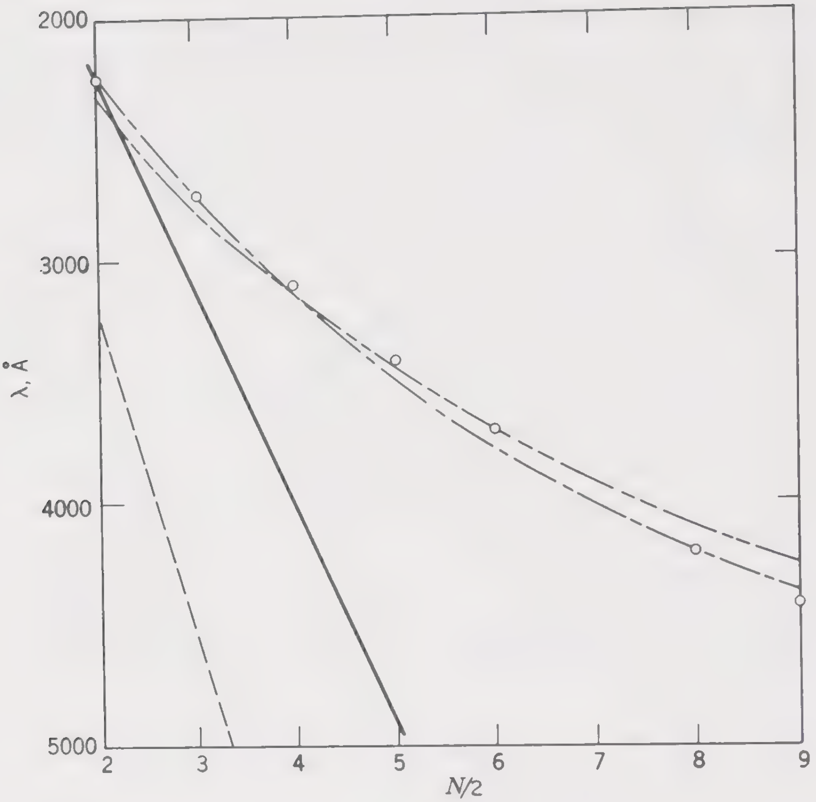

Fig. 4. Variation of long-wavelength absorption band of α,ω dimethylpolyenes: (○) = experimental data; (——) LCAO–MO ($\beta = -4.44$ eV); (---) FEMO ($a = 1.40$ Å); (——–—) LCAO–MO with alternating bond lengths ($\beta_{C=C} = -4.00$ eV, $\beta_{C=C} = -2.88$ eV); (— – – —) FEMO with alternating bond lengths. (After J. N. Murrell, *Theory Electronic of Spectra of Organic Molecules*, Methuen, London, 1963.)

2. FREE-ELECTRON MOLECULAR ORBITAL THEORY (FEMO)

In a conjugated system, some of the electrons appear to have a great freedom of motion. When this is true, as in linear conjugated polyenes, it is assumed that the electrons can be divided into two sets: the mobile (π) electrons and the localized (σ) electrons. The former are those which principally participate in reactions typical of olefins such as bromination. These also account for the lower ionization potentials and longer wavelength absorption of polyenes compared to the corresponding saturated compounds. In the free electron molecular orbital theory (FEMO) only the mobile electrons are explicitly considered. It is assumed that there is no interaction between the σ and π electrons, that each mobile electron can be treated separately, and that there is no repulsion between them.

The model chosen for the theory is a one-dimensional linear potential box. The potential within the box is assumed constant (and equal to zero for convenience), and the potential at the walls and beyond is assumed to be infinitely large. Application of boundary conditions requires that the wave function vanish at the walls. Solution of this problem results in a wave equation of the form

$$\Psi_n(x) = A \sin (n\pi x/L)$$

where A is a constant, n is a quantum number with values of 1, 2, . . ., x is the distance along the box, and L is the length of the box. Associated with each $\Psi_n(x)$ is an energy

$$E_n = (n^2h^2/8mL^2)$$

where h is Planck's constant and m is the mass of the electron. It will be noted that since n has only certain values, the energy is also restricted to certain values, and thus energy quantization naturally evolves. The form of the waves is shown in Figure 3 (Section II-H-1).

Of greatest interest is the energy of the longest wavelength transition since it is the one most easily observed and is responsible for the color of the higher members of the series. This corresponds to the energy difference

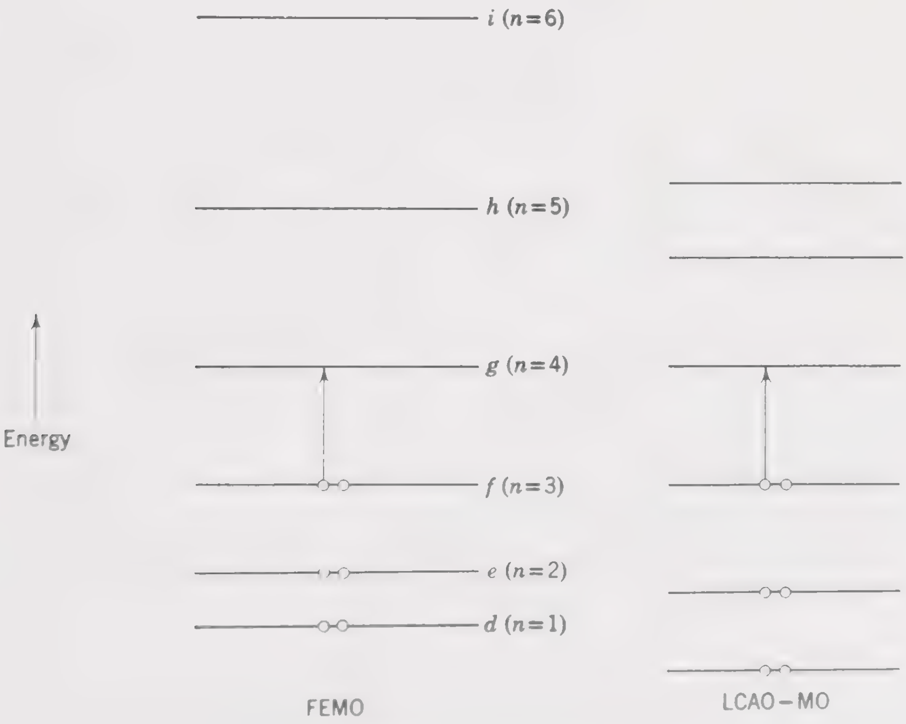

Fig. 5. Energy levels of hexatriene.

between the highest filled ($n = N/2$) and lowest empty ($n = N/2 + 1$) molecular orbital. This energy difference in terms of wavelength is

$$hc/\Delta E = \lambda_{\max} = (8mc/h)a^2N^2/(N+1)$$

where N is the number of atoms and a is the distance between the atoms ($L = Na$). For large N, $\lambda_{\max} \cong (8mc/h)a^2N$. This simple approach properly predicts the red shift of the long wavelength absorption band with lengthening of the polyenes. However, it does not correctly predict the observed fact that for $N > 12$, the wavelength is no longer linearly related to N but levels off to a nearly constant value. Bond alternation may be introduced into the FEMO model by making the constant potential a sinusoidal one with maxima at the single bond centers and minima at the double bond centers (8). The improvement over the simple model is as good as for the LCAO model (see Fig. 4).

The FEMO and LCAO–MO level schemes for hexatriene are compared in Figure 5. The highest filled orbital of FEMO theory is labeled f with lower-lying orbitals denoted as $e, d, c, \ldots$. The lowest unfilled orbital is labeled g with higher energy levels denoted as $h, i, j, \ldots$ (9). The long wavelength absorption band is associated with the transition $f \rightarrow g$ for which $\Delta n = 1$.

I. Other Transitions and Symbols

All the transitions which have been discussed up to this point are those in which an electron has been promoted from one molecular orbital to another. These are called N → V transitions and for most organic compounds are usually $\pi \rightarrow \pi^*$ or, less frequently, $\sigma \rightarrow \sigma^*$ transitions. Another important class of transitions is that in which an electron is promoted from a nonbonding atomic orbital to a molecular orbital. Such a transition is called N → Q. An N → Q or, more specifically, an $n \rightarrow \sigma^*$ transition in HF is

$$1s^2x^2y^2\, di_2{}^2\sigma_1{}^2 \rightarrow 1s^2x^2y^1\, di_2{}^2\sigma_1{}^2\sigma_1{}^{*1}$$

Another type of N → Q transition, the $n \rightarrow \pi^*$ transition, is often found in aromatic compounds. N → Q transitions are readily identified by characteristic solvent shifts (Section IV-E-2).

An electron may be promoted to a level which is high in energy and in which the electron is widely separated from the molecule. In such a case, the molecule appears to the electron as an atom, and its state is essentially atomic. Its energy will normally take on values given by the formula due to Rydberg:

$$\nu = \nu_\infty - R/(n+a)^2$$

where $n = 1, 2, \ldots, \infty$. Here a is an empirical constant. The states are called Rydberg states, and the transition from the ground state of the molecule to the Rydberg state is called $N \rightarrow R$ (see Chapter I, p. 57).

III. THE CHROMOPHORES

A. The Single Bond

1. MOLECULAR HYDROGEN

Molecular hydrogen absorbs far out in the ultraviolet, its longest wavelength bands lying at 1100 Å. The description of this absorption in terms of atomic energy levels, one-electron molecular energy levels, and molecular states runs as follows: The zero of energy of this system is taken to be complete ionization, $2H^+ + 2e$. When one of the electrons is put in the 1*s* orbital on one of the atoms, the resultant system, $H(1s) + H^+ + e$, lies at −13.60 eV.* From a 1*s* orbital on atom A and a 1*s* orbital on atom B, there

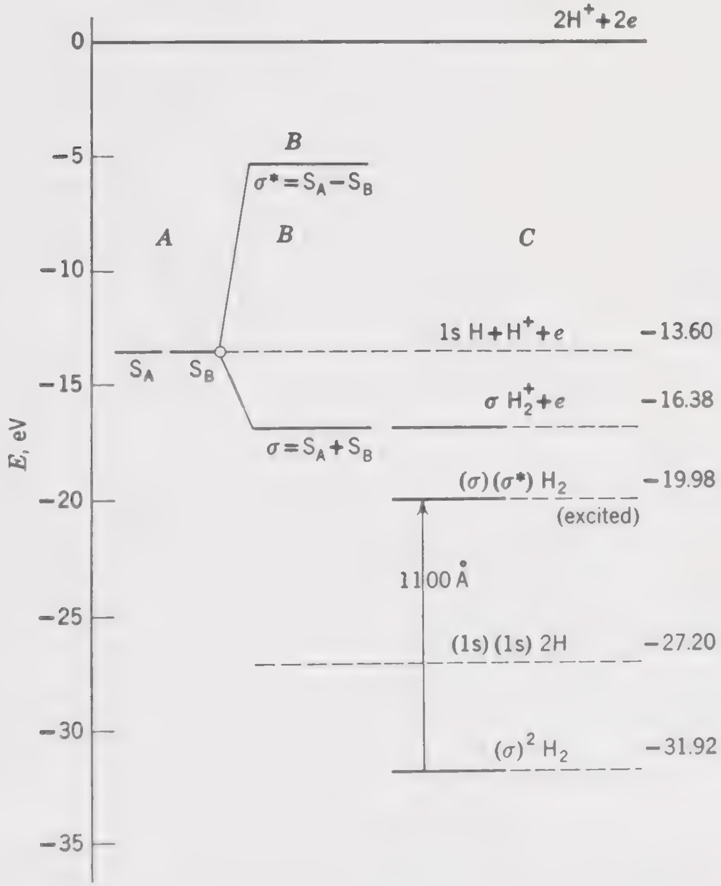
2H⁺+2e
0
−5
−10
−15
−20
−25
−30
−35
E, eV
A
B
C
B
σ* = S_A − S_B
S_A
S_B
σ = S_A + S_B
1s H+H⁺+e
−13.60
σ H₂⁺+e
−16.38
(σ)(σ*) H₂
(excited)
−19.98
1100 Å
(1s) (1s) 2H
−27.20
(σ)² H₂
−31.92

Fig. 6. Energy levels for H_2^+ and H_2.

---

* The kilocalorie is the conventional energy unit for the chemist. This unit is seldom found in the spectroscopic literature, where the wavenumber, cm^{-1}, or the electron volt, eV, is more usual (1 eV = 8068 cm^{-1} = 23.063 kcal/mole).

are formed two one-electron molecular orbitals, $\sigma = 1s_A + 1s_B$ and $\sigma^* = 1s_A - 1s_B$. Placing one electron in the σ orbital yields a state which lies at -16.38 eV, which is 2.78 eV below $H(1s) + H^+ + e$ and so is stable with respect to it. This is the ground state of the hydrogen molecular ion. The σ^* orbital lies some 8 eV above $H(1s) + H^+ + e$ and so is unstable with respect to it. For this reason σ^* is called an antibonding orbital. The two electrons of H_2 are then added to the one-electron molecular orbitals to obtain the various molecular states: $(\sigma)^2$, $(\sigma)^1\ (\sigma^*)^1$ and $(\sigma^*)^2$. The ground state $(\sigma)^2$ lies at -31.92 eV, which is 4.72 eV below the energy of two hydrogen atoms in $1s$ states. This latter quantity, less 0.27 eV for the zero-point energy of vibration, is the binding energy in H_2. The ground state energy of -31.92 eV is just about two times the energy of the hydrogen molecule ion, as is predicted on the basis of the simple molecular orbital theory. This is somewhat of an accident resulting from the cancellation of several large terms (5).

The lowest-lying excited state $\sigma\sigma^*$ of H_2 lies at -19.98 eV which is 11.94 eV above the ground state. The absorption of 1100 Å radiation causes a transition from the ground state to the $\sigma\sigma^*$ state.† It may be written $(\sigma)^2 \rightarrow \sigma\sigma^*$ and is an N → V transition. The next lowest excited state is not $(\sigma^*)^2$ but $\sigma\pi^*$, where $\pi^* = x_A - x_B$. This molecular orbital is formed from excited H_2 atomic orbitals. There are a number of such excited atomic states (region *A* of Fig. 6) which form excited one-electron molecular orbitals. (region *B*) from which are formed excited molecular states (region *C*). The higher energy states often form part of a Rydberg series.

2. PARAFFINS (10)

The ionization energy of methane is 13.0 eV, and its first absorption band is at 1250 Å. To a first approximation, the optical excitation may be thought of as a promotion from a bonding to an antibonding orbital localized in a bond. From the four bond orbitals, $\sigma_i = te_i + \lambda_i s_{Hi}$, where $i = 1$ to 4, there can be formed, by linear combination, four molecular orbitals Ψ'_{2s}, Ψ'_x, Ψ'_y, Ψ'_z, which have the symmetry of the $2s$, x, y, and z atomic orbitals. The electron configuration of the ground state of methane may then be written

$$1s_C{}^2\Psi'_{2s}{}^2\Psi'_x{}^2\Psi'_y{}^2\Psi'_z{}^2 \Bumpeq [\Psi'(A_1)]^2[\Psi'(T_2)]^6$$

The first absorption band has been postulated to arise from an excitation of one of the electrons to $3s$-like orbitals, $\Psi'^*(A_1)$, so that the excited state configuration is

$$[\Psi'(A_1)]^2[\Psi'(T_2)]^5[\Psi'^*(A_1)]^1$$

---

† $\lambda = 10^8/\Delta E(\mathrm{cm}^{-1}) = 10^8\ (\Delta E(\mathrm{eV}) \times 8068)$ Å; $1100 \cong 10^8\ (11.94 \times 8068)$ Å.

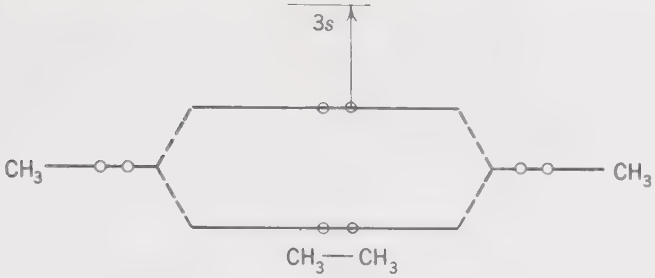

Fig. 7. Diatomic model of ethane.

The ionization energy of ethane is 11.7 eV, and its first absorption band is at 1350 Å. The excitation can be considered to be from a bonding orbital formed from the two carbon tetrahedral hybrids to either the antibonding orbital or to a 3*s*-like orbital. The excitation is thought to lie in the carbon–carbon bond because the absorption is at longer wavelengths, the ionization energy is lower than in methane, and the bond strength is less than that of the carbon–hydrogen bond in methane.

An alternative description is to carry over the methane formulation and consider the optical electrons as lying in levels formed from the interaction of a virtual y orbital from each methyl group (considered to behave as its united atom analog, fluorine). The interaction produces two new levels, one lower and one higher than in methane (see Fig. 7). Both levels are full so that excitation will remove an electron from the higher level; thus both the ionization and the spectral excitation energy should be lower than in methane. This may also be the basis of the explanation of the lower ionization energy and longer wavelength of absorption of the higher acylic hydrocarbons. Octane, for example, has an ionization energy of 10.26 eV and absorbs at 1700 Å.

Cyclopropane absorbs at 1800 Å, a considerably longer wavelength than the corresponding straight-chain compound; however the ionization energy of both compounds is 11.1 eV. This may be rationalized by the statement that the strain decreases the energy of the excited state more than it raises the ground state. More conventionally, one may say that since this system may be treated as a delocalized σ electron compound (11), its absorption should resemble that of ethylene.

B. The Multiple Bond*

In this section those multiple-bonded compounds in which a basic atom is not incorporated in the bond will be considered. Compounds containing multiple bonds have lower ionization energies and absorb at longer wavelengths than those containing only single bonds. This is because the π electrons in the former are not as strongly interacting as the σ electrons, so that the π bonding and antibonding levels are not as widely separated as are the levels of the σ electrons.

---

* For a critique of π electron treatments including those more sophisticated than Huckel theory, see R. G. Parr, *Quantum Theory of Molecular Electronic Structure*, Benjamin, New York, 1963.

1. ETHYLENE (12,13)

Ethylene absorbs strongly at 1610 Å (see Fig. 8 for a typical ethylenic spectrum). Since compounds with normal σ bonds absorb below 1610 Å, the absorption can be attributed to the excitation of π electrons.† The molecular orbitals and their energies are

$$\pi = x_A + x_B \qquad E = \alpha + \beta$$
$$\pi^* = x_A - x_B \qquad E = \alpha - \beta$$

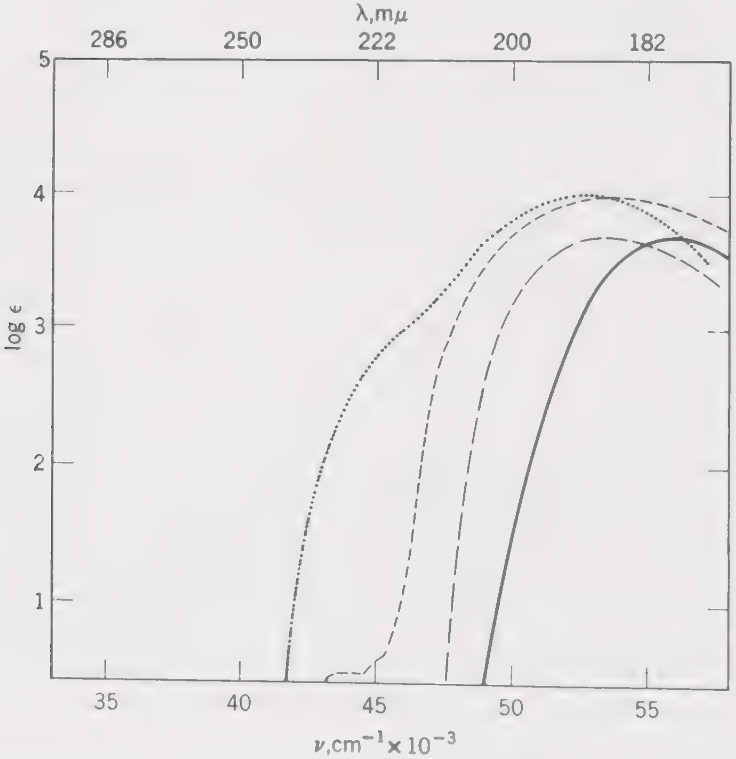

Fig. 8. Low-temperature spectra of olefins: (——) 1-hexene, 77 K; (— —), trimethylethylene, 77 K; (- - -) tetramethylethylene, 77 K; (· · · · ·) tetramethylethylene, room temperature. [After H. B. Klevens and J. R. Platt, Technical Report, Part One, Laboratory of Molecular Structure and Spectra, University of Chicago (1953–54).]

---

† However, see M. B. Robin et al., *J. Chem. Phys.*, **44**, 1803 (1966), for evidence of $\pi \rightarrow \sigma^*$ (C—H bond) transitions centered near 2200 Å in monoolefins.

where $\alpha = \int x_i H x_i \, d\tau$ and $\beta = \int x_i H x_j \, d\tau$. β is assumed to be zero unless i and j are adjacent atoms. The ground state configuration is $\sigma^2\pi^2$ where $\sigma = tr_A + tr_B$ (see p. 329). There are two N → V transitions: $\sigma^2\pi^2 \rightarrow \sigma^2\pi\pi^*$ and $\sigma^2\pi^2 \rightarrow \sigma^2\pi^{*2}$. The first transition is allowed and will give rise to a strong absorption, while the second is forbidden. According to simple molecular orbital theory the $\pi \rightarrow \pi^*$ transition should lie at a longer wavelength than the $\pi^2 \rightarrow \pi^{*2}$ excitation. We attribute the intense 1610-Å band to the single electron transition. At shorter wavelengths there is a series of N → R transitions terminating in the ionization of the ethylene molecule.

On the basis of the assignment of the $\pi \rightarrow \pi^*$ band at 1610 Å and the experimental value of the ionization energy, 10.4 eV, numerical values may be assigned to α and β. The energy of the ethylene cation is $\alpha + \beta$, so the ionization energy of ethylene is

$$I = (\alpha + \beta) - 2(\alpha + \beta) = -(\alpha + \beta) = 10.4 \text{ eV}$$
$$h\nu = (\alpha - \beta) - (\alpha + \beta) = -2\beta = 7.7 \text{ eV}$$

Therefore

$$\beta = -3.9 \text{ eV}$$
$$\alpha = -6.5 \text{ eV}$$

2. THE EFFECT OF BASIC SUBSTITUTION

When a basic atom or group, i.e., an atom or group containing unshared electron pairs, e.g., Cl, OH, SH, or NH_2, is substituted on ethylene, the 1610-Å band shifts to longer wavelengths. The substituent influences the chromophore in two ways: through an inductive (electrostatic) effect and through a resonance (charge delocalization) effect. The description of the resonance effect follows in a straightforward way from simple molecular orbital theory.

We label the basic group in the molecule by X and its coulomb integral by

$$\alpha_X = \alpha + \delta_X \beta$$

where α and β are the coulomb and resonance integrals for carbon, and δ is called the electronegativity parameter.† The value of δ is positive for those groups more electronegative than carbon and negative for those more electropositive.

---

† The resonance integral and overlap integral between X and C are also different (though probably not by such a great extent as α) from that between C and C. In an effort to keep the number of adjustable parameters to a minimum, we shall for the moment place the entire effect of the heteroatom on the value of α_X. Another effect which should be considered is that of the change in α of the carbon atom attached to X through an inductive mechanism. This will also be neglected here for the same reason.

TABLE I

Ionization Potentials of Some Basic Compounds[a]

CH_3—X	H_nX	$I(CH_3—X)$	$I(H_nX)$	$\delta(CH_3—X)$[b]	$\delta(H_nX)$[b]	Best δ[c]
CH_3CH_3[d]	CH_4	11.7	13.1	1.3	1.7	2
CH_3NH_2	NH_3	9.4	10.5	0.7	1.0	1.5
CH_3OH	H_2O	10.9	12.7	1.1	1.6	2
CH_3SH	H_2S	9.4	10.5	0.7	1.0	~1.5
CH_3F	HF	12.7	16.4	1.6	2.6	3
CH_3Cl	HCl	11.4	12.8	1.3	1.6	2
CH_3Br	HBr	10.6	11.7	1.0	1.3	1.5
CH_3I	HI	9.6	10.4	0.8	1.0	—

[a] All values are from electron impact data except for the spectroscopic value for CH_3SH. See F. H. Field and J. L. Franklin, *Electron Impact Phenomena and the Properties of Gaseous Ions*, Academic Press, New York, 1957, p. 105, for references. Units are electron volts.

[b] $\delta = (-\alpha - I)/\beta$, where $\alpha = -6.5$ eV, $\beta = -3.9$ eV, and I is the ionization potential of the respective compound.

[c] Suggested values based on various experimental data. See ref. 6, p. 135.

[d] The methyl group is assumed to behave as a basic group.

Now it should be noted that α_X is primarily a measure of the strength of the binding of the π electron to the basic group. Consequently, for a series of basic groups, one might expect α_X to parallel the ionization energies of compounds containing X. Defined in this way a δ_X scale should be similar to Pauling's electronegativity scale. In Table I the ionization potentials for series of compounds of types CH_3—X and H_nX are listed. Values of δ_X have been computed from the respective ionization potentials of the compounds and values for α and β of carbon.

The secular equation for the monosubstituted ethylene, assuming only resonance interactions, is

$$\begin{vmatrix} \alpha - E & \beta & 0 \\ \beta & \alpha - E & \beta_{CX} \\ 0 & \beta_{CX} & \alpha + \delta\beta - E \end{vmatrix} = 0$$

Setting $x = (\alpha - E)/\beta$ and $\gamma = \beta_{CX}/\beta$

$$\begin{vmatrix} x & 1 & 0 \\ 1 & x & \gamma \\ 0 & \gamma & x + \delta \end{vmatrix} = 0$$

Setting $\gamma = 1$, then $(x + \delta)(x^2 - 1) - x = 0$, which is an unfactorable cubic equation. However, the energies of the molecular orbitals may be obtained for two limiting cases:

a. $\delta = 0$, allyl system:
Then

$$x^3 - 2x = 0$$
$$x = 0, \qquad \pm\sqrt{2}$$

and

$$\begin{aligned} E_3 &= \alpha - \sqrt{2}\beta \text{ (antibonding)} \\ E_2 &= \alpha \qquad\quad\ \text{(nonbonding)} \\ E_1 &= \alpha + \sqrt{2}\beta \text{ (bonding)} \end{aligned}$$

b. $\delta \rightarrow \infty$:
Then x may be neglected, giving

$$\begin{aligned} &(x + \delta)(x^2 - 1) = 0 \\ &E_3 \rightarrow \alpha - \beta \\ &E_2 \rightarrow \alpha + \beta \\ &E_1 \rightarrow \alpha + \delta\beta = \alpha_X \end{aligned}$$

Thus, if inductive effects are neglected, the substituted ethylene system approaches the system ethylene plus a noninteracting heterogroup as $\delta \rightarrow \infty$. For highly electronegative heteroatoms the π electrons (of the lone pair usually) are so tightly bound that they do not delocalize.

For $\delta > 1$, approximate eigenvalues may be obtained from perturbation theory:

$$\begin{aligned} E_3 &\cong \alpha - \beta[1 + \gamma^2/2(1 + \delta)] \\ E_2 &\cong \alpha + \beta[1 + \gamma^2/2(1 - \delta)] \\ E_1 &\cong \alpha + \delta\beta[1 + \gamma^2/(\delta^2 - 1)] \end{aligned}$$

The one-electron energy levels of the monosubstituted ethylene system are shown in Figure 9 as a function of δ for γ, the ratio of the resonance integral for C—X to that for C—C, $=1$.

The basic group contributes two π electrons to the system. The ground state of the monosubstituted ethylene is then $(\Psi'_1)^2(\Psi'_2)^2$, and the first excited state $(\Psi'_1)^2\Psi'_2\Psi'_3{}^*$ (see Fig. 10). From Figure 9 we see that for the basic compound with $\delta \neq \infty$ the excitation energy $E_3 - E_2$ lies between $-\sqrt{2}\beta$ and -2β. The approximate excitation energy from the perturbation theory for $\delta > 1$ is $-2\beta[1 - \gamma^2/2(\delta^2 - 1)]$. According to this model, the greater the δ of the basic group, the greater is the excitation energy, approaching the ethylene value, -2β, as $\delta \rightarrow \infty$. The approximate change of the excitation energy in the basic monosubstituted compound relative to that of ethylene is $\beta[\gamma^2/(\delta^2 - 1)]$ for $\delta > 1$. Thus, OH and NH_2 groups cause a greater shift of the absorption band than does Cl due to the lower δ values of the former. Figure 10 shows an energy level scheme for ethylene and a monosubstituted

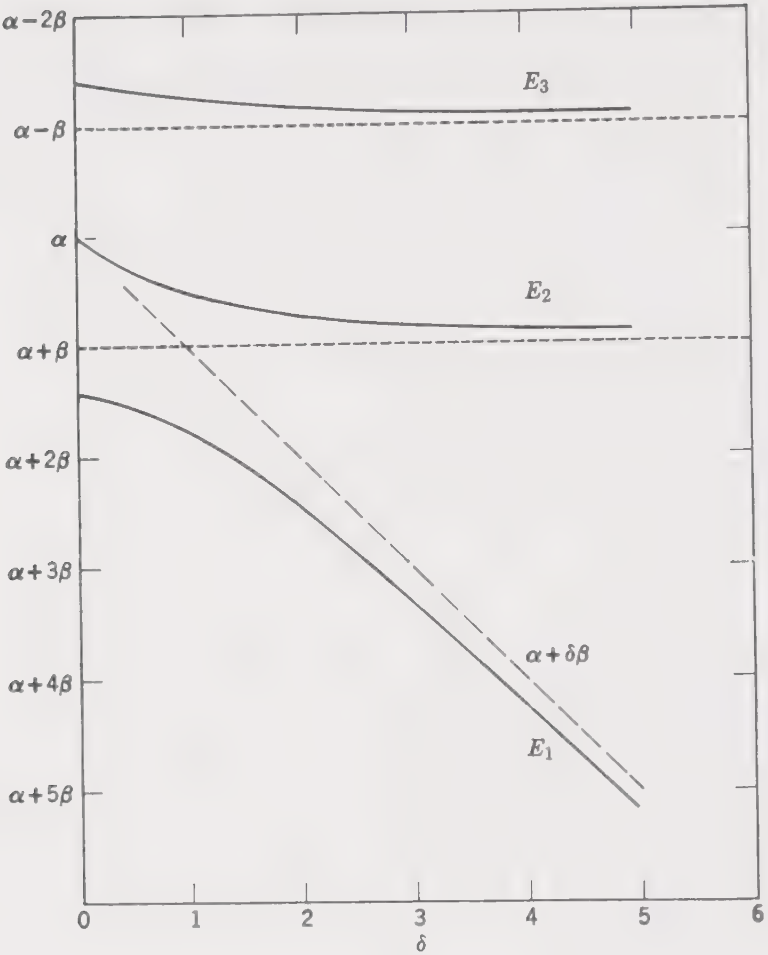

Fig. 9. One-electron energy levels of monosubstituted ethylene.

ethylene with an arbitrary value assumed for δ. According to simple molecular orbital theory the ionization energy of the monosubstituted ethylene is $I = -E_2 < -(\alpha + \beta)$. Thus, the ionization energy of the monosubstituted ethylene is lower than that of ethylene.

The resonance interaction also produces a transfer of charge from the basic group to the ethylenic group. It could be said that in the interaction the basic group is oxidized and the ethylenic group reduced. Intramolecular oxidation and reduction and its relation to color were discussed by Stieglitz as far back as 1923 (14).

The inductive effect is a nonresonance charge transfer process. The charge transfer modifies the electronegativity of the atoms and, consequently, the coulomb integrals for the π electrons. The inductive effect is said to be positive when the substituent becomes positive with respect to the adjacent atom. A

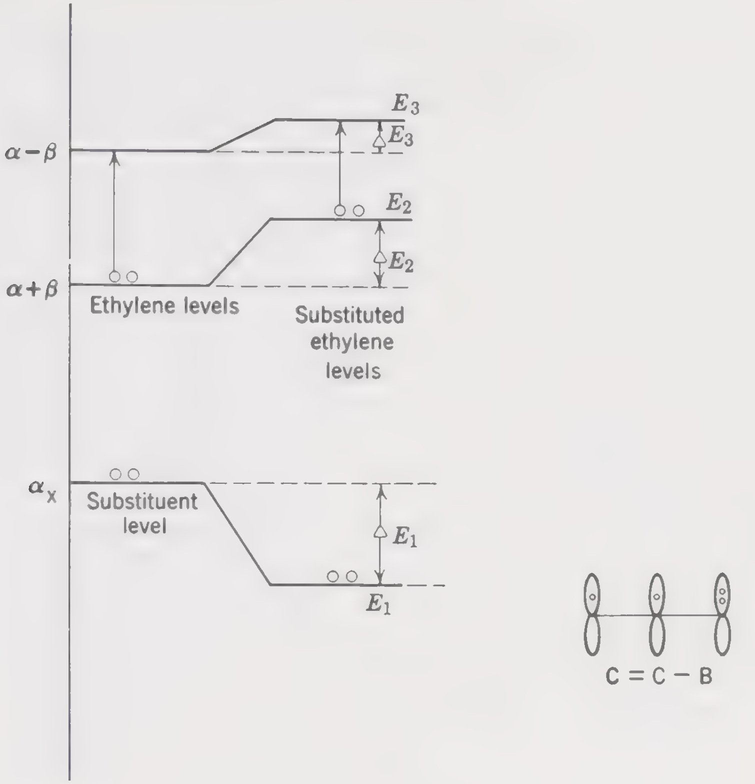

Fig. 10. One-electron levels for a basic substituted ethylene.

positive inductive effect will decrease the ionization energy of the adjacent atom and increase the ionization energy of the substituent. Hence a positive inductive effect will raise α and lower α_X, thereby raising E_2 and E_3 but lowering E_1. Since the long wavelength absorption is correlated with the energy difference $E_3 - E_2$, the inductive effect will have only a small effect on the spectra as long as both E_3 and E_2 are shifted by approximately the same amount. Further, since E_2 is the highest occupied level of the substituted compound in the ground state, a positive inductive effect will decrease the ionization energy relative to that of ethylene.

3. ALKYL SUBSTITUTION: HYPERCONJUGATION

Alkyl substitution also shifts the ethylene absorption to longer wavelengths (see Table II) and lowers the ionization energy. Thus, while the alkyl groups do not possess a formal unshared pair of electrons, in many instances they behave as if they do (see Section III-A-2). We can model them by assigning a virtual unshared pair of electrons on each methyl or methylene group, i.e.,

TABLE II
Long-Wavelength Absorption Bands of Alkyl Substituted Ethylenes

Compound	Band maximum, Å	Ionization energy,[f] eV	Ref.
Ethylene	1614	10.52	a
Methyl-	1730	9.73	b
Ethyl-	1751	9.58	c
n-Propyl-	1767	9.50	c
Isopropyl-	1761	9.51	c
n-Butyl-	1782	9.46	c
1,1-Dimethyl-	1883	9.23	c
cis-Dimethyl-	1754	9.13	c
trans-Dimethyl-	1777	9.13	c
Tetramethyl-[e]	1914		d
Trimethyl-[e]	1887	8.67	d
Cyclohexene[e]	1827	8.95	d

[a] P. G. Wilkinson and H. L. Johnson, *J. Chem. Phys.*, **18**, 190 (1950).

[b] W. C. Price and W. T. Totte, *Proc. Roy. Soc.*, **A174**, 207 (1940).

[c] J. T. Gary and L. W. Pickett, *J. Chem. Phys.*, **22**, 599, 1266 (1954).

[d] W. J. Potts, *J. Chem. Phys.*, **23**, 65 (1955).

[e] Solution spectra in a mixture of 3-methylpentane and isopentane.

[f] Photoionization data from K. Watanabe, T. Nakayama, and J. Mottl, *Final Report on Ionization Potential of Molecules by a Photoionization Method*, Dept. Army No. 5B-99-01-004, ORD-No. TB2-0001-OOR-No. 1624 Dec. 1959; Contract No. DA-04-200-ORD 480 and 737.

$\ddot{C}H_3$, so that they are formally equivalent to the basic groups in many of their properties. This phenomenon is called *hyperconjugation.**

It follows from the concept of the virtual unshared pair of electrons on the alkyl groups and the discussion of the resonance effects in the previous section that alkyl substitution will intensify and shift the spectrum to the red and decrease the ionization energy.

---

* Hyperconjugation is here formulated differently than was done originally by Mulliken, Rieke, and Brown, *J. Am. Chem. Soc.*, **63**, 41 (1941), who consider the methyl group to be the analogue of a triple bond. According to Mulliken, *Rev. Mod. Phys.*, **14**, 265 (1942), hyperconjugation in substituted ethylenes lowers the value of E_3. The model described above is closely related to the united atom model proposed by Burkhardt and Evans, *Mem. Proc. Manchester Lit. Phil. Soc.*, **77**, 37 (1933), in which the methyl group is taken to be the analogue of the fluorine atom. See also *Conference on Hyperconjugation*, V. Shiner and E. Campaigne, Eds., Pergamon Press, New York, 1959.

All the alkyl groups have the same general effect on the properties of ethylene. There are variations due to the differences in the capacities of the several groups to resonate. Methyl appears to be the best resonator. An explanation may be that the bond polarity H^+C^- would make methyl resemble most closely its united atom analog, fluorine. Progressive replacement of hydrogen by methyl groups destroys this resemblance so that the order of hyperconjugation ability, i.e., increasing γ (pp. 232–233), should be methyl > ethyl > isopropyl > *tert*-butyl.

It follows from the concept of the virtual unshared pair of electrons on each methyl group that the various alkyl groups will produce different effects on the spectra and ionization energies. The virtual x orbitals on each methyl or methylene group will interact producing filled molecular orbitals which differ in energy depending upon the number of methyl or methylene groups and their geometrical arrangement. The interaction of these alkyl virtual molecular orbitals with the ethylene molecular orbitals will raise the energy of the ethylene levels, the lower ethylene level being raised more than the upper one. This will decrease the ionization energy and shift the spectrum toward the red. For example, molecular orbital diagrams for the methyl and ethyl substituted compounds are

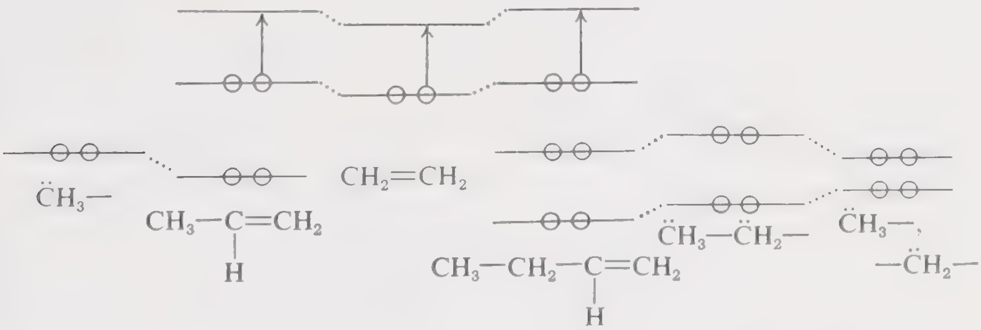

The interaction between the alkyl group orbitals and the ethylene levels will depend upon two factors: the energy difference between the ethylene and alkyl levels and the value of γ for the particular alkyl group. A greater interaction occurs as γ increases and as the energy difference between the levels decreases. Since the order of increasing γ is expected to be methyl > ethyl > isopropyl > *tert*-butyl and that of decreasing energy difference between the alkyl and ethylene orbitals is in the opposite order, these factors oppose one another. Since the observed order of the red shift of the spectrum and decreasing ionization energies is *n*-butyl > isopropyl > ethyl > methyl, it appears that the latter effect is dominant.

No new features are introduced by cyclization. The spectra of cyclopentene and cyclohexene resemble closely the spectra of the disubstituted olefin (see Table II).

4. DIOLEFINS

Diolefins, with double bonds separated by two or more single bonds, absorb in the same region as do the corresponding monoolefins. The absorption of conjugated diolefins lies farther to the red, butadiene absorbing at 1750 and 2170 Å.

Butadiene contains four adjacent x orbitals from which there are formed four molecular orbitals†:

$$\begin{array}{rlrl}
\pi_1 &= bx_A + a(x_B + x_C) + bx_D & E_1 &= \alpha + 1.62\beta \\
\pi_2 &= ax_A + b(x_B - x_C) - ax_D & E_2 &= \alpha + 0.62\beta \\
\pi_3{}^* &= ax_A - b(x_B + x_C) + ax_D & E_3 &= \alpha - 0.62\beta \\
\pi_4{}^* &= bx_A - a(x_B - x_C) - bx_D & E_4 &= \alpha - 1.62\beta
\end{array}$$

where $a = 0.602$ and $b = 0.372$. The energies are calculated from the formula given in Section II-H-1.

For the ground state the π electron configuration is $\pi_1{}^2\pi_2{}^2$. The two absorption bands at 1750 and 2170 Å correspond to the $\pi_2 \rightarrow \pi_4{}^*$ and $\pi_2 \rightarrow \pi_3{}^*$ transitions. In Figure 11 the energy levels and the electronic transitions for

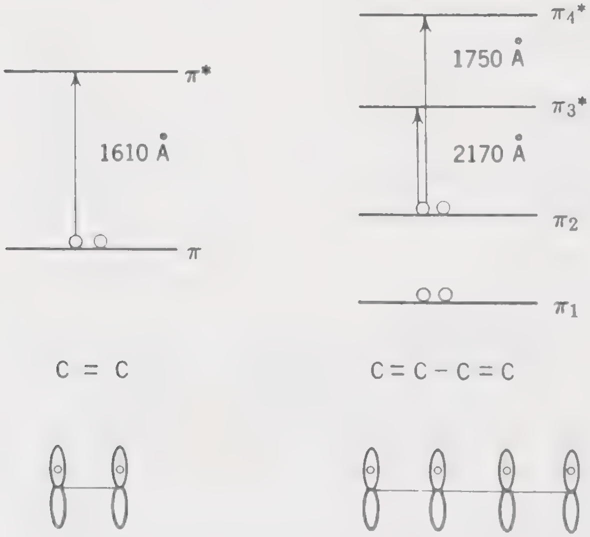

Fig. 11. One-electron energy levels for ethylene and butadiene.

---

† These molecular orbitals give the bond orders in butadiene. C. A. Coulson, *Proc. Roy. Soc.* (*London*), **A169**, 413 (1939), obtains 1.89 for the end bond and 1.45 for the center bond.

both ethylene and butadiene are given. The red shift produced by the vinyl substitution on ethylene arises from the addition to the system of a new level at the energy of each of the two ethylene levels. There is interaction in each pair of levels producing a lower and a higher level. Since the higher member of the lower pair and the lower member of the higher pair are closer together than the original ethylene levels, there is a red shift.

The center bond in butadiene has some double bond character, so there exists the possibility of *cis* and *trans* isomers about this "single" bond (15). The transition moments of the two isomers for the first two transitions, $\pi_2 \rightarrow \pi_3^*$ and $\pi_2 \rightarrow \pi_4^*$, are of some interest. These are, respectively

$$\mathbf{T}_{23} = \int \pi_2 \mathbf{R} \pi_3^* \, d\tau \quad \text{and} \quad \mathbf{T}_{24} = \int \pi_2 \mathbf{R} \pi_4^* \, d\tau$$

Since $\pi_2 = ax_A + b(x_B - x_C) - ax_D$, $\pi_3^* = ax_A - b(x_B + x_C) + ax_D$, and $\pi_4^* = bx_A - a(x_B - x_C) - bx_D$

$$\mathbf{T}_{23} = a^2(\mathbf{R}_A - \mathbf{R}_D) - b^2(\mathbf{R}_B - \mathbf{R}_C) = a^2(\mathbf{R}_A - \mathbf{R}_D) - 2b^2\mathbf{R}_B$$

and

$$\mathbf{T}_{24} = ab\mathbf{R}_A - ab(\mathbf{R}_B + \mathbf{R}_C) + ab\mathbf{R}_D = ab(\mathbf{R}_A + \mathbf{R}_D)$$

The expressions on the right occur because $\mathbf{R}_B = -\mathbf{R}_C$.

Remembering that the **R**'s are vectors directed from the center of the molecule to the respective atoms, it will be noticed that $\mathbf{T}_{23}$ is larger for the *trans* than for the *cis* modification. On the other hand, $\mathbf{T}_{24}$ is zero for the *trans* modification. The absorption at 1750 Å has been associated with the $\pi_2 \rightarrow \pi_4^*$ transition and shows appreciable intensity, so that one concludes that a considerable fraction of the butadiene is in the *cis* form. This band is

TABLE III
Long-Wavelength Absorption Maxima of Some Conjugated Dienes in Ethanol

Compound	Wavelength, Å
Butadiene[a]	2170
1-Methylbutadiene[a]	2235
2-Methylbutadiene[a]	2200
1,4-Dimethylbutadiene[a]	2270
2,3-Dimethylbutadiene[a]	2260
Cyclopentadiene[b]	2380
1,3-Cyclohexadiene[c]	2690

[a] W. J. Bailey and J. C. Goossens, *J. Am. Chem. Soc.*, **78**, 2804 (1956).

[b] D. Peters, *J. Chem. Soc.*, **1959**, 1761.

[c] G. T. Piliugin and S. V. Shinkerenka, *Zh. Obsch. Khim.*, **28**, 1284 (1958).

also strong in cyclopentadiene and cyclohexadiene since they are 100% in the *cis* form.

Alkyl substitution on butadiene also produces a red shift (see Table III). The shifts are so uniform that sets of empirical rules have been devised to predict the band positions of the substituted compounds (16). Cyclopentadiene and cyclohexadiene absorb considerably more to the red of butadiene than would be expected from dialkyl substitution alone (see Figs. 8 and 12). This shift is attributable to cyclic strain which primarily raises the energy of the ground state resulting in a red shift of the spectrum.

5. ACETYLENE (17)

Neglecting the C—H bonds, a simple molecular orbital description of the bonding in acetylene may be formulated as follows. Orbitals of σ symmetry are formed from the two carbon digonal hybrids

$$\sigma = di_{1\mathrm{C}} + di_{2\mathrm{C}}$$
$$\sigma^* = di_{1\mathrm{C}} - di_{2\mathrm{C}}$$

The unhybridized carbon x and y orbitals combine to form perpendicular π orbitals

$$\pi_x = x_1 + x_2$$
$$\pi_y = y_1 + y_2$$
$$\pi_y^* = x_1 - x_2$$
$$\pi_y^* = y_1 - y_2$$

The ground state configuration of acetylene is then $\sigma^2\pi_x^{\ 2}\pi_y^{\ 2}$. Since the perpendicular π_x and π_y orbitals do not interact in the simple molecular orbital theory, their energies will be equal and analogous to those of ethylene

$$E(\pi_x, \pi_y) = \alpha' + \beta'$$
$$E(\pi_x^*, \pi_y^*) = \alpha' - \beta'$$

However, since the C—C bond distance in acetylene is 1.20 Å compared to 1.33 Å in ethylene, β' should be larger than β in ethylene due to the greater overlap of the x or y orbitals at the shorter bond distance.

Acetylene absorbs rather weakly from 2500 to 2100 Å and then more intensely at 1520 to 2100 Å. A number of bands appear in the short wavelength region including initial bands of a Rydberg series at 1520 Å. The longest wavelength band is assigned to a transition to an excited state in which the molecule has assumed a planar, ethylenelike structure with the H atoms in the *trans* position (18). The energy of this excited state may be roughly estimated as the mean of the energies of the ethylene ground-state orbital $(\alpha + \beta)$ and of its first excited-state orbital $(\alpha - \beta)$. If the difference between the α's of ethylene and acetylene is small, then the excitation energy

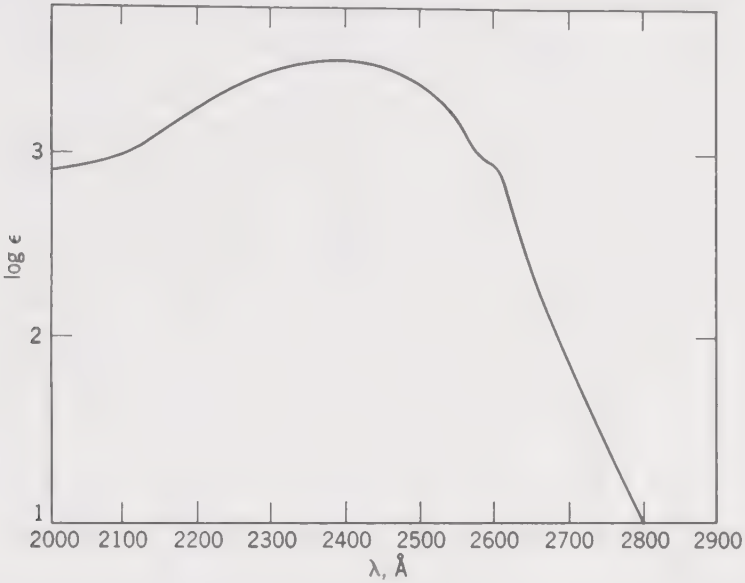

Fig. 12. Spectrum of 1,3-cyclopentadiene in isooctane. (After A. P. I. Ultraviolet Spectrogram 53, Shell Development Company.)

of the first transition in acetylene will be approximately $-\beta'$ (see Fig. 13). Therefore, the long wavelength band in acetylene will lie at longer wavelengths than that in ethylene (-2β). Since β' is greater than β and α' is approximately equal to α, the ionization energy of acetylene (11.4 eV) is larger than that of ethylene (10.6 eV).

C. The Basic Group

Saturated compounds containing atoms with unshared pairs of electrons have lower ionization energies and absorb at longer wavelengths than do saturated hydrocarbons. These facts suggest that in each of these processes

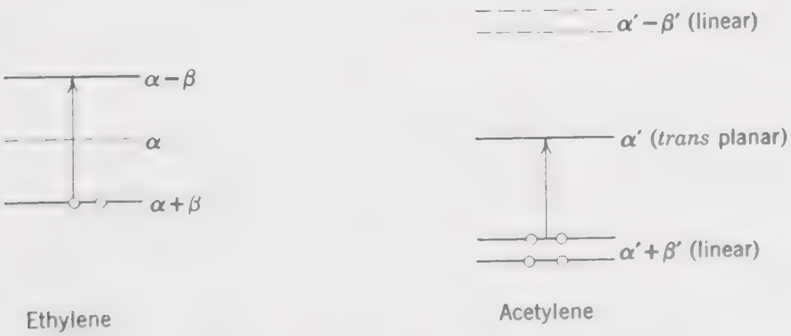

Fig. 13. Molecular levels for ethylene and acetylene.

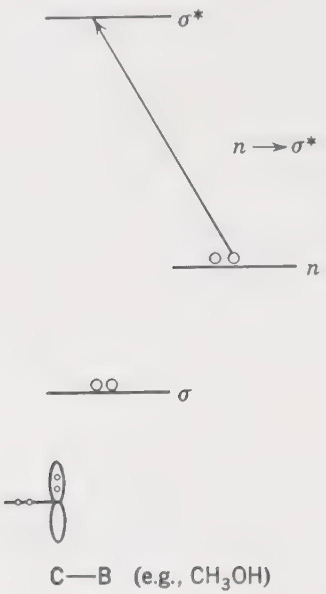

Fig. 14. Energy levels and long-wavelength transition for the basic group.

one of the electrons in a nonbonding orbital is being excited (see Fig. 14). Evidence in support of this interpretation comes from the fact that in a number of the molecules containing halogen the bands appear to be members of Rydberg series with two ionization limits, the separation of which is closely related to that found for the isolated halogen atom (19). This suggests that a nonbonding electron in the halogen atom is excited. Furthermore, if nonbonding electrons are involved in the excitation, a noticeable shift of the absorption band to higher energy should occur upon a change of solvents from nonhydrogen bonding to hydrogen bonding due to the stabilization of the nonbonding level by the hydrogen bond. Such a shift has been observed for alkyl halides (see Table IV) supporting the participation of nonbonding electrons in the excitation. The regions of absorption of the several basic groups also parallel rather closely the ionization energies (see Table V and

TABLE IV

Shift of Long-Wavelength Absorption Band of Alkyl Iodides in Solution, Å[a]

Compound	Vapor	Heptane	Ether	Chloroform	Methanol	Water
Methyl Iodide	2576	2575	2547	2541	2540	2494
Ethyl Iodide	2582	2582	2568	2550	2550	2509
n-Propyl Iodide	2568	2576	2556	2544	2541	2505

[a] K. Kimura and S. Nagakura, *Spectrochim. Acta*, **17**, 166 (1961).

TABLE V

Ionization Energies and Long-Wavelength Absorption Bands of Some Compounds Containing Basic Groups

Compound	Ionization energy,[o] eV	Solvent	λ_{max}, Å	ϵ_{max}	λ_{max}, Å	ϵ_{max}	Ref.
HCl	12.78	Vapor	2300E[p]	Weak	1540	800	a,b
CH_3Cl	11.4	Vapor	1730	Weak	1600		c
		n-Heptane	1770	260	1690	370	d
HBr	11.69	Vapor	2640E[p]		1820		a
CH_3Br	10.7	Vapor	2040	180	1940		e,f
HI	10.4	Vapor	3320E[p]		2170	180	a,g
CH_3I	9.6	Vapor	2570	230	1980, 1940		e,f
H_2O	12.7	Vapor	1670	1480	1500E		h,i
		n-Heptane	1760	1200	1670	2120	d
CH_3OH	10.9	Vapor	1830	150	1590	3000	h,i
		n-Heptane	1780	180	1742	360	d
H_2S	10.5	Hexane	2250	160	1890	1600	j
CH_3SH	9.44	Cyclohexane	2270	140			m
		Vapor			ca. 1840		n
NH_3	10.52	Vapor	1940	5600	1520	Strong	k
CH_3NH_2	9.41	Vapor	2150	600	1940, 1905	2200, 3200	k
CH_3OCH_3	10.5	Vapor	1840	2510	1625	4000	l

[a] A. K. Datta, *Z. Physik.*, **77**, 404 (1932).

[b] J. Romand and B. Vodar, *Compt. Rend.*, **226**, 2062 (1948).

[c] C. R. Zobel and A. B. F. Duncan, *J. Am. Chem. Soc.*, **77**, 2611 (1959); W. C. Price, *J. Chem. Phys.*, **4**, 539 (1936).

[d] H. Tsubomura, K. Kimura, K. Kaya, J. Tanaka, and S. Nagakura, *Bull. Chem. Soc. Japan*, **37**, 418 (1964).

[e] N. Davidson, *J. Am. Chem. Soc.*, **73**, 467 (1951); D. Porret and C. F. Goodeve, *Proc. Roy. Soc. (London)*, **A165**, 31 (1938); P. Fink and C. F. Goodeve, *Proc. Roy. Soc. (London)*, **A163**, 595 (1937).

[f] A. Henrici, *Z. Physik.*, **77**, 35 (1932).

[g] J. Romand and V. Vodar, *Spectrochim. Acta*, **8**, 242 (1956).

[h] A. J. Harrison, B. J. Cederholm, and E. M. Coffin, ONRN8onr 74100, Final Rept., Mount Holyoke (June 1951).

[i] A. J. Harrison, B. J. Cederholm, and M. A. Terwilliger, *J. Chem. Phys.*, **30**, 355 (1959).

[j] H. Ley and B. Arends, *Z. Physik. Chem.*, **15b**, 311 (1931).

[k] E. Tannenbaum, E. M. Coffin, and A. J. Harrison, *J. Chem. Phys.*, **21**, 311 (1953).

[l] A. J. Harrison and D. R. W. Price, *J. Chem. Phys.*, **30**, 357 (1959).

[m] J. C. Morris, W. J. Lanum, R. V. Helm, W. E. Haines, G. L. Cook, and J. S. Ball, *J. Chem. Eng. Data*, **5**, 112 (1960).

[n] W. C. Price, J. P. Teagan, and A. D. Walsh, *Proc. Roy. Soc. (London)*, **A201**, 600 (1956).

[o] All electron impact data except for CH_3SH, which is a spectroscopic value. F. H. Field and J. L. Franklin, *Electron Impact Phenomena and the Properties of Gaseous Ions*, Academic Press, New York, 1957.

[p] Long-wavelength absorption edge.

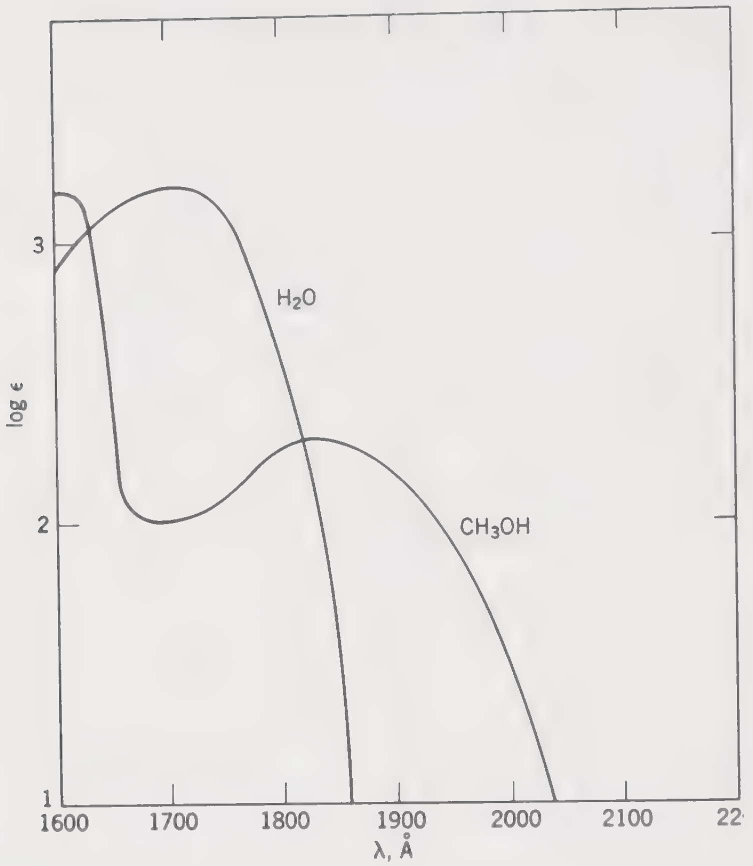

Fig. 15. Vapor spectrum of H_2O and CH_3OH. (After A. J. Harrison, B. J. Cederholm, and E. M. Coffin, ONR Project NR-056-160, Mount Holyoke.)

Fig. 15). The sulfur and nitrogen compounds absorb at longer wavelengths than the analogous oxygen compounds. This is attributable to the higher energy of their nonbonding orbitals as shown by their lower ionization energies.

On excitation the electron may undergo a transition to a state which is localized on the basic atom, or it may go to a molecular state. For highly excited states the distinction between the two types of states is lost, and all become Rydberg or united atom states. Furthermore, while one may conceive of an excitation as being localized on the basic atom, the excitation will almost certainly increase the electronegativity of this atom and consequently increase the amount of the electron transfer from the other atoms associated with it. The net result is then actually excitation to a molecular state. The long wavelength absorption in most of these compounds is probably due to the transition $\sigma^2 y_B{}^2 \rightarrow \sigma^2 y_B \sigma^*$ $(n \rightarrow \sigma^*)$ although $\sigma^2 y_B{}^2 \rightarrow \sigma^2 y_B ns$ is also a possibility (20). In the sulfur-containing compounds the $y_B \rightarrow 3d$ transition is also a possibility (21). For an $n \rightarrow \sigma^*$ transition the intensity should be relatively weak due to the small overlap between the nonbonding and σ^* orbitals.† Experimentally, the molar extinction coefficients of the absorption bands of several basic compounds lie in the rage 200–3000 (22).

The replacement of hydrogen in the basic group hydrides by alkyl groups usually shifts the spectrum toward the red and lowers the ionization energy (see Table V). This is attributable to a positive inductive effect of the alkyl groups which should raise the energy of the nonbonding orbitals but have little effect on the energy of the σ^* orbital. A resonance effect also appears to be operating, since with some bases the band for the methyl compound lies at longer wavelengths than the band for the ethyl compound.

An alternative explanation may be formulated on the basis of the united atom model for the alkyl groups (see Section III-B-3). In the case of the methyl compounds the filled virtual nonbonding orbital of the methyl group will interact with the filled nonbonding orbital of the basic atom to produce two molecular orbitals, one higher and one lower, than the original nonbonding components. Since the higher molecular orbital is occupied, the alkyl compound should have a lower ionization energy (from the MO) than the hydride (from y_B). The $n \rightarrow \sigma^*$ transition should also lie to the red of its position in the hydride since the transition is now from the higher-energy molecular orbital rather than from y_B.

D. The Multiple-Bonded Basic Group

A very large number of important chromophores, for example $>C=O$, $>C=S$, $—NO_2$, $—N=O$, belong to this classification. For these chromophores the transition which is most likely to produce long wavelength absorption is an $n \rightarrow \pi^*$ transition from a nonbonding orbital on the basic atom to an antibonding π^* orbital in the multiple bond, $\sigma^2\pi_x{}^2y_B{}^2 \rightarrow \sigma^2\pi_x{}^2y_B\pi_x{}^*$ (23) (Fig. 16). Since the basic atom B is the more electronegative atom in the bond, x_B will lie lower than x_C. Also x_B and y_B have the same energy, thus it follows that y_B lies at higher energy than the bonding orbital $\pi_x = x_C + \lambda x_B$. The greater height of y_B and the fact that the antibonding π^* orbital lies lower than an antibonding orbital in a single bond (σ^*) puts the absorption corresponding to the $y_B \rightarrow \pi^*$ transition at longer wavelengths than that due to the $\pi \rightarrow \pi^*$ or $y_B \rightarrow \sigma^*$ transition (see Fig. 16).

---

† For $\pi \rightarrow \pi^*$ transitions, the transition moment $\int \pi \mathbf{R} \pi^* d\tau$ contains terms like $\int x_A \mathbf{R} x_A d\tau$, which are relatively large. However, for $n \rightarrow \sigma^*$ or $n \rightarrow \pi^*$ transitions, the transition moment contains only terms of the type $\int y_B \mathbf{R} \sigma^*(\pi^*) d\tau$. These integrals are proportional to overlap integrals between y_B and $\sigma^*(\pi^*)$, which are small.

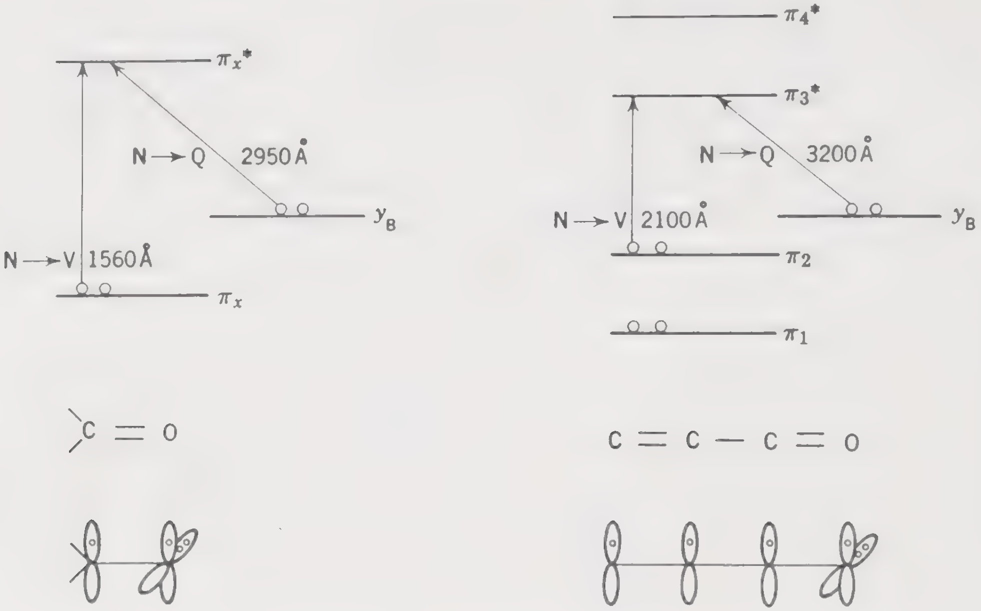

Fig. 16. Energy levels for the carbonyl and conjugated carbonyl groups.

In addition to the transition just discussed, other transitions, such as $n \to \sigma^*$ and $\pi \to \pi^*$, are also observed at shorter wavelengths in the spectra of these compounds. However, the $n \to \pi^*$ transitions are usually easily recognizable by their low intensities, sensitivity of absorption wavelength to solvent effects, and spectral shifts caused by substitution of various groups on the chromophore. The low intensities, even for the symmetry allowed $n \to \pi^*$ transitions, are attributable to the small overlap of the nonbonding and π^* orbitals which are mainly oriented in mutually perpendicular directions. A discussion of the effects of solvents on the $n \to \pi^*$ transitions will be deferred to Section IV-E-2.

1. THE CARBONYL GROUP

Formaldehyde has a strong absorption in the vapor at about 1555 Å which probably corresponds to the $\pi \to \pi^*$, $\sigma^2\pi_x{}^2y_O{}^2 \to \sigma^2\pi_x{}^1y_O{}^2\pi_x{}^*$, transition at 1600 Å in ethylene (Fig. 16). In these cases $\sigma = tr_C + \lambda z_O$ and $\pi_x = x_C + \lambda x_O$. Two other transitions occur in formaldehyde at 1750 and 2950 Å in the vapor (25,26). The latter of these is very weak ($\epsilon = 10$). On the basis of calculations (23), the 1750-Å band has been considered to be an $n \to \sigma^*$ transition. The 2950-Å band has been assigned† as the forbidden $n \to \pi^*$ transition, $\sigma^2\pi_x^2y_O{}^2 \to \sigma^2\pi_x{}^2y_O{}^1\pi_x{}^*$.

---

† In the ground state formaldehyde is planar. In the excited state, however (see ref. 24) a CH bond lies, however, at an angle of 20° to the COH plane.

TABLE VI

$n \rightarrow \pi^*$ Transitions of Saturated Carbonyl Compounds

Compound X_1—CO—X_2	λ_{max}, Å	Substituent effect		ϵ_{max}	Solvent	Ionization energy[a], eV	Ref.
		X_1	X_2				
HCOH	2950			10	Vapor	10.87	b
$HCONH_2$	2050		$+R, -I$	160	Vapor	10.25	b
HCOOH	2050		$+R, -I$	40	Vapor	11.05	b
$HCOOCH_3$	2150		$+R, -I$	70	Isooctane	10.82	k
$HCOC_2H_5$	2930		$+R, +I$	20	Isooctane	9.98	c
$HCOCH_3$	2900		$+R, +I$	10	Vapor	10.21	b
$ClCOCH_3$	2400	$-I, +R$	$+R, +I$	40	Heptane	11.02	j
$BrCOCH_3$	2500	$-I, +R$	$+R, +I$	90	Heptane	10.55	j
NH_2COCH_3	2050	$-I, +R$	$+R, +I$	160	Methanol	9.77	i
$HOCOCH_3$	2000	$-I, +R$	$+R, +I$	60	Vapor	10.37	f
CH_3OCOCH_3	2100	$-I, +R$	$+R, +I$	60	Isooctane	10.27	k
$HSCOCH_3$	2190	$-I, +R$	$+R, +I$	2200	Cyclohexane	10.00	e
CH_3COCH_3	2790	$+I, +R$	$+R, +I$	10	Vapor	9.69	d
$C_2H_5COCH_3$	2780	$+I, +R$	$+R, +I$	20	Isooctane	9.53	g
i-$C_3H_7COCH_3$	2850	$+I, +R$	$+R, +I$	20	Dichloroethane	9.32	h
Cyclohexanone	2850			10	Hexane	9.14	l
Cyclopentanone	2990			20	Hexane	9.26	l

[a] Photoionization values from K. Watanabe, T. Nakayama, and J. Mottl, "Final Report on Ionization Potential of Molecules by a Photoionization Method," Dept. Army No. 5B-99-01-004, ORD No. TB2-0001-00R- no. 1624. Contract no. DA-04-200-ORD 480 and 737 (December, 1959).

[b] K. Bowden, E. A. Braude, and E. R. H. Jones, *J. Chem. Soc.*, **1946**, 948.

[c] A. P. I. Research Project No. 44, Shell Development Company, **I**, 329 (1949).

[d] G. Briegleb and W. Strohmeier, *Z. Naturforsch*, **6b**, 6 (1951).

[e] J. I. Cunneen, *J. Chem. Soc.*, **1947**, 134.

[f] G. Briegleb and W. Strohmeier, *Naturwissenschaften*, **33**, 344 (1946).

[g] R. P. Mariella and R. R. Raube, *J. Am. Chem. Soc.*, **74**, 518 (1952).

[h] M. F. Hawthorne and W. D. Emmons, *J. Am. Chem. Soc.*, **80**, 6398 (1958).

[i] F. Korte and K. H. Lohmer, *Chem. Ber.*, **91**, 1397 (1961).

[j] B. D. Saksena and R. E. Kagarise, *J. Chem. Phys.*, **19**, 994 (1951).

[k] W. D. Closson and P. Haug, *J. Am. Chem. Soc.*, **86**, 2384 (1964).

[l] G. Forster, R. Skrabal, and J. Wagner, *Z. Elektrochem.*, **43**, 290 (1937); S. W. Benson and G. B. Kistiakowsky, *J. Am. Chem. Soc.*, **64**, 80 (1942).

Substitution of alkyl, halogen, or hydroxyl groups for hydrogen shifts the $n \rightarrow \pi^*$ band to shorter wavelengths (see Fig. 17 and Table VI). Both the resonance effect and the inductive effect operate. The resonance effect (R) raises the energy of $\pi_y{}^*$ just as in the substitution on ethylene, but the y_O orbital from which the electron comes is not appreciably affected. Thus the

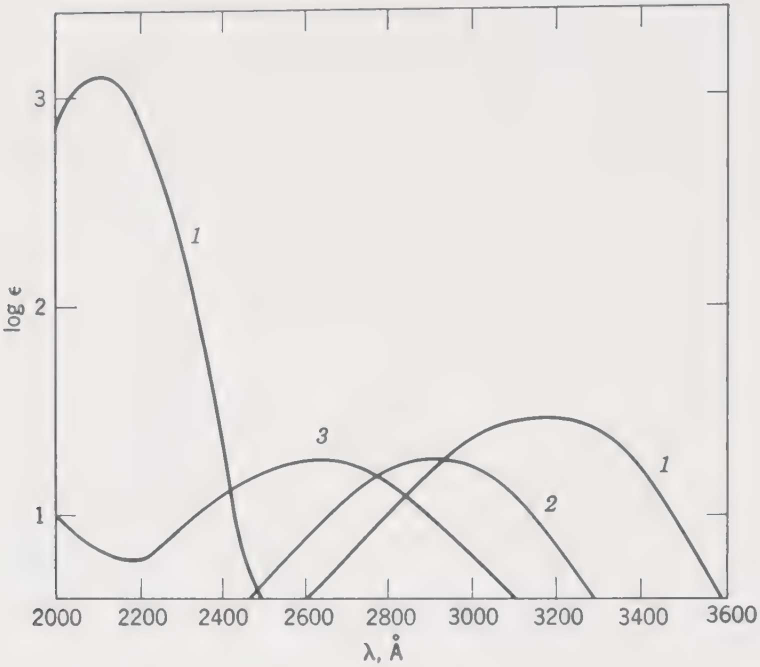

Fig. 17. The spectra in aqueous solution of three compounds containing the carbonyl group: (*1*) acrolein; (*2*) acetaldehyde; (*3*) acetone. (After A.P.I. Ultraviolet Spectrograms 327, 330, and 339, Shell Development Co.)

$n \rightarrow \pi^*$ spectrum is shifted to shorter wavelengths by the resonance effect alone. By a similar argument, the ionization energy does not change appreciably. A positive inductive effect, $(+I)$, as with alkyl substitution, will raise the energy of y_0, which will lower the ionization energy and shift the $n \rightarrow \pi^*$ band to longer wavelengths, thereby partially counterbalancing the resonance effect. A negative inductive effect, as with hydroxyl, halogen, or amino substitution, will lower the energy of y_0, increase the ionization energy, and shift the $n \rightarrow \pi^*$ spectrum to shorter wavelengths. The shifts of the $n \rightarrow \pi^*$ band resulting from substitutional effects are caused by combinations of these effects. In Table VI the effects are summarized for some of the simpler carbonyl compounds. All substituted compounds show shifts of the $n \rightarrow \pi^*$ band to a shorter wavelength, indicating that even if a $+I$ effect occurs, the $+R$ effect is dominant. The cyclic ketones absorb at approximately the same wavelengths as do the acyclic dialkyl ketones.

Substitution of unsaturated groups such as vinyl or phenyl forming a conjugative system with the carbonyl group shifts the $n \rightarrow \pi^*$ band toward the red (see Fig. 18 and Table VII). Since the y_0 orbital energy is relatively constant as judged by the ionization energies, the red shift of the band must be caused by the lowering of the π_x^* level. In the polyene-substituted compounds the π_x^* levels are progressively lowered in energy as the number of

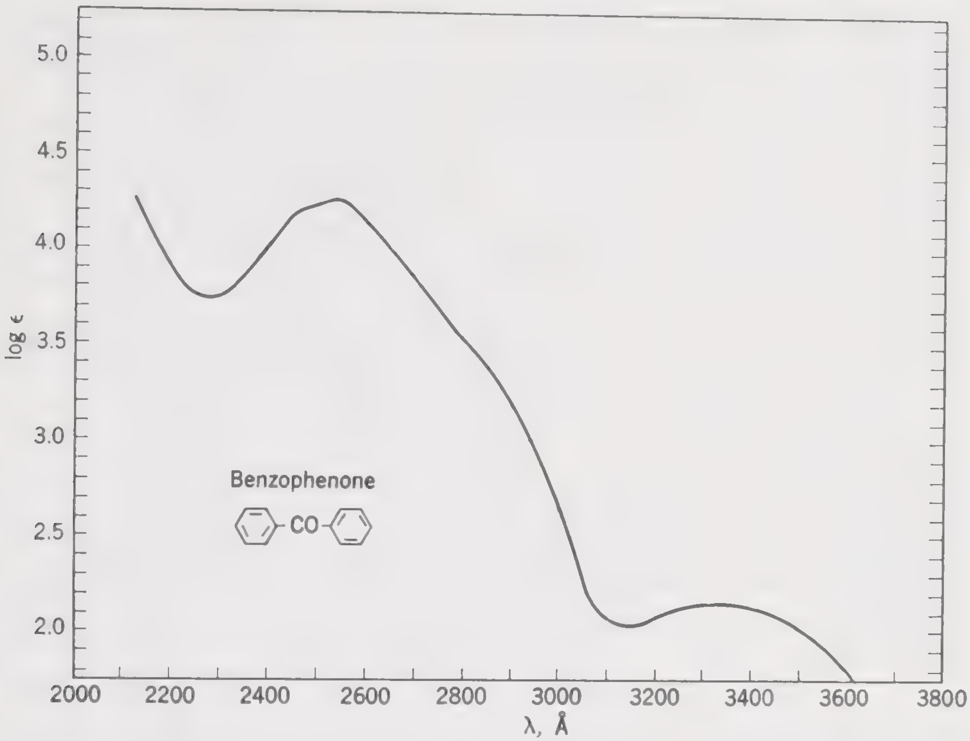

Fig. 18. Spectrum of benzophenone in ethanol. (After R. A. Friedel and M. Orchin, *Ultraviolet Spectra of Aromatic Compounds*, Wiley, New York, 1951.)

TABLE VII

$n \rightarrow \pi^*$ Transitions of Unsaturated Carbonyl Compounds

Compound	Ionization energy,[f] eV	λ_{max}, Å	ϵ_{max}	Solvent	Ref.
$H \cdot CO \cdot H$	10.9	2880	10	Water	a
$H \cdot CO \cdot CH_2 \cdot CH_3$	10.0	2780	10	Water	d
$H \cdot CO \cdot CH{:}CH_2$	10.1	3150	30	Water	b
$H \cdot CO \cdot CH{:}CH \cdot CH_3$	9.73	3100	30	Water	d
$H \cdot CO \cdot CH{:}CH \cdot CH{:}CH_2$	—	3250	50	Ethanol	c
$H \cdot CO \cdot C_6H_5$	9.53	3200	50	Ethanol	d
$C_6H_5 \cdot CO \cdot C_6H_5$	9.75	3300	180	Ethanol	e

[a] R. Bieber and G. Trumpler, *Helv. Chim. Acta*, **30**, 1860 (1947).

[b] API Research Project No. 44, Shell Development Co., **I**, 330 (1949).

[c] E. L. Pippen and M. Nonaka, *J. Org. Chem.*, **23**, 1580 (1958).

[d] N. J. Leonard, R. T. Rapala, H. L. Herzog, and E. R. Blout, *J. Am. Chem. Soc.*, **71**, 2997 (1949).

[e] E. D. Bergmann et al., *Bull. Soc. Chim. France*, [5]**18**, 684 (1951).

[f] Photoionization values.

double bonds increases, just as in the conjugated polyenes mentioned earlier (Section II-H) (see Fig. 16). The red shift produced by the addition of the phenyl group may be regarded as due to an increased conjugative system for the π electrons resulting in a considerable lowering of the lowest antibonding π^* orbital of the carbonyl group.

In the dialdehydes and diketones having two y_0 orbitals and also two π_x^* orbitals of different energy, there is the possibility of four $n \rightarrow \pi^*$ bands. However, the two y_0 orbitals must interact strongly in order to produce distinct $n \rightarrow \pi^*$ bands. This interaction appears to be small even for cyclic *cis*-α,β-diketones since only two $n \rightarrow \pi^*$ transitions are observed in these compounds (27). The two transitions corresponding to $y_0 \rightarrow \pi_4^*$ and $y_0 \rightarrow \pi_3^*$ appear at 2800 Å ($\epsilon = 20$) and 4200 Å ($\epsilon = 10$) in the spectrum of diacetyl in ethanol (28) and at 2800 Å ($\epsilon = 20$) and 4660 Å ($\epsilon = 30$) in the spectrum of camphorquinone (27,29).

The α,β-unsaturated ketones also have a strong $\pi \rightarrow \pi^*$ band in the neighborhood of 2100–2300 Å, which is the analog of the $\pi_2 \rightarrow \pi_3^*$ transition of butadiene (Figs. 11 and 16). The effects of substitution at the α and β positions on the location of this $\pi \rightarrow \pi^*$ band are predictable to a high degree of accuracy through the use of empirical rules (30,31). Similar rules have been formulated for α,β-unsaturated aldehydes (32) and acids (33). These empirical rules have been of great importance in assigning the structures of steroids. They are summarized in Table VIII.

TABLE VIII
Empirical Rules for Position of $\pi \rightarrow \pi^*$ Transition in α,β-Unsaturated Carbonyl Compounds in Ethanol[a]

Type of compound	Basic[a,c] λ_{max}, Å	Additional wavelength change from substitution, Å						
		α				β		γ, δ
		R[b]	OH	Cl	Br	R[b]	OH	R[b]
α,β-Unsaturated ketones	2150	100	350		230	100	350	
α,β-Unsaturated aldehydes	2090	110				110		
α,β-Unsaturated esters or acids	1970	100				100	350	
Dienones	2450	100	350	150	230	120		180

[a] For ring systems, the ring residue at each position is regarded as an alkyl group. If a carbon carbon double bond is exocyclic to a five- or six-membered ring or endocyclic in a five- or seven-membered ring, add 50 Å to the basic λ_{max}. If a [3.1.1]-bicyclo system is part of the conjugated system, add 150 Å to the basic λ_{max}.

[b] R may be an alkyl, ring residue; OAc, or OR group.

[c] If conjugation is extended by a C=C group, add 300 Å to the basic λ_{max}.

2. THE THIOCARBONYL AND SULFOXIDE GROUPS

Compounds containing the thiocarbonyl group exhibit the same type of absorption bands as do those containing the carbonyl chromophore. The $n \rightarrow \pi^*$ bands in the thiocarbonyl compounds are red-shifted compared to those in the carbonyl compounds, e.g., $\lambda_{\max}$ for thiobenzophenone is 5990 Å and for benzophenone 3300 Å (see also Table IX). This red shift of the $n \rightarrow \pi^*$ bands is attributable to the higher energy of the nonbonding sulfur orbital and to a lowering of the $\pi_x{}^*$ orbital due to the smaller electronegativity of sulfur relative to oxygen. The lower energy of the $\pi_x{}^*$ orbital in the thiocarbonyl group also produces a shift of the $\pi \rightarrow \pi^*$ transition to longer wavelengths. This is shown by the appearance of a strong band ($\epsilon = 5000$–$15{,}000$) in the region of 2300–3100 Å in the spectra of thiocarbonates and thiocarboxylic acid derivatives (34). Substitution of basic groups such as NH_2 on the thiocarbonyl group shifts the $n \rightarrow \pi^*$ band to shorter wavelengths analogous to substitutional effects on the carbonyl group (see Table IX). The addition of a phenyl group shifts the $n \rightarrow \pi^*$ absorption band toward longer wavelengths by lowering the energy of the π^* levels as was the situation with the carbonyl group.

TABLE IX
$n \rightarrow \pi^*$ Bands of Thiocarbonyl Compounds

Compound	$\lambda_{\max}$, Å	$\epsilon_{\max}$	Solvent	Ref.
Thiocyclohexanone	5040	~10	Cyclohexane	a
Cyclohexanone	2850	10	Hexane	b
Thioacetamide	3180	60	Water	c
Acetamide	2050	160	Methanol	d
Thiourea	2700	100	Water	c
Thiobenzophenone	5990	630	Isopropyl alcohol	e
Benzophenone	3300	180	Ethanol	f

[a] M. J. Janssen, *Rec. Trav. Chim.*, **79**, 454, 464 (1960).

[b] G. Forster, R. Skrabal, and J. Wagner, *Z. Elektrochem.*, **43**, 290 (1937); S. W. Benson and G. B. Kistiakowsky, *J. Am. Chem. Soc.*, **64**, 80 (1942).

[c] H. Hosoya, J. Tanaka, and S. Nagakura, *Bull. Chem. Soc. Japan*, **33**, 850 (1959).

[d] B. D. Saksena and R. E. Kagarise, *J. Chem. Phys.*, **19**, 994 (1951).

[e] G. Sartori and C. Furlani, *Ann. Chim. (Rome)*, **44**, 95 (1954).

[f] E. D. Bergmann et al., *Bull. Soc. Chim. France*, [5]**18**, 684 (1951).

The sulfoxides, having a pair of nonbonding electrons on the sulfur atom, should also exhibit an $n \rightarrow \pi^*$ band in their absorption spectra. Saturated sulfoxides have a moderately strong band ($\epsilon = 1500$) near 2200 Å in ethanol

(35). A similar band occurs at approximately the same location in the spectra of 2-methylallyl sulfoxide. The solvent dependence of the band maximum indicates that this band corresponds to the expected $n \rightarrow \pi^*$ transition.

3. NITROSO AND NITRO COMPOUNDS

Nitrosomethane has a weak band at 6750 Å in the vapor as compared with 2900 Å for the $n \rightarrow \pi^*$ band in acetaldehyde. This may be assigned as an $n \rightarrow \pi^*$ transition originating from either the nitrogen y_N orbital, the oxygen y_O orbital, or from a level composed of a combination of these two. Energetically, the assignment to the nonbonding molecular orbital seems more reasonable. The effects of substitution of basic or alkyl groups on the position of this band are the same as with the carbonyl group—a shift to shorter wavelengths. Nitrosobenzene absorbs at longer wavelengths (7660 Å) than does nitrosomethane due to the conjugative effect of the phenyl group which lowers the π^* level. Table X lists the $n \rightarrow \pi^*$ transitions of some nitroso compounds. The other $n \rightarrow \pi^*$ transition must occur at shorter wavelengths. Perhaps the weak bands at 3000 Å ($\epsilon = 100$) in t-C_4H_9NO and at 2580 Å ($\epsilon = 420$) in NOCl correspond to this transition. A more intense band is found at 2200–2300 Å in $(CH_3)_2NNO$, n-C_4H_9ONO, and t-C_4H_9SNO which may be a charge-transfer band involving the substituent as donor and the —NO group as acceptor. The $\pi \rightarrow \pi^*$ transition in the NO double bond appears near 1400–1600 Å in NOCl and 1-chloro-1-nitrosocyclohexane (36).

The molecular structure of the nitro group may be formulated as follows, considering only the π electrons (37). The molecular orbitals†

$$\begin{aligned}\pi_{x_1} &= x_{AO} + \lambda x_N + x_{BO}\\ \pi_{x_2} &= x_{AO} - x_{BO}\\ \pi_{x_3}{}^* &= x_{AO} - \eta x_N + x_{BO}\end{aligned}$$

are formed from the two oxygen and one nitrogen x orbitals. Here A and B index the two oxygen atoms. The two oxygen nonbonding y orbitals may interact to yield two nonbonding molecular orbitals

$$\pi_{y_1} = y_A + y_B \quad \text{and} \quad \pi_{y_2} = y_A - y_B$$

In the ground state the electronic configuration is $(\pi_{x_1})^2(\pi_{x_2})^2(\pi_{y_1})^2(\pi_{y_2})^2$ (see Fig. 20). Two $n \rightarrow \pi^*$ transitions, $\pi_{y_1} \rightarrow \pi_{x_3}{}^*$ and $\pi_{y_2} \rightarrow \pi_{x_3}{}^*$, and a $\pi \rightarrow \pi^*$ transition, $\pi_{x_2} \rightarrow \pi_{x_3}{}^*$, are expected in the nitro compounds. From calculations (37), however, it is found that the interaction between the y_A and y_B levels is small so that only one $n \rightarrow \pi^*$ band will be seen in the absorption spectrum. It is interesting to note that the charge densities calculated from

---

† See Figure 3 for the forms of the π_x molecular orbitals.

TABLE X

$n \rightarrow \pi^*$ Bands of Azo, Nitro, and Nitroso Compounds

Compound	λ_{max}, Å	ϵ_{max}	Solvent	Ref.
CH_3NNCH_3	3500	30	Methyl chloride	a
CF_3NNCF_3	3650	120	Methyl chloride	a
$C_6H_5NNCH_3$	4040	90	Cyclohexane	b
cis-$C_6H_5NNC_6H_5$	4320	1300	Isooctane	c
trans-$C_6H_5NNC_6H_5$	4500	400	Isooctane	c
CH_3NO	6750		Vapor	d
t-C_4H_9NO	6650	20	Diethyl ether	f
CF_3NO	6930	20	Vapor	e
$ClNO$	4600	10	Carbon tetrachloride	g
FNO	3110	Weak	Vapor	h
$(CH_3)_2NNO$	3610	130	Petroleum ether	i
n-C_4H_9ONO	3560	90	Petroleum ether	i
t-C_4H_9SNO	3390	980	Heptane	j
C_6H_5NO	7660	40	Hexane	k
CH_3NO_2	2800	10	Isooctane	l
s-$C_4H_9ONO_2$	2700	20	Ethanol	m
$C_6H_5NO_2$	3680	200	Vapor	n

[a] O. Ruff and W. Willenberg, *Chem. Ber.*, **73**, 724 (1940).

[b] P. P. Birnbaum, J. H. Linford, and D. W. G. Style, *Trans. Faraday Soc.*, **49**, 735 (1953).

[c] G. Zimmerman, L. Chow, and U. Paik, *J. Am. Chem. Soc.*, **80**, 3528 (1958).

[d] R. N. Dixon, quoted in J. N. Murrell, *Theory of Electronic Spectra of Organic Molecules*, Methuen, London, 1963, p. 184.

[e] J. Mason, *J. Chem. Soc.*, **1957**, 3904.

[f] E. C. C. Baly and C. H. Desch, *J. Chem. Soc.*, **93**, 1755 (1908).

[g] M. J. Collis, F. P. Gintz, D. R. Goddard, E. A. Hebdon, and G. J. Minkoff, *J. Chem. Soc.*, **1958**, 438.

[h] H. S. Johnson and H. J. Bertin, *J. Mol. Specty.*, **3**, 683 (1959).

[i] R. N. Haszeldine and J. Jander, *J. Chem. Soc.*, **1954**, 691.

[j] G. Kresze and U. Uhlich, *Chem. Ber.*, **92**, 1048 (1959).

[k] A. Buroway et al., *J. Chem. Soc.*, **1955**, 3721.

[l] API Research Project 44, California Research Corporation **I**, 104 (1945).

[m] H. E. Ungnade and R. A. Smiley, *J. Org. Chem.*, **21**, 993 (1956).

[n] E. Merkel, *Z. Elektrochem.*, **63**, 373 (1959).

the molecular orbital approach mentioned are about the same as predicted from the two valence structures:

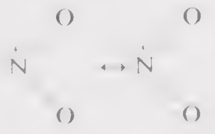

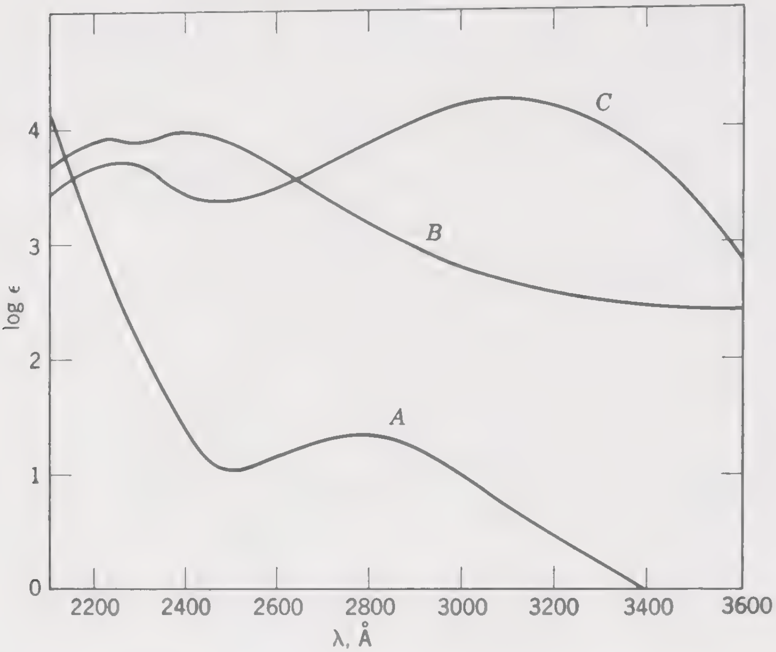

Fig. 19. The spectra of three nitro compounds: (*A*) nitromethane; (*B*) nitropropene-1; (*C*) nitro-1,3-pentadiene. [(*A*) after A.P.I. Ultraviolet Spectrogram 104 (isooctane) (California Research Corporation); (*C*) after E. A. Braude, E. R. H. Jones, and G. G. Rose, *J. Chem. Soc.*, **1947**, 1104 (in ethanol).]

The $n \rightarrow \pi^*$ transition occurs at 2800 Å in nitromethane (see Table X and Figs. 19, 20) at almost the same wavelength as the carbonyl $n \rightarrow \pi^*$ of acetaldehyde. Substitution of a basic group shifts the absorption to shorter

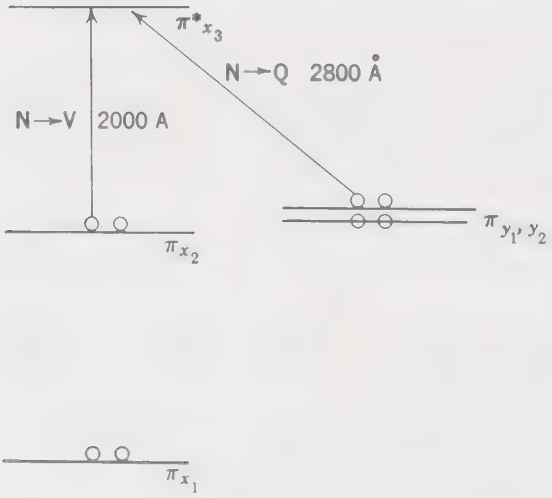

Fig. 20. Energy levels for the nitro group.

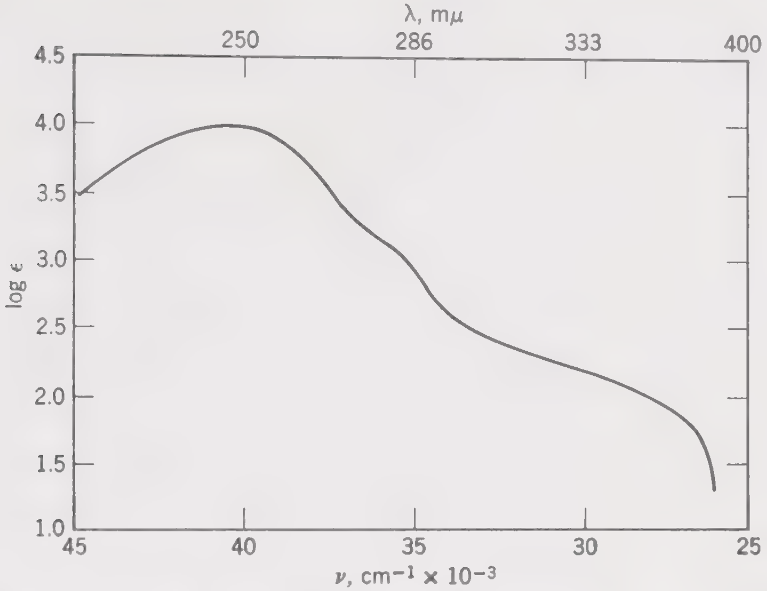

Fig. 21. The absorption spectrum of nitrobenzene in heptane. (After J. N. Murrell, *Theory of Electronic Spectra of Organic Molecules*, Methuen, London, 1963.)

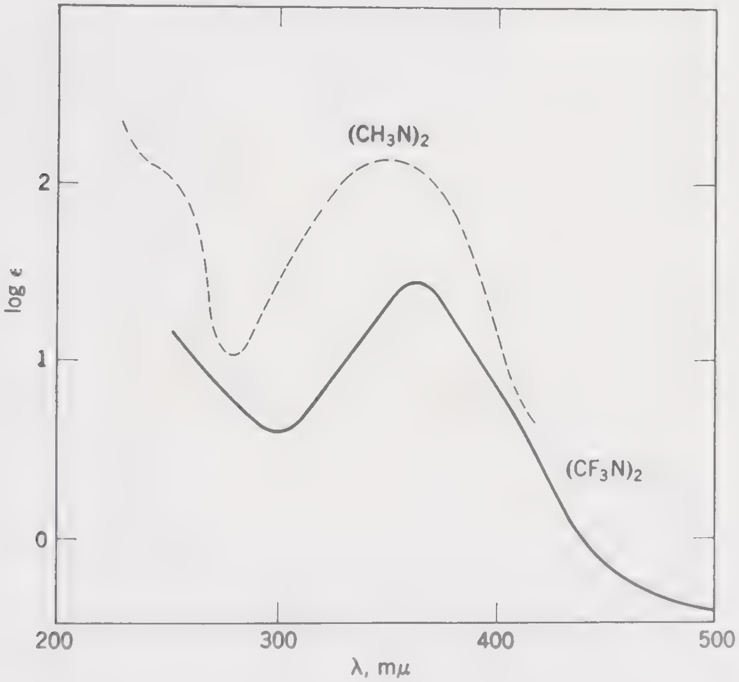

Fig. 22. Spectra of azomethane and hexafluoroazomethane. [From O. Ruff and W. Willenberg, *Chem. Ber.*, **73**, 724 (1940).]

wavelengths while addition of a phenyl group shifts the band toward the visible (Fig. 21). These effects are the same as noted for the carbonyl group and occur for the same reasons. Upon substitution of a vinyl group, the $n \rightarrow \pi^*$ band disappears (38) probably being covered by the more intense $\pi \rightarrow \pi^*$ band which is shifted toward the red. Nitromethane has a strong band at 1980 Å ($\epsilon = 5000$) (39) in the vapor which corresponds to the $\pi_{x_2} \rightarrow \pi_{x_3}^*$ transition. This band is shifted to the red upon addition of basic, conjugated olefin, or phenyl groups. In nitroolefins (hexane solution) it occurs at 2200–2400 Å (Fig. 19) (38), and in nitrobenzene at 2500 Å (40) (Fig. 21) showing the same behavior as the $\pi \rightarrow \pi^*$ band of the carbonyl group.

4. AZO COMPOUNDS

The azo group is similar to ethylene except that instead of two of the ethylene C—H σ bonds it has two nitrogen lone pairs in approximately sp^2 orbitals. There are then two π molecular orbitals

$$\pi_1 = x_A + x_B$$
$$\pi_2^* = x_A - x_B$$

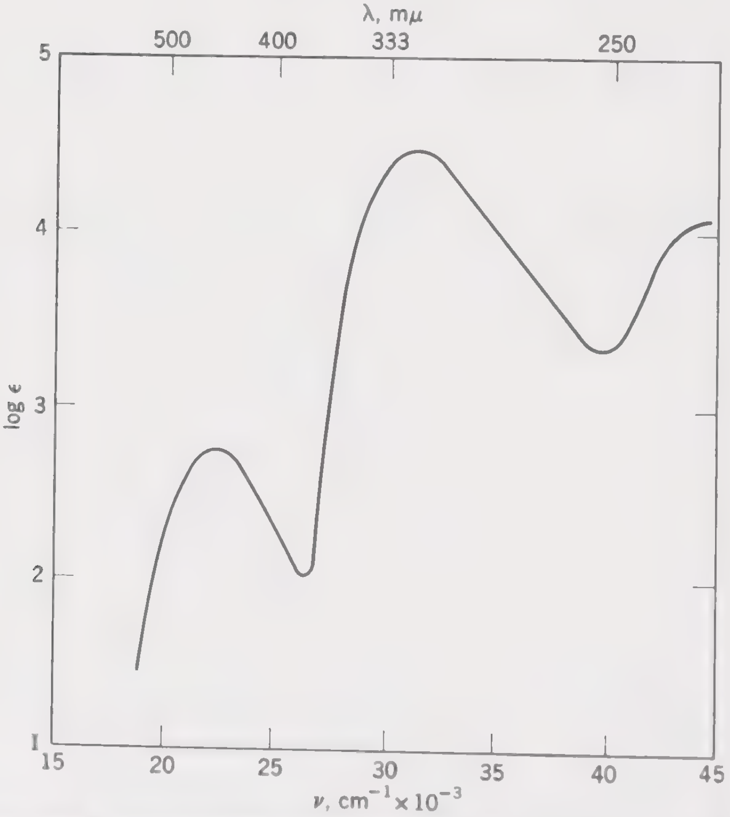

Fig. 23. Spectrum of *trans*-azobenzene in ethanol. [From A. Pongratz, G. Markgraf, and E. Mayer-Pitsch, *Chem. Ber.*, **71**, 1289 (1938).]

and two nonbonding orbitals

$$y_1 = y_A + y_B$$
$$y_2 = y_A - y_B$$

The ground state configuration is $(\pi_1)^2(y_1)^2(y_2)^2$.

Since there are two nonbonding levels, y_1 and y_2, two $n \rightarrow \pi^*$ transitions are expected in the spectra if y_A and y_B interact strongly. However in azomethane only one broad band is observed at 3500 Å (see Table X and Fig. 22) although a weak shoulder also appears near 2500 Å. Substitutional effects on the 3500-Å band are the same as noted in other chromophores having $n \rightarrow \pi^*$ transitions. The $\pi_1 \rightarrow \pi_2^*$ band must occur in the vacuum ultraviolet for azomethane. Substitution of phenyl groups shifts this $\pi \rightarrow \pi^*$ band into the ultraviolet region (Fig. 23). It is at 2600 Å ($\epsilon = 7800$) in phenyl azomethane (cyclohexane solution) (41) and at 2810 Å ($\epsilon = 5300$) and 3200 Å ($\epsilon = 21{,}300$) in *cis*- and *trans*-azobenzene (ethanol solution) (42). The $n \rightarrow \pi^*$ band is also shifted toward the red by a phenyl substitution (Fig. 23).

E. The Benzene Chromophore

1. BENZENE

Benzene absorbs weakly at 2600 and 2000 Å, but strongly at 1800 Å (see Fig. 24). These transitions are assumed to be between molecular orbitals formed from the six π electrons. The secular equation for the six electrons is (see Chapter II, p. 178 *et seq.*)

$$\begin{vmatrix} H_{AA} - E & H_{AB} & 0 & 0 & 0 & H_{AF} \\ H_{AB} & H_{BB} - E & H_{BC} & 0 & 0 & 0 \\ 0 & H_{BC} & H_{CC} - E & H_{CD} & 0 & 0 \\ 0 & 0 & H_{CD} & H_{DD} - E & H_{DE} & 0 \\ 0 & 0 & 0 & H_{DE} & H_{EE} - E & H_{EF} \\ H_{AF} & 0 & 0 & 0 & H_{EF} & H_{FF} - E \end{vmatrix} = 0$$

$H_{AA} = H_{BB}$, etc. $\equiv \alpha$, $H_{AB} = H_{BC}$, etc. $\equiv \beta$.

The molecular orbitals and their energies are (Section II-F):

$$\pi_1 = x_A + x_B + x_C + x_D + x_E + x_F \qquad E_1 = \alpha + 2\beta$$
$$\pi_2 = x_B + x_C - x_E - x_F \qquad E_2 = \alpha + \beta$$
$$\pi_3 = 2x_A + x_B - x_C - 2x_D - x_E + x_F \qquad E_3 = \alpha + \beta$$
$$\pi_4^* = x_B - x_C + x_E - x_F \qquad E_4 = \alpha - \beta$$
$$\pi_5^* = 2x_A - x_B - x_C + 2x_D - x_E - x_F \qquad E_5 = \alpha - \beta$$
$$\pi_6^* = x_A - x_B + x_C - x_D + x_E - x_F \qquad E_6 = \alpha - 2\beta$$

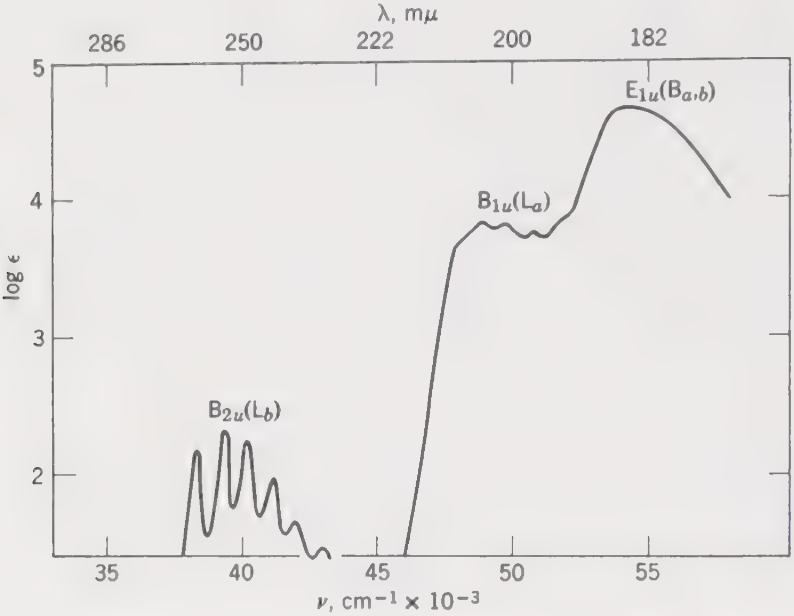

Fig. 24. Spectrum of benzene. [After H. B. Klevens and J. R. Platt, Technical Report, Part 1, Laboratory of Molecular Structure and Spectra, University of Chicago (1953–54).]

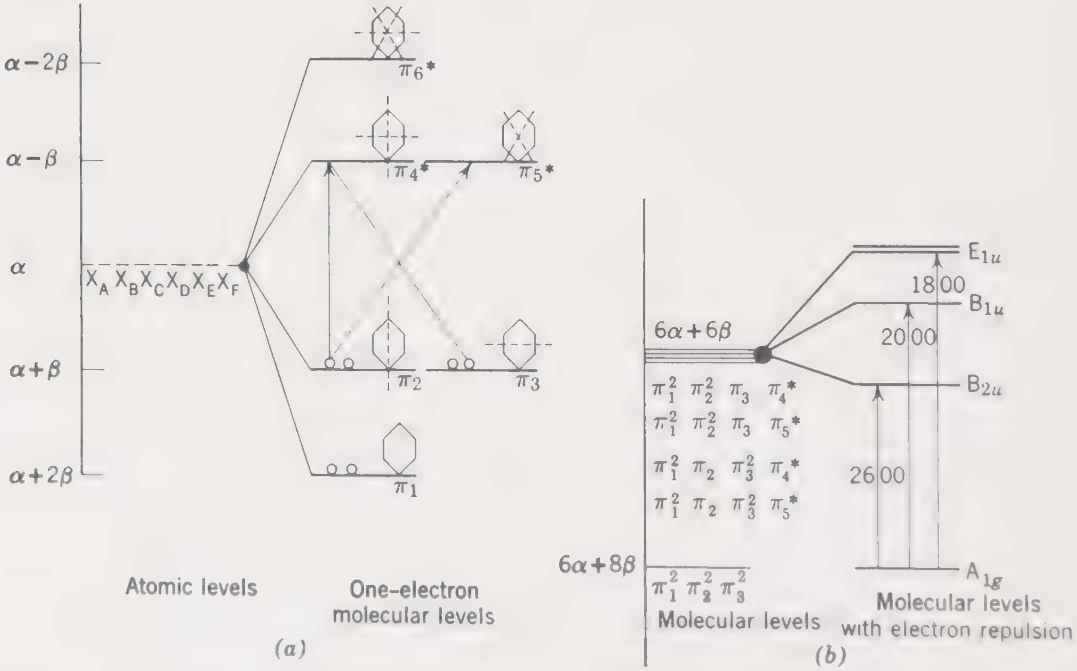
α−2β
α−β
α
α+β
α+2β
X$_A$ X$_B$X$_C$X$_D$X$_E$X$_F$
π$_6$*
π$_4$*
π$_5$*
π$_2$
π$_3$
π$_1$
Atomic levels
One-electron molecular levels
(a)
6α+6β
π$_1^2$ π$_2^2$ π$_3$ π$_4$*
π$_1^2$ π$_2^2$ π$_3$ π$_5$*
π$_1^2$ π$_2$ π$_3^2$ π$_4$*
π$_1^2$ π$_2$ π$_3^2$ π$_5$*
6α+8β
π$_1^2$ π$_2^2$ π$_3^2$
Molecular levels
E$_{1u}$
B$_{1u}$
B$_{2u}$
A$_{1g}$
18|00
20|00
26|00
Molecular levels with electron repulsion
(b)

Fig. 25. Benzene: (*a*) one-electron molecular levels; (*b*) configurations and molecular levels with electron repulsion. The dotted lines on the hexagons indicate the nodal planes in the molecular orbitals.

π_2 and π_3, and π_4^* and π_5^* are degenerate pairs of molecular orbitals (see Fig. 25*a*). That is, each wave function of a degenerate pair is a distinct and independent wave function, but each has the same energy. In benzene, the degenerate molecular orbitals have the same number of nodal planes, but they differ in the orientation of these planes. The ground state configuration for the x electrons is $\pi_1^2\pi_2^2\pi_3^2$. The first excited state is fourfold degenerate since the configurations

$$\pi_1^2\pi_2^2\pi_3\pi_4, \qquad \pi_1^2\pi_2^2\pi_3\pi_5^*, \qquad \pi_1^2\pi_2\pi_3^2\pi_4^*, \quad \text{and} \quad \pi_1^2\pi_2\pi_3^2\pi_5^*$$

all have the same energy.

The introduction of electron repulsion into the theory mixes these configurations,† producing new states (43). These states have been labeled B_{2u}, B_{1u}, and E_{1u}, the labels stemming from the symmetry properties of the wave functions associated with the states. Some, but not all, of the original fourfold degeneracy has been removed since E_{1u} is a twofold degenerate state (see Fig. 25*b*). The forms of the new wave functions are relatively simple. For example

$$(B_{1u}) = \pi_1^2\pi_2^2\pi_3\pi_5^* - \pi_1^2\pi_2\pi_3^2\pi_4^*$$

and has a nodal pattern which resembles that of π_6^*. The nodal diagrams of the states are

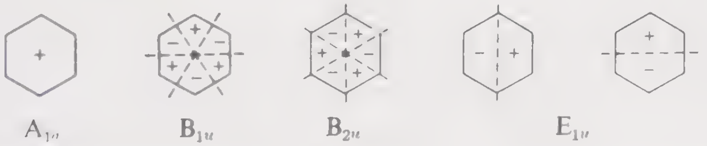

The benzene absorption at 2600 Å is associated with the $A_{1g} \rightarrow B_{2u}$ transition, that at 2000 Å with $A_{1g} \rightarrow B_{1u}$,‡ and that at 1800 Å, with $A_{1g} \rightarrow E_{1u}$ (45) (see Fig. 25). The first two of these transitions are forbidden and, therefore, weak, while the $A_{1g} \rightarrow E_{1u}$ transition is allowed and, therefore, strong. In contrast to most electronic band systems, the vibrational structure of the 2600-Å band is almost completely resolved (see Fig. 26*e*). This permits a more complete analysis of an electronic transition than is normally possible.

The fact that the $A_{1g} \rightarrow B_{1u}$, B_{2u} transitions are forbidden can perhaps be understood by noting the forms of the wave functions given above. It is not possible to generate these forms from the totally symmetric ground state, A_{1g}, by the dipole moment vector which represents radiation. However, certain

---

† Configuration interaction is of particular importance for states which are degenerate in the molecular orbital approximation. However, complete configuration interaction does not alter the relative state positions of Fig. 25*a*. J. Koutecky, K. Hlavaty, and P. Hochmann, *Theoret. Chim. Acta*, **3**, 341 (1965).

‡ A valence bond calculation assigns this band as a forbidden $A_{1g} \rightarrow E_{2g}$ transition (44).

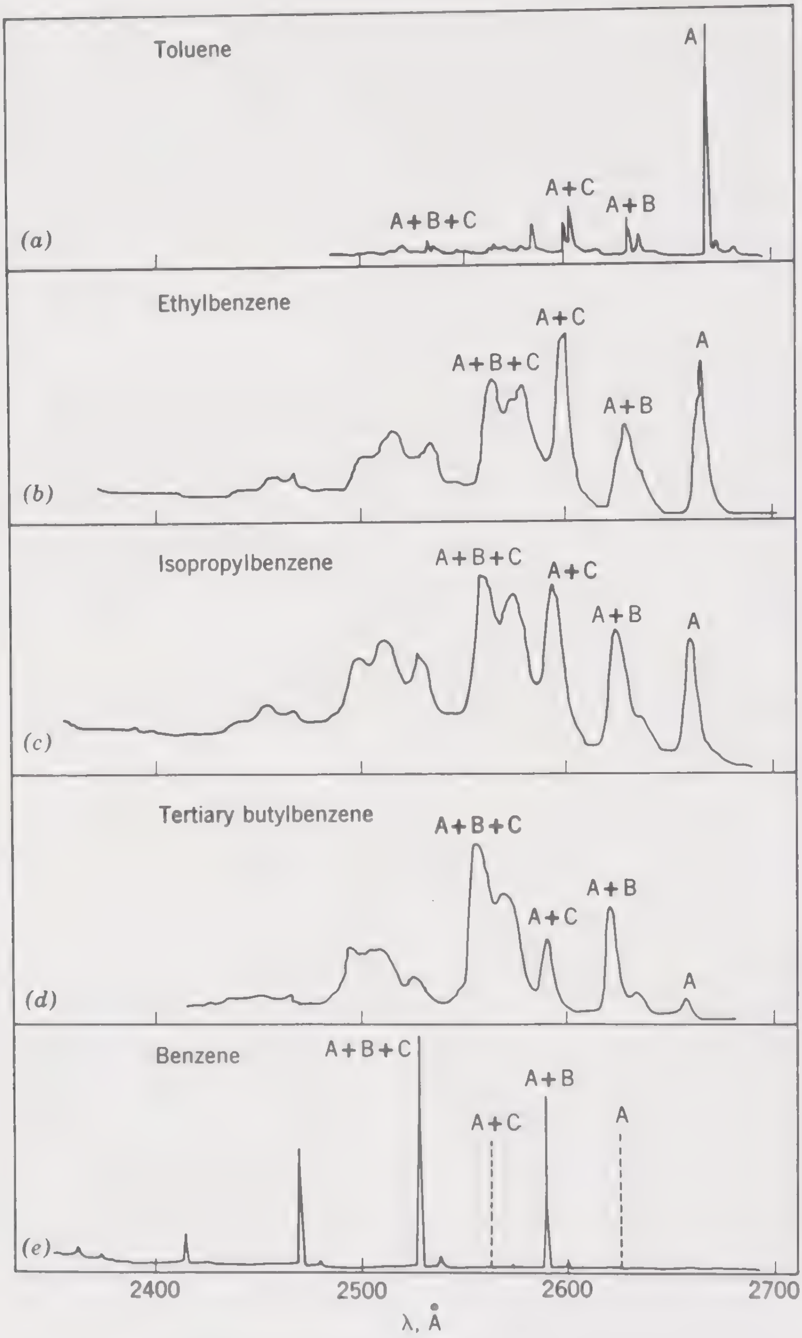

Fig. 26. The vapor spectrum of benzene and some monoalkyl-substituted benzenes. [After F. A. Matsen, W. W. Robertson, and R. L. Chuoke, *Chem. Rev.*, **41**, 273 (1947).]

vibrations which destroy the hexagonal symmetry can break down the selection rule. For the 2600-Å band such a vibration has the form

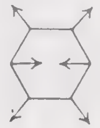

and is designated E_{2g} because of its symmetry. All vibrational bands of any intensity contain the E_{2g} vibration, either alone or in combination. This vibration has a wave number of 520 cm^{-1} in the B_{2u} state and is indicated by the symbol *B* in Figure 26*e*. The symbol *A* indicates the location of the band origin; it would result from a transition to a vibrationless excited state from a vibrationless ground state. Since it does not contain the vibration E_{2g}, it is forbidden. Its location can be calculated after a vibrational analysis is made, and this location is indicated by a dotted line. The symbol C is for an A_{1g} vibration of the form

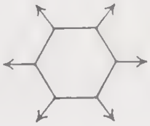

It cannot occur alone but does occur in combination with E_{2g} to give a series of bands A + B, A + B + C, A + B + 2C, etc. Information about the 2000- and 1800-Å bands is meager since they are diffuse and vibrational analysis cannot be made (see Fig. 24). Furthermore, it is probable that N → R transitions are superimposed on the N → V transitions.

The benzene molecular orbitals respond differently to the symmetry operations of the benzene ring—rotation by 60, 120, or 180° or reflection through the various symmetry planes. These properties are of importance in the discussion of the effect of substitution on spectra. In these discussions the convention will be adopted that monosubstitution will always occur at carbon atom A and paradisubstitution at carbon atoms A and D. Of particular interest, then, is the response of the molecular orbitals to reflection through the plane perpendicular to the ring and containing atoms A and D. For the molecular orbitals to describe properly the hexagonal symmetry of benzene, and in particular the fact that benzene is symmetric to reflection through the A–D plane, they must be symmetric or antisymmetric with respect to this reflection. This is necessary because the square of the molecular orbital wave function gives the electron density distribution which must be symmetric to reflection through this plane. This reflection leaves atoms A and D unchanged and interchanges B with F and C with D. It can be seen in Figure 25*a* that π_1, π_3, $\pi_5{}^*$, and $\pi_6{}^*$ are symmetric, and π_2 and $\pi_4{}^*$ are antisymmetric. It can perhaps also be seen that the antisymmetric orbitals cannot contain x_A and x_D since there is no way in which an antisymmetric molecular orbital can be constructed from atomic orbitals which lie in the symmetry plane and which are themselves symmetric with respect to it. These considerations are important in a discussion of the effect of substitution since substitution on carbon atom A and/or D does not (to the molecular orbital approximation) change the energy of the antisymmetric orbitals. There is no interaction because neither π_2 nor π_4 contains x_A or x_D and because the interaction of a substituent with B or with C would cancel, because of difference in sign, against the interaction with E or with F.

2. MONOSUBSTITUTED BENZENES

Basic substitution shifts the benzene absorption at 2600 Å to longer wavelengths and intensifies it (see Fig. 27). Substitution perturbs the benzene ring both by the resonance effect and the inductive effect. The inductive effect, just as in ethylene, is thought to move all levels in the same direction and to approximately the same extent so as to have little effect on the position of the spectrum. For example, the anilinium ion, which carries a positive charge adjacent to the ring and should show an appreciable inductive effect but no

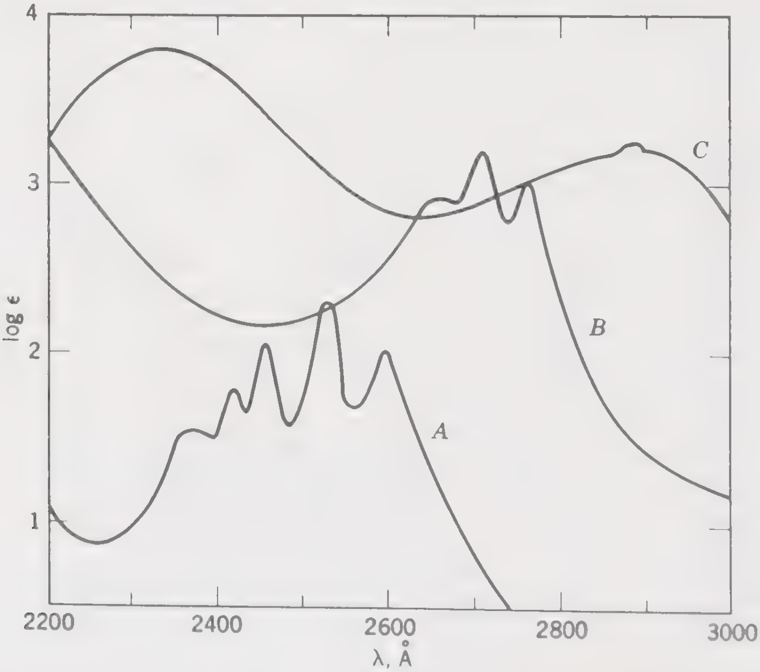

Fig. 27. Spectra of benzene (*A*), phenol (*B*), and aniline (*C*), in isooctane. (After A P I. Spectrogram 39, Shell Development Co., 99, 107, California Research Corp.)

resonance effect, absorbs at almost the same wavelength and with only slightly higher intensity than does benzene. The inductive effect does have an influence on the ionization energy; the positive inductive effect lowers it, and the negative effect increases it.

The resonance effect has a large influence on the spectrum which is describable in terms of molecular orbital theory (46). Calling the substituent S, the secular equation for the x orbitals of a monosubstituted benzene is

$$\begin{vmatrix} H_{\mathrm{SS}}-E & H_{\mathrm{AS}} & 0 & 0 & 0 & 0 & 0 \\ H_{\mathrm{AS}} & H_{\mathrm{AA}}-E & H_{\mathrm{AB}} & 0 & 0 & 0 & H_{\mathrm{AF}} \\ 0 & H_{\mathrm{AB}} & H_{\mathrm{BB}}-E & H_{\mathrm{BC}} & 0 & 0 & 0 \\ 0 & 0 & H_{\mathrm{BC}} & H_{\mathrm{CC}}-E & H_{\mathrm{CD}} & 0 & 0 \\ 0 & 0 & 0 & H_{\mathrm{CD}} & H_{\mathrm{DD}}-E & H_{\mathrm{DE}} & 0 \\ 0 & 0 & 0 & 0 & H_{\mathrm{DE}} & H_{\mathrm{EE}}-E & H_{\mathrm{EF}} \\ 0 & H_{\mathrm{AF}} & 0 & 0 & 0 & H_{\mathrm{EF}} & H_{\mathrm{FF}}-E \end{vmatrix} = 0$$

Two of the orbitals obtained are identical with two of the benzene orbitals π_2 and $\pi_4{}^*$, and possess the same energy, $\alpha + \beta$ and $\alpha - \beta$, respectively. These energy levels are not perturbed by the substituent because a node exists at atom A in each level. The remaining five orbitals, which may be called "symmetrical orbitals," do interact and produce most of the changes associated with substitution on benzene. In obtaining the remaining five levels, it has been assumed that H_{AS} has the same value (β) as do the resonance integrals between adjacent carbon atoms. The quantity H_{SS} may be written as $\alpha + \delta\beta$ (47), where δ is a measure of the difference in electronegativity between the substituent and carbon with respect to x electrons.

In Figure 28 the energy levels are plotted as a function of δ. The ground-state configuration is $\pi_7{}^2\pi_1{}^2\pi_2{}^2\pi_3{}^2$. The frequency of the long wavelength transition is given approximately† by $E_4 - E_3$. It can be seen on inspection that the excitation energy increases with increasing δ approaching that of benzene at large δ. Since δ is a measure of the electronegativity of the substituent with respect to carbon, it should increase as the ionization energy of the substituent increases. The experimental data are summarized in Figure 29. The behavior (48) of —SH is anomalous, as is that of $-\mathrm{SeC_2H_5}$ and $-\mathrm{TeC_2H_5}$ (49). This behavior is probably due to the interaction of d orbitals of the substituent group with the benzene x orbitals. Participation of d orbitals has been shown to contribute to the shift of the 2600-Å band in phenylsilane (50).

---

† Because of the near degeneracy in the excited state and the mixing of levels which occurs when electron repulsion is explicitly included, a more exact expression is $(E_5 - E_2 + E_4 - E_3)/2$.

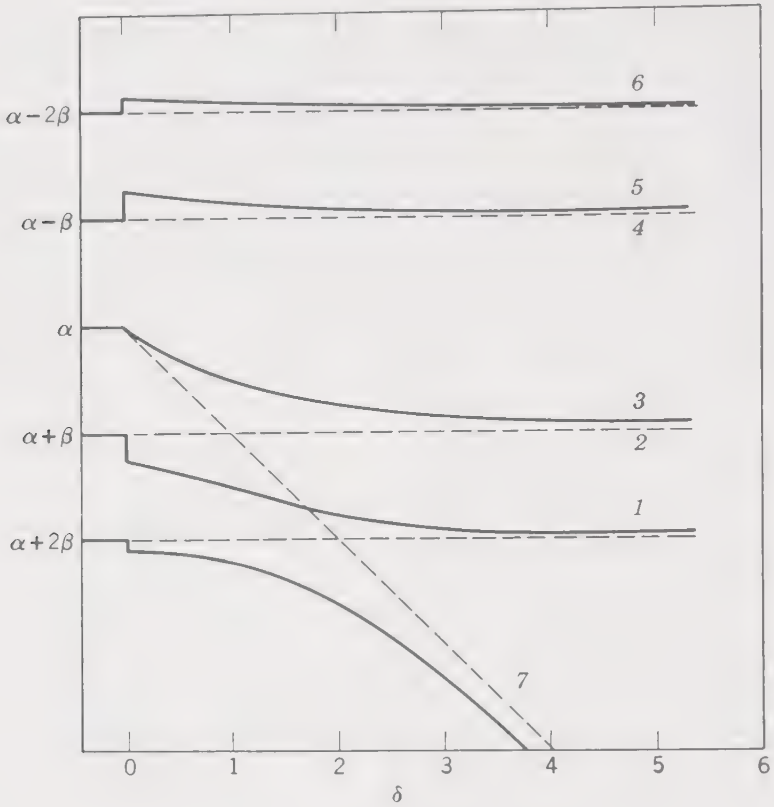

Fig. 28. Energy levels of monosubstituted benzene (46).

The resonance effect (δ small) lowers the ionization energy of the monosubstituted benzene by raising the energy of the highest occupied orbital, π_3. An alternate description is to note that the resonance effect moves negative charge into the ring, thereby lowering the energy required to remove an electron. Experimental evidence for this migration of charge is obtained from the resonance moment (51). Parenthetically, the migrating charge settles at the *ortho* and *para* positions, all basic groups being *ortho-para* directors. Thus, the *ortho para* directing strength of a substituent correlates with the wavelength of absorption.

The $A_{1g} \rightarrow B_{2u}$ transition is forbidden in benzene as a consequence of the hexagonal symmetry of the benzene molecule and in particular of the six π electrons. The migration of charge which accompanies the basic group substitution distorts the hexagonal symmetry and removes some of the forbiddenness from the $A_{1g} \rightarrow B_{2u}$ transition, thereby intensifying the absorption. The greater the migration, the greater the intensification. For example, the phenol spectrum is roughly ten times as intense as the benzene spectrum (52) (see Fig. 27). A strong inductive effect will also intensify the spectrum. For

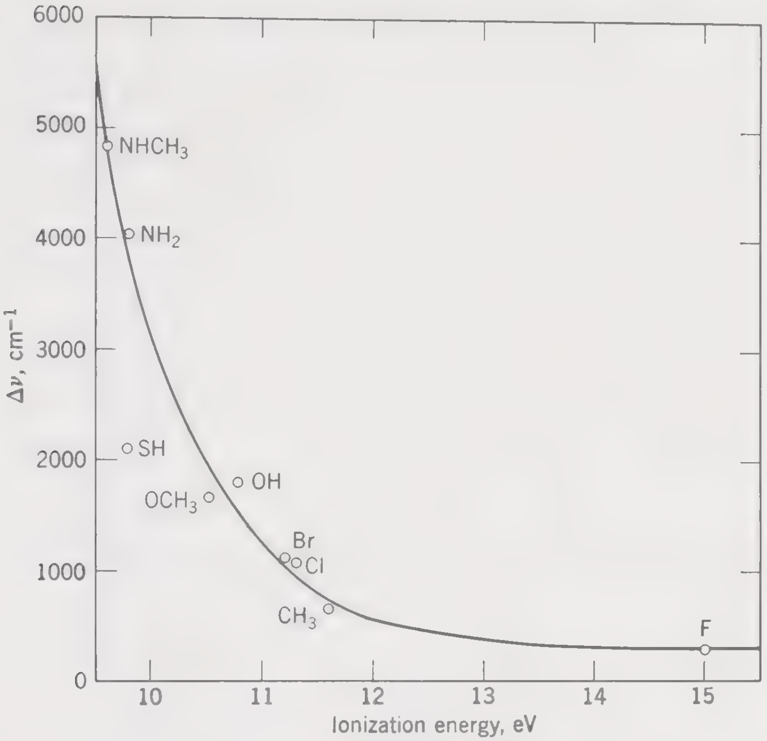

Fig. 29. Wavenumber shift for monosubstitution of benzene plotted against ionization energy of substituent.

example, fluorine, which has a high ionization energy of 12.8 eV in its methyl compound and shifts the spectrum only 605 cm^{-1}, gives three times the intensification of chlorine, which has an ionization energy of 11.3 eV in its methyl compound and shifts the spectrum 1037 cm^{-1} (53) (see Fig. 30).

Accompanying the overall change in intensity, there is a change in the relative intensity of the vibrational bands. The O—O band is missing in the $A_{1g} \rightarrow B_{2u}$ electronic transition of benzene. Further, only those bands occur in the benzene spectrum which contain the E_{2g} vibration. With substitution, the electronic transition is no longer forbidden, so that the O—O and other vibrational bands appear. For substituents which interact strongly with the ring, the new bands may actually be stronger than those containing the E_{2g} vibration (see Fig. 26).

The maximum interaction between substituent and ring is obtained when the π orbitals on the benzene ring and the p orbital on the substituent are parallel. This p orbital is set askew in an *ortho*-substituted dimethylaniline. The wavelength and the intensity of the absorption are decreased relative to dimethylaniline, the spectrum resembling more closely that of benzene itself (54). There is also a corresponding decrease in the resonance moment (55).

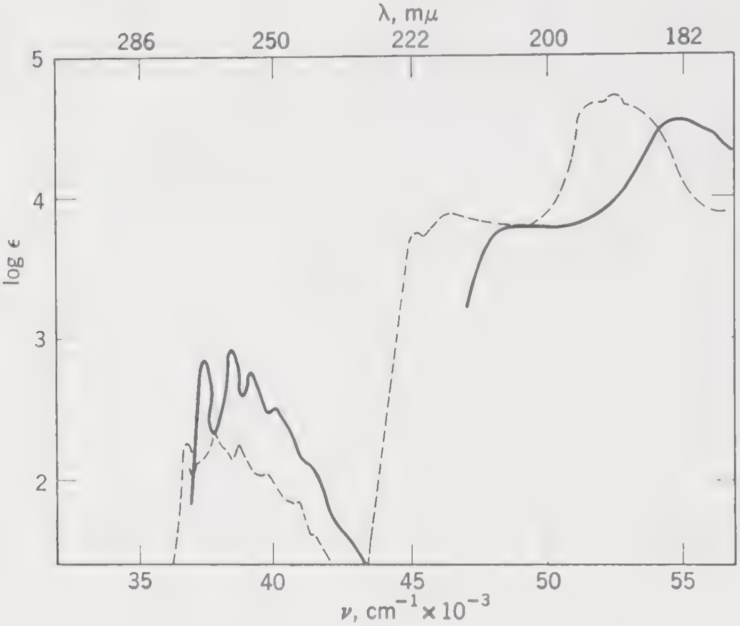

Fig. 30. Spectra of chloro- and fluorobenzene: (– – –) chlorobenzene; (——) fluorobenzene. [After H. B. Klevens and J. R. Platt, Technical Report, Part One, Laboratory of Molecular Structure and Spectra, University of Chicago (1953–54).]

3. ALKYL SUBSTITUTION

Alkyl substitution intensifies and shifts the benzene spectrum toward the red just as does basic group substitution (56). This is additional evidence for hyperconjugation (see Section III-B-3). Of all the alkyl groups, methyl causes the greatest wavelength shift, intensification, and greatest change in the vibrational intensities. The effect decreases progressively as the hydrogens on the methyl group are replaced by alkyl groups (see Fig. 26 and Table XI). This is in contrast to the alkyl substituted ethylenes, where the reverse order of increasing red shift was found.

As the substituent becomes more complex, the spectra become more diffuse. It is thought that the greater complexity gives greater opportunity for the electronic energy of the ring to be converted to vibrational energy in the substituent. This will result in the broadening of the band since the width of an energy state is inversely proportional to the lifetime of the state.

Alkyl substitution reduces the ionization energies of the substituted benzenes in the order methyl, ethyl, *n*-propyl, *t*-butyl (Table XI), i.e., the order of decreasing energy separation between the benzene and virtual ν orbitals on the alkyl groups (pp. 235–237). Thus, it appears that the hyperconjugation effect (γ) does not overcome the effect of decreasing energy separation between benzene and alkyl orbitals.

4. CHLOROALKYL SUBSTITUTION

The series of substituents, CH_3, CH_2CH_3, $CH_2CH_2CH_2Cl$, CH_2CH_2Cl, $CHCl_2$, CH_2Cl, and CCl_3, presents a gradual transition from *ortho–para* direction to *meta* direction, that is, a transition from migration of electrons into the ring to migration of electrons out of the ring. The wavelength shift and intensification with respect to benzene are high at either end of the series and go through a minimum between CH_2CH_2Cl and CH_2Cl (58). The methyl group is considered to carry a virtual x orbital which is coupled to the x orbitals in the benzene ring. There are originally two electrons in this orbital, and the net result of the interaction is that a portion of these migrate into the ring. The trichloromethyl group is thought to possess a similar virtual x orbital on the carbon atom which contains considerably less than two electrons because of the electronegativity of the halogens, so that the net result is migration out of the ring. This effect could be called "negative hyperconjugation." Now migration either into or out of the ring will distort the hexagonal symmetry of the electron density of the original benzene ring and will cause intensification of the spectrum. The observed wavelength shift indicates that the energy level pattern will approximate that for toluene.

5. THE SUBSTITUTION OF UNSATURATED GROUPS

Substitution of unsaturated groups shifts the absorption of the phenyl chromophore toward the red, by the same mechanism as for vinyl substitution on ethylene (see Table XI). The lengthening of the conjugated system narrows the gap between the highest occupied and the lowest unoccupied levels.

The vinyl group shifts the benzene spectrum to about the same extent as does the $-NH_2$ group (see Fig. 31). The effect of the ethynyl group is much less. The y electrons on the ethynyl group do not contribute to the resonance with the benzene ring. They do, however, shorten the $C{\equiv}C$ bond distance in the ethynyl group which makes the resonance integral for the ethynyl electrons larger and reduces the resonance of the ethynyl group with the ring. The cyclopropyl group shows definite unsaturation properties, not only in the shift in the spectrum, but in the intensity and appearance of the spectrum as well (59,60). In the cyclopropyl group the H–C–H angle is forced to be 120°, which is the angle between σ bonds for trigonal hybridization. This would leave an unhybridized p_x orbital on each of the carbon atoms which would then couple with the x orbitals of the benzene ring just as for styrene (61). The cyclopentyl group also exhibits evidences of strain in its spectrum, but to a much smaller extent.

The red shift of the benzene absorption on carbonyl substitution is analogous to that obtained by vinyl substitution. The shift is not as great as in styrene since the orbital on oxygen has a greater electronegativity than

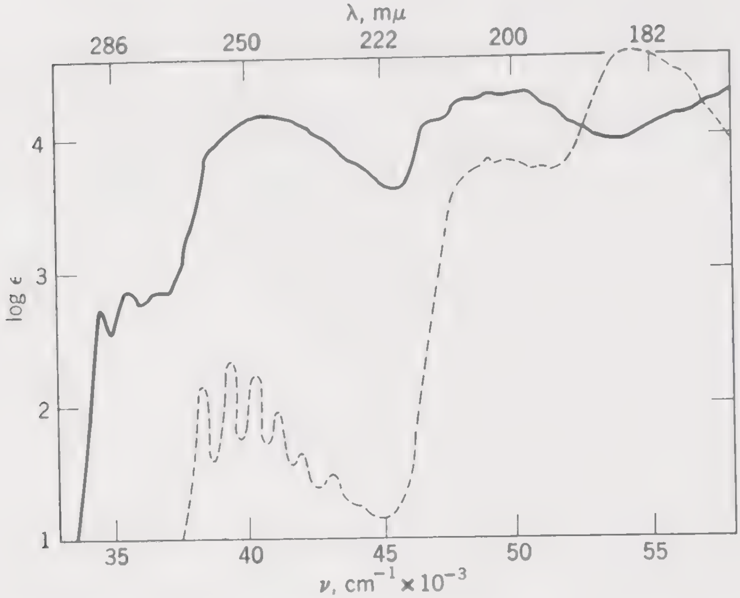

Fig. 31. Spectra of styrene and benzene: (——) styrene; (----) benzene. [After H. B. Klevens and J. R. Platt, Technical Report, Part One, Laboratory of Molecular Structure and Spectra, University of Chicago (1953–54).]

the orbital on carbon, preventing maximum interaction between the carbonyl molecular orbitals and the benzene orbitals.

Substitution of a nitro group on benzene shifts the 2600 Å band by a large amount [λ_{max} = 2880 Å in the vapor (62)], due to its large resonance effect. In addition to the usual bands arising from the benzene and nitro chromophores, there is an additional band observed at 2400 Å (ϵ = 8500) which is attributed to a charge transfer transition between the benzene ring (donor) and the nitro group (acceptor) (62,63) (Fig. 21). Similarly, the aniline spectrum is red shifted so that the 2600-Å maximum of benzene is at 2820 Å (vapor). A charge transfer band is also observed at 2300 Å (ϵ = 8000, vapor) (64), where the amino group is the donor and the benzene ring is the acceptor (63,65) (Fig. 27).

6. POLYSUBSTITUTED BENZENES

In a discussion of polysubstituted benzenes, weakly and strongly interacting substituents must be considered separately. For the weakly resonating substituents the wavelength shift of the 2600 Å band is almost additive, as would be expected from simple perturbation theory (see Section II-G). In contrast, the intensity is vectorially additive. It is proportional to the square of the transition moment **m**, a vector whose direction is that of the electric vector of the light which is absorbed. In the monosubstituted benzenes this

TABLE XI
Wavelength of the O→O Bands and Ionization Energies of Some Substituted Benzenes (56,57,59)

Compound	λ, Å	Ionization energy,[a] eV
Benzene	2624.6	9.25
Toluene	2667.5	8.82
Ethylbenzene	2664.3	8.76
n-Propylbenzene	2665.2	8.72
Isopropylbenzene	2658.7	8.69
n-Butylbenzene	2666.3	8.69
sec-Butylbenzene	2661.0	8.68
tert-Butylbenzene	2655.2	8.68
Cyclohexylbenzene	2659.5	
Cyclopentylbenzene	2670.5	
Cyclopropylbenzene	2712.1	
Phenylacetylene	2748.7	8.82
Styrene	2875.9	8.47

[a] Photoionization values.

direction is parallel to the plane of the ring and perpendicular to the ring-substituent bond. The length of the vector **m** varies with the extent of the resonance interaction of the substituent with the ring. A second substituent adds its vector, $\mathbf{m}_j$, to the vector of the first substituent,* $\mathbf{m}_i$, at an angle equal to that of the angle between the two substituents (66)

$$\Delta\mathbf{I} \propto \mathbf{m}_i^2 + \mathbf{m}_j^2 + \mathbf{m}_i\mathbf{m}_j \ (\textit{ortho, meta})$$
$$\Delta I \propto m_i^2 + m_j^2 + 2m_{ij}m_{ij} \ (\textit{para})$$

where $\Delta\mathbf{I}$ is the change relative to the benzene spectrum. However, the sign of the vector is taken as negative in the B, D, and F positions and positive in the C and E positions, where the carbon atom bearing the first substituent is labeled A, and the other positions in sequence round the ring are indicated by B, C, . . . , F. This change in the sign of the vector comes from the fact that the B_{2u} state has three nodal planes. By convention the transition moment $\mathbf{m}_A$ is taken as positive. Then $\mathbf{m}_B$, $\mathbf{m}_D$, and $\mathbf{m}_F$ are taken as negative; and $\mathbf{m}_C$ and $\mathbf{m}_E$ are taken as positive. Since the intensity is proportional to the square of the transition moment, the relative intensities of the various substituted benzenes with identical substituents may be calculated, with the results given in Table XII. The results agree quite closely with those found experimentally (see Fig. 32). The results for the 1,4 positions (A,D) and for the 1,2,3 positions (F, A, B) are particularly interesting since they could be obtained by no other formulation. They are strong arguments for the assignment of B_{2u} symmetry

---

* The **R** of Section II-A has been replaced by **m** to preserve dimensions.

TABLE XII
Relative Intensities of Substituted Benzenes

Compound	Relative intensity
C_6H_5X	1
1,2-$C_6H_4X_2$	1
1,3-$C_6H_4X_2$	1
1,4-$C_6H_4X_2$	4
1,3,5-$C_6H_3X_3$	0
1,2,3-$C_6H_3X_3$	0
1,2,4-$C_6H_3X_3$	3

to the excited state and for the validity of the quantum mechanical formulation used in this problem. When the substituents are not identical, the vectors are not equal in length but are compounded in the same way. Further, if substituents are not all *ortho–para* or all *meta* directors, the vectors will differ in sign. This follows from the fact that the *ortho–para* directors send charge into the ring, and *meta* directors take charge out of the ring, as was discussed in the section on monosubstituted benzenes.

It has been possible to assign to each group a quantity called the *spectroscopic moment* **m** which has units of (centimeter moles/liter)$^{1/2}$ (67), and from which the increase in the maximum extinction ϵ may be calculated by the vector addition formula given above. In Table XIII are given a few of the assigned spectroscopic moments. These values have also been shown to apply

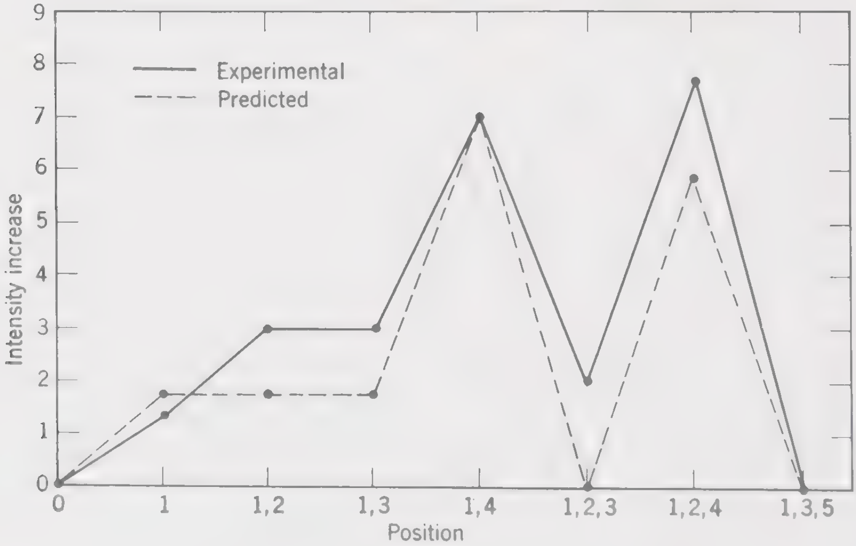

Fig. 32. Intensity of 2600-Å band in chlorobenzenes.

TABLE XIII
Spectroscopic Moments of Substituted Benzenes

Group	Spectroscopic moment, (cm mole/liter)$^{-1/2}$	Group	Spectroscopic moment, (cm mole/liter)$^{-1/2}$
OH	32	*iso*-C_3H_7	6.5
OCH_3	34	*tert*-C_4H_9	5.5
F	20	H	0
CH_3	8	CH_2F	−2
Cl	10	CH_2Cl	−3
C_2H_5	7	NC	−6
Br	10	CHF_2	−11
I	13	SH	27
$CHCl_2$	−11	CN	−18
CF_3	−14	$CHBr_2$	−25
SO_2NH_2	−15	COOH	−27
CCl_3	−17	SO_3H	−42
NH_2	38	CHO	−32
		(N)	−43

to substitution on pyridine and naphthalene. The simple rules for intensification given above do not hold very well for groups which interact very strongly with the ring, e.g., —NH_2 and —NO_2.

Some relatively simple equations for predicting the wavelength shift of the 2600-Å band in di- and trisubstituted benzenes can be derived from perturbation theory (68). The red shift of the absorption maximum relative to the reference maximum of 38,900 cm^{-1} in benzene is given by

$$\Delta\nu = \sum_m l_m + \Big[\sum_m v_m e^{(2\pi i m/3)}\Big]^2$$

TABLE XIV
Equations for Predicting Shifts of 2600-Å Band in Substituted Benzenes

Substitution	Substituent positions m	Formula[a]
Mono	0	$\Delta\nu = l_0 + v_0^2$
Ortho-di-	0,1	$\Delta\nu = l_0 + v_0^2 + l_1 + v_1^2 - v_1v_0 + \tilde{O}$
Meta-di-	0,2	$\Delta\nu = l_0 + v_0^2 + l_2 + v_2^2 - v_0v_2$
Para-di-	0,3	$\Delta\nu = l_0 + v_0^2 + l_3 + v_3^2 + 2v_0v_3$
1,2,4-tri-	0,1,3	$\Delta\nu = l_0 + v_0^2 + l_1 + v_1^2 + l_3 + v_3^2$
		$+ 2v_0v_3 - v_1v_0 - v_1v_3 + \tilde{O}$

[a] $\tilde{O}$ is the *ortho* correction listed in Table XVI.

TABLE XV
l and v Parameters for 2600-Å Band of Substituted Benzenes (69)

Group	l, cm^{-1}	v, (cm^{-1})$^{1/2}$
CH_3	510	8.85
OCH_3	510	31.6
OH	640	31.6
Br	900	3.48
Cl	900	7.27
NH_2	1110	45.5
COOH	1170	−33.2
COO^-	1210	−19.9
CN	1470	−23.1
O^-	2390	40.8
$COCH_3$	3440	−16.4
CHO	3690	−15.5
NO_2	5160	−33.2

where l_m and v_m are parameters characteristic of the particular substituted groups, and the sums are taken over the number of substituents, m (69). The first term in the equation represents the sum of the first-order inductive and second-order resonance contributions to the shifts. The second term is an approximation to the second-order inductive effects which are vector quantities. The exponential expression is a representation of these vector quantities in the complex plane. The particular expressions for the substituted benzenes are listed in Table XIV. Values of l and v for the common substituents are listed in Table XV. These expressions give very good agreement with the observed shifts of the 2600-Å band in the *para*- and *meta*-substituted compounds with a wide range of substituents (70,71), but the *ortho* compounds require an additional correction factor. It appears that the "*ortho*" correction may be due to hydrogen bonding between the substituents and/or steric effects. With the *ortho* corrections the predicted shifts for the 1,2,4-trisubstituted benzenes are also in good agreement with the available data. These corrections are listed in Table XVI. It is interesting to note that electron withdrawing groups have negative values of v, and electron-releasing groups have positive values.

7. THE EFFECT OF SUBSTITUTION ON THE 2000-Å BAND OF BENZENE

Substitution affects the 2000-Å band in much the same way as it does the 2600-Å band. For example, the ratio of the wavelengths of the two bands is approximately 1.25 for most monosubstituted benzenes (70).

For polysubstituted benzenes perturbation equations similar to those

TABLE XVI
Ortho Corrections for 2600-Å Band of Substituted Benzenes[a] (69)

Group A	Group B	$\tilde{O}$, cm^{-1}
CH_3	CH_3	−290
CH_3	NH_2	−400
CH_3	CN	70
CH_3	NO_2	980
OH	OH	260
OH	O^-	590
OH	COOH	730
OH	COO^-	1060
OH	CHO	990
OH	OCH_3	320
OH	NO_2	1540
OH	$COCH_3$	1610
NH_2	NH_2	0
NH_2	COOH	1670
NH_2	COO^-	1070
NH_2	NO_2	3660
Cl	Cl	−50
Cl	COOH	−370
Cl	COO^-	−530
Cl	$COCH_3$	−850
Cl	CHO	680
Cl	NO_2	−290
OCH_3	OCH_3	370
OCH_3	COOH	0
OCH_3	COO^-	−1000
OCH_3	NO_2	710
COOH	COOH	−770
COO^-	COO^-	−600
COO^-	O^-	−630
O^-	$COCH_3$	810
O^-	CHO	1480
O^-	NO_2	1470

[a] Add to equations in Table XIV.

mentioned previously may be used to predict the wavelength shift of the 2000-Å band (69). For the 2000-Å band the second-order inductive effect is small, but the second-order resonance effect is larger than for the 2600-Å band. The expression used to compute the shifts of the 2000-Å band is

$$\Delta\nu = K\Big(\sum_{m} I'_m\Big) + (x_0 - x_3)^2$$

where the I' parameters are similar to the I's of the previous expression but not the same because of the larger second-order resonance effect and neglect of the vector terms representing the second-order inductive effect. K is a parameter depending only on the number of substituents. The second term is only required when substituents are *para* to one another. There appears to be a contribution to the shift of the 2000-Å band caused by mixing with a charge transfer state having a quinoid type structure (63,65)

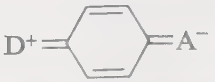

and the second-term corrects for this interaction in the *para*-substituted compounds. The various parameters are listed in Table XVII.

TABLE XVII
Parameters for Shift of 2000-Å Band of Substituted Benzenes (69)

Group	I', $(\mathrm{cm}^{-1})^{1/2}$	x, cm^{-1}	Group	I', cm^{-1}	x, $(\mathrm{cm}^{-1})^{1/2}$
O^-	6580	51.2	COO^-	4490	−25.9
NH_2	5650	44.9	CN	4490	−27.8
OCH_3	3050	25.3	COOH	5650	−32.6
OH	1630	21.5	CHO	9050	−35.1
Br	1510	20.2	$COCH_3$	8350	−35.7
Cl	1400	6.32	NO_2	11890	−47.4
CH_3	710	3.80			

Number of substituents	K
1	1.00
2	0.81
3	0.72

8. PARABENZOQUINONE

p-Benzoquinone is one of the simplest colored compounds. Because of this, the quinoid structure

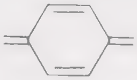

assumed great importance in the early development of color theory. The compound has additional interest because its properties appear to classify it somewhere between an α,β-unsaturated ketone and a disubstituted benzene. *p*-Benzoquinone has a high-intensity band near 2450 Å, a medium-intensity band near 2850 Å, and a broad, low-intensity band near 4450 Å (72,73) (see Fig. 33). There are eight atomic π orbitals in this system from which eight

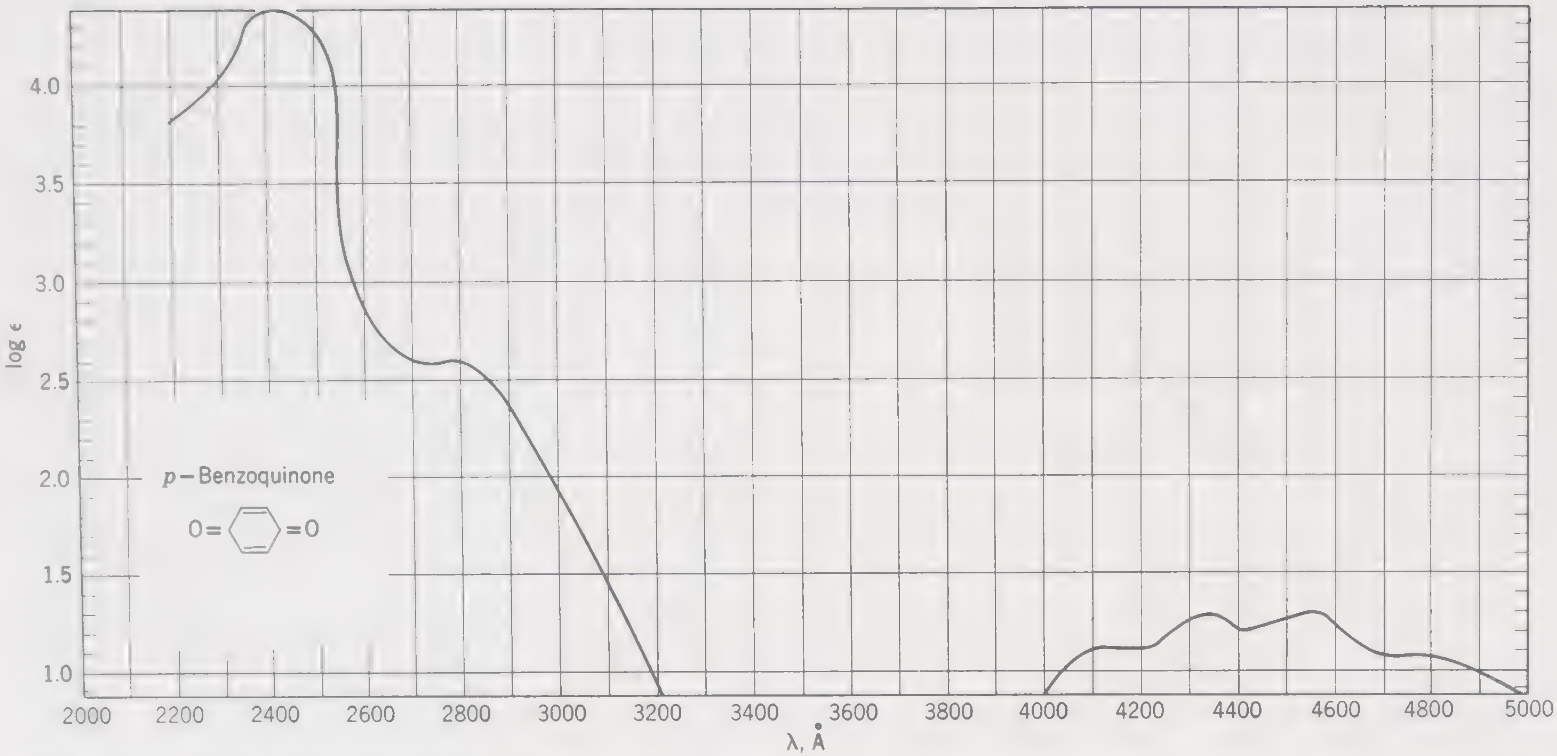

Fig. 33. Spectrum of *p*-benzoquinone in hexane. (After R. A. Friedel and M. Orchin, *Ultraviolet Spectra of Aromatic Compounds*, Wiley, New York, 1951.)

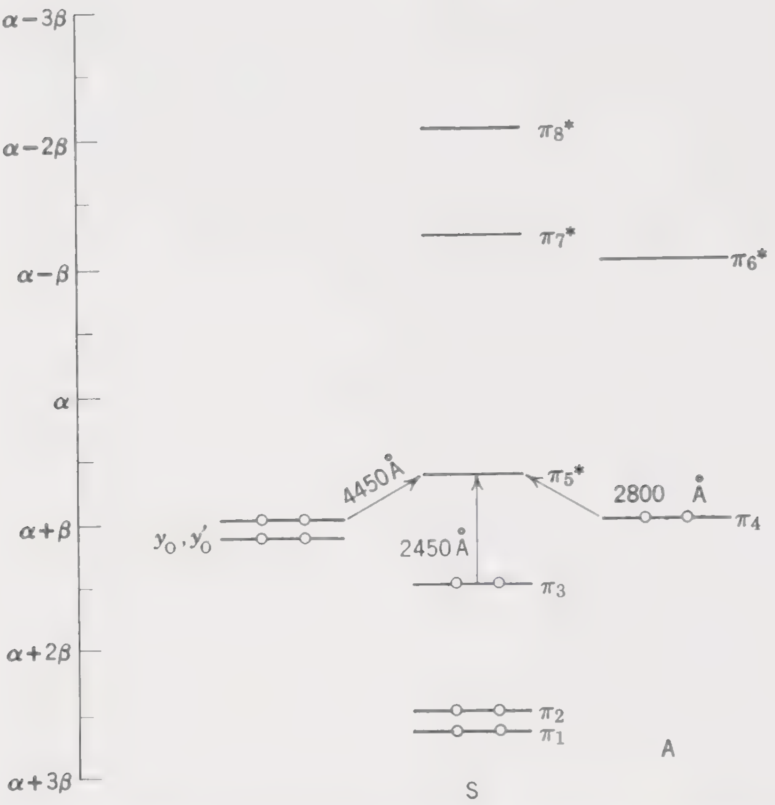

Fig. 34. Energy levels of *p*-benzoquinone: S and A denote molecular orbitals which are symmetrical or antisymmetrical to reflection in the plane through the oxygen atoms and perpendicular to the plane of the ring.

molecular orbitals are formed. Two of these are identical with the π_2 and π_4* molecular orbitals of benzene and have the same energies, $\alpha + \beta$ and $\alpha - \beta$ respectively. The *p*-benzoquinone energy levels given in Figure 34 are calculated† on the assumption that the coulomb integral on oxygen is $\alpha + 2\beta$ and that $\beta_{CO} = \beta_{CC}$ (72,74). Because of the large distance between the two y_0 orbitals, their interaction should be small, and the levels should be degenerate. Configuration interaction may well change the order of some of the levels, but the picture presented is probably correct in its main features (75).

The 4450-Å band which gives *p*-benzoquinone its color is assigned to the $n \rightarrow \pi^*$ transitions, $y_0, y'_0 \rightarrow \pi_5^*$. This band shows the solvent shifts and intensity characteristic of $n \rightarrow \pi^*$ bands (76). The 2450-Å band is assigned to the transition, $\pi_3 \rightarrow \pi_5^*$. The 2800-Å band is assigned to the $\pi_4 \rightarrow \pi_6^*$

---

† The bond orders calculated from molecular orbital theory are: for the O—C bond, 1.80; for the C_1—C_2 bond, 1.34; and for the C_2—C_3 bond, 1.89. These indicate the lack of aromaticity in *p*-benzoquinone (74).

transition. Effects of substituents upon the $\pi \rightarrow \pi^*$ bands may be predicted by perturbation formulas similar to those used for substituted benzenes (75). It is of interest to note that the $n \rightarrow \pi^*$ transition which gives *p*-benzoquinone its color is not the type of transition which gives dyes their intense color. The association of the quinoid structure with color which was made in the early days of the color theory, and which appeared to be sound, apparently was made on an erroneous basis.

F. Condensed-Ring Aromatic Hydrocarbons (77–79)

The polycyclic aromatic hydrocarbons are conveniently divided into two groups for discussion of their spectral properties: the "acenes" and the "phenes." The acenes are linearly condensed systems, the first member of which is naphthalene. The phenes contain an angular or bent system of condensed rings. The first member of this series is phenanthrene. Both the acenes and the phenes belong to the cata-condensed classification, i.e., their empirical formulas are $C_{4n+2}H_{2n+4}$, where n is the number of rings and all of the carbon atoms in the compounds lie on the periphery of the condensed systems.

The absorption spectra of the condensed aromatics normally consist of at least three distinct band systems (see Fig. 35). The intensity of each system increases as its spectral location approaches shorter wavelengths. In a very systematic study of the spectra of these compounds an empirical nomenclature was established for correlating the band systems from one compound to another (77). The strong band lying at shortest wavelength is called the β band, the weaker intermediate wavelength band is called the *para* band, and the very weak band usually lying at longest wavelength is called the α band. This wavelength order is preserved in nearly all of the condensed aromatics; however, in naphthacene and pentacene the α band is located between the β and *para* bands. In the spectra of anthracene and tetracene the weak α band is not easily observed. Another very intense band, β', is found at wavelengths shorter than that of the β band in some of the larger compounds.

The α and β bands appear to be related to one another. In fact the ratio of the wavenumbers of the two bands (ν_β/ν_α) is almost constant at 1.35 in all of the compounds. Both the α and β bands shift moderately to the red upon increased condensation in both the acene and phene series. However in the acenes the *para* band shifts very rapidly to the red upon further annelation. In the phene series the wavelength shift of the *para* band parallels those of the α and β bands (see Fig. 36).

A discussion of the spectra of the benzenoid hydrocarbons may be based upon the simple molecular orbital theory (78). In all aromatic hydrocarbons containing only even membered rings (alternant hydrocarbons) the energy

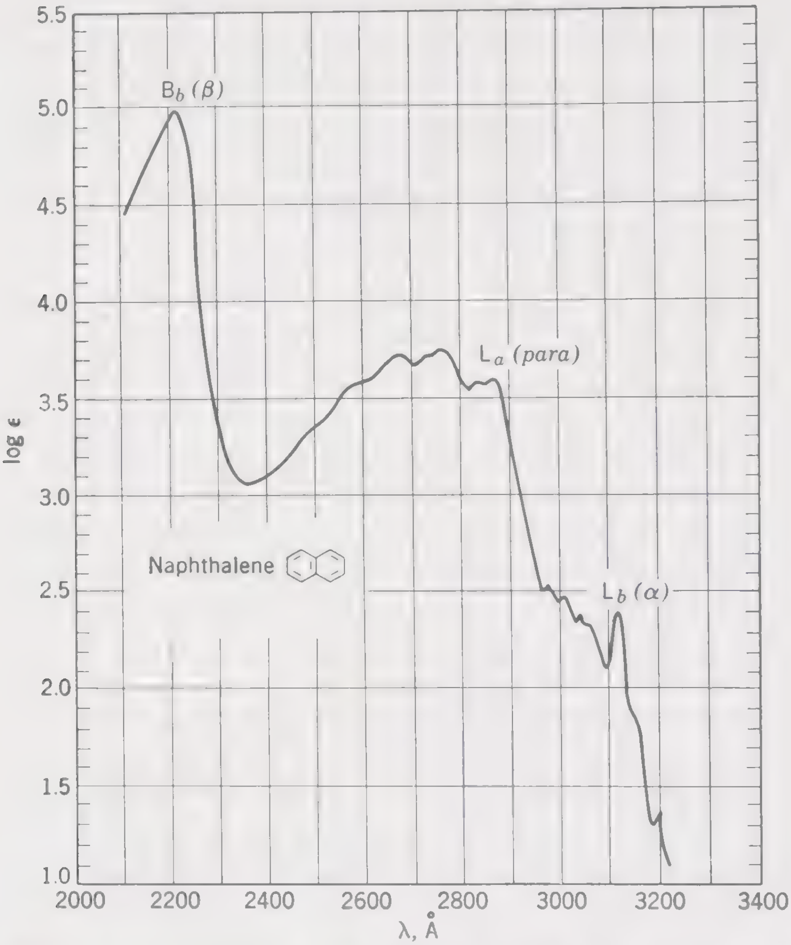

Fig. 35. Spectrum of naphthalene in 95% ethanol. (After R. A. Friedel and M. Orchin, *Ultraviolet Spectra of Aromatic Compounds*, Wiley, New York, 1951.)

levels occur in pairs with energies equally spaced about α, $E_i = \alpha \pm m_i\beta$. The four lowest energy transitions involve excitations from the two highest filled molecular orbitals, Ψ_1 and Ψ_2, to the two lowest-energy unfilled molecular orbitals, Ψ_3^* and Ψ_4^*. The energies of these orbitals are

$$\begin{aligned} \Psi_1: &\quad \alpha + m_1\beta \\ \Psi_2: &\quad \alpha + m_2\beta \\ \Psi_3^*: &\quad \alpha - m_2\beta \\ \Psi_4^*: &\quad \alpha - m_1\beta \end{aligned}$$

where $m_1 > m_2$ and m_1 and $m_2 > 0$. The excitation energies for the transitions $\Psi_1 \rightarrow \Psi_3^*$, $\Psi_1 \rightarrow \Psi_4^*$, $\Psi_2 \rightarrow \Psi_3^*$, and $\Psi_2 \rightarrow \Psi_4^*$ are then $-(m_1 + m_2)\beta$, $-2m_1\beta$, $-2m_2\beta$, and $-(m_1 + m_2)\beta$, respectively. The excited configurations

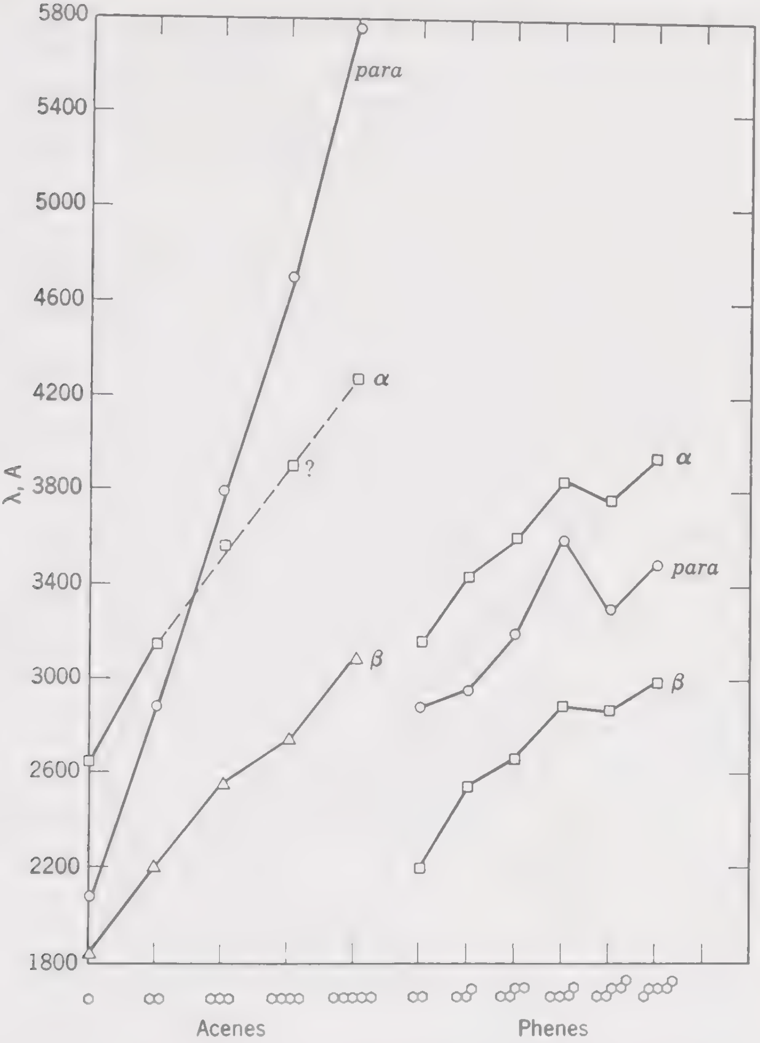

Fig. 36. α, β, and *para* bands of condensed aromatic hydrocarbons.

$\Psi_1^{\,1}\Psi_2^{\,2}\Psi^*_3{}^1$ and $\Psi_1^{\,2}\Psi_2^{\,1}\Psi^*_4{}^1$ have the same energy in this simple approximation. Inclusion of electron repulsion removes this degeneracy and produces two new states, $\Psi^+ = 1/\sqrt{2}(\Psi_1^{\,2}\Psi_2^{\,1}\Psi_4^{\,1} + \Psi_1^{\,1}\Psi_2^{\,2}\Psi_3^{\,1})$, and $\Psi^- = 1/\sqrt{2}(\Psi_1^{\,2}\Psi_2^{\,1}\Psi_4^{\,1} - \Psi_1^{\,1}\Psi_2^{\,2}\Psi_3^{\,1})$, with energies of $-(m_1 + m_2)\beta + C$ and $-(m_1 + m_2)\beta - C$, respectively. In some cases the magnitude of C, which is usually positive, may be large enough to place the Ψ^- state below the $\Psi_1^{\,2}\Psi_2^{\,1}\Psi^*_3{}^1$ state. Because of the pairing properties of the alternant hydrocarbons, the transition moments associated with excitation to the degenerate $\Psi_1^{\,2}\Psi_2^{\,1}\Psi^*_4{}^1$ or $\Psi_1^{\,1}\Psi_2^{\,2}\Psi^*_3{}^1$ states are equal. Thus in the excitation to the Ψ^+ state the transition moments add producing a strongly allowed transition, while the excitation to the Ψ^- state produces a weak transition because of the cancellation of the two oppositely directed transition moments. The excitations $\Psi'_1 \to \Psi'_4{}^*$ and $\Psi'_2 \to \Psi'_3{}^*$ produce moderately intense transitions. Thus, the transitions to the Ψ'^+ and Ψ'^- states are identified with the strong β and weak α bands, respectively. The transitions $\Psi'_2 \to \Psi'_3{}^*$ and $\Psi'_1 \to \Psi'_4{}^*$ are identified with the moderately strong *para* and β' bands.

Although molecular orbital theory may be used to interpret the absorption spectra of the condensed hydrocarbons, we will use a classification based upon a free electron model (79) in the following discussion since correlation of the spectra of different compounds is very simple in this model.

In this free-election model the π electrons are assumed to be confined to the periphery of the molecule which is distorted into a circle. The potential energy is assumed to be constant along this circular perimeter. The energy levels of this model are given by

$$E = q^2h^2/2ml^2$$

where h is Planck's constant, m is the mass of the electron, l is the perimeter length, and q is an integral quantum number measuring angular momentum and having values 0, 1, 2, ... Since electrons may travel either clockwise or counterclockwise around the periphery, all of the energy levels are doubly degenerate except for the one corresponding to $q = 0$.

The highest filled level of the hydrocarbon is denoted as f, and lower filled levels as e, d, c, etc. The lowest unfilled energy level is called a g level with higher energy ones denoted as h, i, j, etc. The lowest energy one electron transition is then denoted as the $f \to g$ transition. Because of the degeneracy of both the f and g levels, the excited electronic configuration f^3g results in four excited states, $B_{a,b}$ and $L_{a,b}$. The B and L component states are degenerate in the free electron model. The nondegenerate ground state is called A. The transitions $A \to B_{a,b}$ are allowed in both the acenes and the phenes, and the transition moment is polarized perpendicular (B_a) or parallel (B_b) to the long axis of the molecule. The $A \to L_{a,b}$ transitions are forbidden and therefore relatively weak in all compounds. The L_a and L_b bands are short- and long-axis polarized, respectively, in the acenes, but these directions are reversed in the phenes. Other low-energy states arise from the excited electronic configuration f^3h, yielding excited states, $C_{a,b}$. The excited configuration e^3f^4g likewise yields other $C_{a,b}$ excited states. The transitions $A \to C_{a,b}$ are allowed in phenes without a center of symmetry, but are forbidden in all acenes. The $A \to C_{a,b}$ transition moments in the phenes are parallel (C_a) or perpendicular (C_b) to the long axis of the compounds. Although the L, C, and B states are each doubly degenerate in the free electron model, they usually have different energies in the actual molecules because of the cross-links and the presence of the carbon nuclei. Benzene is an exception to this.

Due to its high symmetry the B_a and B_b states are degenerate. The absorption spectrum of benzene is classified as follows in the above notation:

$$
\begin{aligned}
2600\ \text{Å}&: \quad A \rightarrow L_b \\
2100\ \text{Å}&: \quad A \rightarrow L_a \\
1850\ \text{Å}&: \quad A \rightarrow B_{a,b}
\end{aligned}
$$

1. NAPHTHALENE (80–83)

Naphthalene has band systems at 3120, 2860, 2210, 1900, and 1690 Å (see Figs. 35 and 37). Using the free electron classification, they are assigned to transitions to the L_b, L_a, B_b, C_b, and B_a states. The orientation of the transition moment may be experimentally determined by using polarized light and suitably oriented crystals. Experiments on naphthalene single crystals do not yield unambiguous results due to resonance interactions between the molecules in the crystal. However, this interaction is diminished in solid solutions of naphthalene in durene, and the spectra show that the two longest wavelength bands have long- (L_b) and short-axis (B_b) polarization, respectively. The 2210-Å band is long-axis polarized (B_b).

The effects of substitution may also help in deciding the polarization of a transition in these compounds. A substituent which exerts a resonance effect will extend the conjugated system of the original compound. Thus a substituent at position 1 which increases the conjugative system of naphthalene in the short-axis direction will primarily affect the bands which are polarized

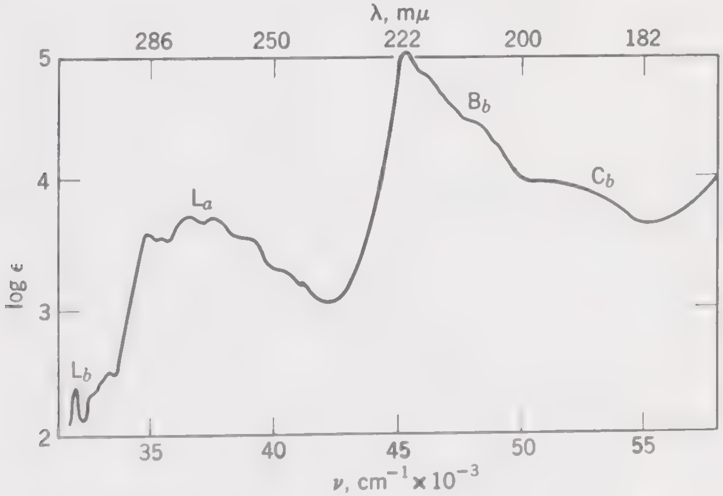

Fig. 37. Naphthalene spectrum. [After H. B. Klevens and J. R. Platt, Technical Report, Part One. Laboratory of Molecular Structure and Spectra, University of Chicago (1953–54).]

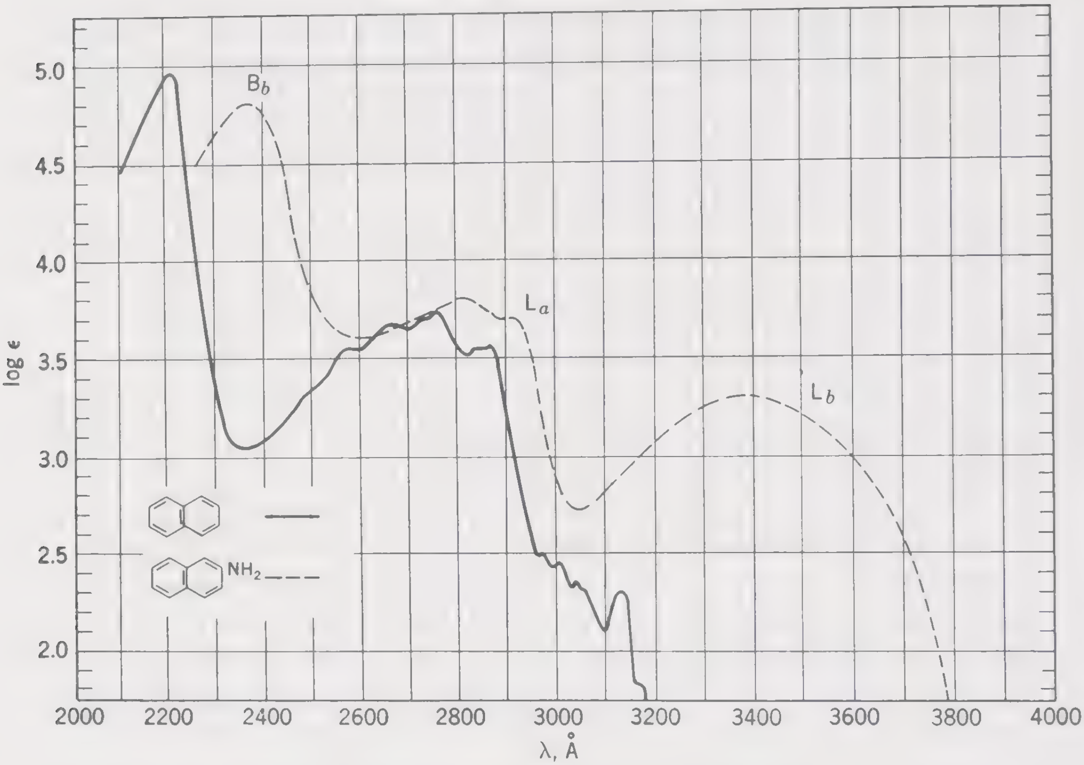

Fig. 38. Spectra of naphthalene (——) and 2-naphthylamine (– – – –). (After R. A. Friedel and M. Orchin, *Ultraviolet Spectra of Aromatic Compounds*, Wiley, New York, 1951.)

in that direction. Substitution at position 2 will affect the long axis-polarized transitions to the greatest extent.

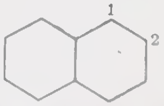

In the spectrum of 2-aminonaphthalene the bands at 3120 and 2210 Å are red shifted, while the band at 2860 Å is almost unaffected (Fig. 38). Similar behavior is also shown by other substituted amino and methyl naphthalenes. These results agree with long axis polarization for the 3120- (L_b) and 2210-Å (B_b) bands and short axis polarization for the 2860- Å (L_a) band. In general the effects of substitution with resonating groups result in a red shift and/or intensification of the bands which are polarized in the directions of extended conjugation.

2. ANTHRACENE (80,84–86)

The absorption spectrum of anthracene is considerably red shifted compared to that of naphthalene (see Fig. 39). The weak L_b band is not clearly

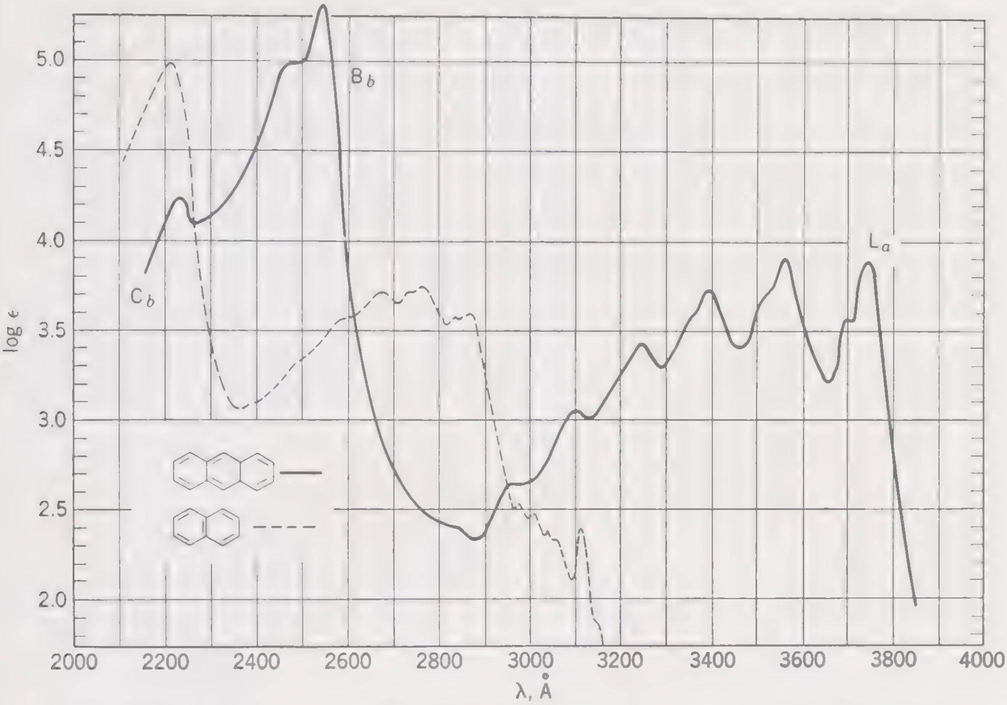

Fig. 39. Spectra of anthracene (——) and naphthalene (----). (After R. A. Friedel and M. Orchin, *Ultraviolet Spectra of Aromatic Compounds*, Wiley, New York, 1951.)

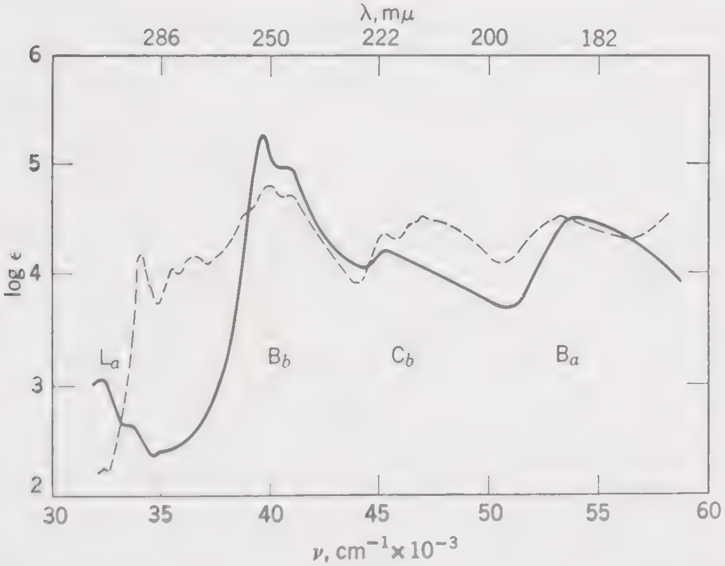

Fig. 40. Spectra of anthracene (——) and phenanthrene (——). [After H. B. Klevens and J. R. Platt, Technical Report, Part One, Laboratory of Molecular Structure and Spectra, University of Chicago (1953–54).]

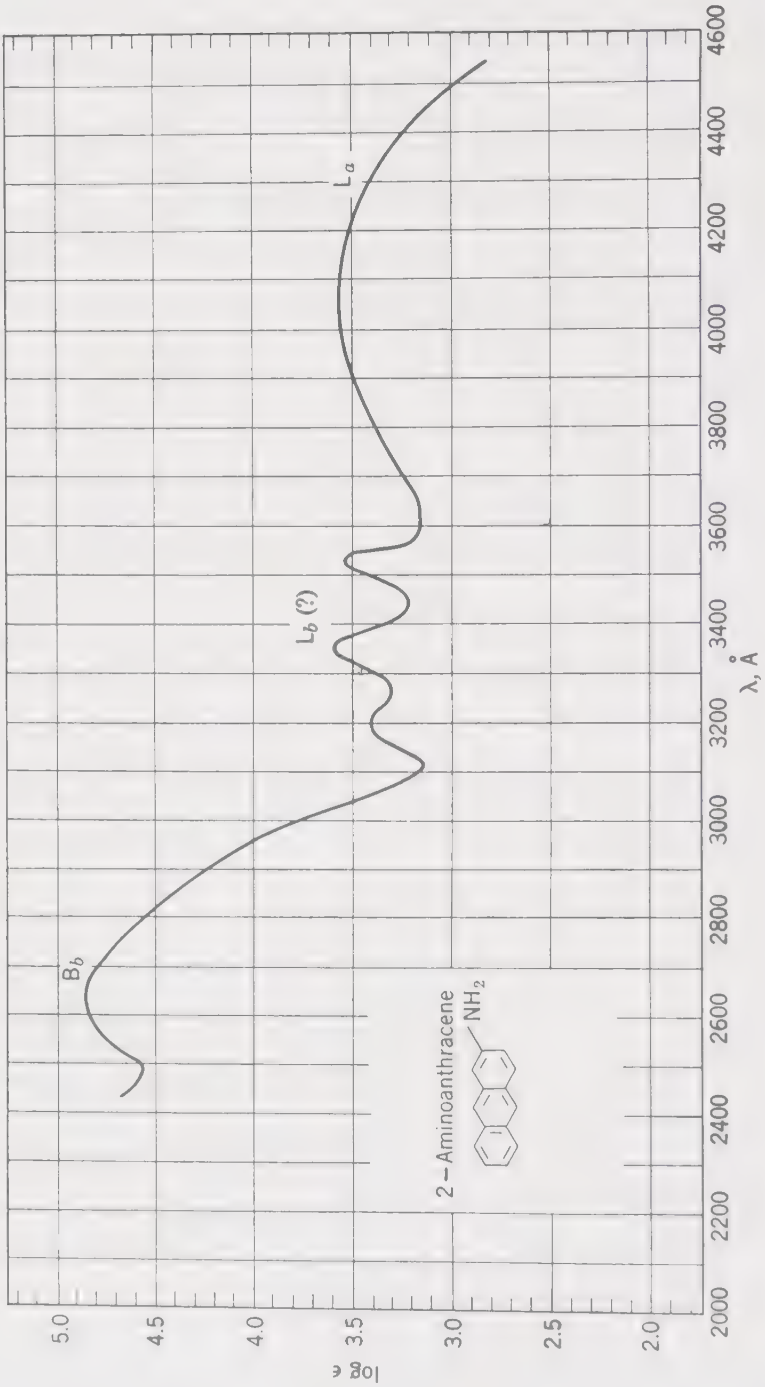

Fig. 41. Spectrum of 2-aminoanthracene in ethanol. (After R. A. Friedel and M. Orchin, *Ultraviolet Spectra of Aromatic Compounds*, Wiley, New York, 1951.)

visible and probably lies under the L_a band which begins at 3780 Å.* The very strong band (ϵ = 180,000) at 2540 Å is assigned to the B_b band. Other strong bands near 2200 and 1860 Å are assigned to the C_b and B_a transitions (Fig. 40). Since anthracene has a center of symmetry, the C_b band should be forbidden; however, its intensity (ϵ = 15,000) is high for a forbidden band. Crystal polarization spectra show that the bands at 3780 and 2450 Å are short and long axis polarized, respectively.

The effects of substitution on the anthracene bands substantiate the polarizations of the L_a and B_b bands. Substitution of methyl groups produces small red shifts of both the L_a and B_b bands. The effect of amino groups is much greater, producing small red shifts of the B_b band but very large red shifts of the L_a band. Another band system begins to become distinct in the spectrum of the 2- and 9-amino anthracene compounds. It occurs at about 3100–3600 Å in 2-aminoanthracene (Fig. 41). From its behavior upon substitution it appears to be long axis polarized, and therefore it may be the L_b band which is masked in the parent compound. The 9- or 10-phenylanthracenes have spectra which are very similar to the respective alkyl-substituted compounds (Fig. 42). Evidently, the phenyl groups are prevented from

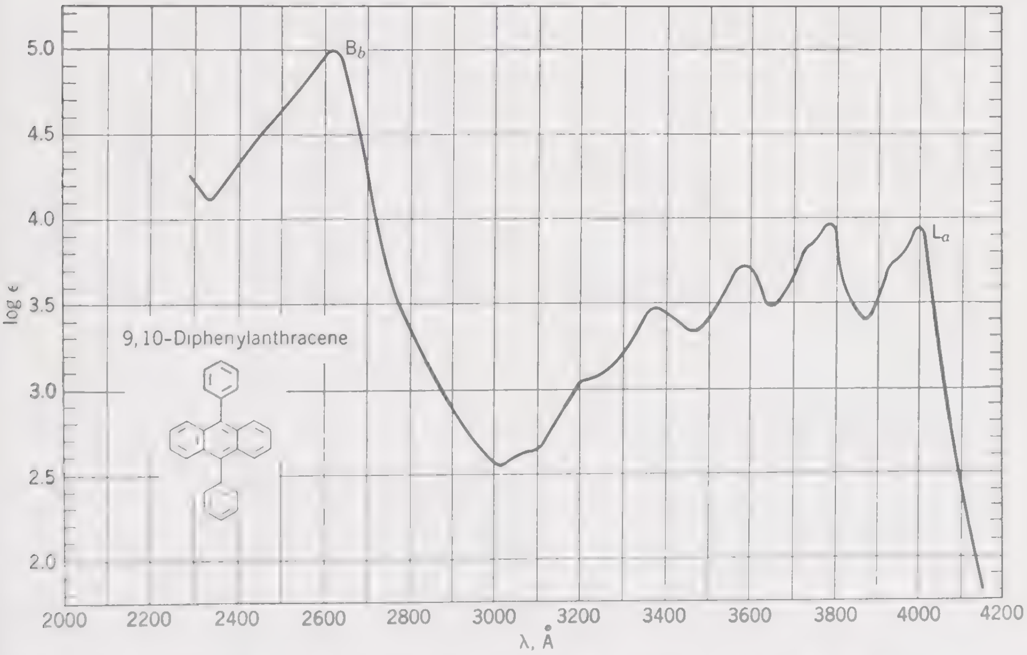

Fig. 42. Spectrum of 9,10-diphenylanthracene in ethanol. (After R. A. Friedel and M. Orchin. *Ultraviolet Spectra of Aromatic Compounds*, Wiley, New York, 1951.)

---

* Studies of the absorption of plane polarized light by anthracene placed in a magnetic field indicate the L_b band lies near 3570 Å. See ref. 85.

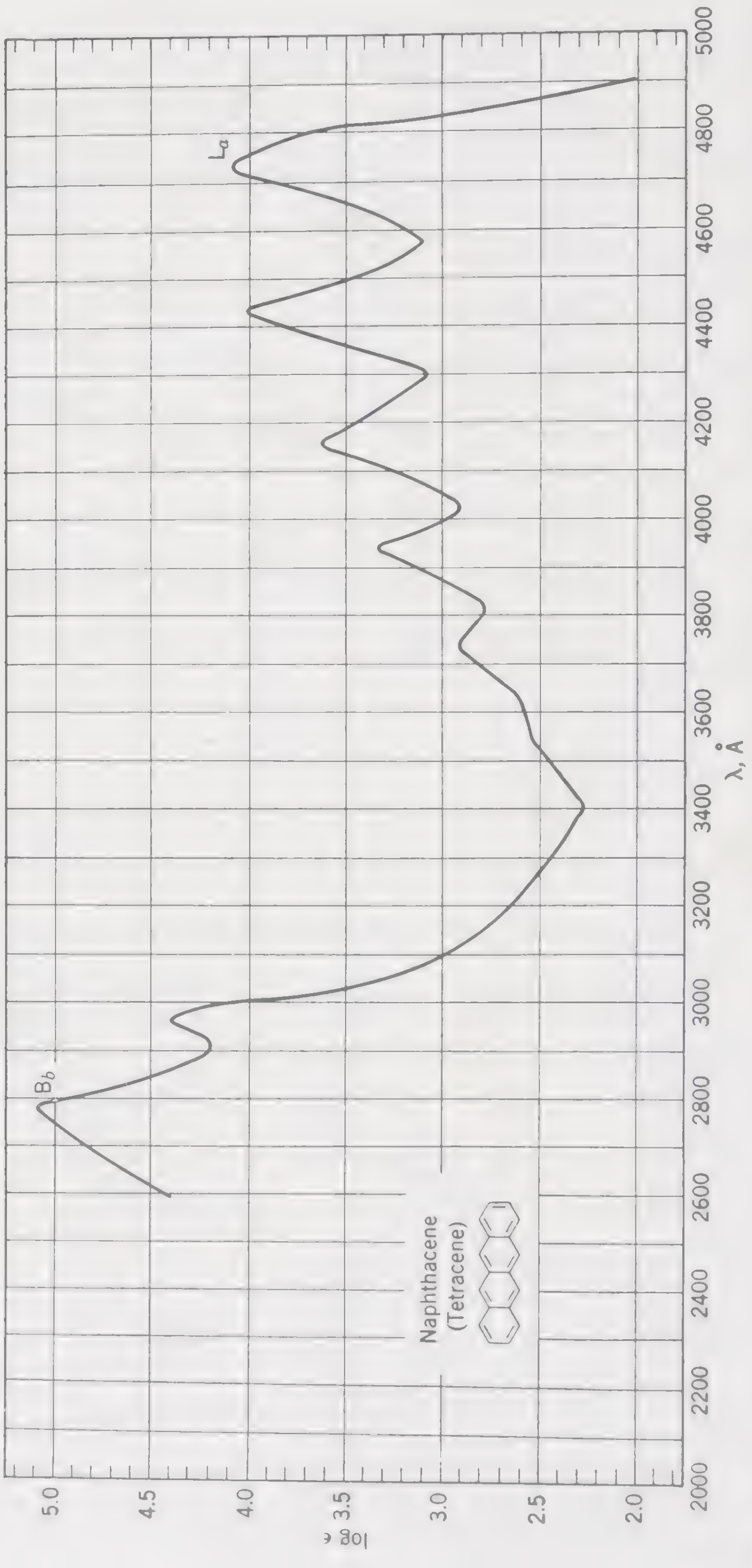

Fig. 43. Spectrum of naphthacene in benzene. (After R. A. Friedel and M. Orchin, *Ultraviolet Spectra of Aromatic Compounds*, Wiley, New York, 1951.)

achieving strong resonance with the anthracene ring by steric interference of the 1,8- or 4,5-hydrogens on the anthracene ring and the 2′- and 6′-hydrogens on the phenyl group.

3. NAPHTHACENE AND HIGHER ACENES (80,87,88)

The absorption band systems of naphthacene occur at 4700 (L_a), 2740 (B_b), 2290 (C_b), 2100 (B_a), 1870 (C_a?), and 1800 Å (?) (Fig. 43). Another band system is reported near 2930 Å which may be the L_b transition. However, its location is at much shorter wavelengths than would be expected from the location of the L_b bands in the other acenes. From Figure 36 the L_b band should be near 3900 Å. Polarized crystal spectra show that the reported bands are polarized in the short- (L_a), long- or short- (L_b?), long- (B_b), and short-axis (C_b) directions.

The absorption spectrum of pentacene is considerably red shifted compared to naphthacene. The L_b band, which was difficult to locate in anthracene and naphthacene, is now visible at 4170 Å due to the large red shift of the L_a band which begins at 5800 Å. The very intense (ϵ = 300,000) B_b band occurs at 3100 Å. Only the position of the long wavelength L_a band at 6930 Å of hexacene is known because of the low solubility and high reactivity of this highly condensed compound in most solvents.

4. PHENANTHRENE AND OTHER PHENES (82,87)

The spectrum of phenanthrene is much like that of its acene isomer anthracene except that the bands are less intense (see Fig. 40). The most intense band, B_b, which is long axis polarized, is much weaker than in anthracene due to the reduction of the length of the conjugative system in the long axis direction by the "bent" ring. The band systems occur at 3530 (L_b), 3030 (L_a), 2540 (B_b), 2120 (C_b), 1870 (B_a), and 1770 (C_a) (Figs. 40 and 44). The L_b band, which was hidden under the L_a band in anthracene, is clearly shown in the phenanthrene spectrum. The C_b band is forbidden in compounds with a center of symmetry; however, phenanthrene does not have a center of symmetry, and accordingly the intensity of the C_b band is double that in anthracene. The spectra of the other phenes—1,2-benzanthracene, chrysene, and 3,4-benzphenanthrene—are similar to that of phenanthrene.

5. IONIZATION ENERGIES AND ELECTRON AFFINITIES (89,90)

The simple molecular orbital theory states that the energy levels of the acenes, phenes, and other condensed aromatic hydrocarbons containing only even membered rings (even alternant compounds) occur in bonding and antibonding pairs, $\alpha + m_i\beta$ and $\alpha - m_i\beta$. The ionization energy of the compound is identified with the energy of the highest filled molecular orbital, $(\alpha + m_i\beta)$.

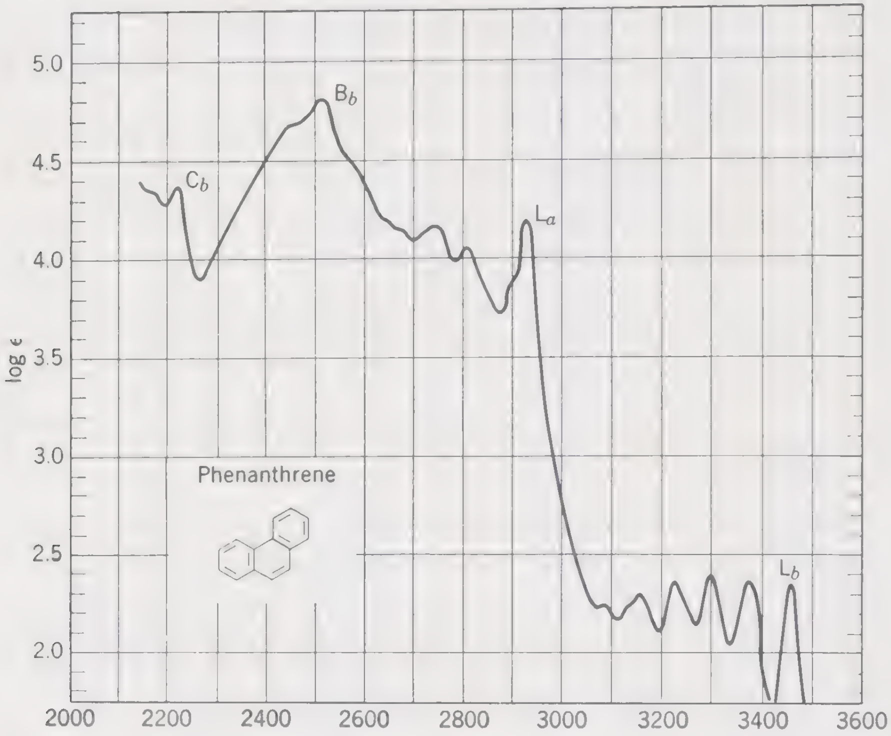

Fig. 44. Spectrum of phenanthrene in cyclohexane. (After R. A. Friedel and M. Orchin, *Ultraviolet Spectra of Aromatic Compounds*, Wiley, New York, 1951.)

and the electron affinity with the energy of the lowest empty molecular orbital, $\alpha - m\beta$. Since the long-wavelength absorption band in these compounds can be associated with the difference in energy of the $\alpha - m\beta$ and $\alpha + m\beta$ levels, $-2m\beta$; a linear relationship between the band position and the ionization potentials or electron affinities of these compounds should result (see Fig. 45). Such correlations are found to hold (see Fig. 46) and are useful for prediction of ionization energies and electron affinities of the aromatic compounds (89,90).

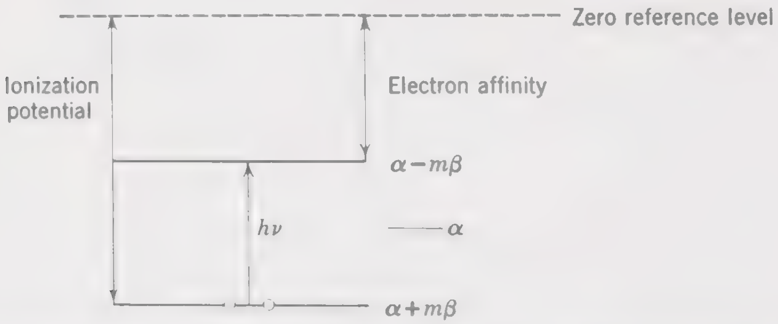
Zero reference level
Ionization potential
Electron affinity
$\alpha - m\beta$
$h\nu$
α
$\alpha + m\beta$

Fig. 45. Relationship between ionization potential, electron affinity, and long-wavelength absorption in alternate aromatic hydrocarbons.

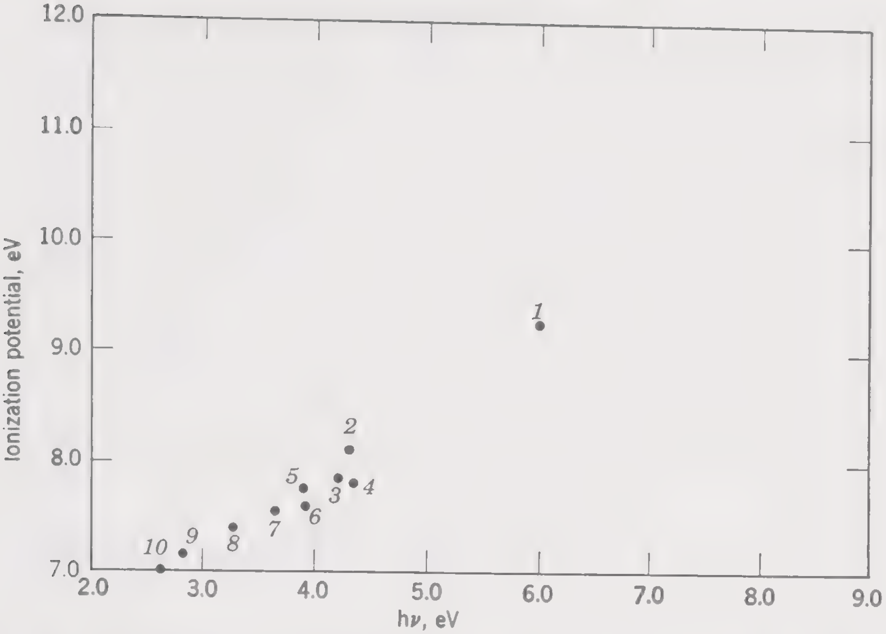

Fig. 46. *Para* band energy versus ionization energy: (*1*) benzene; (*2*) naphthalene; (*3*) phenanthrene; (*4*) triphenylene; (*5*) chrysene; (*6*) benzo (c) phenanthrene; (*7*) pyrene; (*8*) anthracene; (*9*) perylene; (*10*) tetracene.

6. AZULENE (91)

Azulene, unlike its colorless isomer naphthalene, is blue. The spectra of the two isomers are similar except that the bands of azulene are shifted considerably to the red, particularly the long wavelength L_b band which gives azulene its color (Fig. 47). The bands of azulene may be classified in the free electron model as L_b (7000 Å), L_a (3570 Å), B_b (2690 Å), C_b (2360 Å), and B_a (1930 Å). The direction of the transition moment in azulene is the same as given for the phenes, B_a (parallel to short axis), B_b (long axis), C_a (short axis), C_b (long axis), L_a (long axis), and L_b (short axis). The C_b band, forbidden in naphthalene because of its center of symmetry, is allowed in azulene and is twice as intense as in naphthalene.

The substitution of alkyl groups on azulene shifts the long wavelength L_b band to the red or to the blue depending upon the position of substitution. 1, 3, 5, or 7 substitution gives rise to a red shift while 2, 4, 6, or 8 substitution causes a blue shift.

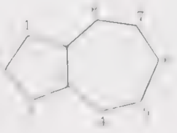

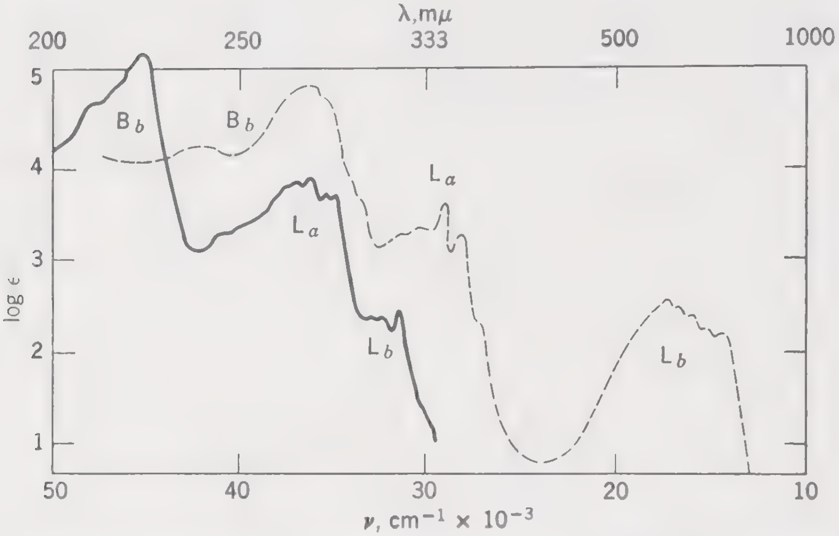

Fig. 47. Spectra of azulene (----) and naphthalene (——). (After J. N. Murrell, *Theory of Electronic Spectra of Organic Molecules*, Methuen, London, 1963.)

The shift of the L_b band upon polyalkylsubstitution is given by the sum of the shifts of the particular monosubstituted azulenes (92). The blue or red shifts of the L_b band of azulene caused by alkyl substitution are in contrast to the red shifts produced by alkyl groups in the even alternant aromatic hydrocarbons. This effect is attributed to the inductive effect of the alkyl group. In the even alternant ring compounds the electron densities in the ground and excited states are equal and the same at each carbon atom (93). Thus, to a very good approximation the result of an inductive effect on the ground and excited states is equal and produces no band shift, the shifts being due primarily to the resonance (hyperconjugation) effect. However, in azulene the electron densities are not equal at different positions in the ring and also change upon excitation. The 1, 3, 5, and 7 positions have decreased electron densities upon excitation, while the 2, 4, 6, and 8 positions have increased electron densities. The $+I$ effect of an alkyl group at positions 1, 3, 5, or 7 will lower the transition energy and cause a red shift of the L_b band. Substitution at the 2, 4, 6, or 8 positions will have the opposite effect. The resonance effect is of less importance in azulene than in the even membered ring hydrocarbons. This can be seen in the relatively small shift of the L_b band induced by a phenyl group in azulene as compared to the effect of a phenyl group on the naphthalene spectrum. The behavior of the azulene ultraviolet bands upon alkyl substitution is different from that of the L_b band. An alkyl substitution always gives rise to a red shift of these bands, substitution in the five-membered ring giving a greater shift than substitution in the seven-membered ring.

G. The Heterocyclics

1. SATURATED HETEROCYCLICS (94–96)

The five- and six-membered oxygen heterocyclics, tetrahydrofuran and tetrahydropyran, absorb at about 1740 and 1870 Å ($\epsilon = \sim 2000$; ~ 800). Dioxane has only one band which is at 1800 Å; however, its intensity is much greater ($\epsilon = 6300$) than the bands in the monooxygen compounds (Table XVIII). These spectra resemble quite closely the spectra of the saturated acyclic ethers, and there seems to be no reason to doubt that these absorptions are caused by the conventional N → Q ($n \rightarrow \sigma^*$) transition. The σ^* molecular orbital involved in these transitions is probably the antibonding molecular orbital arising from the carbon–oxygen single bond. The three-membered ring ethylene oxide absorbs at 1690 and 1710 Å. It has been shown that the epoxy group resembles cyclopropane in its ability to conjugate with unsaturated systems. It appears that oxygen is behaving like a CH_2 group and that the changes in hybridization accompanying this behavior bind the "nonbonding" electrons more tightly, thus moving the $n \rightarrow \sigma^*$ transition to shorter wavelengths.

The saturated nitrogen heterocyclics—pyrrolidine, piperidine, and piperazine—absorb at longer wavelengths than the oxygen compounds, presumably due to the higher energy of the nonbonding electrons in the nitrogen

TABLE XVIII
Absorption Bands of Saturated Heterocyclic Compounds

Compound	Ionization energy, eV	λ_{max}, Å	ϵ	λ_{max}, Å	ϵ	Solvent	Ref.
Ethylene oxide	10.6	1690	3800	1710	3700	Vapor	a
Tetrahydrofuran	9.5	1720	2500	1870	800	Vapor	b
Tetrahydropyran	9.3	1760	2000	1870	630	Vapor	b
Dioxane	9.1	1800	6300			Vapor	b
Pyrrolidine	8.6	1710	2500	1960	1900	Vapor	c
Piperidine	8.5			1980	3500	Vapor	c
Piperazine	8.5			1960	4700	Vapor	c
Thiacyclobutane	8.9	2190	560	2750	25	Isooctane	d
Thiacyclopentane	8.5	2195	800	2500	30	Isooctane	d
Thiacyclohexane	8.4	2100	1800	2300	180	Ethanol	e

[a] T. K. Liu and A. B. F. Duncan, *J. Chem. Phys.*, **17**, 241 (1949).

[b] L. W. Pickett, N. J. Hoeflich, and T. K. Liu, *J. Am. Chem. Soc.*, **73**, 4865 (1951).

[c] L. W. Pickett, M. E. Corning, G. M. Wieder, D. A. Semenow, and J. M. Buckley, *J. Am. Chem. Soc.*, **75**, 1618 (1953).

[d] W. E. Haines, R. V. Helm, C. W. Bailey, and J. S. Ball, *J. Phys. Chem.*, **58**, 270 (1954).

[e] E. A. Fehnel and M. Carmack, *J. Am. Chem. Soc.*, **71**, 84 (1949).

compounds as shown by their lower ionization energies. The sulfur heterocyclics absorb at even longer wavelengths (Table XVIII) for the same reason. The spectra of the nitrogen and sulfur compounds are shifted to shorter wavelengths in polar solvents supporting the assignment of the bands to $n \rightarrow \sigma^*$ transitions.

2. UNSATURATED FIVE-MEMBERED HETEROCYCLICS

The unsaturated five-membered heterocyclics have absorption bands in the region 1900–2500 Å (Table XIX). The spectra of pyrrole and furan are similar to those of cyclopentadiene and divinyl ether (Fig. 48). However, the bands of the heterocyclics lie at shorter wavelength than in cyclopentadiene due to the conjugation of the more electronegative heteroatom. The band of the oxygen and nitrogen heterocyclics is shifted to longer wavelengths and is less intense in thiophene and selenophene; moreover, a second, more intense band appears

TABLE XIX
Absorption Bands of Unsaturated Heterocyclic Compounds

Compound	Ionization energy, eV	λ_{max}, Å	ϵ	λ_{max}, Å	ϵ	Solvent	Ref.
Cyclopentadiene	8.6	1910	2800	2390	3000	*n*-Heptane, hexane	a
Furan	8.9	2070	4700			*n*-Heptane, hexane	a,b
Divinyl ether		2035	15,000			Vapor	c
Pyrrole	8.2	2070	8700			*n*-Heptane, ethanol	a,b
Thiophene	8.9	2280	4900	2310	7400	*n*-Heptane, ethanol	a,d
Selenophene		2320	3300	2510	5250	Hexane	e
Imidazole		2080	5000			Ethanol	f
Pyrazole		2110	3400			Ethanol	f
Isoxazole		2110	4000			Ethanol	f
Thiazole		2400	4000			Ethanol	f

[a] H. B. Klevens and J. R. Platt, Technical Report, Laboratory of Molecular Structure and Spectra, Part 1, University of Chicago (1953–54).

[b] K. Bowden, E. A. Braude, and E. R. H. Jones, *J. Chem. Soc.*, **1946**, 948.

[c] A. J. Harrison, C. L. Gaddis, and E. M. Coffin, *J. Chem. Phys.*, **18**, 221 (1950).

[d] S. Gronowitz, *Arkiv Kemi*, **13**, 239 (1958); L. Chierice and G. Pappalardo, *Gazz. Chim. Ital.*, **88**, 453 (1958).

[e] G. Leandri, A. Mangini, F. Montanari, and R. Passerini, *Gazz. Chim. Ital.*, **85**, 769 (1955).

[f] D. S. Noyce, E. Ryder, and B. H. Walker, *J. Org. Chem.*, **20**, 1681 (1955).

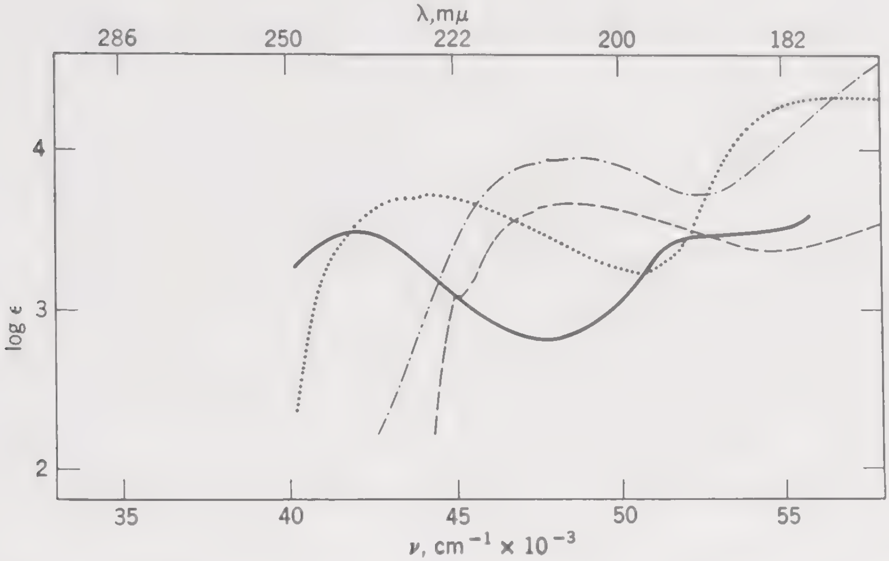

Fig. 48. Spectra of unsaturated five-membered heterocyclics: (——) cyclopentadiene; (– – – –) furan; (—·—·) pyrrole; (·····) thiophene. [After H. B. Klevens and J. R. Platt, Technical Report, Part One, Laboratory of Molecular Structure and Spectra, University of Chicago (1953–54).]

in these compounds. Both of these bands may be attributed to $\pi \rightarrow \pi^*$ transitions between the molecular orbitals formed from the diene orbitals and the heteroatom orbitals. The wavelengths of the spectra parallel the increasing participation of the heteroatom orbital in conjugation with the diene and consequent increasing aromatic character of these compounds. The five-membered ring compounds containing two heteroatoms, imidazole, pyrazole, and isoxazole, show only one absorption band near 2100 Å. This band is shifted to 2400 Å in thiazole (Table XIX). Although $n \rightarrow \pi^*$ transitions are expected in these compounds, none have been reported.

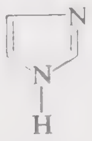
Imidazole

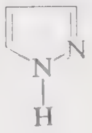
Pyrazole

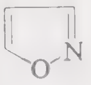
Isoxazole

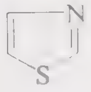
Thiazole

The heterocyclic compounds composed of a five-membered ring fused to benzene or other aromatic hydrocarbons have spectra which are similar to those of their carbocyclic analogs. The carbocyclic analogs are determined by replacing the heteroatom by a —C=C— group. Thus, the spectrum of thianaphthene is similar to that of naphthalene (see Fig. 49). The similarity of

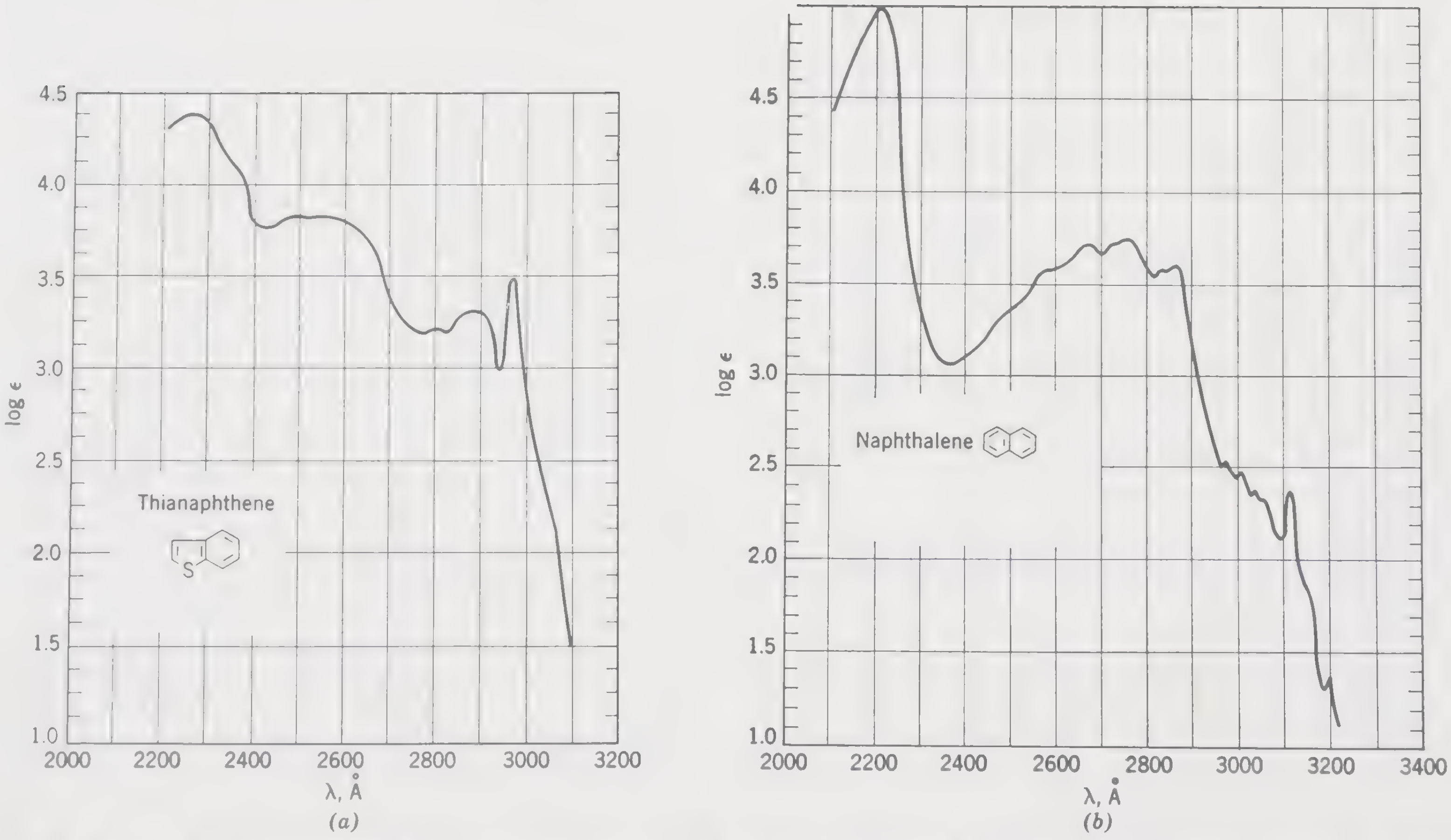

(*a*) (*b*)

Fig. 49. Spectra of (*a*) thianaphthene and (*b*) naphthalene in 95% ethanol. (After R. A. Friedel and M. Orchin, *Ultraviolet Spectra of Aromatic Compounds*, Wiley, New York, 1951.)

the spectra increases as the size of the condensed heterocyclic compound increases.

3. AZA AROMATIC HETEROCYCLICS (97–99)

The absorption spectrum of pyridine is very similar to its carbocyclic analog benzene (Fig. 50), indicating that the nitrogen atom introduces only a small perturbation on the benzene levels. The forbidden 2600-Å band (L_b) of benzene is allowed in pyridine because of the reduction of the benzene hexagonal symmetry by the nitrogen atom. This band is accordingly more intense than in the benzene spectrum. The L_a and $B_{a,b}$ bands of benzene are shifted to shorter wavelengths in pyridine and also in the diazines (Fig. 51). In the diazines and *s*-tetrazine the L_b band occurs at about 2400–2600 Å. However,

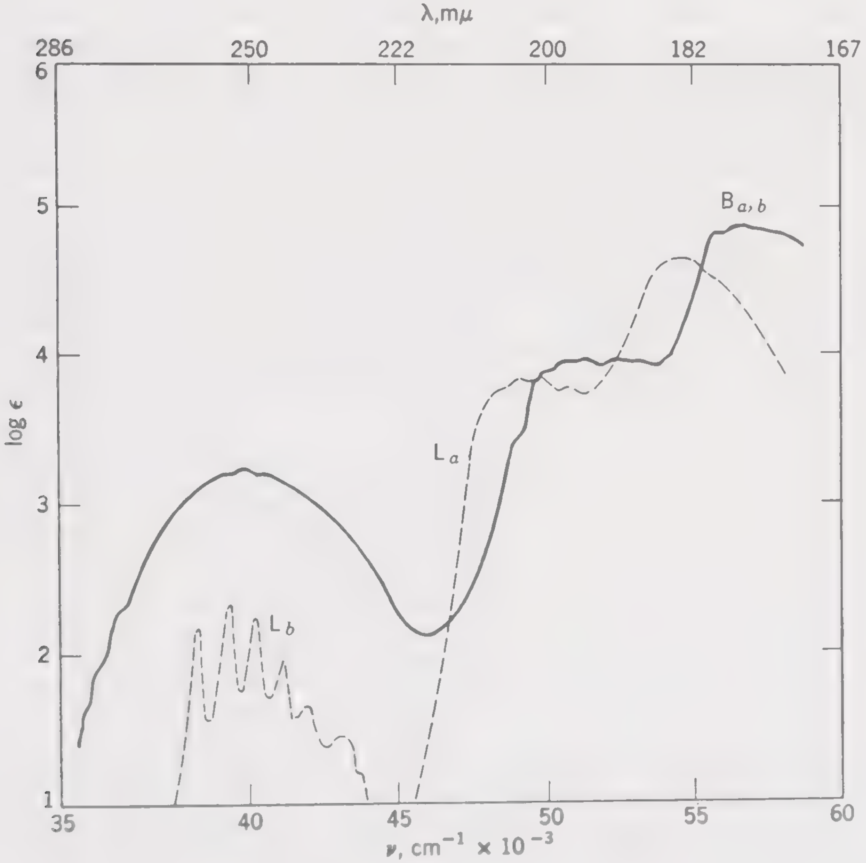

Fig. 50. Spectra of pyridine (———) and benzene (----). [After H. B. Klevens and J. R. Platt, Technical Report, Part One, Laboratory of Molecular Structure and Spectra, University of Chicago (1953–54).]

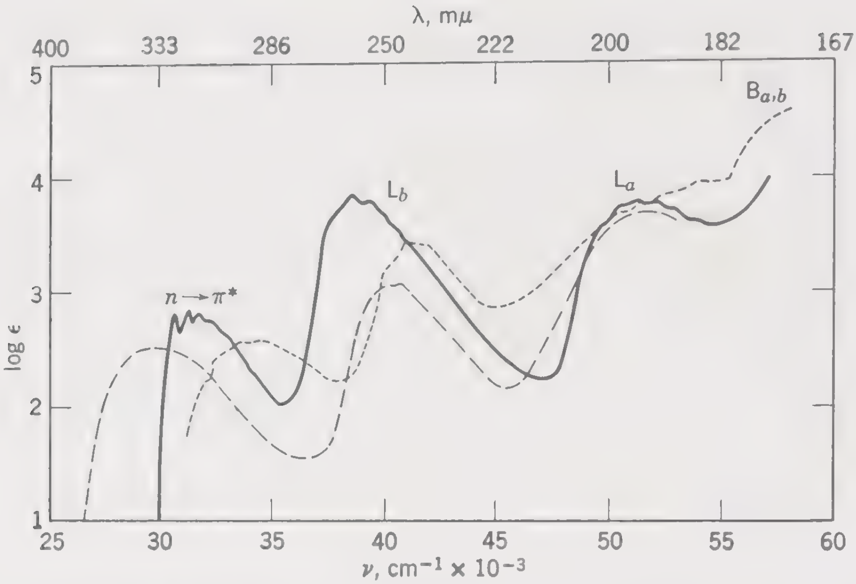

Fig. 51. Spectra of diazines: (— —) pyridizine; (----) pyrimidine; (——) pyrazine. [After H. B. Klevens and J. R. Platt, Technical Report, Part One, Laboratory of Molecular Structure and Spectra, University of Chicago (1953–54).]

in *s*-triazine this band is at 2220 Å (Table XX). The shifts of this band depend upon the contribution of the nitrogen x orbitals to the molecular orbitals of the ground and excited states of the particular aza compound. These contributions are determined by the symmetry of the particular compound and of

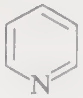

Pyridine

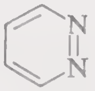

Pyridazine

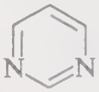

Pyrimidine

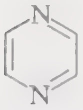

Pyrazine

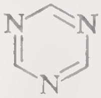

s-Triazine

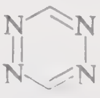

s-Tetrazine

the molecular orbitals, and therefore the contributions and the band shifts vary from one compound to the next. Because of the particular symmetry of *s*-triazine, the L_b band is forbidden ($\epsilon = 150$) just as in benzene. The spectra of monoaza condensed aromatic compounds, such as quinoline, isoquinoline, and acridine, generally resemble those of the carbocyclic compounds. The resemblance usually becomes less noticeable as more nitrogen atoms are

TABLE XX
Long-Wavelength Bands of Azabenzenes[a]

	L_b		$n \rightarrow \pi^*$		
Compound	λ_{max}, Å	ϵ_{max}	λ_{max}, Å	ϵ_{max}	Ionization energy, eV
Benzene	2540	110			9.3
Pyridine	2510	2000	~2700	~450	9.3
Pyridazine	2460	1300	3400	320	8.9
Pyrimidine	2430	2030	2980	330	9.5
Pyrazine	2600	5600	3280	1040	9.3
s-Triazine	2220	150	2720	890	10.0
s-Tetrazine	2520	2150	3200	30	
			5420	830	

[a] S. F. Mason, *J. Chem. Soc.*, **1959**, 1204, 1247; solvent, cyclohexane.

introduced, reflecting the changes in the molecular symmetry of the compound.

The azaaromatic compounds, unlike the five-membered ring heterocyclics, have a nonbonded pair of electrons in a nitrogen sp^2 orbital, which lies in the plane of the ring and is essentially perpendicular to the π and π^* molecular orbitals. Accordingly, weak $n \rightarrow \pi^*$ transitions are expected in these compounds. Since the nonbonding orbital lies at higher energy than the highest filled π molecular orbital, the $n \rightarrow \pi^*$ transition is expected to be the band occurring at longest wavelength. However, in pyridine the $n \rightarrow \pi^*$ transition is not clearly seen in solution, occurring as a shoulder on the L_b band in the 2700–2900-Å region. It is identified by its characteristic shift in hydroxylic solvents.

The $n \rightarrow \pi^*$ transitions of the diaza benzenes occur as distinct bands in the 3000–3400-Å region due to the blue shift of the L_b and the red shift of the $n \rightarrow \pi^*$ bands. The $n \rightarrow \pi^*$ band of *s*-triazine is at 2720 Å. *s*-Tetrazine appears to have two $n \rightarrow \pi^*$ bands, one near 3200 Å and the other at 5420 Å (97). Since the polyazines have more than one n orbital, more than one $n \rightarrow \pi^*$ band may occur. However, the n orbitals do not interact unless they are adjacent in the particular compound as in pyridazine and *s*-tetrazine, where two distinct $n \rightarrow \pi^*$ bands would be expected. Usually the nonbonding interaction is so small that distinct bands are not observed except for the case of *s*-tetrazine. However, the presence of the unresolved $n \rightarrow \pi^*$ bands is evident from the greater intensity of the $n \rightarrow \pi^*$ bands of the tri- and tetraazines. The intensity of the $n \rightarrow \pi^*$ bands of the aza aromatic compounds is much greater than that of the corresponding bands in the carbonyl compounds since the overlap of the sp^2 lone pair hybrid and the π^* orbital is greater than the overlap between an x_0 and $\pi_y{}^*$ orbital in carbonyl compounds.

IV. SPECIAL TOPICS

A. Complexes

1. CHARGE TRANSFER COMPLEXES (100)

A complex is a loose reversible association of two or more distinct chemical components. Often the complex formation is accompanied by a shift in absorption or by the appearance of a new absorption band. It is the latter feature of complex formation which is to be discussed in this section. For example, benzene complexes with iodine, producing a new absorption band at 2900 Å (101) (see Fig. 52). Iodine complexes with a wide variety of organic compounds—aromatics, olefins, and those containing basic groups (102–106).

It has been proposed that in these complexes one component behaves as a Lewis acid (A) and the other as a Lewis base (B) (107). The system is roughly described as a resonance hybrid between a no-bond state A,B and a dative state A^-,B^+ with wave functions ψ_{NB} and ψ_D, and energies W_{NB} and W_D, respectively. To form the dative state from the no-bond state, it is necessary to supply an amount of energy:

$$W_D - W_{NB} = I_B - E_A - e^2/r + \phi$$

where I_B is the ionization potential of the base, E_A is the electron affinity of the acid, e^2/r is the coulomb energy due to the charge separation r in the

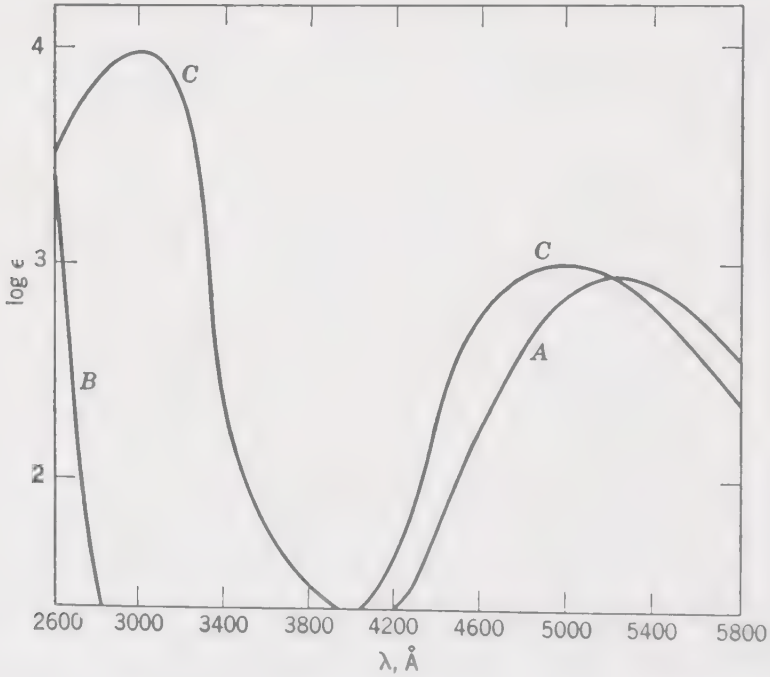

Fig. 52. The spectra of iodine (*A*), benzene (*B*), and the benzene iodine complex (*C*).

complex, and ϕ is the difference between the other energy quantities of the two states. If the resonance integral between the no-bond and dative states is β, then, by perturbation theory, the energy in the actual ground state, Ψ_N, derived from the interacting no-bond and dative states is

$$\Psi_N \cong \psi_{NB} \qquad E_N = W_{NB} + \beta^2/(W_{NB} - W_D)$$

and that for the excited state, Ψ_E (see Section II-G and Fig. 2):

$$\Psi_E \cong \psi_D \qquad E_E = W_D - \beta^2/(W_{NB} - W_D)$$

The binding energy of the complex in its ground state is then given by $\beta^2/(W_{NB} - W_D)$ and the frequency of absorption by

$$h\nu = W_D - W_{NB} - 2\beta^2/(W_{NB} - W_D)$$

For complexes formed from the same acid, one may write

$$h\nu = I_B + D + 2\beta^2/(I_B + D)$$

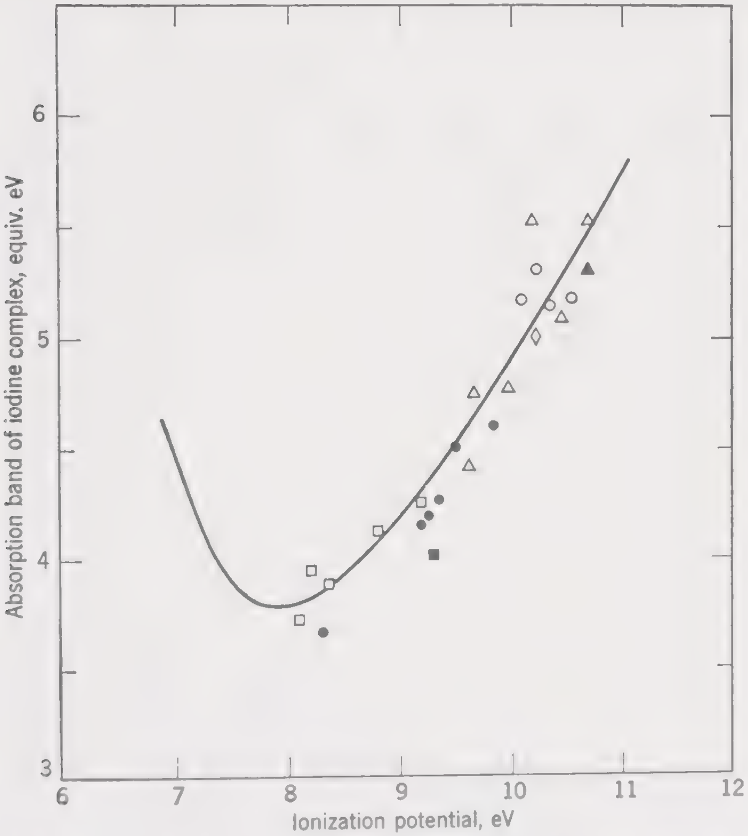

Fig. 53. The frequency of absorption of the iodine complex plotted against the ionization energy of the base (116): (○) saturated hydrocarbons; (●) olefins; (□) aromatics; (△) alkyl halides; (▲) alcohols; (◇) ethers; (■) thioethers.

where $D = -E_A - e^2/r + \phi$, both β and D being regarded as approximately constant.

In Figure 53 $h\nu$ is plotted versus I_B values for a number of iodine complexes. The curve is drawn for $\beta = 1.3$ and $D = 6$ eV, both of which are quite reasonable values. The large increase in the frequency at low ionization energy is a consequence of the use of perturbation theory. It is interesting to note that saturated hydrocarbons behave as bases. Br_2, ICl, SO_2, $COCl_2$, and $C_6H_3(NO_2)_3$ have been studied, in addition to I_2, and shown to act as acids toward bases (108,109).

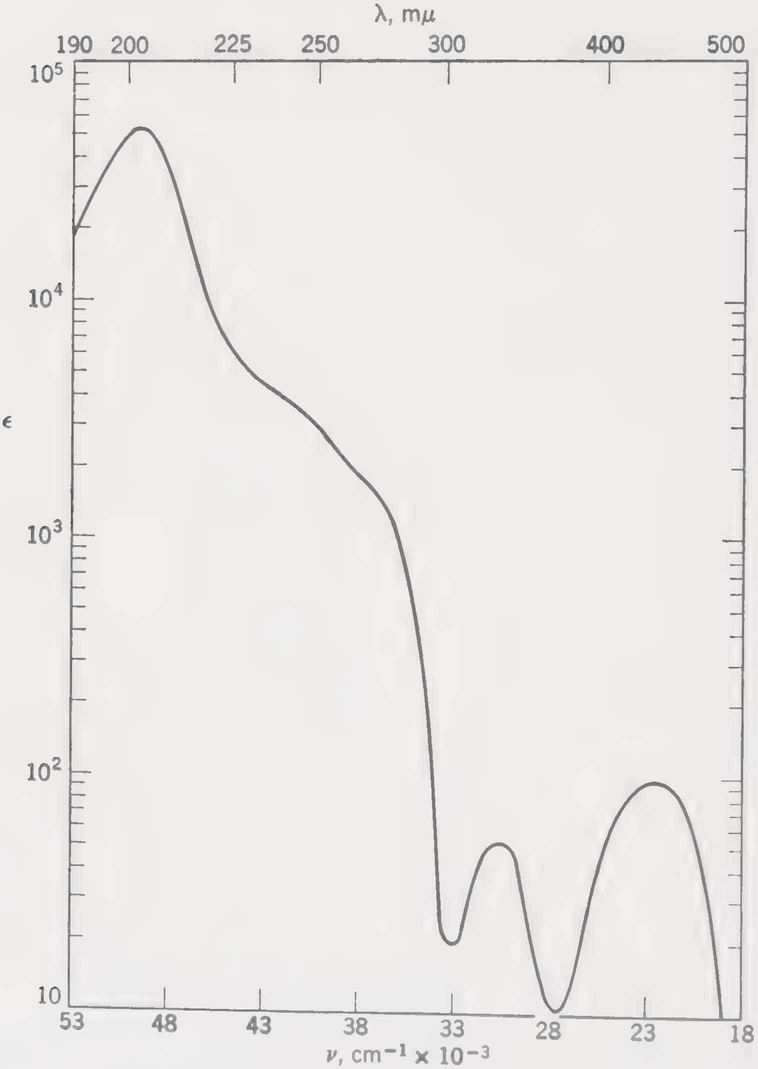

Fig. 54. Absorption spectrum of ferrocene in cyclohexane (113).

2. ORGANOMETALLIC COMPLEXES (110)

There are a very large number of colored stable complexes between organic molecules and transition elements or rare earths. In most of these, however, the weak, long-wavelength absorption is due to forbidden transitions involving the excitation of the *d* or *f* electrons of the metal ion perturbed by the organic ligands and not excitation in the organic part of the complex.

The dicyclopentadienyl and diarene "sandwich" complexes are examples of colored transition metal complexes. The red-orange iron complex, ferrocene (dicyclopentadienyl iron), is the best known of these compounds. The weak visible absorption bands of ferrocene at 3240 and 4400 Å (Fig. 54) are attributed to transitions between the 3*d* orbitals of the ferrous ion which are split by the ligand field potential of the two $C_5H_5^-$ groups (111–113). In a calculation where the ligand field potential was approximated by a cylindrical potential, the energy of the *d* orbitals was given as $\epsilon(d_{z^2}) < \epsilon(d_{xz,yz}) < \epsilon(d_{x^2,y^2,xy})$ (114). However, it has been shown from Mossbauer studies (115) and analysis of the absorption spectrum (111) that this *d* orbital arrangement is incorrect and that the correct order is $\epsilon(d_{xy,x^2-y^2}) < \epsilon(d_{z^2}) < \epsilon(d_{xz,yz})$. In the molecular orbital description of ferrocene (113,116), the bonding is due to interaction of the iron 3*d*, 4*s*, and 4*p* orbitals with appropriate molecular orbitals composed of the $2p$–π carbon orbitals of the rings. The molecular point group is D_{5d}, with A and E representations. The highest filled and lowest empty molecular orbitals are primarily 3*d* orbitals (70–100%), and the *d*-*d* description of the weak transitions is still valid.* The visible bands are

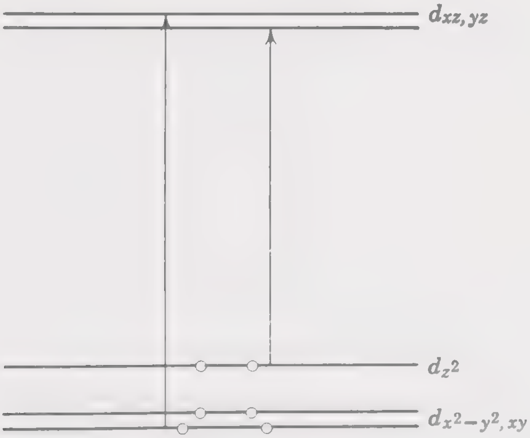

Fig. 55. Ligand field levels of ferrocene.

---

* In an atom $d \leftrightarrow d^*$ transitions are forbidden due to the $g \leftrightarrow g$ rule. In a molecule with inversion symmetry like ferrocene, this rule still holds.

assigned to forbidden transitions between the filled iron d_{z^2} A_{1g} and essentially $d_{x^2-y^2}$, d_{xy} E_{2g} orbitals and the empty, antibonding, essentially d_{xz}, d_{yz} E_{1g} orbitals (Fig. 55) (112,113). Because of the degenerate *d* orbitals, configuration interaction is important in these compounds, as for benzene (Section III-E-1).

B. Hydrocarbon Ions and Radicals

The simple molecular orbital description of carbonium ions (**1**), free radicals (**2**), and carbanions (**3**) is the same. The σ bonds are sp^2 hydrids, and an unhybridized *x* orbital lies perpendicular to the plane of the group. This

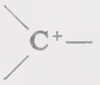
(1)

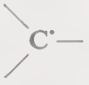
(2)

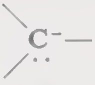
(3)

nonbonding *x* orbital is unoccupied, occupied by one electron, and filled in the carbonium ion, radical, and carbanion, respectively. The molecular orbitals of these groups should be very similar except for small differences caused by the varying electronegativity of the carbon. The simplest hydrocarbon radical, $CH_3\cdot$, has a series of Rydberg bands in the 1300–1510 Å region and at 2160 Å arising from the nonbonding *x* orbital promotion to a highly excited *ns* or *nd* level. The lower energy $\sigma(C—H) \rightarrow x$ promotion is theoretically forbidden and has not been observed.

1. SIMPLE CARBONIUM IONS (117,118)

For many years the aliphatic carbonium ion has been postulated as an intermediate in many acid-catalyzed reactions. Recently the existence of tertiary and some secondary carbonium ions in SbF_5 and $FSO_3H–SbF_5$ has been proved by NMR spectra (118). The addition of small amounts of olefins or aliphatic alcohols to sulfuric acid results in an absorption band near 3000 Å, the tail of which causes the yellow color of the solution (119) (see Fig. 56). This band might be due to aliphatic carbonium ions or to oxidized allylic ions. Similar absorption bands have been attributed to the simple *t*-alkyl cations (120,121). However, this band in the spectra of the carbonium ions is probably due to small amounts of alkenyl cations which absorb at about this wavelength (117,118) since a reinvestigation of the alkyl cations in FSO_3H-SbF_5 shows no bands at wavelengths longer than 2100 Å.

The methyl cation is stabilized by substituting cyclopropyl groups for the hydrogen atoms, probably by resonance interaction of the carbonium *x* orbital and the bent "banana" bonds of the cyclopropyl groups. Methylcyclopropylcarbonium ion has a band at 2980 Å (ϵ = 11,000), dicyclopropylmethyl cation at 2700 Å (ϵ = 12,000), and tricyclopropylmethyl

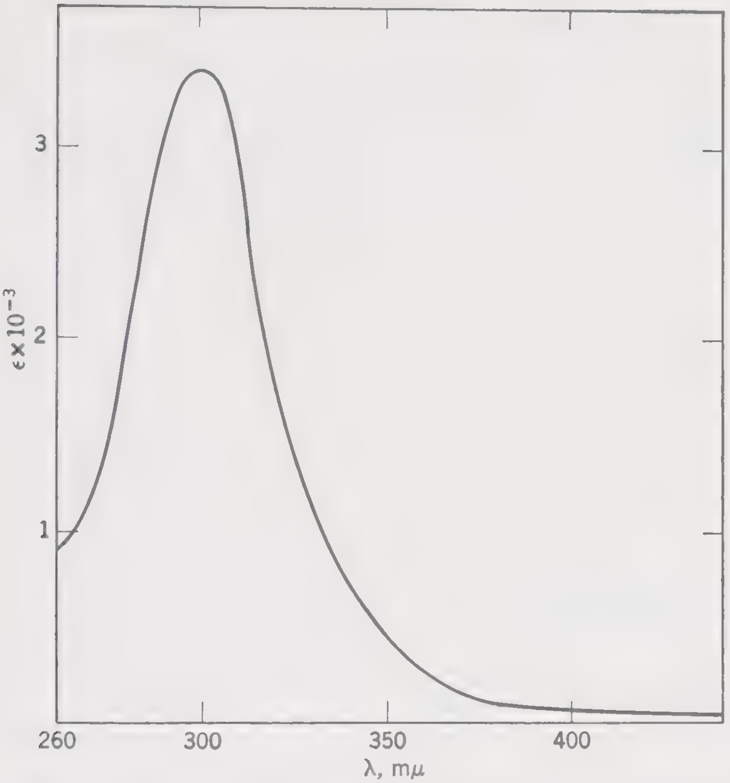

Fig. 56. The spectrum of $10^{-4}M$ solution of octene in 96% sulfuric acid (119).

cation absorbs at 2700 Å (ϵ = 22,000). The alkenyl cations absorb at approximately 3000 Å (Fig 56). The effect of increasing ring size of the cycloalkenyl cations is a shift of the absorption band toward the visible, similar to the shifts in cyclic dienes. The pentamethyl or tetramethyl derivatives of the cyclobutenyl, cyclopentenyl, and cyclohexenyl cations absorb at 2450, 2990, and 3140 Å, respectively.

2. AROMATIC IONS AND RADICALS

The benzene molecule has remarkable stability and a characteristic electronic spectrum by virtue of its circular, planar array of six π orbitals with six electrons. It is natural then to ask whether other systems possess such stability and such a spectrum. Elementary reasoning would lead one to expect that cyclobutadiene and cyclooctatetrene should have these properties. In both of these compounds there must be a considerable departure from the 120° angle of benzene, which, it will be remembered, arises naturally from the sp^2 hybridization. This will reduce the resonance energy, the stability, and the aromaticity. Cyclobutadiene has not been isolated, and cyclooctatetrene is puckered and has no aromatic properties (122). The five- and seven-membered rings would not depart quite so far from the 120° angle. These do not form a completely conjugated system, but the conversion of the saturated atom into a carbanion or a carbonium ion would introduce an x orbital on that atom, and the resultant species would be completely conjugated. The resonance energies of some of these ions have been calculated by molecular orbital theory and found to be $(CH)_5{}^-$, -2.48β; $(CH)_5{}^+$, -1.24β; $(CH)_7{}^+$, -3.00β; and $(CH)_7{}^-$, -2.12β (123). The cycloheptatrienylium carbonium ion (tropylium ion) has been prepared and its bromide shown to be symmetrical, and the ion to have the absorption characteristics of a single ring aromatic system (124): $\lambda_{\max} = 2750$ ($\epsilon = 4400$) (L_a) and 2170 Å ($\epsilon = 41{,}000$) ($B_{a,b}$). The cyclopentadienide derivative, 1-methyl-2,3,4,5-tetracarbomethoxy cyclopentadienide, has absorption bands at 2700 ($\epsilon = 34{,}000$) and 3080 ($\epsilon = 14{,}000$) (125). The cyclooctatetraene radical anion and dianion are probably both planar aromatic systems. The latter has the L_a band at 3400 Å ($\epsilon = 3000$) and the $B_{a,b}$ band at 2750 Å ($\epsilon = 10{,}000$). In C_8H_8 and $C_7H_7{}^+$ there is no transition corresponding to the L_b band of C_6H_6.

The phenyl-substituted ions and radicals are relatively stable due to a resonance interaction between the x orbitals of the phenyl group and the central carbon x orbital. The benzyl and triphenylmethyl ions and radicals have molecular orbitals such that a nonbonding orbital occurs along with the paired bonding and antibonding molecular orbitals with energies, $\alpha \pm m_i\beta$. This nonbonding orbital is filled in the anion, empty in the cation, and half filled in the radical. The absorption spectra of the ions and radicals should be very similar, involving, in all three forms, low energy transitions $f \rightarrow g$ and in the radical a low energy transition $e \rightarrow f$, as well as a higher energy $f \rightarrow h$ transition in the cation or $e \rightarrow g$ transition in the radical and anion. The transitions in the ions involving nonbonding orbitals are charge-transfer transitions since the nonbonding orbital is localized on the methyl group and the other molecular orbitals are primarily on the rings. The diphenylmethyl cation and anion absorb at 4410 Å (in sulfuric acid) (126) and 4340 Å (in diethyl ether), respectively (127). The triphenylmethyl cation, anion, and radical have bands at 4410 and 4340 Å (128); 4750 and 4100 Å (127); and 3400 Å (129), respectively. The benzyl anion absorbs at 2590 Å ($\epsilon = 24{,}000$) in a tetrahydrofuran solution (130), and the radical has a strong band at 3000 Å and a weaker band near 4500 Å.

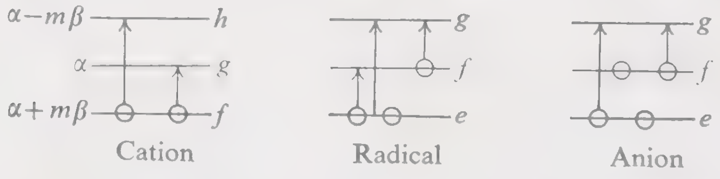

Cation Radical Anion

For even alternate aromatics such as benzene and naphthalene the bonding and antibonding molecular orbitals occur in pairs with energies, $\alpha \pm m_i\beta$, as previously noted. The ions of such compounds should have spectra which are very similar to those of the neutral hydrocarbons except that a new long wavelength band should be seen in the spectra of the ions. This band will correspond to the $g \rightarrow h$ or $e \rightarrow f$ transition in the anion and cation, respectively. Since both excitation energies are equal in the simple molecular orbital approach, the spectra of the anion and cation should be very similar. Experimentally the spectra of the cations and anions of perylene, tetracene,

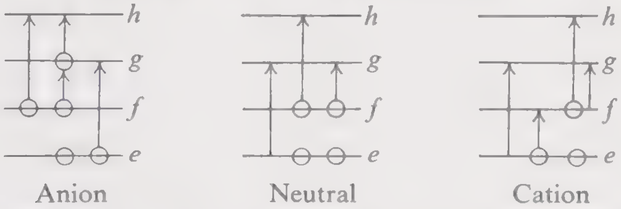

pyrene, and anthracene are almost identical (131) (Fig. 57). These spectra are also very similar to the spectra of the parent hydrocarbons except for the long wavelength $g \rightarrow h$ or $e \rightarrow f$ transition in the ions.

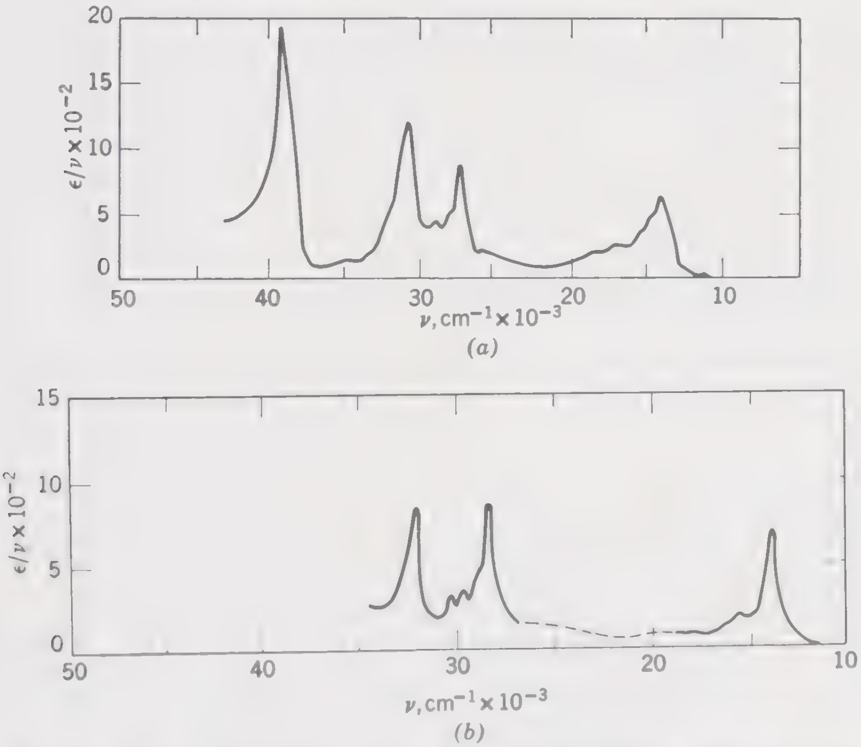

Fig. 57. Spectra of anthracene ions: (*a*) anthracene anion in tetrahydrofuran; (*b*) anthracene cation in CF_3COOH-H_2OBF_3, contacted with air. (After ref. 131.)

C. Dyes and Other Extended Conjugated Systems

Theories of dye color have been continuously proposed since the first dye was synthesized. While these theories appear unsophisticated and incomplete by present standards, many of them reveal certain aspects of the present theory with surprising clarity. Witt, in 1876, called attention to the fact that every dye then known contained at least one of the following groups:

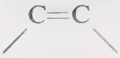

—N=O

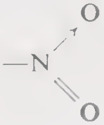

—N=N—

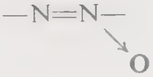

These groups all carry x orbitals on adjacent atoms. The x orbitals interact weakly compared to the orbitals in σ bonds, so that the bonding molecular orbital lies higher, and the antibonding orbital lies lower than in a saturated compound. Consequently, both N → V and N → Q transitions lie at longer wavelengths for compounds containing these groups than in completely saturated compounds.

Witt also suggested that certain groups called *auxochromes*, $—NH_2$, —OH, $—SO_3H$, and $—CO_2H$, intensify the color of the chromophores. These groups also contain x orbitals, which, however, normally lie lower in energy than do the chromophore orbitals. The auxochrome orbitals push the chromophore levels upward, the bonding more than the antibonding, and so produce a red shift, at least in N → V transitions. Later, Stieglitz postulated that the auxochromes were oxidized and the chromophores reduced. Molecular orbital theory shows that the auxochrome normally donates some electron density to the chromophore, that is, the auxochrome is oxidized and the chromophore reduced.

In 1888, Armstrong proposed that the quinoid structure or something close to it must be possessed by a compound before it can be colored. This idea is based in part on the fact that the simple compound *p*-benzoquinone is colored. In Section III-E-8 it was suggested that the color of *p*-benzoquinone is due to an N → Q transition, the band being fairly weak compared to some of the N → V transitions. It is highly probable that the latter are the analogs of the transitions which produce the bright, visible color in many dyes. A particularly weak link in the Armstrong argument is the fact that iminoquinone and diiminoquinone are colorless even though they possess the quinoid structure. The explanation probably hinges on the tightness of binding of the unshared electron pair on the imino group since one of these electrons must be excited in an N → Q transition. It should be pointed out that since some of the *p* orbital character of nitrogen in the iminoquinones is used up in the formation of the double bond, the unshared pair must have considerable *s* character and so be strongly bonded to the nitrogen. The fact that diazomethane is colored cannot be used as a strong argument against the above explanation since it has a strained configuration.

Just after the turn of the century, it was recognized that a molecule which could assume several distinct quinoid structures was likely to be colored. Phenylene blue is an example:

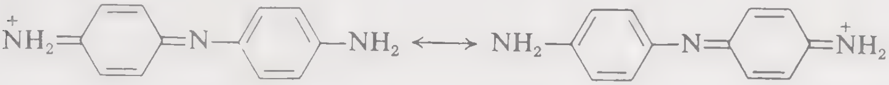

This concept is very much like the resonance theory developed thirty years later by Bury, Pauling, and others. The terms "oscillation" and "rhythmic rearrangement" were used by classical analogy instead of "resonance," and the concept was, of course, without quantum mechanical basis.

Molecular orbital theory, on the other hand, does not assign definite valence structures. Each carbon and nitrogen atom contributes one π orbital to the molecular orbitals which extend over the whole molecule. While an exact calculation of the positions of the absorption bands of phenylene blue cannot be made, the lowest unfilled and the highest filled molecular orbitals lie close enough together so that one would predict that such a system should absorb in the visible. It is interesting to note that bond orders of the several bonds in the molecule as calculated from its molecular orbitals show some quinoid character in both benzene rings, while the calculated electron densities show that the terminal nitrogen atoms carry a small positive charge, in agreement with the resonance picture given above. One may summarize by saying that, in compounds for which the possibility exists of writing several distinct quinoid structures, there is also the possibility of the existence of a large number of interacting π orbitals, which produce molecular orbitals with energies close enough together to give absorption in the visible region.

As a general rule, the greater the amount of conjugation the more deeply colored the compound. The long wavelength absorption of all polyenes

$$R_1\text{—}(CH{=}CH)_n\text{—}R_2$$

shifts toward the red as n increases. The functional form of the dependence of wavelength upon n depends on the nature of the end groups, R_1 and R_2. For certain cyanine dyes, in which $R_1 = R_2$, there is a linear dependence of wavelength upon n (132). The dye series

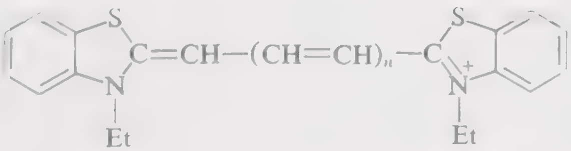

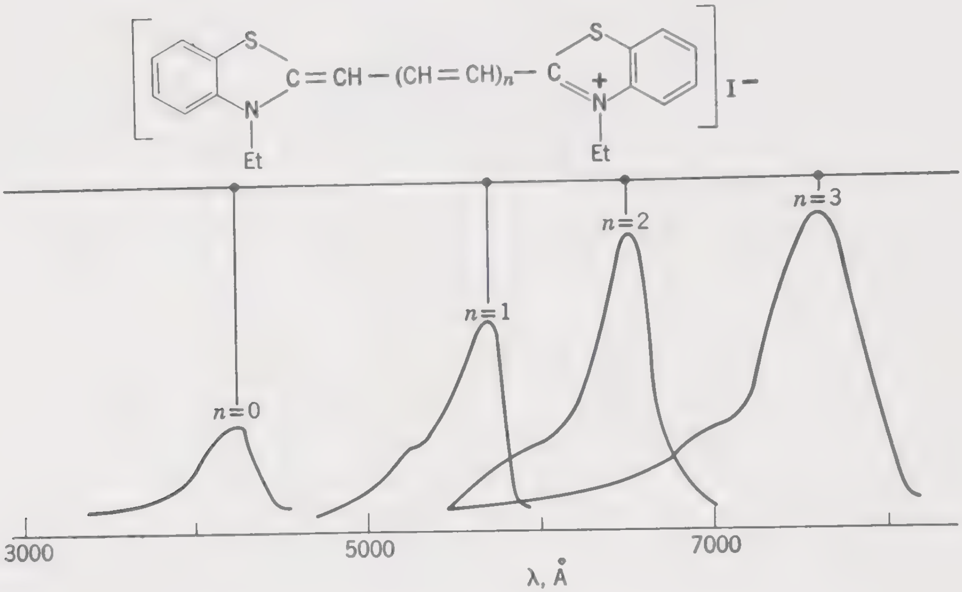

Fig. 58. The spectra of a series of cyanine dyes (132).

exhibits this behavior (see Fig. 58). If R_1 is not very different from R_2, the linear dependence of the wavelength on n is preserved, and, further, the wavelength is the mean of the wavelengths of $R_1—(CH=CH)_n—R_1$ and $R_2—(CH=CH)_n—R_2$. The linear relation appears to be the exception rather

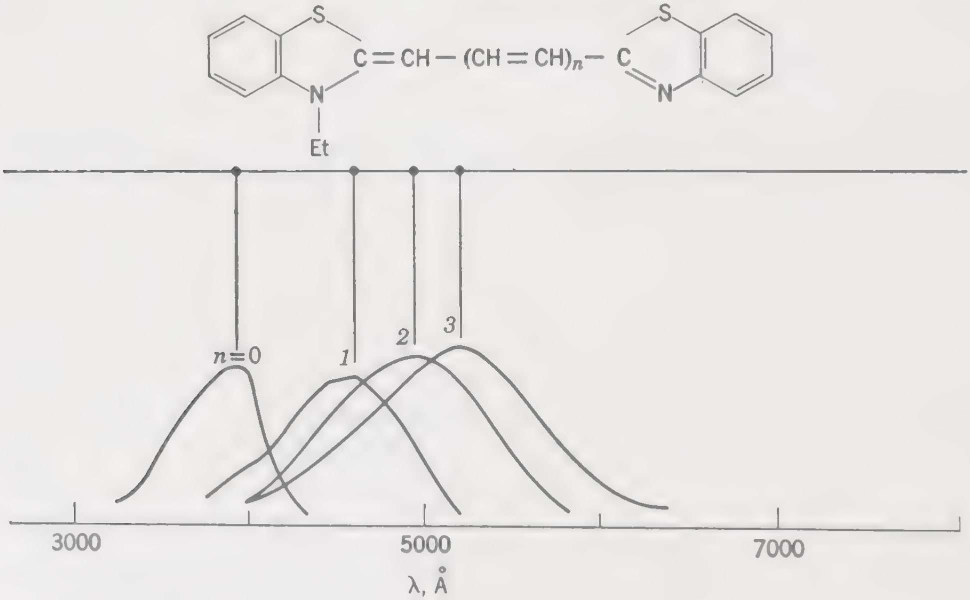

Fig. 59. The spectra of a series of anhydro base dyes (132).

than the rule. There follow three series of polyenes for which the wavelength does not vary linearly with *n*:

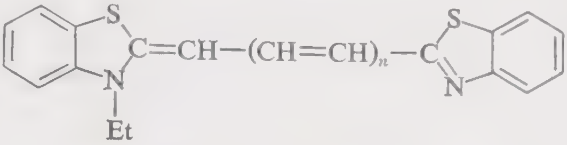

$$\mathrm{Me_2\overset{+}{N}{=}CH{-}(CH{=}CH)_n{-}NMe_2}$$

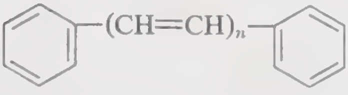

The first series differs from the previous dye in that one of the nitrogen atoms is bonded to only two other atoms and so cannot assume the charged quaternary structure. The spectra of this and the second series appear to converge to a definite wavelength at large *n* (see Fig. 59). The wavelength of maximum absorption of the diphenyl polyenes varies with the square root of *n*.

The molecular orbital theory predicts for simple polyenes a linear variation of wavelength with *n* (see Section II-H-1). Molecular orbital calculations on the second dye (133), taking the coulomb integral on nitrogen to be $\alpha + 0.58\beta$, give the observed convergence as well as good numerical agreement.

The merocyanine dyes are unsymmetrical dyes which contain a basic heterocyclic nucleus linked through a conjugated chain to an acidic nucleus. They are uncharged but have high dipole moments. The ground and excited states of these dyes have different electron densities, and the absorption maxima and intensities are very solvent dependent (134). The absorption band of compounds such as **1** shifts toward the red in more polar solvents while the spectra of compounds like **2** shift toward the blue. Other dyes exhibit first a red and then a blue shift with increasing polarity of the solvent. For example, **3** first shows a red shift upon diluting a pyridine solution with water. Upon further dilution a blue shift is observed. At some intermediate solvent composition addition of a small amount of water scarcely shifts the spectrum. It might be said that both the ground and excited states have equal polarities in this particular solvent. However, since the pyridine, water, and the dye

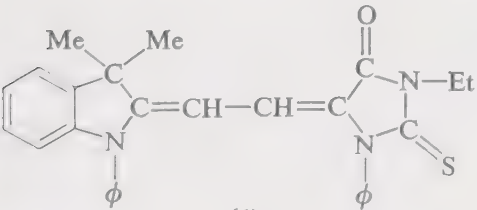

(1)

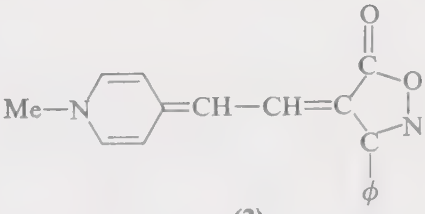

(2)

are hydrogen bonded, this behavior may be due to a shift in the equilibrium between the various hydrogen bonded species.

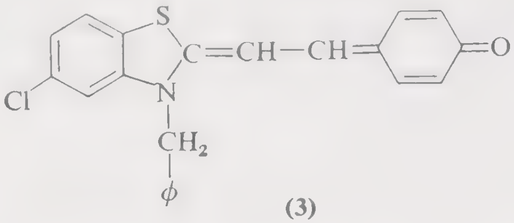

(3)

The compounds discussed previously in this chapter usually obey the Beer-Lambert law. For dyes, especially in aqueous solution, this is not always true. In Figure 60 are given the molar extinction coefficients of 1,1′-diethyl-2,2′-cyanine chloride in $1.3 \times 10^{-5} M$ and in $1.4 \times 10^{-2} M$ aqueous solution (135,136). The solid curve in Figure 60 is typical of the absorption spectrum

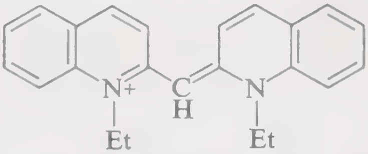

of many dyes dissolved in organic solvents, when Beer's law is followed, and in very dilute aqueous solution. The spectrum, dominated by a strong main maximum on the long wavelength side, usually accompanied by a subsidiary maximum or shoulder about 1300 cm^{-1} hypsochromic to the main band, appears to be that of the monomeric form of the dye in its solvent environment, but free from interaction with other dye molecules. The structure in this spectrum probably represents vibrational components of a vibronic spectrum. As the concentration of the dye in aqueous solution is increased at room temperature, the main monomeric maximum decreases in intensity, and a new band appears on the short wavelength side, usually at a wavelength somewhat less than that of the vibrational subband. An increase in temperature causes the spectrum of the more concentrated aqueous solution to revert toward that of the monomer. For a number of dyes, including methylene blue (137,138), rhodamine B (139), acridine orange (140), proflavine (141), and the series of cyanine dyes in Figure 58 (142), it has been shown that the new band can be attributed to a dimer, since the concentrations of monomer and dimer can be determined from an analysis of the spectrum and are found to obey the law of mass action, $c_m^2/c_d = K$, appropriate to a monomer-dimer equilibrium. The mass law, in this form, sometimes holds only over a limited range of concentration, above which broadening of the dimer band or the appearance of new bands at still shorter wavelength indicates the formation of aggregates containing more than two monomeric units.

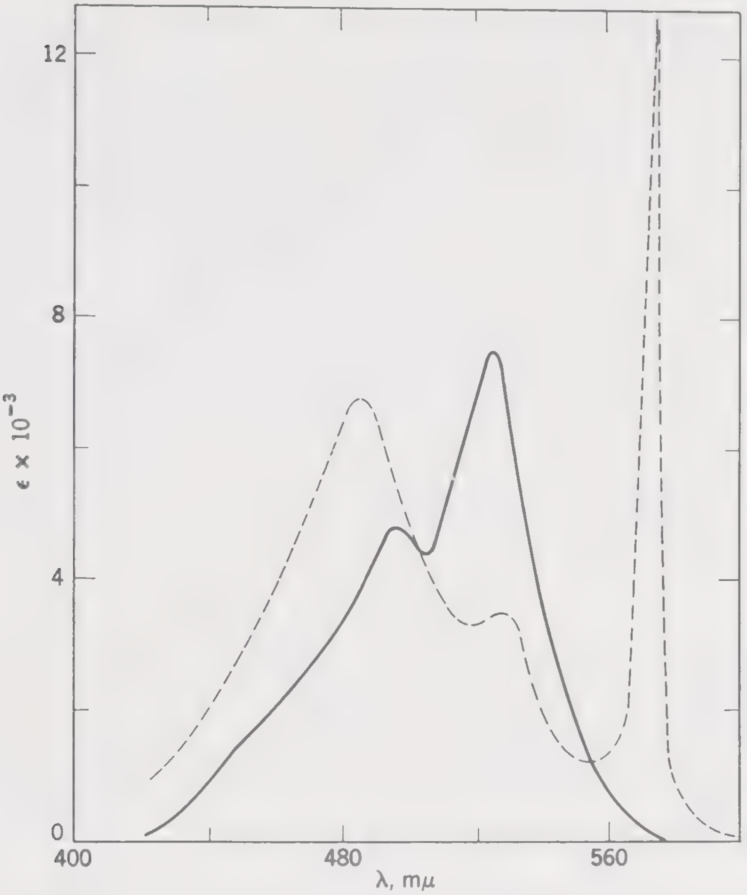

Fig. 60. The spectrum of 1,1′-diethyl-2,2′-cyanine chloride at 1.3×10^{-5} (——) and $1.4 \times 10^{-2}M$ (---) aqueous solution (147).

The structure of many dye molecules is essentially a flat coplanar arrangement of their skeletal atoms in heterocyclic or aromatic rings with sometimes a coplanar connecting conjugated chain, and it seems likely that the dimer consists of a sandwich arrangement of the two monomers with their planes parallel. The component monomers in the dimer of a cationic dye, such as those referred to in the last paragraph, or of an anionic dye like fluorescein, must be held together against the electrostatic repulsion of similar charges. The effect of the high dielectric constant of water in diminishing this repulsion is, no doubt, a main reason for strong dimerization in aqueous solution, although dimers are not observed in organic solvents of equally high or higher dielectric constant. At low temperatures, however, dimerization of dyes is observed in alcohol (144).

An interesting feature of the spectrum of dye dimers is that it is double-banded—the strong band on the short wavelength side of the monomeric maximum is accompanied by a feebler band on the long wavelength side (not to be confused with the intense sharp band on the long wavelength side of the monomeric maximum of the dye illustrated in Fig. 60). The bathochromic component of the dimeric spectrum is usually concealed partially in the long wavelength tail of the monomer in equilibrium with the dimer, but its presence can be shown, on analysis of the spectrum, by subtracting the monomeric absorption from the total absorption of the equilibrium mixture.

We shall outline the theoretical treatments (143–145) that have been applied to account for the main features of the dimeric absorption spectrum. The ground state electronic eigenfunction of a dimer containing two identical monomers described by eigenfunctions ψ_A and ψ_B can be written

$$\Psi_g = \psi_A \psi_B$$

When the dimer has absorbed one photon, its excited state is derived from the degenerate functions

$$\Phi_1 = \psi_A \psi_B^* \quad \text{and} \quad \Phi_2 = \psi_A^* \psi_B$$

in which the excitation, indicated by the asterisk, is considered to reside in one or other of the linked monomers. The degenerate functions do not describe stationary states; in the actual dimer, the excitation is distributed over both monomeric components, and the energy exchange interaction splits the electronically excited state of the dimer into the linear combinations of the degenerate functions:

$$\Psi_I = 1/\sqrt{2}(\Phi_1 + \Phi_2)$$
$$\Psi_{II} = 1/\sqrt{2}(\Phi_1 - \Phi_2)$$

in a manner quite analogous to the electron exchange interaction in, for example, the hydrogen molecular ion.

The relative positions of the excited dimer levels I and II must now be determined, along with their separation in energy and the selection rules for radiational transitions from the ground state to the excited states of the dimer. The perturbing potential causing the splitting is taken to be the interaction of point multipoles in the unperturbed monomers, of which, in the case of dye monomers with strong absorption bands, the dipole-dipole interaction alone need be considered. This interaction varies inversely as the cube of the distance between the dipoles. On this basis it is shown (144,145) that the perturbing interaction occurs between the transition dipole moments of the individual monomers and that, when identical monomers are coupled in a sandwich arrangement, the energy of the degenerate state is lowered by the interaction by the amount

$$\Delta E = \mathbf{M}^2 / r_{AB}{}^3$$

where **M** is the transition dipole moment of the isolated monomer and r_{AB} is the distance between the interacting transition moments in the dimer. The higher of the dimeric excited states is an equal energetic amount above the degenerate level, hence the separation between states I and II is $2\mathbf{M}^2/r_{AB}^3$. The transition moment **M** of the monomer acts along the direction of the conjugated chain joining the two heterocyclic nuclei and in the molecular plane.

Which of the states Ψ'_I or Ψ'_{II} is the lower in energy depends on the phase relations of the directions in which the transition moments act. If the nodeless function Ψ'_I is taken as the lower state, the coupled transition moments must act in opposite directions, $\mathbf{M}_B = -\mathbf{M}_A$ for identical monomers, since this is the condition for the existence of an attractive force between the transition moments in a sandwich arrangement of the monomers. The negative sign of the function Ψ'_{II} is associated with a node which corresponds to a change in the phase relations of the directions of the interacting transition moments; in this mode of interaction, they vibrate so as to act in the same phase and repel each other, with a consequent increase of energy.

To determine the intensity of the transitions from the ground to the excited states of the dimer, we must evaluate the corresponding transition moments for the dimer. These are found to be (144,145) combinations of the individual monomeric transition moments:

$$\mathbf{M}_I = 1/\sqrt{2}(\mathbf{M}_A + \mathbf{M}_B)$$
$$\mathbf{M}_{II} = 1/\sqrt{2}(\mathbf{M}_A - \mathbf{M}_B)$$

where the suffixes I and II indicate transitions from the ground state to states Ψ'_I and Ψ'_{II}, respectively. Since for identical dimers in the sandwich arrangement the relation between the individual transition moments consistent with the state Ψ'_I being of lower energy is $\mathbf{M}_B = -\mathbf{M}_A$, the transition moment $\mathbf{M}_I$ is zero and $\mathbf{M}_{II} = 2\mathbf{M}/\sqrt{2}$. The radiational transition from the ground state to the lower, stabilized dimeric state is therefore forbidden for a homogeneous dimer in the sandwich arrangement. The integrated intensity of the short-wavelength dimeric band corresponding to $\mathbf{M}_{II}$ is, under the approximations of the theory, equal to twice that of the unperturbed monomeric band.

For a symmetrical sandwich dimer with parallel chromophores, this theory then predicts a strong absorption band at a shorter wavelength than the monomeric maximum, a weak band, of zero intensity under the conditions assumed in the theory, at a longer wavelength than the monomeric maximum, the separation between the two bands being proportional to the integrated intensity of the monomeric band and inversely proportional to the cube of the separation of the coupled monomers. These predictions are qualitatively in accord with observations on dimer spectra. The double-branched nature of the observed bands has already been described. The fact that the dimeric band of long wavelength, although usually feeble, is observable, probably indicates some asymmetry in the dimeric sandwich. It has also been shown for the dye series of Figure 58 that the separation between the two dimeric bands increases with the length of the chromophoric chain (142). This is consistent with the prediction of greater separation with increasing intensity of monomer absorption, since the intensity is known to increase with an increase in the length of the conjugated chain joining the heterocyclic nuclei in these dyes. It can therefore be concluded that the dimers of dye molecules with a planar configuration do indeed contain the monomers in a sandwichlike arrangement.

Mixed dimers can be formed from nonidentical monomers, such as cyanine dye monomers of different chain length or containing different heterocyclic nuclei (142). The mixed dimers show the same essential features as homogeneous dimers. Consistent with the greater asymmetry of the mixed dimer, the intensity of the long wavelength component of its absorption band is greater than that of the long wavelength branch of either of the parent homogeneous dimers.

The intense sharp absorption band at about 5730 Å, on the long wavelength side of the monomeric band near 5200 Å in the aqueous solution of the quinocyanine dye illustrated in Figure 60 appears at very high concentrations at which the solution is a semirigid gel. This type of band, frequently called a J band, first observed by Jelley (135) and by Scheibe (136,146,147), is found in concentrated aqueous solutions of a relatively small number of dyes, mostly cyanines containing the quinoline or other heterocyclic nucleus. In solution the J band is associated with a nematic state in which a number of monomeric units seem to be aggregated to form threadlike polymers held together by the van der Waals attraction between parallel monomeric planes in a card pack arrangement threaded by the axis. The narrow band is polarized along the direction of the axis of the aggregate, i.e., in a direction inclined to the direction of the monomeric chromophore and its corresponding transition moment (146). An increase in temperature breaks down the aggregate structure, the J band first diminishing in intensity as the temperature is gradually raised in favor, first, of aggregates of the type already described, absorbing at shorter wavelengths than the monomer, and ultimately only the monomeric spectrum remains. Some dyes adsorbed on silver halide crystallites exhibit the J band and sensitive photographic plates to the corresponding wavelengths, although this type of absorption is not necessary to cause sensitization (147).

With regard to the interpretation of the J band, an important theoretical point is that if two monomers in an excited dimer were arranged head to tail to form a linear dimer instead of the sandwichlike dimer already discussed, the excited state I of lower energy requires that the interacting monomeric transition moments vibrate in the same direction, as otherwise the interaction would be repulsive. Correspondingly, in the upper state II the directions are opposite (143,145). Hence, for the linear interaction of the monomeric transition moments, the radiational transition from the ground to the lower excited state of the dimer will be intense, while that to the upper state will be weak or forbidden. Dimers of this nature do not seem to have been observed among dyes, as is to be expected because of the relatively weak van der Waals forces between planar molecules in head to tail array. If, however, a linear array of interacting transition moments can be found in the J aggregate, the strong J band, bathochromic to the molecular band, could be understood. In the case of the multimonomeric polymer, the head to tail interaction gives rise to a band of energy levels instead of to the dimeric pair. However, the selection rule for the polymer is the same as that for the linear dimer; the strong absorption band involves a transition to the lowest level of the band of excited levels, when the individual interacting transition moments vibrate in the same direction. Such a linear array of transition moments parallel to the axis of the aggregate would be realized if the individual monomers were strung along the axis in a card pack arrangement with parallel planes, with the chromophores inclined at an angle α to the axis under 90°. For this model, McRae and Kasha have shown (148) that if α exceeds 55°, the polymer behaves as a sandwichlike aggregate. In this case the strong absorption band is displaced to the shorter wavelengths from the monomeric band. If less than 55°, i.e., when the molecular planes and the chromophores become more nearly parallel to the axis, the polymer behaves as a linear array of transition moments, for which the strong absorption band is at longer wavelengths than the monomeric band. This last model seems to describe essential features of the spectrum of the *J* aggregate, but the detailed structure of this form of dyes is still uncertain.

The strong tendency of dyes to polymerize and to be adsorbed to polar surfaces seems to be another manifestation, besides the color, of the nonlocalization of the electrons occupying the π orbitals. The intramolecular mobility of these electrons is equivalent to high polarizability in the direction of the chain length of the dye molecule, with the result that the dispersion forces between dye molecules are high, leading to ready aggregation, especially in media of high dielectric constant, and to ready adsorption by surfaces.

D. Porphyrins (149), Chlorophylls (150), and Other Natural Pigments

An important class of naturally occurring pigments, including hemin, chlorophyll, and phthalocyanines, is based structurally upon the fused pyrrole rings of the porphin system (Fig. 61). The porphin ring is composed of four pyrrole rings connected by CH bridges and is remarkedly aromatic in

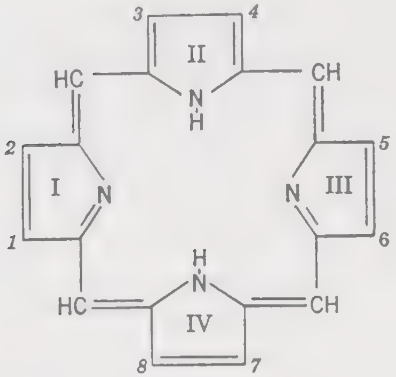

Fig. 61. Structure of porphin.

character. The absorption spectra of free base porphins consist of an intense band near 4000 Å (ϵ = 300,000–600,000), called the Soret band, and four moderately intense bands (ϵ = 5000–30,000) in the 5000–6600 Å region (Fig 62). The free base porphins are often empirically classified as etio, rhodo, or phyllo, depending upon the appearance of the long-wavelength spectra (151). When the free base porphin is converted into a more symmetrical metal com-

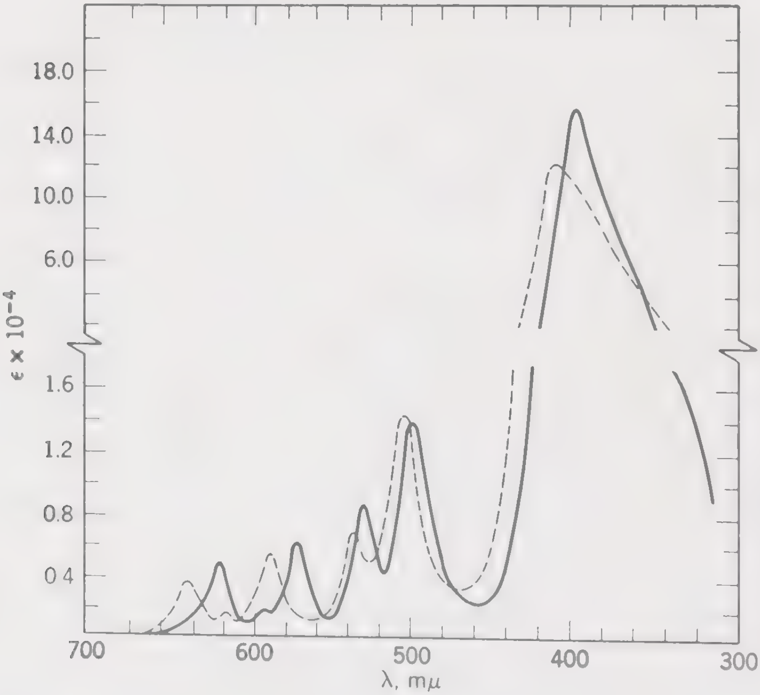

Fig. 62. Spectra of etioporphyrin II (——) and *n*-methyletioporphyrin II (– – –) [From J. Erdman and A. Corwin, *J. Am. Chem. Soc.*, **68**, 1885 (1946).]

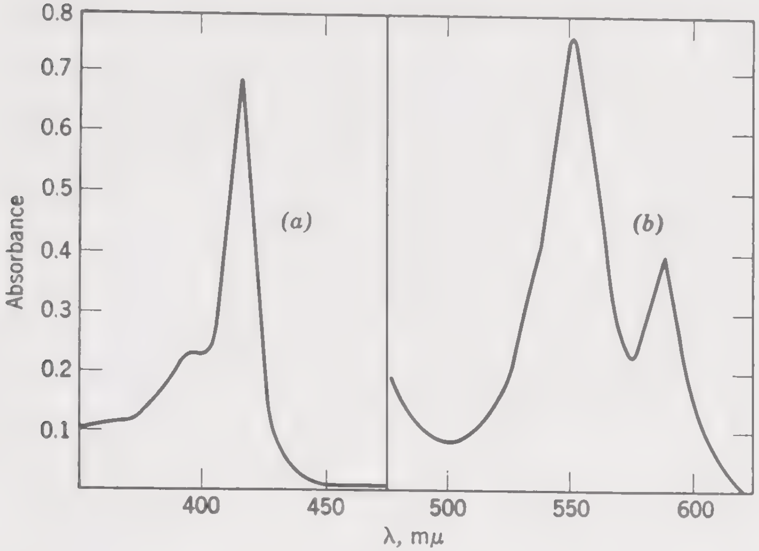

Fig. 63. Spectra of Sr^{2+} mesoporphyrin IX dimethyl ester: (*a*) 0.1 mm path length; (*b*) 2.0 mm path length. [From R. S. Becker and J. B. Allison, *J. Phys. Chem.*, **67**, 2669 (1963).]

plex, the four-band system in the visible region is converted into a predominantly two-band system. Due to the decreased symmetry of the free base porphins, as compared to the metallo complexes, the degenerate excited state of the metalloporphyrins is split into two components in the free base compounds giving rise to the four-band spectrum (Fig. 63). If the metal is changed within a fixed porphin skeleton, the intensity of the long wavelength band varies and the entire spectrum is shifted (152,153). The visible bands are attributed to $\pi \rightarrow \pi^*$ transitions between the highest filled orbital f and the lowest unfilled orbital g, which is doubly degenerate in the metalloporphyrins. The Soret band is assigned to the $e \rightarrow g$ transition. The spectra of the reduced porphins, chlorins and tetrahydroporphins, are similar to the other porphins. However the Soret band is less intense than in the porphins, and the long wavelength band is much more intense. Metal complexation does not simplify the visible spectra as much as in the porphin derivatives (154).

The chlorophylls are magnesium complexes of porphin derivatives. Their spectra are similar to the free base porphins with the Soret band in the 4000–4500 Å region and the less intense visible system in the 5000–7500-Å region (Fig. 64). Similar compounds such as pheophytins, pheophorbides, and chlorophyllides have spectra like those of the chlorophylls (150,155). The tetraazatetrabenzporphins or phthalocyanines exist both as free bases and as a variety of colored metal complexes. The spectra of these compounds are similar to the other porphins (156).

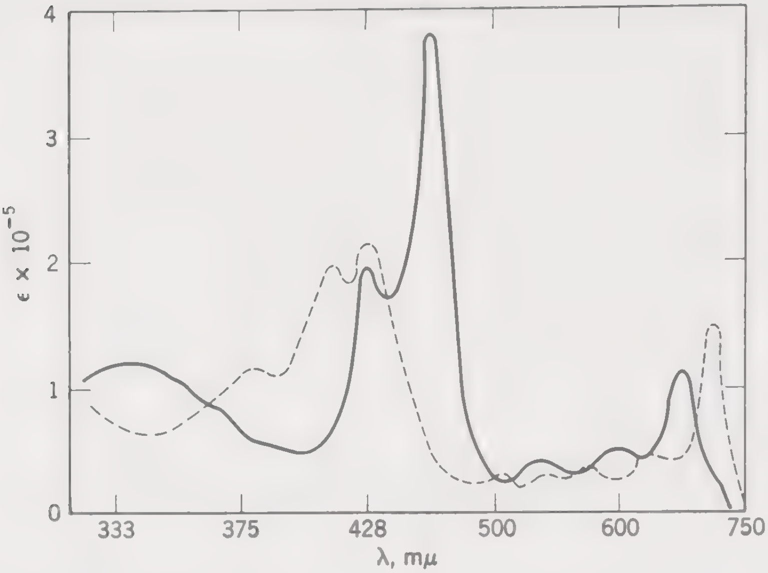

Fig. 64. Spectra of chlorophylls: (——) chlorophyll *b*; (-----) chlorophyll *a*.

An important class of polyenes, which has been extensively studied, is the carotenoids. This class contains carotene, a pigment from carrots; lycopene, a pigment from tomatoes; xanthophyll, a pigment from green leaves; zeaxanthin, a pigment from corn; fucoxanthin, a pigment of brown algae; capsanthin, a pigment of paprika; astacin, a pigment of lobster shells; and many others. Lycopene contains forty carbon atoms, eleven double bonds, and has a molar extinction coefficient of 150,000 at 4500 Å (see Fig. 65).

Many different *cis trans* modifications are possible, not only about the double bonds, but also about the single bonds as well, since they possess

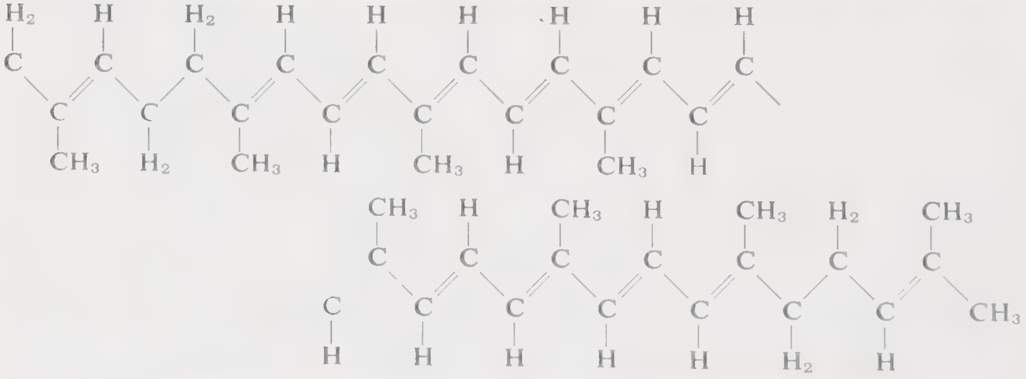

some double-bond character. It will be remembered from the discussion of conjugated diolefins in Section III-B-4 that the transition moment for the first excitation is larger in the *trans* than in the *cis* modification. On the other

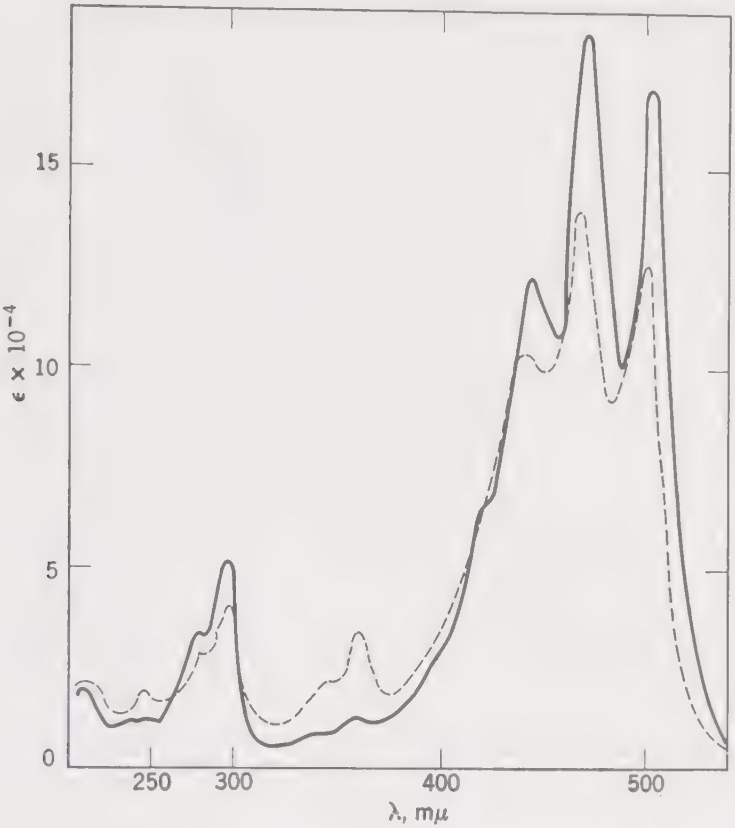

Fig. 65. The spectrum of lycopene before (solid line) and after (broken line) treatment with iodine (157).

hand, the transition moment is zero for the second excitation in the *trans* modification. In a polyene the same rules would apply to a completely *trans* isomer as apply to the *trans* modification of butadiene. If the polyene has a *cis* configuration at the center bond only, the same rules would apply as for the *cis* modification of butadiene. For *cis* configurations away from the center bond, the effect is smaller. It has been found that the absorption at 4600 Å is strongest in the natural lycopene (Fig. 65) (157). After reflux or treatment with iodine, the band becomes weaker and a new band appears at 3500 Å. If the new band may be assigned to the second excitation, one may conclude that the natural lycopene is mainly *trans* and that either of the two treatments effects a certain amount of *trans–cis* conversion. In strong support of this argument is the fact that another isomer, neolycopene, has a fairly strong band at 3500 Å, as well as at 4600 Å. On treatment of this substance with iodine, the intensity of the 3500-Å band decreases and that of the 4600-Å band increases (see Fig. 66). It appears that the neolycopene is predominantly in the *cis* form and that the iodine catalyzes a *cis–trans* conversion.

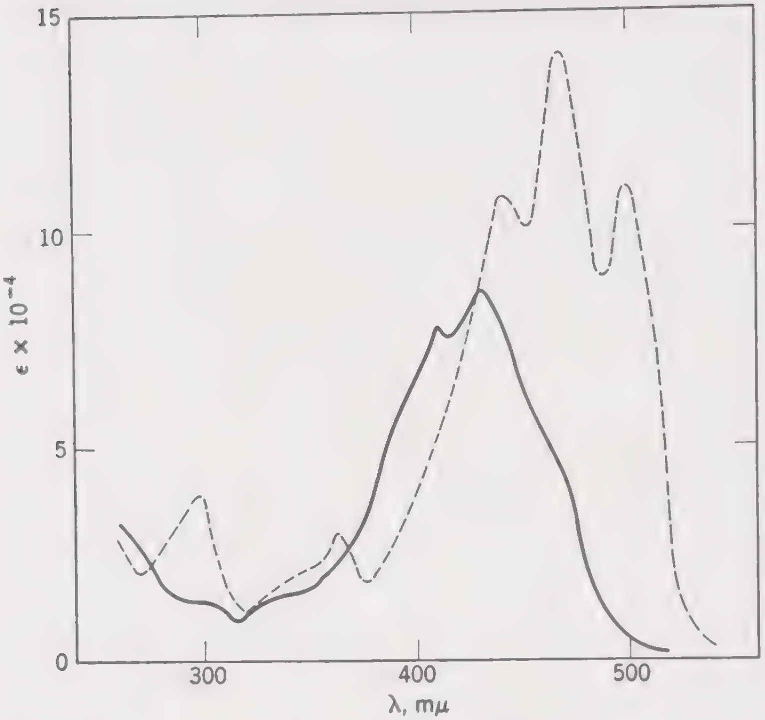

Fig. 66. The spectrum of *cis*-lycopene before (solid line) and after (broken line) treatment with iodine (157).

E. The Effect of Environment

The discussion of absorption spectra in terms of energy levels and transition probabilities applies ideally to isolated molecules. If a molecule is subjected to forces from neighboring molecules, the wave length, the intensity, the band breadth, and the vibrational pattern of the absorption band may be changed. Electronic spectra may be obtained in many different environments: vapor state, liquid state, solid state, and liquid and solid solution. Since the intermolecular forces differ in each environment, the spectrum of a chromophore may change depending upon the particular environment (see Fig. 67).

The low pressure vapor spectrum approaches most closely the spectrum of the isolated molecule. Here the spectra with highest resolution are most frequently obtained. Often the vibrational structure and occasionally the rotational structure can be resolved. At higher pressures or in high partial pressures of a foreign gas the bands are broadened. The width of an energy level is given by $\Delta E \sim h/\Delta\tau$. Here $\Delta\tau$ is the lifetime of the excited state which is decreased by collisions. The effectiveness of a collision is determined by the intermolecular forces such as dipole dipole, dipole induced dipole, and induced dipole induced dipole forces. These forces are in turn determined by

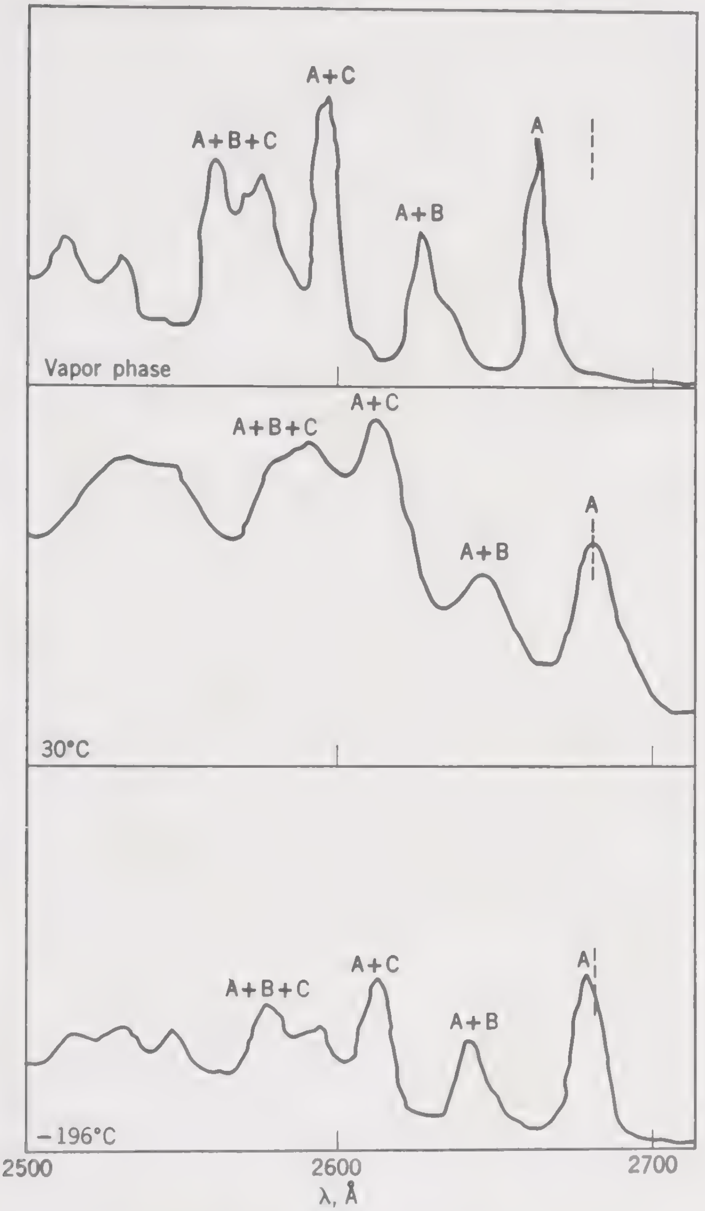

Fig. 67. The spectrum of ethylbenzene in the vapor and in nonpolar solution at two temperatures. The solvent used was a mixture of propane and cyclohexane. The dotted line marks the approximate center of the 30°C solution peak. (From W. F. Hamner, Ph.D. thesis, University of Texas, 1950.)

the polarizabilities and the dipole moments of the interacting molecules. Helium with a low polarizability and zero dipole moment exerts only a small influence on a vapor spectrum.

At higher pressures or in the presence of high partial pressure of a nonpolar foreign gas, the spectrum of a nonpolar molecule is also generally shifted to the red. There appear to be two effects contributing to this shift, one dependent upon the polarizability of the foreign gas and another with unknown dependence. Normally the polarizability dependent shift is dominant, yielding a red shift. However, in foreign gases with very low polarizability the other effect may become evident, e.g., benzene vapor shows a blue shift with increasing helium pressure (158). An explanation of the polarizability dependent effect is that the process of excitation may be regarded as producing a separation of charge. The presence of neighboring molecules generally reduces the amount of work required for charge separation thus producing a red shift. In this process the neighboring molecules are polarized, and the shift is therefore sometimes called the polarization red shift. The magnitude of this red shift depends upon the intensity of the particular transition and the polarizability or refractive index of the medium. An approximate expression for this shift to lower frequencies is given by

$$\Delta\nu = A\mathbf{Q}^2[(K-1)/(2K+1)]$$

Here A is a constant, $\mathbf{Q}$ is the transition moment, and K is the dielectric constant of the medium which is a measure of its polarizability. In addition to the polarization red shift there may be additional effects which produce shifts of the absorption spectrum. These shifts are due to changes in the intermolecular forces between the chromophore molecules in the ground and excited states and the surrounding molecules. The magnitude and direction of these effects depend upon the dipole moments and polarizabilities of the chromophore and interacting molecules.

1. SOLVENT EFFECTS (159–161)

The shifts of absorption bands occurring upon a change from vapor to solution or from one solvent system to another are the result of differences in solvation energies of the solute in the ground and excited states. The shift $\Delta\nu = \nu_{\text{sol}} - \nu_{\text{vap}}$ is equal to the difference in the solvation energies of the solute in the ground and excited states, $S_G - S_E$. Likewise, the shift of an absorption band of a chromophore in solution caused by a change of solvent is given by the difference between the respective shifts from vapor to each

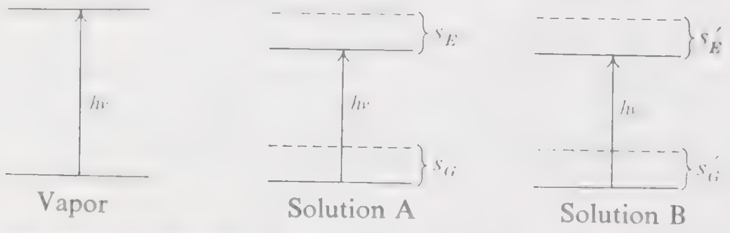

solvent system or alternantly by the change in the difference of solvation energies, $S_G - S_E$, in each solvent system.

$$\Delta\nu_{S'-S} = \nu'_{\text{sol}} - \nu_{\text{sol}} = \nu'_{\text{sol}} - \nu_V - (\nu_{\text{sol}} - \nu_V) = (S'_G - S'_E) - (S_G - S_E)$$

where the dashed symbols refer to one solvent, the undashed, to the other, and ν_V is the frequency of the chromophore in the vapor state. The solvation energies include induced dipole–induced dipole interactions between nonpolar solutes and solvents, induced dipole–dipole forces between polar solutes and nonpolar solvents or vice versa, and dipole–dipole interactions between polar solutes and solvents. In addition to these intermolecular forces there are two effects classified as Franck-Condon effects which sometimes affect the solvation energies. The Franck-Condon effects are of two kinds, orientation and packing strain.

Orientation strain may arise when a ground state molecule is surrounded by a cage of oriented solvent molecules which are arranged in positions of minimum potential energy for the ground state of the solute. Upon excitation, according to the Franck-Condon principle, the solvent molecules remain in this same configuration which may not correspond to the equilibrium state for the excited molecule. Depending upon the change in the dipole moment of the solute upon excitation, this orientation strain may increase or decrease the excited state solvation energy. Orientation strain is to be expected in cases where both solute and solvent are polar and where the solute dipole moment is changed upon excitation. If excitation alters the amount of hydrogen bonding between solute and solvent, then orientation strain is also expected. Packing strain is expected to occur in cases where the molecule in the excited state is substantially larger than in the ground state. The excited state molecule will be compressed in effect by the ground state solvent arrangement resulting in an excited state energy which is higher than the equilibrium energy. Since most organic molecules do not change size to any great extent upon excitation, packing strain is normally negligible compared to the other effects.

The spectra of nonpolar solutes in nonpolar solvents are shifted to the visible compared to their vapor spectra (Table XXI). This is due to the polarization red shift as mentioned previously. The expression for the polarization shift always predicts a red shift upon going from vapor to solution which is larger for allowed transitions and more polar solvents. The magnitude of this general red shift is rather small for a nonpolar solute and solvent. Since the solute does not have a dipole moment in either the ground or excited states, there are no solute–solvent orientation forces and therefore no orientation strain in the excited state. Some packing strain may occur in the smaller organic molecules. For the usual case of increased size in the excited state, packing strain would result in a shift toward the ultraviolet region (blue shift).

TABLE XXI

Shifts of Maximum Absorption of Aromatic Hydrocarbons in Various Solvents[a]

Solvent	Anthracene		Naphthalene		Naphthacene	
	^1L_a ($f = 0.1$)	^1B_b ($f = 2.3$)	^1L_a ($f = 0.2$)	^1L_b ($f = 0.002$)	^1L_a ($f = 0.1$)	^1B_b ($f = 1.9$)
Perfluoromethyl-cyclohexane[b]	521	1051	485			
C_5H_{12}	866	1756	928	171	854	1338
$C_5H_{11}Cl$	976	1925	1060	188	968	1535
$C_7H_{15}OH$	991	1976	1237	195	994	1438
$C_8H_{17}NH_2$	1023	2067	1119	228	1033	1657
C_4H_9Br	1028	2111	1151	212	1044	1709
$C_8H_{17}SH$	1054	2193	1188	250	1080	1777
C_6H_6	1103			252	1116	
C_3H_7I	1159			270	1156	
C_5NH_5	1201			271	1249	
CS_2	1625				1556	

[a] Data are in reciprocal centimeters. Unpublished data from Humble Oil and Refining Co., Baytown, Texas. We wish to thank Dr. B. H. Johnson for these data.

[b] The shifts are red shifts in solution referred to the vapor data. Vapor values used are: anthracene—^1L_a (3624.5 Å); ^1B_b (2406.0 Å); naphthalene—^1L_a (2678.8 Å); ^1L_b (3080.7 Å); naphthacene—^1L_a (4500.4 Å); ^1B_b (2635.7 Å). f is the oscillator strength.

However, unless the packing strain is larger than the general polarization shift, a total red shift will be observed.

The case of a solution of a nonpolar solute in a polar solvent is similar to the situation of a nonpolar solute in a nonpolar solvent (Table XXI). Since the solute is nonpolar, no orientation strain will occur. There may be slight packing strain since the polar solvent molecules may interact among themselves to form a cage around the solute molecule. The polarization red shift will be the dominant effect observed, but it may be reduced by the smaller blue shift arising from packing strain.

The situation with a polar solute in a nonpolar solvent is complicated by the occurrence of solute dipole–induced dipole interactions with the solvent. Again, since the solvent is nonpolar, there will be no appreciable orientation strain. The primary contributions to the total shift are from the general polarization red shift and the differences of the dipole–induced dipole interactions in the excited and ground states. If the solute dipole moment increases upon excitation, the dipole–induced dipole interactions will be greater in the excited state than in the ground state, and a red shift will result. Likewise, for a decrease in the solute dipole moment, a blue shift is expected. The resulting total shift of the band for a solute with decreasing dipole moment may be either red or blue depending upon the relative magnitudes of the two effects. However, for a solute with increasing dipole moment, which is the normal behavior in N → V transitions of most organic compounds; the total shift should always be toward the red since it is composed of the polarization red shift and the dipole–induced dipole red shift. If the dipole moment does not change upon excitation, the polarization red shift will be dominant.

Shifts of absorption spectra of polar solutes in polar solvents are predominantly due to differential dipole–dipole interactions between the solute and solvent in the ground and excited states and to orientation strain in the excited state. If the dipole moment is not changed upon excitation, there will be no orientation strain. The orientation strain which occurs upon a change of dipole moment of the solute will result in a blue shift if the solute dipole decreases and a red shift if the dipole increases upon excitation. For the case where the solute dipole moment does not change upon excitation, the dipole–dipole interactions will be the same in both excited and ground states, and the polarization red shift will be dominant. If the solute dipole moment increases upon excitation, the dipole–dipole forces will be stronger in the excited than in the ground state, and a red shift should result. This red shift is superimposed upon the general polarization red shift and the orientation strain red shift resulting in an overall red shift. However, if the solute dipole moment decreases upon excitation, a blue shift is predicted from the change in dipole–dipole forces. This is superimposed upon the general polarization red shift and the orientation strain blue shift. The total shift will usually be a blue shift since the sum of the dipole–dipole and orientation shifts should be greater than the polarization red shift. It should be emphasized that these shifts are all relative to the vapor spectrum.

2. THE CLASSIFICATION OF TRANSITIONS BY SOLVENT EFFECTS (162,163)

The effect of changing the solvent system upon the position of the bands in an absorption spectrum may often be used to classify the bands as $\pi \rightarrow \pi^*$, $n \rightarrow \pi^*$, or $n \rightarrow \sigma^*$. Usually, the solvents used in such a study are a nonpolar one such as hexane and a polar, or more commonly a hydroxylic solvent such as an alcohol or water. If a band shifts to shorter wavelengths upon a change of solvent from hexane to alcohol, it is called a "blue shift band"; if it shifts to the red, a "red shift band" (162). The blue shift bands are attributed to $n \rightarrow \pi^*$ or $n \rightarrow \sigma^*$ transitions, and the red shift bands to $\pi \rightarrow \pi^*$ transitions. The validity of these generalizations follow from the previous discussion of general solvent effects and considerations of the effect of hydrogen bonding on the spectra (164).

For a nonpolar solute undergoing a $\pi \rightarrow \pi^*$ transition, the shift of the band upon a change from a nonpolar to polar solvent depends upon the difference in the polarization red shifts in the two solvents. Since this shift is larger in polar solvents than in nonpolar solvents, a red shift will be observed. If a polar solute undergoes a $\pi \rightarrow \pi^*$ excitation, then the band shift upon a change from a nonpolar to polar solvent will depend upon the difference between the polarization red shift and dipole–dipole shift in the polar solvent and the polarization red shift and dipole–induced dipole shift in the nonpolar solvent. In the majority of cases the dipole moment of the molecule will be greater in the excited state and both the dipole–dipole and dipole–induced dipole shifts will be red shifts. Since the dipole–dipole and polarization red shifts in the polar solvent will be greater than the shifts in the nonpolar solvent, a red shift will be observed (Fig. 68).

The verification of a blue shift band as a transition involving a nonbonding orbital also follows from the general discussion of solvent effects. In the majority of molecules having nonbonding electrons, the nonbonding electrons are localized upon the more electronegative atom of a polar group. Upon excitation the localized nonbonding electron is delocalized over the less electronegative atoms over which the excited orbital (π^* or σ^*) extends. Thus, the dipole moment of the polar molecule is reduced in the excited state. The shift of such a band upon a change from a nonpolar to polar solvent will depend upon the difference between the dipole–dipole and orientation strain blue shifts in the polar solvent and the polarization red shift and dipole–induced dipole blue shift in the nonpolar solvent. Since the interactions in the polar solvent will be stronger than those in the nonpolar solvent, a blue shift will be observed. A similar explanation may be used if hydrogen bonding

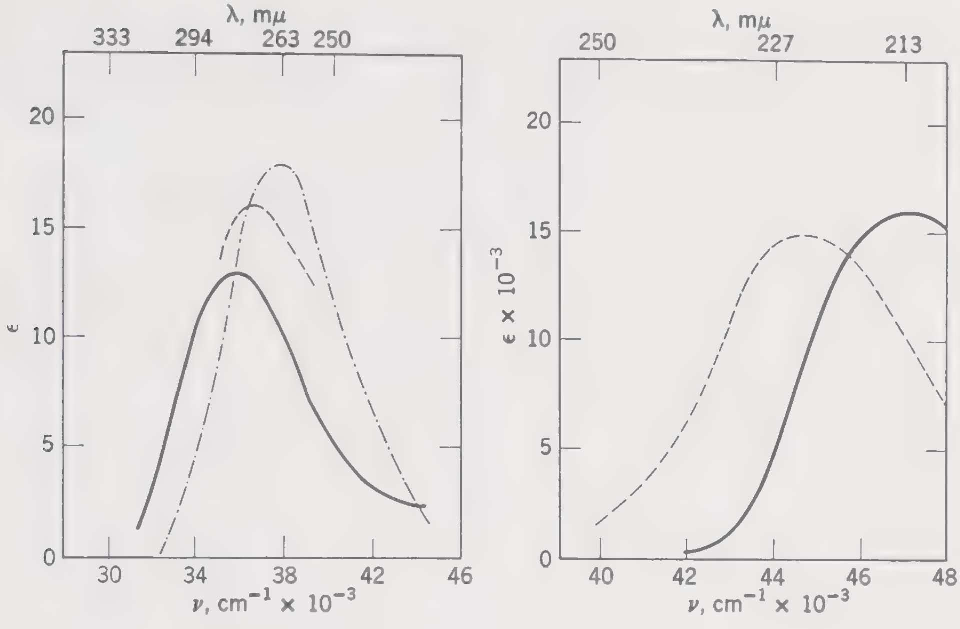

(a) (b)

Fig. 68. Solvent effects on: (*a*) the $n \rightarrow \pi$ band of acetone, (——) heptane, (– – –) ethanol, (–·–) water; (*b*) the $\pi \rightarrow \pi^*$ band of crotonaldehyde, (——) heptane, (– – –) water (160).

between the nonbonding electrons and the solvent occurs. The hydrogen bonding which stabilizes the ground state will be weakened by the shift of electron density away from the nonbonding center upon excitation, and a blue shift of the band will be observed relative to the band position in a non-hydrogen bonding solvent (Fig. 68). Since it may be possible to have an $n \rightarrow \sigma^*$ or $n \rightarrow \pi^*$ transition in which the excited state has a greater dipole moment than the ground state, the best indication of the involvement of nonbonding electrons in a transition is a large blue shift of the suspected band upon solution in a strong acid solution which is capable of binding the nonbonding electrons by protonation.

3. THE EFFECTS OF TEMPERATURE AND PRESSURE

An increase in pressure affects the spectrum of a compound by changing the dielectric constant, index of refraction, and density of the solvent. The band shifts induced by pressure changes depend upon the solvent properties and intensities of the bands for nonpolar solutes and also upon the change in dipole moment for polar solutes. Since different electronic transitions normally have different intensities, the band shifts caused by increased pressure are different for each transition. Thus, in some compounds the pressure induced band shifts may be used to distinguish between electronic transitions. In the spectrum of azulene a band located at 2956 Å near the B_b transition has been assigned to a transition other than the B_b transition (165). Experimentally the two bands show different behavior upon changing the pressure of the system thus verifying the assignment of the 2956-Å band as a separate transition (166) (see Fig. 69).

A change in temperature may affect the spectrum of a compound by altering the properties of the solvent, such as refractive index, dielectric constant, and density, and also by causing a redistribution of intensity among the vibrational bands. In the case of a nonpolar solute dissolved in a nonpolar solvent there are two opposing shifts operating (167,168). Upon decreasing the temperature of the system, a red shift occurs because of the increased density of the solvent and increased solute–solvent interactions. Opposing this red shift is a blue shift due to decreased population of the higher vibrational levels of the ground state resulting from the lower temperature. Transitions between these higher vibrational levels in the ground state and the excited state vibrational levels are called "hot bands" since they disappear upon lowering the temperature. The observed band shift depends upon the relative magnitudes of the polarization red shift and the hot band blue shift. Since the red shift is intensity dependent, absorption bands of different intensities will exhibit different temperature dependent shifts. This behavior may be used to distinguish between closely spaced electronic transitions or in some cases to reveal bands in low-temperature spectra which may be hidden under stronger bands in room-temperature spectra.

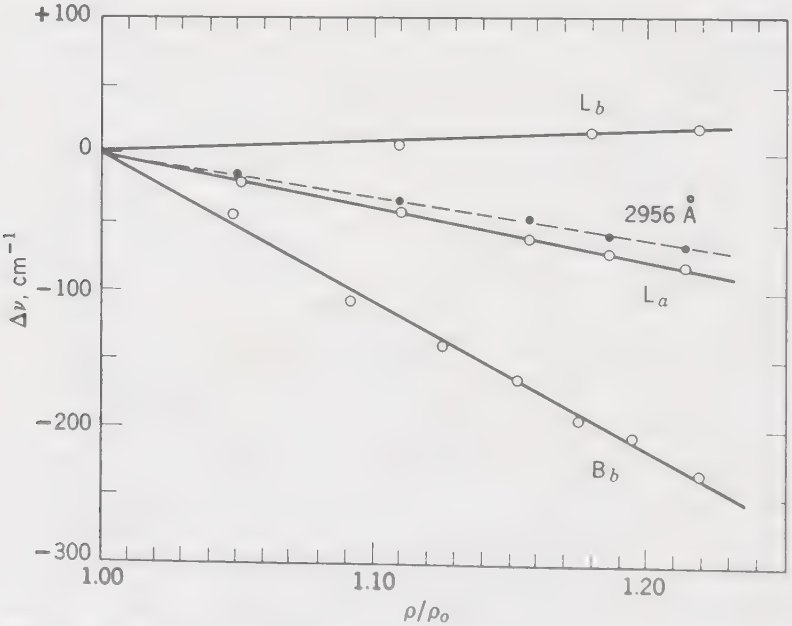

Fig. 69. Effect of pressure upon the spectrum of azulene in pentane. ρ/ρ_0 is the relative density of pentane at various applied pressures (166).

List of Symbols

ϕ = General atomic orbital
Ψ = General molecular orbital

s_A	*s* orbital on atom A
z_A	*p* orbital with orientation in the direction of the bond
x_A	*p* orbital with orientation perpendicular to the bond and perpendicular to the plane of the molecule if there is one
y_A	*p* orbital with orientation perpendicular to the bond and lying in the plane of the molecule if there is one

$di_A = s_A + \lambda z_A$	Digonal orbital
$tr_A = s_A + \lambda z_A + \lambda' y_A$	Trigonal orbital
$te_A = s_A + \lambda x_A + \lambda' y_A + \lambda'' z_A$	Tetrahedral orbital

The principal quantum number is added to the atomic orbital symbol to indicate an excited atomic state, e.g., $5s_A$.

MOLECULAR ORBITALS

σ	Any bonding molecular orbital made from combinations on separate atoms of *s*, *z*, *tr*, and *te*, e.g., $= s_A + \lambda tr_B$
π	A bonding molecular orbital formed from *y* or *x*, e.g., $\pi_y = y_A + y_B$
$(\ )^*$	Any antibonding molecular orbital, e.g., $\sigma^* = s_A - \eta tr_B$

TRANSITIONS

N → V	From a bonding orbital in the ground state of a molecule to a higher energy orbital formed from the same atomic orbitals, e.g., $s_A + s_B \rightarrow s_A - s_B$. For transitions between π orbitals these are often called $\pi \rightarrow \pi$ or $\pi \rightarrow \pi^*$.
N → Q	From a nonbonding orbital localized on an atom to an antibonding orbital or other higher energy orbital, e.g., $y_B \rightarrow s_A - \lambda z_B$. For transitions to π orbitals these are often called *n* (nonbonding) $\rightarrow \pi$ or $n \rightarrow \pi^*$.
N → R	From an orbital in the ground state to one of high enough energy for the molecule ion core to resemble an atomic ion. Such a transition is often the member of a series which terminates in ionization. The wave numbers of the bands in the series can often be represented by $\nu = \nu_\infty - R/(n + a)^2$ where ν_∞ is the ionization energy in cm^{-1} and *a* is approximately constant.

INTEGRALS

$\alpha = \int x_A H x_A \, d\tau$	Coulomb integral for *x* orbitals on carbon
$\alpha + \delta\beta = \int x_A H x_A \, d\tau$	Coulomb integral for *x* orbitals on elements other than carbon (for δ positive the element is more electronegative than carbon)
$\beta = \int x_A H x_B \, d\tau$	Resonance integral for *x* orbitals on carbon
$S = \int x_A x_B \, d\tau$	Overlap integral for *x* orbitals on carbon
$J = \int \phi_A(1)\phi_B(2)(e^2/r_{12})\phi_A(1)\phi_B(2) \, d\tau$	Coulomb integral
$K = \int \phi_A(1)\phi_B(2)(e^2/r_{12})\phi_A(2)\phi_B(1) \, d\tau$	Exchange integral

General References

C. A. Coulson, *Valence*, 2nd ed., Oxford University Press, London, 1961.

A. Streitwieser, Jr., *Molecular Orbital Theory for Organic Chemists*, Wiley, New York, 1961.

L. N. Ferguson, *Modern Structural Theory of Organic Chemistry*, Prentice Hall, New York, 1963, Chap. 5.

A. E. Gillam and E. S. Stern, *An Introduction to Electronic Absorption Spectroscopy in Organic Chemistry*, Arnold, London, 1960.

G. Herzberg, *Electronic Spectra and Electronic Structure of Polyatomic Molecules*, Van Nostrand, New York, 1966.

J. N. Murrell, *The Theory of the Electronic Spectra of Organic Molecules*, Methuen, London, 1963.

C. Sandorfy, *Electronic Spectra and Quantum Chemistry*, Prentice Hall, Englewood Cliffs, 1964.

H. H. Jaffe and M. Orchin, *Theory and Applications of Ultraviolet Spectroscopy*, Wiley, New York, 1962.

S. F. Mason, *Quart. Rev.*, **15**, 287 (1961).

A. J. Scott, *Interpretation of Ultraviolet Spectra of Natural Products*, Pergamon Press, New York, 1964.

Collections of Spectra and Spectral Data

"Ultraviolet Spectral Data," American Petroleum Institute Research Project 44, Carnegie Institute and U.S. Bureau of Standards.

R. A. Friedel and M. Orchin, *Ultraviolet Spectra of Aromatic Compounds*, Wiley, New York, 1951.

Landolt-Bornstein, *Zahlenwerte and Funktionen*, Vol. I, Part 3, Springer, Berlin, 1951, pp. 248–320.

L. Lang, Ed., *Absorption Spectra in the Ultraviolet and Visible Region*, Hungarian Academy of Science, Part I, 1959, Part II, 1961, Part III, 1962, Part IV, 1963.

M. J. Kamlet, Ed., *Organic Electronic Spectral Data*, Vol. I, Interscience, New York, 1960.

H. E. Ungnade, Ed., *Organic Electronic Spectral Data*, Vol. II, Interscience, New York, 1960.

J. P. Phillips and F. C. Nachod, Eds., *Organic Electronic Spectral Data*, Vol. IV, Interscience, New York, 1963.

O. H. Wheeler and L. A. Kaplan, Eds., *Organic Electronic Spectral Data*, Vol. III, Interscience, New York, 1966.

References

1. See for example: LiH: J. C. Browne and F. A. Matsen, *Phys. Rev.*, **135**, 1227 (1964), $He_2(^3\Sigma_u^+)$: R. D. Poshusta and F. A. Matsen, *Phys. Rev.*, **132**, 307 (1963); He_2^+: P. N. Reagan, J. C. Browne, and F. A. Matsen, *Phys. Rev.*, **132**, 304 (1963).
2. See I. Fischer-Hjalmars, *Theoret. Chim. Acta*, **4**, 332 (1966) and references listed therein.
3. G. R. Taylor and R. G. Parr, *Proc. Natl. Acad. Sci.*, **38**, 154 (1952).
4. R. G. Parr, *Quantum Theory of Molecular Electronic Structure*, Benjamin, New York, 1963.

5. C. A. Coulson, *Valence*, 2nd ed., Oxford Univ. Press, London, 1961; J. N. Murrell, S. F. Kettle, and J. M. Tedder, *Valence Theory*, Wiley, New York, 1965.
6. A. Streitwieser, Jr., *Molecular Orbital Theory for Organic Chemists*, Wiley, New York, 1961; L. Salem, *Molecular Orbital Theory of Conjugated Systems*, Benjamin, New York, 1966.
7. J. E. Lennard-Jones and C. A. Coulson, *Trans. Faraday Soc.*, **35**, 811 (1939); C. A. Coulson and H. C. Longuet-Higgins, *Proc. Roy. Soc.* (*London*), **A192**, 16 (1947).
8. H. Kuhn, *J. Chem. Phys.*, **17**, 1198 (1949); *Fortschr. Chem. Org. Naturstoffe*, **17**, 404 (1959).
9. J. R. Platt, *J. Opt. Soc. Am.*, **43**, 252 (1953); *Radiation Biology*, A. Hollaender, Ed., McGraw-Hill, New York, 1956, p. 71.
10. R. S. Mulliken, *J. Chem. Phys.*, **3**, 517 (1935); G. Moe and A. B. F. Duncan, *J. Am. Chem. Soc.*, **74**, 3140 (1952); J. E. Lennard-Jones and G. G. Hall, *Discussions Faraday Soc.*, **10**, 18 (1951).
11. R. D. Brown, *J. Chem. Phys.*, **45**, 1482 (1966).
12. D. P. Craig, *Proc. Roy. Soc.* (*London*), **A200**, 272, 401 (1950).
13. P. G. Wilkinson and R. S. Mulliken, *J. Chem. Phys.*, **23**, 1895 (1955); W. J. Potts, *J. Chem. Phys.*, **23**, 65 (1955).
14. J. Stieglitz, *Proc. Natl. Acad. Sci.*, **9**, 303 (1923).
15. R. S. Mulliken, *Rev. Mod. Phys.*, **14**, 265 (1942); R. S. Rasmussen, D. D. Tunnicliff, and R. R. Brattain, *J. Chem. Phys.*, **11**, 433 (1943).
16. R. B. Woodward, *J. Am. Chem. Soc.*, **64**, 72 (1942).
17. R. S. Mulliken, *J. Chem. Phys.*, **3**, 517 (1935); *Can. J. Chem.*, **36**, 10 (1958); G. Moe and A. B. F. Duncan, *J. Am. Chem. Soc.*, **74**, 3136 (1952); C. K. Ingold and G. W. King, *J. Chem. Soc.*, **1953**, 2702; K. K. Innes, *J. Chem. Phys.*, **22**, 863 (1954). A. D. Walsh, *J. Chem. Soc.*, **1953**, 2260.
18. C. K. Ingold and G. W. King, *J. Chem. Soc.*, **1953**, 2725; K. K. Innes, *J. Chem. Phys.*, **22**, 863 (1954).
19. W. C. Price, *J. Chem. Phys.*, **4**, 539 (1936); R. S. Mulliken, *Phys. Rev.*, **47**, 413 (1935).
20. R. S. Mulliken, *Phys. Rev.*, **61**, 277 (1942) and earlier papers; see ref. 22 for further discussion.
21. H. H. Jaffe and M. Orchin, *Theory and Applications of Ultraviolet Spectroscopy*, Wiley, New York, 1962, p. 476.
22. K. Kimura and S. Nagakura, *Spectrochim. Acta*, **17**, 166 (1961); H. Tsubomura, K. Kimura, K. Kaya, J. Tanaka, and S. Nagakura, *Bull. Chem. Soc. Japan*, **37**, 417 (1964).
23. R. S. Mulliken, *J. Chem. Phys.*, **3**, 564 (1935); H. L. McMurry, *J. Chem. Phys.*, **9**, 231, 241 (1941); J. W. Sidman, *Chem. Rev.*, **58**, 689 (1958); M. Kasha, "Nature and Significance of $n \to \pi^*$ Transitions," *Light and Life*, W. D. McElroy and B. Glass, Eds., Johns Hopkins Press, Baltimore, 1961.
24. G. W. Robinson and V. E. Digiorgio, *Can. J. Chem.*, **36**, 31 (1958); J. C. D. Brand, *J. Chem. Soc.*, **1956**, 858.
25. G. Fleming, M. M. Anderson, A. J. Harrison, and L. W. Pickett, *J. Chem. Phys.*, **30**, 351 (1959).
26. A. D. Cohen and C. Reid, *J. Chem. Phys.*, **24**, 85 (1956).
27. N. J. Leonard and P. M. Mader, *J. Am. Chem. Soc.*, **72**, 5388 (1950).
28. R. T. Holman, W. O. Lundberg, and G. O. Burr, *J. Am. Chem. Soc.*, **67**, 1669 (1945).

29. R. A. Ford and F. Parry, *Spectrochim. Acta*, **12**, 78 (1958).
30. R. B. Woodward, *J. Am. Chem. Soc.*, **63**, 1123 (1942).
31. L. F. Fieser and M. Fieser, *Steroids*, Reinhold, New York, 1959.
32. L. K. Evans and A. E. Gillam, *J. Chem. Soc.*, **1943**, 565.
33. A. T. Nielsen, *J. Org. Chem.*, **22**, 1539 (1957).
34. M. J. Janssen, *Rec. Trav. Chem.*, **79**, 454, 464 (1960).
35. H. P. Koch, *J. Chem. Soc.*, **1950**, 2892.
36. M. Tanaka, J. Tanaka, and S. Nagakura, *Bull. Chem. Soc. Japan*, **39**, 766 (1966).
37. K. L. McEwen, *J. Chem. Phys.*, **32**, 1801 (1960).
38. E. A. Braude, E. R. H. Jones, and G. G. Rose, *J. Chem. Soc.*, **1947**, 1104.
39. S. Nagakura, *Mol. Phys.*, **3**, 152 (1960).
40. R. N. Jones and G. D. Thorn, *Can. J. Res.*, **27B**, 828 (1949).
41. P. P. Birnbaum, J. H. Linford, and D. W. G. Style, *Trans. Faraday Soc.*, **49**, 735 (1953).
42. P. Grammaticakis, *Bull. Soc. Chim. France*, **15**, 975 (1948).
43. M. G. Mayer and A. L. Sklar, *J. Chem. Phys.*, **6**, 645 (1938); A. L. Sklar, *Rev. Mod. Phys.*, **14**, 232 (1942).
44. D. P. Craig, *Proc. Roy. Soc. (London)*, **A200**, 401 (1950).
45. T. M. Dunn and C. K. Ingold, *Nature*, **176**, 65 (1955); F. A. Matsen, W. W. Robertson, and R. L. Chuoke, *Chem. Rev.*, **41**, 273 (1947).
46. F. A. Matsen, *J. Am. Chem. Soc.*, **72**, 5243 (1950); L. Goodman and H. Shull, *J. Chem. Phys.*, **27**, 1388 (1957); H. Baba, *Bull. Chem. Soc. Japan*, **34**, 76 (1961); J. N. Murrell, *Proc. Phys. Soc. (London)*, **A68**, 969 (1955); *J. Chem. Phys.*, **25**, 1143 (1956).
47. G. W. Wheland and L. Pauling, *J. Am. Chem. Soc.*, **57**, 2086 (1935).
48. W. W. Robertson and F. A. Matsen, *J. Am. Chem. Soc.*, **72**, 5248 (1950).
49. K. Bowden and E. A. Braude, *J. Chem. Soc.*, **1952**, 1068.
50. L. Goodman, A. H. Konstam, and L. H. Sommer, *J. Am. Chem. Soc.*, **87**, 1012 (1965).
51. L. Pauling, *Nature of the Chemical Bond*. Cornell Univ. Press, 2nd ed., Ithaca, 1940.
52. A. L. Sklar, *J. Chem. Phys.*, **7**, 984 (1939).
53. W. W. Robertson and F. A. Matsen, *J. Am. Chem. Soc.*, **72**, 5252 (1950).
54. W. R. Remington, *J. Am. Chem. Soc.*, **67**, 1838 (1945). W. G. Brown and H. Reagan *ibid.*, **69**, 1032 (1947).
55. C. E. Ingham and G. C. Hampson, *J. Chem. Soc.*, **1939**, 981.
56. F. A. Matsen, W. W. Robertson, and R. L. Chuoke, *Chem. Rev.*, **41**, 273 (1947).
57. K. Watanabe, T. Nakayama, and J. Mottl, *Final Report on Ionization Potential of Molecules by a Photoionization Method* (December, 1959) Dept. Army No. 5B-99-01-004, ORD-no. TB2-0001- no. 1624; Contract No. DA-64-200-ORD 400 and737.
58. W. F. Hamner and F. A. Matsen, *J. Am. Chem. Soc.*, **70**, 2482 (1948).
59. W. W. Robertson, J. F. Music, and F. A. Matsen, *J. Am. Chem. Soc.*, **72**, 5260 (1950).
60. M. T. Rogers, *J. Am. Chem. Soc.*, **69**, 2544 (1947).
61. A. D. Walsh, *Trans. Faraday Soc.*, **45**, 179 (1949); T. M. Sugden, *Nature*, **160**, 367 (1947); J. F. Music and F. A. Matsen, *J. Am. Chem. Soc.*, **72**, 5256 (1950).
62. S. Nagakura, M. Kojima, and Y. Maruyama, *J. Mol. Spectry.*, **13**, 174 (1964).
63. S. Nagakura and J. Tanaka, *J. Chem. Phys.*, **22**, 236 (1954).
64. K. Kimura, H. Tsubomura, and S. Nagakura, Tech. Rept. A115, Institute for Solid State Physics, University of Tokyo (May, 1964).
65. H. C. Longuet-Higgins and J. N. Murrell, *Proc. Phys. Soc. (London)*, **A68**, 601 (1955); J. N. Murrell, *ibid.*, **A68**, 969 (1955).

66. A. L. Sklar, *Rev. Mod. Phys.*, **14**, 232 (1942).
67. J. R. Platt, *J. Chem. Phys.*, **19**, 263 (1951); J. Petruska, *J. Chem. Phys.*, **34**, 1120 (1961).
68. Th. Förster, *Z. Naturforsch.*, **2a**, 149 (1947); J. Petruska, *J. Chem. Phys.*, **34**, 1111 (1961); *Ibid.*, **34**, 1120 (1961); P. E. Stevenson, *J. Mol. Spectry.*, **15**, 220 (1965).
69. P. E. Stevenson, *J. Mol. Spectry.*, **15**, 220 (1965).
70. L. Doub and J. M. Vandenbelt, *J. Am. Chem. Soc.*, **69**, 2714 (1947).
71. L. Doub and J. M. Vandenbelt, *J. Am. Chem. Soc.*, **71**, 2414 (1949); *ibid.*, **77**, 4535 (1955).
72. E. A. Braude, *J. Chem. Soc.*, **1945**, 490.
73. S. Nagakura and A. Kuboyama, *J. Am. Chem. Soc.*, **76**, 1003 (1954), H. Hartmann and E. Lorenz, *Z. Naturforsch.*, **7a**, 360 (1952).
74. C. A. Coulson, *Valence*, 2nd ed., Oxford Univ. Press, London, 1961; see also T. Anno, I. Matsubara, and A. Sado, *Bull. Chem. Soc. Japan*, **30**, 168 (1957).
75. P. E. Stevenson, *J. Mol. Spectry.*, **17**, 58 (1965); L. E. Orgel, *Trans. Faraday Soc.* **52**, 1172 (1956).
76. H. McConnell, *J. Chem. Phys.*, **20**, 700 (1952); S. Nagakura, *Bull. Chem. Soc. Japan*, **25**, 124 (1952).
77. E. Clar, *Aromatische Kohlenwasserstoffe*, 2nd ed., Springer, Berlin, 1952.
78. M. J. S. Dewar and H. C. Longuet-Higgins, *Proc. Phys. Soc.* (*London*), **A67**, 795 (1954). See ref. 4 for more advanced theoretical treatments.
79. J. R. Platt, *J. Chem. Phys.*, **17**, 484 (1949).
80. H. B. Klevens and J. R. Platt, *J. Chem. Phys.*, **17**, 470 (1949).
81. D. S. McClure, *J. Chem. Phys.*, **22**, 1668 (1954).
82. D. P. Craig and J. R. Walsh, *J. Chem. Phys.*, **24**, 471 (1956).
83. Y. Hirshberg and R. N. Jones, *Can. J. Res.*, **27B**, 437 (1949); W. L. Mosby, *J. Am. Chem. Soc.*, **75**, 3348 (1953); A. S. Bailey, K. C. Bryant, R. A. Hancock, S. H. Morrell, and J. C. Smith, *J. Inst. Petrol.*, **33**, 503 (1947); E. Heilbronner, U. Frolicher, and P. A. Plattner, *Helv. Chim. Acta*, **32**, 2479 (1049); R. A. Morton and A. J. A. de Gouveia, *J. Chem. Soc.*, **1934**, 916; B. J. Adair, J. W. Cook, and D. T. Gibson, *J. Chem. Soc.*, **1953**, 8.
84. D. P. Craig and P. C. Hobbins, *J. Chem. Soc.*, **1955**, 2302, 2309.
85. J. G. Foss and M. E. McCarville, *J. Chem. Phys.*, **44**, 4350 (1966).
86. R. N. Jones, *J. Am. Chem. Soc.*, **67**, 2127 (1945).
87. R. S. Becker, I. S. Singh, and E. A. Jackson, *J. Chem. Phys.*, **38**, 2144 (1963); G. C. Morris, *J. Mol. Spectry.*, **18**, 42 (1965).
88. A. Bree and L. Lyons, *J. Chem. Soc.*, **1960**, 5206; J. Tanaka, *Bull. Chem. Soc. Japan*, **38**, 86 (1965).
89. G. Briegleb, *Angew. Chem.*, **76**, 326 (1964) and references therein.
90. A. T. Watson and F. A. Matsen, *J. Chem. Phys.*, **18**, 1305 (1950); I. Bergman, *Trans. Faraday Soc.*, **50**, 829 (1954); R. S. Becker and W. E. Wentworth, *J. Am. Chem. Soc.*, **85**, 2210 (1963).
91. D. E. Mann, J. R. Platt, and H. B. Klevens, *J. Chem. Phys.*, **17**, 481 (1949).
92. P. A. Plattner, *Helv. Chim. Acta*, **24**, 283 (1941); P. A. Plattner and E. Heilbronner, *Helv. Chim. Acta*, **30**, 910 (1947).
93. C. A. Coulson and G. S. Rushbrooke, *Proc. Cambridge Phil. Soc.*, **36**, 193 (1940).
94. T. K. Liu and A. B. F. Duncan, *J. Chem. Phys.*, **17**, 241 (1949).
95. L. W. Pickett, N. J. Hoeflich, and T. K. Liu, *J. Am. Chem. Soc.*, **73**, 4865 (1951); L. W. Pickett, M. E. Corning, G. M. Wieder, D. A. Semenow, and J. M. Buckley, *J. Am. Chem. Soc.*, **75**, 1618 (1953).

96. W. E. Haines, R. V. Helm, C. W. Bailey, and J. S. Ball, *J. Phys. Chem.*, **58**, 270 (1954); E. A. Fehnel and M. Carmack, *J. Am. Chem. Soc.*, **71**, 84 (1949).
97. S. F. Mason, *J. Chem. Soc.*, **1959**, 1204, 1247; J. E. Parkin and K. K. Innes, *J. Mol. Spectry.*, **15**, 407 (1965).
98. M. Kasha, "Nature and Significance of $n \rightarrow \pi^*$ Transitions," *Light and Life*, W. D. McElroy and B. Glass, Eds., Johns Hopkins Press, Baltimore, 1961.
99. F. Halverson and R. C. Hirt, *J. Chem. Phys.*, **13**, 1165 (1949); **19**, 711 (1951).
100. R. S. Mulliken and W. B. Person, *Ann. Rev. Phys. Chem.*, **13**, 107 (1962); S. P. McGlynn, *Chem. Rev.*, **58**, 1113 (1958); G. Briegleb, *Electronen-Donator-Acceptor-Komplexe*, Springer, Berlin, 1961.
101. H. A. Benesi and J. H. Hildebrand, *J. Am. Chem. Soc.*, **71**, 2703 (1949).
102. R. M. Keefer and L. J. Andrews, *J. Am. Chem. Soc.*, **72**, 4677, 5170 (1950); **73**, 462 (1951).
103. S. Fried and K. M. Sancier, *J. Am. Chem. Soc.*, **74**, 1273 (1952).
104. J. S. Ham, J. R. Platt, and H. McConnell, *J. Chem. Phys.*, **19**, 1301 (1951).
105. S. H. Hastings, J. L. Franklin, J. C. Schiller, and F. A. Matsen, *J. Am. Chem. Soc.*, **75**, 2900 (1953).
106. G. Briegleb and J. Czekalla, *Angew. Chem.*, **72**, 401 (1960).
107. R. S. Mulliken, *J. Am. Chem. Soc.*, **74**, 811 (1952); *J. Phys. Chem.*, **56**, 801 (1952).
108. D. M. G. Lawrey and H. McConnell, *J. Am. Chem. Soc.*, **74**, 6175 (1952).
109. H. McConnell, J. S. Ham, and J. R. Platt, *J. Chem. Phys.*, **21**, 66 (1953).
110. L. E. Orgel, *An Introduction to Transition-Metal Chemistry, Ligand Field Theory*, Methuen, London, 1960; C. K. Jorgensen, *Absorption Spectra and Chemical Bonding in Complexes*, Pergamon Press, London, 1962.
111. D. R. Scott and R. S. Becker, *J. Chem. Phys.*, **35**, 516 (1961); **35**, 2246 (1961); *J. Organometal. Chem.*, **4**, 409 (1965).
112. D. A. Levy, Ph.D. dissertation, Cambridge University, 1960.
113. D. R. Scott, Ph.D. dissertation, University of Houston, January, 1965.
114. F. A. Matsen, *J. Am. Chem. Soc.*, **81**, 2023 (1959).
115. R. L. Collins, *J. Chem. Phys.*, **42**, 1072 (1965).
116. See F. A. Cotton, Ed., *Progress in Inorganic Chemistry*, Vol. I, Interscience, New York, 1959, p. 78; L. L. Lohr, Ph.D. dissertation, Harvard University, 1963; R. D. Fischer, *Theor. Chim. Acta*, **1**, 418 (1963).
117. N. C. Deno in S. G. Cohen, A. Streitwieser, Jr., and R. W. Taft, Eds., *Progress in Physical Organic Chemistry*, Vol. 2, Interscience, New York, 1964, p. 129.
118. G. A. Olah, W. S. Tolgyesi, S. J. Kuhn, M. E. Moffatt, I. J. Bastien, and E. B. Baker, *J. Am. Chem. Soc.*, **85**, 1328 (1963); G. A. Olah and C. U. Pittman in *Advances in Physical Organic Chemistry*, Vol. 4, V. Gold, Ed., Academic Press, New York, 1966, p. 305.
119. J. Gonzales-Vidal, E. Kohn, and F. A. Matsen, *J. Chem. Phys.*, **25**, 181 (1956).
120. J. Rosenbaum and M. C. R. Symons, *Proc. Chem. Soc.*, **1959**, 92.
121. J. Rosenbaum and M. C. R. Symons, *Mol. Phys.*, **3**, 205 (1960).
122. L. Craig, *Chem. Rev.*, **49**, 103 (1951).
123. E. Hückel, *Z. Physik.*, **70**, 204 (1931).
124. W. von E. Doering and L. H. Knox, *J. Am. Chem. Soc.*, **76**, 3203 (1954); see also A. W. Johnson, *J. Chem. Soc.*, **1954**, 1331.
125. R. C. Cookson, J. Hudee, and B. Whitear, *Proc. Chem. Soc.*, **1961**, 117.
126. V. Gold and F. L. Tye, *J. Chem. Soc.*, **1952**, 2173, 2181, 2184.
127. R. Grinter and S. F. Mason, quoted in S. F. Mason, *Quart. Rev.*, **15**, 287 (1961).

128. N. C. Deno, J. J. Jaruzelski, and A. Schriesheim, *J. Org. Chem.*, **19**, 155 (1954); *J. Am. Chem. Soc.*, **77**, 3044 (1955).
129. L. C. Anderson, *J. Am. Chem. Soc.*, **57**, 1673 (1935).
130. F. J. Hopton and N. S. Hush, *Mol. Phys.*, **6**, 209 (1963).
131. G. J. Hoijtink, N. H. Velthorst, and P. J. Zandstra, *Mol. Phys.*, **3**, 533 (1960); W. I. Aalbersberg, G. J. Hoijtink, E. L. Mackor, and W. P. Weijland, *J. Chem. Soc.*, **1959**, 3049, 3055; other papers by Hoijtink and co-authors.
132. L. G. S. Brooker, *Rev. Mod. Phys.*, **14**, 275 (1942).
133. M. J. S. Dewar, *J. Chem. Soc.*, **1950**, 2329.
134. L. G. S. Brooker et al., *J. Am. Chem. Soc.*, **73**, 5332, 5350 (1951).
135. E. E. Jelley, *Nature*, **138**, 1009 (1936).
136. G. Scheibe, *Angew. Chem.*, **50**, 51 (1937).
137. E. Rabinowitch and L. Epstein, *J. Am. Chem. Soc.*, **63**, 69 (1941).
138. K. Bergmann and C. T. O'Konski, *J. Phys. Chem.*, **67**, 2169 (1963).
139. T. Förster and E. König, *Z. Elecktrochem.*, **61**, 344 (1956).
140. V. Zanker, *Z. Physik. Chem.*, **200**, 250 (1952).
141. G. R. Haugen and W. H. Melhuish, *Trans. Faraday Soc.*, **60**, 386 (1964).
142. W. West and S. Pearce, *J. Phys. Chem.*, **69**, 1894 (1965).
143. T. Förster, *Fluoreszenz Organischer Verbindungen*, Vandenhoeck and Ruprecht, Göttingen, 1951, p. 254.
144. G. Levinson, W. T. Simpson, and W. Curtis, *J. Am. Chem. Soc.*, **79**, 4314 (1957).
145. E. G. McRae and M. Kasha, in *Physical Processes in Radiation Biology*, L. Augenstein, R. Mason, and B. Rosenberg, Eds., Academic Press, 1964, p. 23.
146. G. Scheibe, *Z. Elektrochem.*, **47**, 73 (1941); **52**, 283 (1958).
147. *Theory of the Photographic Process*, 3rd ed., K. E. C. Mees and T. H. James, Eds., Macmillan, New York, 1966, p. 244 *et seq.*
148. E. G. McRae and M. Kasha, *J. Chem. Phys.*, **28**, 721 (1958).
149. M. Gouterman, *J. Chem. Phys.*, **30**, 1139 (1959); *J. Mol. Spectry.*, **6**, 138 (1961); J. R. Platt in *Radiation Biology*, Vol. III, A. Hollander, Ed., McGraw-Hill, New York, 1956, Chapter 2.
150. F. P. Zscheile and C. L. Comar, *Bot. Gazz.*, **102**, 463 (1941); D. G. Harris and F. P. Zscheile, *ibid.*, **104**, 515 (1943); J. H. Smith and A. Benitez, *Modern Methods of Plant Analysis*, Springer, Berlin, 1955, p. 143; E. I. Rabinowitch, *Photosynthesis and Related Processes*, Vol. I, II (1), II (2), Interscience, New York, 1945, 1951, 1956.
151. A. Stern and H. Wenderlein, *Z. Physik. Chem.*, **A175**, 405 (1936); **A176**, 91 (1936); **A177**, 40 (1936).
152. G. D. Dorough, J. R. Miller, and F. M. Huennekens, *J. Am. Chem. Soc.*, **73**, 4315 (1951); A. Stern and M. Dezeli, *Z. Physik. Chem.*, **180A**, 131 (1937).
153. J. B. Allison, Ph.D. dissertation, University of Houston, 1962; J. B. Allison and R. S. Becker, *J. Phys. Chem.*, **67**, 2675 (1963).
154. G. D. Dorough and F. M. Huennekens, *J. Am. Chem. Soc.*, **74**, 3974 (1952).
155. C. S. French, in *Handbuch der Pflanzenphysiologie*, W. Ruhland, Ed., Springer, Berlin, 1960, p. 252.
156. R. P. Linstead, *J. Chem. Soc.*, **1953**, 2873.
157. L. Zechmeister, A. L. deRosen, W. A. Schroeder, A. Polgár, and L. Pauling, *J. Am. Chem. Soc.*, **65**, 1940 (1943).
158. W. W. Robertson and A. D. King, *J. Chem. Phys.*, **31**, 473 (1959).
159. N. S. Bayliss, *J. Chem. Phys.*, **8**, 292 (1950).
160. N. S. Bayliss and E. G. McRae, *J. Phys. Chem.*, **58**, 1002, 1006 (1954).

161. E. G. McRae, *J. Phys. Chem.*, **61**, 562 (1957); S. Basu in *Advances in Quantum Chemistry*, Vol. 1, P. O. Lödwin, Ed., Academic Press, New York, 1964, p. 145.
162. H. McConnell, *J. Chem. Phys.*, **20**, 700 (1952).
163. M. Kasha, *Discussions Faraday Soc.*, **9**, 14 (1950).
164. G. J. Brealey and M. Kasha, *J. Am. Chem. Soc.*, **77**, 4462 (1955); G. C. Pimentel, *J. Am. Chem. Soc.*, **79**, 3323 (1957).
165. R. Pariser, *J. Chem. Phys.*, **25**, 1112 (1956).
166. W. W. Robertson and A. D. King, *J. Chem. Phys.*, **34**, 2190 (1961).
167. B. Oksengorn, *Compt. Rend.*, **242**, 2324 (1956).
168. W. W. Robertson, *J. Chem. Phys.*, **33**, 362 (1960).

CHAPTER IV

FLUORESCENCE AND PHOSPHORESCENCE SPECTROSCOPY

Ralph S. Becker
Department of Chemistry, University of Houston, Houston, Texas

I. Introduction . . . 338
  A. General Difference between Fluorescence and Phosphorescence . . . 338
  B. Important Characteristics of Excited States . . . 341
    1. Energy . . . 342
    2. Lifetime . . . 342
    3. Quantum Yield . . . 345
    4. Polarization . . . 347
II. Fluorescence . . . 348
  A. Nature of Fluorescence . . . 348
  B. Relationship between Absorption Intensity and Lifetime . . . 351
  C. Solvent Effects . . . 353
    1. General . . . 353
    2. Specific Examples . . . 356
  D. Aliphatic and Unsaturated Compounds . . . 357
  E. Aromatic Hydrocarbons and Substituted Derivatives . . . 358
    1. Aromatic Hydrocarbons . . . 358
    2. Substituted Aromatic Compounds . . . 365
  F. Aromatic Molecules with n,π^* States . . . 369
  G. Heterocyclic Compounds and Compounds of Biological Interest . . . 371
    1. Heterocyclic Compounds . . . 371
    2. Compounds of Biological Interest . . . 374
  H. Metal Complexes . . . 377
  I. Charge-Transfer Complexes . . . 389
  J. Physical Chemistry of the Lowest Excited Singlet State . . . 392
III. Phosphorescence and the Triplet State . . . 395
  A. The Nature of Phosphorescence . . . 395
    1. Spin–Orbit Coupling and Transition Probability . . . 395
    2. Intercombinations . . . 397
  B. Paramagnetism of the Phosphorescent State . . . 399
  C. Aromatic Hydrocarbons, Substituted Aromatic Hydrocarbons, and the Intramolecular Heavy Atom Effect . . . 403
    1. Aromatic Hydrocarbons . . . 403
    2. Substituted Aromatic Hydrocarbons and the Intramolecular Heavy Atom Effect . . . 407
  D. Molecules with n,π^* States . . . 414
    1. Carbonyl Molecules . . . 414
    2. Heterocyclic Compounds . . . 418
  E. Metal Complexes . . . 421

F. Singlet → Triplet Transitions and Enhancement by External Perturbations 427
  1. Singlet → Triplet Transitions 427
  2. Enhancement of Singlet → Triplet Transition by External Perturbations 430
G. Triplet → Triplet Absorption 433
H. Effect of External Perturbations on Characteristics of the Triplet . . . 439
I. Intermolecular Energy Transfer and Photochemistry 443
  1. Aromatic Hydrocarbons 443
  2. Carbonyls 444
  3. Miscellaneous 448
J. Additional Topics 449
  1. Physical Chemistry of the Lowest Excited Triplet State 449
  2. Enhancement of Phosphorescence by Aggregation and Molecular Excitons 450
References 452

I. INTRODUCTION

A. General Difference between Fluorescence and Phosphorescence

Fluorescence and phosphorescence are processes in which radiation is emitted by molecules or atoms that have been excited by the absorption of radiation. The initial state of the molecule before excitation is usually the ground electronic state. As a result of the emission from electronic excited states, the molecule returns to the ground electronic state, although frequently to a vibrationally excited form of that electronic state. A basis for much of the theoretical description and analysis of these phenomena is afforded by molecular orbital theory. The molecule has a set of molecular orbitals, and these are filled with electrons beginning with the lowest energy orbital and according to the Pauli exclusion principle. Any state notation for the molecule is obtained by first taking the product of the appropriate characteristics over all the electrons in the orbitals as in atoms (Chapter II). In the case of a diatomic molecule, the state potential energy curve is a function of internuclear distance only (Chapter II). In a polyatomic molecule, the situation is not so simple but a similar picture is adequate in the sense that it represents a cross section of the potential diagram.

It was mentioned in Chapters II and III that an electron in an atom or molecule behaves as if it generates two types of magnetic moments and mechanical angular momenta. One is associated with its motion about the nucleus, the other pictorially visualized as originating in a "spin" of the electron, the value of the spin angular momentum of a single electron being $1/2(h/2\pi)$. As an illustrative example, consider a molecule like butadiene, whose spectral features are approximately determined by four π electrons, one on each carbon atom. According to molecular orbital theory (Chapters II, III) the molecule contains four molecular orbitals, to each of which can be assigned two electrons of opposite spin. The ground state of the molecule can be derived by adding the electrons one at a time to the orbitals, beginning with the lowest. Thus, in the ground state of the example cited, the four π electrons are assigned in pairs to the two lowest orbitals, the spins of the two electrons in a given orbital being of opposite sign (Fig. 1). The resultant spin, S, of the ground state is therefore zero and the multiplicity of the state is singlet (Chapter II, Section I-D). An excited state is derived by removing one of the electrons from the uppermost filled orbital of the ground state to a vacant orbital of higher energy and if the spin of the excited electron is conserved in this process, the total spin of the excited state is zero and the multiplicity is again singlet (Fig. 1*b*). If, however, as in Figure 1*c*, the spin of the excited electron is no longer opposed to that of the odd electron left in the second orbital, the total spin is unity. The multiplicity is $2S + 1 = 3$ and the excited state is a triplet.

State multiplicities are important since the nature of the emission processes depends on them. If the states from which the emission originate and

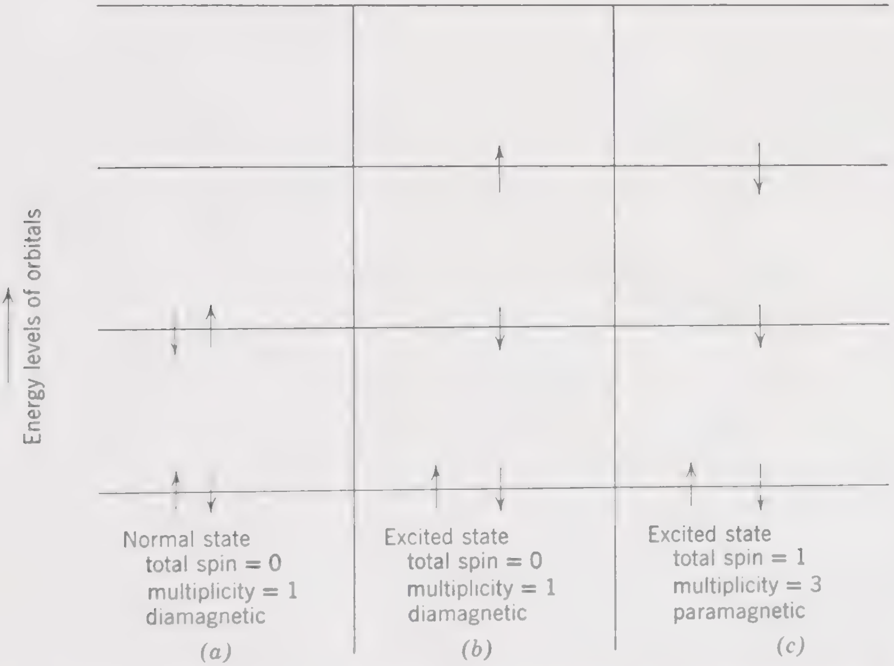
Energy levels of orbitals
Normal state
total spin = 0
multiplicity = 1
diamagnetic
(a)
Excited state
total spin = 0
multiplicity = 1
diamagnetic
(b)
Excited state
total spin = 1
multiplicity = 3
paramagnetic
(c)

Fig. 1. π Electron orbitals for butadiene (diagrammatic). In the normal state (*a*), the two lowest orbitals are each occupied by two electrons of opposite spin, yielding a singlet state. In the excited state (*b*), one of the electrons has been raised to the next higher level without change in spin, yielding an excited singlet state. In state (*c*), excitation is accompanied by a change in spin of one of the electrons, yielding an excited triplet state. The energy of the state derived from the orbitals in *c* is less than that derived from the orbitals in *b*.

terminate have the same multiplicity, the emission is called fluorescence. This process most commonly occurs between the first excited singlet and ground state singlet. However, if the states from which the emission originate and terminate differ in spin ($\Delta S \geq 1$), then the emission is known as phosphorescence. The states of principal concern to us relative to phosphorescence will be the triplet and ground state singlet. Because highly probable transitions can occur only when $\Delta S = 0$, phosphorescence emissions have relatively long lifetimes (10^{-3} to 10 sec) while fluorescences have relatively short lifetimes (10^{-7} to 10^{-10} sec). More detail concerning these emissions will be given in succeeding sections.

In Chapter II, Section I-D, it was pointed out that the magnetic interaction between the spin and orbital motion of an electron in an atom was very small for light atoms and that, if several electrons were present, the individual spins coupled to form a resultant spin, S, and the individual orbital momenta coupled to form a resultant orbital angular momentum, L, and that these two vectors coupled to form a resultant total angular momentum, J. Only a discrete number of relative orientations of the spin and orbital momenta is allowed; for example, if $L = 1$ and $S = 1$, three orientations are possible, giving rise to three energy levels. The state corresponding to these values of L and S is therefore a triplet, the individual members of which are generally only slightly separated from each other. Thus, the He atom and the atoms of the second group of elements in the periodic table have, in addition to the singlet levels corresponding to opposed spins of the two optical electrons, sets of triplet levels, the separation of which is very small in He and Be and increases rapidly with increasing atomic number. According to Hund's rule, the triplet levels associated with a given orbital angular momentum are lower in energy than the corresponding singlet levels. Moreover, when the interaction between the orbital motion and the spin is small, there will be little perturbation in an electronic transition which could cause a change in spin; hence, in the lighter members of the group of atoms with two optical electrons, there will be a very low probability of singlet ↔ triplet transitions. In atoms of higher atomic number, the interaction between the spin and orbital momenta becomes relatively large, so that during an electronic transition the perturbation can change the spin. Thus, spectral lines involving a change in multiplicity become relatively intense in heavy atoms. For example, the well-known ultraviolet mercury line of wavelength 2537 Å is associated in absorption with the transition from the $^1S_0$ ground level to the middle level, $^3P_1$, of the first excited ^3P state.

The case is similar in simple molecules and in molecules with conjugated chains. For every excited singlet level with paired (antiparallel) spins, there is a corresponding triplet level usually of lower energy with two parallel spins. If all the atoms in the molecule are light, e.g., H, C, N, and O, transitions be-

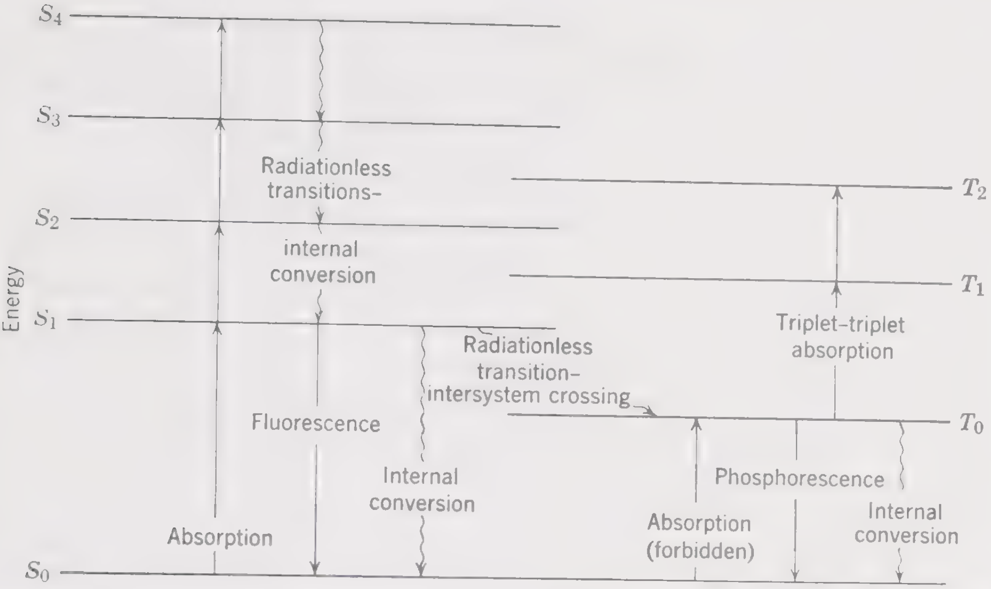
S_4
S_3
S_2
S_1
S_0
Energy
Radiationless transitions-
internal conversion
Radiationless transition-
intersystem crossing
Fluorescence
Internal conversion
Absorption
T_2
T_1
T_0
Triplet-triplet absorption
Phosphorescence
Absorption (forbidden)
Internal conversion

Fig. 2. Schematic state energy level diagram—S is singlet and T is triplet. The S_0 state is the ground state and the subscript numbers identify individual states.

tween the ground singlet to the excited triplet states will be very improbable and the corresponding absorption will be extremely weak. On the other hand, if the molecule contains heavy atoms such as Br, I, or heavy metals, the singlet ↔ triplet transitions can be expected to become stronger (see Section III-A).

The ground state of most stable molecules containing an even number of electrons is diamagnetic because of the arrangement of the electrons into pairs with opposed spin magnetic moments. Thus, the ground state for most molecules is singlet (O_2 is an exception, for example). A molecule excited to the triplet state is paramagnetic by virtue of the total spin magnetic moment of the two unpaired electrons. Finally, it should be reemphasized that the rigorous differentiation between fluorescence and phosphorescence is the nature of the states between which the emission occurs (see Fig. 2). For fluorescence the multiplicities of the states are the same (most commonly from the first excited singlet state to the singlet ground state). For phosphorescence the multiplicities of the states are different (most commonly from the lowest triplet state to the singlet ground state).

B. Important Characteristics of Excited States

There are four characteristics that can be associated with a molecular emission. They are: (*1*) energy, (*2*) lifetime, (*3*) quantum yield, and (*4*) polarization. Before proceeding to a detailed discussion of each of these, it will be helpful to consider qualitatively some aspects of the emission processes. Upon electronic excitation to any state above the first excited singlet, deexcitation occurs commonly to the lowest excited singlet state. From this state there can occur fluorescence emission or continued deexcitation to the ground state with no emission, crossing to the triplet state or any combination of these (Figs. 2 and 3). If the triplet is occupied, phosphorescence and/or deexcitation to the ground state with no emission can occur. Because the lowest triplet is below the lowest excited singlet state, phosphorescence occurs at longer wavelength than does fluorescence. The shape of the fluorescence spectrum often resembles that of the absorption band of longest wavelength, with approximately a mirror-image relationship between the intensities of emission and absorption as a function of wavelength. Frequently, the fluorescence spectrum is located immediately adjacent to the longest wavelength absorption band on the long wavelength side. Sometimes a larger wavelength interval is found between the absorption and emission spectrum. The long wavelength displacement of the fluorescence with respect to the absorption is referred to as the "Stokes shift." Further details regarding shape, intensity, and the magnitude of the Stokes shift are discussed in subsequent sections.

1. ENERGY

The energy associated with an emission process is the easiest of the characteristic quantities to determine. In essence the fluorescence spectrum is produced by exciting the molecule by radiation from some external energy source followed by the emission of a photon by the excited molecule. The energy, E, emitted in the transition associated with any wavelength of the fluorescence spectrum is given by the Bohr relation $E = h\tilde{\nu}$, where $\tilde{\nu}$ is the frequency of the emitted radiation. Of course, the vibrational band of highest energy in the emission spectrum corresponds to the energy of the excited state (relative to the ground state). This corresponds to the emission origin and represents the transition from the zero vibrational level of the excited state to the zero vibrational level of the ground state. Any other energy would include vibrational energy as shown in Figure 3.

2. LIFETIME

The second characteristic of an excited state, its mean lifetime, is somewhat more difficult to measure, particularly when it is short (10^{-7} to 10^{-10} sec). Observations show that the fluorescence decays after the withdrawal of the

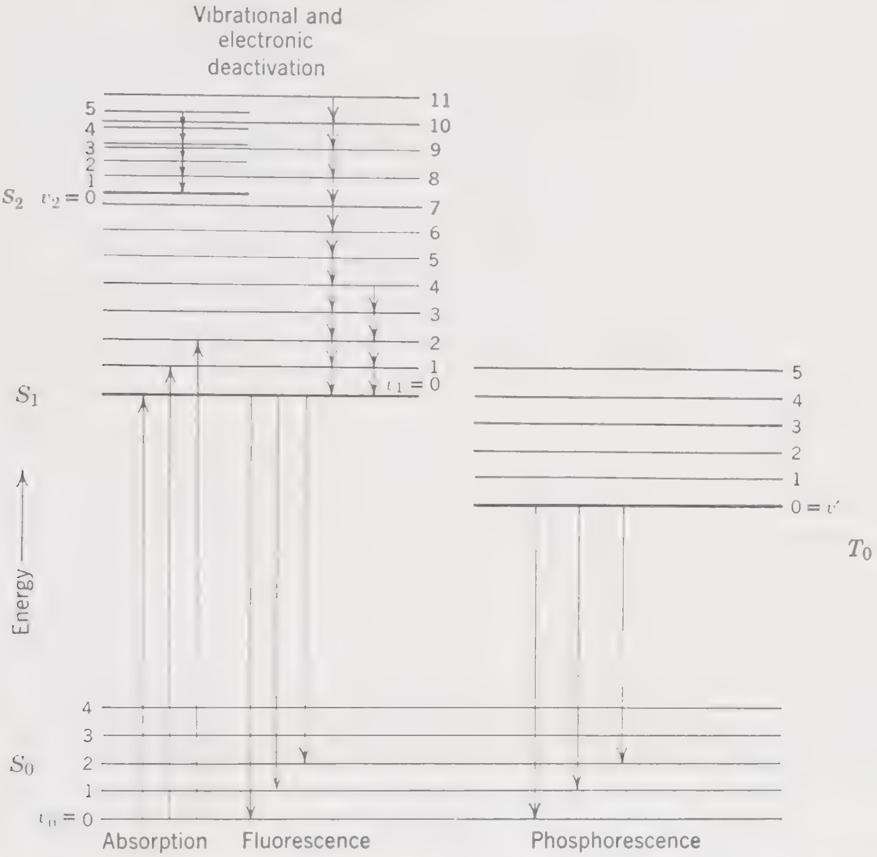
Vibrational and electronic deactivation
S_2 $v_2 = 0$
1
2
3
4
5
11
10
9
8
7
6
5
4
3
2
1
$v_1 = 0$
S_1
Energy
5
4
3
2
1
$0 = v'$
T_0
4
3
S_0
2
1
$v_0 = 0$
Absorption
Fluorescence
Phosphorescence

Fig. 3. Schematic energy level diagram showing electronic states and associated vibrational levels.

exciting source, according to a first-order rate equation, i.e., exponentially with the time,

$$I = I_0 e^{-t/\tau} \tag{1}$$

where I_0 is some initial intensity at an arbitrary time zero, I is the intensity at some later time, t, and τ is a constant. When the time t over which the decay is measured is equal to τ, the intensity has fallen to $1/e$ of its initial value. τ is defined as the mean decay time for the emission process, or the mean life of the excited state. Of course, there are relations between the rate constants and the lifetime τ. One relation is

$$k_F = 1/\tau_0 \quad \text{or} \quad \tau_0 = 1/k_F \tag{2}$$

where k_F refers to the rate constant for fluorescence and τ_0 is the corresponding intrinsic or natural lifetime. The observed lifetime τ will equal τ_0 only in the absence of any deactivating processes both internal and external. The observed lifetime, τ, is determined by all the deactivational processes and can be expressed as $\tau = 1/\Sigma k_i$. Thus, the actually observed mean lifetime may differ from the natural lifetime. For fluorescence the relationship is: $\tau_0\varphi_0 = \tau$ where τ is the observed lifetime of the emission in the absence of external quenching and φ_0 is the quantum yield of the fluorescent emission in the absence of any external quenching processes (Section I-B-3). External quenching results from collisions between the solute molecule and any other molecule. It is known that internal deactivational processes must shorten the lifetime from its value in the absence of such deactivational processes. One way this can be shown is from the effect of substitution of deuterium for hydrogen on aromatic hydrocarbons. In the deuterium compounds, the lifetimes are notably longer than those containing hydrogen (for more details see Section III-C-1).

In the case of phosphorescence, the decay also follows the first-order rate equation. The intrinsic or natural lifetime for phosphorescence emission is also defined in the same way as for fluorescence,

$$\tau_0 = 1/k_P \tag{3}$$

where k_P is the rate constant for phosphorescence. However, the relationship between the quantum yields and the intrinsic and observed lifetimes is not quite so simple as in the case of fluorescence. If we define k_{IC} as the rate constant for internal conversion (vibrational deactivation of electronic energy) between S_1 and S_0 and k_{IS} as the rate constant for intersystem crossing between S_1 and T_0 (Fig. 2), then the intrinsic lifetime of phosphorescence is related to the observed lifetime as follows:

$$\tau_0 = \tau\left(\frac{k_{IS}}{k_{IC} + k_{IS}}\right)\frac{1 - {\varphi_0}^F}{{\varphi_0}^P} \tag{4}$$

where ${\varphi_0}^F$ and ${\varphi_0}^P$ are the quantum yields of fluorescence and phosphorescence in the absence of external quenching respectively (see Section I-B-3). Often it is assumed that internal conversion occurs only from the triplet state and then the relationship is simplified to

$$\tau_0 = \tau\left(\frac{1 - {\varphi_0}^F}{{\varphi_0}^P}\right) \tag{5}$$

The experimental procedures for measuring decay times vary according to the order of magnitude of the decay. Shutter type arrangements are the simplest. The emission can be detected by the use of an arrangement allowing periodic entrance of the exciting radiation to the sample through one shutter and passage of the emitted radiation to a detector through a second shutter. The latter shutter normally opens and closes with the same frequency as the first but is delayed in time. If the luminescence persists for a period up to 10^{-3} sec after the removal of the exciting radiation, mechanical shutters consisting of slots in rotating disks or cylinders can be used, as in the Becquerel phosphorescence (1). The fluorescence of dyes decays in some 10^{-8} sec after removal of the exciting radiation and for such periods mechanical shutters are replaced by electrooptical shutters without moving parts. One such device is a Kerr cell placed between crossed Nicol prisms. The cell contains a liquid, such as nitrobenzene, of high dipole moment and high polarizability, which becomes doubly refracting in an electric field. The arrangement transmits light when the field is applied and is opaque when the field is zero and therefore acts as a shutter of very low inertia. The light exciting the fluorescent system is passed through one such shutter and the fluorescence passes through a similar shutter which can be actuated a minute fraction of a microsecond later. It is sometimes not necessary to have a second Kerr cell.

Another procedure to measure lifetimes employs a method known as phase shift. In this method, the exciting light is sent through a water tank in which standing waves are being generated by a vibrating quartz crystal. The wave pattern diffracts the light and the diffraction image of one slit is focused on another. The emergent modulated light is split so that a small part goes to a reference detector and the remainder to the sample. The lifetime is determined by first scattering the light that normally would go to the sample, to a second detector and the phase relation between the signals is measured. The sample is then put into place. The emitted fluorescence is modulated in intensity according to the excitation modulation but is delayed in phase by an angle which is related to the observed fluorescence lifetime by Eqs. 6 and 2:

$$\tan \Delta\Phi = 2\pi f \tau \tag{6}$$

where f is the frequency of modulation and $\Delta\Phi$ is the angular delay in the phase. This technique permits measurement in the nanosecond (10^{-9} sec) range.

3. QUANTUM YIELD

The quantum yield is the most difficult characteristic to measure. This is particularly true when absolute quantum yields are desired. It is somewhat more simple to obtain information on relative quantum yields. In general the quantum yield of an emission is defined as the number of quanta emitted per exciting quantum absorbed. Therefore,

$$\varphi^F = \frac{\text{number of fluorescence quanta emitted}}{\text{number of quanta absorbed (in excitation to) to a singlet excited state}}$$

The quantum yield of phosphorescence is defined as:

$$\varphi^P = \frac{\text{number of phosphorescence quanta emitted}}{\text{number of quanta absorbed (in excitation to) to a singlet excited state}}$$

In the case of phosphorescence, because of the forbidden character of the direct absorption $S_0 \rightarrow T_0$ (Fig. 2), excitation usually occurs via a singlet state. The quantum yields become intrinsic, $\varphi_0{}^F$, $\varphi_0{}^P$, when they are measured in the absence of external quenching by collision processes.

In the absence of photochemical reaction (such as self-decomposition) the following expression is valid:

$$\sum_i \varphi_0{}^i = \varphi_0{}^F + \varphi_0{}^P + \varphi_0{}^I = 1 \tag{7}$$

where $\varphi_0{}^I$ is the quantum yield for internal conversion by vibrational deactivation (radiationless deactivation between electronic states, see Figs. 2 and 3.) In many cases $\varphi_0{}^I$ may be small and for the sake of discussion let it be considered to be zero. Then

$$\varphi_0{}^F + \varphi_0{}^P = 1 \tag{8}$$

This equation points up the important fact that these are *complementary* in nature. Even though phosphorescence may not be seen (as in a fluid solution) the triplet state *is still occupied* to a degree dependent upon the intrinsic quantum yield. This has important significance if the triplet state is involved in following photochemical process. Other concepts and expressions involving quantum yields are discussed later (see Sections I-B-2 and III-A-2).

In the case of collisional bimolecular quenching (external quenching) the general relation between lifetime and quantum yields is

$$\frac{\tau_Q}{\tau} = \frac{\varphi}{\varphi_0} \tag{9}$$

where τ_Q is the observed lifetime in presence of external quenching, τ is the lifetime in the absence of external quenching and φ_0 is as previously defined and φ is the observed quantum yield in the presence of quenching. Thus, the observed τ_Q is

$$\tau_Q = \left(\frac{\varphi}{\varphi_0}\right)\tau \tag{10}$$

For example, if $\varphi_0 = 0.3$ and $\varphi = 0.03$ then the observed lifetime will be 0.1 of the lifetime in the absence of quenching. Collisions effectively shorten the lifetime.

Relative quantum yields are commonly measured with a rhodamine B quantum counter (3). The rhodamine dye is excited by the fluorescence of the sample which is fed to a photomultiplier whose signal is compared with a standard signal from a photocell. The intensities are converted to relative quanta sec^{-1}. Further details are available in the literature (3–5). The problem of reabsorption and reemission of the primary fluorescence has also been considered (3). Absolute quantum efficiencies (3,6–8) can be determined by measuring the sample emission with a calibrated photomultiplier and by comparing this with the response to a known portion of the light scattered from a block of magnesium oxide substituted for the sample and illuminated by the same source.

In the remainder of this chapter, it will be assumed that external quenching is absent, except when stated otherwise.

4. POLARIZATION

It is known that, in general, transitions will be allowed only for certain orientations of the electric vector of the incident radiation. An electronic transition is allowed providing

$$\int \psi_e \mathbf{M} \psi_{e'} \, d\tau \neq 0$$

where ψ_e and ψ_e' are electronic wave functions, **M** is the dipole moment operator, and $d\tau$ is the element of volume in terms of the electronic coordinates. In group theoretical language, the integral will be nonzero if the direct product of the integrand $\psi_e \mathbf{M} \psi_e'$ transforms or has a component that transforms like the totally symmetric irreducible representation of the group (p. 163 *et seq.*). If, for example,

$$\int \psi_e M_z \psi_{e'} \, d\tau$$

where M_z is the component of **M** along the z axis, transforms like the totally symmetric representation, then the transition will be polarized along the z direction. For example, the z direction may be perpendicular to the plane of an aromatic hydrocarbon such as naphthalene. The component of the dipole moment M_x, M_y and M_z transform like translational displacements which are denoted T_x, T_y, and T_z in group theory tables. With this knowledge we can say that if the direct product of $\psi_e \psi_{e'}$ transforms like T_x, T_y, or T_z then the transition is allowed and is polarized along the x, y, or z axis. For example in H_2O (Group C_{2v}) the transitions $A_1 \leftrightarrow A_1$, $A_2 \leftrightarrow A_2$ and $B_1 \leftrightarrow B_1$ are allowed and polarized along the z axis.

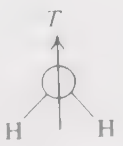

II. FLUORESCENCE

A. Nature of Fluorescence

The simplest examples of fluorescence are afforded by monatomic vapors at low pressure. Sodium atoms, for example, in their ground state, $^2S_0$, absorb the well-known D lines and are thus excited to the states $^2P_{1/2}$ and $^2P_{3/2}$, reverting, after a mean life of 1.6×10^{-8} sec, to the ground state with the emission in all directions of the D lines. This type of fluorescent emission, in which the wavelengths of the emission and absorption lines coincide, is called *resonance radiation.* The term is derived from the classical (prequantum) concept that absorption resulted from a resonance between the frequency of the exciting light and an electronic frequency within the atom.

Resonance spectra can be observed in diatomic molecules at very low pressure in the gaseous state. On excitation by monochromatic radiation emission is not confined to the absorbed frequency. Transitions occur from the excited state (a particular rotational state of a particular vibrational state of the excited electronic state) to rotational states of a number of vibrational states of the ground electronic state. Thus, the "resonance spectrum" of a diatomic molecule consists of a series of lines, one coinciding with the absorption line, the others at longer wavelengths representing the return to higher vibrational levels of the ground state. The intervals between the principal members of the series therefore represent energy differences between vibrational levels in the ground state.

An important question arises regarding the number of possible excited singlet states from which the fluorescence may originate. Absorption can occur to any of the excited states S_1, S_2, S_3, etc. However, fluorescence emission occurs in almost every case from the lowest excited state S_1 (Figs. 2 and 3). Moreover, the vibrational level origin within S_1 is the zero level. Thus, the lowest energy band in absorption and the highest energy band in emission should coincide. This is in fact quite true for vapor but may not be true for solutions (see Section II-C). An exceptional case is that of azulene for which the fluorescence emission is from the second excited singlet level rather than from the first.

In general, the lifetimes of excited states of singlet character can be expected to range from 10^{-7} to 10^{-9} sec. However, associated with each state there are vibrations whose lifetime can be expected to range from 10^{-11} to 10^{-13} sec. Moreover, in a complex molecule there are large numbers of excited states which, it may be recalled, are actually potential energy surfaces. These may be represented in a cross-sectional sense as shown in Figure 6 of Chapter 1. Once excitation has occurred to a vibrational level of some relatively high singlet state, say S_3, the molecule immediately begins vibrating and an extremely rapid vibrational cascading process starts through the vibrational levels associated with the excited state (Figs. 2 and 3).

It may well be that the potential energy surface for S_3 is crossed or cut by that for S_2. Some vibrational level of S_2 will then be isoenergetic or nearly so with that of S_3 (for example, level *8* of S_1 and level *1* of S_2 in Fig. 3). In this case there is a high probability that during the next and succeeding vibrations, the molecule will be vibrating in a manner appropriate to that for S_2. As the cascading continues, S_1 may cross S_2 and the above process repeated until finally the vibrational cascading or *internal conversion* process has carried the molecule to the lowest vibrational level of the lowest excited electronic state S_1. From here the molecule emits to various vibrational levels of the ground state and the typical fluorescence band results as in Figure 4. It is important to note that the potential energy curves need *not* actually cross, but that they be sufficiently close so that they interact strongly or "mix," thereby ultimately providing a pathway for the energy loss just described. From experimental results, it is quite evident that the deactivational process as described above occurs with an extremely high probability, since emissions other than from S_1 are almost nonexistent. Thus, electronic energy is transformed and lost as vibrational energy by *internal conversion*. Also it is highly likely that part of the energy loss associated with internal conversion occurs during collisions of the excited molecules with other molecules. The proportion of the energy lost in this way is not known. However, the transformation from high to low excited electronic states occurs not only in fluid media, but also in rigid media in which the number of collisions must be severely diminished.

If it happens that the ground state and lowest excited state potential energy curves cross or mix, the fluorescence intensity may be weak or absent. The molecules can also lose energy from the first excited state by collisions. For example, the fluorescence intensity or quantum yield often increases with an increase in the solvent viscosity. The implication is that fewer collisions or restricted freedom of molecular motion will decrease the number of molecules whose excitation energy is degraded before emission can occur.

The rules relating the shape of an absorption spectrum and the Franck-Condon principle also apply to the general shape of fluorescence spectra. There have been numerous accounts in the literature of the approximate mirror image relationship between absorption and emission (for example, Fig. 4). This can occur if the vibrations in the excited state are comparable to those in the ground state. Differences in the dipole orientation or in hydrogen bonding between the two states can modify this relationship. The mirror image relationship is therefore not to be considered as general and its existence will be one of the characteristics of the emission useful in the interpretation of the process.

Finally, it is worthwhile to consider the case of azulene. Excitation of azulene results in fluorescence emission from the second excited singlet state

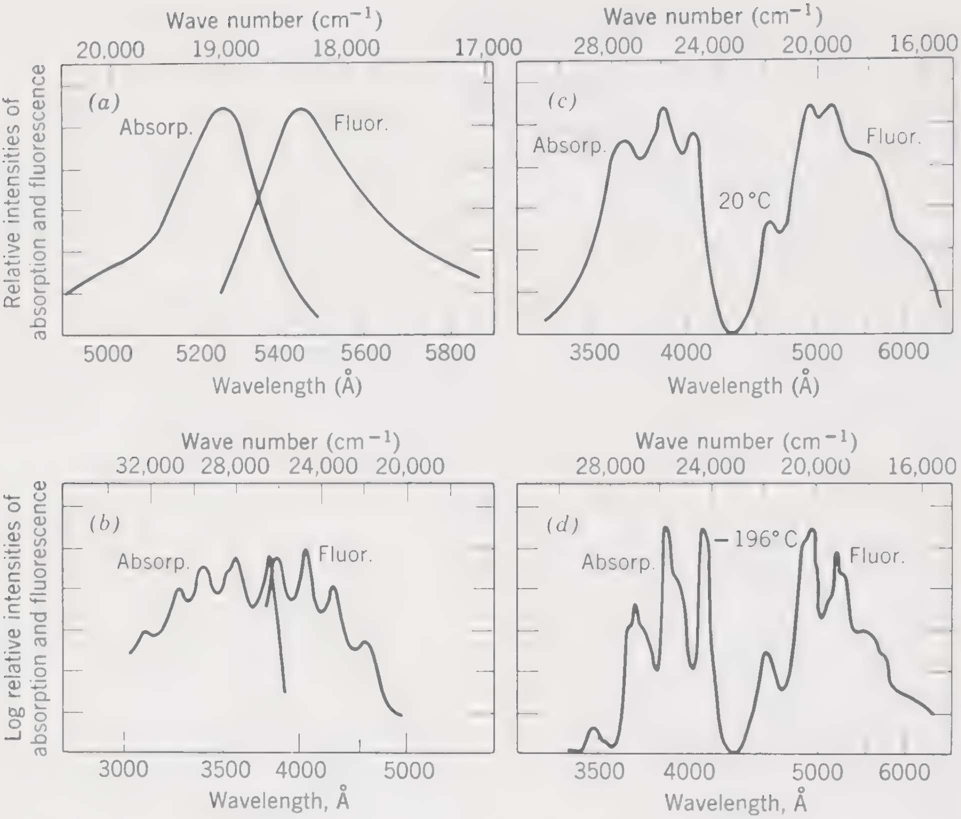

Fig. 4. Approximate mirror-image relation between absorption and fluorescence spectra: (*A*) fluorescein (8a); (*B*) anthracene in dioxane (8b); (*C*) diphenyloctatetraene in xylene at 20°C (8c); and (*D*) same as (*C*) at −196°C (8c).

and moreover no phosphorescence occurs (9,10). This could be interpreted in several ways. Excitation into the second state is not followed by internal conversion to the first state because of the differences in energy and symmetry characteristics between them. That is, they do not cross or mix. Secondly, excitation into the first band results in internal conversion to the ground state (thus no fluorescence) because of crossing of the potential curves (9). Also, it is possible that as an alternative explanation crossing occurs from the first excited singlet to the triplet level (10) and thus the population in the potentially fluorescent state is converted to the equivalent occupation of the triplet state. It has been suggested that phosphorescence has not been observed because of difficulty of observing the expected long wavelength emission (10), or because the lowest triplet state lies above the lowest excited singlet; hence, occupation of the former is vanishingly small (9). The observations on emission are inadequate to clarify completely the peculiarities of the azulene fluorescence. Oxygen perturbed singlet → triplet absorption (see Section

III-F-2) indicates that the lowest triplet state is either higher than the first excited singlet state or only very slightly lower (11).

B. Relationship between Absorption Intensity and Lifetime

We shall deal here with the fundamental relation between the transition probabilities for induced and spontaneous emission. Although the results have been expressed in various ways, the following is a general expression (Chapter I, p. 53):

$$\frac{1}{\tau_0} = A_{2\to 1} = \frac{8\pi 2303 c\nu^2 n^2}{N} \frac{g_1}{g_2} \int \epsilon \, d\nu \tag{11}$$

where $A_{2\to 1}$ is the Einstein coefficient for spontaneous emission from the excited to the ground state, c is the velocity of light, *in vacuo*, ν is the energy of the transition in cm^{-1}, n is the refractive index of the surrounding medium, g_1 and g_2 are the degeneracies of the lower and upper states, ϵ is the molecular (or molar) extinction coefficient and N is Avogadro's number. The integration is taken over an entire absorption band. Again, the actually observed lifetime τ will agree with τ_0 providing there are no other deactivational modes present other than emission being considered.

In general, the equation can be accurately applied to an atomic system where the absorption and emission have the same wavelength and applied approximately to molecular systems. A modification of the equation can be made for molecular systems for which the transition of concern is highly allowed (2). It will be worthwhile to briefly pursue the basis for the above equation and the modifications.

There are several ways of deriving the relationships between the Einstein probability coefficients for absorption and emission. The following abbreviated development is one of them for discrete states. Figure 5 defines the coefficients as the induced absorption coefficient, B_{12}, the induced emission

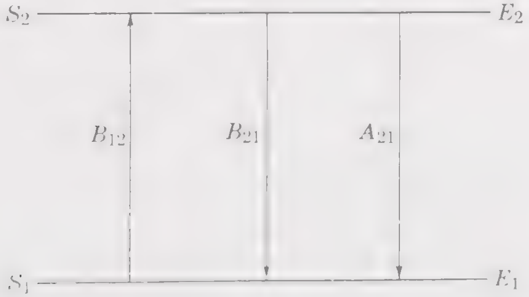

Fig. 5. Relation among the Einstein coefficients.

coefficient, B_{21}, and the spontaneous emission coefficient, A_{21}. The rate of absorption from state 1 to state 2 is

$$n_1 B_{12} \rho_v \tag{12}$$

where n_1 is the number of molecules state 1 and ρ_v is the radiation density as given by Planck's blackbody radiation law. The rate of emission from state 2 to state 1 is

$$n_2(A_{21} + B_{21}\rho_v) \tag{13}$$

where n_2 is the number of molecules in state 2. For a given radiation density, the probabilities of induced emission and of absorption are assumed to be equal. At equilibrium, Eq. 12 is equal to Eq. 13. Also, the number of molecules in the states is determined by the Boltzmann distribution law and ρ_v by the blackbody law, resulting in the following equation:

$$A_{21} = \frac{8\pi h \nu^3 n^3}{c^3} \frac{g_1}{g_2} B_{12} \tag{14}$$

The coefficient B_{12} can be expanded in terms of the probability of a transition from state 1 to state 2 to give

$$B_{12} = \frac{2303}{hn\,N} \int \epsilon \, d\nu \tag{15}$$

Substitution of Eq. 15 into Eq. 14 will give Eq. 11.

In the case of molecular systems, the electronic states are not discrete because of vibrations and moreover the vibrational fine structure has breadth. Therefore, transitions can occur over a range of frequencies or energies. Additional modifications are therefore required. The final equation for an allowed transition can generally be written as (2)

$$\frac{1}{\tau_0} = A_{21} = \frac{8\pi \times 2303 c n^2}{N\langle \nu_f^{-3}\rangle_{av}^{-1}} \frac{g_1}{g_2} \int \epsilon \, d \ln \nu \tag{16}$$

where the integral is over the entire electronic absorption band and $\langle \nu_f^{-3}\rangle_{av}^{-1}$ is the reciprocal of the mean value of ν^{-3} in the fluorescence spectrum. If the absorption was sharp and the fluorescence and absorption occurred at the same wavelength the integral could be considered constant. Therefore, a factor of $1/\nu$ could be extracted from under the integral and $\langle \nu_f^{-3}\rangle_{av}^{-1}$ becomes ν^3 and the equation becomes identical to equation 11.

The $\langle \nu_f^{-3}\rangle_{av}^{-1}$ can be most accurately evaluated by plotting intensity (relative quanta at each frequency) vs. frequency in cm^{-1} and ν^{-3} times the intensity vs. frequency (cm^{-1}). The ratio of the areas under these curves gives $\langle \nu_f^{-3} \rangle_{av}^{-1}$ with good accuracy (2). Also, a mean frequency can be estimated from the emission curve, the value cubed and taken as $\langle \nu_f^{-3} \rangle_{av}^{-1}$.

The formula holds for moderately strong transitions ($\epsilon \cong 8000$) and where there is not a large change in configuration in the excited state. The latter implies ideally that the maximum intensity lies at the 0–0 band. Presumably if it is near this, say up to the 0–3 band, the formula is valid (2). In the case of weak, but not symmetry forbidden transitions, the correct order of magnitude may be expected from the equation. It would appear that the error may range from 4 to 10%. In the case of the first absorption band of benzene, symmetry forbidden, the calculated lifetime is estimated to be approximately 16% too long (2).

Table I gives some fluorescence lifetimes and compares the observed values to those calculated from equation 16. The calculated values include the consideration of the fluorescence quantum yields (2). It is worthwhile to emphasize that both absorption and emission must be measured in the same solvent in order to compare observed and calculated lifetimes.

TABLE I
Comparison of Observed and Calculated Lifetimes (nsec) (2)

Compound	Solvent	Obs.	Calc.	Error (%)
Perylene	Benzene	4.79	4.29	−10
Acridone	EtOH	11.80	12.06	+2
9-Aminoacridine	EtOH	13.87	15.43	+11
9-Aminoacridine	EtOH–HCl	14.07	14.19	+1
9-Aminoacridine	H_2O	16.04	16.40	+2
9-Aminoacridine	H_2O–HCl	15.45	16.67	+8
Fluorescein	H_2O–NaOH	4.02	4.37	+9
Rhodamine *b*	EtOH	6.16	6.01	−2
Rubrene	Benzene	16.42	22.42	+37

C. Solvent Effects

1. GENERAL

The first point, an important one, to be considered is the relationship between the energy of the 0–0 band in absorption and emission. It will be recalled that this is the vibrational band of lowest energy in absorption and of highest energy in emission (Fig. 3). The discussion will not deal with cases in which the electronic transition is symmetry forbidden in which case therefore, the 0–0 band is missing in absorption. Even in this case, the 0–0 band can occur in solution although absent for the pure solute in the vapor state. Ideally, it would be expected that the absorption and emission bands would coincide since the energy change is identical. Figure 4 gives some examples of near coincidence and noncoincidence of these frequencies.

If the solvent and solute are such that one is polar and the other is nonpolar or if both are nonpolar, the frequency shifts in absorption and emission are predicted to be the same. The quantitative expressions for the shifts are equivalent (12,13). Therefore, the 0–0 bands should coincide or very nearly do so. This results from considerations similar to those given earlier. The situation is illustrated in Figure 6. The important factor in these cases is that there is no or very little difference in energy between the Franck-Condon state and the equilibrium state. Thus, the state attained by absorption and that from which emission originates are nearly the same. Further, it will be recalled that in these cases the polarization term (induced dipole–induced dipole term) and dipole–induced dipole terms are the principal contributing

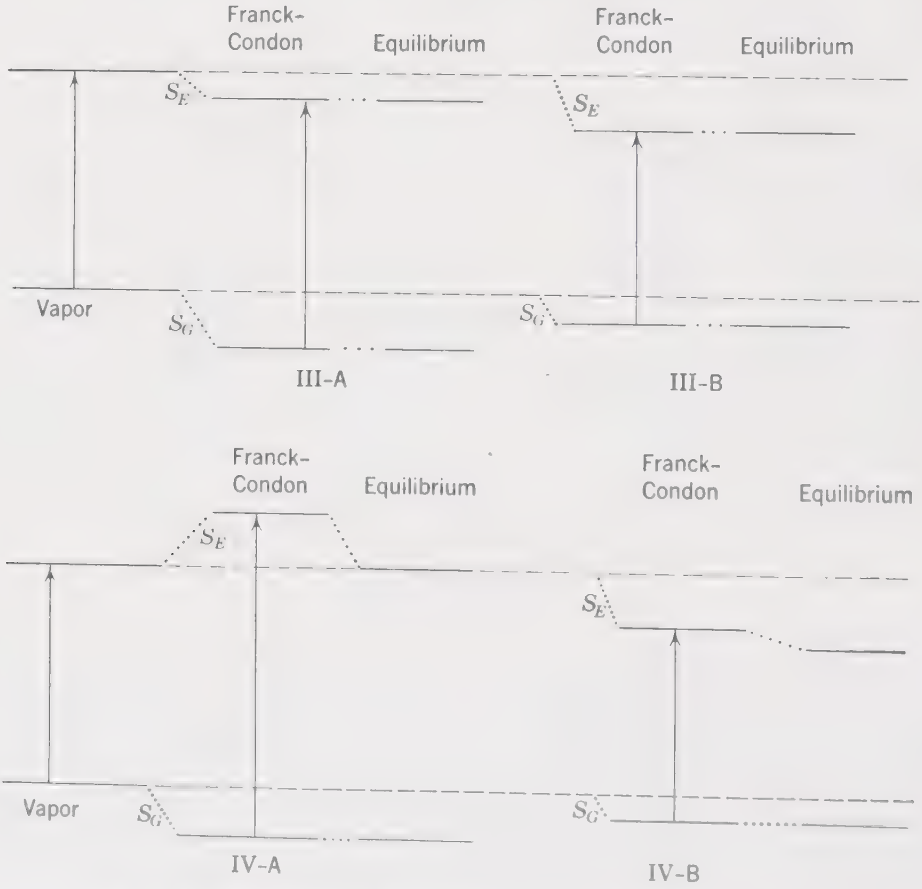
Franck-Condon
Equilibrium
S_E
S_G
Vapor
III-A
Franck-Condon
Equilibrium
S_E
S_G
III-B
Franck-Condon
Equilibrium
S_E
S_G
Vapor
IV-A
Franck-Condon
Equilibrium
S_E
S_G
IV-B

Fig. 6. Energy diagrams for various solute–solvent interactions.

factors in the solvent–solute interaction. Therefore, no orientation strain occurs; hence, the Franck-Condon and equilibrium states are nearly the same.

When the solute and solvent are both polar the situation in fluorescence is more complicated just as it is for absorption. In the simplest instance, if there is negligible dipole reorientation in the excited state, the frequency shift for fluorescence is the same as that for absorption. Again, the quantitative expressions for the shifts are identical. In this case, the 0–0 bands in the two processes should be the same or nearly so. This situation could arise when a rigid solvent is employed. In a rigid solvent, the relaxation times are several orders of magnitude greater than the lifetime of the excited state. However, if the solvent is fluid, relaxation is much more rapid and is generally completed in a time less than the lifetime of the emitting state. When this is true, it can be assumed that complete dipole reorientation occurs. Therefore, absorption will occur to the metastable Franck-Condon state but emission will occur from the equilibrium state. The representation of this difference can be seen in Figure 6 for cases IV-A and IV-B. The quantitative expression for the $\Delta\nu$ in absorption is different from that in emission and the 0–0 bands will not coincide. The final relationship expressing this difference is (13)

$$\begin{aligned}\nu(\text{abs}) - \nu(\text{emiss}) = {} & \left[\frac{D-1}{D+2} - \frac{n_0{}^2-1}{n_0{}^2+1}\right] \\ & + \left\{\frac{2}{hc}\,\frac{(\alpha_0^u - \alpha_i^u)[3(\mathbf{M}_{00}^u)^2 - 5(\mathbf{M}_{ii}^u)^2 + 2\mathbf{M}_{00}^u \cdot \mathbf{M}_{ii}^u]}{a^6}\right\} \\ & \times \left[\frac{D-1}{D+2} - \frac{n_0{}^2-1}{n_0{}^2+2}\right]^2 \qquad (17)\end{aligned}$$

where $\mathbf{M}_{00}^u$ and $\mathbf{M}_{ii}^u$ represent the dipole moment of the solute molecule in the ground and excited states, respectively, a is an effective cavity radius appropriate to the solvent, D is the static dielectric constant of the solvent, n_0 is the solvent refractive index at zero frequency and α_0^u and α_i^u are the polarizabilities of the solute molecule in its ground and excited states respectively.

In actual fact, instead of predicting the shift to be expected, one often calculates the excited state dipole moments from the equation by using the experimentally determined shift. In many cases, the second term can often be neglected. This term originates in the induced dipole–dipole interaction (solute–solvent). If the solvent is not highly polar, the induced dipole–dipole terms can be considered to make a negligible contribution to the shift. Thus, an estimate of the excited state dipole can be made from experimental shift data and the known ground state dipole moment. Other expressions similar to equation 17 have been used to estimate excited state dipole moments (14), and other methods have been proposed (15).

2. SPECIFIC EXAMPLES

Perhaps the most important topic here is that regarding molecules in which $n \leftrightarrow \pi^*$ transitions occur. It is important to note that in most cases in which the n,π^* singlet state is the lowest excited state, the emission that occurs is phosphorescence. This is by far the most common situation among molecules containing a carbonyl group and in aza aromatic compounds. Therefore, most of the discussion regarding $n \leftrightarrow \pi^*$ transitions is appropriate to the section on phosphorescence. However, some compounds of the type noted above do fluoresce and the effect of the solvent is important. More details of particular cases are considered in Section II-F.

One of the first studies relative to the effect of a solvent on fluorescence involved chlorophyll (16). Earlier work (17) had shown qualitatively that the fluorescence of the chlorphylls in benzene was extremely weak, but that the addition of small amounts of hydroxylic solvents increased the intensity. Changes were also noted in the long wavelength absorption band. More complete studies (16) at low temperature show that the chlorophylls in hydroxylic solvent systems fluoresce strongly. However, if dry chlorophylls are dissolved in a dry hydrocarbon solvent, the usual fluorescence is absent but a new and intense phosphorescence occurs at longer wavelength. Simultaneous with this change in emission, a new shoulder develops on the long wavelength absorption band of the chlorophylls. This result could be interpreted in terms of the reversal of the n,π^* and π,π^* singlet states (16). In a hydroxylic solvent, the emission would occur primarily as fluorescence from the π,π^* singlet. In a dry hydrocarbon solvent, the n,π^* singlet state would lie lowest and complete or nearly complete spin–orbital coupling would carry the molecule to the lowest n,π^* triplet from which phosphorescence emission would occur. It has also been proposed that the new long-wavelength emission may be due to dimers (18). However, it has been shown that at the same and even higher concentrations of nonspecially dried chlorophylls in the same hydrocarbon solvent, no similar emission occurs (19). It has also been observed (20) that these solvent effects did not occur when the metal was removed from chlorophyll, where it seems that solvent attachment to the metal was required for them to occur. Pertinent to this point, is the fact that an analog of chlorophyll, a Mg porphyrin, apparently does show solvent complexing directly to the metal (21). There are some problems in this interpretation since normally it would be expected that complete internal conversion would occur from the n,π triplet to the lower π,π^* triplet state. Further investigation would appear to be worthwhile. Very recently, the emission has been assigned as originating from an unsolvated chlorophyll monomer (21a).

Interesting cases concerning n,π^* states are those of acridine (22) and quinoline (23). Opinion has varied as to whether acridine fluoresces. The problem of the fluorescence of this molecule has largely centered around the nature of the solvent required. Several workers have noted that water or hydroxylic solvents are necessary for fluorescence. However, acridine does fluoresce in solvents not containing water or hydroxylic solvents at low temperature (22). A combined study of low-temperature absorption and emission further shows that the n,π^* singlet state is not the lowest state (22). Also of importance is the fact that at low temperatures a tricomplex can be formed with acridine even when it is protonated. Moreover, protonated acridine also shows fluorescence considerably to the red of acridine (the absorption in part is also considerably displaced to the red). Here the specific effect of solvents, including protonation, are important.

Finally, the case of quinoline is interesting (see Section II-F for more detail). Although the absorption of quinoline and naphthalene appear to be similar, the emissions may be quite different (23). In hydrocarbon solvents, quinoline is nonfluorescent but shows some phosphorescence (similar to that of naphthalene). However, in hydroxylic solvents, a fluorescence appears similar to that for naphthalene while the intensity of phosphorescence is lowered. In this and the acridine cases just cited it is very important to note the specific roles that solvents play. Solvent effects can be dramatic and a complete change in the nature of the emission can occur with a change of solvent.

Another important aspect of solvents is the nature of the matrix formed when they are cooled. Certain pure hydrocarbons and mixtures of these with many other solvents produce clear glasses when cooled to low temperature (77°K). Excitation of the solute results in the usual fluorescence with associated rather broad vibrational fine structure. However, in the case of certain aliphatic hydrocarbon solvents and aromatic hydrocarbon solutes, interesting changes can occur. In the spectral effects just discussed functional group characteristics of the solvent played dominant roles. In the case of the hydrocarbons, the physical characteristics of the solvent molecule are important. Russian investigators have been the most active in this subject area (24). At low temperature (77°K) the emission spectra of aromatic hydrocarbons such as naphthalene dissolved in aliphatic hydrocarbons such as heptane, show remarkably fine, quasilinear vibrational structure. This effect is discussed in greater detail in Section II-E-1.

D. Aliphatic and Unsaturated Compounds

Certain polyacetylene derivatives show fluorescence, phosphorescence, or both in a rigid glass at low temperature (25). For example, fluorescence is observed for diethyltetraacetylene and diphenylacetylene. Phosphorescence is observed for these as well as others such as diphenyldiacetylene (no fluorescence) and dihydroxytriacetylene (no fluorescence). The fluorescences originate in the 3000–4350-Å region while the phosphorescences originate in the 4550–5900-Å region. The lifetimes of the latter emission vary from 0.01 to 5 sec. Some solutions of aliphatic derivatives presumably show fluorescence under high energy excitation as with γ rays (26). For example, bromoform, tetrachloroethylene, and dimethylformamide show weak emission. Some other compounds such as diphenylmethane, tetraisobutylene, 1,6-diphenyl-1,3,5-hexatriene show somewhat stronger emission, particularly the latter. In other cases such as aromatic compounds, a generally good correlation of luminescence intensity from γ excitation and ultraviolet excitation exists (26).

Generally, fluorescence occurs from butadiene and hexatriene, with phenyl substitution or, in some cases, with methyl additions (27). Quantum yields of fluorescence are as high as 0.43 and as low as zero; usually they are different in benzene and in heptane, being lower in benzene with some exceptions. The emission spectra vary in location from the ultraviolet to the visible. The simplest hexatriene derivative, 1,6-diphenylhexatriene, emits in the deep blue spectral region. The addition of methyl groups to this compound to form the 5-methyl- or the 4,5-dimethyl derivatives causes a marked decrease in the quantum yields (5 to 30-fold). In fact, in the dimethyl derivative, fluorescence seems not to occur in benzene. Other substituted derivatives such as the 1,5-diphenyl-6-(2-pyridyl)hexatriene show no emission.

As the number of phenyl substitutions increases on a butadiene parent, the spectrum moves into the visible. In addition, the tetraphenyl (1,1,4,4-) derivative has the highest fluorescence quantum yield. The lifetimes of fluorescence for the 1,1,4,4-tetraphenylbutadiene and 1,6-diphenylhexatriene derivatives are 2.5 and 7.1×10^{-9} sec, respectively, in heptane (shorter in benzene).

E. Aromatic Hydrocarbons and Substituted Derivatives

1. AROMATIC HYDROCARBONS

Aromatic hydrocarbons (see Fig. 7) are fluorescent in solution. The spectral position depends on the longest wavelength of absorption. Benzene emits in the ultraviolet and a progressive movement of the emission to the visible occurs through the linear polyacenes—anthracene emitting in the blue, naphthacene in the green, and pentacene in the red regions. This is in agreement with the predictions of molecular orbital theory. Especially at low temperatures there is well-defined vibrational structure in the emission spectra. The quantum yields of fluorescence increase with increasing number of rings from a value of 0.26 (6) for benzene to about 0.46 (28) for anthracene [however, later data indicate a lower value of approximately 0.3 (3)] and then diminish to a low value at pentacene. At least in the case of benzene and

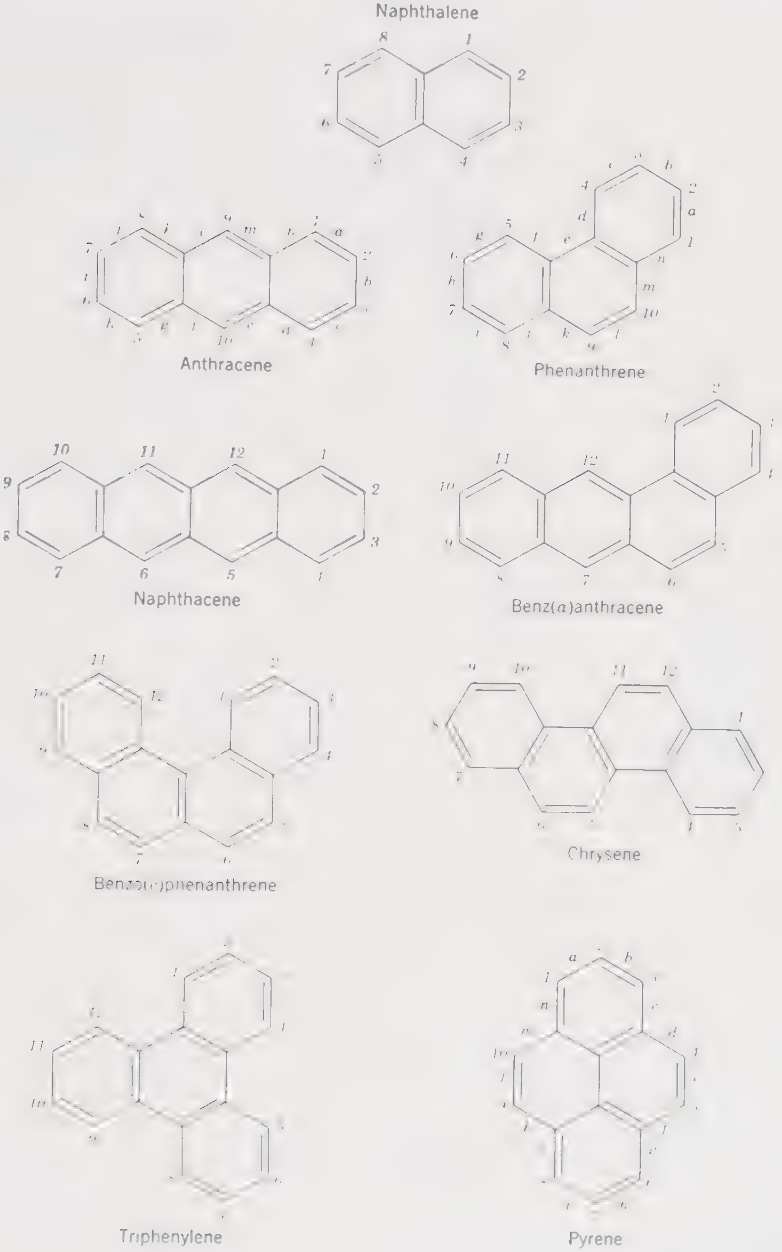
Naphthalene
Anthracene
Phenanthrene
Naphthacene
Benz(a)anthracene
Benzo(c)phenanthrene
Chrysene
Triphenylene
Pyrene

Fig. 7. Structures of various aromatic hydrocarbons.

naphthalene, the quantum yields are dependent somewhat on the concentration, as well as on the frequency of the exciting radiation. Table II gives some values. It must be emphasized that in comparing quantum yields, it is very important to consider factors such as correction for reabsorption, solvent and concentration as well as exciting frequency. The neglect of correction for

TABLE II

Absolute Quantum Yields for Fluorescence for Some Hydrocarbons and Derivatives

Compound	$\varphi^{a,c}$	$\varphi_0^{a,b,c}$
Anthracene	0.241(B), 0.241(P), 0.249(A), 0.323(HC), 0.36(H)	0.256(B), 0.316(P), 0.270(A), 0.328(HC)
Perylene	0.800(B), 0.790(P), 0.840(A)	0.890(B)
9-Bromoanthracene	0.050(B), 0.024(P), 0.019(A)	0.052(B)
9,10-Diphenylanthracene	0.840(B), 0.83(P), 0.81(A)	0.84(B), 0.81(A)
9-Cyanoanthracene	0.796(B), 0.660(P), 0.740(A)	0.878(B)
Benzene	0.26[d], 0.20[g]	
Fluorobenzene	0.24[d]	
Naphthalene	0.55[d]	
Triphenylene	0.04[d]	
9,10-Dimethylanthracene	0.81(B)[e]	0.81(B)
9,10-Dichloroanthracene	0.56[h]	
1-Fluoronaphthalene	0.84[f]	
1-Chloronaphthalene	0.058[f]	
1-Bromonaphthalene	0.0016 ± 0.0005[f]	
1-Iodonaphthalene	$<$0.0005[f]	
1-Methylnaphthalene	0.85 ± 0.19[f]	
1-Naphthaldehyde	$<$0.0001[f]	
1-Nitronaphthalene	$<$0.0001[f]	

[a] Solvents: B = benzene, P = petroleum ether, A = ethyl alcohol, H = hexane, AE = alcohol–ether, 2:1 by volume, HC = paraffin hydrocarbon (paraffin), EPA = ether–isopentane–ethyl alcohol, 5:5:2 by volume.

[b] Extrapolated to infinite dilution.

[c] All data above benzene, except where noted, at room temperature from reference 3, corrected for reabsorption.

[d] Reference 6, all in EPA at 77 K. Reabsorption considered negligible, some data slightly concentration dependent.

[e] Reference 7, room temperature.

[f] Reference 45, all in AE at 77 K. Based on absolute φ_F naphthalene of 0.55 from reference 6.

[g] Reference 152.

[h] Reference 29b, 21°C in alcohol.

[i] Reference 29b, 21°C in hexane, 0.28 in alcohol as a standard.

reabsorption can result in appreciable error—as high as 50% if 30–50% of the absorption spectrum overlaps the fluorescence spectrum and if the fluorescence quantum yield is high (29). The nature of the solvent can sometimes have a dramatic effect on the yield. For example, 9-methyl-10-chloromethylanthracene shows a φ_F of 0.09 in benzene and 0.73 in ethanol (uncorrected for reabsorption) (7). In the case of the parent hydrocarbons, the effect is not so marked but is nonetheless present (8). At least in certain cases, for example, anthracene in ethanol and fluorene in ethanol or hexane, the φ_F is independent of wavelength over a quite wide range of wavelengths (3).

Data on fluorescence lifetimes are less plentiful than those on phosphorescence, although there are a fair number on microcrystalline hydrocarbons (29). Some typical values of fluorescence lifetimes are shown in Table III. In some cases (pyrene; benz(*a*)pyrene in microcrystalline state) it is doubtful if the lifetime is inherent to the free molecule. The fluorescence spectra (29) of these compounds show characteristics of a dimer type of complex between excited and unexcited molecules and thus the emission lifetime in a microcrystalline state may possibly be associated with this aggregate. Although peculiarities of the spectra have been pointed out (29) and general molecular interaction considered, apparently this specific possibility was not considered. Studies on the fluorescence spectra of benz(*a*)pyrene, pyrene, coronene, and perylene also suggest that the excited dimer may participate in the emission. Such dimer complexes are discussed later in this section. The crystalline monomethyl derivatives of benz(*a*)anthracene have lifetimes of approximately 10 nsec except that the 8 and 11 derivatives show considerably longer lifetimes (~ 100 nsec). In the latter cases, there is again an indication of a fluorescence different from that of the others attributable to an excited-unexcited pair.

TABLE III
Fluorescent Lifetimes of Hydrocarbons

Compound	Observed lifetime (nsec)
Anthracene	6.4,[a] 6.5[b]
Phenanthrene	5.7[b]
Benz(*a*)anthracene	6.1,[a] 60[b]
Chrysene	17.6,[a] 50[b]
Pyrene	46.5,[a] ~400[b]
Perylene	7.9[b]
para-Terphenyl	5.5,[a] 1.3[b]
Benz(*a*)pyrene	8.6[a]
Benzene	2000,[c] 590[d]
Naphthalene	500[c]

[a] Microcrystalline state from reference 29.

[b] From reference 29a in EPA (5 parts ether–5 parts isopentane–2 parts ethyl alcohol) at 77 K.

[c] A. Dammers-de-Klerk, *Chem. Weekblad*, **54**, 281 (1958).

[d] J. Donovan and A. B. F. Duncan, *J. Chem. Phys.*, **35**, 1389 (1961); in vapor phase extrapolated to zero pressure.

Crystalline monomethyl-substituted benzo(*c*)phenanthrenes have lifetimes in the 20 nsec range. The fluorescence lifetimes of the first seven hydrocarbons in an alcohol ether hydrocarbon solvent at 77°K listed in Table III are not altered by perdeuteration of the hydrocarbon (29a). This indicates that essentially there is no internal conversion to the ground state from the first excited singlet state. Further, at least in the case of anthracene, the lifetime is the same at room temperature. Since the rate constant for fluorescence emission is not expected to be temperature dependent, this indicates that the rate constant for intersystem crossing is unlikely to vary with temperature. However, the rate constant for fluorescence emission does show a very slight temperature dependence (29b). Further, the sum of the rate constants for internal conversion and intersystem crossing show no temperature dependence. In contrast, for 9,10-dichloranthracene the sum of these same rate constants shows a strong temperature dependence. However, the emission rate constant shows only a slight temperature dependence (29b). In summary, the results on anthracene, despite the very small variation of the emission rate constant, quite clearly show that essentially all the rate constants considered are temperature independent and thus, the quantum yield of fluorescence should be temperature independent. This appears to be true (29b).

Just as in the case of the linear polyacenes, the spectral location of the fluorescence of hydrocarbon isomers depends on the location of the longest wavelength absorption. In the isomeric tetracyclic compounds this depends qualitatively on the number of "bends" in the molecule. Thus, linear naphthacene emits in the green beginning at approximately 4750 Å; benz(*a*)anthracene (one bend), at 3800 Å, chrysene and benzo(*c*)phenanthrene, two bends, at 3600 Å and 3700 Å, respectively; and finally triphenylene, at 3450 Å (30). The general trend is in accord with the deductions from molecular orbital theory. The intensity of fluorescence varies considerably among the tetracyclic isomers. Benz(*a*)anthracene and naphthacene are the strongest emitters and triphenylene is the weakest. In compounds containing larger systems such as five or six rings, the fluorescence is usually at longer wavelengths, with some exceptions. For example, one of the benzochrysenes apparently emits at shorter wavelengths than does benz(*a*)anthracene (31).

Partial hydrogenation of the molecule can cause a significant shift of the emission toward the blue or ultraviolet region of the spectrum. Hydrogenation of linearly condensed ring hydrocarbons at sites which reduce the number of rings in conjugation may cause visible fluorescence to disappear as the absorption band and the fluorescence are displaced into the ultraviolet region. For example, 9,10-dihydroanthracene contains two disconnected benzene rings and the blue fluorescence of anthracene is replaced by ultraviolet fluorescence similar to that of benzene (32). Similarly, the fluorescence of pure fluorene is limited to the ultraviolet region and, in agreement with the structure, is similar in position to that of biphenyl; however, the quantum yield of fluorescence for fluorene is considerably higher. Similarly, the emission spectrum of pentacene begins at approximately 5800 Å while that of one of the dihydro derivatives begins at approximately 3850 Å.

One of the interesting developments regarding the emission spectra of aromatic hydrocarbons is the possibility of obtaining unusually well-resolved fine structure. This is accomplished by cooling solutions in aliphatic hydrocarbon to 77°K or below, where the mixture becomes a frozen crystalline solution. Depending upon the dimensions of the solute and solvent molecules, the resulting fluorescence can be quasilinear in nature with bands as narrow as 10 cm^{-1}. Detailed studies of this aspect of the emission of aromatic hydrocarbons include those on naphthalene, anthracene, benz(*a*)anthracene, benz(*a*)pyrene, coronene, perylene, pyrene, and other compounds (24,33,34). Certain aliphatic alcohols can also be used as solvents for the development of this effect. The linelike structure is presumed to arise because an aromatic hydrocarbon replaces an aliphatic hydrocarbon at a lattice site and thereby exists in a state that can be described as an oriented gas molecule. Thus, the spectra are of the unperturbed system corresponding to free molecules. The ideal situation results when the dimensions of the solute and solvent molecules are comparable so that the solute molecule can occupy a definite position in the host lattice with minimum deformation. For example, the emission spectrum of naphthalene in pentane shows quasilinear structure, but is more diffuse in hexane and heptane. If the solvent molecule is too small, a similar situation arises. The broader, diffuse spectra that can result tend to be similar to those obtained in clear, rigid glass solvent systems. There can be a variation in the number of lines and their intensity, depending upon the solvent and temperature. The variations in part appear to originate from the fact that there are local differences in the crystal field surrounding different molecules. Also, the rate of freezing of the mixture is important. Slow freezing results in the loss of some short wavelength components and weakening of some long wavelength components. This probably results from formation of rotational isomers (34). Under slow freezing it is more likely that a greater proportion of the molecules will be in the stablest conformation and the spectrum will be simple. Such fine-line spectra can be used to determine structural details of the emitting molecule (34).

One factor which requires consideration when studying the fluorescence of aromatic hydrocarbons is the effect of solute concentration. In the cases of anthracene and phenanthrene, for example, there is considerable separation of the 0-0 bands of the absorption and fluorescence spectra when the concentration is high ($10^{-3}\,M$) in cyclohexane. However, at low concentration ($< 10^{-6}\,M$) there is near perfect coincidence of the 0-0 bands (35). It should be noted however that this effect does not always occur since in certain solvents, such as ethanol, dioxane, and benzene, a separation at low concentration still may exist (50–110 cm^{-1}). The closest coincidences are obtained with aliphatic hydrocarbon solvents. In some cases, there is a still wider separation between the 0–0 bands even when low concentrations are used. For example in biphenyl the separation is 445 cm^{-1} at $10^{-7}M$. In *trans-trans*-diphenyloctatetraene, the separation is even larger (1675 cm^{-1}) (35). This is not surprising in view of the fact that the structures in the ground and excited states may be quite different (moreover, photoisomerization can occur). Solvent interactions with the excited state can be appreciably different from those in the ground state.

At high concentrations of hydrocarbons, entirely new spectral characteristics can arise (36–39). In the case of pyrene at approximately $10^{-4}M$, only a structured fluorescence spectrum is observed in the ultraviolet–violet region. However, as the concentration is increased to about $10^{-2}M$, the structured fluorescence becomes very weak and a new, broad structureless fluorescence spectrum occurs in the blue region. This transformation can also be seen at an intermediate concentration (36). The spectral change can be interpreted in terms of the formation of dimers formed by the combination of one excited and one unexcited pyrene molecule (36,37). Of course, in order for emission to occur from this species, it must form within the lifetime of the excited state of the pyrene molecule. The fluorescence of the monomer and dimer can be quenched with certain molecules (37). The formation of excited dimers or *excimers* in this way is by no means universal. The best known case is probably pyrene. The existence of such *excimers* depends on whether the lifetime of the excited state molecule is long enough for dimer formation, whether the dimer dissociates rapidly, and whether the intermolecular interaction energy is sufficient to cause quenching of the dimer fluorescence. The lifetime of the monomeric pyrene fluorescence in deoxygenated cyclohexane is approximately 2.9×10^{-7} sec in the absence of external quenching. The observed lifetime is near this only at concentrations less than $0.5 \times 10^{-3}M$. At higher concentrations, dimers are formed and the lifetime is 4.0×10^{-8} sec and is independent of concentration (39). There is also evidence for a similar type emission from crystalline hydrocarbons, as mentioned earlier (40). In these cases, pyrene in particular shows a crystal lattice in which there are essentially pairs of almost completely overlapping molecules. The fluorescence spectrum of the crystalline pyrene exhibits a broad structureless band in the visible similar to that known for dimers in solution. Other molecules having lattices in which there is very high molecular overlap also show this phenomenon (perylene, benz(*a*)pyrene, and coronene).

Finally, it is worth mentioning again the interesting situation in the hydrocarbon azulene (a nonalternate). Here, fluorescence occurs from the second excited singlet state and no phosphorescence occurs (see Section II-A).

2. SUBSTITUTED AROMATIC COMPOUNDS

Substitutions may alter the fluorescence of a parent molecule by their effect on the position, quantum yield (see Table II) and lifetime of fluorescence. The best known examples of the effects of substitution are on benzene. Therefore the following discussion will refer to this as the parent and to other aromatics where appropriate.

The amino, methylamino, and dimethylamino groups cause large red shifts of the benzene fluorescence (2700–3100 Å) with generally enhanced intensity. In aqueous solution, the fluorescence maxima of the amino and methylamino occur in the 3500-Å region with maximum intensity at $pH = 7–10$ and essentially zero intensity at $pH = 1$ (41). This indicates that the cation is nonfluorescent. Similar group substitutions appear to produce intensity enhancement in naphthalene (fluorescence from ~3000–3600 Å).

Alkyl substitution on both benzene and naphthalene cause small red shifts of the absorption bands and so correspondingly for the fluorescence. The quantum efficiency of the ultraviolet fluorescence of toluene (~2700–3200 Å) and the xylenes is higher than that of benzene while that of hexamethyl benzene is lower. In the case of anthracene, the yield depends quite noticeably on the position of substitution. At low temperature, the 9-methyl derivative has φ_F near 0.9 (0.8–0.95, depending on the solvent) while the 2-methyl has a φ_F similarly varying from 0.2 to 0.3 (42). Multiple alkyl substitution causes differences in quantum yields which again depend on the relative positions of substitutions (43). The quantum yields of 9-alkyl-substituted anthracenes seems quite independent of the chain length (methyl through propyl) (44).

Halogens have a varying effect in several respects. The monofluoro derivatives have their emission near the same wavelength as the parent hydrocarbon and at approximately the same intensity. In benzene and naphthalene, the fluorescence is red-shifted and the intensity progressively decreases in going from chlorine to bromine as a substituent. The iodo compound is not fluorescent (45). As will be discussed in further detail later in the chapter, the probability of radiationless transitions to the lowest triplet state (intersystem crossing) increases with the atomic number of the halogen. This competes with the fluorescence process and, in effect, is a quenching mechanism. In addition, fluorescence can be quenched by photochemical processes which result in rupture of the carbon–halogen bond. Iodobenzene is particularly affected because of the low bond strength. Thus, the lower fluorescence is probably due in some part to the competing predissociation process. In the case of anthracene, there is more sensitivity to position of substitution (42,46). For example, 9,10-dichloroanthracene has a quantum yield near 1 at low temperatures whereas that of the 1,5 derivative is only about 0.1. Moreover φ_F of the 9,10 derivative shows a steep temperature dependence while that of the 1,5 compound does not (42). It appears to be a generalization that disubstitution on the 9 and 10 positions notably increases the quantum yields over that of any other disubstituted derivative (42,43,46). Substitution in the 9 and 10 positions by two halogen atoms or one halogen and an alkyl group results in fluorescence maxima in nearly identical positions (47). Also, dialkyl or dihalo substituents in the 9 and 10 positions give fluorescence maxima in almost the same region.

The introduction of hydroxyl or methoxyl into the benzene nucleus shifts the fluorescence to longer wavelengths. It is probable that the quantum yields are increased over that of benzene. In aqueous solutions of the hydroxy compounds the quantum yields may vary markedly with the pH. For example, phenol fluoresces in neutral and acidic solutions but not at $pH > 12$. Thus, the anion appears to be incapable of fluorescence while the neutral molecule is fluorescent. Moreover, anisole fluoresces quite uniformly throughout the entire pH range (41). This gives added support to the conclusion that it is the phenolate anion that is nonfluorescent. Although more discussion is given later, it appears that in the case of naphthols (the 1- and 2-mono derivatives) that the neutral molecules and the anions do fluoresce, at least in aqueous solutions to $pH = 13.3$ (48). Moreover, in one case (the 2 derivative) the fluorescence intensity of the anion is greater than that of the un-ionized form. The dihydroxy compounds show fluorescence, as do their singly charged anionic forms in basic aqueous solution (49). Further, one of the double charged anions (the 1,3 derivative) shows fluorescence (48). The reasons for the differences among these compounds is not clear. Further there are conflicting data on the mononaphthols (41,48). There does not appear to be any fundamental reasons for the differences between the anions of phenol and the naphthols. The monomethyl-substituted phenols (the cresols) and disubstituted derivatives all show fluorescence in aqueous solution at low concentration ($\sim 10^{-4} M$) which is red-shifted from that of phenol. The fluorescence intensity is high from $pH = 1$–7 and becomes zero at $pH = 15$. In general, methyl substitution lowers the intensity with respect to that of phenol except for *p*-cresol. The dihydroxy benzenes, catechol, resorcinol, and quinol fluoresce (41). Like phenol, these compounds to not fluoresce at $pH = 13$.

As the pH is lowered, they begin to fluoresce weakly at $pH = 10$–11, where the concentration of the uncharged molecular species first becomes appreciable. It thus appears that both the singly charged and the doubly charged anions of the dihydroxybenzenes are nonfluorescent.

The carboxyl group causes a definite red shift of the fluorescence. Moreover, it causes a substantial if not complete quenching of the fluorescence of benzene (at least in aqueous solution at all pH values) (41). This effect can be compensated for by the additional substitution of hydroxyl or amino groups. For example, salicylic acid, *m*- and *p*-hydroxybenzoic and *o*- and *p*-amino-benzoic acids all show fluorescence. In aqueous solution at concentrations $<10^{-4}M$ the *o*-, *m*-, and *p*-hydroxy benzoic acids appear not to fluoresce as neutral species (41). The *o*-hydroxy derivative shows fluorescence as the mono- and dianion whereas in the other cases only the dianion was found to fluoresce. An increase in concentration could modify these results to some degree although probably not change the essential qualitative order of relative intensity. More complicated acids such as hydroxyphenylacetic acid fluoresce (41). In general, at concentrations of $\sim 5 \times 10^{-5}M$ in aqueous solutions, those acids which do not contain the phenol grouping do not fluoresce (for example, phenylacetic acid). In those cases in which the hydroxy group is present, the acids fluoresce only as the monoanion.

The sulfonic acid group, SO_3H, or the sulfonate ion, SO_3^{2-}, usually exerts little influence on the absorption or fluorescence of aromatic compounds and the group can be introduced if a water-soluble fluorescent compound is desired.

The presence of a quinone structure generally results in quenching of fluorescence. Benzoquinone and anthraquinone do not fluoresce in solution, although anthraquinones containing hydroxyl groups capable of forming hydrogen bridges with the carbonyl oxygen are fluorescent (for example 1,4-dihydroxyanthraquinone).

In benzene and naphthalene, the $C{\equiv}N$ group increases fluorescence efficiency without appreciably changing the wavelength. In anthracene, the cyano group in the 9 position greatly enhances the fluorescent yield (Table II). Styrene, $C_6H_6CH{=}CH_2$, fluoresces in the ultraviolet with greater efficiency than benzene with displacement to longer wavelengths. Of the stilbenes, 1,2-diphenylethylenes, the *cis* compound shows much lower fluorescence intensity than does the *trans*-stilbene. The *trans* derivative fluoresces relatively strongly and the spectrum is characterized by well-resolved vibrational structure extending into the visible region. During irradiation *cis*-stilbene is continuously converted to *trans*-stilbene, the fluorescence of which gradually becomes evident. The introduction of amino, hydroxy, and alkoxy substituents into *trans*-stilbene causes displacement of the absorption bands to longer wavelengths, and the corresponding fluorescence extends into the blue region of the spectrum.

Related to the above subject is the consideration of the azobenzenes and azonaphthalenes. Azobenzene has no luminescence to about 7000 A. The azo compounds do luminesce when substituents are able to form intra- or intermolecular hydrogen bonds (49). The *o*-hydroxyazo compounds fluoresce only in solutions of normal hydrocarbons at 77 K and as solids at both room and low temperature. The *o*-aminoazo compounds do not fluoresce in solution. The *o*- and *p*-hydroxy-, and *p*-aminoazo compounds show fluorescence as solids at both room and low temperature. However, methylation of the hydroxy or the amino groups in the *o*- and *p*-positions causes fluorescence to disappear. The *o*-hydroxyazonaphthalene also shows fluorescence. In general, it appears that without substitution, the excited state energy can be dissipated by torsional vibration modes. However, with *o*-hydroxy groups, a hydrogen bond can form to the azo group giving coplanarity and increased rigidity, thus at least reducing torsional dissipation of energy. This apparently is not the entire answer since the *p*-hydroxy compound does fluoresce even if only weakly. More detailed study is necessary in order to completely clarify the situation.

The nitro group tends to repress fluorescence strongly. Nitrobenzene, the nitronaphthalenes, the nitrophenols, and picric acid do not fluoresce. As with iodo-substituted compounds, the nitro group does not necessarily completely quench the fluorescence if the molecule contains a substituent tending to intensify fluorescence. For example, 1-nitro-2-naphthylamine is fluorescent as are some dyes containing the nitro group, although the quantum efficiency of fluorescence is low.

The fluorescence of methyl-substituted isomeric tetracyclic aromatic hydrocarbons, is generally red-shifted from that of the parent molecule (19). This is in agreement with the changes in absorption and is in accord with the predictions of molecular orbital theory. In addition, there is considerable variation in intensity among a given methyl-substituted series such as the benz(*a*)anthracenes. The 7-methyl derivative appears to be the strongest emitter while the 3- and 9-methyl derivatives appear to be the weakest (19).

Substitution of aromatic rings in hydrocarbons such as anthracene causes red shifts. In addition, phenyl disubstitution in the 9 and 10 positions causes a large increase of the fluorescence quantum yield ($\varphi_F \sim 1$).

The effect of substituting within the ring to produce heterocyclic compounds depends on the heteroatom. Introduction of nitrogen commonly shifts the fluorescence to the red. The introduction of NH or O for CH_2 in fluorene to give carbazole and dibenzofuran results in a red shift. In the case of indene, substitution to give the nitrogen analog indole and the oxygen analog benzofuran causes a slight blue shift in the former and fluorescence apparently is absent in the latter (50). Again, in these cases, as additional benzene rings are linearly condensed, the spectrum shifts to the red. An interesting effect of substitution, from both physical and spectral points of view concerns the *p*-polyphenylenes (51). This series begins with biphenyl and includes *p*-terphenyl, etc. As the number of unsubstituted rings increases, a limiting absorption maximum of about 3450 Å is reached, the maximum of biphenyl being at 2500 Å. The maximum of fluorescence also reaches a limiting value. The absorption of the methyl-substituted series also converges but to a shorter absorption limit of approximately 2900 Å; the fluorescence also converges. If the *p*-polyphenyl compounds are modified by oxygen bridging between adjacent benzene rings, the absorption maxima undergo a significant red shift. For example, *p*-terphenyl has a maximum at 2800 Å while the trioxido *p*-terphenyl has a maximum at 3650 Å. This occurs presumably because internal rotation of the benzene rings is prevented and the *p*-orbital overlap is increased with consequent extension of the total π system for the oxido compounds.

F. Aromatic Molecules with n,π^* States

Fluorescence usually does not occur in compounds that have $n \rightarrow \pi^*$ transitions as the lowest energy transition. The reason is that almost complete intersystem crossing takes place from the lowest n,π^* singlet state to a triplet from which phosphorescence occurs (see Section III-D). An example of this occurs in benzophenone. However, it is known that some simpler molecules, such as formaldehyde, biacetyl, and acetone, do fluoresce weakly even when the n,π^* state is the lowest excited state.

Usually when n,π^* states exist, this state is that of lowest excitation energy in the singlet series. Thus it is usually to be expected that molecules with $n \rightarrow \pi^*$ transitions lowest will not fluoresce but will phosphoresce. This is usually but not always true. Moreover, there are exceptions regarding the omnipresence of phosphorescence even when the n,π^* singlet state is lowest. Nonetheless, the exceptions are few and the generalization is useful.

It might be best to proceed with an outstanding exception to the association of phosphorescence with molecules which have the n,π^* singlet states lowest. The molecules *sym*-tetrazine and dimethyl tetrazine have lowest excited singlet states of the n,π^* type. However, the emissions from these molecules are fluorescences with lifetimes estimated to be less than 10^{-5} sec (52). It is possible that no π,π^* triplet state lies between the n,π^* singlet and triplet and that, moreover, there is no direct coupling between the latter states. In any case, it would appear that with a short lifetime as is indicated for the fluorescence, the intersystem crossing to the triplet is not sufficiently competitive with the fluorescence radiative path.

Until very recently, pyrazine (a 1,4-diazine) and pyrimidine (a 1,3-diazine) were considered as prime examples of molecules with an n,π^* singlet state as the lowest excited state and showing only phosphorescence. However, these molecules do exhibit fluorescence (52a,52b). The fluorescence lifetime in the case of pyrimidine is 1.5×10^{-9} sec. This is very short compared to that estimated for *sym*-tetrazine. Pyradazine (a 1,2-diazine) also shows a fluorescence with a short lifetime (2.6×10^{-9} sec) and no phosphorescence (52a). In all cases, fluorescence occurs in hydrocarbon solvents. However, pyrazine does not exhibit fluorescence in a hydroxylic solvent (52b). Similar information is not available for the other diazines. It is also worth noting that deuteriation causes a notable increase on the quantum yield of fluorescence for pyridazine but not pyrimidine. This would seem to indicate that there is internal conversion from the n,π^* singlet state to the ground state (see Section III-C-1 for further discussion regarding the effects of deuterium substitution). As another example, 9,10-diazaphenanthrene is known to fluoresce (53) although its lowest excited singlet state is n,π^*.

In systems where the n,π^* singlet state is lowest and moreover where it is below the π,π^* triplet, presumably the only mode for intersystem crossing is n,π^* (singlet) → n,π^* (triplet). To the first approximation, the spin–orbit coupling between these configurations is forbidden. Thus, the rate constant would be low and comparable to that for fluorescence (23) and fluorescence, rather than phosphorescence, would occur. Further details regarding intersystem crossing will be discussed in Section III-A.

Another area of interest concerns the reversal of the energy order of excited states and its consequence. This topic has already been partly described in Section II-C-2, which is on specific solvent effects. The first investigation concerning this problem was relative to chlorophylls (16). This is discussed in Section II-C-2.

Quinoline has an emitting triplet of π,π^* type (23). This molecule shows fluorescence and phosphorescence in a hydroxylic solvent but only phosphorescence in a hydrocarbon solvent at low temperatures. The phosphorescence of quinoline is stronger than that of naphthalene in the hydroxylic system. The principal reason for this is that intersystem crossing from the lowest π,π^* singlet to an n,π^* triplet is quite probable. In fact, this probability is higher than that for the π,π^* (singlet) → π,π^* (triplet) intersystem crossing in naphthalene. Further, in quinoline, internal conversion occurs to the π,π^* triplet followed by phosphorescence.

The nature of the solvent can be very important in determining the emission characteristics of carbonyl compounds. For example, pyrene-3-aldehyde does not fluoresce at room temperature in heptane or diethyl ether; however, it does fluoresce with very low intensity in acetonitrile and with moderate intensity in alcohols and acetic acid (54). Accompanying this increase in intensity is a red shift of the fluorescence and loss of vibrational structure. The appearance or nonappearance of fluorescence in a compound such as pyrene-3-aldehyde is likely to depend on the relative location of the n,π^* state and the lowest π,π^* state. If the n,π^* singlet is lower than the π,π^* singlet state, intersystem crossing from the n,π^* singlet to a triplet state will be probable with consequent quenching of fluorescence. Solvents such as alcohols apparently induce fluorescence because they lower the energy of the π,π^* state below that of the n,π^* state, while solvents like chloroacetic acid appear to raise the n,π^* state above the π,π^* state, thereby also inducing fluorescence (54). Apparently phosphorescence has been seen at low temperatures (< 160 K) in a hydrocarbon solvent and assigned as originating from the π,π^* triplet (54). Without further evidence, this assignment is questionable. The interaction of solvents such as alcohols is assumed to involve principally the excited state, while for chloroacetic acid, the ground state is the one assumed to be primarily affected. Other aldehydes as naphthalene-1-aldehyde and phenanthrene-9-aldehyde show no fluorescence in hydrocarbon or hydroxylic solvents. However, naphthalene-2-aldehyde and anthracene-9-aldehyde like pyrene-3-aldehyde, are fluorescent in ethanol but nonfluorescent in heptane. Pyrene-4-aldehyde and tetracene-9-aldehyde are fluorescent in both ethanol and heptane (54).

In conclusion, it appears that most aromatic carbonyl-containing compounds are not fluorescent but do exhibit phosphorescence. These include benzophenone, acetophenone, anthraquinone, etc. Also, although most aromatic heterocyclics show a strong phosphorescence, many show at least a weak fluorescence. In some cases, fluorescence (vs. solely phosphorescence) can be induced by utilizing a hydroxylic solvent (as in the case of quinoline) while in other cases, this type solvent suppresses fluorescence (pyrazine). Particularly because of the emission behavior of the diazines, the theoretical understanding of radiative and nonradiative processes in such molecules will have to undergo review.

Most aromatic nitro-containing compounds appear not to fluoresce but do exhibit phosphorescence. Some examples of these are nitrobiphenyl, dinitronaphthalene, nitrofluorene, etc.

G. Heterocyclic Compounds and Compounds of Biological Interest

1. HETEROCYCLIC COMPOUNDS

Certain aromatic *N*-heterocyclic compounds have already been discussed with special references to the existence of n,π^* states. Here, more compounds and more complex cases will be considered. Solutions of the heterocyclic molecules pyridine, pyrrole, furan, thiophene, and benzofuran do not fluoresce. However, benzopyrrole, indole (**1**), does fluoresce in a buffered water solution (55). The quantum yield in neutral aqueous solution is 0.40 (29). It is possible to make many monoaza derivatives of indole. The complete series of 2-, 3-, 4-, 5-, 6-, and 7-monoazaindoles show fluorescence in buffered water solutions at concentrations of 10^{-5} to 10^{-6} *M* (55). The cation of each

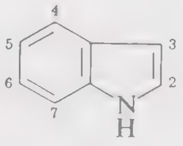

(**1**)

of these derivatives is also fluorescent. The fluorescence maxima are in the ultraviolet (~ 3100–3900 Å) except for the 4 and 5 derivatives, which fluoresce at about 4100 Å. The aza substitution causes a relative red shift of the fluorescence maximum, except for the 2 and 3 derivatives. Among these compounds there is quite a variation in the intensity of fluorescence in spite of the fact that the absorption intensities of at least some of the compounds are comparable and that the spectral location of the fluorescence maxima are the same. It is of further interest to note that in the monoaza derivatives, substitution in the pyrrole portion shifts the maximum toward shorter wavelengths whereas substitution in the benzene portion causes a shift to longer wavelength. In ethanol, the fluorescence maximum for indole is at a slightly shorter wavelength than that of the carbocyclic analog indene (2800 Å vs. 2900 Å). Also, all of the neutral monoazaindoles show fluorescence in 95% ethanol and all maxima occur in the ultraviolet. Usually, compared to indole, the fluorescence maximum of the aza derivatives is displaced to longer wavelengths, but to shorter wavelengths for the 2- and 3-substituted compounds.

The diazaindoles all have fluorescence maxima in the ultraviolet, whether in water or ethanol. This is also true of the cations. The 2,3- and 3,5-diazaindoles have maxima very near to that of the parent indole while the spectrum of the 3,4 derivative is displaced to the shorter wavelengths. Among the diaza compounds, there is no apparent regularity of shift if both nitrogen atoms are in the pyrrole portion or if one is in each portion and moreover over different positions in the two rings. The pyrrole-substituted monoazaindoles and the 3,4-diazaindole have fluorescence more intense than the parent indole while that of the others is weaker.

One triazaindole (3,5,7-), or purine, has a fluorescence maximum (~ 3700 Å in aqueous solution, 3500 Å in alcohol) at longer wavelengths than indole, or than the diaza compounds mentioned above or than pyrrole-substituted monoaza compounds. The cation shows no fluorescence. The intensity appears to be weaker than for all the other cases except for the 2,3-diazaindole. In conclusion, the substitution of one nitrogen in the pyrrole portion causes a marked blue shift but the substitution of two restores the maximum to a position near that of the parent indole. One nitrogen substituted in the benzene portion always causes a red shift. The effect of one in each portion depends on the position of substitution. The substitution of two nitrogens in the benzene portion is capable of more than compensating for the blue shift produced by substitution in the pyrrole portion.

Acridine fluoresces in pure nonhydroxylic and hydroxylic solvents, beginning at about 3900 Å (22). Substitution in the 9 position of acridine by alkyl groups, olefinic groups, aromatic groups, or combinations causes little change in the absorption spectra. However, when NH_2, OH, or $N(CH_3)_2$ groups are substituted in the aromatic portion of a styryl substituent on acridine, there are notable changes in absorption with accompanying changes in the fluorescence polarization curve (56). Substitution in the 9 position by OH to produce acridone gives a compound which fluoresces in the region from 4000 to 5000 Å. Apparently little association occurs in dioxane or alcohol up to high concentration although some quenching does occur. An increase in polarity of the solvent causes a red shift as does transformation to the cationic form (57).

Proflavine or 3,6-diaminoacridine cation (**2**) has a strong fluorescence at

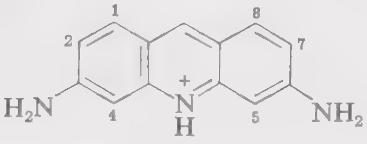

(**2**)

~4750 Å at low temperature (−180 C) and a broader maximum at ~4900 Å at room temperature in 95% ethyl alcohol (58). Substitution in the 2,7 positions by fluorine, chlorine, and bromine causes a progressive red shift of the maximum. At the same time, the quantum yield of fluorescence at −180 C progressively decreases while the quantum yield of phosphorescence increases.

Coumarin (**3**) has a fluorescence maximum at 3515 Å in 95% ethanol (59).

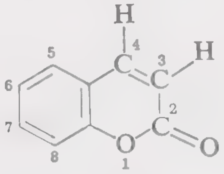

(**3**)

Methyl substitution causes a red shift of the maximum and also both hydroxyl and methoxyl substituents cause relatively large red shifts, hydroxyl producing the larger effect. The shifts also depend on the position of substitution. Electron-withdrawing groups in the 3 position and electron-donating groups in the 7 position enhance the fluorescence intensity.

The fluorescence of the hydroxyquinolines depends on the position of substitution and the pH of the aqueous solution (41). The 5- and 8-hydroxy derivatives do not fluoresce and 6-hydroxyquinoline fluoresces weakly. The 2-hydroxy derivative shows uniform fluorescence independent of pH if excitation occurs in the 3250 Å region but decreases at high pH (~14) if excited at ~2800 Å. The other derivatives all fluoresce but the intensity depends on the pH and in some cases, on the wavelength of the exciting light.

Finally, a heterocyclic polyene, triazacyclooctatetriene shows yellow fluorescence (60).

2. COMPOUNDS OF BIOLOGICAL INTEREST

There has been a vast increase in the information and interest in molecules of biological interest. These include amino acids, various heterocyclic compounds, and proteins. It will not be possible to consider all cases but some representative cases will be discussed.

Three aromatic amino acids, phenylalanine (**4**), tyrosine (**5**), and tryptophan (**6**) in neutral water solutions show broad, structureless fluorescence in the ultraviolet with maxima at approximately 2800, 3000, and 3500 Å, respectively. The quantum yields are 4% for structure **4**, 21% for structure **5**, and 20% for structure **6**. It is probable that energy transfer can occur from structure **4** to **5** to **6** and from all the aromatic amino acids to the heme group of hemeproteins (61). The fluorescence of tyrosine is at a plateau maximum between pH 4 and 9 (62). The fluorescence of tryptophan is maximum at a pH between 10 and 11. Particularly in the case of tyrosine, there is a very rapid fall in fluorescence intensity above and below the pH values noted. In the case of tryptophan the fluorescence intensity decreases rapidly above and below 10.5 but levels off on the low pH side until a pH of 3 is reached, when it decreases again. Several compounds related to tyrosine, such as phenol and tyrosine methyl ester, show the same dependence of fluorescence intensity on pH. Also, some derivatives of tryptophan act like tryptophan. In the case of tyrosine, removal of the side chain, acetylation, or removal of the carboxyl have little affect on the quantum yield. However, glycylation of the amino group or esterification of the carboxyl decreases the quantum yield to 1/3 or 1/4 of the value of tyrosine. In the case of tryptophan when the side chain is removed (to produce indole), or when the side chain is short and has no carboxyl group, the fluorescence quantum yield is increased. However, glycyla-

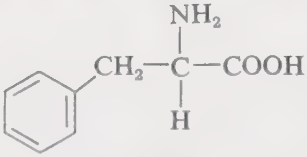

(**4**)

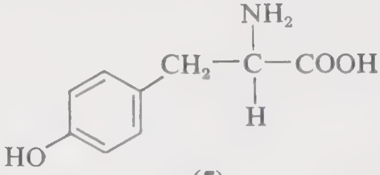

(**5**)

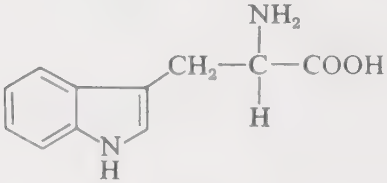

(**6**)

tion or esterification produces a decrease in quantum yield parallel to that found for tyrosine (62). Quenching by bases seems to occur via a mechanism involving transfer of hydrogen from nitrogen to the hydroxyl ion (62). This conclusion is supported by the *lack* of quenching in N-methylindole in base up to $5N$. However, indole derivatives show no fluorescence in $1N$ sodium hydroxide. The proton transfer presumably occurs in the first excited state to produce an anion which is deactivated principally or totally by radiationless modes. Tyrosine and phenol are nonfluorescent as the anions ($\mathrm{pH} > 10$). However, substitution of the hydroxyl, for example, to give an ether, delays quenching until the pH exceeds 14.

The principal importance of the fluorescence of tryptophan and tyrosine is in the analysis of proteins. Proteins are subjected to hydrolysis and the content of these amino acids is determined by their fluorescence spectra. High analytical accuracy is achieved, particularly for tryptophan. Many metabolites of these have been investigated using fluorescence techniques with excellent results.

Further investigation (63) shows that tryptophan has two sets of emission, each of which is composed of a short-lived and long-lived component. Excitation of tryptophan in frozen aqueous solution at 3500 Å produces a blue short-lived emission ($\sim$4500 Å) and a green long-lived emission ($\sim$5000 Å). Excitation at 2800 Å gives a fluorescence in the ultraviolet ($\sim$3500 Å) and a very weak long-lived emission in the green ($\sim$5000 Å). These results are unusual. When excited in a frozen glucose or methanol solution at 2800 Å, the ultraviolet fluorescence still exists but now a blue phosphorescence replaces the weak green one. Excitation at 3500 Å still gives a short-lived blue emission and a long-lived green one. Certain compounds are good quenchers. The amino acid cysteine quenches the ultraviolet fluorescence with little enhancement of the long-lived blue emission. Both trinitrobenzene and dinitrophenol quench all of the tryptophan emission. Riboflavin and folic acid are also effective. These latter four results probably occur because of energy transfer to the triplet state of the electron acceptor molecules since the emission observed is essentially that of the complexing agents themselves (63).

Other amino acids have very little or no fluorescence. However, in several cases, the amino acids have been reacted with another molecule to give products showing high fluorescence (64). Among such reactants are histamine, histidine, and arginine. The fluorescence properties of proteins and protein complexes have been actively investigated. Many proteins show fluorescence as a broad structureless band in the ultraviolet with maxima generally in the 3000 3500-Å region (65,66). Nucleic acids also show fluorescence (67). The proteins include myoglobin, pepsin, ovalbumin, hemoglobin, fibrinogin, insulin, and others. The quantum yields of fluorescence of a group of 21 proteins in water vary from 0% (1 case) to 15%. For those proteins soluble in an organic solvent, such as propane 1,2-diol, the quantum yields increase except in the one case where fluorescence was originally absent. The proteins containing phenylalanine along with other aromatic groups show no fluorescence of phenylalanine. Also tyrosine fluorescence is detectable only in the absence of tryptophan moieties. In proteins containing tryptophan, fluorescence of this moiety only is observed, regardless of the energy of the exciting light. This is true even when the absorption is principally due to tyrosine and the number of phenylalanine and tyrosine moieties far outnumber those of tryptophan. There appears, however, to be little energy transfer from tyrosine to tryptophan; instead, tyrosine fluorescence is largely quenched by interactions probably involving hydrogen bonding of phenolic groups to nearby carboxyl groups. Cysteine or the peptide linkage in general make no contribution to protein fluorescence.

The shape and position of the fluorescence spectrum of tyrosine does not depend on pH, whereas for tryptophan, there is a shift of about 50 Å to the red at pH above 8. The intensity of the fluorescence of both compounds decreases with increasing temperature. Some proteins containing tryptophan show a notable decrease in the intensity of the fluorescence characteristic of tryptophan as the temperature is increased.

If a prosthetic group is attached to a protein, it is generally found that the fluorescence is considerably weaker than for the protein without the prosthetic group. These include such species as myoglobin, hemoglobin, and carbon monoxide complexes with myoglobin (68,69). At least in some cases, it is known that the energy is utilized to produce photochemical changes. When an enzyme is complexed with a coenzyme, the intensity of fluorescence of the complex is usually greater than that of the coenzyme itself; however, it is generally lower than for the protein itself (at least in dehydrogenases) (70).

Another area receiving wide attention is the chemical binding of a dye to a protein to give a complex that emits fluorescence in the visible region (68, 71–74). Probably the most commonly used dye is 1-dimethylaminonaphthalene-5-sulfonyl chloride which binds to the protein by reacting with the amino groups to produce sulfonamides. Normally, excitation is accomplished via the protein absorption band and emission occurs by energy transfer in the visible region. This technique, with modification of the dye, has been used in the fluorescent antibody technique (64). Other "dyes" such as protoporphyrin have also been used to give a complex with a protein which fluoresces red (64).

Many other molecules such as vitamin A (a polyene), riboflavin (an *N*-heteroaromatic), pyridine nucleotides, other vitamin condensate products, carbohydrate condensate products, steriods in acid media, etc., show fluorescence.

H. Metal Complexes

A great variety of metal complexes, including the π or sandwich type, and those with porphyrin, chlorophylls, 8-hydroxyquinoline, phthalocyanines, and others fluoresce. As in prior cases, some of the discussion overlaps with that of phosphorescence. This aspect will be mentioned where necessary but the details are described in the sections devoted to phosphorescence.

When considering the kind of emission to be expected from a metal complex, several salient factors must be considered. The broad considerations are: (*1*) the nature of the ligand, (*2*) the nature of the metal, (*3*) the nature of the perturbation—that is, does the metal perturb the ligand levels or does the ligand perturb the metal levels, (*4*) solvent interactions, (*5*) temperature. In the first place, an obviously important point is the emission characteristics of the uncomplexed parent molecule. With regard to the metal, an important point is its position in the periodic table—important categories are: the transition elements, the rare earths, and the remainder. In addition, of great importance is the diamagnetic or paramagnetic nature of the metal ion and its oxidation state. The third consideration is one of great importance, since the nature of the excited states and their intercombination is largely determined by the nature of the perturbation. Solvent interaction arises but exerts a dominant effect only in particular instances. As usual the solvent may shift the position of the emission and modify its appearance. The temperature is particularly important because of its effect on the viscosity of the solvent. This, in turn, affects the collisional deactivation of excited states and thus both the intensity and nature of the emission. Also, the temperature affects the fine structure character of the emission. The importance of these factors and others that will be developed, in effecting characteristics of the emission spectra cannot be overemphasized. Many investigations, particularly earlier ones, produced incorrect results because of a lack of understanding of certain general basic premises. Much of the discussion will center around restricted types of compounds but the results are generally applicable to a broader consideration of various types of complexes.

Probably the metallo complexes which have been most completely investigated are those of the porphyrins (75–83) and porphyrinlike compounds [including the chlorophylls (16,17,79,84–89) and phthalocyanines (79,90)]. Table IV presents the spectral results for 22 metal porphyrins (80–83). From the table, one striking fact is found: *no transition metal porphyrin fluoresces, whatever the oxidation state of the metal may be*. This fact alone is very useful, although earlier work had indicated contrary results in a few cases. This knowledge is of great value in the analysis of a single component or a system of components containing metal complexes by a fluorescence technique. This applies to synthetic problems, as well as *in vitro* or *in vivo*

TABLE IV

Luminescence and Lifetime Data for Various Metalloporphyrins (81,82)

Compound	Atomic number of metal atom	Fluorescence		Phosphorescence		Singlet–triplet separation[b] (cm^{-1})	Triplet state lifetime (msec)
		Position of 1st band (Å)	Relative intensity[a,c]	Position of 1st band (Å)	Relative intensity[a,c]		
Mesoporphyrin IX dimethyl ester	—	6175	vs	7515	vw	2871	14
Be mesoporphyrin IX dimethyl ester complex	4	6065	vs	Not observed	—	—	12
Mg etioporphyrin II	12	5815	s	7150	w	3247	160
Ca mesoporphyrin IX dimethyl ester	20	5870	s	7200	m	3313	63
Zn mesoporphyrin IX dimethyl ester	30	5715	m	7010	m	3126	83
Sr mesoporphyrin IX dimethyl ester	38	5890	vw	7365	m	3482	7
Cd mesoporphyrin IX dimethyl ester	48	5820	w	7260	m	3223	7
Sn mesoporphyrin IX dimethyl ester	50	5715	w	7020	s	3087	21
Ba mesoporphyrin IX dimethyl ester	56	5960	vw	7495	s	3201	8
Hg mesoporphyrin IX dimethyl ester	80	Absent	—	7845	w	4578	≤ 0.5
Pb mesoporphyrin IX dimethyl ester	82	Absent	—	7910	vw	4655	≤ 0.5
Mn(+2)mesoporphyrin IX dimethyl ester	25	Absent		7520	vw	3816	< 0.5

Mn(+3) acetate mesoporphyrin IX dimethyl ester	25	Absent	6580	—	~2000	—
Fe(+2)mesoporphyrin IX dimethyl ester	26	Absent	6805	vw	3647	<0.5
Fe(+3) acetate mesoporphyrin IX dimethyl ester	26	Absent	6815	vw	~2400	—
Co(+2)mesoporphyrin IX dimethyl ester	27	Absent	6720	w	3294	<0.5
Co(+3)chloride mesoporphyrin IX dimethyl ester	27	Absent	6815	w	~2900	—
VO(+2)mesoporphyrin IX dimethyl ester	23	Absent	7095	w	~3380	<0.5
Cu(+2)mesoporphyrin IX dimethyl ester	29	Absent	6820	vs	3228	0.10
Ni(+2)mesoporphyrin IX dimethyl ester	28	Absent	6810	vw	3464	11
Pd(+2)mesoporphyrin IX dimethyl ester	46	Absent	6580	vs	3099	2.0
Pt(+2)mesoporphyrin IX dimethyl ester	78	Absent	6380	vs	2931	0.14

---

[a] These intensities are assigned relative to the parent whose fluorescent intensity is considered vs (very strong); and s (strong), m (medium), w (weak), and vw (very weak).

[b] Calculated as the frequency difference between the absorption band at longest wavelength and the phosphorescence band of shortest wavelength. The frequency shift between the longest wavelength absorption band at room temperature and the shortest wavelength fluorescence band at low temperature is at most 200 cm^{-1} and usually 100 cm^{-1} or less.

[c] No fluorescence exists for any of the transition metal complexes considered.

study of biochemical or biological systems. The detailed discussion of the reasons for these observations will be postponed until Sections III-A and E on phosphorescence. At present it will merely be stated that transition metal ions cause complete quenching of fluorescence. Intersystem crossing from the singlet excited states to the triplet states is in general favored by the presence of centers of high atomic number (the metal ions in our case). Thus, the fluorescence intensity of metal complexes varies greatly with the metal ion, generally decreasing with increasing atomic number.

Unfortunately, the relation between fluorescence and the atomic number of the metal in these complexes is not completely clear cut. For example, among the metallo complexes of the groups, II-A, II-B, and IV-A diamagnetic divalent metals (Be, Mg, Ca, Sr, Ba; Zn, Cd, Hg; Sn, Pb), two are nonfluorescent (Hg and Pb) which is something probably not expected. Although within the II-A and II-B series the general expectation of decreasing fluorecence intensity with increasing atomic number is followed, the fluorescence of the strontium ($Z = 38$) and barium ($Z = 56$) complexes seems unduly weak. Lead and mercury ions have unusually large ionic and covalent radii. The location and shape of the absorption spectra of the lead and mercury complexes are different from those of the other compounds, particularly in the case of lead. Also the energy separation between the lowest singlet and triplet is unusually large (Table IV). All these factors point to an unusual bonding scheme. The metals are very probably not coplanar with the rest of the porphyrin ring structure. This factor plus the high atomic number provide quenching mechanisms for the fluorescence via intersystem crossing to the triplet state and internal conversion to the ground state from both the singlet and triplet states. This is strongly supported by the lack of fluorescence and the unusually weak phosphorescence. Weak phosphorescence of lead and mercury complexes would normally be unexpected, since such high atomic number centers should induce a high probability of crossing to the triplet, with consequent strong phosphorescence.

With regard to the anomalies exhibited by Sr and Ba porphyrin complexes, the lowering of the fluorescence intensity in passing from the calcium to the strontium derivative is abnormally large but the barium complex shows little further decrease despite an atomic number increase of 18 (Table IV). The ionic and covalent radii of barium are large, in fact larger than those of lead and mercury ions. Despite this, the barium complex fluoresces and moreover, it also phosphoresces strongly (Table IV). The absorption spectrum of the barium complex is normal, while those of lead and mercury are abnormal in spite of the larger size of the Ba^{2+} ion. Because of the low electronegativity of barium, the complex is probably essentially ionic. Hence, since little distortion is to be expected, the absorption spectrum is normal. The emission data can be explained similarly. That is, the barium acts essentially as an external perturbation (strong because of its proximity). Accordingly, fluorescence is highly, though not completely, quenched, because of intersystem crossing to a triplet and equally important, there is not a high degree of internal conversion to the ground state since a strong phosphorescence exists. The strontium complex appears to have a total quantum yield which is lower than for the barium complex and this probably results from geometric distortion with consequent increased total internal conversion to the ground state. Even in the zinc-cadmium comparison, the overall quantum yield appears to decrease with increasing ionic size. Here again, molecular distortion caused by the cadmium ion may play a role.

Several salient points emerge from these facts. Diamagnetic metal complexes can, in general, both fluoresce and phosphoresce. General trends appear regarding the relationship of the atomic number of the metal of the complex and the intensity of fluorescence—metals of high atomic number are the more efficient in quenching. Geometric distortion of the complex can result in internal conversion from the excited states to the ground state with consequent weakening of either or both fluorescence and phosphorescence. Phosphorescence appears to be the most affected by such distortions (see Section III-E). In addition, the electronegativity of the metal ions can play an important role in determining the nature of the metal–porphyrin bonding. This manifests itself by effects on the intensity of either or both types of emission. Because of the complexity of the various effects, it is obvious that it is difficult to accurately predict a result, but these considerations may be used as a guide relative to what might be expected in other metallic complexes containing similar ions.

As has already been mentioned, Table IV shows that none of the metalloporphyrins containing ions of transition metals is fluorescent, whatever the state of oxidation of the ion. Silver porphyrins also seem to be nonfluorescent. Even if the transition metal ion and its complex is diamagnetic, no fluorescence is found. Earlier work (78) indicated fluorescence of both the nickel and silver compounds, but the observed fluorescence probably originated from some of the parent porphyrin as impurity. The main difference between these complexes and those of the divalent ions already discussed lies in the nature of the perturbation. In the transition metal complexes, the ligand field splits the *d* levels of the ions. Split levels of appropriate symmetry can combine with ligand orbitals ultimately to produce additional states. Hence, additional couplings can occur and thereby promote a high degree of intersystem crossing to the triplet states. Moreover, the presence of new states between the usual porphyrin states and the ground state increases the probability of internal conversion. In the diamagnetic metal complexes not containing transition metal ions, the metal ion perturbs the ligand levels. This results in modification of the usual porphyrin energy states but *not* in the introduction of new states. Although parameters such as atomic number, electronegativity, etc. must still be considered, the major difference in results lies in the nature of the principal perturbation. That is, does the metal perturb the porphyrin levels, as in the complexes containing diamagnetic ions, or does the porphyrin perturb the metal levels, as in the transition metal complexes?

The phthalocyanines are closely related to the porphyrins (Fig. 8). Earlier work on these compounds was limited to the magnesium derivative (90). The parent compound and most of the metal derivatives are blue in color. They have intense absorption bands, one occurring in the red region. The parent fluoresces in the deep red (6920 Å) as does the magnesium derivative (6705 Å) (79). The zinc derivative also has a red fluorescence (6730 Å) (79,80). The tin derivative fluoresces (19). However, the nickel, cobalt, and copper derivatives show no emission to approximately 10,000 Å (19). Here again, it is interesting that the complexes of the transition metal ions show no fluorescence. Although phosphorescence has not been found for any of the metallo derivatives or for the parent itself, it is probable that in the case of the copper derivative, a phosphorescence exists in a not easily accessible spectral region (beyond 9600 Å).

Another class of molecules related to the porphyrins are the chlorophylls (Fig. 8). There are a great many variations of these depending on the nature of the outer-ring substitution, modifications in the pentacyclic ring, etc. Figure 8 gives the structure of a few pertinent compounds.

The principal parent could be considered to be pheophytin and the others derivatives of it. Pheophytin, chlorophylls *a* and *b*, the ethyl chlorophyllides and pheophorbides all emit fluorescence in the red region (approximately 6600–7000 Å). It will be recalled that the chlorophylls have a typical strong absorption in the red and blue regions. The absorption in the red is more intense than the usual porphyrin absorption in the green-yellow region. The modification of the region of absorption and thereby the region of fluorescence occurs principally because of the addition of two hydrogen atoms to one of the porphyrin pyrrole rings and the addition of the pentacyclic ring between one pyrrole ring and a methine carbon. Chlorophyll *a* or *b* have attracted greatest attention because of their participation in photosynthesis. These are already metallo derivatives (Mg). Quantum yields of fluorescence for both chlorophylls vary with the solvent from 0.32 in methanol to 0.35 in pyridine for chlorophyll *a* and from 0.084 in methanol to 0.16 in ethyl ether for chlorophyll *b* (91). The quantum yields *in vivo* are considerably lower, as for chlorophyll *a*, for which the values *in vivo* range from 0.015 to 0.027 (91). The lifetimes of fluorescence of chlorophyll *a* in different solvents at room temperature ranges from 5.1 to 7.8×10^{-9} sec. For chlorophyll *a* *in vivo* the lifetime is approximately one-quarter that *in vitro*. Calculations have been made of quantum yields based on the formula $\varphi = \tau/\tau_0$ and compared to the measured ones (92). The comparison was favorable.

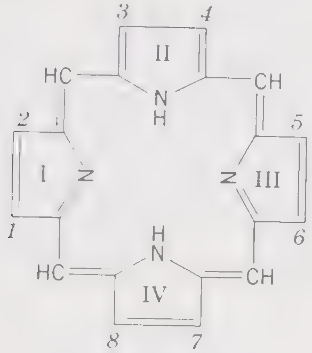

Porphyrin nucleus

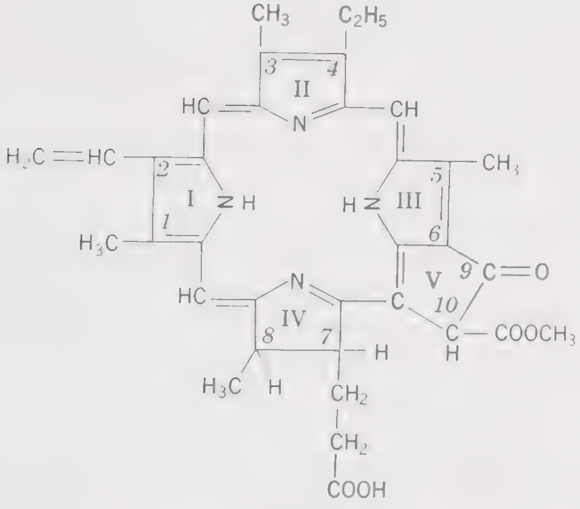

Pheophorbide *a*

Fig. 8. Structures of porphyrins and chlorophylls and their derivatives: (*1*) Mesoporphyrin IX, dimethyl ester-1,3,5,8-tetramethyl-2,4-diethyl-6,7-di(methyl propionate) porphyrin. (*2*) Metalloporphyrin—same as porphyrin with metal complexed in center. (*3*) Phthalocyanine—same as porphyrin except methine carbons are replaced by nitrogen atoms and four phenyl groups are fused at positions 1,2; 3,4; 5,6; and 7,8. (*4*) Chlorophyll *a*—same as pheophorbide *a* except magnesium complexed in center of ring and propionic acid residue in position 7 is esterified with phytol alcohol ($C_{20}H_{39}OH$). (*5*) Chlorophyll *b*—same as chlorophyll *a* except that a formyl group is substituted for the methyl group at position 3. (*6*) Ethyl chlorophyllide—same as a chlorophyll except there is ethyl rather than phytol esterification on the propionic acid residue.

The copper derivatives of pheophytin *b*, pheophorbide *a*, and chlorophyllide *a* are not fluorescent (16,79) while the cadmium derivative of the chlorophyllide *a* is (19). The zinc chlorophyllide derivative also shows fluorescence (19). Here again, it appears as if transition metal derivatives show no fluorescence. These derivatives do show phosphorescence which is strongest in the copper complex (16,19,79).

Several of the metal derivatives of 8-hydroxyquinoline have been investigated (93,94). The discussion of the rare earth complexes will be postponed until later. The aluminum, gallium, iridium, zinc, cadmium, magnesium, and lead and trivalent thallium fluoresce at room temperature in solution. However, the divalent paramagnetic copper, nickel, cobalt, and manganese complexes do not fluoresce at room temperature in solution or in the solid state. At a low temperature (77°K) in a rigid glass, the first group mentioned also shows fluorescence. The divalent cobalt, nickel, and manganese complexes shows a barely detectable luminescence under the same conditions. The divalent copper complex shows a definite luminescence at low temperature. It is probable that this luminescence is a phosphorescence. The absence of emission at room temperature by the transition metal complexes would be understandable if the emission were phosphorescence; this would be quenched at room temperature by collisional deactivation. The appearance of emission as phosphorescence in a rigid glass would be similarly understandable because of the absence of quenching. Two other transition metal complexes of 8-hydroxyquinoline, the ferric and chromic derivatives do not show fluorescence. Impurities or photolytic decomposition products could account for the barely detectable emission observed in the cobalt, nickel, and manganese complexes.

Another very important class of metal complexes comprises those derived from rare earth ions. In such complexes there is a rather high probability of *intra*molecular energy transfer between the ligand and the ion (95–98). When rare earth complexes are excited, a variety of spectral emissions can occur. The emission can be essentially line emission from the rare earth cation, molecular band fluorescence and phosphorescence, or combinations of both band and line emission. In the latter case, one or the other of the emissions can predominate. The nature of the principal emission depends both on the nature of the trivalent rare earth ion and the type of ligand in the complex. Some important ligands are benzoylacetone, dibenzoylmethane, tribenzoylmethane, 8-hydroxyquinoline and methyl derivatives, *o*-hydroxybenzophenone and acetylacetone. In certain cases, the instability of the complexes presents problems, since spurious emission may occur from the chelating molecule and its anion. Moreover, intermediate species in which mono- or dichelates are involved complicate the results (98).

The anhydrous chlorides of all the rare earth ions show a line fluorescence by direct excitation of the ions (99). If however, the hydrated crystals are excited, only five of the rare earth ions emit. When coordinated with water only Gd^{3+}, Tb^{3+}, and Eu^{3+} emit strongly, Sm^{3+} and Dy^{3+} emit weakly and others show only very weak or no fluorescence (100). Absorption spectra of nearly all the rare earth ions are known for the free gaseous ionic crystal and solution states. The linelike fluorescence originates from transitions within the 4*f* levels.

The possible number of transitions within the rare earth ion depends upon the electron configuration. Thus, it is possible to separate the ions into broad classes according to the number of transitions possible. In the first group (I) are the lanthanum (La^{3+}) and lutetium (Lu^{3+}) ions in which the *f* orbitals are emptied and filled, respectively. No transitions can originate from states resulting from *f* orbital configurations. The gadolinium (Gd^{3+}) ion, with an f^7 configuration, is also included in this group since no transitions in the visible or near-infrared regions exist. In the second group (II) are the cerium (Ce^{3+}) and ytterbium (Yb^{3+}) ions where because of a single *f* electron or 13*f* electrons, respectively, only one transition can occur. Finally, in the third group (III) are all of the other +3 valence ions in which multiple transitions can occur. In the latter case, it would seem that many state origins would exist and, therefore, many emissions. However, it is known that this is not true and emissions originate from only a few states designated *resonance* levels. This circumstance provides a fortunate situation for interpreting the final results in the chelated complexes.

The spectral characteristics of the chelates may now be considered. The chelates of the first group of rare earth ions show only molecular band emission. Figure 9 will be helpful in considering the results. In Group I, the rare earth ion levels are above the possible lowest singlet and triplet levels of the ligands. No linelike emission results but only molecular bandlike emission is seen. In these cases, the principal effect of the metal substitution is to perturb the ligand. This perturbation is manifested in several ways including effects on intensity and position of absorption and emission, on the nature of the emission (whether fluorescence or phosphorescence) on decay times and quantum yields of the emissions. These factors will vary depending on the ligand and magnetic characteristics of the ion. In the complexes with dibenzoylmethane, all three ions of Group I show phosphorescence but only in the case of Gd^{3+} is this the sole type of emission (95). The relative intensity of fluorescence to phosphorescence depends on the solvent. The lifetime of the triplet emission is shortest for Gd^{3+} and longest for Lu^{3+}. Complexes with the benzoylacetonate, tribenzoylmethide, anthranilate, and the 8-hydroxyquinolate ions also show both molecular fluorescence and phosphorescence (101).

Of the chelates in Group II (Ce^{3+}, Yb^{3+}), only Yb^{3+} complexes have been studied in any detail. Complexes of Yb^{3+} with ligands, such as those given above, result in both line and molecular band emission (101).

The nature of the emission of the rare earths that comprise Group III, depends on the ligand (95,98,101). For example, dysprosium (Dy^{3+}) complexes with benzoylacetone and tribenzoylmethane give line emission (fluorescence). However, complexes with dibenzoylmethane and 8-hydroxyquinoline give molecular band emission only, while complexes with anthranilate ion

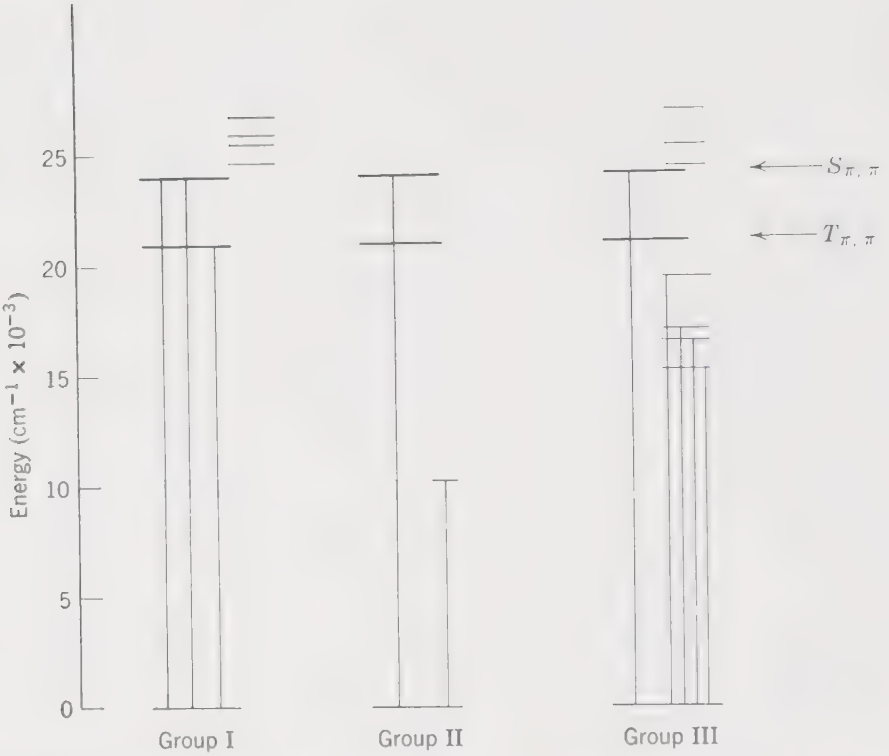

Fig. 9. Schematic energy level diagram for rare-earth ions (light lines) and ligands (dark lines) (98).

give a combination of band and lines. Other rare earth ions with these ligands give line, band or a combination depending upon the ligand (101). (All emission data in Groups II and III refer to rigid glasses at 77°K.) Europium (Eu^{3+}) salicylaldehyde, and *m*-nitrobenzoylacetonate show only line emission (95). The intensity of the fluorescence in benzene increases as the temperature decreases to a greater extent than does that of europium nitrate in water over the same range. In addition, the intensity of fluorescence of the solid increases vastly (150-fold) upon temperature reduction to 90°K whereas that of solid europium chloride hexahydrate changes very little (twofold). The fluorescence intensity of the nitrobenzoylacetonate is considerably greater than that of the aldehyde complex. The effect of solvent upon the intensity is quite pronounced, since the intensity is considerably weaker in alcohol solutions than in benzene. However, the intensity in alcohol can be increased by cooling. At 90°K, the quantum yield of fluorescence of europium *m*-nitrobenzoylacetonate is high (approximately 0.85) and although the quantum efficiency varies greatly with temperature, the lifetime does not. This indicates that the principal quenching occurs before excitation of the ion.

Finally, the efficiency of intramolecular energy transfer from the ligand to the ion is decreased as the complex becomes more ionic.

The results given earlier for Groups II and III can be explained in terms of transfer of energy from the lowest triplet state to rare earth ion levels and ultimately to the resonance level (98,101). On the basis of this approach, for the Group I complexes, the ion states could not be occupied since they lie higher than the lowest triplet of the ligand. Further, in the case of Yb^{3+} in Group II, the resonance level lies below any of the ligand triplets; therefore it can be occupied with a resultant line emission (bands appear also). It would appear that because of the large energy gaps occurring in this case, the intercombination between the states is sufficiently slow for the rate constant for emission from the triplet state to be competitive with that one responsible for occupation of the ion state. In Group III, Figure 9 shows that the ion resonance level may be below, equal to, or above the possible triplet states. Thus, the emission could occur either as lines, molecular bands, or combinations (101). Again it would appear that the presence of lines only instead of a combination of lines and molecular bands would depend upon the relative magnitude of the appropriate rate constants as noted earlier. Moreover, since the presence of an ion resonance level below the various ligand triplets can result in either lines or combinations of lines and bands for a given rare earth ion, some specific properties of the ligands must be important. It would appear that variation in the state mixings is a dominant feature. The importance of state mixing is further emphasized by the fact that with two different rare earth ions whose resonance levels are below those for the triplet of a given ligand, only lines will result in one case whereas a combination will result in the other.

Other possibilities for energy transfer may be as likely, if not more likely (102,103). From lifetime data, it appears as if the triplet level from which energy transfer occurs to an ion level is not the one from which phosphorescence occurs (the lowest triplet) (102). The transfer may be from a higher vibrational level of the lowest triplet or from a higher triplet (102). There is some incongruity in these statements. Another mechanism could be involved particularly in those cases where the lowest triplet level is below the ion resonance level (the emitting level). Energy transfer could occur from a higher ligand triplet to a higher ion level followed by internal conversion to the ion resonance level which would be quenched by the lower chelate triplet (no resonance fluorescence) (103). It has been possible to directly excite an ion resonance level and show that if there is a lower lying triplet, ion resonance fluorescence is quenched; however, if there is no lower triplet the resonance fluorescence is observed (103).

The effect of quenchers on certain europium and europium chelates offers some further information. Most of the quenching in the europium chelates appears to occur only when the energy matching criterion between the triplet of the chelate and that of the quencher is fulfilled regardless of Eu^{3+} levels (103a). Chelated ion emission decreases with increasing quencher concentration to a value of approximately 10% of the initial value. If it is assumed that the unquenched ion emission does not come from another species whose triplet is lower than that of the quencher, then energy transfer occurs to ion levels higher than the lowest triplet of the ligand and is not quenched by it. Such results indicate that mechanisms involving energy transfer from triplet state of the ligand to rare earth ion levels rather than from the ligand singlet to rare earth ion levels are more probable (103a).

In nearly all of the considerations given heretofore, it is assumed that the phosphorescence that arises, along with the sensitized rare earth ion emission, is from the same species that gives rise to the ion emission. It can be shown that for certain gadolinium and samarium complexes, spurious phosphorescence results. This most likely occurs from ligand negative ions (103b). Thus, it is important that such a possibility be taken into account in analysis of any data which will eventually lead to a mechanistic proposal.

In terbium and europium chelates, there are three principal sources of electronic energy loss (103c). These include losses in the singlet or triplet ligand levels, the upper rare earth ion levels, and the rare earth ion emitting level. For example, in the case of several different europium chelates, the efficiency of emission from the $^5D_0$ ion level is appreciably higher if the $^5D_0$ level is directly excited compared with either excitation into the ligand or higher ion levels (103c). The losses from the upper ion levels appear to occur via direct nonradiative transitions to the ground state.

In certain terbium chelates, fluorescence is strong at low temperatures (77°K) but absent at room temperatures. This is particularly noticeable if the ligand triplet states lie energetically close to the $^5D_4$ ion emitting level. If there is a large energy separation such as for the acetylacetonate where the triplet is appreciably higher than the $^5D_4$ level, the fluorescence lifetime is constant throughout the temperature range. These and similar considerations for some europium chelates provide good evidence for thermal quenching of the emitting ion level occurring via excitation to the triplets. This may occur even if the triplet is appreciably higher in energy than the emitting ion level (1500–2500 cm^{-1}) (103c).

In general, the efficiency of emission from chelated rare-earth ions is greater than that from unchelated ones probably because the radiative rate constant is increased by the ligand in contrast to any appreciable protection against quenching (103c). Further, the lifetime of fluorescence of europium (unchelated) varies over a certain temperature range. This temperature dependent quenching can be accounted for because of either interaction of the ion with hydrogen vibrations of the solvents or thermal population of the next higher ion level (the $^5D_1$) (103d).

Thus, it appears as if the simple mechanism first postulated concerning energy transfer (98,101) is too restrictive. It is likely that state mixing and other considerations as noted earlier are indeed important.

Solution mixtures of rare earth ions and ketones show emission of the ion (104,105). In one case (104), two different rare earth salts dissolved in pure solvents, such as acetophenone, benzophenone, and acetone, gave absorption spectra essentially the same as those of the pure solvent. More concentrated solutions show absorptions typical of the ions. Excitation by wavelengths absorbed principally by the solvent results in characteristic line fluorescence of the rare earth ion. It is postulated that a weakly bonded ketone ion complex is formed in which, upon excitation of the ketone, energy transfer occurs to the ion. When the n,π^* singlet state of benzophenone is excited in a mixture of benzophenone and europium tris-hexafluoroacetylacetonate, characteristic Eu^{3+} red lines are observed (105). This would indicate an intermolecular triplet–triplet energy transfer between the sensitizer and the complex followed by intramolecular energy transfer to the rare earth ion states (providing no complex with the sensitizer exists). The intensity of the presumed sensitized emission is affected by temperature, concentration, and the presence of oxygen.

Little work has been published on the sandwich or π complexes, the best known of which are those between transition metals and the ligands cyclopentadiene or benzene. Nickelocene and ferrocene apparently show no emission at wavelengths shorter than 10,000 Å, no matter what state is excited (106). Ferrocene appears to emit a weak phosphorescence at 77°K (106) and at 20°K in a variety of matrixes, including argon, xenon, nitrogen and methane (106a). Dibenzene chromium likewise shows no emission up to 10,000 Å either in fluid solution at room temperature or in a rigid medium at low temperature, although it possesses at least one very intense absorption band in that region (107), nor is there any photodecomposition. Titanocene dichloride shows an unassigned emission in the red (19). In summary then, transition metal complexes with cyclopentadiene or benzene appear not to fluoresce and phosphoresce only feebly. Most of the excitation energy must be internally converted.

I. Charge-Transfer Complexes

In this section we shall be concerned with complexes which involve hydrocarbons as electron donors and a variety of other molecules as acceptors (for example, anthracene trinitrobenzene). The general nature and the absorption spectra of such charge-transfer complexes have been discussed in Chapter III, Section IV-A-I.

Complexes involving trinitrobenzene and various aromatic hydrocarbons at low temperature (77°K) show emission. Because the emission of the complex resembled that of the free donor hydrocarbon, it could be assumed that the emission was only the phosphorescence of the donor (108,109). However, if the trinitrobenzene (TNB)–anthracene and TNB–phenanthrene complexes are excited at room temperature in fluid solution, emission is also observed (110). The emission spectrum is a mirror image of the absorption spectrum. Many other examples of such mirror image relationships also exist for various other hydrocarbons with a variety of donors (111,112). Moreover, the lifetime of the emission of many complexes at both room and low temperature is between 10^{-8} and 10^{-9} sec (see Table V). These facts strongly indicate that the emission is not phosphorescence but is in fact the charge transfer fluorescence. Moreover, if the emission were a phosphorescence from the free hydrocarbon, its energy should not change to any significant degree in different complexes involving the same donor hydrocarbon and various acceptors. However, if the emission is a charge-transfer fluorescence, the energy of the emission will depend upon the location of the charge-transfer absorption. Thus, as the electron affinity of the acceptor changes, the absorption band will move to longer wavelengths with increased electron affinity of the acceptor, as will the emission. Data on six different hydrocarbon donors and six different acceptors are in complete accord with the conclusion that the emission represents the charge-transfer fluorescence.

In many instances, the charge-transfer fluorescence is overlapped by phosphorescence (112–114), as in the case of aromatic hydrocarbon–TNB complexes. The emission band system is found to consist of two parts, a strong

TABLE V

Lifetimes of Emission of Some Donor Acceptor Complexes at Room and Low Temperature[a]

	Acceptor			
	Trinitrobenzene		Tetrachlorophthalic anhydride	
Donor	20°C	−190°C	20°C	−190°C
Hexamethylbenzene	2.6×10^{-9}sec		7.7×10^{-9}sec	11.0×10^{-9}sec
Durene		3.6×10^{-9}sec	8.1	6.8
Anthracene	5.0		4.3	
Naphthalene			2.6	2.3
Phenanthrene	3.6		3.0	
Benz(*a*)anthracene			7.3	

[a] J. Czekalla, A. Schmillin, and K. Mager, *Z. Elektrochem.*, **61**, 1053 (1957), **63**, 623 (1959).

charge-transfer fluorescence and a weak emission nearly identical to the phosphorescence of the free uncomplexed hydrocarbon. Since the energy of the charge-transfer fluorescence depends in part on the electron affinity of the acceptor, a change in acceptor presumably could move the fluorescence relative to the phosphorescence so that they would be separated. This can be accomplished in a series of complexes in which various hydrocarbon donors are complexed with tetrachlorophthalic anhydride (112). The location and fine structure of the phosphorescence spectrum shows that it differs from that of the free uncomplexed hydrocarbon. In the crystalline complex, the phosphorescence spectrum is red-shifted and the vibrational frequencies lowered compared to that of the free hydrocarbon (112,114). The frequency lowering is more pronounced in the crystal than in solution (112). Further, the lifetime of the phosphorescence of the complex is shorter than that of the free hydrocarbon, especially so in the case of the crystal (see Table VI). It is also worth noting the general decrease in the lifetime of the phosphorescent state when the bromoanhydride is the acceptor compared to the chloroanhydride. More will be said about this later (see Section III-C-2). The importance of the facts just discussed is that they indicate that the observed phosphorescence emission is probably not that of the free uncomplexed hydrocarbon as first thought (113) and that complete dissociation does not occur. If dissociation did occur then the simplified energy scheme given in Figure 10 would be appropriate. Intersystem crossing would occur near the crossing of the excited singlet (E) and triplet (T) states, which is dissociative for the triplet state. Thus, the complex might be expected to largely dissociate and emission to occur from the uncomplexed hydrocarbon (see region of $r = \infty$ in Fig. 10). However, as discussed above, the spectrum is not that of the free hydrocarbon. One possible explanation is that the surplus energy of the dissociative triplet is dissipated and the complex reforms in its triplet state with emission from this state (113). Further, the emission process ($T \rightarrow S$ phosphorescence) is

TABLE VI

Phosphorescence Lifetimes of Some Hydrocarbons and Their Complexes (112)

		Acceptor			
		Tetrachlorophthalic anhydride		Tetrabromophthalic anhydride	
	Donor in solution[a]	Solution[a]	Crystal	Solution[a]	Crystal
Durene	5.9 sec	0.25 sec	0.002 sec	0.0095 sec	0.0012 sec
Hexamethylbenzene	5.6	0.0085	0.0011	0.0047	0.001
Naphthalene	2.4	0.16	0.45	0.29	0.029
Phenanthrene	3.6	1.8	0.25	0.36	0.019

[a] In *n*-propyl ether–isopentane (3:1) at 190°C; crystal at same temperature.

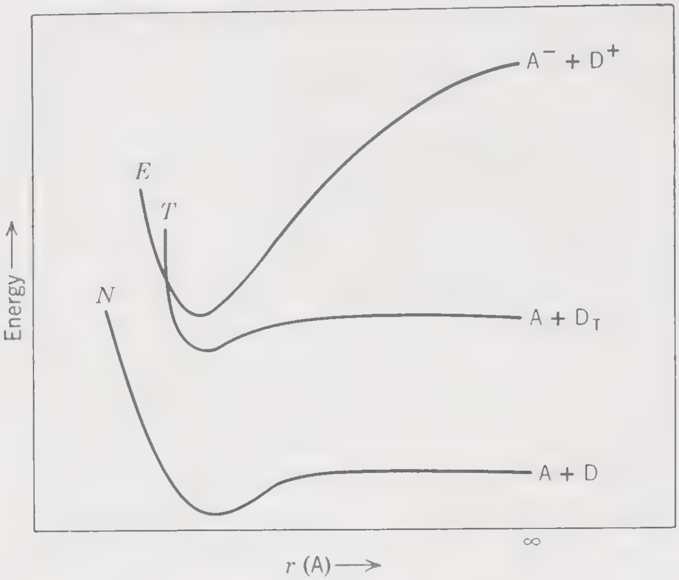

Fig. 10. Potential energy curves for the ground (*N*), excited singlet (*E*) and triplet (*T*) states for a donor (D)–acceptor (A) complex.

largely localized on the hydrocarbon component. It would appear that with better knowledge of other possibilities for the shape of the appropriate potential energy curves and their crossing points, different mechanisms could evolve. These may represent better descriptions of the true situation.

J. Physical Chemistry of the Lowest Excited Singlet State

An interesting question is what effect electronic excitation has on certain chemical properties. Of particular interest is the change in the pK of acids and bases in the excited singlet state compared to that in the ground state (115–120). In addition, changes occur for molecules in triplet states (121,122). Table VII summarizes data for a considerable number of molecules.

The pK_a of acridine in the ground state is 5.5 whereas in the first excited state it increases to 10.6 (118). Thus, acridine is a very much stronger base in the excited state than in the ground state. However, the monoazabenzene relative pyridine has about the same pK_a in both the ground and first excited states (118). The molecule 2-naphthylamine shows a change from pK_a = 4.1 in the ground state to -2 in the excited state and thus becomes a considerably stronger acid. Apparently indole becomes a stronger acid in the excited state. In Section II-G-2 it was noted that in basic solutions, the fluorescence of indole is quenched. This would indicate that this occurs because of proton transfer while in the excited singlet state.

TABLE VII

pK_a Values in Various Electronic States[a]

Molecule	p$K_a^{S_0}$	p$K_a^{S_1}$	pK_a^{T}	
Acridine	5.5	10.6	5.6[b]	—[b]
Quinoline	5.1		6.0	5.8
2-Naphthylamine	4.1	−2	3.3	3.1
N,*N'*-Dimethyl-1-naphthylamine	4.9		2.7	2.9
Phenol	10	4.0[c]		8.5[c]
p-Methylphenol	10.3	4.3[c]		8.6[c]
p-Chlorophenol	9.4	3.2[c]		8.0[c]
2-Naphthol	9.5	3.1	8.1	7.7
2-Naphthoic acid	3.7	10–12	4.0	4.2
1-Naphthoic acid	3.7	10–12	3.8	4.6
m-Bromophenol	9.0	3.8[c]		
m-Chlorophenol	9.1	3.0[c]		

[a] S_0 is ground singlet state, S_1 is first excited singlet state, and T is lowest triplet state.

[b] First column from flash photolysis data and second column from phosphorescence data.

[c] E. Wehry and L. Rogers, *J. Am. Chem. Soc.*, **87**, 4234 (1965).

The ammonium salts of aromatic amines are very strong acids in the first excited state with pK values between −2 and −6. Based on the reaction

$$(\mathrm{ArNH_3^+})^* \cdot \mathrm{HOR} \underset{k_r}{\overset{k_f}{\rightleftharpoons}} \mathrm{ArNH_2^*} \cdot \mathrm{H_2OR^+}$$

$k_f \gg k_r$, where the asterisk indicates the electronically excited state and k_f and k_r are the rate constants for the forward and reverse reactions respectively. Acidic alcohol solutions of the ammonium compound show fluorescence of the amine at room temperature. However, if the temperature is lowered, the fluorescence of the ammonium compound appears and the intensity of that of the amine decreases. The temperature at which this occurs depends on the nature of the alcohol. This effect presumably arises because the configurational changes of the alcohol solvent associated with the proton transfer become rate determining at different temperatures, depending on the alcohol.

Hydroxy-substituted benzenes and naphthalenes also show large variation in pK_a values between the ground state and first excited state (Table VII) (123). The 2-naphthol shows a ΔpK of 6.3 between the two states in both aqueous and glycerine solutions. Phenol shows a greater ΔpK in the glycerol solutions than in aqueous solution (Table VII).

The determination of the pK in the excited state involves both the absorption and fluorescence spectra (116,123). It can also be determined from the variation in the fluorescence quantum yields as a function of the pH (116). The former procedure requires the pK of the molecule in the ground state be known. The determination is based on the energy diagram shown in Figure 11 and thermodynamic quantities from the equilibria appropriate to a phenol or acid:

$$\mathrm{ROH} + \mathrm{H_2O} = \mathrm{RO^-} + \mathrm{H_3O^+}$$
$$\mathrm{ROH^*} + \mathrm{H_2O} = (\mathrm{RO^-})^* + \mathrm{H_3O}$$

The appropriate equations are

$$\Delta E + E_d{}^* = \Delta E' + E_d \tag{18}$$

where E_d and $E_d{}^*$ are the heats of dissociation in the ground and excited states and ΔE and $\Delta E'$ are the energy differences between the ground and first excited singlet states for the undissociated acid and anion, respectively (Fig. 11).

$$E_d - E_d{}^* = (\Delta G + T\Delta S) - (\Delta G^* + T\Delta S^*) \tag{19}$$

If $\Delta S = \Delta S^*$, then

$$\Delta G - \Delta G^* = -RT \ln \frac{K_a}{K_a{}^*} = \Delta E - \Delta E' \tag{20}$$

where the K values are the dissociation constants in the appropriate state. Then

$$\mathrm{p}K_a - \mathrm{p}K_a{}^* = \frac{\Delta E - \Delta E'}{2.303RT} \tag{21}$$

In the case of pK_a values for the excited singlet state, the ΔE and $\Delta E'$ are estimated from the longest wavelength absorption maximum and the fluorescence maximum (123) by

$$\Delta E = h\nu = \frac{h\nu_A + h\nu_F}{2} \tag{22}$$

$$\Delta E' = h\nu' = \frac{h\nu_A{}' + h\nu_F{}'}{2} \tag{23}$$

where the subscript A refers to absorption and F to fluorescence. Thus, from a known value for pK_a of the ground state (p$K_a^{S_0}$), the p$K_a{}^*$ of the excited singlet (p$K_a^{S_1}$) can be determined (see Table VII).

For the phenols, the increase in acidity is extremely large (~6 pK units for cresol and ~6.2 pK units for chlorophenol). In some cases a molecule normally considered an acid in the ground state becomes a base (or very weak acid) in the first excited state. For example, the pK_a value of both 1- and 2-naphthoic acid changes from approximately 4 in the ground state to 10–12

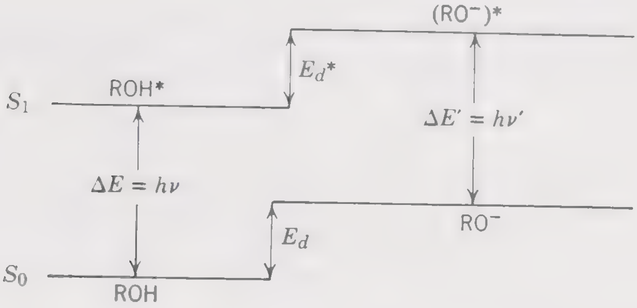

Fig. 11. Schematic thermochemical diagram for determination of excited singlet pK_a values (123).

in the excited singlet state. Some calculations on naphthol and phenol indicate that such an increase in pK for the excited state is to be expected. Certainly more effort should be made to understand effects of substituents such as those described.

III. PHOSPHORESCENCE AND THE TRIPLET STATE

A. The Nature of Phosphorescence

1. SPIN–ORBIT COUPLING AND TRANSITION PROBABILITY

In order to have a better understanding of phosphorescence and triplet states, we shall first discuss spin–orbit coupling. In light atoms or molecules containing light atoms, the spin angular momentum of the electrons can be considered as a quantized independent quantity. Its value must be conserved during a transition (pure L–S coupling). The total wave function for a system can be written

$$\Psi_t = \Phi\Gamma \tag{24}$$

where Φ and Γ are the space and spin parts of the total function. The ordinary Hamiltonian does not contain any terms involving the spin. The transition probability between two states, based on the transition moment integral, is

$$P = \left| k \int_{-\infty}^{+\infty} \Psi_n \mathbf{M} \Psi_m \, d\tau \right|^2 \tag{25}$$

where the integration is over all space and $\mathbf{M}$ is the electric dipole operator ($e\mathbf{r}$). If the complete wave function (Eq. 24) is substituted into Eq. 25, the integral vanishes ($= 0$) if states m and n have different multiplicities. This happens because integration over the spin coordinates when the spin functions Γ are different gives zero. In other words the spin functions are orthogonal

$$\left(\int \Gamma_1 \Gamma_2 \, d\Gamma = 0\right)$$

Spin–orbit coupling effectively mixes some singlet character into triplet states and some triplet character into singlet states, thus destroying their pure character and orthogonal nature. The spin–orbit interaction causes a small term to appear in the Hamiltonian operator:

$$H_{\text{total}} = H_{\text{ord}} + H_{\text{rep}} + H_{\text{SO}} \tag{26}$$

where the terms in the total Hamiltonian are the ordinary Hamiltonian, one including electron repulsions and the additional one for spin–orbit interaction. The spin–orbit interaction part is introduced as a relativistic correction. The greatest contribution to spin–orbit interaction occurs when an electron is closest to the nucleus and is moving with relativistic velocity.

The properties of the spin–orbit operator can be deduced for any nuclear potential field but the properties are most easily seen for a spherical field (appropriate to an atom), which can be used as an approximation for molecules. The spin–orbit Hamiltonian has the form

$$H_{\text{SO}} = \sum_i \sum_j - C r_{ij}{}^{-1} \frac{dV(r_0)}{dr_i} (l_{xi}s_{xi} + l_{yi}s_{yi} + l_{zi}s_{zi}) \tag{27}$$

where r_{ij} is the distance of the ith electron from the jth nucleus and l and s are the orbital and spin operators of the ith electron. The sums are over all electrons and nuclei. The magnitude of spin-orbit interaction depends on an average value of $1/r \, dV/dr$ for the electron. Moreover, for a bare nucleus $V = Ze/r$ and $1/r \, dV/dr = -Ze/r^3$. For a nucleus surrounded with electrons, the electrostatic potential changes more rapidly with r because of the fast change in shielding by the electrons as the nucleus is approached. Thus, the spin-orbit interaction tends to be large in atoms of high atomic number and for orbits that penetrate the core more deeply.

One component of the spin–orbit Hamiltonian for molecules, assuming a central field potential, may be written

$$H_{\text{SO}}^{x} = \frac{1}{2n} \sum_i^n \sum_k^n (Al_{xi} + Al_{xk})(s_{xi} + s_k) + \frac{1}{2n} \sum_i^n \sum_k^n (Al_{xi} - Al_{xk})(s_{xi} - s_{xk}) \tag{28}$$

where $A = \sum_j^m \frac{1}{r_{ij}} \cdot \frac{dV(r_{ij})}{dr_{ij}}$

j is a particular nucleus, and r_{ij} is the distance from the electron i to the nucleus j and the sum is over all electrons and nuclei. This equation is more complete than Eq. 27 since it includes spin–orbit coupling of electron i with the repulsive field of electron k. The second term, because of the symmetry of its spin part, leads to mixing of states of different multiplicity and gives magnitude to the $S \leftrightarrow T$ transition moment integral. If it is assumed that only some particular singlet mixes strongly with a pure triplet, then

$$\int \Psi_S' | e\mathbf{r} | \Psi_T' \, d\tau = \frac{\Psi_S^P | H' | \Psi_T{}^0}{E_T{}^0 - E_S^P} \left(\int \Psi_S^P | e\mathbf{r} | \Psi_S{}^0\right) d\tau \tag{29}$$

where the Ψ_S' and Ψ_T' are the perturbed singlet and triplet states, Ψ_S^P is the perturbing singlet state, $\Psi_S{}^0$ and $\Psi_T{}^0$ are the unperturbed singlet and triplet, $E_T{}^0$ and E_S^P are the energies of the unperturbed triplet and perturbing singlet and H' is the spin–orbit Hamiltonian, one component of which is given in Eq. 28. The part $\Psi_S^P | H' | \Psi_T{}^0$ is proportional to $\zeta_{n,l}$, the spin–orbit coupling factor which for hydrogenlike atoms is

$$\frac{e^2h^2}{2m^2c^2a_0{}^3} \frac{Z^4}{n^3(l + 1)(l + \frac{1}{2})l} \tag{30}$$

Thus, it can be seen that the intensity of the $S \leftrightarrow T$ transition is "stolen" from the $S^0 \leftrightarrow S^P$ transition. Since the transition probability is proportional to $(\int \Psi_S' | e\mathbf{r} | \Psi_T' \, d\tau)^2$, the $S \leftrightarrow T$ probability is dependent on Z^8 and $1/\tau^6$. This particularly strong Z and τ dependence applies to molecules as an approximation only since a central field potential was assumed. Nevertheless, there is a strong dependence on Z and τ. The development of H_{SO} for fields other than spherical has been made (124).

2. INTERCOMBINATIONS

In Figure 2 the essential intercombination processes involving states of different multiplicity are shown. The term intersystem crossing has been coined to describe the internal conversion (or radiationless transition) process that depends on spin–orbit coupling (125). This crossing is commonly between the first excited singlet and the lowest triplet (the $S_1 \rightarrow T_0$ transition, see Figure 2). The radiative intercombination process is phosphorescence and involves the transition $T_0 \rightarrow S_0$ (Fig. 2). The intersystem crossing ratio $\chi = q_P/q_F$ has been used as a measure of the population of a triplet state relative to the lowest excited singlet state (S_1) where q_P and q_F are the quantum yields of fluorescence and phosphorescence respectively (125). The fraction of molecules leaving S_1 to T_0 will depend on the ratio of the appropriate rate constants and can be expressed as

$$\Phi_{\mathrm{IS}} = \frac{k_{\mathrm{IS}}}{k_{\mathrm{F}} + k_{\mathrm{IS}} + k_{\mathrm{IC}}} \tag{31}$$

where k_{IS} and k_F and k_{IC} are the intersystem, fluorescence and internal conversion ($S_1 \rightarrow S_0$) rate constants respectively. Often, k_{IC} is considered small compared to other rate constants. Also, the ratio is not equal to χ.

It will be recalled that a direct transition from $S_0 \rightarrow T_0$ is forbidden in the absence of spin–orbit coupling because of spin orthogonality. Of course, in the presence of spin–orbit coupling this process becomes less forbidden but is still an extremely unlikely process compared to any transition involving no change in multiplicity. It is even considerably weaker than any symmetry forbidden process involving no change in multiplicity. Thus, it is not feasible to attempt to excite phosphorescence emission by utilizing the $S_0 \rightarrow T_0$ absorption transition.

As has been implied earlier, the procedure to excite phosphorescence is to utilize $S_0 \rightarrow S_1$, or higher transitions followed by intersystem crossing from S_1 to the triplet followed by phosphorescence. It may be asked why this process is more successful than $S_0 \rightarrow T_0$ since, without spin–orbit coupling, both are forbidden. At first glance one might expect that even with spin–orbit coupling $S_0 \rightarrow T_0$ and $S_1 \rightarrow T_0$ would be about equally probable. The important factor which this neglects is that the transition moment integral between the perturbed states, which, in the presence of spin–orbital coupling, constitute the actual S_0, S_1, and T_0 states of the molecule, also depends on the energy difference between the triplet and singlet states concerned. Therefore, since T_0–S_0 energy differences are commonly of the order of 20,000 cm^{-1} and S_1–T_0 energy differences are commonly of the order of 3000–9000 cm^{-1}, the intersystem crossing probability ($S_1 \rightarrow T_0$) is considerably greater than the direct transition from the ground state to T_0.

It is generally true that radiative processes involving intercombinations (phosphorescence) are of the order of 10^{-6} of those involving no multiplicity differences. This means that the lifetimes for phosphorescence are as a general rule some million times greater than those for fluorescences. The rate constant for the intersystem crossing process is of the order of 10^7 sec^{-1} (or corresponds to a lifetime of 10^{-7} sec). Since the general order of fluorescence lifetimes is 10^{-8}–10^{-9} sec, one can see the considerable difference in the $S_1 \rightarrow T_0$ and $T_0 \leftrightarrow S_0$ transition probabilities. Although the $S_1 \rightarrow T_0$ process is slower than the $S_1 \rightarrow S_0$ process, it is fast enough to compete with the fluorescence process and give triplet state occupation. It is important to point out that in many cases the relative rates for the $S_1 \rightarrow S_0$ and $S_1 \rightarrow T_0$ processes can be altered to be strongly in favor of the $S_1 \rightarrow T_0$ process with consequent high or even total occupation of the triplet state with a resulting complete absence of fluorescence. This can be accomplished by the introduction of a high atomic numbered center, a paramagnetic center, or by having a molecule in which the S_1–S_0 transition is weak (the fluorescence will have a long lifetime). In any of these cases, the intersystem crossing rate constant may be equal to or considerably larger than that for fluorescence. More details and examples on these points will be given in later sections.

Finally, the effect of paramagnetic ions or molecules should be considered. In the case of paramagnetic ions, the systems of particular interest are the metalloorganic complexes containing such ions. For these ions, the spin momentum alone need be considered. Because of this spin momentum, there exists an extremely strong inhomogeneous magnetic field. This would be as strong as, if not stronger than, any similar field created by a high atomic numbered center. Thus, if would be expected that complete or nearly complete spin–orbit coupling would occur in complexes containing paramagnetic ions. This would in turn increase the probability of intersystem crossing to such a degree that it would dominate the probability for $S_1 \rightarrow S_0$ emission (fluorescence would be quenched). Thus, phosphorescence might be expected to be the sole emission. This is borne out by experiments (see Section III-E).

The interest in the effect of paramagnetic molecules primarily centers around their effect on the $S_0 \rightarrow T_0$ absorption of other molecules. In these cases, the perturbation is an external one. Oxygen (O_2) represents the best-known paramagnetic molecule. Although the known perturbing influence of O_2 is probably not solely the result of a magnetic effect, this factor appears to be of consideration (see Section III-F-2).

B. Paramagnetism of the Phosphorescent State

An important problem is to prove that the phosphorescent state is indeed the spectroscopic triplet state. Early work gave reasonably clear indication of this. Lewis and Calvin (126) and Lewis, Calvin, and Kasha (127) showed that fluorescein in a boric acid glass at 25°C became paramagnetic on exposure to light, returning to its normal diamagnetic state in the dark. In this medium, fluorescein is present as the cation **(7)** with an absorption maximum at 4390 Å and a strong yellow phosphorescence with a mean life of about 2 sec. In contrast the well-known anion has an absorption maximum at 4920 Å, with a high quantum yield of green fluorescence. As a result of the long life of the phosphorescent state before emitting and the high quantum yield, indicating little radiationless deactivation, a relatively large fraction of the fluorescein

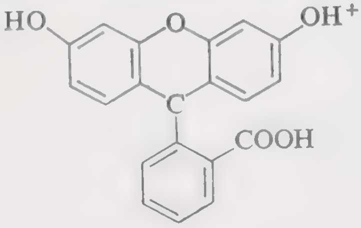

(7)

TABLE VIII

Some Phosphorescent Spectral Characteristics of Aromatic Hydrocarbons

Compound	Point group	Wavelength origin (Å)	Measured lifetimes[a] in seconds	Quantum yields P	Quantum yields F	S_1–T_0 separation (cm^{-1})	S_2–T_0 separation[j] (cm^{-1})
Benzene	D_{6h}	3390	7.0[b] (21)[b]	0.26[g] 0.20[h]	0.26[g] 0.20[h]	8600	
Naphthalene	D_{2h}	4695	2.2 ± 5%[e]; 2.6[b] (11)[b]; 2.1 ± 0.1[f]; 3.0[k]; 2.25[l]	0.1[g]	0.55[g]	10,700	
Anthracene	D_{2h}	6700	0.04[c]		0.32[l]	11,700	
Phenanthrene	C_{2v}	4605	3.3 ± 0.2[d]; 3.8[e]; 3.50[l]	0.9[n]	0.12[n]	6700	
Benz(*a*)anthracene	C_s	5950	0.3 ± 0.1[d]		0.20[o]	9300	11,100
Benzo(*c*)phenanthrene	C_{2v}	5000	2.5[m]			6900	10,600
Chrysene	C_{2h}	4975	2.5 ± 0.1[d]		0.23[o]	7600	11,200
Triphenylene	D_{3h}	4200	15.9 (29)[b]; 13.3[k]	0.60[g]	0.04[g]	5500	10,700
Pyrene	D_{2h}	5880	0.2		~1[p]	9900	12,900
Dibenz(*a*,*h*)anthracene	C_{2h}	5465	~1[c]; 1.5 ± 0.1[d]			7000	
Coronene	D_{6h}	5235	9.4 ± 0.2[d]; 7.9[k]			4500	
Fluorene	C_{2v}	4210	4.9 ± 0.2[d]		0.70[o]	9400	
Biphenyl	D_{2h}	4385	3.6[d]				

[a] Numbers in parenthesis are the natural lifetimes found by assuming all radiationless or photochemical processes occurred from the triplet state as given in reference 6.

[b] Reference 6 in EPA (5-ether 5-isopentane and 2-alcohol) at 77°K.

[c] Reference 133, from measurement of triplet–triplet absorption in glycerine at $-25°C$. In tetrahydrofuran, anthracene is ~0.1 sec and dibenzanthracene is 1.2 sec.

[d] Reference 134, in EPA at 77°K.

[e] Reference 135, in EPA at 77°K. Essentially, no difference existed in isooctane and heptane.

[f] Reference 136, based on EPR data in durene at 77°K.

[g] Reference 6, in EPA at 77°K. Some slight dependence on concentration and frequency of excitation.

[h] Reference 152, in EPA at 77°K.

[i] Reference 3, room temperature in heavy paraffin.

[j] Results are based on unpublished data of R. S. Becker, University of Houston, in EPA or 3-methylpentane.

[k] Reference 129 based on EPR data at 77°K in mixed alcohol solution.

[l] G. von Foerster, *J. Chem. Phys.*, **40**, 2059 (1964). Naphthalene and phenanthrene in EPA (slight variation in other solvents).

[m] E. Clar and M. Zander, *Chem. Ber.*, **89**, 749 (1956).

[n] R. Kellogg and R. Bennett, *J. Chem. Phys.*, **41**, 3842 (1964), in cellulose.

[o] M. Windsor and W. Dawson, at 23°C, private communication, 1967.

[p] B. Stevens, M. Thomas, and J. Jones, *J. Chem. Phys.*, **46**, 405 (1967), at 77°K.

molecules can be maintained in the excited phosphorescent state. As many as 88.5% of the molecules can be in the excited state. The magnetic measurements were made by means of a modified Theorell magnetic microbalance and it was shown that the illuminated phosphor became paramagnetic, reverting to the diamagnetic state in the dark. From estimates of the concentration of dye molecules in the excited state, the molar paramagnetic susceptibility of the excited state was found to agree, within an estimated maximum experimental error of 13%, with the observed susceptibility of the ground state of the oxygen molecule (known to be $^3\Sigma$).

However, further evidence of the paramagnetic nature of the phosphorescent state has been sought by the search for paramagnetic resonance of this state which would, of course, provide additional unequivocal evidence for its triplet nature. An electron paramagnetic resonance (EPR) absorption of the phosphorescent state of naphthalene has been observed (128). This was obtained from single crystals of a solid solution of naphthalene in durene. The spectra are due to transitions between neighboring sublevels of the triplet. The triplet electronic degeneracy is removed by magnetic dipole–dipole interaction. In the presence of an external magnetic field, there are different energy levels and transitions are possible between them (see Fig. 12). The levels result from the different possible spin orientations relative to the external field. Further results are available not only on single crystals but on rigid glass solutions of some aromatic hydrocarbons. Triphenylene, 1,3,5-triphenylbenzene, coronene, and naphthalene all exhibit EPR spectra in their phosphorescent state in rigid glasses of primary alcohols at 77°K (129). The decay times are 13.3, 5.1, 7.9, and 3.0 sec, respectively. These should be the same as the lifetimes of the phosphorescences. They are in fact similar, though not identical (see Table VIII, Section III-C-1). This may result from the difference in solvents.

In addition to hydrocarbons, other molecules show EPR spectra in their phosphorescent state. Several ketones, such as aminobenzophenone, phenyl-

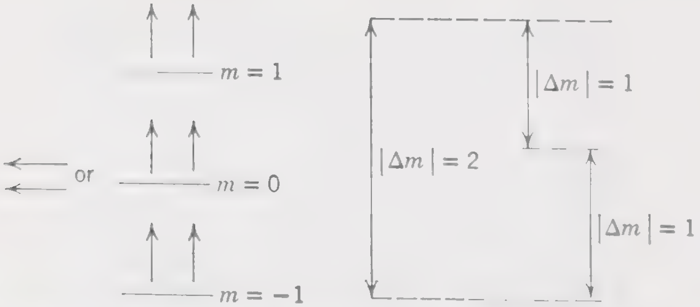

Fig. 12. Schematic diagram showing components of a triplet level and relative spin orientations.

benzophenone, and others in rigid glasses of alcohols at 77°K, show such absorption (130). The decay time for aminobenzophenone is close to that observed for phosphorescence (0.41 sec). Also *N*-ethylacridone exhibits EPR absorption in the phosphorescent state at 77°K in a rigid glass (131). A single crystal solid solution of quinoxaline (1,4-diazanaphthalene) in durene at 77°K shows an EPR absorption in its phosphorescent state (132). The lifetime of the EPR signal is estimated to be 0.2 ± 0.1 sec while that from phosphorescence is 0.25 ± 0.02 sec.

It is now obvious from the preponderance of evidence that the phosphorescent state and triplet state are, in fact, one and the same.

C. Aromatic Hydrocarbons, Substituted Aromatic Hydrocarbons, and the Intramolecular Heavy Atom Effect

1. AROMATIC HYDROCARBONS

Many aromatic hydrocarbons phosphoresce in rigid media (glasses) at low temperature (77°K). Benzene, the simplest member of this series, has received the most intensive study. Considerable information is available for hydrocarbons containing up to four rings, but less for those containing more. Table VIII gives data on the spectral location, lifetime, and quantum yield for some hydrocarbons. As for fluorescence, the phosphorescence wavelength of the linear polyacenes increases as the number of rings increases, consistent with expectations from molecular orbital theory. Napththacene is estimated to have a phosphorescence beginning at beyond 10,000 Å. Also, it is worthy of note that the lifetime decreases as the number of rings increases (benzene through anthracene).

In the tricyclic and isomeric tetracyclic hydrocarbons, the origin of the phosphorescence spectra, like that of the fluorescence, decreases in wavelength with an increase in the number of bends in the molecular skeleton. This is also consistent with predictions from molecular orbital theory. Also, it will be noted that the lifetimes increase as the number of bends increases (this also represents an increase in the symmetry elements). On the basis of the relation of the lifetimes, it would be expected that benzo(*c*)phenanthrene would have a longer lifetime than benz(*a*)anthracene. It is interesting to note that the nonisomeric pyrene has properties very similar to benz(*a*)anthracene except for the S_2–T_0 separation. It can be seen that the S_1–T_0 separation is not consistent among the isomers; however, the S_2–T_0 is amazingly consistent. Moreover, this is true among the monomethyl derivatives of a given individual parent molecule as well as between the monomethyl derivatives of different parent molecules (see later in this section).

The five-ring dibenzanthracene (C_{2h}) has characteristics quite similar to its C_{2h} counterpart in the tetracyclics (chrysene). The six-ring coronene (D_{6h})

shows a resemblance in lifetime to its D_{6h} counterpart benzene. However, the other characteristics vary. Finally, fluorene fits in between benzene and naphthalene which is not unexpected. Essentially, the benzene portions are isolated but some interaction does occur, giving the molecule a "benzene-naphthalene hybrid" character. Among the alternate hydrocarbons, the general trend in lifetime is to increase with an increase in the symmetry elements (the tricyclics do not fit well).

The lowest triplet state in benzene is B_{1u} (137). The assignment for the lowest triplet state of naphthalene is still in question. The phosphorescence has been shown to be polarized parallel to the second singlet–singlet electronic transition (and thus in the plane) as well as perpendicular to the plane of the molecule (138,139). Even if it were polarized in-plane (and thus presumably B_{3u}) a clear decision cannot be made without detailed analysis because of vibronic mixing of the two lowest singlet states. In phenanthrene, the phosphorescence is polarized perpendicular to the plane (138–140). The triplet state is assigned as B_1 (140).

For the tetracyclics, little polarization data exist. However, in the case of chrysene, it appears that the phosphorescence is polarized perpendicular to the plane (139,141). In one case, this conclusion is based on the fact that the polarization is negative relative to the first two transitions in absorption. These are quite surely polarized in-plane (142). Table VIII shows that in the isomeric tetracyclics, the S_2–T_0 separation is remarkably constant. Moreover, this is true for all the monomethyl derivatives. For example, in benz(*a*)-anthracene, the variation is from 10,920–11,220 cm^{-1}. It has been implied that this indicates that the triplet state has the same symmetry as the second excited singlet state (142,143). There are other indications that triplets in some cases may be polarized in-plane (144). These would appear to conflict with the above results on naphthalene and chrysene at least. Moreover, it has been generalized that the phosphorescence is polarized perpendicular to the plane for all polyacenes (139,141). Thus, the conflict would appear to extend to all the tetracyclics and to naphthalene. Presumably, the polarization data are correct. Nevertheless, the triplet state assignment based on the S_2–T_0 separation could still be correct since the perturbing states responsible for the results on polarization (strong out-of-plane and weak in-plane) may be able to mix only with that particular triplet state. It is worthwhile to note the significance of the out-of-plane polarization for phosphorescence. The implication is that it is *not* the (π,π^*) singlet and triplets that mix but rather (π,σ) or Rydberg singlets with (π,π^*) triplets. In addition, the ground state could mix with (π,σ) triplets (139,141).

It can be seen from Table VIII that the total quantum yield of emission for several hydrocarbons is quite high. Moreover, there is significant variation among the quantum yields of phosphorescence, although unfortunately, few data are available. This fact makes it difficult to generalize on the relationships between the symmetry, number of rings, and quantum yields. However, a few comments can be made. Despite the fact that quantitative data do not exist for benz(*a*)anthracene, the intensity of phosphorescence for triphenylene is strong, while that for benz(*a*)anthracene is weak (19). The qualitative order for triphenylene is that phosphorescence is about ten times stronger than fluorescence, while the intensity order is reversed for benz(*a*)anthracene (19). Quantitative data support the qualitative data for triphenylene (see Table VIII). Further, the qualitative data indicate that the intensity of phosphorescence in triphenylene is approximately equal to that of fluorescence in benz(*a*)-anthracene. Thus, for benz(*a*)anthracene it would be predicted that $\varphi_F =$ 0.2–0.5 and $\varphi_P = 0.02$–0.1. For benz(*a*)anthracene, where the phosphorescence is weak, the lifetime is some 50 times shorter than in the case of triphenylene where it is strong. This short lifetime could be partly accounted for by radiationless transitions out of the triplet state if this is occupied to a relatively high degree, but other factors, such as symmetry of the states and the degree of spin-orbit coupling, probably contribute.

Another point of interest is the effect of deuteration on the spectral characteristics of the hydrocarbons. The lifetime of perdeuteriated benzene in solid matrices of CH_4, Ar, Kr, and Xe at 4.2°K is 22, 26, 1, and 0.07 sec, respectively. Ordinary benzene has a lifetime of 16, 16, 1, and 0.07 sec, respectively in the same system (145,146). The lifetime of perdeuteriated naphthalene is also longer than that of ordinary naphthalene (136,147). Deuteriated naphthalene in deuteriated durene at 77°K shows a mean lifetime in the decay of the paramagnetic resonance signal, originating from the triplet state of 16.9 ± 0.7 sec, considerably longer than that of ordinary napththalene in ordinary durene at 77°K, 2.1 ± 0.1 sec. Ordinary naphthalene in deuteriated durene has a lifetime near the 2.1 sec value. A parallel situation also exists for perdeuteriated anthracene and ordinary anthracene (145). It has been suggested that the normal phosphorescence originating from intramolecular perturbation is highly vibrationally induced (145,148). The intensity behavior of the 0–0 band of phosphorescence of benzene in the above matrices adds support to this premise (149,150); the band is strong in Kr and Xe and weak or absent in the matrices of lower molecular weight. In CH_4 and Ar, the spectrum is that arising from the inherent intramolecular perturbation. In Kr and Xe, the effect of the external perturbation (intermolecular heavy atom effect) predominates over the intramolecular perturbation as can be seen from both the effect on the lifetimes and intensity behavior of the 0 → 0 band. However, the effect of deuterium in lengthening the lifetime of several hydrocarbons also points to the fact that phosphorescence (in the absence of external perturbation) is vibrationally induced. The presence of a radiationless transition between the triplet and ground states for benzene and naphthalene is consistent with quantum yield data (6). The combination of quantum yield data, isotopic effect and solvent perturbation data provide strong evidence for the fact that the normal phosphorescence in hydrocarbons is vibrationally induced.

Although a detailed analysis of the foregoing topic is beyond the scope of this book, certain deductions are worth mentioning. These assume that radiationless transitions from the lowest excited singlet ground state are unimportant. Also, estimates of vibrational factors and spin–orbit coupling terms are uncertain. Nevertheless, by using calculated values for the latter, establishing limits for the former, using calculated values for some of the higher triplets, and carrying out a vibrational analysis on the phosphorescence of benzene in the matrices, the principal operating mechanism for the intramolecular perturbation in benzene can be deduced (151). The results indicate that the two most likely mechanisms involve either indirect interaction of the $^1B_{2u}$ state with the triplets via vibronic mixing between the $^1B_{2u}$ and $^1E_{1u}$ states and spin–orbit mixing of the $^1E_{1u}$ and $^3E_{1u}$ or vibronic mixing within the triplet manifold of $^3E_{1u}$ with $^3B_{1u}$. The former mechanism appears to be the more likely (151). Questions of natural lifetime are important. These depend on the known quantum yields and measured lifetimes. It will be recalled that the true or natural radiative lifetime would be that expected in the absence of radiationless modes. Based on absolute quantum yields and assuming all radiationless modes originate in the triplet state, a lifetime of 21 sec can be calculated for benzene (6). Newer quantum yield data give a longer value of 28 ± 4 sec (152). Deuteriation experiments indicate a lower limit of 26 sec. Thus, the radiative lifetime can be given as 28 ± 2 sec. The question of the existence of a significant probability for a radiationless mode between the first excited singlet and ground state has been considered (152). Assuming a true radiative phosphorescence lifetime of 26 sec, then the difference between this value and the 28 sec lifetime arises because of some singlet to ground state radiationless process ($S_1 \rightarrow S_0$). A quantum yield of about 0.06 (upper limit) can be calculated for this radiationless process.

Lower limits are established on the assumption that for some deuterated hydrocarbons, the measured lifetime is the same as the natural lifetime. At least for perdeutero naphthalene the radiationless transition is not totally quenched by perdeuteration (152a). This means that the measured lifetime is not the natural lifetime (the former is shorter than the latter). It is usually assumed that the rate of internal conversion between singlet excited states is very much more rapid than that for internal conversion from excited singlets to triplets. Conflicting data on this point, based on measurements of the ration of phosphorescence to fluorescence intensities excited by absorption to the first and higher excited singlet states, have been reported for hexahelicene (153) and for chrysene (152b).

The phosphorescence spectra of aromatic hydrocarbons shows a dramatic increase in structure when studied in certain crystalline saturated aliphatic hydrocarbons at low temperature. Fluorene in heptane at 77°K shows fine line structure (see Sections II-C and E) for both fluorescence and phosphorescence (154). The fluorescence spectrum begins at 3015 Å and the phosphorescence at 4069 Å in heptane. In octane, phosphorescence begins with an intense band at 4203 Å and ends near 5800 Å. It is likely that the spectrum originating at 4203 Å in octane is intrinsic, and that shorter wavelength lines are caused by impurities. It is interesting to compare the spectra of the isomers benz(*e*)- and benz(*a*)pyrene (155). The benz(*e*)pyrene has a fluorescence spectrum beginning at 3763 Å and extending to approximately 4500 Å and phosphorescence from 5366 Å to 6500 Å in heptane at 77°K. The origin of phosphorescence for benz(*a*)pyrene is at considerably longer wavelength, (6820 Å vs. 5366 Å for benz(*e*)pyrene), while the fluorescence emission of the benz(*a*) derivative is only some 250 cm^{-1} lower in energy compared to the energy difference of 3960 cm^{-1} in phosphorescence. In addition, the benz(*e*)pyrene shows a mirror symmetry relationship which is not present for the benz(*a*)pyrene. Further, the 0–0 band of fluorescence in the benz(*e*) derivative is weak, whereas it is the most intense band in the benz(*a*) derivative. Finally, for benz(*e*)pyrene, if the temperature is lowered to 4°K, not only do the lines further sharpen but some of the lines present at 77°K split up into new, even finer lines. Several seven-membered ring compounds show fine-line structure in aliphatic hydrocarbons at low temperature (156). These include a tribenzpyrene and a benzonaphthylpyrene. The phosphorescence spectra begin at 6100 and 4900 Å, respectively, and the sharpness of the lines is not the same in all solvents. For example, hexane is the best solvent for sharp lines for the tribenzo derivative while octane is the best for the benzonaphthyl derivative. Again, it appears quite certain that the phenomenon is a molecular one and not the result of crystallization, etc., as was discussed in the section on fluorescence.

2. SUBSTITUTED AROMATIC HYDROCARBONS AND THE INTRAMOLECULAR HEAVY ATOM EFFECT

The lifetime of phosphorescence of the halobenzenes decreases with increasing atomic number of the halogen (see Table IX). This is in line with expectation based on the discussion in Section III-A concerning the dependance of singlet ↔ triplet transition probability on atomic number. However, the quantum yield of the phosphorescence is not so simply dependent on the atomic number. In the fluoro derivative phosphorescence is absent, it is weak in the chloro case, still weaker in the bromo derivative and absent in iodobenzene. In these cases, several factors must be taken into account, including the ratio of the fluorescence and internal conversion rate constants to the intersystem crossing rate constant. Even if the triplet state were relatively highly occupied, the $T_0 \rightarrow S_0$ internal conversion rate constant could be larger than the radiative one, resulting in a low quantum yield. A detailed understanding of these cases is still lacking. It is interesting that multiple chloro substitution, up to four chlorine atoms, has negligible effect on the lifetime. Moreover, isomeric substitution (*ortho* and *para*) does not alter the lifetime. Furthermore, multiple bromo substitution seems to have little effect on the lifetime and, in fact, it is possible that the lifetime even may increase somewhat. Here again, there is no real understanding of the phenomena.

Benzoic acid shows a relatively strong blue-violet phosphorescence in ethanol at low temperature (origin at 3670 Å) (157). The phosphorescence varies in location and intensity depending upon the solvent, being weakest in petroleum ether. The general spectrum is similar to that of toluene. The phosphorescence spectrum of methyl benzoate is similar to that of the acid in all solvents. Thus, since the ester will exist as a monomer, it is quite certain that the spectrum of the acid also represents that of the monomer. The phosphorescence spectrum of benzoic acid in benzene at 90°K contains strong out-of-plane vibrational bands indicative of reduced molecular symmetry and molecular deformation, compared with the unsubstituted compound. The similar compound, benzamide, has a blue phosphorescence in ethanol and benzene, although it is weaker in the latter solvent. Also, the lifetime is shorter (~1 sec vs. ~5 sec). It is noteworthy that no out-of-plane vibrations are observed in this case. Since the molecular structure of all three of the compounds is expected to be similar, it appears that benzamide is not deformed in benzene at low temperature. Nitrobenzene, in addition to having no fluorescence, shows only a very weak phosphorescence.

By comparison, an examination of the halonaphthalenes is of value. In the 1-substituted compounds there is a progressive decrease in τ_P as the atomic number of the halogen increases. The quantum yield of phosphorescence increases notably from the fluoro to the chloro compound and then undergoes only minor changes, although that of the iodo compound is the highest (see Table IX). The quantum yields of fluorescence decrease regularly as the atomic number increases. However, the total quantum yield of the fluoro compound is over two times that of any of the others. Further, the decrease in φ_F from the fluoro to the chloro compound is about 14-fold while the increase in φ_P is only about fivefold. Obviously, there is a substantial increase in the rate constant of some radiationless process or processes. Between the chloro and the bromo compounds the change in φ_P is insignificant but the decrease in φ_F is about 35-fold, and between the bromo and iodo compounds, φ_P increases again about 30% but the φ_F decreases by a factor of 3 or more. Several general conclusions can be drawn from these results. First, the intersystem rate constant increases notably relative to the fluorescence rate constant in going from the fluoro to the chloro derivative. Second, $\chi = \varphi_P/\varphi_F$ undergoes a rapid increase as the atomic number of the halogen increases (~ 0.07 for the fluoro to > 1000 for iodo compound). Third, the probability or rate constant for emission (based on τ_P) does not, in general, increase as rapidly in magnitude as the intersystem rate constant. As was noted earlier, there is an increase in a radiationless mode or modes in going from the fluoro to the chloro derivative. These modes are still present and are even more probable in going from the chloro to the bromo derivative since φ_F decreases greatly. Proceeding from the bromo to the iodo derivative, the increase in φ_P is greater than the decrease in φ_F indicating a decrease in the probability of a radiationless mode or modes of deactivation. The increase in φ_F from naphthalene to fluoronaphthalene with essentially no change in φ_P points to a decrease in the rate constant for internal conversion from $S_1 \rightarrow S_0$.

In the case of the 2-halo-substituted naphthalene, the lifetime of phosphorescence is almost the same as for the 1-halo derivatives. Thus, it is apparent that the position of substitution is relatively unimportant in its effect on the radiative probability. Unfortunately, quantum yield data are not available for further comparison. The assignment of the triplet states in the 2-halonaphthalenes cases is still not clear. Earlier indications were that the symmetry of the triplets were the same as that of the ground states (158). Emission, in the 0–0 band, is negatively polarized and thus is polarized greatly out of the molecular plane for all halo derivatives. In the 1-halo compounds except for the 0–0 band, the polarization is positive and its magnitude is sensitive to the nature (atomic number) of the halogens. Thus, except for the 0–0 band, the emission is in-plane and is possibly caused by mixing of in-plane states involving the halogen atom. In the 2-halo compounds, except for the 0–0 band, the polarization is negative and does not depend upon the nature of the halogen; however, it is sensitive to the wavelength of excitation. The indication is that a possible perturbing in-plane state is a charge-transfer σ,σ^* state in the carbon–halogen portion of the molecule (159). Here again, the assignment of the triplet is uncertain as is the mechanism of the enhancement of spin–orbit coupling.

In other derivatives of naphthalene, varying results are obtained. The substitution of methyl in the 1 position enhances the φ_F but has little effect on φ_P or τ_P. The spectral characteristics are very similar to those of the 1-fluoro derivative. Other groups in the 1 position have a more marked influence. This is particularly true for the aldehyde group, by which φ_F is strongly decreased, φ_P is decreased somewhat and τ_P is also decreased (Table IX). In the original discussion of the aldehyde (41) it is inferred that energy is transferred to a triplet with no further explanation. In the aldehyde it is likely that an n,π^* singlet state is lowest and intersystem crossing to a triplet is complete or nearly so. The reason for this is discussed in Section III-D-1. However, there

TABLE IX

Spectral Characteristics of Some Substituted Aromatic Hydrocarbons

Compound	Origin of phosphorescence (Å)	Measured τ_P[a,b] (sec)	φ_P	φ_F
Benzene	3390	7.0	0.26,[c] 0.20[d]	0.26,[c] 0.20[d]
Toluene	3460	8.8, 8[e]		
Durene		5.7,[f] 6.40		
Hexamethylbenzene		~5.7,[f] 8.55		
Aniline	3730	4.7		
Phenol	3495	2.9		
Anisole	3545	3.0		
Fluorobenzene	Absent			0.22[c]
Chlorobenzene		0.004	0.06[c]	
Bromobenzene		~0.0001	<0.03[c]	
Iodobenzene	Absent			
o-Dichlorobenzene		0.018		
p-Dichlorobenzene		0.016		
p-Dibromobenzene		0.003		
1,3,5-Trichlorobenzene		0.022		
1,3,5-Tribromobenzene		0.00074		
1,2,4,5-Tetrachlorobenzene		0.018		
1,2,4,5-Tetrabromobenzene		0.00055		
Benzoic acid	3675	2.5		
Hexachlorobenzene	4130			
Naphthalene	4695[a,g]	2.6, 2.3[g]	0.1,[f] 0.051[g]	0.55[c]

(continued)

must be highly probable radiationless quenching modes associated with the triplet state of the aldehyde, as is shown by the low quantum yield of phosphorescence, and the large decrease, by a factor of about 30, in the lifetime compared to that of naphthalene. This decrease would be expected if the degree of occupation of the first excited singlet state of naphthalene, responsible for the fluorescence, were converted, in the aldehyde, to a parallel degree of triplet state occupation that disappeared radiationlessly. Consistent with this explanation is the fact that for the 1-hydroxy derivative, in which the n,π^* singlet state is not expected to be that of lowest energy, there is no decrease in φ_F compared to naphthalene. In fact, it is increased by about 50%, and only a small decrease in φ_P and in τ_P occurs. The total luminescence quantum yield is increased in the naphthol (Table IX). Of course, in the aldehydes some quanta could be lost by a radiationless process originating in the excited singlet state, although this process is probably much less important than that described above. The phosphorescence of naphthaldehyde apparently originates from a π,π^* triplet state and not from an n,π^* state (160).

Substitution of a nitro group in the 1 position causes a large decrease in

TABLE IX (*continued*)

Compound	Origin of phosphorescence (Å)	Measured $\tau_P{}^{a,b}$ (sec)	φ_P	φ_F
1-Methylnaphthalene	4760 (4810^g)	2.5, 2.1^g	0.044^g	0.85^g
2-Methylnaphthalene				
1-Aminonaphthalene	5265	1.5		
1-Hydroxynaphthalene	4855^g	1.9	0.036^g	0.76
2-Hydroxynaphthalene		1.3		
2-Carboxynaphthalene	4875	2.5		
1-Nitronaphthalene	5195^g	0.049	0.083^g	0.0001^g
1-Fluoronaphthalene	4730^g	1.5	0.056 ± 0.009^g	$0.84 + 0.08^g$
1-Chloronaphthalene	4830^g	0.30, 0.29^g	0.30 ± 0.06^g	0.058 ± 0.005^g
1-Bromonaphthalene	4830^g	0.018	0.27 ± 0.04^g	0.0016 ± 0.0005^g
1-Iodonaphthalene	4880^g	0.0025, 0.002^g	0.38 ± 0.06^g	0.0005^g
2-Fluoronaphthalene	4695			
2-Chloronaphthalene	4740	0.47		
2-Bromonaphthalene	4760	0.02		
2-Iodonaphthalene	4760	0.0025		
1-Naphthaldehyde	5060^g	0.08^g	0.02^g	$< 0.0001^g$
Biphenyl	4385	3.6		
o,o'-Difluorobiphenyl	3890	0.88		
p,p'-Difluorobiphenyl	4350	3.2		

---

[a] In EPA (see Table VIII) at 77°K unless noted otherwise.

[b] All data from reference 6 except where noted; consult reference for error limits.

[c] Reference 134.

[d] Reference 152, in EPA at 77°K.

[e] Pure toluene at 4°K; Y. Kanda and H. Sponer, *J. Chem. Phys.*, **28**, 798 (1958).

[f] Reference 135 in EPA at 77°K. Lifetimes show concentration and solvent dependence.

[g] In ethanol ether (2:1) at 77°K; V. Ermolaev and K. Svetashev, *Opt. Spectry. USSR (English Transl.)*, 7, 399 (1959). All quantum yields based on φ_F for naphthalene of 0.55. Error is 5–10% on τ_P.

φ_F, a slight decrease in φ_P and a large decrease in τ_P. These facts, again, indicate the presence of strong deactivational modes, the most important of which is probably between the emitting triplet and ground states. Unfortunately, only lifetime data exist for amino substitution and this indicates a slight decrease in τ_P. The real effect of the substituent cannot be evaluated. The decreases in τ_P caused by hydroxy and amino substitution in naphthalene are parallel to those in benzene. Of the fourteen possible nitro-substituted 1- and 2-naphthylamines, only three show phosphorescence while the others fluoresce (161). It is interesting that in several cases the fluorescence maxima are at longer wavelength than some of the phosphorescence maxima. This is unusual and although there may be explanations, it would seem that further substantiation would be worthwhile. A series of dinitro naphthalenes also show phosphorescence (as do the 1- and 2-mono derivatives). In these compounds, the origins vary from ~6000 to ~5000 Å (161). The spectra all show structure near the origin except for the 1,2 and 2,3 derivatives, in which steric interactions apparently cause broadening. Naphthalene derivatives containing only the nitro group presumably do not fluoresce.

Finally, biphenyl and some derivatives show interesting properties. The sterically hindered *o,o'*-difluoro compound exhibits a rather large blue shift (~3000 cm^{-1}) of its phosphorescence origin as well as a fourfold decrease in τ_P compared to the unsubstituted compound. On the other hand, the *p,p'*-difluoro derivative resembles biphenyl both in the position of the origin and in τ_P. The latter result is parallel to the case of naphthalene where the same substituted atom had little effect on either the origin or τ_P of phosphorescence, although the φ_F did increase. Further study of such cases would be interesting.

In addition to those hydrocarbons noted above, methyl-substituted tetracyclic aromatic hydrocarbons show emission (19,162). For the twelve monomethylbenz(*a*)anthracenes, the origin of phosphorescence is displaced to longer wavelength (by some 600 cm^{-1}) from that of the parent hydrocarbon at 16,800 cm^{-1} or 5950 Å. The intensity of fluorescence within the monomethyl derivatives varies about 10-fold—that of the 7-methyl derivative being the strongest. Phosphorescence is considerably weaker than the fluorescence in all cases. The separation S_1–T_0 varies from 8900 to 9400 cm^{-1} while for S_2–T_0 it is 10,700–11,400 cm^{-1}. Several dimethyl derivatives show red shifts of the origin from that of the unsubstituted compound, the 7,12 derivative showing the largest (~1200 cm^{-1}). In the methylbenzo(*c*)phenanthrenes (parent origin at 20,000 cm^{-1} or 5000 Å) the shifts are all to the red but the maximum shift caused by the methyl group is less than that for benzanthracenes. One tetramethyl derivative shows a large red shift (~1700 cm^{-1}). The intensities of fluorescence and of phosphorescence are about the same in the parent. The S_1–T_0 separation varies from 6500–7500 cm^{-1} while for the S_2–T_0, it is 10,400–10,900 cm^{-1}. In the 1-methyl derivative, the S_1–T_0 separation is largest and probably results from steric interaction. For the methylchrysenes (parent origin at 20,100 cm^{-1} or 4975 Å) the shifts are to the red, but again are relatively small. The S_1–T_0 separation is 7400–7800 cm^{-1} while for the S_2–T_0 it is 10,900–11,200 cm^{-1}. The largest value is for the parent in this case. The intensities of fluorescence and phosphorescence are approximately equal in the parent. In the methyltriphenylenes (parent origin at 23,800 cm^{-1} or 4200 Å) the shifts are to the red. The intensity of phosphorescence is considerably greater than that of fluorescence in the parent and derivatives. The S_1–T_0 separation is 5400–5500 cm^{-1} while it is 10,700–10,800 cm^{-1} for the S_2–T_0. In the methylpyrenes (parent origin at 17,000 cm^{-1}), the S_1–T_0 separation is 9700–10,100 cm^{-1} while for the S_2–T_0 it is

12,600–13,000 cm^{-1} (the largest value is for the parent). It is worth summarizing several facts about the methyl derivatives and the parents (19). The variation among the separations (S_1–T_0 or S_2–T_0) for the methyl derivatives within one series is minor. More important, between the series all of the S_2–T_0 separations are comparable, while there is considerable variation for the S_1–T_0 separations. The nonisomeric pyrene has an S_2–T_0 separation considerably larger than that for the other hydrocarbons. The small variance in the S_2–T_0 separation for the isomeric hydrocarbons would seem to indicate the same symmetry for these two states.

Although the following discussion does not involve the heavy atom effect due to substitution on the hydrocarbon, it is concerned with this effect for complexes of the hydrocarbons. It is possible to form charge-transfer complexes of hydrocarbons with various acceptors (see Section II-I). Complexes of naphthalene and acenapthene with trinitrobenzene, and acenaphthene with halo-substituted phthalic anhydrides, show an increase in the quantum yield ratio φ_P/φ_F (163). It is suggested that the increase in the ratio of phosphorescence to fluorescence indicates an increase in the gross probability for the intersystem crossing between the excited singlet and triplet states of the donor hydrocarbon. The gross increase is postulated to arise principally because of a more probable radiationless process involving an intermediate charge-transfer state, ($S_{1_D} \rightarrow$ charge-transfer state $\rightarrow T_D$), where the suffix D represents the donor. Further, the ratio of φ_P/φ_F for naphthalene–tetrahalophthalic anhydride complexes increases as the atomic number of the halogen increases (163). This indicates the presence of a heavy atom effect in addition to the enhancement resulting from the perturbations present in the charge-transfer complex.

To summarize, the effect of halo substitution on benzene is such that a progressive increase in the atomic number of the halogen results in a progressive decrease in τ_P. Moreover, φ_P decreases as well. Multiple halogen substitution has little effect on τ_P. Substitution of a methyl group and multiple methyl groups has little effect on τ_P. A similar result occurs for substitution of an amino group. Hydroxyl or carboxyl substitution decreases τ_P by a factor of 2–3.

For the naphthalene compounds, an increase in the atomic number of the substituted halogens decreases τ_P, as for those of benzene, but increases φ_P relative to the parent naphthalene. In the latter respect, the effect of the substitution is different from that in benzene. In addition, except for fluorobenzene, halogenation causes a notable decrease in φ_F. In all cases except fluorine, radiationless transition modes are introduced. The progressive decrease in τ_P as a function of the atomic number of the halogen is independent of the position of substitution. A methyl group has little effect on τ_P and φ_P, but increases φ_F, thus reducing the probability for deactivation by a radiationless mode. An aldehyde group effectively quenches completely fluorescence and decreases τ_P and φ_P. A dramatic decrease in φ_{total} shows the introduction of strong radiationless modes which appear to be principally in the triplet manifold ($T_0 \rightarrow S_0$). A hydroxy or amino group causes a small reduction in τ_P. The former substitution also causes a small reduction in φ_P but a notable (50%) increase in φ_F and φ_{total}. Thus, the probability for a radiationless mode or modes has been decreased. The position of substitution of the hydroxyl has little effect on τ_P. A nitro group, in effect, completely quenches fluorescence, increases φ_P slightly, and decreases τ_P. The φ_{total} decreases showing the introduction of strong radiationless modes; further the principal one appears to originate in the triplet state. Finally, a carboxyl group has little or no effect on τ_P. It can be seen that certain general trends appear in both series but in many respects, there are differences.

The effect of methyl groups on the spectroscopic properties of tetracyclic compounds is variable. The strongest influence is noted on the molecule of lowest symmetry, benz(*a*)anthracene. The second singlet–triplet separation (S_2–T_0) is remarkably constant for all derivatives of all of the isomeric tetracyclics. This is not true for the first singlet–triplet (S_1–T_0) separation.

D. Molecules with n,π^* States

In this section we shall consider two major classes of molecules: the carbonyl type and the heterocyclic type. Usually phosphorescence is expected from molecules of these types although there are certainly exceptions (see Section II-F). One reason for this expectation is that because of the forbidden nature of the $n \rightarrow \pi^*$ absorption, the lifetime of the $\pi^* \rightarrow n$ fluorescence emission is expected to be relatively long. Thus, the probability for intersystem crossing to a triplet should be high and only phosphorescence should occur. This will happen when the n,π^* singlet state is the lowest of the excited singlet states. However, because the energy difference between the n,π^* singlet and π,π^* singlet states is often small, the nature of the solvent is often important in determining which will be lower. Therefore, some molecules will show different emission characteristics depending upon the solvent.

1. CARBONYL MOLECULES

In Table X, spectral properties of a large number of aldehydic and ketonic carbonyl compounds are given. In addition, there are data on aromatic acids. For example benzoic, phthalic, and gallic ($C_6H_2(OH)_3COOH$) acids emit phosphorescence beginning at 4051, 4600, and 4295 Å, respectively (164).

One case of interest is biacetyl since it shows both fluorescence and phosphorescence in the gas phase, in dilute solution and in a rigid glass. In these phases, the φ_F is 0.0023, 0.01, and >0.005, respectively (165); the φ_P is 0.145, 0.007, and 0.23, respectively (165,166); the lifetime of phosphorescence is 0.0018 (167), 0.001 (168), and 0.00225 sec (134), respectively. The ratio of $\varphi_P \varphi_F$ undergoes large changes, being 64 (169) in the gas phase, 7.5 in benzene solution, and quite high in the rigid medium (165). Other values of φ_F in different fluid solvents are about 0.01. The natural lifetime calculated, assuming that intersystem crossing is virtually complete, is approximately 0.01 sec in all three phases. There is considerable interest in biacetyl in terms of energy transfer or sensitization phenomena (see Section III-I).

An interesting effect is noticeable when the alkyl chain on one side of a diketone is increased. In a series of 2,3-aliphatic diketones beginning with biacetyl and ending with 2,3-octanedione, the intensity of phosphorescence decreases as the alkyl chain length increases (169a). However, the relative intensities of the fluorescences are approximately the same and weak. The phosphorescences all have a maximum in the 5240–5340-Å region while the fluorescences occur in the 4660–4760-Å region. At 77°K the phosphorescences are very intense and the fluorescences are essentially absent. The phosphorescences can be sensitized by benzophenone.

It will be recalled that the solvent can play an important role in determining the nature of the emission because if the n,π^* singlet and π,π^* singlet states are close together they may be reversed in energy relative to one another by a change in solvent. This affects the probability of intersystem crossing to the triplet state and thus the relative intensity of fluorescence and phosphorescence. In cases such as benzophenone or benzaldehyde, it is likely that no hydrogen bonding (hydroxlic) solvent can increase the energy of the n,π^* singlet state to a value above that of the π,π^* singlet state; and thus intersystem crossing to a triplet is very probable in all solvents with consequent sole emission of phosphorescence. One reason why intersystem crossing is so likely when the n,π^* singlet is lowest compared to that when the π,π^* singlet is lowest is the following. The intensity of all $n \rightarrow \pi^*$ singlet transitions is very weak (for example, in benzaldehyde $\epsilon_{\max} \approx 1.4$). Therefore, in accord with equation (11), the emission lifetimes expected are long. Thus, upon excitation to higher π,π^* singlet excited states, for which the intensity of absorption is high, internal conversion occurs to the lowest n,π^* singlet state. With a low rate constant for fluorescence, the intersystem rate constant can be and usually is significantly faster than the fluorescence. Thus, the triplet state is highly or completely occupied, little or no fluorescence occurs, and phosphorescence is the sole emission. The quantum yield can be high or low depending on competing internal conversion modes to the ground state and photochemical reactions (see Table X). This explanation does not include all factors, but some of these will be included in the discussion of heterocyclic compounds for which more calculations and experimental detail are available.

TABLE X

Phosphorescence Spectral Properties of Aromatic Carbonyl Compounds

Molecule[a]	Origin (Å)	φ_P	τ_P[b] (sec)
Benzophenone 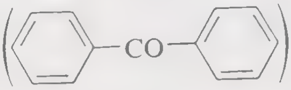	4125	0.75[b]	0.0077, 0.006[b]
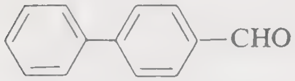	4750		
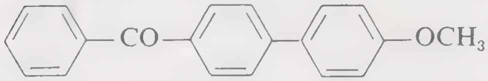	4855	0.50 ± 0.10	0.48 ± 0.02
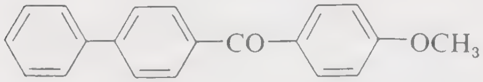	4658	0.65 ± 0.06	0.28 ± 0.02
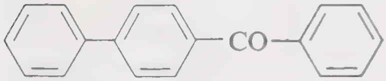	4710	0.47 ± 0.05	0.30 ± 0.02
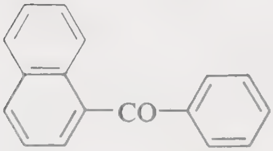	4975	0.25 ± 0.03	0.74 ± 0.03
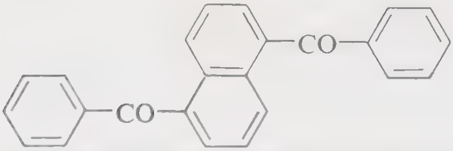	5020	0.29 ± 0.03	0.56 ± 0.02

(continued)

In the case of pyrene-3-aldehyde and certain other molecules as noted earlier (see Section II-F), the relative intensity of fluorescence varies with the solvent because of the effect just discussed. Presumably, the phosphorescence intensity of pyrene-3-aldehyde would also vary with the solvent but this is not known (54). However, the phosphorescence does appear at low temperature in hydrocarbon glasses (see Section II-F). Another example of the effect of solvent concerns the chlorophylls (16). Here at low temperatures, if the chlorophylls are dry and are excited in a dry hydrocarbon, a phosphorescence results (at 7550 Å for chlorophyll *a*). However, if only a very small amount of a hydroxylic solvent is added, this particular phosphorescence disappears and the usual fluorescence appears. Also, another phosphorescence is known to be at lower energy (at 8850 Å for chlorophyll *a*) and is different from the assigned phosphorescence occurring for dry chlorophylls in dry hydrocarbons (16,170).

TABLE X (*continued*)

Molecule[a]	Origin (Å)	φ_P	$\tau_P{}^{b}$ (sec)
Naphthalene	4705	$0.05 + 0.005$	2.3 ± 0.1
1-Naphthaldehyde	5065	0.03 ± 0.01	0.08 ± 0.01
2-Naphthaldehyde	4810	0.03 ± 0.01	0.35 ± 0.02
2-Acetylnaphthalene	4815	0.05 ± 0.01	0.97 ± 0.03
2-Chloro-1-naphthaldehyde	5195	0.06 ± 0.02	
Benzaldehyde[c]	3970		0.0015
Acetophenone	3870	0.63^{b}	0.008, 0.0023
Ethylphenylketone[c]			0.0037
o-Hydroxybenzaldehyde[c]	4065		
Carbazole[c]	4085		7.25
Benzoin[c]	3900		2–4
Biacetyl		$0.23^{d}(\varphi_F = >.005)^{d}$	0.00225^{b}
p-Phenylbenzophenone[e]			0.32 ± 0.01
p-Aminobenzophenone[e]			0.40
p,p'-Bis(dimethylamino)benzophenone[e]			0.27 ± 0.02
p-Dimethylaminobenzophenone[e]			0.35 ± 0.03
p,p'-Dimethoxybenzophenone[e]			0.065 ± 0.007
Dimethyl ketone[b]			0.0006
Methylethyl ketone[b]			0.00085
Diethyl ketone[b]			0.00126
Diisopropyl ketone[b]			0.0037
Di-*t*-butyl ketone[b]			0.0086
Methyl-β-naphthyl ketone[b]	4830		0.95

[a] All data above dotted line from reference 171.

[b] Reference 6 in EPA at 77 K. Benzophenone quantum yield varies, depending on concentration.

[c] Reference 221.

[d] Reference 165 at 77 K. The phosphorescence shows both wavelength and concentration dependence. $\varphi_F = 1.03 \times 10^{-2}$ in benzene at 25°C.

[e] Reference 172 at 77°K.

The carbonyl compounds above the benzaldehyde and below benzophenone in Table X like benzophenone, do not fluoresce but their phosphorescence lifetimes are quite different from those of benzophenone. Moreover, the phosphorescence spectral origin is red-shifted compared to that of benzophenone. In fact, the emission spectra resemble those of other derivatives of biphenyl or naphthalene. This, at first consideration, is surprising particularly for those molecules with a benzophenonelike moiety. For example, the emission of 2-acetyl-naphthalene looks very similar to that of 1-chloronaphthalene in both origin and shape. Further, the phosphorescence spectrum does not contain the $1600-1700\ \mathrm{cm}^{-1}$ carbonyl vibration as does that of benzophenone but an aromatic ring frequency vibration of approximately

1400 cm^{-1}. The results indicate that excitation results in occupation of the n,π^* singlet state followed by intersystem crossing to a triplet state and then emission from a π,π^* triplet state (171), rather than from the n,π^* triplet, as for benzophenone.

In addition, photochemical reactivity has been used as a criterion for the assignment of the lowest energy state (172,173). In certain substituted benzophenones, in contrast to benzophenone itself, photoreduction to the pinacol cannot be observed (Section III-I). This could arise if the lowest triplet state of the photochemically unreactive compounds were of π,π^* character rather than of n,π^* character; the charge distribution (diradical type), consistent with high photochemical activity, would then not exist and the capacity of the oxygen site to abstract hydrogen would be lost. Certain ketone and aldehyde sensitizers do not cause racemization of optically active alcohols. It appears that the photochemically unreactive group of ketones and aldehydes may have lowest triplet states of π,π^* character. For more detailed discussion of the molecules involved see Section III-I.

Finally other molecules, such as camphorquinone, do show n,π^* phosphorescence in the visible spectral region in a hydrocarbon glass at 77°K, with a lifetime of 7.1×10^{-3} sec. Here there is a question as to the specific assignment because of the presence of two orbitals containing n electrons. This situation arises also in other cases such as biacetyl and in diazaheterocyclic compounds.

2. HETEROCYCLIC COMPOUNDS

In Table XI, some spectral properties of heterocyclic compounds are given. There has been a great interest in such compounds both with regard to their absorption and emission spectra. Considerable theoretical effort has been devoted to a better understanding of the nature of the $n \leftrightarrow \pi^*$ transitions and spin-orbit coupling in these molecules (23,124,174–180). Heterocyclic compounds that do not show phosphorescence include pyridine, pyrrol, furan, and thiophene. However, at least in the case of pyridine, oxygen perturbation studies show that a singlet–triplet transition exists at approximately 3350 Å (181). Further, solvent studies indicate that the triplet state is of π,π^* type rather than n,π^* type.

Pyrazine and dimethylpyrazine both show phosphorescence at 3850 and 3800 Å, respectively (182). In addition, both show singlet–triplet absorption; the unsubstituted compound shows better resolved fine structure both in absorption and emission. The principal point of interest regarding these molecules is the nature of the triplet state. The triplet state could be the analog of the benzene triplet but displaced by the nitrogen perturbation, or it could be of the n,π^* type. The intensity of the transition plus the presence of a 0–0 band in absorption indicates that it is not a symmetry-forbidden tran-

TABLE XI

Phosphorescence Spectral Properties of Some Heterocyclic Compounds

Molecule	Origin (Å)	φ_P	τ_P (sec)
Pyridazine	4250[f]	vw[f]	
Pyrimidine	3540	s[f]	0.01
Pyrazine	3850	vs[f]	0.020[a]
sym-Triazine	3790[c]	vvw[f]	0.044[i]
2,4,6-Triphenyl-*s*-triazine	4060[j]		1.1[j]
Quinoxoline	4650[d]		0.25[d]
Fluorene[b]	4080		4.9[a], 6.9[c]
Dibenzofuran[b]	4080		5
Carbazole[b]	4070		10, 7.6[c]
Indene	4050		1
Thianaphthene[b]	4160		0.5
Indole[b]	4040		5, 6.3[c]
9,10-Dihydroacridine			3.5
9,10-Diazaphenanthrene	7700[e]		
o-Phenanthroline[g] (1,9-Diazaphenanthrene)	4502		1.6
Quinoline[h]	4570	0.19	1.3

[a] Reference 134.

[b] R. Heckman, *J. Mol. Spectry.*, **2**, 27 (1958) in EPA at 77°K.

[c] V. Ermolaev, *Opt. Spectry. USSR* (*English Transl.*), **11**, 266 (1961), in ethanol ethyl ether (2:1) at 77°K.

[d] In EPA or durene at 77°K, lifetime in durene

[e] E. Lippert, *Luminescence of Organic and Inorganic Materials*, H. Kallmann and G. Spruch, Eds., Wiley, New York, 1962, p. 274.

[f] Reference 178 quoted as relative intensities. Reference 52a indicates pyridazine has no phosphorescence in a hydrocarbon solvent.

[g] Reference 122.

[h] Reference 186 in hydroxylic solvent.

[i] Reference 185a.

[j] Reference 185b.

sition. Theory predicts the n,π^* triplet to be near the experimentally determined location. Further, since it is predicted that upon conjugative substitution a π,π^* triplet level is shifted to the red, while an n,π^* triplet is expected to be blue-shifted (174), the data for the dimethyl derivative support the assignment of the triplet as n,π^* ($^3B_{2u}$). The vibrational fine structure indicates that the σ orbitals of nitrogen rehybridize upon $n \rightarrow \pi^*$ excitation.

An important consideration in the case of the azines is the nature of solvent interaction and its effect on the absorption and emission spectra. An interesting case in point is pyrimidine, although the following discussion is not restricted to that molecule; for example, pyrazine also fits the situation (183). Pyrimidine exhibits phosphorescence in both hydrocarbon and hydroxylic glasses (~3540 Å) which is assigned as originating from an n,π^* triplet state

($^3B_1$). Moreover, the hydrochloride salt has a phosphorescence in a hydroxylic glass virtually identical with that of the free base, whose detailed emission spectra is essentially independent of the nature of the solvent. Of further importance is the fact that the emission spectrum of pyrimidine in a hydroxylic glass does not bear a mirror image relationship to the absorption spectrum associated with the $n \rightarrow \pi^*$ transition in a hydroxylic glass but to the spectrum in a hydrocarbon glass. Thus, the solute–solvent interaction in the excited state must be similar to that in a hydrocarbon glass. This supports the view that hydrogen bonding is essentially absent in the excited state. There is no doubt that the pyrimidine hydrochloride has a strong hydrogen bond in the ground state. However, the emission spectrum is similar to the absorption spectrum of the pyrimidine base in a hydrocarbon solvent and not to that of the hydrochloride. These facts definitively show that a hydrogen bond is either absent or very weak in the n,π^* triplet state for both the base and its hydrochloride. Furthermore, the spectral evidence just referred to indicates that the hydrogen bond is absent in the n,π^* singlet state. In the light of these facts, the shift expected in absorption upon going from a hydrocarbon to a hydroxylic solvent depends upon both the stabilization energy of the ground state (resulting from the solvent interacting with the nonbonding electrons) and the Franck-Condon destabilization energy in the excited state. These interactions will result in an overall blue shift. On the other hand, since the emission data show that the hydrogen bond is weak or absent in both the excited state and the ground state (after excitation in rigid media), the spectral shift in emission will depend only upon the Franck-Condon destabilization energy in the ground state. This will result in a small red shift. It is likely that these results are general for $n \rightarrow \pi^*$ transitions in *N*-heterocyclic compounds (183).

In addition to the above considerations, polarization data, coupled with theoretical calculations and experimental results on particular *N*-heterocyclics, have improved the understanding of the reason for increased spin-orbit coupling in these types of molecules. Theoretical prediction based on the symmetry properties of the singlet and triplet spin functions predict that the mixing of n,π^* singlet and triplet states is forbidden by symmetry (23,184). Further, theory predicts that the $n \leftrightarrow \pi^*$ triplet–singlet transition for both pyrazine and pyrimidine (124,184) should be polarized in the molecular plane, as is experimentally verified (184,185). Also, theoretical considerations predict that the degree of spin-orbit coupling between n,π^* singlet and n,π^* triplet states is approximately 1000 times less than that between n,π^* singlet and π,π^* triplet states (23). If an n,π^* singlet state is lowest, the above consideration plus the lack of good overlap between the vibrational wave functions of the n,π^* singlet and the n,π^* triplet states indicates that the intersystem crossing may well proceed to a π,π^* triplet state. This could account for the fluorescence of 9,10-diazaphenanthrene and *sym*-tetrazine. In these molecules, the interaction between adjacent nitrogen atoms could lead to a large splitting of the n,π^* states such that an n,π^* singlet could be below the lowest π,π^* triplet. Thus, the $S_1(n,\pi^*) \rightarrow T_0(n,\pi^*)$ process would be the only crossing pathway but it would have a large prohibition factor (~ 1000) relative to crossing to the π,π^* triplet state. Therefore, the $S_1(n,\pi^*) \rightarrow S_0$ rate could be competitive and fluorescence would result (23).

The situation for *sym*-triazine and derivatives depends upon the nature of the substitution (185a,b). The parent *sym*-triazine and the trimethyl derivatives have lowest excited singlet and triplet states of n,π^* type (185a,b) and exhibit weak phosphorescences ($\tau \approx 0.5$ sec). Phenyl and phenylmethyl-substituted *sym*-triazines also exhibited phosphorescences (at approximately 4070 Å) with lifetimes varying between 1.1 and 1.9 sec. The lowest excited triplet for these latter molecules is of π,π^* type (185b). The lowest excited singlet appears not to have been assigned.

In the case of quinoline, only phosphorescence occurs in a hydrocarbon solvent while both fluorescence and phosphorescence are present when the solvent is hydroxylic (23,186). The quantum yield of phosphorescence is 0.19 in alcohol–ether hydroxylic solvents (186). Further, from calculated rate constants for internal conversion and fluorescence, it has been qualitatively suggested that the n electrons play the important role in spin–orbit coupling. More quantitative considerations of the problem clarifies some of the important details (23). In the hydroxylic solvent, the π,π^* singlet state is lowest. Further, the phosphorescence of naphthalene is similar in both intensity and lifetime to that of quinoline. However, the fluorescence rate constant for quinoline is expected to be about 10 times greater than that for naphthalene. Thus, some mechanism must be responsible for enhancing the intersystem rate constant for quinoline. It is postulated that the presence of an n,π^* triplet between the lowest π,π^* singlet and triplet states is responsible for the enhancement (23). Quinoxaline exhibits phosphorescence in a hydroxylic glass. The phosphorescence is highly out-of-plane polarized. The emitting state is assigned as a π,π^* triplet with which an n,π^* singlet and/or σ,π^* states have mixed.

In conclusion, it appears that when the emitting triplet state is of n,π^* type, the mixing singlet state is likely to be of π,π^* type. However, if the emitting triplet state is of π,π^* type, the mixing singlets are likely to be of n,π^* and/or σ,π^* type. However, exceptions appear to exist.

E. Metal Complexes

One of the most completely studied series of metal complexes involves the porphyrins (79–82). Table IV gives the results obtained for a large group including closed-shell diamagnetic ions, open-shell diamagnetic, and open-shell paramagnetic transition ion metalloporphyrins. The discussion will be divided between the derivatives of the nontransition metal ions and the transition metal ions because of the significant differences in the nature of the ions involved.

Within one group of diamagnetic nontransition metal ions, it might be expected that their complexes would exhibit reasonably smooth trends in the quantum yield of phosphorescence and the lifetime. The reason for this is that with parallel electronic configurations, the spin–orbit coupling would be expected to increase progressively with the atomic number of the perturbing metal ion. A glance at Table IV will show that this is not true and in some cases the deviation from expectation is great. The following discussion will thus be illuminating regarding the qualifications that must accompany generalized statements concerning the enhancement of spin–orbit coupling by the parameters upon which it normally depends.

The first series exemplifying the problem is that containing the Group II-A ions (Mg^{2+}, Ca^{2+}, Sr^{2+}, Ba^{2+}). Even though there is a trend towards decreasing τ_P with increasing atomic number, there is a notable leveling off and in fact a possible reversal of the lifetime at Ba. In addition, the intensities of phosphorescence level off between Ca to Sr while the intensities of fluorescence can undergo a marked and sudden decrease at the same point in the series. For the most part, the quantum yields of fluorescence and phosphorescence are not complementary. We shall deal only with the more marked deviations from regular trends. The first concerns the notable decrease in the intensity of fluorescence, the lack of change in the intensity of phosphorescence, and the ninefold decrease in τ_P when proceeding from the Ca to the Sr derivative. The increase in the atomic number could account for the decrease in fluorescence (by an increase in spin-orbit coupling and parallel increase in intersystem crossing to the triplet), but not for the lack of change in the intensity of phosphorescence. Further analysis shows that there must have been an increase in the rate constant for a radiationless transition of the excited singlet or triplet state in the Sr^{2+} compared to the Ca derivative. The location of this deactivation mode is not clear from this consideration alone but the cause is more discernible. These ions differ mostly in their size, and thus it is likely that the deactivating mode in the Sr compound is a result of geometrical distortion by the large ion.

Consideration of the Sr and Ba compounds will further clarify the situation. For Ba, it is interesting that despite a continued increase in ionic size, the fluorescence intensity does not change, the phosphorescence intensity increases and the τ_P is equal to or larger than that for the Sr compound. This is puzzling at first sight if one postulates molecular distortion as the cause of the loss of luminescence, since, the Ba ion being the largest of the metal ions considered in Table IV, distortion would be a maximum in the Ba complexes; nevertheless luminescence is increased. An analysis of all pertinent data (82, 83) reveals that the electronegativity of Ba is sufficiently small that the complex can be best described as one in which the Ba is not covalently but rather ionically bonded. Thus, Ba acts as a noncovalently bonded perturbation with a consequent reduction in any molecular distortion that might have been expected relative to the Sr complex.

The concept of increased probability of radiationless transition as a result of geometrical distortion is supported by further data on the luminescence of the complexes of porphyrins with the metals of Groups II-B (Zn, Cd, Hg) and IV-A (Sn, Pb). As is shown in Table IV the fluorescence intensity of the Cd derivative is much less than that of the Zn complex, although the phosphorescence of the two complexes is about the same, while for the Hg compound, in which the metal has very large ionic and covalent radii, fluorescence is absent and phosphorescence weaker than for the Cd complex. It is clear that with increasing size of the metal the rate constant of one or more modes of radiationless deactivation to the ground state increases. And absorption data (82,83) point strongly to a distortion from nonplanarity in the complexes containing large metal atoms as the cause. Comparison of the emission properties of the Sn and Pb complexes points to the same conclusion. The large Pb atom quenches the fluorescence, which is of moderate strength in the Zn complex and also greatly reduces the intensity and the lifetime of the phosphorescence.

In summary, the data quite clearly establish the fact that geometrical distortion increases the probability of radiationless transitions to the ground state. It also appears that this occurs principally between the triplet and ground states (82). In addition to distortion, it is necessary to consider the effect of metal ion electronegativity and electronic configuration. Any of these, but particularly metal size and its effect on geometrical distortion, may counteract and even reverse the trend expected from an increase in atomic number.

Special considerations arise when the metal ion, as in the Ni, Pd, Pt subgroup, contains unfilled *d* orbitals (81). In passing from the Zn to the Ni complex (with a decrease in atomic number) the moderately intense fluorescence of the Zn complex is completely quenched, with also a sharp decrease in the intensity of phosphorescence. A moderate decrease in lifetime also occurs. Clearly in the Ni complex, the probability of radiationless transitions to the ground state is greatly increased; nevertheless there is little change in the ionic or covalent radius and in the electronegativity (81). The outstanding difference between the Zn and Ni ions is the presence of unfilled *d* orbitals in Ni. The presence in the Ni complex of an intermediate ligand field triplet state between the ground state and the normal π-triplet state of porphyrin and geometrical distortion appear to be the factors responsible for the increased probability of a radiationless transition to the ground state (81,187). This transition appears to occur from the normal π-triplet state of the porphyrin via the ligand field triplet state (81).

The spectral changes occurring among the complexes of the Ni subgroup are also very interesting. None of the complexes fluoresce. The very weak intensity of phosphorescence of the Ni compound is greatly increased in the Pd compound but then stays nearly the same for the Pd compound despite an increase of atomic number of 32 (see Table IV). The phosphorescence lifetime progressively decreases but a much larger change occurs between the Pd and Pt compounds, even though the atomic number change is the same as that between the Ni and Pd complexes. It is obvious that in this sequence the rate constant for the radiationless mode present in the Ni compound has been markedly decreased. Consideration of all pertinent information leads to the conclusion that it is probable that intersystem crossing to the triplet state is complete in all of these cases (via indirect coupling through new states) (Section II-H) but that because of the variable location of an intermediate ligand field triplet, the probability for radiationless transitions varies in the series, being strong in the Ni compound (81,187). The molecular geometry of the Ni complex is probably also an important consideration. In addition, despite essentially complete intersystem crossing, the rate constant for emission from the triplet to the ground state singlet appears to depend strongly on the atomic number. Thus, two different factors are involved in the mixing of the functions that determine the occupation of the triplet state compounds and the lifetimes (81). The difference in lifetime between the Pd and Pt compounds compared to the Ni and Pd complexes is very likely caused by the increased quantum yield between the Ni and Pd derivatives which offsets the expected decrease in lifetime associated with an increase in the atomic number of the perturbing metal atom.

Turning now to complexes of porphyrins with transition metal ions that contain varying numbers of *d* electrons, one sees from Table IV that in all cases fluorescence is absent, the phosphorescence intensity is weak and the phosphorescence lifetime is short. It is very likely that intersystem crossing is complete in these cases also, for reasons similar to those for the Ni subgroup (81). Also, the low quantum yield of phosphorescence results from the presence of an intermediate ligand field state associated with strong radiationless deactivating modes except for the Cu complex. The paramagnetic nature of the ions and the radiationless modes are responsible for the short lifetimes. The Ag complex represents a unique and unusual case since neither fluorescence nor phosphorescence exists. The 2+ oxidation state for Ag is not common so that either a ligand field state or charge-transfer state must be located at a position such that there is a very high probability for a radiationless transition (81). It may be possible that an emission does occur from the Ag complex but beyond the region of normal investigation ($\sim$10,000 Å).

In conclusion, it can be seen that even in those complexes where essentially complete spin–orbit coupling exists, the expected strong phosphorescence may not appear. Other factors can dominate and cause gross deviation from expectation. Moreover, complexes containing diamagnetic metal ions of almost identical atomic number can show very different emission spectral characteristics because of strongly modifying factors, such as the presence of ligand field levels. Even among the complexes containing diamagnetic ions from the same groups in the periodic system, significant deviations of the emission characteristics from those expected from simple considerations of atomic weight can arise. The other important parameters to consider are geometrical distortion and electronegativity of the ion. Further, triplet state lifetimes among groups of transition metal complexes may depend on a significantly different factor than that responsible for occupation of the state. Finally, there is *no* fluorescence for any of the transition metal complexes. The varying behavior (particularly that different from expectation) exhibited by the metal complexes forewarn us of the danger of making *a priori* predictions of emission spectral characteristics from inadequate premises.

Other metal complexes that show phosphorescence are those of the chlorophylls and their derivatives (see Fig. 8 for structural formulas) (79,170). Both chlorophyll *a* and chlorophyll *b* show weak phosphorescence in a rigid glass at 77°K. The spectra occur at 8850 and 8750 Å respectively, and originate from a π,π^* triplet (79,170). In addition, both these chlorophylls show stronger phosphorescence when dry and in a dry hydrocarbon solvent at low temperature (16) at 7750 and 7330 Å for chlorophylls *a* and *b*, respectively. Ethyl chlorophyllide also shows a weak phosphorescence. The copper ethyl chlorophyllide *a* and copper pheophytin *b* both show intense phosphorescence at 8635 and 8740 Å, respectively (170). In these latter cases it should be noted that the emissions are considerably stronger than in the chlorophylls which are Mg derivatives. This is expected because of the strong spin–orbit coupling caused by the paramagnetic copper ion.

Metallo complexes of quite different ligands show some similarity as well as some differences compared with those of the porphyrins and chlorophyll type. Oxine (8-hydroxyquinolene) and variously substituted oxines show only fluorescence of varying quantum yield at 80°K (187a). In closed-shell metal oxinates, the ligand localized fluorescence yield is only somewhat affected by atomic number. However, a marked affect does occur with high atomic number metals. Phosphorescence is observed for the Pb and Bi complexes; however, the total quantum yield undergoes a substantial reduction (187a). Transition metal chelates show a markedly reduced quantum yield of fluorescence and apparently no phosphorescence. If the metallo complex is a selenooxinate, some notable differences appear. Although the total quantum yield is generally smaller than for the oxinates, phosphorescence is observed for closed shell metals and for Ni. Both the total and phosphorescence quantum yield increases between the Zn and Cd derivatives (fluorescence appears to be absent for the Cd derivative and very weak for the Zn chelate).

The interesting case of the rare earth complexes has been described in certain respects earlier (see Section II-H). The chelating anions of particular interest include benzoylacetonate, dibenzoylmethide, tribenzoylmethide, 8-hydroxyquinolate, and some others. The effect of rare earth ions in enhancing phosphorescence of certain organic chelating agents was first considered some time ago (188). The lifetimes of phosphorescence of various rare earth complexes of dibenzoylmethane show no simple relation with atomic number or size of the metal ion. Table XII shows the lifetimes for some complexes of dibenzoylmethane. The effectiveness of the atomic number in promoting spin–orbit coupling depends to a significant extent upon the closeness of approach of the optical electrons to the nucleus. It will be recalled that spin–orbit coupling depends strongly both on the atomic number and on the distance of the electrons from the nucleus. The distance of approach will depend upon the electron configuration to some extent, as is apparently the case for the Lu and La complexes, where, despite the higher atomic number of Lu, the La complex has shorter lifetime (see Table XII). The Gd complex exhibits no fluorescence and its phosphorescence has a very short lifetime. In this case, the results are consistent with those to be expected because of the paramagnetic nature of the ion; that is, spin–orbit coupling must be effectively complete because of the strong inhomogeneous magnetic field provided by the ion. Further, there is little variation in the location of the triplet level of certain of the rare earth complexes. The average position of the triplet level of rare earth complexes with dibenzoylmethane is 20,520 cm^{-1} (4880 Å) with a maximum deviation of 250 cm^{-1} (Table XII) (98,101,188).

TABLE XII

Lifetimes of Phosphorescence for Some Dibenzoylmethide Complexes (188)

Metal	Atomic number of metal	τ_P (sec in alc)	Origin of phosphorescence spectra
Al	13	0.70	20,900 cm^{-1} (4785 Å)
Sc	21	0.39	20,600 cm^{-1} (4855 Å)
Y	39	0.24	20,350 cm^{-1} (4915 Å)
Lu	71	0.10	20,350 cm^{-1} (4915 Å)
La	57	0.06	20,250 cm^{-1} (4940 Å)
Gd	64	0.002	20,350 cm^{-1} (4915 Å)

TABLE XIII

Location of Triplet States for Some Rare Earth Complexes (101)

Metallo chelate	Average location of triplet state origin[a]
Benzoylacetonate (La,Sm,Gd,Dy,Tm,Yb,Lu)	21,480 cm^{-1} (4655 Å)
Dibenzoylmethide (La,Sm,Eu,Gd,Dy,Tm,Yb,Lu)	20,520 cm^{-1} (4870 Å)
Tribenzoylmethide (Gd,Dy)	20,765 cm^{-1} (4815 Å)
Anthranilate[b] (La,Sm,Eu,Gd,Tb,Dy,Tm,Yb,Lu)	22,135 cm^{-1}[a] (4520 Å)
8-Hydroxyquinolate (La,Gd,Lu)	17,760 cm^{-1} (5630 Å)
2-Methyl-8-hydroxyquinolate (La,Gd,Lu)	18,000 cm^{-1} (5555 Å)

[a] Maximum deviation throughout 500 cm^{-1} or less.

[b] This corresponds to the maximum of phosphorescence and not the origin.

If salts of dibenzoylmethane are compared within a series containing metals of similar electronic configuration (same periodic group), then the phosphorescence lifetimes decrease with increasing atomic number (188). This is interesting in comparison to the porphyrin complexes where, for example, the Ca, Sr, Ba complexes do not follow such a trend. The difference is partly due to the considerably different geometric characteristics of the complexes. However, this comparison brings up a valuable point; that is, generalizing on the consequences of certain considerations such as the effect of atomic number on spin–orbit coupling must be qualified, even within a series containing metal ions of a parallel electronic configuration.

The location of the lowest triplet level of many rare earth ion complexes depends significantly upon the nature of the organic chelating agent (98,101, 189). Table XIII shows the average location of the lowest triplet state for several different rare earth chelates. A given rare earth complex with various ligands may show only band emission, line emission, or a combination of both (see Section II-H). In certain complexes, such as those with La, Lu, and Gd, only molecular band emission is observed, no matter what chelating agent is involved (98,101,189). The origin of the line emission was discussed earlier (see Section II-H).

F. Singlet → Triplet Transitions and Enhancement by External Perturbations

No attempt will be made to cover all cases involving singlet–triplet absorption but only representative situations to elucidate the process. This will also apply to examples of external perturbations.

1. SINGLET → TRIPLET TRANSITIONS

If the phosphorescence of organic compounds represents the radiation emission accompanying the transition of a molecule from an excited triplet state to the normal singlet, it follows that the corresponding absorption process, involving a transition from the normal singlet to the excited triplet state should also be observable, although it will usually be very weak. The low intensity of most singlet → triplet absorption spectra demands long path lengths of concentrated solutions or of the pure liquid for their observation, and even then, detection of the forbidden transition depends on adequate separation from the long wavelength edge of the stronger singlet → triplet absorption spectrum. Care must be taken to avoid interpreting the absorption of impurity as the singlet → triplet absorption. One of the criteria for singlet → triplet absorption is the near correspondence of the 0–0 absorption band with the 0–0 phosphorescence band for the compound in dilute solid solution. Normally, the same type of approximate mirror image relationship between the singlet → triplet absorption bands and the phosphorescence bands exists as for the normal singlet → singlet absorption spectrum and the fluorescence spectrum.

The intensity of the singlet → triplet absorption is governed by, among other factors, the spin–orbit interaction, and in a series of like molecules the intensity of this absorption will increase with the atomic number of substituting atoms. Figures 13 and 14 show some typical singlet → triplet absorption curves for 1-chloronaphthalene (190) and for heterocyclic compounds (191). In the case of the halohydrocarbons, the effect of the increased atomic number of the halogen is to increase the integrated intensity or *f* number of

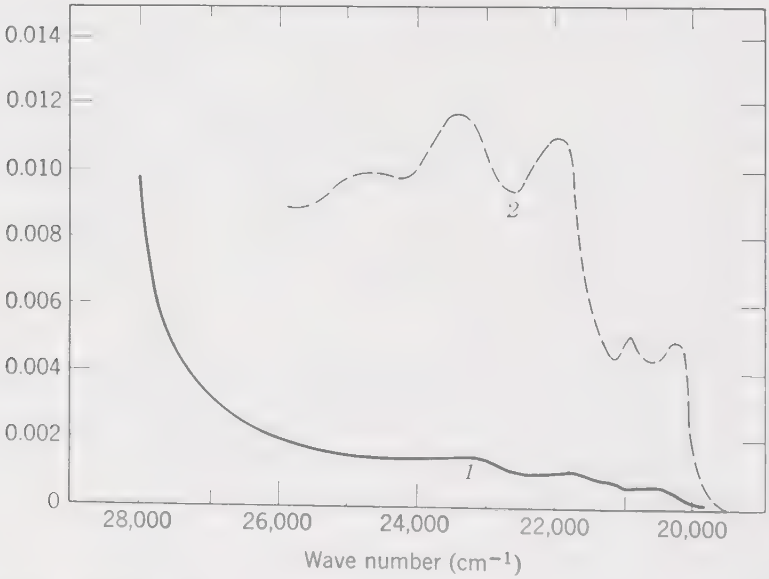

Fig. 13. Singlet → triplet absorption of 1-chloronaphthalene (190): (*1*) alone, and (*2*) in ethyl iodide, 1:2 by volume.

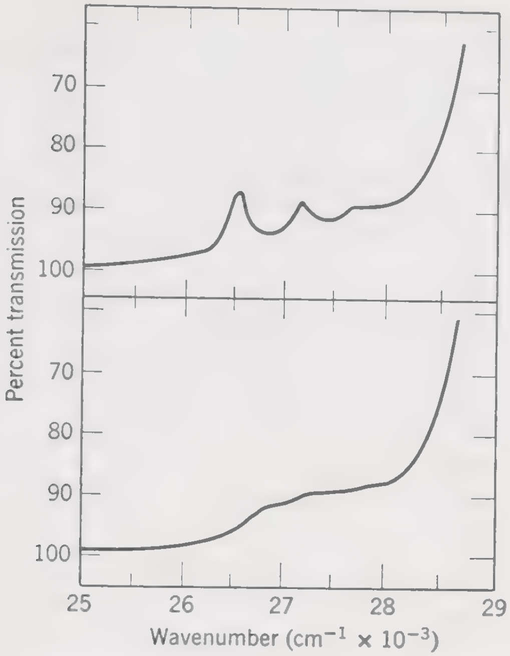

Fig. 14. Singlet → triplet absorption curves: Pyrazine (upper) and 2,5-dimethylpyrazine (lower) at room temperature (191).

the absorption. This is in accord with the theoretical expectations from increased spin–orbit coupling.

In the case of pyrazine it is possible that the singlet → triplet transition could be either of $\pi \rightarrow \pi^*$ ($A_{1g} \rightarrow {}^3B_{3u}$) or $n \rightarrow \pi^*$ ($A_{1g} \rightarrow {}^3B_{2u}$) type. A theoretical calculation predicts that absorption corresponds to an intercombinational $n \rightarrow \pi^*$ type (191). However, this is not unequivocal proof. A substitutional perturbation is predicted to lower the energy of the π,π^* triplet state and raise the energy of the n,π^* triplet state thus producing a blue shift of the singlet → triplet absorption (192,193). A dimethylpyrazine shows a blue shift in absorption of approximately 300 cm^{-1} in comparison with the parent compound. If the transition were of $n \rightarrow \pi^*$ type, a blue shift of 100 cm^{-1} would be predicted while a red shift of 1000 cm^{-1} would be predicted for one of $\pi \rightarrow \pi^*$ type. The phosphorescence is also blue-shifted by a comparable amount. Thus, the transition is assigned as one of $n \rightarrow \pi^*$ triplet type (191). The absorption and emission spectra show a dominant vibration of about 615 cm^{-1}. This is significant in terms of the nature of the transition. The excitation out of the n orbital (sp^2 hybrid) would be expected to result in some rehybridization in the excited state. Thus, the principal vibration generated would be one of angular distortion since the carbon–nitrogen–carbon angle is associated with the hybridization of σ orbitals on the nitrogen (191). This should apply to all $n \rightarrow \pi^*$ transitions in diazines, singlet → singlet as well as singlet → triplet. Also, chloropyrazine shows both an enhancement and blue shift of the singlet → triplet transitions relative to that for pyrazine.

Calculation predicts that for pyridine, the $n \rightarrow \pi^*$ singlet → triplet transition will be at higher energy than the $\pi \rightarrow \pi^*$ transition (191). Perturbation studies with O_2 (194) have permitted location of the lowest singlet → triplet transition, which is found to be in harmony with the prediction that it should be of $\pi \rightarrow \pi^*$ type.

Finally, a ketone, biacetyl, shows singlet → triplet absorption in various solvents (195). The band has no structure and occurs near 5000 Å. The intensity depends on the solvent, being strongest in heptane and weakest in pyridine among the solvents studied. Generally, solvents containing oxygen and nitrogen lower the intensity, as is true also for the lowest singlet → singlet absorption. The dichloro- and dibromo-substituted compounds show no singlet → triplet absorption. This may arise because of a red shift and intensification of the tail of the closely adjacent singlet → singlet transition.

Another interesting method to determine the singlet → triplet absorption spectra is from the phosphorescence excitation spectrum. That is, the determination of the changes in intensity of phosphorescence as a function of the exciting wavelength in the region of the singlet → triplet absorption. For example, α-bromonaphthalene exhibits a moderately resolved excitation spectrum (thus, absorption) in the 4900–3700-Å region at 77°K (195a).

2. ENHANCEMENT OF SINGLET → TRIPLET TRANSITION BY EXTERNAL PERTURBATIONS

The enhancement of spin–orbit coupling by heavy atoms with the consequent increase in the probability of singlet → triplet transitions can be effected by external perturbations by molecules containing heavy atoms as well as by internal perturbations by heavy atoms within the absorbing or emitting molecule. The first example was the remarkable effect of ethyl iodide as solvent on the singlet → triplet absorption of 1-chloronaphthalene illustrated in Figure 13 (190). The singlet → triplet absorption of α-chloronaphthalene alone, which extends into the violet region of the spectrum is so feeble that the liquid appears colorless and the bands are barely detectable in the long wave tail of the first singlet → singlet absorption band in the ultraviolet. Pure ethyl iodide is also colorless, but a mixture of one part of α-chloronaphthalene and two parts of ethyl iodide by volume is distinctly yellow. The spectrum in the violet shows a well-defined vibrational structure, similar in appearance and intensity to the singlet → triplet absorption spectrum of β-iodonaphthalene. There is no evidence of compound formation of the ordinary kind. The generality of this phenomenon has been well established.

The principal questions involve the nature of the mechanism responsible for the result. Part of the problem revolves around the fact that several different classes of molecules or atoms produce a similar effect.

The first mechanism proposed for the action of ethyl iodide involved an increase in the spin orbital coupling by magnetic perturbation by the iodine atom in the heavy atom effect on collision with the α-chloronaphthalene (190). Evidence, however, of the formation of weak charge-transfer complexes between haloaromatic compounds and propyl iodide (196) raises the possibility that such complexes may participate in the singlet → triplet enhancement. Considerable enhancement of singlet → triplet absorption bands of many aromatic, heterocyclic, acetylinic, and olefinic compounds (see Fig. 15) can be effected by introducing O_2 at high pressure, and at the same time stronger absorption bands appear at shorter wavelengths than the singlet → triplet bands, but at longer wavelengths than the normal bands of the organic molecule alone (11,194,198). These latter O_2-induced bands can be attributed to charge-transfer bands between the organic molecule as donor and the O_2 as acceptor (194,198). Perturbing molecules in the doublet state, as NO, as well as in the triplet state, as O_2, are effective in enhancing singlet → triplet absorption (198). It appears that in the enhancement of singlet → triplet absorption by O_2, the magnetic moment of the perturber exercises an insignificant effect, or one of minor importance (197,199). The effect principally

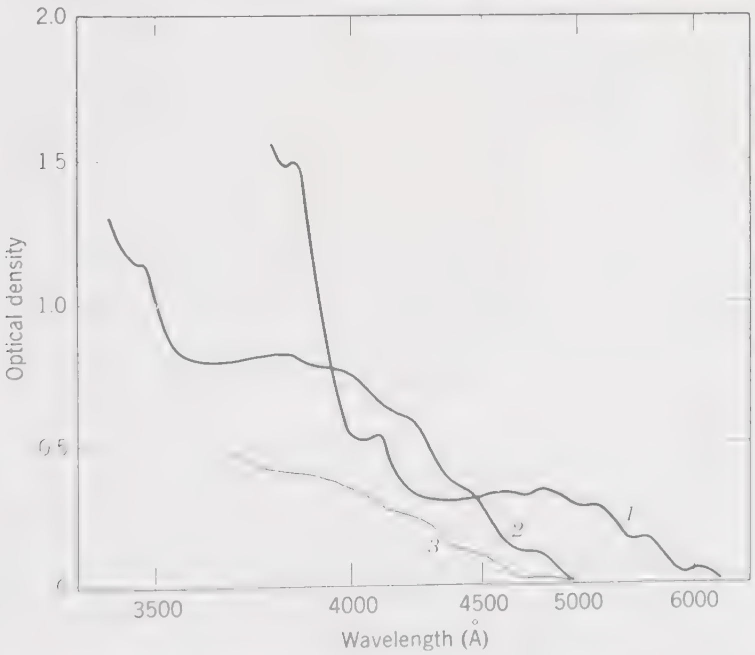

Fig. 15. Singlet → triplet absorption of (1) hexatriene and (2) butadiene in chloroform solutions with oxygen at 130 atm, and (3) butadiene in ethyl iodide solution (198).

depends on the formation of a charge-transfer complex between the O_2 and the organic molecule. The mixing between the singlet and triplet states that produces the increased absorption occurs through the mediation of a charge-transfer excited state. Interaction between a charge-transfer excited state and the triplet state of the organic molecule in the complex causes intensity to be borrowed by the singlet → triplet band from the charge-transfer band, the intensity of the latter coming at least partly from the strong singlet → singlet transition of the organic molecule. First-order perturbation theory shows that the dipole strength of charge-transfer transition has a finite value because electron exchange between the perturbing molecule and the organic molecule results in a nonvanishing exchange interaction between certain excited states (199). The dipole strength of the singlet → triplet transition depends on the magnitude of the exchange terms and the dipole strength of the singlet → singlet transition. According to these considerations the important factor in determining the singlet → triplet intensity is the electron exchange between the donor and the acceptor.

Nevertheless, enhancement of singlet → triplet absorption of 1-chloronaphthalene by xenon at pressures from 100–200 atm suggests that a true "heavy atom effect" may exist (200). The effects of ethyl iodide, oxygen, and xenon on the enhancement are compared in Figure 16. If the extinction coefficients of the chloronaphthalene are computed on the assumption that the absorption is to be wholly ascribed to a 1:1 complex, the relative effects of xenon:ethyl iodide:oxygen are approximately in the ratio 1:10:1000. It is quite possible that the enhancement caused by ethyl iodide and oxygen involves charge-transfer complexes with the aromatic molecule, as already described. It is doubtful that xenon could form a complex of sufficiently long life for an enhancement mediated by charge-transfer to be effective. The relatively small effect of xenon compared with those of ethyl iodide and oxygen may indicate the relative magnitude of a collision-induced heavy atom magnetic perturbation in contrast to the greater perturbation via charge transfer. If this is so, a small proportion of the observed effect of ethyl iodide must be attributed to the heavy atom effect and a pure magnetic component in the effect of oxygen is to be anticipated because of the paramagnetic nature of this molecule.

Several other examples of perturbation of the singlet → triplet transition exist. For example, enhancement of absorption occurs in the case of biacetyl when ethyl iodide is the solvent (195). No vibrational structure is seen. Also, ethyl iodide causes a notable enhancement in the case of *trans*-stilbene (201). Some vibrational structure does appear which is also noted when O_2 is the perturbing agent.

In conclusion, it is quite evident that it is highly probable that two mechanisms can operate—one involving charge-transfer states and the other

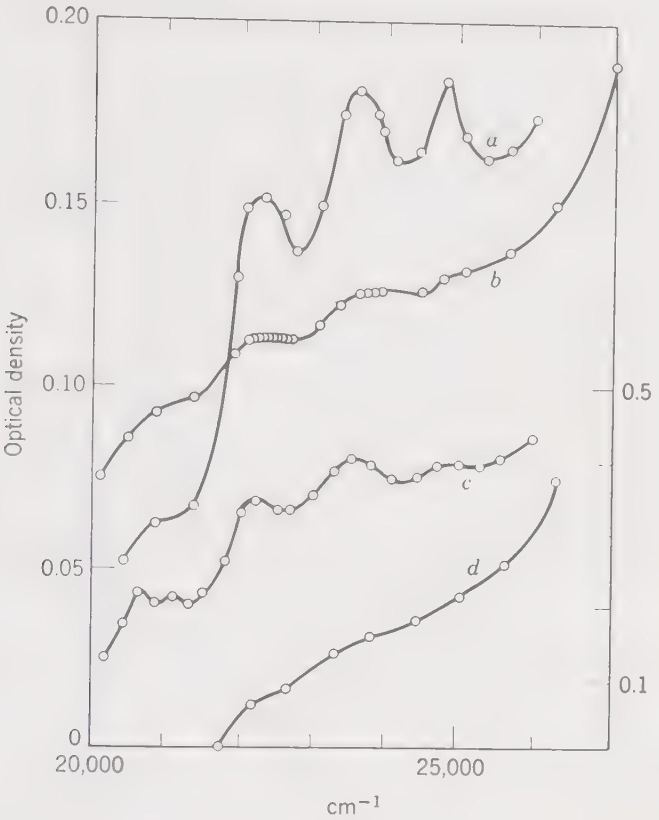

Fig. 16. Absorption spectra of 1-chloronaphthalene with different perturbing solvents (198): (*a*) 1-chloronaphthalene–ethyl iodide mixture; (*b*) 1-chloronaphthalene–xenon (143 atm); (*c*) 1-chloronaphthalene–oxygen (30 atm, optical density scale at right side of diagram); and (*d*) pure 1-chloronaphthalene.

a true magnetic effect. It is likely that both operate when alkyl halides are the perturbers. Also, it would appear that both probably operate when O_2 is the external perturbing agent. On the other hand, when Xe is the perturbing agent, the magnetic effect would appear to predominate. With alkyl halides or O_2 the magnetic effect is very probably of minor importance.

G. Triplet → Triplet Absorption

Triplet → triplet absorption can occur via excitation from the lowest triplet to the higher ones. This is observable in many cases because the lifetime of the lowest triplet is sufficiently long to allow for the existence of a reasonable concentration of molecules in this excited state.

The observation of triplet → triplet absorption is commonly accomplished by flashing a sample in fluid solution followed by scanning and recording

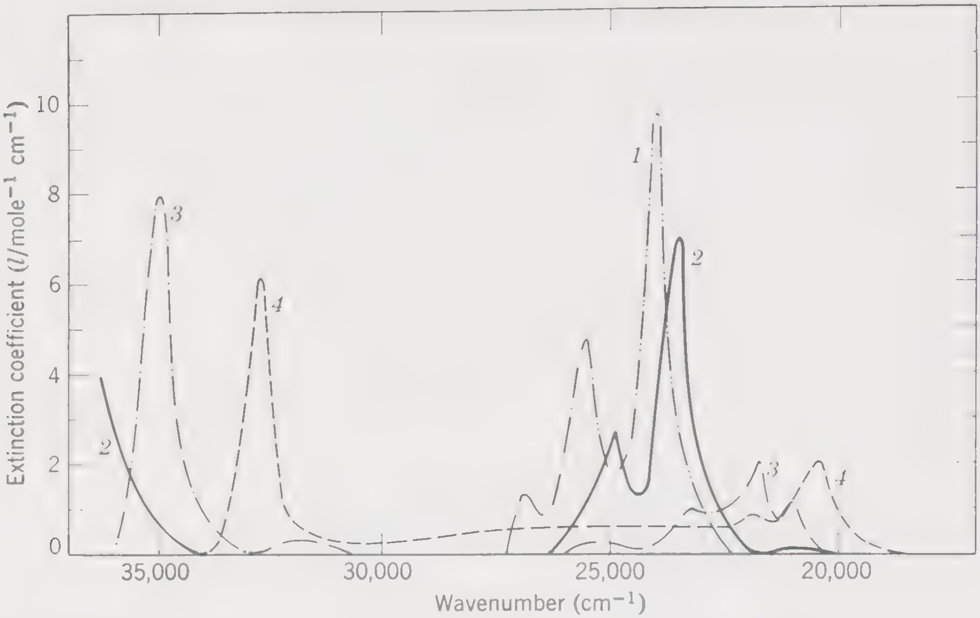

Fig. 17. Triplet–triplet absorption of (*1*) naphthalene; (*2*) anthracene; (*3*) naphthacene; and (*4*) pentacene (203).

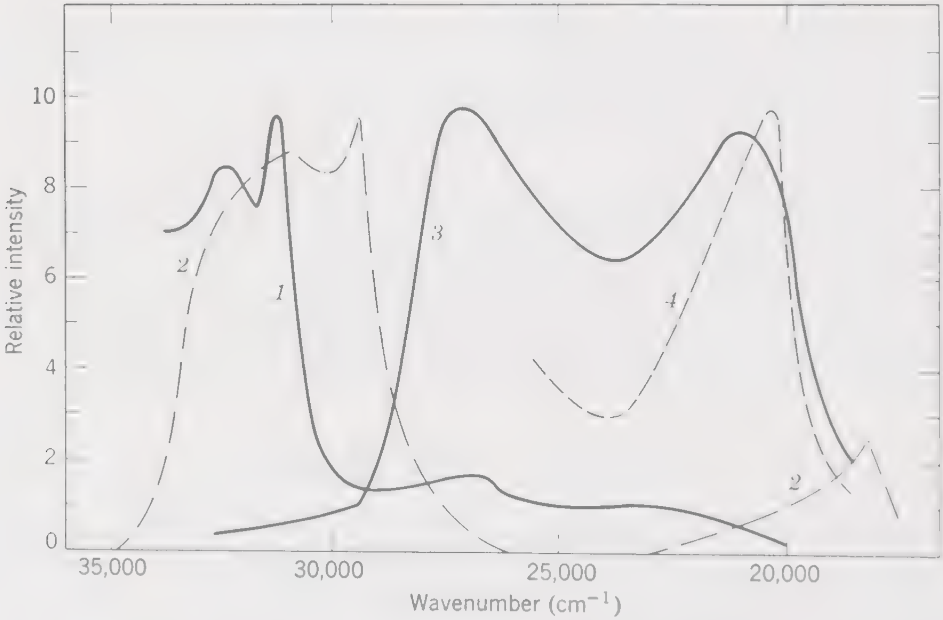

Fig. 18. Triplet–triplet spectra of (*1*) benzaldehyde; (*2*) benzophenone; (*3*) benzoin; and (*4*) benzil (203).

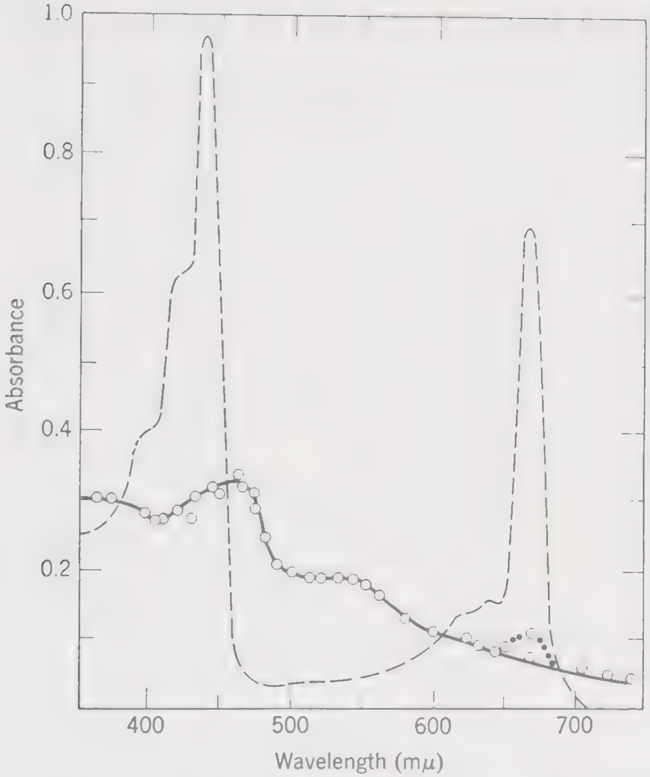

Fig. 19. Absorption spectra of chlorophyll *a*: singlet–singlet absorption (– – –) and triplet–triplet absorption (——) (202).

(202). The flash excitation method and its application to solutions permits observation of triplet → triplet spectral decay processes and chemical reactions of excited molecules. The technique can be used to study states having lifetimes longer than approximately 3×10^{-6} sec (202). Many molecules have been studied by this technique, including aromatic hydrocarbons, and their derivatives (203,204), porphyrins (205), chlorophylls (202,206,207), aldehydes and ketones (203,207), and dyes (206,208,209). In addition to the triplet → triplet absorption, the decay kinetics of the triplet state can be ascertained.

Some typical triplet → triplet absorption spectra are shown in Figures 17–20. In addition, Table XIV shows the location of excited triplet levels for some molecules determined by triplet → triplet absorption. Of course, the wavelengths of the absorption origins can be determined from the data in Table XIV. The maximum conversion to the triplet varies greatly, being as low as a few percent and as high as 95%. For the linear polyacenes, except benzene, there are two strong transitions which progressively move to longer wavelengths as the number of condensed rings increases (203). In several of

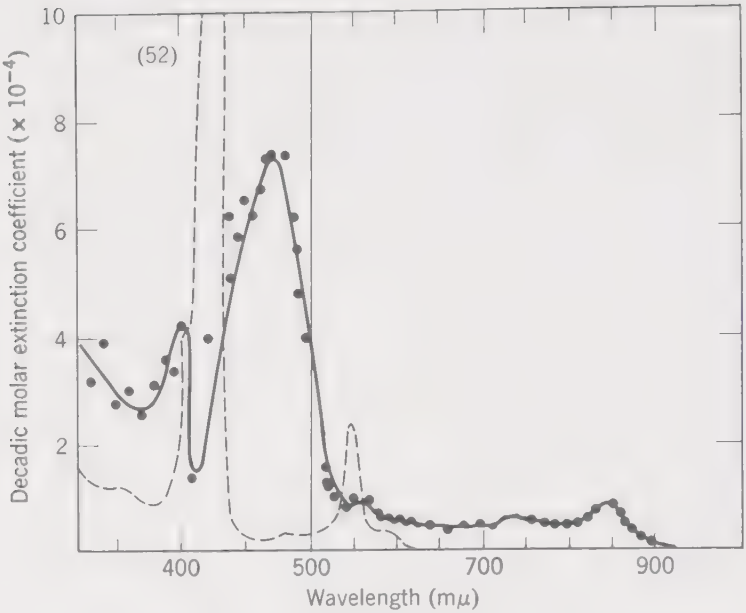

Fig. 20. Absorption spectra of zinc tetraphenylporphyrin: singlet–singlet (– – – –) and triplet–triplet (——) (205).

the hydrocarbons, other weaker transitions exist. The first strong transition (in the 17,000–27,000 cm^{-1} region) shows some vibrational structure (see Figure 17). The second strong transition is in the 33,600–38,000 cm^{-1} region. As was stated above, no triplet → triplet absorption has been found for benzene. Tentative assignments of the excited triplets of the strong transitions are $^3B_{1g}^-$ and $^3A_{1g}^-$, respectively, based on agreement with earlier intensity and energy predictions (209). The reasons for the observed absence of triplet–triplet absorption transitions in benzene in fluid solutions is not completely clear. However, the lifetime of the lowest triplet state in fluid solution (hexane) is at least as short as that of the lowest excited singlet state ($\sim 2 \times 10^{-8}$ sec) (209); therefore, the triplet state decays so rapidly that the concentration would be vanishingly small.

Other aromatic hydrocarbons also show triplet → triplet absorption (203). All of the tetracyclic aromatic hydrocarbons have two strong absorption regions similar to the linear hydrocarbons. Benz(*a*)anthracene seems to show the most marked vibrational structure, whereas chrysene and benzo(*c*)-phenanthrene show little. Also, the latter two differ from the others in that the lower energy strong transition is more intense than the higher energy one. The oscillator strengths of the transitions decrease as the number of "bends" in the structure increase. This is somewhat similar to the case of the normal singlet → singlet transitions. Higher hydrocarbons, such as dibenzanthracene and coronene, also show triplet → triplet transitions. Biphenyl and fluorene

TABLE XIV

Location of Some Excited Triplet States (cm^{-1}) (203)

Compound	T_0	T_1 (weak)	T_2 (strong)	T_3 (weak)	T_4 (strong)
Benzene	29,400	—	—	—	—
Naphthalene	21,300	—	45,400	—	59,800
Anthracene	14,700	36,070	38,280	—	50,400
Naphthacene	10,250	31,250	31,990	42,150	45,280
Pentacene	8000	27,000	28,400	34,000	40,790
Phenanthrene	21,600	40,830	42,390	—	—
Benz(*a*)anthracene	16,500	35,020	37,120	—	48,250
Chrysene	19,800	—	37,340	—	44,740
Benzo(*c*)phenanthrene	20,600	—	39,940	—	45,600
Triphenylene	23,800	—	47,160	—	52,700
Pyrene	16,800	36,050	40,840	—	44,560
Dibenz(*a*,*h*)anthracene	18,300	—	37,080	41,880	49,000
Perylene	12,600	—	33,090	—	48,300
Coronene	19,100	38,160	40,790	—	—
α-Chloronaphthalene	21,200	—	44,900	—	—
α-Hydroxynaphthalene	20,500	39,730	46,180	—	—
β-Bromonaphthalene	21,100	—	45,050	—	—
Benzaldehyde	25,200	48,500	56,450	—	—
Acetophenone	26,000	—	61,530	—	—
Benzophenone	24,400	42,750	53,900	—	—
Benzil	21,600	42,160	47,900	—	—
Benzoic acid	27,200	—	58,450	—	—
Diphenyl	22,800	—	49,930	—	—
Diacetyl	19,700	—	51,250	—	—

show one strong absorption in the 4000 Å region and fluorene has one additional weaker transition at longer wavelength.

Many derivatives of these hydrocarbons show triplet → triplet absorption (203). Alkyl, halo, hydroxy and amino derivatives of benzene show no such absorption. The only benzene derivatives that show triplet → triplet absorption are those containing a carbonyl group, such as benzaldehyde, acetophenone, benzoic acid, and benzamide. However, in the latter two cases the transitions are considerably weaker than in the other derivatives which show absorption. None of the spectra show much vibrational structure but benzaldehyde and benzophenone exhibit the most. Two aliphatic ketones, acetone, and biacetyl also show triplet → triplet absorption but with no structure.

Many derivatives of naphthalene and anthracene show triplet → triplet absorption (203). The lower energy strong transition (~4000–3300 Å) of many derivatives of naphthalene, for example, bromo, methyl, and hydroxy derivatives, look very similar to that of naphthalene. Other cases are quite similar except for some variation in wavelength or clarity of structure (sulfonic acid, ether, and chloro derivatives). In all cases, the intensities of the transitions are comparable. Particularly in 1-naphthol, a moderately strong longer wavelength transition occurs (~5000 Å). In a monochloro- and a dichloroanthracene, the band intensities are quite comparable and they occur at nearly the same position as in anthracene (~4350 Å).

Both chlorophylls *a* and *b* show triplet → triplet absorption (see Fig. 19 for chlorophyll *a*). The spectrum of chlorophyll *a* has less detailed structure than does that of chlorophyll *b*. The former has two maxima (~4620 and 5300 Å) and the latter has five maxima (~3800, 4450, 4850, 5500, and 6050 Å). The strongest occur at 4620 and 4850 Å, respectively (202). The absorption continues to about 8000 Å and then decreases to a flat low value to about 10,000 Å (205). Tetraphenylporphyrin shows four maxima (~3900, 4300, 6900, and 7800 Å, see Fig. 20). The Zn derivative also shows four maxima which are all red-shifted relative to the parent porphyrin (see Fig. 20) (205). In a general way, the absorption spectra of Zn protoporphyrin and Mg phthalocyanine bear a resemblance to those of the chlorophylls (206). That is, a strong blue band (similar to the strong blue or Soret band of the singlet → singlet transition) exists and absorption continues to the red with some band structure. In general, however, the porphyrins show lower triplet → triplet absorption in the yellow-green region than do the chlorophylls. Also, the infrared band in the porphyrins is more distinctive than in the chlorophylls. No triplet → triplet absorption occurs for the divalent transition metal complexes of porphyrins (Cu^{2+}, Fe^{2+}, Co^{2+}, Ni^{2+}) or chlorophylls (Cu^{2+}) (205,206). This is most likely attributable to the short lifetime of the triplet state (82,83) with accompanying low triplet concentration and therefore, vanishingly small absorption.

Several dyes exhibit triplet → triplet absorption spectra (207,208). Retinene, a *p*-toluidene complex of retinene, rhodopsin (207), and acridine orange (208) show absorption. Retinene has one very strong band ($\epsilon \sim 80{,}000$) with a maximum at approximately 4500 Å. The singlet singlet maximum is about one-half as intense and is at shorter wavelengths (~3750 Å). The *p*-toluidene complex shows a strong maximum ($\epsilon \sim 45{,}000$) to the green of retinene (at ~5000 Å) and a minor maximum (~3500 Å) (207). In retinene, the amount of conversion to the triplet state varies with the solvent, being as low as 1.7% and as high as 11% (in this case the conversion is equivalent to quantum yield defined as percent triplet formed from the excited singlet) (207). Acridine orange shows a strong triplet → triplet absorption band and some further absorption whose shape and wavelength depend on the solvent (208). In acidic solvents, acridine orange has a strong band near 4900 Å with additional rather undefined absorption extending toward 3500 and 10,000 Å. In basic solvents, a slightly weaker maximum occurs near 4300 Å, with absorption extending to the wavelengths previously noted. In addition rather clear but significantly weaker maxima occur near 5800 and 3600 Å.

Finally, it appears that molecules such as β-carotene, p-benzoquinone, and p-nitroaniline do not show triplet → triplet absorption.

H. Effect of External Perturbations on Characteristics of the Triplet

In this section we shall be particularly concerned with effects of external heavy metal ions and certain solvents on the lifetime of the triplet state, as determined by the flash–excitation method.

This method permits the study of quenching of triplet states in fluid solution in contrast to the highly viscous or rigid media necessary for the observation of phosphorescence. In Section III-G it was stated that triplet → triplet absorption was absent in transition metal complexes of porphyrins and chlorophylls. This lack of absorption was attributed to the expected short lifetime of the triplet because of high spin–orbit coupling. The lifetimes of the triplet states of anthracene and chlorophylls vary significantly in the presence of quenchers. They are notably shortened in the presence of *external* Ni^{2+}, Co^{2+}, and Cu^{2+} ions, but other ions such as Mn^{2+} and Nd^{2+} have only minor effect (202). From lifetime data, it is possible to evaluate bimolecular quenching constants involving the molecule in the triplet excited state and the quenching metal ions (205). In the case of anthracene, the quenching constants for Cu^{2+}, Cr^{3+}, Ni^{2+}, and Co^{2+} are in the neighborhood of 10^8 l mole^{-1} sec^{-1}. For the porphyrins, the values are smaller, except for Cu^{2+}. The quenching constant for Ni^{2+} on the triplet state of the zinc complex of tetraphenyl porphyrin in pyridine solution is the same as for the uncomplexed porphyrin.

The Mn^{2+} ion quenches less than other transition metal ions and particularly less than the Cu^{2+} ion, approximately 100–200 times less, depending on the solvent. Rare–earth ions are weaker quenching agents than Mn^{2+}, not only for anthracene but also for the porphyrins and chlorophylls. The addition of water to tetrahydrofuran causes a particularly marked decrease in the quenching constant for Ni^{2+}, Cr^{3+}, and Co^{2+} which levels off with increasing concentration of water. Addition of water to pyridine solutions has less effect. In aqueous solution, potassium iodide is comparable to the more effective transition metals as a quencher of the triplet state but Zn^{2+} ion has no effect.

The near absence of quenching effects by Gd^{3+} and Mn^{2+}, both of which have high spin magnetic moments, shows that the quenching by Ni^{2+}, Cr^{3+}, and Cu^{2+} is not caused by simple magnetic perturbation. Further evidence for this conclusion comes from observations on the quenching of the fluorescence of β-naphthalene sulfonic acid by various transition and rare earth ions (205). The quenching appears to involve a charge-transfer intermediate formed from the triplet molecule and the quenching ion. The potential energy curve of the ionic charge-transfer complex is assumed to cross that of the ground state metal ion–organic molecule complex; therefore, internal conversion from the excited to the ground state is probable. An alternative mechanism involves the decomposition of the charge-transfer complex to a pair of one-electron oxidation–reduction products which then return to the initial state by relatively slow back reactions.

Further evidence for the existence of an intermediate charge-transfer complex in quenching by metal ions comes from quenching data on the anthracene triplet (210). In the quenching of the anthracene triplet by cupric chloride, the value in pyridine solution of the bimolecular quenching constant k in the equation $-dC^*/dt = kC^*Q$ (where C^* is the concentration of triplet anthracene and Q is that of the quencher) is intermediate between those in ethylene diamine and in *o*-phenanthroline solution. The differences in rate of quenching reflect the effect on the quenching ion of replacing pyridine in the $CuCl_2 \cdot 2$-pyridine complex by the other ligands with the ethylene diamine complex showing the lowest quenching constant. Known charge-transfer reactions involving reduction of inorganic ions by a given reducing ion solvated in different ways show marked differences in rate with the nature of the solvate. The effects parallel those observed in triplet quenching, suggesting the participation of a charge-transfer intermediate in the quenching process.

A different quenching mechanism involves energy transfer upon collision of the type (211,212):

$$\mathrm{M}^*(T) + \mathrm{Q(multiplet)} \rightarrow \mathrm{M}(S) + \mathrm{Q(multiplet)} \qquad (32)$$

where $\mathrm{M}^*(T)$ and $\mathrm{M}(S)$ are the donor or quenchable molecules in their excited triplet and ground state singlet respectively and Q is the quencher molecule. When the triplet energy level of the quencher (acceptor) is significantly lower than that of the donor, the energy transfer is diffusion controlled and apparently no long range transfer occurs. When the triplet state energy levels are similar, the energy transfer is less likely. If the triplet level of the quencher molecule is higher than that of the donor no quenching occurs. These results are reflected in the quenching rate constants. This mechanism should result in excitation of the quencher triplet and thus, triplet → triplet absorption should be observable in the quencher or acceptor molecule. This can be observed in many cases where acceptors are normally a hydrocarbon or halo derivative and the donors are hydrocarbons or their halo derivatives and ketones (212). It is interesting that quenching of hydrocarbon triplets by hydrocarbon quenchers apparently does not require an intermediate complex to be formed (212).

For comparable quenchers (paramagnetic ions) acting on aromatic hydrocarbons, there does appear to be a difference in concept regarding the mechanism of quenching (for one mechanism see earlier discussion in this section). Another mechanism involves the general process as given in equation 32 where the multiplicity change may occur without either energy transfer or other change in the quencher molecule (211). This process is independent of the magnetic susceptibility of the quencher (providing it is not of singlet character). Two major groups would exist. One is that in which a relatively stable collision complex (with quenchers as O_2, NO, and aromatic triplets) is formed, followed by dissociation into products with altered spin and for which there is a statistical probability for the overall process. The other is one in which the energy of the complex with respect to reactants is small compared with kT energy. The difference in quenching rates will depend on the life of the collision complex and the strength of the spin–spin interaction. Well-shielded electrons of quencher ions would be expected to interact less with electrons of the excited molecule. Therefore, a combination of these factors could account for the observed variable quenching rates (of metal ions of the first transition series and ions of the lanthanides). It is true that in the two major mechanisms, a complex of some sort is postulated. The problem of characterizing it may be largely only a semantic one. The details of the language used to describe the ultimate fate of the complex differ but the difference does not appear to be serious.

The one consideration that may have to be resolved is the fact that quenching rates for diamagnetic quenchers can be comparable to those with unpaired electrons (213). This could presumably be explained by energy transfer involving

$$\mathrm{M}^*(T) + \mathrm{Q}(S) \rightarrow \mathrm{M}(S) + \mathrm{Q}(T) \tag{33}$$

as discussed above (Eq. 32) (212). Thus, it would appear likely that at least two principal mechanisms operate, depending upon the nature of the quencher. The only real problem is whether the particular mechanism as represented by Eq. 33 involves a complex (205) or does not involve a complex (211).

Another large area of concern is the perturbation effects of solvents containing a heavy atom. The lifetimes of certain phthalimides is generally lower in propyl bromide than in any other of about 20 solvents (214). Several other molecules appear to have both their lifetime and intensity of phosphorescence modified by a solvent system containing a heavy atom (215). For example, a series of dinitronaphthalenes show an increase in intensity and a decrease in lifetime of phosphorescence when the solvent is a mixture of an alcohol and 20% ethyl iodide, compared with the values in the pure alcohols at 77 K. A similar phenomenon occurs for *N*,*N*-dimethyl-4-nitroaniline, coumarin, and acid fluorescein (215). It is probable that this effect is real although the lifetimes of at least certain phthalimides undergoes a large variation depending on the solvent (214). Also it is interesting that the lifetimes of all the cases mentioned above in the ethyl iodide solvent system are about the same (0.005–0.008 sec). This is somewhat puzzling.

A series of 1-monohalonaphthalenes in various propyl halide solvents (cracked glasses) exhibit notable differences (196) in lifetime (see Table XV). The lifetimes are given as first observable because of the nonexponential nature of the decay in the cracked glass systems (146). The decrease in lifetime produced by substitution of chlorine on naphthalene is less than that produced by the external perturbation of napththalene by iodine (as propyl iodide). In addition, the heavier the halogen of the halide, the shorter is the lifetime of the halonaphthalene. These data provide good evidence for a true heavy atom perturbation. This would be an additional perturbation to that proposed in terms of charge-transfer mixing of the singlet and triplet states of the aromatic hydrocarbon by the alkyl iodide–hydrocarbon complex (197). The effect of various alkyl halides on the singlet → triplet absorption intensity is also in harmony with the low temperature lifetime data. This is further support for the proposition that a heavy atom effect is operative in addition to the charge-transfer mixing (196).

Considerable care must be exercised in relating changes with the nature of the heavy atom in an external perturbing solvent. The nonexponential nature of the decay curves indicate the nonuniformity of the various regions of the glasses. Further, the different halides may modify the density and geometry characteristics of the glassy matrix. If the mechanism of external spin–orbit coupling is of the electron exchange types, the latter have exponential dependency on internuclear distances. Thus, for example, factors other than atomic number must be considered. Furthermore, the relative effect of an external heavy atom perturbation on the rate constants of triplet emission (k_P) and internal conversion (k_P^{IC}) is $k_P > k_P^{\mathrm{IC}}$ (152a). Further, the effect on k_P^{IC} compared with the intersystem crossing rate constant (k_{IS}) is not clear because of the lack of quantitative data (152a).

TABLE XV

First Observable Lifetimes of Some Compounds in Different Solvents (196)

Compound	EPA	Propyl-chloride	Propyl-bromide	Propyl-iodide
Np	2.6 sec	0.52 sec	0.14 sec	0.076 sec
1-FNp	1.4	0.17	0.10	0.029
1-ClNp	0.23	0.075	0.059	0.023
1-BrNp	0.014	0.0073	0.0069	0.0063
1-INp	0.0023	0.0014	0.0012	0.009

Another type of external perturbing agent is a solid matrix of a rare gas such as argon, krypton, or xenon (149). In the case of benzene, the lifetime of phosphorescence in CH$_4$, Ar, Kr, and Xe (at 4.2°K) is 16, 16, 1, and 0.07 sec, respectively. The phosphorescence in Kr and Xe shows a strong band near 29,500 cm^{-1} which is probably the 0–0 band. This band is either weak or absent in the other matrices (lower atomic or molecular weight solvents) and other intensity differences exist between the matrices. Further, the quantum yield ratio of fluorescence: phosphorescence is effectively zero in Ar, Kr, and Xe but above one in the methane. The result for perdeuterated benzene in the same matrices is quite parallel to that in benzene itself. The external perturbation produced by CH$_4$ and Ar appears to be relatively small while for Kr and Xe, it is larger than the intramolecular one. The spectrum in Ar or CH$_4$ would be that resulting from *lack* of external perturbation. It has been suggested that the intramolecular phosphorescence mechanism is highly vibrationally induced (148,150). The behavior of the 0–0 band and the effect of deuteration (see Section III-C-1) in the two sets of matrices support this view (150).

I. Intermolecular Energy Transfer and Photochemistry

The variety of molecules and systems studied involving energy transfer and photochemistry is extremely large. Only certain examples will be discussed in order to illustrate certain points of interest involving triplet states. The triplet states of many molecules can be occupied in high yields as for example those of benzene 18% (216), anthracene 13% (216), triphenylene 95% (216a), and benzophenone 100% (216a). Of course, these will vary under specific conditions. Also, in other cases, higher as well as lower quantum efficiency of occupation are possible.

1. AROMATIC HYDROCARBONS

Among the hydrocarbons, anthracene is probably one of the best understood. If anthracene solutions are irradiated in the absence of oxygen, the product is dianthracene. However, if oxygen is present, the product is the bridged peroxide. Further, the irradiation of anthracene in CCl$_4$ gives detectable quantities of the 9-chloro and 9,10-dichloro derivatives (217). Flash photolysis studies show that anthracene in the triplet state is deactivated by reaction with oxygen at nearly every encounter. This reaction with oxygen does not occur with unexcited anthracene. Photodimerization results when anthracene is in its excited singlet state while the oxidation (to the peroxide) occurs when anthracene is in the triplet state. Other linear polyacenes, such as naphthacene, also exhibit peroxide formation parallel to that for anthracene. The reactions indicate some charge localization in the 9 and 10 position in the triplet state, which could be viewed in this case as a classical biradical corresponding to a spectroscopic triplet. However, it should be noted that this classical picture is not a complete or accurate description and should not be taken as a general relation.

Anthracene photooxidation occurs fastest in carbon disulfide. The exact reason for this is not known but it appears that some sort of energy transfer occurs which facilitates the formation of anthracene triplets (217). Further, the nature of a substitution and solvent play important roles which may alter the role of any one process. For example, in 9,10-diphenylanthracene, the quantum yield of photooxidation depends both on the oxygen and hydrocarbon concentration (218) while for anthracene itself, the yield is quite independent of the oxygen concentration. This plus data on the fluorescence yield and lack of dimerization in systems without oxygen indicate that the phenyl substituents prevent solvent interactions because of steric reasons. This is further supported by the fact that heavy atom-containing solvents enhance the rate of photooxidation. Therefore, a likely mechanism involves an increased singlet–triplet conversion by oxygen perturbation which always results in photooxidation (217). Finally, the amount of quenching by oxygen and the amount of peroxide formed are quite parallel in benzene and some of its derivatives (219). However, this is not true for anthracene. At low concentrations, 9-methylanthracene shows a considerably higher quantum yield of fluorescence in the absence of oxygen than with the oxygen present although the quantity of peroxide formed (in the presence of the oxygen) is extremely small (220). Thus, oxygen is quenching fluorescence although the expected chemical reaction does not occur.

2. CARBONYLS

Another important type of molecule participating in photochemistry is that containing the carbonyl group. Here we shall be concerned with *inter*molecular triplet–triplet energy transfer. This does not mean that such transfers are excluded for hydrocarbons. For example in Section III-H, it was noted that quenching of a hydrocarbon triplet could be accomplished by other hydrocarbons or their derivatives and that this involved triplet–triplet energy transfer. In fact in this same section (III-H), reference is also made to ketones. However, it seems more appropriate to stress them here.

a. Energy Transfer. The earliest observation on triplet–triplet energy transfer principally involved aldehyde or ketone donors and hydrocarbons or their derivatives as acceptors (221). When benzaldehyde and naphthalene are in a rigid glass solution at 77°K, irradiation at a wavelength where the absorption of napthahalene is nonexistent still results in phosphorescence of naphthalene. The irradiation is in a region where the aldehyde does have absorption. Napththalene alone irradiated at the same wavelengths does not emit phosphorescence. The mechanism involves excitation of the donor (benzaldehyde) triplet with subsequent sensitization of the acceptor (naphthalene) triplet followed by phosphorescence emission of the acceptor. The process cannot occur by the trivial mechanism of emission reabsorption since the acceptor has no absorption in the region of the donor emission. Further, it would be expected that the mean lifetime of phosphorescence of the donor would be shortened by virtue of the radiationless transfer to an acceptor. This is true for many combinations of sensitizers and acceptors. In addition, in some cases, the quantum yield of emission of the acceptor is greater by sensitization than by direct excitation. The relative probability of transfer from donors to acceptors varies. For example, for the benzophenone–naphthalene system the relative probability is 0.75 while for carbazole–naphthalene, it is 2.3 (221).

Another method for detecting triplet energy transfer involves the observation of triplet → triplet absorption of the acceptor molecule (222). For example, a mixture of benzophenone–naphthalene or biacetyl–benz(*a*)-anthracene when flashed in the region of the donors only (the ketones) results in the observation of triplet → triplet absorption of the acceptors. In addition, no fluorescence of the acceptors is noted, thus proving that the formation of the triplet state of the acceptor does not occur via its singlet state. Moreover, both by this procedure and the one just previously discussed, triplet energy transfer does not occur if the acceptor triplet level lies above that of the donor triplet. The energy transfer process can be represented as

$$D^*(\text{triplet}) + A(\text{singlet}) \rightarrow D(\text{singlet}) + A^*(\text{triplet})$$

where D and A represent donor and acceptor respectively. Experimental evidence indicates the mechanism for energy transfer is best explained by an exchange interaction involving overlap of electron charge clouds.

Considerable interest regarding triplet energy transfer centers around the benzene-biacetyl system. In this case, benzene is the donor and biacetyl is the acceptor. A number of molecules which have triplet states higher than that of biacetyl sensitize the phosphorescence of biacetyl in solution (223). It is also possible to sensitize biacetyl *fluorescence* with benzene in solution (224). Further, benzene sensitizes biacetyl phosphorescence in the gas phase giving a moderate increase in the quantum yield ratio of phosphorescence to fluorescence (225,226). In fluid solution, however, it is found that benzene does not sensitize the phosphorescence of biacetyl (227). The similarity of the phosphorescence quantum yield in solution, vapor, and rigid media suggests that the yield of triplet should be comparable in these phases. Also, since the phosphorescence of biacetyl can be sensitized in a rigid medium it would seem likely that the energy transfer process would occur in fluid solution at almost each collision. Thus, it appears that the most likely explanation is that the lifetime of the benzene triplet is very short and comparable to that of the singlet ($\sim 2 \times 10^{-8}$ sec). However, other information based primarily on the concentration dependence of the intensity ratio of biacetyl phosphorescence to benzene fluorescence (instead of biacetyl fluorescence which would be the usual case, for example see references 224 and 225), indicates some triplet transfer from benzene to biacetyl does occur (228). With one assumption, the lower limit of lifetime of the triplet benzene is estimated to be $\sim 10^{-6}$ sec. The difference in these results likely resides in the inherent difference in sensitivity of the methods.

Finally, triplet energy transfer can occur in plastics at room temperature as well as at low temperature (77°K). The results on the lifetime of decay of naphthalene at various concentrations and in the presence of benzophenone apparently rule out the formation of donor–acceptor complexes. However, the results do not support or refute the fact that the mechanism of transfer is by exchange interactions.

b. Photochemistry. Since the early observations of photochemical activity of benzophenone–alcohol systems exposed to sunlight (230), a vast literature has accumulated on the photochemistry of systems containing benzophenone and other ketones and aldehydes, such as biacetyl or benzaldehyde. In this section we shall review some of the salient points in the modern photochemical discussion of these reactions. We will only be concerned with some of the reactions involving ketones and aldehydes.

One of the interesting problems is the photochemistry of benzophenone in various alcohols in the *absence* of oxygen. The first concern will be with the primary photochemical steps:

$$\Phi_2CO + h\nu \rightarrow \Phi_2CO^* \tag{34}$$

$$\Phi_2CO^* + RH \rightarrow \Phi_2COH\cdot + R\cdot \tag{35}$$

The points to be considered are the nature of the excited state of benzophenone and the proof of the existence of the ketyl radical. Flash photolysis experiments on benzophenone confirm that the transient produced is the ketyl radical (231). The initial photochemical reactions of benzophenone could be the following (231):

$$\Phi_2CO + h\nu \rightarrow \Phi_2CO^* \quad (S, \text{singlet}) \tag{36}$$

$$\Phi_2CO^*(S) \rightarrow \Phi_2CO^* \quad (T, \text{triplet}) \tag{37}$$

$$\Phi_2CO^*(T) \rightarrow \Phi_2CO \tag{38}$$

$$\Phi_2CO^*(S) + RH \rightarrow \Phi_2COH\cdot + R\cdot \tag{39}$$

$$\Phi_2CO^*(T) + RH \rightarrow \Phi_2COH\cdot + R\cdot \tag{40}$$

The important question to resolve is whether reaction 39 or 40 is the correct one. It is known that naphthalene can quench the triplet state of benzophenone (212). When benzophenone is flashed in the presence of naphthalene ($\sim 10^{-3}M$) no ketyl radical is detected. Also, benzophenone, when irradiated in the presence of naphthalene in isopropyl alcohol does not produce any benzopinacol. It thus appears quite certain that reaction 39 is unimportant and that the important spectroscopic state is the triplet in the primary photochemical steps (reactions 34 and 35).

The next problem concerns the following steps that lead to the product benzopinacol. It appears that ketyl radicals dimerize to give the benzopinacol. The detailed behavior of the reaction appears to depend on the degree of absence of oxygen. That is, if air is excluded during the reaction (except for that initially present in the reaction vessel), the reaction in isopropyl alcohol proceeds as follows (232):

$$\Phi_2CO^* + Me_2CHOH \rightarrow \Phi_2COH\cdot + Me_2COH\cdot \tag{41}$$

$$Me_2COH\cdot + \Phi_2CO \rightarrow \Phi_2COH\cdot + Me_2CO \tag{42}$$

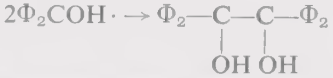

$$2\Phi_2COH\cdot \rightarrow \Phi_2\underset{\displaystyle OH}{\overset{}{C}}-\underset{\displaystyle OH}{\overset{}{C}}-\Phi_2 \tag{43}$$

In systems containing some initial residual oxygen and irradiated with low intensity light, the quantum yield is reduced to about one-half. The quantum yield for benzopinacol is 0.93 at 3660 Å (at high intensity) in oxygen-free solutions. The quantum yield for acetone is 0.92 at 3660 Å and 0.99 at 3130 Å and is independent of the quantity of oxygen in solution. If oxygen is "totally absent," then the detailed reaction mechanism appears to require an intermediate of the type $\Phi_2COHOC\Phi_2\cdot$ which forms a dimer which then splits to produce benzopinacol and two benzophenone molecules (232). If oxygen is present during the reaction, the yield of benzopinacol is reduced to zero even though the yield of acetone is not reduced. In addition, hydrogen peroxide is produced and benzophenone is not consumed in the reaction. Mechanisms for the reaction have been suggested (232).

Biacetyl also undergoes photochemical reaction in hexane containing oxygen (233). The reaction appears to produce acetic acid. The mechanism presumably involves the triplet state of biacetyl reacting with the solvent by hydrogen extraction to produce a radical which then reacts with oxygen to form a peroxide. Following this, hydrogen extraction from the solvent occurs giving a product which splits to give two molecules of acetic acid. The triplet state of biacetyl is quenched by a photochemical reaction involving hydrogen abstraction from such molecules as primary and secondary amines, phenols, and aldehydes as well as alcohols (234).

A considerable number of other reactions utilizing benzophenone as a sensitizer are known. Ethyl pyruvate can undergo photochemical decomposition to acetaldehyde, carbon monoxide, and a small amount of carbon dioxide. In the presence of benzophenone as a sensitizer, the same products result but the quantum yield is higher (235). The decomposition of diazomethane is photosensitized by benzophenone to give triplet methylene radical. The addition of this to cyclohexene gives products which differ primarily in the relative quantities formed compared to those formed by the addition of singlet methylene (formed by direct irradiation of diazomethane). Further, many carbonyl molecules, including benzophenone, acetone, biacetyl, and naphthaldehyde, have been examined as photosensitizers for *cis-trans* isomerization (236). Energy transfer occurs at nearly every collision between a triplet and acceptor molecule if the transfer is exothermic (triplet of acceptor below that of donor). For example, 9-anthraldehyde (low lying triplet) will *not* isomerize *cis*-piperylene while biacetyl will.

Of a large number of substituted benzophenones irradiated in an alcohol, some can be photoreduced to pinacols and some cannot (172). For example, *m*- and *p*-methyl, *o*-, *m*-, *p*-chloro-, *o*,*p*-dimethoxy-, and *p*-methoxybenzophenones give pinacols while nitro-*o*-hydroxy-*p*-methoxy-, *o*-amino-, *p*,*p*′-bis-(dimethylamino), *o*,*p*-dihydroxy benzophenones give no (or very low quantum yields of) pinacols. In certain cases, such as the *o*-amino, hydroxy, or methyl derivatives, it appears that upon irradiation photoenolization occurs. This may be responsible, at least in part, for the lack of reactivity since the enols are apparently not photoreducible to the pinacol. If the above groups are replaced by methoxy or carboxy groups, the *inter*molecular hydrogen abstraction capability is restored and photoreduction can occur. Although this may account for the results in some cases, it is probably not a satisfactory explanation for the behavior of such molecules as *p*-amino- and *p*,*p*′-bis-(dimethylamino)benzophenone. In these cases it is postulated that the lowest triplet state is not of n,π^* character but of π,π^* type. Presumably, the difference in charge distribution in these cases would be such that the diradical type distribution expected for the n,π^* triplet state would not exist and the chemical reactivity of the oxygen site (to extract hydrogen) would be absent. Other evidence based on racemization involving aldehydes and ketones and optically active alcohols, indicates that certain ones of the ketonic sensitizers do not give racemization (173). In one case, β-acetophenone, it is presumed that the phosphorescence has its origin from a π,π^* triplet (237). It is generally thought that the unreactive group of ketones and aldehydes have lowest π,π^* triplet states (173). Certain anthraquinones undergo photochemical reaction (1-chloro and 1,5-dichloro) while others do not (1,8-; 1,5-; 1,4-dihydroxy). It is probable or possible that either or both photoenolization and the nature of the triplets are responsible for the results.

3. MISCELLANEOUS

In this part we shall consider some further examples in order to show the breadth of interest in the subject of photochemistry.

A unique approach involves irradiation into the multiplicity forbidden $S \rightarrow T$ absorption band. For example, if the system benzene-nitric oxide is excited with light in the 2900–3400 Å region, both *o*-nitrophenol and 2,4-dinitrophenol are formed (238). The quantum yield of each of these products is about ~0.012 when the mixed system is irradiated with light of 3130 Å. Also, if dry benzene with oxygen at 100 atm is irradiated in the same regions as above, phenol and probably *o*-benzoquinone are produced. The quantum yield of phenol is approximately 0.03. In each case it appears that the benzene is excited to the triplet and reacts with the O_2 or NO in the ground state.

There are quite a few examples of photochemically induced *cis-trans* isomerizations such as that of *p*-dimethylaminocinnamic acid nitrile (p-$(CH_3)_2N—C_6H_4—CH{=}CH—CN$). The *cis* and the *trans* forms are interconvertible and the sum of the quantum efficiencies is unity (239). It is postulated that in both cases the intermediate state is a triplet of very short lifetime.

The photoisomerization mechanism for the conversion of *trans*-stilbene to its *cis* form and that suggested for certain of its derivatives are not simple (240). There is strong evidence for the fact that stilbene does not directly isomerize in the lowest excited singlet state or in the lowest excited triplet state. Apparently there are two paths for isomerization—one of which has a small activation energy and the other involving a singlet to excited triplet crossing. The latter involves those stilbenes with heavy atom substituents. It would appear that the crossing is not to the lowest triplet but to a higher one which still lies at or below the first excited singlet (240).

J. Additional Topics

1. PHYSICAL CHEMISTRY OF THE LOWEST EXCITED TRIPLET STATE

The general discussion will center around the pK values of a number of molecules in the lowest excited triplet state. In particular we shall be concerned with the pK_a values of a number of organic acids and bases. In Section II-J, the general basis for the determination of pK values of excited states was given. In the particular case of the determination of the pK for a triplet state, the ΔE and $\Delta E'$ values are determined differently than for the case of a singlet state. Here the ΔE and $\Delta E'$ represent the difference in energy between the lowest triplet and ground state of the acid and conjugate base respectively (241). These can be determined from the location of the 0–0 band of the phosphorescence of the two forms (or short wavelength limit). From the known pK_a of the ground state, the pK_a of the triplet can be determined from (241)

$$\mathrm{p}K_a{}^{\mathrm{G}} - \mathrm{p}K_a{}^{\mathrm{T}} = \frac{\Delta E_{\mathrm{HA}} - \Delta E_{\mathrm{A}}}{2.303RT} \qquad (44)$$

TABLE XVI

pK_a Values in Various Electronic States[a] (241,122,123)

Molecule	pK_a^{G}	pK_a^{T}		p$K_a^{\mathrm{S}_1}$
Acridine	5.5	5.6[b]	—[b]	10.6
Quinoline	5.1	6.0	5.8	—
2-Naphthylamine	4.1	3.3	3.1	−2
N,*N*-Dimethyl-1-naphthylamine	4.9	2.7	2.9	—
Phenol	10	—	8.5[c]	4.0[c]
p-Methylphenol	10.3	—	8.6[c]	−4.3[c]
p-Chlorophenol	9.4	—	8.0[c]	3.2[c]
2-Naphthol	9.5	8.1	7.7	3.1
2-Naphthoic acid	3.7	4.0	4.2	10–12
1-Naphthoic acid	3.7	3.8	4.6	10–12
o-Phenanthroline	4.85	6.7	6.7	—
o-Phenanthroline-H$^+$	−1.4	−3.8	−3.8	—

[a] G is ground singlet state, S_1 is first excited singlet state, and T is lowest triplet state.

[b] Third column from flash photolysis data and fourth column from phosphorescence data.

[c] E. Wehry and L. Rogers, *J. Am. Chem. Soc.*, **81**, 4234 (1965)

where superscript G and T refer to the ground and triplet states, and the subscripts HA and A refer to the acid and conjugate base, respectively. Table XVI gives some pK_a values for both the excited singlet and triplet states. From the data in Table XVI it is worth noting that the pK_a in the triplet state is similar to that of the ground state while the pK_a for the excited singlet is considerably different from that of the ground state (~ 4 to ~ 10). The *o*-phenanthrolene molecule shows the greatest difference in the pK_a of the ground and triplet states (~ 2) (122) while *p*-chlorophenol shows the greatest difference between the excited singlet and ground states (123).

It should also be noted that pK_a values of the triplet state can be determined by direct observation of the triplet → triplet absorption spectra of the acid and conjugate base (241).

2. ENHANCEMENT OF PHOSPHORESCENCE BY AGGREGATION AND MOLECULAR EXCITONS

Although it is beyond the scope of this book to deal with the details of exciton theory, certain aspects of it are important. In particular, we shall only be concerned with exciton theory relative to its application to molecular aggregates and deductions pertinent to enhancement of phosphorescence. For details, the excellent works of Kasha (242,243), McRae (242,244), and

Simpson et al. (245) should be consulted; see also Chapter II, page 312. Consider an aggregate of molecules in which an excited electron is strongly bound to a specific molecular center. As a beginning point, the excited states of the molecular aggregate may be described in terms of the excited states of the component molecules. One description of the excited molecular aggregate involves a superposition of the collective excited states which describes the excitation in terms of a traveling wave packet of excitation known as an *exciton*.

We shall consider the case of linear polymers. The polymer is presumed to consist of *N* molecular units. Before excited state interaction, degeneracy exists being *N*-fold in character. After the perturbation (electrostatic) resulting from the intermolecular dipole–dipole interaction of the transition dipoles, an exciton band of *N* individual exciton states is produced. Another way to describe this is that the upper state of each monomer 0–0 transition is expanded by *N*-fold aggregation into *N*-fold band of levels or states. The band width is directly proportional to the intensity of the corresponding 0–0 component of the monomer absorption (242). Figure 21 shows exciton bands and states appropriate to various geometrical arrangements of the molecules within aggregates. Schemes II and III represent the arrangements which are most likely approached in real aggregates. We are interested in the energy of exciton states, the band width and the dipole selection rules (the $S_0 \rightarrow S_1$ transition moment in particular). Quantitative equations for determining the band width and transition moment integrals have been developed (242). Also, appeal to an electrostatic vector model permits a qualitative development of

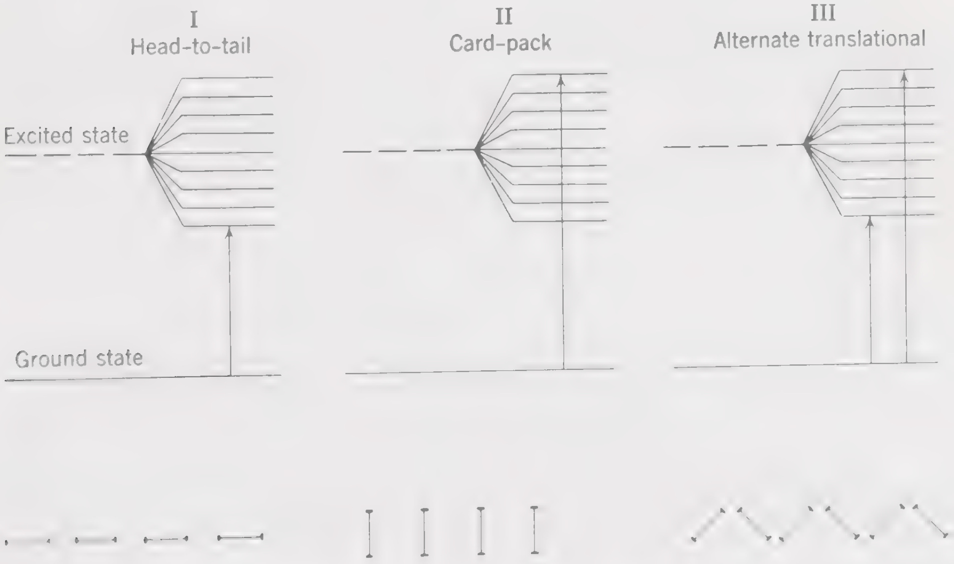

Fig. 21 Diagrammatic energy level scheme for exciton band structures in linear molecular polymers with various geometrical arrangements of transition dipoles (243).

the energy of the exciton states and selection rules (243) (see also Chapter III, Section IV-C).

In Figure 21, the vertical arrows represent those transitions which are allowed (ground state → exciton state). The band width for the singlet states of aggregates of dye molecules can be quite large ($\sim 1000\ \text{cm}^{-1}$) depending upon the geometrical arrangement of the molecules within the aggregate system (242). On the other hand, the triplet band width is virtually zero because of the forbidden nature of the spin-intercombination selection rule. However, the order of magnitude of the splitting in the singlet band is comparable to that present between the lowest singlet and triplet states of several dye monomers. Because of this, the intersystem rate constant would be expected to increase. In addition, the rate constant for fluorescence is important. In the cases of Schemes I and III, the rate constant for fluorescence is effectively unchanged from that of the monomer. However, in Scheme II, the lowest transition is forbidden and therefore the rate constant for fluorescence is significantly decreased. Thus, the enhancement of phosphorescence for the aggregate relative to the monomer is expected in all three schemes for fluorescence. The maximum effect will occur in Scheme II because of the forbidden character of the $S_0 \leftrightarrow S_1$ transition. A parallel discussion exists for the case where the aggregate is composed of two molecules (dimer).

References

1. G. Lewis and M. Kasha, *J. Am. Chem. Soc.*, **66**, 2100 (1944).
2. S. Strickler and R. Berg, *J. Chem. Phys.*, **37**, 814 (1962).
3. W. Melhuish, *J. Phys. Chem.*, **65**, 229 (1961).
4. E. Bowen, *Trans. Faraday Soc.*, **50**, 97 (1954).
5. G. Weber and F. Teale, *Trans. Faraday Soc.*, **53**, 646 (1957).
6. E. Gilmore, G. Gibson, and D. McClure, *J. Chem. Phys.*, **20**, 829 (1952); **23**, 399 (1955).
7. W. Melhuish, *New Zealand J. Sci. and Tech.*, **37B**, 142 (1955).
8. G. Weber and F. Teale, *Trans. Faraday Soc.*, **54**, 640 (1958).

8a. E. L. Nichols and E. Merritt, *Phys. Rev.*, **31**, 376 (1910).
8b. G. Kortüm and B. Finckh, *Z. Physik. Chem.*, **B52**, 263 (1942).
8c. K. W. Hausser, R. Kuhn, and E. Kuhn, *Z. Physik. Chem.*, **B29**, 417 (1935).

9. M. Beer and H. Longuet-Higgins, *J. Chem. Phys.*, **23**, 1390 (1955).
10. G. Viswanath and M. Kasha, *J. Chem. Phys.*, **24**, 574 (1956).
11. D. Evans, *J. Chem. Soc.*, **1960**, 1735.
12. N. Mataga, Y. Kaifu, and M. Koizumi, *Bull. Chem. Soc. Japan*, **29**, 115 (1956).
13. E. McRae, *J. Phys. Chem.*, **61**, 562 (1957).
14. N. Mataga, Y. Kaifu, and M. Koizumi, *Bull. Chem. Soc. Japan*, **29**, 465 (1956).
15. E. Lippert, *Z. Physik. Chem. (N.F.)*, **6**, 125 (1956); *Z. Naturforsch.*, **10a**, 541 (1955).
16. J. Fernandez and R. Becker, *J. Chem. Phys.*, **31**, 467 (1959).
17. R. Livingston, W. Watson, and J. McArdle, *J. Am. Chem. Soc.*, **71**, 1542 (1959).
18. R. Livingston, *Quart. Rev.*, **14**, 174 (1960).
19. R. Becker, unpublished, University of Houston.

20. V. Evstigneev, A. Gavrilova, and A. Krasnovski, *Dokl. Akad. Nauk SSSR*, **70**, 261 (1950).
21. J. Allison and R. Becker, *J. Phys. Chem.*, **67**, 2675 (1963); J. Miller and G. Dorough, *J. Am. Chem. Soc.*, **74**, 3977 (1952).
21a. S. Broyde and S. Brady, *J. Chem. Phys.*, **46**, 3334 (1967).
22. S. Ladner and R. Becker, *J. Phys. Chem.*, **67**, 2481 (1963).
23. M. El-Sayed, *J. Chem. Phys.*, **38**, 2834 (1963); **36**, 573 (1962).
24. E. Shpol'skii and R. Personov, *Opt. Spectry. USSR* (*English Transl.*), **8**, 172 (1960) and references therein; T. Bolotnikova *ibid.*, **7**, 138 (1959).
25. M. Beer, *J. Chem. Phys.*, **25**, 745 (1956).
26. M. Furst, H. Kallmann, and F. Brown, *J. Chem. Phys.*, **26**, 1321 (1957).
27. A. Nitkitin and M. Galanin, *Opt. Spectry. USSR* (*English Transl.*), **6**, 226 (1959).
28. E. Bowen and A. Williams, *Trans. Faraday Soc.*, **35**, 765 (1939).
29. J. Birks and A. Cameron, *Proc. Roy. Soc.*, **249**, 207 (1959).
29a. J. Laposa and E. Lim, *J. Chem. Phys.*, **42**, 3025 (1965).
29b. W. Ware and B. Baldwin, *J. Chem. Phys.*, **43**, 1194 (1965).
30. R. Becker, unpublished, University of Houston.
31. C. Karr, *Appl. Spectry.*, **13**, 15 (1959).
32. H. Ley and H. Specker, *Z. Wiss. Phot.*, **38**, 13, 96 (1939).
33. T. Bolotnikova, *Izv. Akad. Nauk SSSR Ser. Fiz*, **23**, 29 (1959).
34. E. Shpol'skii, *Soviet Phys. Usp.* (*English Transl.*), **3**, 372 (1960) and references therein.
35. M. Nakamizo and Y. Kanda, *Spectrochim. Acta*, **19**, 1235 (1963).
36. T. Förster and K. Kasper, *Z. Elektrochem.*, **59**, 976 (1955).
37. K. Kasper, *Z. Physik. Chem.*, **12**, 55 (1957).
38. A. Dammers-de-Klerk, *Mol. Phys.*, **1**, 141 (1958).
39. J. Birks and I. Munro, *Luminescence of Organic and Inorganic Materials*, H. Kallmann and G. Spruch, Eds, Wiley and Sons, New York, 1962, pp. 230–234.
40. B. Stevens, *Spectrochim. Acta*, **18**, 439 (1962).
41. R. Williams, *J. Roy. Inst. Chem.*, **83**, 611 (1959).
42. E. Bowen and J. Sahu, *J. Chem. Phys.*, **63**, 4 (1959).
43. A. Cherkasov, *Opt. Spectry. USSR* (*English Transl.*), **7**, 211 (1959).
44. A. Cherkasov and T. M. Vember, *Opt. Spectry. USSR* (*English Transl.*), **6**, 319 (1959).
45. V. Ermolaev and K. Switashev, *Opt. Spectry. USSR* (*English Transl.*), **7**, 399 (1959).
46. M. Furst, H. Kallmann, and F. Brown, *J. Chem. Phys.*, **26**, 1321 (1957).
47. A. Cherkasov, *Opt. Spectry. USSR* (*English Transl.*), **6**, 315 (1959).
48. D. Hercules and L. Rogers, *Spectrochim. Acta*, **393**, (1959).
49. R. Nurmukhametov, D. Shigorin, Y. Kozlov, and V. Puchov, *Opt. Spectry. USSR* (*English Transl.*), **1**, 327 (1961).
50. B. Van Duuren, *Anal. Chem.*, **32**, 1436 (1960).
51. H. Wirth, *Luminescence of Organic and Inorganic Materials*, H. Kallman and G. Spruch, Eds., Wiley, New York, pp. 226.
52. M. Chowdhury and L. Goodman, *J. Chem. Phys.*, **36**, 548 (1962).
52a. B. Cohen, H. Baba, and L. Goodman, *J. Chem. Phys.*, **43**, 2902 (1965);
52b. L. Logan and I. Ross, *J. Chem. Phys.*, **43**, 290 (1965).
53. E. Lippert, *Angew. Chem.*, **23**, 695 (1961).
54. D. K. Bredereck, T. Förster, and H. Oesterlin, *Luminescence of Organic and Inorganic Materials*, H. Kallman and G. Spruch, Eds, Wiley and Sons, Inc., New York, 1962, p. 161.
55. T. Adler, *Anal. Chem.*, **34**, 685 (1962).

56. V. Zanker and A. Reichel, *Z. Elektrochem.*, **63**, 1133 (1959).
57. A. Kilimov and V. Voloshina, *Opt. Spectry. USSR* (*English Transl.*), **12**, 362 (1962).
58. V. Zanker and W. Toerber, *Z. Angew. Phys.*, **14**, 43 (1962).
59. C. Wheelock, *J. Am. Chem. Soc.*, **81**, 1348 (1959).
60. H. Beyer and T. Pyl, *Angew. Chem.*, **68**, 374 (1956).
61. F. Teale and G. Weber, *Biochem. J.*, **65**, 476 (1956).
62. A. White, *Biochem. J.*, **71**, 217 (1959).
63. E. Fujimori, *Biochim. Biophys. Acta*, **40**, 251 (1960).
64. S. Udenfriend, *Fluorescence Assay in Biology and Medicine*, Academic Press, New York, 1962.
65. F. Teale, *Biochem. J.*, **76**, 381 (1960).
66. Y. Vladimirov, *Dokl. Akad. Nauk SSSR*, **136**, 960 (1961).
67. L. Agroskin, *Dokl. Akad. Nauk SSSR*, **131**, 1440 (1960).
68. G. Weber and F. Teale, *Discussions Faraday Soc.*, **27**, 1 (1959) and references therein.
69. V. Shore and A. Pardee, *Arch. Biochem. Biophys.*, **60**, 100 (1956).
70. V. Velick, *J. Biol. Chem.*, **233**, 1455 (1958).
71. G. Weber, *Advan. Protein Chem.*, **8**, 415 (1953).
72. C. Chadwick, P. Johnson, and E. Richards, *Nature*, **186**, 239 (1960) and references therein.
73. R. Steiner and A. McAlister, *J. Polymer Sci.*, **24**, 105 (1957).
74. H. Uehleke, *Naturwissenschaften*, **45**, 87 (1958).
75. C. Dhere and O. Biermacher, *Compt. Rend.*, **202**, 442 (1936) and references therein.
76. A. Stern and F. Pruckner, *Z. Physik. Chem.*, **185A**, 140 (1939); **180A**, 321 (1937) and references therein.
77. F. Hourowitz, *Ber. Deut. Keram. Ges.*, **68**, 1795 (1935).
78. V. Albers, H. V. Knorr, and D. Fry, *J. Chem. Phys.*, **10**, 700 (1942); H. Knorr and V. Albers, *Phys. Rev.*, **57**, 347 (1940).
79. R. Becker and M. Kasha, *J. Am. Chem. Soc.*, **77**, 3669 (1953).
80. J. Allison and R. Becker, *J. Chem. Phys.*, **32**, 1410 (1960).
81. R. Becker and J. Allison, *J. Phys. Chem.*, **67**, 2662 (1963).
82. R. Becker and J. Allison, *J. Phys. Chem.*, **67**, 2669 (1963).
83. J. Allison and R. Becker, *J. Phys. Chem.*, **67**, 2675 (1963).
84. C. Dhere and A. Raffy, *Compt. Rend.*, **200**, 1367 (1935) and references therein.
85. F. Zscheile and P. Harris, *J. Phys. Chem.*, **47**, 623 (1943).
86. E. Rabinowitch, *Photosynthesis and Related Processes*, Vol. 1, Interscience, New York, 1945; Vol. 2, Part 1 (1951); Vol. 2, Part 2 (1956).
87. F. Johnson, Ed., *The Luminescence of Biological Systems*, Am. Assoc. Adv. Sci., Washington, D. C. (1955).
88. H. Gaffron, Ed., *Research in Photosynthesis*, Interscience, New York (1957).
89. C. French, J. Smith, H. Virgin, and R. Airth, *Plant Physiol.*, **31**, 369 (1956).
90. V. Gachkovskii, *Chem. Abstr.*, **45**, 41b (1951).
91. P. Latimer, T. Bannister, and E. Rabinowitch, *Science*, **124**, 3222 (1956).
92. S. Brody and E. Rabinowitch, *Science*, **125**, 555 (1957).
93. W. Ohnesorge and L. Rogers, *Spectrochim. Acta*, **14**, 27, 41 (1959).
94. O. Popovych and L. Rogers, *Spectrochim. Acta*, **16**, 49 (1960).
95. S. Weissman, *J. Chem. Phys.*, **10**, 214 (1942); P. Yuster and S. Weissman, *J. Chem. Phys.*, **17**, 1182 (1949).
96. A. N. Sevechenko and A. Trofimov, *J. Exp. Theoret. Phys. (USSR)*, **21**, 220 (1951), A. Sevechenko and A. Morachevsky, *Izv. Akad. Nauk SSSR Ser. Fiz.*, **15**, 628 (1951)

97. G. Crosby and M. Kasha, *Spectrochim. Acta*, **10**, 377 (1958).
98. G. Crosby, R. Whan, and J. Freeman, *J. Phys. Chem.*, **66**, 2493 (1962) and references therein.
99. F. Varsany and G. Dieke, *J. Chem. Phys.*, **31**, 1066 (1959).
100. G. Dieke and L. Hall, *J. Chem. Phys.*, **27**, 465 (1957).
101. G. Crosby, R. Whan, and R. Alire, *J. Chem. Phys.*, **34**, 743 (1961).
102. J. Freeman and G. Crosby, *J. Phys. Chem.*, **67**, 2717 (1963).
103. M. Kleinerman, personal communication, American Optical Co., 1964.
103a. M. Bhaumik and M. El-Sayed, *J. Chem. Phys.*, **42**, 787 (1965).
103b. M. Bhaumik, L. Ferder, and M. El-Sayed, *J. Chem. Phys.*, **42**, 1843 (1965).
103c. W. Dawson, J. Kropp, and M. Windsor, *J. Chem. Phys.*, **45**, 2410 (1966) and references therein.
103d. J. Kropp and W. Dawson, *J. Chem. Phys.*, **45**, 2419 (1966) and references therein.
104. E. Matovich and C. Suzuki, *J. Chem. Phys.*, **39**, 1442 (1963).
105. M. El-Sayed and M. Bhaumik, *J. Chem. Phys.*, **39**, 2391 (1963).
106. D. Scott and R. Becker, *J. Chem. Phys.*, **35**, 516 (1961); D. Feuerbacher and R. Becker, unpublished, University of Houston.
106a. J. Smith and B. Meyer, private communication, University of Washington, 1968.
107. R. Becker and J. Bushman, unpublished, University of Houston.
108. C. Reid, *J. Chem. Phys.*, **20**, 1212, 1214 (1952).
109. N. Moodie and C. Reid, *J. Chem. Phys.*, **22**, 252 (1954).
110. A. Bier and J. Ketelaar, *Rec. Trav. Chim.*, **73**, 264 (1954).
111. J. Czekalla, G. Briegleb, N. Hure, and H. Vahlensieck, *Z. Elektrochem.*, **63**, 715 (1959) and references therein.
112. G. Briegleb, *Elektronen-Donator-Acceptor-Komplexe*, Springer-Verlag, Berlin, 1961, pp. 82–94 and references therein.
113. S. McGlynn and J. Boggus, *J. Am. Chem. Soc.*, **80**, 5096 (1958).
114. S. McGlynn, J. Boggus, and E. Elder, *J. Chem. Phys.*, **32**, 357 (1960).
115. T. Förster, *Z. Elektrochem.*, **54**, 42 (1950).
116. A. Weller, *Z. Elektrochem.*, **56**, 662 (1952).
117. A. Weller, *Z. Elektrochem.*, **60**, 1144 (1956).
118. A. Weller, *Z. Elektrochem.*, **61**, 1956 (1957).
119. A. Weller, *Z. Physik. Chem.* **3**, 238 (1955).
120. A. Weller, *Discussions Faraday Soc.*, **27**, 28 (1959).
121. G. Jackson and G. Porter, *Proc. Roy. Soc.* (*London*), **260A**, 13 (1961).
122. J. Brinen, D. Rosebrook, and R. Hirt, *J. Phys. Chem.*, **67**, 2651 (1963).
123. W. Bartok, P. Lucchesi, and N. Snider, *J. Am. Chem. Soc.*, **84**, 1842 (1962).
124. E. Clementi and M. Kasha, *J. Mol. Spectry.*, **2**, 297 (1958).
125. M. Kasha, *Discussions Faraday Soc.*, **9**, 14 (1950).
126. G. N. Lewis and M. Calvin, *J. Am. Chem. Soc.*, **67**, 1232 (1945).
127. G. N. Lewis, M. Calvin, and M. Kasha, *J. Chem. Phys.*, **17**, 804 (1949).
128. C. Hutchinson and B. Mangum, *J. Chem. Phys.*, **29**, 952 (1958).
129. M. de Groot and J. van der Waals, *Mol. Phys.*, **3**, 190 (1960).
130. L. Piette, J. Sharp, T. Kuwana, and J. Pitts, *J. Chem. Phys.*, **36**, 3094 (1962).
131. D. Shigorin, N. Volkova, A. Pisknov, and A. Gurevich, *Opt. Spectry. USSR* (*English Transl.*), **12**, 369 (1962).
132. J. Vincent and A. Maki, *J. Chem. Phys.*, **39**, 3088 (1963).
133. G. Jackson and R. Livingston, *J. Chem. Phys.*, **35**, 2182 (1961).

134. D. S. McClure, *J. Chem. Phys.*, **17**, 905 (1949).
135. D. Olness and H. Sponer, *J. Chem. Phys.*, **38**, 1779 (1963).
136. C. A. Hutchinson and B. W. Mangum, *J. Chem. Phys.*, **32**, 1261 (1960).
137. G. Robinson and R. Frosch, *J. Chem. Phys.*, **37**, 1962 (1962); **38**, 1187 (1963).
138. R. Williams, *J. Chem. Phys.*, **30**, 233 (1959).
139. V. Krishna and L. Goodman, *J. Chem. Phys.*, **37**, 912 (1962).
140. T. Azumi and S. McGlynn, *J. Chem. Phys.*, **37**, 2413 (1962) and references therein.
141. M. El-Sayed, *Nature*, **197**, 481 (1963).
142. R. Becker, I. Singh, and E. Jackson, *J. Chem. Phys.*, **38**, 2144 (1963).
143. H. Klevens and J. Platt, *J. Chem. Phys.*, **17**, 470 (1949); J. Platt, *J. Chem. Phys.*, **17**, 484 (1949).
144. S. McGlynn, M. Padhye, and M. Kasha, *J. Chem. Phys.*, **23**, 593 (1955).
145. M. Wright, R. Frosch, and G. Robinson, *J. Chem. Phys.*, **33**, 934 (1960).
146. G. Robinson, *J. Mol. Spectry.*, **6**, 58 (1961).
147. M. de Groot and J. van der Waals, *Mol. Phys.*, **4**, 189 (1961).
148. D. Craig, *J. Chem. Phys.*, **18**, 236 (1950).
149. M. Wright, R. Frosch, and G. Robinson, *J. Chem. Phys.*, **33**, 934 (1960).
150. G. Robinson and R. Frosch, *J. Chem. Phys.*, **37**, 1962 (1962) and references therein.
151. G. Robinson and R. Frosch, *J. Chem. Phys.*, **38**, 1187 (1963).
152. E. Lim, *J. Chem. Phys.*, **36**, 3497 (1962);
152a. S. Siegel and H. Judeekis, *J. Chem. Phys.*, **42**, 3060 (1965).
152b. S. Strickler and M. O'Dwyer, private communication, 1967.
153. M. O'Dwyer, M. El-Bayoumi, and S. Strickler, *J. Chem. Phys.*, **36**, 1395 (1962).
154. R. Nurmukhametov and G. Goleov, *Opt. Spectry. USSR* (*English Transl.*), **13**, 384 (1962).
155. E. Shpol'skii, L. Klimova, and R. Personov, *Opt. Spectry. USSR* (*English Transl.*), **13**, 188 (1962).
156. A. Khesine, *Opt. Spectry. USSR* (*English Transl.*), **10**, 319 (1961).
157. Y. Kanda, R. Shimada, and Y. Takenoshita, *Spectrochim. Acta*, **19**, 1219 (1963).
158. J. Sidman, *J. Chem. Phys.*, **25**, 229 (1956).
159. M. El-Sayed and T. Pavlopoulpos, *J. Chem. Phys.*, **39**, 1899 (1963).
160. V. Ermolaev and K. Svetashev, *Usp. Fiz. Nauk*, **3**, 423 (1960)-translation.
161. J. Corkell and I. Graham-Bryce, *J. Chem. Soc.*, **1961**, 3893.
162. Y. Hirshberg, *Anal. Chem.*, **28**, 1954 (1956).
163. N. Christodouleas and S. McGlynn, *J. Chem. Phys.*, **40**, 166 (1964).
164. B. Piatnitskii, *Dokl. Akad. Nauk SSSR*, **1**, 451 (1956)-translation.
165. J. Dubois and F. Wilkinson, *J. Chem. Phys.*, **39**, 899 (1963).
166. G. Almy and P. Gillette, *J. Chem. Phys.*, **11**, 188 (1963).
167. W. Kaskan and A. Duncan, *J. Chem. Phys.*, **18**, 427 (1950).
168. H. Backstrom and K. Sandros, *Acta Chem. Scand.*, **12**, 823 (1958).
169. H. Okabe and W. Noyes, *J. Am. Chem. Soc.*, **79**, 801 (1952)
169a. H. Richtol and F. Klappmeier, *J. Chem. Phys.*, **44**, 1519 (1966).
170. I. Singh and R. Becker, *J. Am. Chem. Soc.*, **82**, 2083 (1960).
171. V. Ermolaev and A. Terenin, *Soviet Phys.*, **3**, 423 (1960).
172. J. Pitts, H. Johnson, and T. Kuwana, *J. Phys. Chem.*, **66**, 2456 (1962) and references therein.
173. G. Hammond and P. Leermakers, *J. Am. Chem. Soc.*, **84**, 207 (1962).
174. L. Goodman and H. Shull, *J. Chem. Phys.*, **22**, 1138 (1954); **27**, 1388 (1957).
175. J. Sidman, *Chem. Rev.*, **58**, 698 (1958).
176. L. Goodman and R. Harrell, *J. Chem. Phys.*, **30**, 1131 (1959) and references therein.

177. J. Brinen and L. Goodman, *J. Chem. Phys.*, **31**, 482 (1959).
178. L. Goodman, *J. Mol. Spectry.*, **6**, 109 (1961).
179. D. Kearns and M. El-Bayoumi, *J. Chem. Phys.*, **38**, 1508 (1963).
180. M. El-Sayed and G. Robinson, *J. Chem. Phys.*, **34**, 1849 (1961).
181. D. Evans, *J. Chem. Soc.*, **1957**, 3885.
182. L. Goodman and M. Kasha, *J. Mol. Spectr.*, **2**, 58 (1958).
183. V. Krishna and L. Goodman, *J. Am. Chem. Soc.*, **83**, 2042 (1961).
184. V. Krishna and L. Goodman, *J. Chem. Phys.*, **36**, 2217 (1962).
185. M. El-Sayed and R. Brewer, *J. Phys. Chem.*, **39**, 1623 (1963)
185a. J. Paris, R. Hirt, and R. Schmitt, *J. Chem. Phys.*, **34**, 1851 (1961);
185b. J. Brinen, J. Koren, and W. Hodgson, *J. Chem. Phys.*, **44**, 3095 (1966).
186. V. Ermolaev and I. Kotlyar, *Opt. Spectry. USSR* (*English Transl.*), **9**, 183 (1960).
187. M. Gouterman, *J. Mol. Spectry.*, **6**, 138 (1961).
187a. D. Bhatnazar and L. Forster, *Spectrochim. Acta*, **21**, 1803 (1965).
188. P. Yuster and S. Weissman, *J. Chem. Phys.*, **17**, 1182 (1949).
189. R. Whan and G. Crosby, *J. Mol. Spectry.*, **8**, 315 (1962).
190. M. Kasha, *J. Chem. Phys.*, **20**, 71 (1952).
191. L. Goodman and M. Kasha, *J. Mol. Spectry.*, **2**, 58 (1958).
192. L. Goodman and H. Shull, *J. Chem. Phys.*, **27**, 1388 (1957).
193. L. Goodman and H. Shull, *J. Chem. Phys.*, **22**, 1138 (1954).
194. D. Evans, *J. Chem. Soc.*, **1957**, 3885.
195. L. Forster, *J. Chem. Phys.*, **26**, 1761 (1957).
195a. W. Rothman, A. Chase, and P. Kearns, *J. Chem. Phys.*, **43**, 1067 (1965).
196. S. McGlynn, M. Reynolds, G. Daigre, and N. Christodouleas, *J. Phys. Chem.*, **66**, 2499 (1962).
197. H. Tsumbora and R. Mulliken, *J. Am. Chem. Soc.*, **82**, 5966 (1960).
198. D. Evans, *Nature*, **173**, 536 (1956); *J. Chem. Soc.*, **1957**, 1351; *Proc. Roy. Soc.* (*London*), **255A**, 55 (1960).
199. G. Hoytink, *Mol. Phys.*, **3**, 67 (1960).
200. A. Grabowska, *Spectrochim. Acta*, **19**, 307 (1963).
201. R. Dyck and D. McClure, *J. Chem. Phys.*, **36**, 2326 (1962).
202. H. Linschitz and K. Sarkanen, *J. Am. Chem. Soc.*, **80**, 4826 (1958).
203. G. Porter and M. Windsor, *Proc. Roy. Soc.* (*London*), **245A**, 238 (1958) and references therein.
204. D. Craig and I. Ross, *J. Chem. Soc.*, **1954**, 1589.
205. H. Linschitz and L. Pakkarinen, *J. Am. Chem. Soc.*, **82**, 2411 (1960).
206. R. Livingston and E. Fujimori, *J. Am. Chem. Soc.*, **80**, 5610 (1958).
207. S. Claesson, L. Lindquist, and B. Holmstrom, *Nature*, **183**, 661 (1959); E. Abrahamson, R. Adams, and V. Wulff, *J. Phys. Chem.*, **63**, 441 (1959); W. Dawson and E. Abrahamson, *ibid.*, **66**, 2542 (1962).
208. G. Blauer and H. Linschitz, *J. Phys. Chem.*, **66**, 453 (1962).
209. R. Pariser, *J. Chem. Phys.*, **24**, 250 (1956).
210. C. Steel and H. Linschitz, *J. Phys. Chem.*, **66**, 2577 (1962).
211. G. Porter and M. Wright, *Discussions Faraday Soc.*, **1959**, 18.
212. G. Porter and F. Wilkinson, *Proc. Roy. Soc.* (*London*), **264A**, 1 (1961).
213. E. Fujimori and R. Livingston, *Nature*, **180**, 1036 (1957).
214. E. Viktorova, I. Zhmyreva, V. Kolobkov and A. Saganenko, *Opt. Spectry. USSR* (*English Transl.*), **9**, 181 (1960).
215. I. Graham-Boyce and J. Corkell, *Nature*, **186**, 965 (1960).

216. G. Porter, *Proc. Chem. Soc.*, **1959**, 291 and references therein.
216a. A. Lamola and G. Hammond, *J. Chem. Phys.*, **43**, 2129 (1965).
217. R. Hochstrasser and G. Porter, *Quart. Rev.*, **14**, 146 (1960) and references therein.
218. R. Livingston, *J. Chem. Phys.*, **55**, 887 (1958).
219. E. Bowen and R. Williams, *Trans. Faraday Soc.*, **35**, 765 (1939).
220. A. Cherkasov and T. M. Vember, *Opt. Spectry. USSR (English Transl.)*, **6**, 503 (1959).
221. A. Terenin and V. Ermolaev, *Trans. Faraday Soc.*, **52**, 1042 (1956).
222. G. Porter and F. Wilkinson, *Luminescence of Organic and Inorganic Materials*, H. Kallmann and G. Spruch, Eds., Wiley, New York, 1962, p. 132.
223. H. Backstrom and K. Sandros, *Acta Chem. Scand.*, **14**, 48 (1960).
224. J. Dubois and B. Stevens, *Luminescence of Organic and Inorganic Materials*, H. Kallmann and G. Spruch, Eds., Wiley, New York, 1962, p. 115.
225. H. Ishikawa and W. Noyes, *J. Am. Chem. Soc.*, **84**, 1502 (1962).
226. H. Ishikawa and W. Noyes, *J. Chem. Phys.*, **37**, 583 (1962).
227. J. Dubois and F. Wilkinson, *J. Chem. Phys.*, **38**, 2541 (1963).
228. S. Lipsky, *J. Chem. Phys.*, **38**, 2786 (1963).
229. K. Essential and R. Murashige, *J. Chem. Phys.*, **39**, 2108 (1963).
230. G. Ciamincian and P. Silber, *Ber. Deutsch. Chem. Ges.*, **33**, 2911 (1900).
231. G. Porter and F. Wilkinson, *Trans. Faraday Soc.*, **57**, 1686 (1961).
232. J. Pitts, R. Letsinger, R. Taylor, J. Patterson, G. Recktemvala, and R. Martin, *J. Am. Chem. Soc.*, **81**, 1068 (1959) and references therein.
233. B. Stevens and J. Dubois, *J. Chem. Soc.*, **1962**, 2813.
234. H. Backstrom and K. Sandros, *Acta Chem. Scand.*, **12**, 832 (1958)
235. G. Hammond, P. Leermakers, and N. Turro, *J. Am. Chem. Soc.*, **83**, 2395 (1961).
236. G. Hammond, N. Turro, and P. Leermakers, *J. Phys. Chem.*, **66**, 1144 (1962).
237. V. Ermolaev and A. Terenin, *J. Chim. Phys.*, **1958**, 698.
238. W. Kemula and A. Grabowska, *Nature*, **188**, 224 (1960) and references therein.
239. E. Lippert and W. Leeder, *J. Phys. Chem.*, **66**, 2430 (1962).
240. R. Dyck and D. McClure, *J. Chem. Phys.*, **36**, 2326 (1962).
241. G. Jackson and G. Porter, *Proc. Roy. Soc. (London)*, **260A**, 13 (1961).
242. E. McRae and M. Kasha, *J. Chem. Phys.*, **28**, 721 (1958) and references therein.
243. M. Kasha, *Radiation Res.*, **20**, 55 (1963) and references therein.
244. E. McRae, *Australian J. Chem.*, **14**, 329 (1961); 344 (1961); 354 (1961) and references therein.
245. W. Simpson, G. Levinson, and W. Curtis, *J. Am. Chem. Soc.*, **79**, 4314 (1957).

AUTHOR INDEX

Numbers in parentheses are reference numbers and show that an author's work is referred to although his name is not mentioned in the text. Numbers in *italics* indicate the pages on which the full references appear.

A

Aalbersberg, W. I., 305(131), *335*
Abrahamson, E., 435(207), 438(207), *457*
Adair, B. J., 281(83), *333*
Adams, R., 435(207), 438(207), *457*
Adler, T., 371(55), *453*
Agroskin, L., 375(67), *454*
Airth, R., 377(89), *454*
Albers, V., 377(78), 381(78), *454*
Aldersley, J. B., 67(84), *101*
Alire, R., 385–387(101), 389(101), 426 (101), 427(101), *455*
Allen, L. C., 172(29b), 177(29), *197*
Allinger, J., 70(107), 71(107), *102*
Allinger, N. L., 70(107), 71(107), *102*
Allison, J., 317, *335*, 356(21), 377(80–83), 378(81,82), 382(80), 421(80–82), 423(81, 83), 424(81), 425(81), 438(82,83), *453*, *454*
Almy, G., 415(166), *456*
Anderson, L. C., 304(129), *335*
Anderson, M. M., 71(99), *101*, 246(25), *331*
Andrews, L. J., 298(102), *334*
Angus, W. R., 155(13), *196*
Anno, T., 276(74), *333*
Arends, B., 61(45), 71(110), *100*, *102*, 243
Armitage, J. B., 69(92,93), *101*
Armstrong, R., 80(139), *102*
Arnold, L. B., Jr., 24(13), *99*
Aten, C. F., 22(9), *99*
Azumi, T., 54(33), *100*, 404(140), *456*

B

Baba, H., 263(46), 264(46), *332*, 369(52a), 419(52a), *453*
Backenköhler, F., 76(136), 79(136), *102*
Backstrom, H., 415(168), 445(223), 447 (234), *456*, *458*
Bailey, A. S., 281(83), *333*
Bailey, C. R., 155(13), *196*
Bailey, C. W., 291, *334*
Bailey, W. J., 67(83), *101*, 239
Baker, E. B., 302(118), *334*
Balasobramanian, A., 70(117), 72(117), *102*
Baldwin, B., 362(29b), *453*
Ball, J. S., 243, 291, *334*
Baly, E. C. C., 253
Bannister, T., 382(91), *454*
Barnett, M. P., 179(38), 181(38), *197*
Bartok, W., 393–395(123), 450(123), *455*
Bastien, I. J., 302(118), *334*
Basu, S., 322(161), *336*
Bauer, S. H., 22(9), *99*
Bayliss, N. S., 322(159,160), 327(160), *335*
Beaven, G. H., 90(163), *103*
Becker, R. S., 199, 287(87,90), 288(90), 301(111), 317, *333–335*, 337, 356(16,19, 21,22), 357(22), 362(30), 368(19), 370 (16), 372(22), 377(16,79–83), 378(81, 82), 382(19,79,80), 383(16,19,79), 389 (19,106,107), 401, 404(142), 405(19), 412(19), 413(19), 416(16,170), 421(79–82), 423(81–83), 424(81), 425(16,79,81, 170), 438(82,83), *452–456*
Beer, M., 350(9), 357(25), *452*, *453*
Ben-Efraim, D. A., 64(65), *101*
Benesi, H. A., 298(101), *334*
Benitez, A., 315(150), 317(150), *335*
Bennett, R., 401
Benson, S. W., 247, 251
Berg, R., 55, *100*, 351–353(2), *452*
Bergman, I., 287(90), 288(90), *333*
Bergmann, E. D., 249, 251
Bergmann, K., 310(138), *335*
Bertin, H. J., 253
Beyer, H., 374(60), *454*
Bhatnazar, D., 425(187a), *457*
Bhaumik, M., 388(103a,103b), 389(105), *455*

Bieber, R., 249
Bielecki, J., 71(109), *102*
Bier, A., 390(110), *455*
Biermacher, O., 377(75), *454*
Bird, R. B., 20(8), *99*
Birge, R. T., 41(28), *100*
Birks, J., 360(29), 361(29), 364(39), 371(29), *453*
Birnbaum, P. P., 253, 257(41), *332*
Birss, F. W., 178(32), *197*
Blauer, G., 435(208), 438(208), *457*
Blout, E. R., 65(69), 77(69), *101*, 249
Boggus, J., 390(113,114), 391(113,114), *455*
Bohlmann, F., 65(67), 69(89,91), *101*
Bolotnikova, T., 357(24), 363(24,33), *453*
Booker, H., 66(79), 67(79), *101*
Bowden, K., 68(85), *101*, 247, 263(49), 292, *332*
Bowen, E., 27(20), *100*, 347(4), 358(28), 365(42), 366(42), 444(219), *452*, *453*, *458*
Brady, S., 356(21a), *453*
Brand, J. C. D., 246(24), *331*
Brattain, R. R., 239(15), *331*
Braude, E. A., 68(85), *101*, 247, 254, 256(38), 263(49), 274(72), 276(72), 292, *332* *333*
Brealey, G. J., 70(119), *102*, 326(164), *336*
Bredereck, D. K., 370(54), 371(54), 416(54), *453*
Bree, A., 287(88), *333*
Brewer, R., 420(185), *457*
Briegleb, G., 247, 287(89), 288(89), 298(100,106), *333*, *334*, 390(111,112), 391(112), *455*
Brinen, J., 392(122), 418(177), 419(122, 185b), 421(185b), 450(122), *455*, *457*
Brinton, R. K., 86(151), *103*
Brode, W. R., 3(1), *99*
Brody, S., 382(92), *454*
Brooker, L. G. S., 68(88), 97(183), *101*, *103*, 307(132), 308(132), 309(134), *335*
Brown, F., 358(26), 365(46), 366(46), *453*
Brown, G. H., 25(16), *99*
Brown, R. D., 229(11), *331*
Brown, W. G., 97(181), *103*, 236, 265(54), *332*
Browne, J. C., 201(1), *330*
Broyde, S., 356(21a), *453*
Brunings, K. L., 97(182), *103*
Bryant, K. C., 281(83), *333*
Buckley, J. M., 291, *333*
Buckley, S. W., 61(49), *100*
Burawoy, A., 77(131), *102*
Burkhard, G. V., 67(84), *101*
Burkhardt, G. N., 236
Buroway, A., 253
Burr, G. O., 73(125), 75(125), *102*, 250(28), *331*
Bushman, J., 389(107), *455*

C

Calvert, J. G., 71(98,103,112,113), 86(145,148,149), *101*
Calvin, M., 25, 65(72), 74(127), 94, *99*, *101–103*, 187, *198*, 399, *455*
Cameron, A., 360(29), 361(29), 371(29), *453*
Campaigne, E., 236
Carmack, M., 61(46), *100*, 291, *334*
Carr, E. P., 62(55,57), *100*
Cederholm, B. J., 61(43), *100*, 243, 244
Chadwick, C., 376(72), *454*
Chako, N. Q., 191(69), *198*
Chase, A., 430(195a), *457*
Cherkasov, A., 365(43,44), 366(43,47), 444(220), *453*, *458*
Chernick, C. L., 168(26), *197*
Chierice, L., 292
Chisholm, D. A., 19(7), *99*
Chow, L., 253
Chowdhury, M., 369(52), *453*
Christodouleas, N., 413(163), 431(196), 442(196), *456*, *457*
Chuoke, R. L., 259(45), 260, 266(56), 269(56), *332*
Ciamincian, G., 446(230), *458*
Claassen, H. H., 168(26), *197*
Claesson, S., 435(207), 438(207), *457*
Clar, E., 91, 93, *103*, 277(77), *333*, 401
Clark, C. H. D., 41, *100*
Clementi, E., 397(124), 418(124), 420(124), *455*
Closson, W. D., 247
Coffin, E. M., 61(48), *100*, 243, 244, 292
Cohen, A. D., 70(100), *101*, 246(26), *331*

Cohen, B., 369(52a), 419(52a), *453*
Collins, R. L., 301(115), *334*
Collis, M. J., 253
Comar, C. L., 315(150), 317(150), *335*
Condon, E. U., 30, *100*
Cook, C. L., 69(90,92,93), *101*
Cook, G. L., 243
Cook, J. W., 281(83), *333*
Cookson, R. C., 70(115), *102*, 304(125), *334*
Coolidge, A. S., 176(31), *197*
Corkell, J., 411(161), 412(161), 441(215), *456*, *457*
Corning, M. E., 61(49), *100*, 291, *333*
Corwin, A. W., 97(182), *103*, 316
Cotton, F. A., 299(116), 301(116), *334*
Coulson, C. A., 182, 184, 187(51), *197*, 208(5), 221(7), 228(5), 238, 276(74), 290(93), *330*, *331*, *333*
Craig, D. P., 94(168), *103*, 179, 181, *197*, 230(12), 259(44), 281(82), 282(84), 287(82), *331–333*, 405(148), 435(204), 443(148), *456*, *457*
Craig, L., 304(122), *334*
Crawford, M. F., 19(7), *99*
Crosby, G., 384(97,98), 385(98, 101), 386(98,101), 387(98,101,102), 389(98,101), 426(98, 101), 427(98,101,189), *455*, *457*
Cunneen, J. I., 247
Curtis, W., 311–313(144), *335*, 451(245), *458*
Czaja, R. F., 70(107), 71(107), *102*
Czekalla, J., 298(106), *334*, 390, *455*

D

Daigre, G., 431(196), 442(196), *457*
Dammers-de-Klerk, A., 361, 364(38), *453*
Dandegaonker, S. H., 70(115), *102*
Dannenberg, H., 66(80), *101*
Datta, A. K., 243
Davidson, N., 243
Dawson, W., 388(103c,103d), 401, 435(207), 438(207), *455*, *457*
Deno, N. C., 302(117), 304(128), *334*, *335*
Dent, S. G., Jr., 97(183), *103*
Desch, C. H., 253
Dewar, M. J. S., 277(78), 309(133), *333*, *335*
Dezeli, M., 317(152), *335*
Dhere, C., 377(75,84), *454*
Dieke, G., 384(99,100), *455*
Digiorgio, V. E., 246(24), *331*
Dixon, R. N., 253
Doering, W. v. E., 304(124), *334*
Donle, H. L., 71(108), *102*
Donovan, J., 361
Dorfman, L., 66(81), *101*
Dorough, G. D., 317(152,154), *335*, 356(21), *453*
Doub, L., 272(70,71), *333*
Douglas, A. E., 167(21), *197*
Dressler, K., 167(20), 169(20), *197*
Dubois, J., 414(165), 415(165), 417(165), 445(224,227), 446(224), 447(233), *456*, *458*
Duncan, A. B. F., 61(50a), *100*, 105, 168(23a–c), 178(32), 194(78), *197*, *198*, 228(10), 240(17), 243, 291, *331*, *333*, 361, 415(167), *456*
Dunn, T. M., 181(40), *197*, 259(45), *332*
Dyck, R., 432(201), 449(240), *457*, *458*

E

Edlén, B., 5, *99*
El-Bayoumi, M., 406(153), 418(179), *456*, *457*
Elder, E., 390(114), 391(114), *455*
Ellington, P. S., 63(60), *100*
El-Sayed, M., 356(23), 357(23), 370(23), 388(103a,103b), 389(105), 404(141), 409(159), 418(23,180), 420(23,185), 421(23), *453*, *455–457*
Emmons, W. D., 247
Entwhistle, N., 69(92), *101*
Epstein, L., 310(137), *335*
Erdman, J., 316
Ermolaev, V., 360(45), 365(45), 410(160), 411, 417(171), 418(171), 419, 421(186), 444(221), 445(221), 448(237), *453*, *456–458*
Evans, D., 351(11), 418(181), 430(194), 431(11,194,198), 433(198), *452*, *457*
Evans, L. K., 66, 67(79), 77(130,133), 78(133), 80(133), 81(133), *101*, *102*, 250(32), *332*
Evans, M. G., 236
Evstigneev, V., 356(20), *453*

Ewing, G. E., 13(5,6), *99*
Eyring, H., 108(1), 129, 145(9), 149(11), *196*

F

Fehnel, E. A., 61(46), *100*, 291, *334*
Ferder, L., 388(103b), *455*
Ferguson, L. N., *330*
Fernandez, J., 356(16), 370(16), 377(16), 383(16), 416(16), 425(16), *452*
Feuerbacher, D., 389(106), *455*
Field, F. H., 232, 243
Fields, M., 65(69), 77(69), *101*
Fieser, L. F., 66, 93(165), *101*, *103*, 250 (31), *332*
Fieser, M., 66, *101*, 250(31), *332*
Finckh, B., 350(8b), *452*
Fink, P., 243
Fischer, R. D., 299(116), 301(116), *334*
Fischer-Hjalmars, I., 201(2), *330*
Fisher, M. I., 69(87), *101*
Fleming, G., 71(99), *101*, 246(25), *331*
Foerster, G. v., 401
Förster, T., 271(68), 310(139), 312(143), 315(143), *333*, *335*, 364(36), 370(54), 371(54), 392(115), 416(54), *453*, *455*
Ford, R. A., 250(29), *332*
Forster, G., 72(121), *102*, 247, 251
Forster, L., 73(124), *102*, 425(187a), 430 (195), 432(195), *457*
Foss, J. G., 282(85), 285(85), *333*
Frame, H., 25(14), 90(161), *99*, *103*
Franck, J., 29, *100*
Franck, R. L., 80(139), *102*
Franklin, J. L., 232, 243, 298(105), *334*
Freeman, J., 384–386(98), 387(98,102), 389(98), 426(98), 427(98), *455*
Freiberg, L. A., 70(107), 71(107), *102*
French, C., 317(155), *335*, 377(89), *454*
Fried, S., 298(103), *334*
Friedel, R. A., 85, *103*, 249, 275, 278, 282–286, 288, 294, *330*
Frolicher, U., 281(83), *333*
Frosch, R., 404(137), 405(145,149,150), 406(151), 443(149,150), *456*
Fry, D., 377(78), 381(78), *454*
Fujimori, E., 375(63), 435(206), 438(206), 441(213), *454*, *457*
Furlani, C., 251
Furst, M., 358(26), 365(46), 366(46), *453*

G

Gachkovskii, V., 377(90), 382(90), *454*
Gaddis, C. L., 292
Gaffron, H., 377(88), *454*
Galanin, M., 358(27), *453*
Gary, J. T., 62(56), *100*, 236
Gavrilova, A., 356(20), *453*
Gaydon, A. G., 27(17), *99*
Gibson, D. T., 281(83), *333*
Gibson, G., 347(6), 358(6), 360(6), 401 (6), 406(6), 411(6), 417(6), *452*
Gillam, A. E., 66, 67(79,84), 77(130,133), 78(133), 79(138), 80(133), 81(133), 82 (144), 85, *101*, *102*, 250(32), *330*, *332*
Gillette, P., 415(166), *456*
Gilmore, E., 347(6), 358(6), 360(6), 401 (6), 406(6), 411(6), 417(6), *452*
Gintz, F. P., 253
Goddard, D. R., 253
Godfrey, M., 89(159), *103*
Goeppert-Mayer, M., 165(17), 178–180, *196*
Gold, V., 304(126), *334*
Goleov, G., 407(154), *456*
Gonzales-Vidal, J., 302(119), 303(119), *334*
Goodeve, C. F., 61(51), *100*, 243
Goodfriend, P. L., 178(32), *197*
Goodman, L., 263(46,50), 264(46), *332*, 369(52,52a), 404(139), 418(174,176–178,182), 419(52a,174,178,183), 420 (183,184), 428(191), 429(191–193), 430 (191), *453*, *455–457*
Goossens, J. C., 67(83), *101*, 239
Gouterman, M., 315(149), *335*, 424(187), *457*
Gouveia, A. J. A. de, 281(83), *333*
Grabowska, A., 432(200), 449(238), *457*, *458*
Graham, B., 25(16), *99*
Graham-Bryce, I., 411(161), 412(161), 441 (215), *456*, *457*
Grammaticakis, P., 257(42), *332*
Grinter, R., 89(159,160), *103*, 304(127), *334*
Gronowitz, S., 292
Groot, M. de, 401(129), 402(129), 405 (147), *455*, *456*
Grossmann, P., 71(109a), 72(109a), *102*
Gurevich, A., 403(131), *455*

H

Haines, W. E., 243, 291, *334*
Hale, J. B., 155(13), *196*
Hall, G. G., 228(10), *331*
Hall, L., 384(100), *455*
Halverson, F., 95(174), *103*, 295(99), *334*
Ham, J. S., 298(104), 300(109), *334*
Ham, N. S., 188, *198*
Hamer, F. M., 68(87), *101*
Hammond, G., 418(173), 443(216a), 448 (173,235,236), *456*, *458*
Hamner, W. F., 267(58), 321, *332*
Hampson, G. C., 265(55), *332*
Hancock, R. A., 281(83), *333*
Harrell, R., 418(176), *456*
Harris, P., 377(85), *454*
Harrison, A. J., 61(43,44,48), 62(57), 71 (99,101), *100*, *101*, 243, 244, 246(25), 292, *331*
Harrison, G. R., 3(1), *99*
Hartmann, H., 274(73), *333*
Hartree, D. R., 117(4), *196*
Hastings, S. H., 298(105), *334*
Haszeldine, R. N., 253
Haug, P., 247
Haugen, G. R., 310(141), *335*
Hausser, K. W., 65(68,70,71), 77(132), *101*, *102*, 350(8c), *452*
Hawthorne, M. F., 247
Hebdon, E. A., 253
Heckman, R., 419
Heilbronner, E., 89(159,160), *103*, 281 (83), 290(92), *333*
Helm, R. V., 243, 291, *334*
Henri, V., 71(109), *102*, 191(70), *198*
Henrici, A., 243
Hercules, D., 366(48), *453*
Herold, W., 71(102,111), *102*
Hershberg, E. B., 93(165), *103*
Herzberg, G., 38(26), 61(50), *100*, 120(5, 6), 121(7), 128(8), 145, 153(12), 167(19), *196*, *197*, *330*
Herzfeld, K. F., 185, *198*
Herzog, H. L., 249
Hess, L. D., 78(135), *102*
Hildebrand, J. H., 298(101), *334*
Hindley, N. C., 67(84), *101*
Hirayama, K., 65(73,74), *101*
Hirshberg, Y., 281(83), *333*, 412(162), *456*
Hirt, R. C., 95(174,175), *103*, 295(99), *334*, 392(122), 419(122,185a), 421(185a), 450(122), *455*, *457*
Hlavaty, K., 259
Hobbins, P. C., 282(84), *333*
Hochmann, P., 259
Hochstrasser, R., 443(217), 444(217), *458*
Hodgson, W., 419(185b), 421(185b), *457*
Hoeflich, N. J., 291, *333*
Hoffer, M., 65(68), 77(132), *101*, *102*
Hoijtink, G. J., 305(131), *335*
Holdsworth, R. S., 194(78), *198*
Hollaender, A., 226(9), *331*
Hollas, J. M., 167(21), *197*
Holleman, G. W., 13(6), *99*
Holman, R. T., 73(125), 75(125), *102*, 250 (28), *331*
Holmstrom, B., 435(207), 438(207), *457*
Hopton, F. J., 304(130), *335*
Hosoya, H., 251
Hourowitz, F., 377(77), *454*
Hoytink, G., 431(199), 432(199), *457*
Hudee, J., 304(125), *334*
Hückel, E., 178(33), 182, 186, *197*, 304 (123), *334*
Huennekens, F. M., 317(152,154), *335*
Hure, N., 390(111), *455*
Hush, N. S., 304(130), *335*
Hutchinson, C., 401(136), 402(128), 405 (136), *455*, *456*

I

Ingham, C. E., 265(55), *332*
Ingold, C. K., 155, 167(18), 181(40), *196*, *197*, 240(17,18), 259(45), *331*, *332*
Innes, K. K., 167(18,19), *197*, 240(17,18), 295(97), 297(97), *331*, *334*
Ishikawa, H., 445(225,226), 446(225), *458*
Ito, M., 95(176), *103*

J

Jackson, E., 287(87), *333*, 404(142), *456*
Jackson, G., 392(121), 401(133), 449(241), 450(241), *455*, *458*
Jacobs, L. E., 191(71), *198*
Jaffe, H. H., 245(21), *330*, *331*
Jahn, H. A., 167, *197*
James, H. M., 176(31), *197*

James, T. H., 311(147), 314(147), *335*
Jander, J., 253
Janssen, M. J., 73(114), *102*, 251, *332*
Jaruzelski, J. J., 304(128), *335*
Jelley, E. E., 310(135), 314, *335*
Johnson, A. W., 304(124), *334*
Johnson, F., 377(87), *454*
Johnson, H., 417(172), 418(172), 448 (172), *456*
Johnson, H. L., 236
Johnson, H. S., 253
Johnson, P., 376(72), *454*
Jones, E. R. H., 69(90,92,93), *101*, 247, 254, 256(38), 292, *332*
Jones, J., 401
Jones, L. C., Jr., 62(59), 63(59), *100*
Jones, R. N., 93, 94, *103*, 256(40), 281 (83), 282(86), *332*, *333*
Jorgensen, C. K., 301(110), *334*
Judeekis, H., 406(152a), 442(152a), *456*

K

Kagarise, R. E., 71(110a), 73–75(110a), *102*, 247, 251
Kahn, A. V., 27(22), *100*
Kaifu, Y., 354(12), 355(14), *452*
Kallmann, H., 358(26), 365(46), 366(46), *453*
Kamlet, M. J., *330*
Kanda, Y., 363(35), 364(35), 408(157), 411, *453*, *456*
Kaplan, L. A., *330*
Karo, A. M., 172(29b), 177(29), *197*
Karr, C., 362(31), *453*
Kasha, M., 27(22), 54, 59(39), 70(116, 119), 95(173), *100*, *102*, *103*, 245(23), 246(23), 295(98), 312(145), 313(145), 315, 326(163,164), *331*, *334–336*, 345 (1), 350(10), 377(79), 382(79), 383(79), 384(97), 397(124,125), 399, 404(144), 418(124,182),) 420(124), 421(79), 425 (79), 428(190,191), 429(191), 430(190, 191), 431(190,) 450, 451(242,243), *452*, *454–458*
Kaskan, W., 415(167), *456*
Kasper, K., 364(36,37), *453*
Kauzmann, W., 47(32), *100*
Kaya, K., 243, 245(22), *331*
Kayser, H., 5, *99*
Kearns, D., 179(39), *197*, 418(179), *457*
Kearns, P., 430(195a), *457*
Keefer, R. M., 298(102), *334*
Kellogg, R., 401
Kemula, W., 449(238), *458*
Ketelaar, J., 390(110), *455*
Kettle, S. F., 208(5), 228(5), *331*
Khesine, A., 407(156), *456*
Kilimov, A., 373(57), *454*
Kimball, G. E., 108(1), 129, 145(9), 149 (11), *196*
Kimura, K., 60(52), 61(52), *100*, 242, 243, 245(22), 268(64), *331*, *332*
King, A. D., 322(158), 328(166), *335*, *336*
King, G. W., 167(18), *197*, 240(17,18), *331*
Kistiakowsky, G. B., 24(13), *99*, 247, 251
Klappmeier, F., 415(169a), *456*
Kleinerman, M., 387(103), *455*
Klevens, H. B., 59(40), *100*, 184, 187, *198*, 230, 258, 266, 268, 281, 282(80), 283, 287(80), 289(91), 292, 293, 295, 296, *333*, 404(143), *456*
Klimova, L., 407(155), *456*
Knorr, H. V., 377(78), 38(78), *454*
Knox, L. H., 304(124), *334*
Kobayshi, M., 88(156), *103*
Koch, H. P., 61(47), *100*, 252(35), *332*
König, E., 310(139), *335*
Kohn, E., 302(119), 303(119), *334*
Koizumi, M., 354(12), 355(14), *452*
Kojima, M., 268(62), *332*
Kolobkov, V., 441(214), 442(214), *457*
Konstam, A. H., 263(50), *332*
Koren, J., 419(185b), 421(185b), *457*
Korte, F., 247
Kortüm, G., 86(150), *103*, 350(8b), *452*
Kosower, E. M., 71(106), 96(178,179), *102*, *103*
Kotlyar, I., 419(186), 421(186), *457*
Koutecky, J., 259
Kozlov, Y., 366(49), 367(49), *453*
Kranendonk, J. van, 20(8), *99*
Krasnovski, A., 356(20), *453*
Kresze, G., 253
Krishna, V., 404(139), 419(183), 420(183, 184), *456*, *457*
Kropp, J., 388(103c,103d), *455*
Kuboyama, A., 274(73), *333*
Kuhn, E., 350(8c), *452*

Kuhn, H., 188, *198*
Kuhn, J., 226(8), *331*
Kuhn, R., 65(68,70,71), 77(132), *101*, *102*, 350(8c), *452*
Kuhn, S. J., 302(118), *334*
Kuraishi, T., 95(176), *103*
Kuwana, T., 403(130), 417(172), 418(172), 448(172), *455*, *456*
Kwiatek, J., 80(139), *102*

L

Labhart, H., 81(141), *102*
Ladner, S., 356(22), 357(22), 372(22), *453*
Lake, J. S., 71(101), *101*
Lamola, A., 443(216a), *458*
Landolt-Bornstein, *330*
Lang, L., *330*
Lanum, W. J., 243
Laposa, J., 361(29a), 362(29a), *453*
Latimer, P., 382(91), *454*
Lawrey, D. M. G., 300(108), *334*
Layton, F. M., Jr., 188(66), *198*
Leach, S., 27(19), *99*
Leandri, G., 292
LeBel, N. A., 70(107), 71(107), *102*
Leckie, A. H., 155(13), *156*
Leeder, W., 449(239), *458*
Leermakers, P., 418(173), 448(173,235, 236), *456*, *458*
Lennard-Jones, J. E., 182, *197*, 221(7), 228(10), *331*
Leonard, N. J., 73(126), 74, 75(126), *102*, 249, 250(27), *331*
Letsinger, R., 447(232), *458*
Levinson, G., 311–313(144), *335*, 451(245), *458*
Levy, D. A., 301(112), 302(112), *334*
Lewis, G. N., 25, 54, 65(72), 94, *100*, *101*, *103*, 187, *198*, 345(1), 399, *452*, *455*
Ley, H., 61(45), 71(110), *100*, *102*, 243, 362(32), *453*
Liehr, A. D., 168(24,25), *197*
Lim, E., 360(152), 361(29a), 362(29a), 401(152), 406(152), 411(152), *453*, *456*
Lindquist, L., 435(207), *457*
Linford, J. H., 253, 257(41), *332*
Linschitz, H., 435(202,205,208,) 436(205), 438(202,205,208), 439(202,205), 440(210), 441(205), *457*
Linstead, R. P., 317(156), *335*
Lippert, E., 355(15), 370(53), 419, 449(239), *452*, *453*, *458*
Lipsky, S., 446(228), *458*
Liu, T. K., 168(23c), *197*, 291, *333*
Livingston, R., 356(17,18), 377(17), 401(133), 435(206), 438(206), 441(213), 444(218), *452*, *455*, *457*, *458*
Lloyd, R. A., 27(20), *100*
Locke, J. L., 19(7), *99*
Logan, L., 369(52b), *453*
Lohmer, K. H., 247
Lohr, L. L., 299(116), 301(116), *334*
Longuet-Higgins, H. C., 168(24,27), 169(28), 184, *197*, 268(65), 274(65), 277(78), *332*, *333*, 350(9), *452*
Lord, R. C., 3(1), *99*
Lorenz, E., 274(73), *333*
Lothian, G. E., 3(1), *99*
Loufbourow, J. L., 3(1), *99*
Lucchesi, P., 393–395(123), 450(123), *455*
Lüthy, A., 62(62), 77(129), *101*, *102*
Lundberg, W. O., 73(125), 75(125), *102*, 250(28), *331*
Lykos, P. G., 186, *198*
Lyons, L. E., 94(168), *103*, 287(88), *333*

M

McAlister, A., 376(73), *454*
McArdle, J., 356(17), 377(17), *452*
McCapra, F., 27(19a), *100*
McCarville, M. E., 282(85), 285(85), *333*
McClure, D. S., 94, *103*, 281(81), *333*, 347(6), 358(6), 360(6), 401(6,134), 406(6), 411(6,134), 415(134), 417(6), 419(134), 432(201), 449(240), *452*, *456–458*
McConnell, H., 70(118), 71(118), *102*, 276(76), 298(104), 300(108,109), 326(162), *333*, *334*, *336*
MacDonald, J. C. F., 19(7), *99*
McEwen, K. L., 252(37), *332*
McGlynn, S. P., 54(33), *100*, 298(100), *334*, 390(113,114), 391(113,114), 404(140,144), 413(163), 431(196), 442(196), *455–457*
Mackor, E. L., 305(131), *335*
McMurry, H. L., 70(95a,95b), 73(95a, 95b), 75–77(95b), 194(77), *198*, 245(23), 246(23), *331*

McRae, E. G., 312(145), 313(145), 315, 322(160,161), 327(160), *335*, *336*, 354 (13), 355(13), 450, 451(242), *452*, *458*
McVicker, W. H., 27(18), *99*
Mader, P. M., 73(126), 74, 75(126), *102*, 250(27), *331*
Mager, K., 390
Maki, A., 403(132), *455*
Malhotra, S. S., 68(86), *101*
Mangini, A., 292
Mangum, B., 401(136), 402(128), 405 (136), *455*, *456*
Mann, D. E., 184, *198*, 289(91), *333*
Mannhardt, H., 65(67), *101*
Margenau, H., 112(3), *196*
Mariella, R. P., 77(134), *102*, 247
Markgraf, G., 256
Marsh, J. K., 27(18), *99*
Martin, R., 447(232), *458*
Maruyama, Y., 268(62), *332*
Mason, J., 253
Mason, S. F., 73(123), 95(177), 96(177, 180), *102*, *103*, 295(97), 297, 304(127), *330*, *334*
Mataga, N., 354(12), 355(14), *452*
Matovich, E., 389(104), *455*
Matsen, F. A., 185, *198*, 199, 201(1), 259 (45), 260, 263(46,48), 264(46), 265(53), 266(56), 267(58,59,61), 269(56,59), 287 (90), 288(90), 298(105), 301(114), 302 (119), 303(119), *330*, *332–334*
Matsubara, I., 276(74), *333*
Mayer, M. G., 259(43), *332*
Mayer-Pitsch, E., 256
Meakins, G. D., 63(60), *100*
Mecke, R., 160(14), *196*
Mees, K. E. C., 311(147), 314(147), *335*
Melhuish, W. H., 310(141), *335*, 346(3), 347(3,7), 358(3), 360(3), 361(3,7), 401 (3), *452*
Mellon, M. G., 3(1), *99*
Merkel, E., 253
Merritt, E., 350(8a), *452*
Meyer, B., 389(106a), *455*
Miller, J. R., 317(152), *335*, 356(21), *453*
Minkoff, G. J., 253
Mizushima, W., 95(176), *103*
Moe, G., 168(23a,23c), *197*, 228(10), 240 (17), *331*
Moffatt, M. E., 302(118), *334*
Moffitt, W. E., 168(24,25), *197*
Montanari, F., 292
Moodie, N., 390(109), *455*
Morachevsky, A., 384(96), *454*
Morrell, S. H., 281(83), *333*
Morris, G. C., 287(87), *333*
Morris, J. C., 243
Morse, P. M., 40(27), 41, *100*
Morton, R. A., 281(83), *333*
Mosby, W. L., 281(83), *333*
Moskowitz, J. W., 179(38), *197*
Mottl, J., 236, 247, 269(57), *332*
Mulliken, R. S., 44(30), 55, 62(53,54), 70 (94), *100*, *101*, 183, 184(49), 189, 192–196, *197*, *198*, 228(10), 230(13), 236, 239(15), 240(17), 242(19), 244(20), 245 (23), 246(23), 298(100,107), *331*, *334*, 431(197), 442(197), *457*
Munro, I., 364(39), *453*
Murgenan, H., 214
Murphy, G. M., 112(3), *196*, 214
Murrell, J. N., 88(157), 89(159), *103*, 208 (5), 224, 228(5), 255, 263(46), 264(46), 268(65), 274(65), 290, *330–332*
Music, J. F., 185(54), *198*, 267(59,61), 269(59), *332*

N

Nachod, F. C., *330*
Nagakura, S., 60(52), 61(52), 86(146), 88 (155,156), *100*, *103*, 242, 243, 245(22), 251, 252(36), 256(39), 268(62–64), 274 (63,73), 276(76), *331–333*
Nakamizo, M., 363(35), 364(35), *453*
Nakayama, T., 236, 247, 269(57), *332*
Nichols, E. L., 350(8a), *452*
Nielsen, A. T., 81, *102*, 250(33), *332*
Nitkitin, A., 358(27), *453*
Nonaka, M., 249
Nordheim, G., 22(11), *99*, 165(16), *196*
Noyce, D. S., 292
Noyes, W., 415(169), 445(225,226), 446 (225), *456*, *458*
Nurmukhametov, R., 366(49), 367(49), 407(154), *453*, *456*

O

O'Donnell, C. M., 54(33), *100*
O'Dwyer, M., 406(152b,153), *456*
Öpik, V., 168(24), *197*

Oesterlin, H., 370(54), 371(54), 416(54), *453*
Ohnesorge, W., 384(93), *457*
Okabe, H., 415(169), *456*
O'Konski, C. T., 310(138), *335*
Oksengorn, B., 328(167), *336*
Olah, G. A., 302(118), *334*
Olness, D., 401(135), 411(135), *456*
Orchin, M., 85, *103*, 245(21), 249, 275, 278, 282–286, 288, 294, *330*, *331*
Orgel, L. E., 276(75), 277(75), 301(110), *333*, *334*
Orloff, D., 183(47), *197*
Orloff, H., 183(47), *197*
Orloski, R., 81(140), *102*
O'Shaughnessy, M. T., 90(162), *103*

P

Paddock, E., 191(70), *198*
Padhye, M., 404(144), *456*
Paik, U., 253
Pakkarinen, L., 435(205), 436(205), 438 (205), 439(205), 441(205), *457*
Pappalardo, G., 292
Pardee, A., 376(69), *454*
Paris, J., 419(185a), 421(185a), *457*
Pariser, R., 185, *198*, 328(165), *336*, 435 (209), 436(209), *457*
Parkin, J. E., 295(97), 297(97), *334*
Parr, R. G., 179, 181, 185, 186, *197*, *198*, 201, 204(3), 205(4), 229, *330*
Parry, F., 250(29), *332*
Passerini, R., 292
Paton, J. W., 96(179), *103*
Patterson, J., 447(232), *458*
Pauling, L., 35(25), *100*, 110(2), 182, 188 (67), *196–198*, 263(47), 264(51), 319 (157), 320(157), *332*, *335*
Pavlopoulpos, T., 409(159), *456*
Pearce, S., 310(142), 314(142), *335*
Person, W. B., 55, *100*, 298(100), *334*
Personov, R., 357(24), 363(24), 407(155), *453*, *456*
Peters, D., 239
Petruska, J., 270(67), 271(68), *333*
Phillips, J. P., *330*
Piatnitskii, B., 414(164), *456*
Pickett, L. W., 25(14), 61(49), 62(56), 71 (99), 90(161), *99–101*, *103*, 191(70), *198*, 236, 246(25), 291, *331*, *333*
Piette, L., 403(130), *455*
Piliugin, G. T., 239
Pimentel, G. C., 70(120), 71(120), *102*, 326(164), *336*
Pippen, E. L., 249
Pisknov, A., 403(131), *455*
Pittman, C. U., 302(118), *334*
Pitts, J. N., Jr., 71(98,103,112,113), 78 (135), 86(145,148,149), *101*, *102*, 403 (130), 417(172), 418(172), 447(232), 448 (172), *455*, *456*, *458*
Platt, J. R., 59(40), *100*, 184–187, 191(71), *197*, *198*, 226(9), 230, 258, 266, 268, 270(67), 277(79), 280(79), 281, 282(80), 283, 287(80), 289(91), 292, 293, 295, 296, 298(104), 300(109), 315(149), *331*, *333–335*, 404(143), *456*
Plattner, P. A., 281(83), 290(92), *333*
Polgár, A., 64(66), *101*, 319(157), 320 (157), *335*
Pongratz, A., 256
Pople, J. A., 70(97), *101*, 169(28), 194 (79), *197*, *198*
Popovych, O., 384(94), *454*
Porret, D., 61(51), *100*, 243
Porter, G., 392(121), 434–437(203), 440 (211,212), 441(211,212), 443(216,217), 444(217), 445(222), 446(231), 447(231), 449(241), 450(241), *455*, *457*, *458*
Poshusta, R. D., 201(1), *330*
Potts, W. J., Jr., 45(31), 59(41), 62(58), *100*, 230(13), 236, *331*
Price, D. R. W., 61(44), *100*, 243
Price, H. A., 80(139), *102*
Price, W. C., 57(38), 64(64), *100*, *101*, 236, 242(19), 243, *331*
Pruckner, F., 377(76), *454*
Pryce, M. H. L., 168(24), *197*
Puchov, V., 366(49), 367(49), *453*
Pullman, A., 60(42), *100*, 188(67), *198*
Pullman, B., 60(42), *100*, 188(67), *198*
Pyl, T., 374(60), *454*

R

Rabinowitch, E., 310(137), 315(150), 317 (150), *335*, 377(86), 382(91,92), *454*
Raffy, A., 377(84), *454*
Raisin, C. G., 155(13), *196*
Rajogopolan, S., 66(77), *101*

Ramsay, D. A., 12, *99*, 167(20), 169(20), *197*
Rao, C. N. R., 70(117), 72(117), *102*
Rapala, R. T., 249
Rasmussen, R. S., 239(15), *331*
Raube, R. R., 77(134), *102*, 247
Reagan, H., 97(181), *103*, 265(54), *332*
Reagan, P. N., 201(1), *330*
Recktemvala, G., 447(232), *458*
Rector, C. W., 184, *197*
Reichel, A., 373(56), *454*
Reichstein, T., 71(104), *102*
Reid, C., 70(100), *101*, 246(26), *331*, 390 (108,109), *455*
Reinebeck, L., 27(19), *99*
Remington, W. R., 265(54), *332*
Reynolds, M., 431(196), 442(196), *457*
Richards, E., 376(72), *454*
Richtol, H., 415(169a), *456*
Rieke, C. A., 44(30), *100*, 183(47), 184 (49), 189(68), 194(68), *197*, *198*, 236
Robertson, W. W., 185(54), *198*, 259 (45), 260, 263(48), 265(53), 266(56), 267 (59), 269(56,59), 322(158), 328(166,168), *332*, *335*, *336*
Robin, M. B., 230
Robinson, G. W., 246(24), *331*, 404(137), 405(145,146,149,150), 406(151), 418 (180), 442(146), 443(149,150), *456*, *457*
Rodebush, W. H., 90(162), *103*
Rössler, G., 76(136), 79(136), *102*
Rogers, L., 366(48), 384(93,94), 393, 450, *453*, *454*
Rogers, M. T., 267(60), *332*
Romand, J., 243
Roothaan, C. C. J., 172(30), 179, 183, *197*
Rose, G. G., 254, 256(38), *332*
Rosebrook, D., 392(122), 419(122), 450 (122), *455*
deRosen, A. L., 319(157), 320(157), *335*
Rosenbaum, J., 302(120,121), *334*
Ross, I. G., 179(37), 181, *197*, 369(52b), 435(204), *453*, *457*
Rothman, W., 430(195a), *457*
Rotzler, G., 71(104), *102*
Ruedenberg, K., 188, *198*
Ruff, O., 253, 255
Rumpf, K., 160(14), *196*
Rushbrooke, G. S., 182, *197*, 290(93), *333*
Ryder, E., 292

S

Sack, R. A., 168(24), *197*
Sackter, E., 191(70), *198*
Sado, A., 276(74), *333*
Saganenko, A., 441(214), 442(214), *457*
Sahu, J., 365(42), 366(42), *453*
Saksena, B. D., 71(110a), 73–75(110a), *102*, 247, 251
Salem, L., 201(6), 208(6), 232(6), *331*
Sancier, K. M., 298(103), *334*
Sandorfy, C., *330*
Sandros, K., 415(168), 445(223), 447 (234), *456–458*
Sarkanen, K., 435(202), 438(202), 439 (202), *457*
Sartori, G., 251
Scheibe, G., 61(50), 67(82), 76(136), 79 (136), *100–102*, 310(136), 314, *335*
Schiller, J. C., 298(105), *334*
Schmillin, A., 390
Schmitt, R., 419(185a), 421(185a), *457*
Schriesheim, A., 304(128), *335*
Schroeder, W. A., 319(157), 320(157), *335*
Schüler, H., 27(19), *99*
Schwarz, W. M., Jr., 96(179), *103*
Scorez, J. A., 96(179), *103*
Scott, A. J., *330*
Scott, D. R., 199, 300(113), 301(111,113), 302(113), *334*, 389(106), *455*
Seliger, H. H., 27(21), *100*
Semenow, D. A., 61(49), 62(57), *100*, 291, *333*
Sevechenko, A., 384(96), *454*
Sharp, J., 403(130), *455*
Sheinker, Y. N., 86(153), *103*
Sherman, J., 182(44), *197*
Shigorin, D., 366(49), 367(49), 403(131), *453*, *455*
Shimada, R., 95(176), *103*, 408(157), *456*
Shiner, V., 236
Shinkerenka, S. V., 239
Shoppee, C. W., 74(128), *102*
Shore, V., 376(69), *454*
Shpol'skii, E., 357(24), 363(24,34), 407 (155), *453*, *456*

Shull, H., 263(46), 264(46), *332*, 418(174), 419(174), 429(192,193), *456*, *457*

Sidman, J. W., 70(97), 94(171), *101*, *103*, 194(79), *198*, 245(23), 246(23), *331*, 409 (158), 418(175), *456*

Siegel, S., 406(152a), 442(152a), *456*

Silber, P.., 446(230), *458*

Simpson, W. T., 187, 188, *198*, 311–313 (144), *335*, 451, *458*

Singh, I. S., 287(87), *333*, 404(142), 416 (170), 425(170), *456*

Sklar, A. L., 22(11), *99*, 165(16,17), 178–180, 185, *196*, *198*, 259(43), 264(52), 269(66), *332*, *333*

Skrabal, R., 72(121), *102*, 247, 251

Slater, J. C., 172(29a), 177(29), 178(34), *197*

Smakula, A., 64(64a), 65(68,70,71), 67 (64a), 77(132), *101*, *102*

Smiley, R. A., 253

Smith, J., 377(89), 389(106a), *454*, *455*

Smith, J. C., 281(83), *333*

Smith, J. H., 315(150), 317(150), *335*

Snider, N., 393–395(123), 450(123), *455*

Sommer, L. H., 263(50), *332*

Sondheimer, F., 64(65), *101*

Specker, H., 362(32), *453*

Sponer, H., 22, 41(28), *99*, *100*, 164(15), 165(16), *196*, 401(135), 411, *456*

Sprague, R. H., 97(183), *103*

Steel, C., 440(210), *457*

Steiner, R., 376(73), *454*

Stern, A., 316(151), 317(152), *335*, 377 (76), *454*

Stern, E. S., 82(144), 85, *102*, *330*

Stevens, B., 364(40), 401, 445(224), 446 (224), 447(233), *453*, *458*

Stevenson, P. E., 271(68), 272–274(69), 276(75), 277(75), *333*

Stewart, A. W., 27(18), *99*

Stich, K., 71(104), *102*

Stieglitz, J., 234, *331*

Streitwieser, A., Jr., 201(6), 208(6), 232 (6), *330*, *331*

Strickler, S., 55, *100*, 351–353(2), 406 (152b,153), *452*, *456*

Strohmeier, W., 247

Stucklen, H., 62(55), *100*

Style, D. W. G., 253, 257(41), *332*

Sugden, T. M., 267(61), *332*

Sun, H., 168(23a), *197*

Suzuki, C., 389(104), *455*

Svetashev, K., 410(160), 411, *456*

Switashev, K., 360(45), 365(45), *453*

Symons, M. C. R., 302(120,121), *334*

T

Takenoshita, Y., 408(157), *456*

Tanaka, J., 88(155,156), *103*, 243, 245(22), 251, 252(36), 268(63), 274(63), 287(88), *331–333*

Tanaka, M., 252(36), *332*

Tannenbaum, E., 61(48), *100*, 243

Taylor, G. R., 204(3), *330*

Taylor, L. W., 62(59), 63(59), *100*

Taylor, R., 447(232), *458*

Teagan, J. P., 243

Teale, F., 347(5,8), 361(8), 374(61), 375 (65), 376(68), *452*, *454*

Tedder, J. M., 208(5), 228(5), *331*

Teller, E., 22(10,11), *99*, 164(15), 165(16), 167, *196*, *197*

Terenin, A., 417(171), 418(171), 444(221), 445(221), 448(237), *456*, *458*

Terwilliger, M. A., 61(43), *100*, 243

Thomas, M., 401

Thomson, J. W., 155(13), *196*

Thorn, G. D., 256(40), *332*

Toerber, W., 373(57), *454*

Tolgyesi, W. S., 302(118), *334*

Totte, W. T., 236

Trajmar, S., 13(5), *99*

Trofimov, A., 384(96), *454*

Trumpler, G., 249

Tsubomura, H., 243, 245(22), 268(64), *331*, *332*

Tsumbora, H., 431(197), 442(197), *457*

Tunnicliff, D. D., 239(15), *331*

Turner, D. W., 63(61), *101*

Turro, N., 448(235,236), *458*

Tye, F. L., 304(126), *334*

U

Udenfriend, S., 375(64), 376(64), *454*

Uehleke, H., 376(74), *454*

Uhlich, U., 253

Ungnade, H. E., 253, *330*

Urbanski, T., 86(147), *103*

V

Vahlensieck, H., 390(111), *455*
Vandenbelt, J. M., 272(70,71), *333*
Van Duuren, B., 368(50), *453*
Van Zandt, G., 97(183), *103*
Varsany, F., 384(99), *455*
Velick, V., 376(70), *454*
Velthorst, N. H., 305(131), *335*
Vember, T. M., 365(44), 444(220), *453*, *458*
Viktorova, E., 441(214), 442(214), *457*
Vincent, J., 403(132), *455*
Virgin, H., 377(89), *454*
Viswanath, G., 350(10), *452*
Vittum, P. W., 25(16), *99*
Vladimirov, Y., 375(66), *454*
Vodar, B., 243
Volkert, G., 71(108), *102*
Volkova, N., 403(131), *455*
Volman, D. H., 86(151), *103*
Voloshina, V., 373(57), *454*
deVries, L., 81(140), *102*

W

Waals, J. van der, 401(129), 402(129), 405(147), *455*, *456*
Wagner, J., 72(121), *102*, 247, 251
Wagnière, G., 81(141), *102*
Walker, B. H., 292
Walsh, A. D., 62(63), 64(64), 70(96), *101*, 240(17), 243, 267(61), *331*, *332*
Walsh, J. R., 281(82), 287(82), *333*
Walter, G. F., 25(14), 90(161), *99*, *103*
Walter, J., 108(1), 129, 145(9), 149(11), *196*
Ware, W., 362(29b), *453*
Watanabe, K., 236, 247, 269(57), *332*
Watson, A. T., 287(90), 288(90), *333*
Watson, W., 356(17), 377(17), *452*
Weber, G., 347(5,8), 361(8), 374(61), 376 (68,71), *452*, *454*
Wehry, E., 393, 450
Weijland, W. P., 305(131), *335*
Weinstock, B., 168(26), *197*
Weissberger, A., 25(16), 26, *99*
Weissler, G. L., 168(23a), *197*
Weissman, S., 384–386(95), 426(188), 427 (188), *454*, *457*
Weller, A., 392(116–120), 393(116), 394 (116), *455*
Welsh, H. L., 19(7), *99*
Wenderlein, H., 316(151), *335*
Wentworth, W. E., 287(90), 288(90), *333*
Wepster, B. M., 89(158), 97(158), *103*
West, T. F., 79(138), *102*
West, W., 1, 310(142), 314(142), *335*
Whan, R., 384(98), 385–387(98,101), 389 (98,101), 426(98,101), 427(98,101,189), *455*, *457*
Wheeler, O. H., *330*
Wheelock, C., 373(59), *454*
Wheland, G. W., 182(44), *197*, 263(47), *332*
White, A., 374(62), 375(62), *454*
White, F. C., 97(183), *103*
Whitear, B., 304(125), *334*
Whiting, M. C., 68(86), 69(90,92,93), *101*
Wieder, G. M., 61(149), *100*, 291, *333*
Wilkinson, F., 414(165), 415(165), 417 (165), 440(212), 441(212), 445(222,227), 446(231), 447(212), *456–458*
Wilkinson, P. G., 62(53), *100*, 230(13), 236, *331*
Willenberg, W., 253, 255
Williams, A., 358(28), *453*
Williams, R., 365–367(41), 373(41), 404 (138), 409(41), 444(19), *452*, *453*, *456*
Wilson, C. L., 155(13), *196*
Wilson, E. B., 35(25), *100*, 110(2), *196*
Windsor, M., 388(103c), 401, 434–437 (203), *455*, *457*
Winstein, S., 81(140), *102*
Winston, H., 94(169), *103*
Wirth, H., 368(51), *453*
Witt, O. N., 56, *100*
Wolf, K. L., 71(102,105), 86(152), *102*, *103*
Wolovsky, R., 64(65), *101*
Wood, F. L., 74(127), *102*
Woodward, R. B., 66, 76, 79(137), *101*, *102*, 240(16), 250(30), *331*, *332*
Wright, M., 405(145,149), 440(211), 441 (211), 443(149), *456*, *457*
Wu, G. S., 71(106), *102*
Wulff, V., 435(207), 438(207), *457*

Y

Yuster, P., 384–386(95), 426(188), 427(188), *454*, *457*

Z

Zander, M., 401
Zandstra, P. J., 305(131), *335*
Zanker, V., 310(140), *335*, 373(56,58), *454*
Zechmeister, L., 64(66), *101*, 319(157), 320(157), *335*
Zhmyreva, I., 441(214), 442(214), *457*
Zimmerman, G., 253
Zobel, C. R., 61(50a), *100*, 168(23b), *197*, 243
Zscheile, F. P., 315(150), 317(150), *335*, 377(85), *454*

SUBJECT INDEX

A

Absorbance, 8
  molar, 46
Absorption, pressure-induced, 20
  of radiation, 2, 3
    theory, 37, 46, 49, 146, 189, 268–272, 351, 395, 427, 433, 450 (see also *Selection rules*)
Absorption band, α-band of aromatic hydrocarbons, 277, 279
  β-band of aromatic hydrocarbons, 277, 279
  half width, 54
  "hot," 328
  x and y, 94
Absorption coefficient, 191
  integrated, 191 (see also under *Extinction coefficient*)
Absorption spectrum, see *Spectrum, absorption*. For spectra of compounds, see under individual compounds.
Absorptivity, molar, 8
Acenes, absorption spectra, 287
Acetaldehyde, absorption spectrum, 70, 71, 247, 248
  ionization energy, 247
Acetamide, absorption spectrum, 71, 72, 247, 251
  ionization energy, 247
Acetic acid, absorbtion spectrum, 71, 247
  ionization energy, 247
Acetic anhydride, absorption spectrum, 71
Acetone, absorption spectrum, 71, 243, 247, 248
  fluorescence, 369
  ionization energy, 243, 247
  phosphorescence, 417
  as solvent, 98
  solvent effects on spectrum, 72, 327
Acetone–acetyl-, absorption spectrum, 71
  rare earth complexes, 384
Acetone–benzoyl-, rare earth complexes, fluorescence, 485
Acetone–ethylidene-, absorption spectrum, 77
Acetone–phenyl-, absorption spectrum, 86, 88
Acetonitrile, as solvent, 98
Acetophenone, absorption spectrum, 86, 88
  phosphorescence, 417
  triplet states of, 437
Acetyl bromide, absorption spectrum, 71, 247
  ionization energy, 247
Acetyl chloride, absorption spectrum, 71, 72, 247
  ionization energy, 247
Acetylene, absorption spectrum, 167, 240
  electronic configuration, 240
  hybridization in, 210
  ionization energy, 241
  molecular orbitals of, 240
Acetylene–phenyl-, absorption spectrum, 69, 269
  ionization energy, 269
Acid anhydrides, absorption spectrum, 71
Acid chlorides, absorption spectrum, 71, 72, 74, 247
Acids, aliphatic, absorption spectra, 71
Acridine, absorption spectrum, 95, 296
  fluorescence, 356, 357, 372
  pK_a of excited states, 393, 450
Acridine–9-amino-, fluorescence, 353
Acridine–dihydro-, phosphorescence, 419
Acridine orange, triplet-triplet absorption, 438
Acridine orange dimer, absorption spectrum, 310
Acridone, fluorescence, 353, 373
Acrolein, absorption spectrum, 76, 77, 248
Acrylic acid, absorption spectrum, 81
Aldehydes, absorption spectra, 71, 75, 77, 246 *et seq.*
Alcohols, absorption spectra, 60, 242
Aliphatic compounds, fluorescence, 357
Alkyl halides, absorption spectra, 33, 59, 60, 242

Allyl alcohol, absorption spectrum, 62
Allyl system, molecular orbitals, 233
Alternant hydrocarbons, 287, 288, 305, 404
Amides, absorption spectra, 71, 247
Amines, absorption spectra, 60, 243
Ammonia, absorption spectrum, 243
  ionization energy, 232, 243
Angstrom (unit), 4
Angular momentum, 110, 117, 128, 139
Aniline, absorption spectrum, 86, 88, 262, 268
  charge-transfer band, 268
  fluorescence, 365
  phosphorescence, 410
Anilines–nitro-, absorption spectra, 97
Anilines–nitrodimethyl-, absorption spectra, 87, 89
Anilinium ion, absorption spectrum, 86, 88, 262
Anisole, fluorescence, 366
  phosphorescence, 410
Anthracene, absorption spectrum, 92, 282, 283
    solvent effects on, 324
  fluorescence, 350, 358, 360, 361, 400
  fluorescence quantum yield, 358, 360, 400
  phosphorescence, 400
  photodimerization, 443
  photooxidation, 444
  triplet states of, 437
  triplet-triplet absorption, 434
Anthracenes–amino-, absorption spectra, 284
Anthracene anion, absorption spectrum, 305
Anthracenes–benz-, absorption spectra, 92, 287
  triplet states of, 437
Anthracene–benz(*a*)-, fluorescence, 361, 362, 400
  phosphorescence, 400, 412
Anthracene–9-bromo-, fluorescence, 360
Anthracene cation, absorption spectrum, 305
Anthracene–9-cyano-, fluorescence, 360
Anthracene–dibenzo(*a*,*h*)-, phosphorescence, 400
Anthracenes–dichloro-, fluorescence, 365
Anthracece–dimethyl-, fluorescence, 360
Anthracene–9,10-diphenyl, absorption spectrum, 285
Anthracenes–methyl-, fluorescence, 365
Aromatic amino acids, fluorescence, 374
Aromatic compounds, absorption spectra, 85, 258 *et seq.*, 277 *et seq.*
  fluorescence, 358, 365 *et seq.*
  phosphorescence, 400, 403, 407 *et seq.*
  triplet states, 437
Aromatic free radicals, absorption spectra, 303
Aromatic hydrocarbons, absorption spectra, 277 *et seq.*
  fluorescence, 358 *et seq.*
  fluorescence lifetime, 361
  fluorescence quantum yield, 360
  ionization energy, 287
  molecular orbitals, 278 *et seq.*
  molecular states, 280
  phosphorescence, 391, 400, 403 *et seq.*
  phosphorescence lifetimes, 391, 400
  phosphorescence quantum yields, 400
  quasi-linear fluorescence spectra, 363
Aromatic ions, absorption spectra, 303, 304
Atomic orbital, 108, 329
Auxochrome, 68, 220, 306
Auxochromic effect of dialkylamino group, 68
Azides, alkyl, absorption spectra, 85
Azo compounds, absorption spectra of alkyl derivatives, 83, 84, 255, 257
  molecular orbitals, 253, 256
  n-π^* bands of, 253
Azulene, absorption spectrum, 289, 290
    pressure effect on, 327, 328

B

Balmer series, 107
Beer's Law, 8, 45
Benzaldehyde, absorption spectrum, 86, 249
  phosphorescence, 417
  triplet states of, 437
  triplet-triplet absorption, 439
Benzaldehyde–*o*-hydroxy-, phosphorescence, 417

Benzaldehydes–nitro-, absorption spectra, 87
Benzamide, phosphorescence, 408
Benzene, absorption spectrum, 13, 22–24, 86, 92, 165, 166, 181, 257 *et seq.*, 268, 269, 281, 295
    effect of alkyl substitution, 260, 266
    effect of chloralkyl substitution, 267
    effect of unsaturated groups, 267
  electronic configurations, 258
  fluorescence, 358, 361, 400, 410
  fluorescence lifetime, 361
  fluorescence quantum yield, 358, 400, 410
  ionization energy, 269
  molecular orbitals, 178, 179, 183, 185, 219, 257, 258
  phosphorescence, 400, 406, 410
  photochemical reactions, 449
  as solvent, 98
  symmetry of, 155
  triplet states, 404, 437
Benzenes–amino-, fluorescence, 365
Benzenes–azo-, absorption spectra, 87, 90, 253, 256, 297
  fluorescence, 367
Benzenes–bromo-, phosphorescence, 410
Benzenes–butyl-, absorption spectra, 260, 269
  ionization energy, 269
Benzenes–chloro, absorption spectra, 86, 266
    intensities, 270
    phosphorescence, 410
Benzene–cyano-, absorption spectrum, 86
  fluorescence, 367
Benzene–cyclohexyl-, absorption spectrum, 269
Benzene–cyclopentyl, absorption spectrum, 269
Benzene–cyclopropyl-, absorption spectrum, 269
Benzene–ethyl, absorption spectrum, 260, 269
  effect of temperature and solvent, 321
  ionization energy, 209
Benzene–fluoro-, absorption spectrum, 266
  fluorescence, 360, 410
Benzene–hexamethyl, absorption spectrum, 86
  phosphorescence, 391, 410
    of charge-transfer complexes, 391
Benzene–iodine complex, charge transfer spectrum, 298
Benzene–iodo-, absorption spectrum, 86
  fluorescence, 365
  phosphorescence, 410
Benzene metal complexes, phosphorescence, 389
Benzene–nitro-, absorption spectrum, 86, 97, 252, 253, 255, 256, 268
  charge transfer band, 268
  phosphorescence, 408
Benzene–nitroso-, absorption spectrum, 87, 253
Benzenes–propyl-, absorption spectra, 260, 269
  ionization energy, 269
Benzenes, substituted, absorption spectra, 271 *et seq.*
  molecular orbitals, 185, 263 *et seq.*
    transition moments, 269 *et seq.*
Benzil, triplet states of, 437
  triplet-triplet absorption, 434
Benzoic acid, phosphorescence, 408, 410, 414
  triplet states of, 437
Benzoic acids–amino-, fluorescence, 366
Benzoic acids–hydroxy-, fluorescence, 366
Benzoin, phosphorescence, 417
  triplet-triplet absorption, 439
Benzophenone, absorption spectrum, 86, 249, 251
  energy transfer from, 445
  phosphorescence, 416, 417
  photochemical reactions, 418, 446–448
  as photochemical sensitizer, 447, 448
  triplet states of, 437
  triplet-triplet absorption, 434
Benzophenone–*o*-hydroxy-, rare earth complexes of, 384
p-Benzoquinone, absorption spectrum, 274, 275
  molecular orbitals, 276
  n-π^* transition, 276
Benzpinacol, 447
Benzylamine, absorption spectrum, 86
Benzyl anion, absorption spectrum, 304

Biacetyl, absorption spectrum, 73, 75, 250
  fluorescence, 369, 414
  phosphorescence, 414, 415, 417
  photochemical oxidation, 447
  sensitized fluorescence, 445
  sensitized phosphorescence, 446
  singlet-triplet absorption, 430
  triplet states of, 437
Biphenyls, absorption spectrum, 87, 90
  phosphorescence, 400, 411, 412
  triplet states of, 437
Biphenyls–fluoro-, phosphorescence, 411
Bohr's frequency equation, 9, 10, 13
Born–Oppenheim approximation, 10, 125, 163
Bromine molecule, electronic states, 131
Bromoform, absorption spectrum, 61, 243
  fluorescence, 358
  ionization energy, 243
Butadiene, absorption spectrum, 64, 66, 76, 238, 239
  fluorescence of aromatic derivatives, 358
  intensity of absorption, 195
  molecular orbitals, 238, 338, 339
  singlet-triplet absorption, 431
  transition moments, 239
Butadiene–diethylamino-, absorption spectrum, 68
Butadiene–tetraphenyl-, fluorescence, 358
t-Butane–nitro-, absorption spectrum, 253
Butenes, absorption spectrum, 62, 236
1-Butene-2-methyl-, absorption spectrum, 62
s-Butyl nitrate, absorption spectrum, 253

C

Camphor, absorption spectrum, 71
Camphor quinone, absorption spectrum, 75, 250
  phosphorescence, 418
Carbanions, absorption spectra, 302
Carbazole, phosphorescence, 417, 419
Carbonium ions, absorption spectra, 302, 303
Carbon monoxide, rotational spectrum, 15
Carbon tetrachloride, as solvent, 98
Carbonyl compounds, absorption spectrum, 70, 247 *et seq.*
  characterizing derivatives, absorption spectra, 82
  energy levels, 246
  energy transfer from, 444
  n-π^* transitions, 247
  phosphorescence, 414 *et seq.*
  phosphorescence lifetime, 417
  unsaturated, absorption spectra, 76, 77, 248, 249
Carboxylate ion, absorption spectrum, 72
β-Carotene, absorption spectrum, 64, 318
Carotenoids, absorption spectra, 318 *et seq.*
Cata-condensed hydrocarbons, 91
  free electron model of, 186
Catechol, fluorescence, 366
Character (of a group), 144, 146, 147, 149, 150, 152, 153, 158, 164
Charge density, 126, 127
Charge transfer absorption spectra, 193, 252, 268, 298 *et seq.*
Charge transfer complexes, 298 *et seq.*, 440
  fluorescence, 389 *et seq.*
  phosphorescence, 391, 413
  potential energy curves, 392
Chelates, see *Metal complexes*
Chemiluminescence, 27
Chlorins, absorption spectra, 317
Chloroform, absorption spectrum, 243
  ionization energy, 243
  as solvent, 98
Chlorophylls, absorption spectra, 315 *et seq.*, 318
  fluorescence, 356, 382
    solvent effect, 356
  phosphorescence, solvent effect, 416
  structure of, 383
  triplet-triplet absorption, 435, 438
Chromophore, 56, 201, 220, 306
Chrysene, absorption spectrum, 287
  fluorescence, 361, 362, 400
  phosphorescence, 400
  triplet states of, 437
Cinnamic acids, absorption spectra, 87, 89

Cis-absorption band, 65, 195
Cis- and *trans*-isomers, butadiene, 239
  carotenes, 318
  fluorescence, 367
  intensity of absorption bands, 65, 195, 196
  photochemical interconversion, 449
Citral, absorption spectrum, 77
Class (group theory), 158
Closed shell, 119
Combination bands, 19, 160
  selection rule, 160
Configuration, electronic, 119, 120, 131, 202
  even, 123
  odd, 123
Configurational interaction, 176, 180
Conjugated systems, absorption spectra, 63, 306 *et seq.*
    effect of chain length, 221, 222, 308
  molecular orbital theory, 221 *et seq.*
Conjugative red shift, 221, 308
Coronene, absorption spectrum, 92
  fluorescence, 361
  phosphorescence, 400, 403
  triplet states of, 437
Correlation, electron, 176
Coulomb integral, 115, 116, 231, 329
Coumarin, fluorescence, 373
Cresols, fluorescence, 366
Crotonaldehyde, absorption spectrum, 77, 327
    solvent effects on, 327
Crotonic acid, absorption spectrum, 81
Cyanine dyes, absorption spectra, 98, 307 *et seq.*, 311
Cyclohexadiene, absorption spectrum, 65, 239, 241
Cyclohexane, as solvent, 98
Cyclohexane–3-methylene-, absorption spectrum, 65
Cyclohexanone, absorption spectrum, 71, 247, 251
  ionization energy, 247
Cyclohexene, absorption spectrum, 62, 236
  ionization energy, 236
Cyclooctatetraene, non-aromaticity of, 303
Cyclooctatetraene–triaza-, fluorescence, 374
Cycloparaffins, absorption spectra, 69
Cyclopentadiene, absorption spectrum, 239, 240, 292, 293
  ionization energy, 292
Cyclopentadienyl metal complexes, absorption spectra, 301
  fluorescence, 389
Cyclopentanones, absorption spectra, 71, 78, 247
  ionization energy, 247
Cyclopentene, absorption spectrum, 238
Cyclopropane, absorption spectrum, 229

D

Decapentaene, absorption spectrum, 64
Degenerate state, 112, 130
Deuteration, effect on phosphorescence, 405
Diatomic molecule, correlation between molecular and atomic terms, 130
  dissociation energy, 137
  electronic spectrum, 21, 138
  molecular orbital theory, 124 *et seq.*, 211, 219
  resonance emission spectrum, 348
  rotational spectrum, 14, 132, 134
  symmetry, 129
  transition moment, 213
  vibrational eigenfunctions, 36
  vibrational energy, 35, 132, 134
  vibrational spectrum, 17, 19, 132
Diazo compounds, alkyl, absorption spectra, 83, 84
Dienes, absorption spectra, 65, 67, 239
Diethyl ether, as solvent, 98
Digonal orbitals, 210
Di-isoamyldisulfide, absorption spectrum, 61
Dimers (dye), absorption spectra, 310 *et seq.*
  emission spectra, 451, 452
  mixed, 314
  transition moment of, 313
Dimethylamine, absorption spectrum, 61
Dimethyl sulfide, absorption spectrum, 61
  as solvent, 98
1,4-Dioxane, absorption spectrum, 291
  as solvent, 98

Diphenylmethyl, absorption spectrum, 304

Dipole moment, 46, 47, 120, 170, 175, 309, 321
  of excited states, 355
  of transition, see *Transition moment*

Dipole radiation, 163

Dipole strength, 37, 50, 53, 190

Dispersion, 2

Dissociation energy, see *Energy dissociation*

Disulfides, absorption spectra, 60

Divinyl ether, absorption spectrum, 292

Dodecahexaene, absorption spectrum, 64

Durene, charge transfer complexes, phosphorescence, 391
  phosphorescence, 391, 410

Dyes, absorption spectra, 306 *et seq.*
  J-absorption band, 314

Dye aggregates, 310, 451, 452
  absorption spectra, 310, 314
  emission of, 451, 452

Dysprosium ion, fluorescence, 384

E

Eigenfunction, 34, 108, 203
  antisymmetric, 112, 113, 115
  atomic, 122
  classification, 145
  electronic, 169
  even, 130, 135
  odd, 130, 135
  orthogonal, 109
  symmetrical, 112, 113
  symmetry of, 135
  vibrational, 36

Eigenvalue, 111, 210

Eigenvector, 210

Einstein (unit), 6

Einstein coefficients, 51, 52, 351, 352

Electric moment, see *Dipole moment*

Electron configuration, see *Configuration*

Electron, nonbonding, 59 (see also *Orbital nonbonding*)

Electrons in molecules, classification, 57, 58, 126 *et seq.*, 194, 209, 230 (see also *Molecular orbitals*)

Electron volt (unit), 7

Electronegativity, 231–233

Electronic transitions, polarization of, 93, 94, 347

Emission of radiation, theory of, 46, 49, 342–345, 395

Emission spectra, see *Spectra emission*

Energy, dissociation, 41, 137, 175 (see values under individual compounds)
  electronic, 10, 20, 21, 120, 204, 205
  of excited states, 342
  orbital, 202, 207
  rotational, 10, 132, 133
  vibrational, 10
  zero point, see *Zero point energy*

Energy level, width, 320 (see also *Absorption band, half width*)

Energy of molecules, separability, see *Born–Oppenheim approximation*

Energy transfer, from carbonyl compounds, 444
  and photochemistry, 443 *et seq.*
  in rare earth complexes, 387

Ergostatriene, absorption spectrum, 66

Esters, absorption spectra, 71, 247

Ethane, absorption spectrum, 229
  energy levels of, 229
  ionization energy, 229, 232

Ethane–dibromo-, absorption spectrum, 61

Ethane–di-iodo-, absorption spectrum, 61

Ethanol, as solvent, 98

Ethers, absorption spectra, 60

Ethyl acetate, absorption spectrum, 71

Ethyl iodide, absorption spectrum, 242

Ethyl methyl ketone, absorption spectrum, 247
  ionization energy, 247

Ethyl phenyl ketone, phosphorescence, 417

Ethylene, absorption spectrum, 62, 230, 236
    effect of substituents, 231 *et seq.*
  energy levels, 233 *et seq.*
  hybridization in, 209
  ionization energy, 236
  structure, 167

Ethylene–dichloro-, symmetry, 153

Ethylene–tetrachloro-, fluorescence, 358

Ethylene–tetramethyl-, absorption spectrum, 62, 230

Ethylene–trimethyl-, absorption spectrum, 230
Ethylene oxide, absorption spectrum, 291
Ethylenic compounds, absorption spectra, 236 (see also *Olefins*)
  ionization energy, 236
Europium ion, fluorescence, 384
Europium ion complexes, fluorescence, 386, 388
Even function, 122
Exchange integral, 116, 206, 329
Excimer, 361
  fluorescence, 361, 364
Excited states, acid-base behavior, 392, 449, 450
Exciton, 450–452
External conversion, 344
Extinction coefficient (molar), 8, 44
  integrated, 48, 53, 352

F

f-value, see *Oscillator strength*
Fenchone, absorption spectrum, 71
Ferrocene, absorption spectrum, 301
  molecular orbitals, 301
  phosphorescence, 389
Flash photolysis, 439
Fluorene, absorption spectrum, 87, 91
  fluorescence, 400
  phosphorescence, 400, 407, 419
Fluorescein, fluorescence, 350
Fluorescence, 27, 338 *et seq.*, 348 *et seq.*
  decay time, see *Fluorescence lifetime*
  effect of aggregation, 452
  effect of deuteration, 362, 369, 370
  effects of solvents, 353 *et seq.*, 370
  effect of temperature, 362
  sensitized, 445
Fluorescence lifetime, 342–345, 348, 351–358, 361
  of aromatic hydrocarbons, 361
  measurement, 345
Fluorescence quantum yield, 344 *et seq.*, 360, 410, 411
  of aromatic hydrocarbons, 360, 410, 411
  measurement, 346, 360
Fluorescence quenching, 346 (see also *Internal conversion*, *External conversion; Transition, radiationless*)
Fluorescence spectra, mirror image relation, 349, 350
Force constant, 18, 133
Formaldehyde, absorption spectrum, 70, 71, 246, 247, 249
  fluorescence, 369
  ionization energy, 247, 249
  structure, 167
Formamide, absorption spectrum, 247
  ionization energy, 247
Formamide–dimethyl-, fluorescence, 358
  as solvent, 98
Formic acid, absorption spectrum, 247
  ionization energy, 247
Franck–Condon principle, 22, 28–33, 45, 69, 71, 163, 323, 349
Franck–Condon state, 354, 355
Free electron model, 186, 187, 224 *et seq.*, 280
Furane, absorption spectrum, 292, 293
  ionization energy, 292
Furane–tetrahydro-, absorption spectrum, 291
  as solvent, 98

G

Gadolinium ion, fluorescence, 384
Gallic acid, phosphorescence, 414
Gerade (even) states, 139, 145, 148, 202, 217
Glyoxal, absorption spectrum, 73, 75
Group theory, 139, 140, 145, 213
  multiplication table, 143, 214, 215

H

Harmonic oscillator, 30, 35, 133
Heavy atom effect on intersystem crossing, 405, 407, 408, 413, 430–433, 441, 442
Helium atom, orbital theory, 113, 204 *et seq.*
Heptane, as solvent, 98
Heterocyclic compounds, absorption spectra, 95, 291 *et seq.*
  fluorescence, 368, 371 *et seq.*
  phosphorescence, 418 *et seq.*
Hexacene, absorption spectrum, 92
Hexadecaoctaene, absorption spectrum, 64

1,5-Hexadiene, absorption spectrum, 62, 63
Hexane, as solvent, 98
1,3,5-Hexatriene, absorption spectrum, 64
  fluorescence of aromatic derivatives, 358
  molecular orbitals of, 225
  singlet-triplet absorption, 431
1,3,5-Hexatriene–diphenyl, fluorescence, 358
Hexene, absorption spectrum, 62, 230
Hund's rule, 340
Hybridization of atomic orbitals, 209
Hydrocarbons, condensed ring absorption spectra, 91, 277 *et seq.*
  saturated, absorption spectra, 59, 228
Hydrogen atom, Bohr theory of, 106
  quantum mechanical theory of, 108, 203 *et seq.*
  spectrum, 107
Hydrogen bromide, absorption spectrum, 243
  ionization energy, 232, 243
Hydrogen chloride, absorption spectrum, 243
  ionization energy, 232, 243
  rotation-vibration spectrum, 17
Hydrogen cyanide, structure, 167
Hydrogen fluoride, electronic configuration, 208, 209
  electronic transitions, 226
  ionization energy, 232
Hydrogen iodide, absorption spectrum, 243
  ionization energy, 232, 243
Hydrogen molecule, electron states of, 131, 227
  intensities, 192
  molecular orbital theory, 227
  ortho-form, 137
  para-form, 137
  symmetry properties, 136
Hydrogen molecule ion, molecular orbitals, 126, 127, 227
Hydrogen sulfide, absorption spectrum, 243
  ionization energy, 232, 243
Hydroquinone, fluorescence, 366
Hyperconjugation, 235 *et seq.*, 266, 267
  in benzene compounds, 266, 267

I

Icosadecaene, absorption spectrum, 64
Imidazole, absorption spectrum, 292
Indene, phosphorescence, 419
Indole, fluorescence, 371
  phosphorescence, 419
  pK_a of excited states, 392
Indoles–aza-, fluorescence, 371
Inductive effect, 234, 262, 263
Intensity, of electronic transitions, 121, 189
  of molecular spectra, 44, 45, 146, 351 *et seq.* (see also *Selection rules*)
  of substituted benzene spectra, 269 *et seq.*
  units, 7
  of vibronic bands, 36, 39, 163
Internal conversion, 344, 346, 349, 350, 362
Intersystem crossing, 397
  effect of oxygen, 399
  effect of paramagnetic perturbations, 399
  heavy atom effect on, 398, 431–433
  solvent effect, 356, 357, 414, 415, 441, 442
Inversion, 142, 202
Iodine complexes, charge transfer spectra, 298
Iodoform, absorption spectrum, 61
Ionization energy, of aliphatic compounds, 232
  of aromatic hydrocarbons, 287
  and charge-transfer spectra 299
  of heterocyclic compounds, 292
  of substituted benzenes, 269
Isomers, *cis* and *trans*, absorption spectra, 65, 73, 89, 90
Isooctane, as solvent, 98
Isopropanol, as solvent, 98
Isoquinoline, absorption spectrum, 296
Isoxazole, absorption spectrum, 292

J

j,j-coupling, 118
Jahn-Teller effect, 167, 168

K

Kayser (unit), 5
Kerr cell, 345

Ketene, absorption spectrum, 72
Ketones, absorption spectra, 71, 74–78, 250 (see also *Carbonyl compounds*)
  aliphatic, phosphorescence, 417
Kilokayser (unit), 5

L

Laplace operator, 108
Lifetime, of excited states, 53, 55, 342, 351 *et seq.*, 398 (see also *Fluorescence lifetime; Phosphorescence lifetime*)
Lophine, chemiluminescence, 27
Lorentz–Lorenz equation, 48
Luminal, chemiluminescence, 27
Lycopene, absorption spectrum, 319, 320
Lyman series, 107

M

Matrix element, 50
Matrix operators, 214
Matrix representation of Hamiltonian function, 210
Maxwell–Boltzmann equation, 51
Mercaptans, absorption spectra, 60, 243
Merocyanine dyes, absorption spectra, 309
    effect of solvents, 309
Mesityl oxide, absorption spectrum, 77
Metal complexes, absorption spectra, 301
  fluorescence, 377 *et seq.*
Metalloporphyrins, absorption spectra, 317
Methane, hybridization in, 209
  ionization energy, 228, 232
  orbital theory, 218
  symmetry of, 218
Methane–azo-, absorption spectrum, 253, 255
Methane–dibenzoyl-rare earth complexes,
  flurorescence, 385, 386
Methane–dibenzoyl-metal complexes, phosphorescence, 426
Methane–diphenyl-, fluorescence, 358
Methane–nitro-, absorption spectrum, 253–256
Methane–nitroso-, absorption spectrum, 252, 253
Methane–nitrosotrifluoro-, absorption spectrum, 253
Methane–tribenzoyl-, rare earth complexes of, 385
Methanol, absorption spectrum, 61, 243, 244
  ionization energy, 232, 243
  as solvent, 98
Methyl acetate, absorption spectrum, 247
Methylamine, absorption spectrum, 61, 243
  ionization energy, 232, 243
Methyl benzoate, phosphorescence, 408
Methyl bromide, absorption spectrum, 61
  ionization energy, 232
Methyl chloride, absorption spectrum, 61
  ionization energy, 232
Methyl ethyl ketone, phosphorescence, 417
Methyl fluoride, ionization energy, 232
Methyl formate, absorption spectrum, 247
Methyl iodide, absorption spectrum, 61, 242
  ionization energy, 232
Methyl mercaptan, absorption spectrum, 61, 242
  ionization energy, 232, 243
Methyl–triphenyl-, absorption spectrum, 304
Methyl vinyl ketone, absorption spectrum, 77
Methylene blue, dimer absorption spectrum, 310
Millimicron (unit), 4
Mirror image relation, in fluorescence spectra, 349, 350
  in phosphorescence spectra, 428
Molecular orbital, for homopolar diatomic molecule, 212
  for polyatomic molecules, 221
  See *Orbital, molecular*
Moment of inertia, 14
Morse's equation, 40
Multiplicity, 118, 121, 208, 213, 339

N

n,π^* states, fluorescence of, 369
  phosphorescence of, 369, 411
n,π^* transitions, See under transitions
n,π^* triplet state in heterocyclic compounds, 419

Nanometer (unit), 4
Nanon (unit), 4
Naphthacene, absorption spectrum, 92, 286, 287, 294
  fluorescence, 362
  phosphorescence, 403
  triplet states of, 437
1-Naphthaldehyde, fluorescence, 360, 411, 417
  phosphorescence, 411, 417
1-Naphthaldehyde–2-chloro-, phosphorescence, 417
Naphthalene, absorption spectrum, 92, 278, 281–283, 290
    solvent effects, 324
  charge-transfer complexes, phosphorescence, 391
  fluorescence lifetime, 361
  fluorescence quantum yield, 360, 400, 410
  phosphorescence, 391, 400, 410, 417
  triplet states of, 437
  triplet-triplet absorption, 434
Naphthalene–2-actyl-, phosphorescence, 417
Naphthalene–1-amino-, phosphorescence, 411
Naphthalene–2-amino-, absorption spectrum, 282
Naphthalenes–bromo-, phosphorescence, 409, 411
Naphthalene–1-bromo-, fluorescence, 360
Naphthalene–2-bromo, triplet states of, 437
Naphthalenes–chloro, phosphorescence, 409, 411
Naphthalene–1-chloro-, fluorescence, 360, 411
  singlet-triplet absorption, 428, 433
  triplet states of, 437
Naphthalene–1-fluoro-, fluorescence, 360, 411
  phosphorescence, 411
Naphthalenes–iodo-, phosphorescence, 411
Naphthalene–1-iodo-, fluorescence, 360
Naphthalenes–methyl-, phosphorescence, 409, 411
Naphthalene–1-methyl-, fluorescence, 360
Naphthalene–1-nitro-, fluorescence, 360, 411
  phosphorescence, 411
Naphthoic acids, phosphorescence, 411
  pK_a of excited states, 393, 450
Naphthols, fluorescence, 360, 411
  phosphorescence, 411
1-Naphthol, triplet states of, 437
2-Naphthol, pK_a of excited states, 393, 450
Naphthylamines, pK_a of excited states, 393, 450
Natural pigments, absorption spectra, 315 *et seq.*
Nickelocene, luminescence, 389
Nitrates, alkyl, absorption spectra, 83
Nitro compounds, absorption spectra, 83, 253 *et seq.*
  fluorescence, 368
  n-π^* bands of, 253
  phosphorescence, 271
Nitro group, energy levels, 254
  molecular structure, 252
  quenching effect on fluorescence, 368
Nitrogen molecule, configuration of, 132
Nitroso compounds, n-π^* bands, 253
Nitrosyl chloride, absorption spectrum, 252, 253
Nitrosyl fluoride, absorption spectrum, 253
Nonbonding electrons, 242
Nucleic acids, phosphorescence, 375

O

Octatetraene, absorption spectrum, 64
Octatetraene–diphenyl, fluorescence, 350
Octene, absorption spectrum in sulfuric acid, 303
Odd functions, 122
Odd states, see *Ungerade*
Olefins, absorption spectra, 62, 230
Operator, 108
  dipole moment, 307
  Hamiltonian, 109, 111, 203, 204
  Laplace, 108
Optical density, 8
Orbital, 57, 108, 202
  antibonding, 132, 212, 228, 233
  atomic, 108, 111, 202
  bonding, 132, 212, 233

  classification of, 57, 109, 130–132, 139, 145, 226
  energy, 111, 202, 210
  molecular, 58, 126, 127, 170, 171, 178, 179, 183, 185, 208, 210, 219, 221, 225, 227, 238, 253, 256–258, 276, 329, 338, 339
  nonbonding, 57, 58, 132, 233
  π, 58, 218
  σ, 58, 208, 217
  theory, 108 *et seq.*, 202 *et seq.*
Ortho-forms of diatomic molecules, 137
Oscillator, anharmonic, 31
  harmonic 30, 34, 35, 133–135
  strength, 47, 48, 50, 52–54, 191, 195
Overlap integral, 38, 182
Overtone bands, 18, 19, 160
  selection rules, 161, 162
Oxalic acid, absorption spectrum, 75
Oxalyl chloride, absorption spectrum, 74, 75
Oximes, absorption spectrum, 82
Oxine, see *Quinoline–8-hydroxy-*
Oxygen-induced absorption bands, 431, 433
Oxygen molecule, dissociation energy, 137
  potential energy curves, 125
  singlet states, 27, 125
  symmetry properties, 136
  triplet states, 125

P

P-branch, 17, 18, 134
Para-band, in aromatic hydrocarbons, 277, 279
Para-forms of diatomic molecules, 137
Paraffins, molecular orbital theory, 228 *et seq.*
Parity, 122
Pauli principle, 112, 113, 115, 119, 131
Pentacene, absorption spectrum, 92, 287
  triplet states of, 437
  triplet-triplet absorption, 434
1,3-Pentadiene–nitro-, absorption spectrum, 254
1,4-Pentadiene, absorption spectrum, 62
Peri-condensed hydrocarbons, 91
Perturbation theory, 219, 220
Perylene, fluorescence, 353, 360, 361
  triplet states of, 437
Phenanthrene, absorption spectrum, 92, 283, 287, 288
  fluorescence, 361, 400
  phosphorescence, 391, 400
    of charge-transfer complexes, 391
  pK_a of triplet state, 450
Phenanthrene–benzo(*c*)-, fluorescence, 361, 362
  phosphorescence, 400
  triplet states of, 437
Phenanthrene–9,10-diaza-, phosphorescence, 419
o-Phenanthroline, phosphorescence, 419
Phenazine, absorption spectrum, 95
Phenes, 277
Phenol, absorption spectrum, 26, 86, 262, 264
  fluorescence, 366
  phosphorescence, 410
  pK_a of excited states, 393, 450
Phenol–*p*-chloro-, pK_a of excited states, 393
Phenol–*p*-methyl-, pK_a of excited states, 393
Phenolate ion, absorption spectrum, 86, 88
Phenylalanine, fluorescence, 374
Phenylhydrazones–2,4-dinitro, absorption spectra, 82
Pheophytin, fluorescence, 382
Phosphorescence, 27, 338, 340, 344 *et seq.*, 395 *et seq.*
  effect of aggregation, 452
  effect of deuteration, 405
  effect of solvents, 419, 420 (see also under *Intersystem crossing*)
  lifetime, 344, 345, 418
  quantum yield, 344, 345, 410, 411, 418
  sensitized, 446
Phosphorescent state, paramagnetism of, 399, 402
Phosphoroscope, 345
Photochemical sensitization, 447, 448
Photon, 6
Phthalic acid, phosphorescence, 414
Phthalocyanines, absorption spectra, 317
  fluorescence, 382
Phthalocyanine metal complexes, fluorescence, 382

Piperazine, absorption spectrum, 61, 291
Piperidine, absorption spectrum, 61, 291
Planck constant, 9
Polarity, of heteropolar diatomic molecule, 221
Polarization of transitions, 347
Polarizability, 47, 48, 146, 147
Polyacetylenes, absorption spectra, 69
  fluorescence, 357
  phosphorescence, 357
Polyatomic molecules, spectra of, 139 *et seq.*
  molecular orbital theory, 139 *et seq.*, 221 *et seq.*
Polyenes, absorption spectra, 64, 223–225, 307
  transition moment in, 223
Polyene aldehydes, absorption spectra, 76, 77
Polyene ions, absorption spectra, 68
  molecular orbitals of, 187
p-Polyphenylenes, fluorescence, 368
Porphin, molecular orbitals of, 184
Porphins–tetrahydro-, absorption spectrum, 317
Porphyrins, absorption spectra, 315 *et seq.*
  fluorescence, 378
  phosphorescence, 378, 379
  structure, 383
  triplet state lifetimes, 378, 379
  triplet-triplet absorption, 438
Porphyrin metal complexes, fluorescence, 377–379
  phosphorescence, 378, 422 *et seq.*
  triplet-triplet absorption, 436, 438
Potential energy curves, 28–30, 125, 349, 392
  Morse's equation for, 40
Predissociation, 42, 43
Proflavin, dimer absorption spectrum, 310
  fluorescence, 373
Progression (spectral), 21, 137
Propene–2-methyl-, absorption spectrum, 62
Propene-1–nitro-, absorption spectrum, 254
Propionyl aldehyde, absorption spectrum, 247
  ionization energy, 247
n-Propyl iodide, absorption spectrum, 242
i-Propyl methyl ketone, absorption spectrum, 247
  ionization energy, 247
Proteins, fluorescence, 375
Protein-dye complexes, fluorescence, 376
Purine, fluorescence, 372
Pyrazine, absorption spectrum, 96, 296, 297
  fluorescence, 369
  ionization energy, 297
  phosphorescence, 419, 420
  singlet-triplet absorption, 429
Pyrene, absorption spectrum, 92
  excimer, fluorescence, 364
  fluorescence, 361, 400
  phosphorescence, 400
  triplet states of, 437
Pyrene-3-aldehyde, fluorescence, 370
  phosphorescence, 416
Pyrene–benzo-, fluorescence, 361, 407
  phosphorescence, 407
Pyridazine, absorption spectrum, 96, 292, 296, 297
  fluorescence, 369
  ionization energy, 297
  phosphorescence, 419
Pyridine, absorption spectrum, 96, 295, 297
  ionization energy, 297
  pK_a of excited states, 392
  triplet state, 418
Pyridine ethiodide, absorption spectrum, 96
Pyrimidine, absorption spectrum, 96, 296, 297
  fluorescence, 369
  ionization energy, 297
  phosphorescence, 419, 420
Pyrogallol, chemiluminescence of, 27
Pyrrole, absorption spectrum, 292, 293
  ionization energy, 292
Pyrrolidine, absorption spectrum, 291

Q

Q-branch, 17

Quantum defect, 107
Quantum number, for atoms, 109 *et seq.*, 203
  rotational, 14
  vibrational, 76
Quantum yield of fluorescence or phosphorescence, see *Fluorescence*, etc., *quantum yield*
Quaternary ammonium salts, pK_a of excited states, 393
Quenching, of fluorescence, 387
  of triplet state, 439–441
Quinoid theory of color, 306
Quinoline, absorption spectrum, 95, 296
  fluorescence, 370
  phosphorescence, 419, 421
  pK_a of excited states, 393, 450
Quinolines–hydroxy-, fluorescence, 373
Quinoline–8-hydroxy-, metal complexes of, fluorescence, 384, 425
    phosphorescence, 425
Quinoxoline, phosphorescence, 419, 421

R

R-branch, 17, 18, 134
Radiation, energy of, 6
  frequency of, 2, 4, 5
  magnetic dipole, 55
  quadrupole, 55
  scattering of, 2
  units of, 4, 6
  velocity of, 2, 5
  wavelength of, 2
  wavenumber of, 5
    vacuum correction, 5
Rare earth ions, electronic transitions, 385, 386
  complexes, fluorescence, 384, 385
    phosphorescence, 384, 385, 426
    triplet states of, 426, 427
  fluorescence, 384
Red shift (spectral) in solvents, 323
Reduced mass, 14, 106
Refractive index, 2
Renner effect, 169
Representation of a group, 143–145, 150, 158, 215
Resonance effect, 231, 236, 247, 262–264
Resonance integral, 231, 329
Resonance levels of rare earth ions, 385
Resonance radiation, 348
Resonance spectrum, 348
Resorcinol, fluorescence, 366
Retinine, triplet-triplet absorption, 438
Rhodamine B, fluorescence, 353
  quantum counter, 346
Rhodopsin, triplet-triplet absorption, 438
Riboflavin, fluorescence, 376
Rigidity, effect of, see *Spectrum*
Rotational energy, 132, 133
Rotational spectrum, see *Spectrum*
Rotational states, symmetry of, 136
Rotational structure, 11, 12
Rubrene, fluorescence, 353
Russell–Saunders coupling, 118, 135
Rydberg (unit), 106
Rydberg constant, 107
Rydberg states, 226, 244
Rydberg transition, see under *Transition*

S

Salicylic acid, fluorescence, 366
Samarium ion, fluorescence, 384
Schroedinger equation, 35, 108, 203
Selection rules, 50, 121, 134, 135, 146, 147, 152, 159, 204, 208, 215
  for atomic transitions, 121, 204
  for infrared and Raman transitions, 146, 147, 152, 159
  for multiplicity, 135, 208, 213
  for rotation, 134
Selenophene, absorption spectrum, 292
Self consistent field, for atoms, 117
  for molecules, 172
Semicarbazones, absorption spectra, 82
Sequence (spectral), 21
Similarity transformation (group theory), 215
Singlet state, 207, 339
  lifetime of, 348
Soret band, of porphines, 316, 317
Space quantization, 119
Spectrophotometry, 3
Spectrum, absorption 37 (see under individual compounds)
  of atoms, analysis of, 124
  collections of, 330
  continuous, 13, 33
  effect of environment, 320 *et seq.*
  effect of molecular rigidity, 25

Spectrum (continued)
  effect of pressure, 327
  effect of solvent, 25, 59, 70, 72, 76, 79, 191, 242, 309, 320 *et seq.*, 353 *et seq.*
  effect of temperature, 22, 327
  electronic, 11, 20, 21, 105 *et seq.*, 130 *et seq.*, 140, 169, 189, 200 *et seq.*
  emission, 27
  nature of, 2, 9
  predissociation, 42
  rotational, 10–14, 134
  triplet-triplet absorption, 433, 437
  vibrational, 10, 11, 19, 132
  vibration-rotation, 15, 16
  vibronic, 13, 36, 163 *et seq.*
    intensities in, 36
Spectroscopic moment, 270 *et seq.*
Spin (electronic), 108, 111, 128, 207, 338, 339
  in diatomic molecule, 128
  nuclear, 136
Spin functions, 111, 115
Spin orbital, 108, 111
Spin-orbit coupling, 395 *et seq.*, 420
Solvent, for absorption spectroscopy, 59, 98
Solvent effects on spectra, see under *Spectra*
Stereo-isomers, see under *Cis- and trans-isomers*
Steric effects on spectra, 89, 96 (see also under *Cis- and trans-isomers*)
Steroids, absorption spectra, 63, 66
  fluorescence, 376
Stilbenes, absorption spectra, 87
  fluorescence, 367
  photoisomerization, 449
Styrene, absorption spectrum, 87, 268, 269
  fluorescence, 367
  ionization energy, 269
Succinic acid, absorption spectrum, 71
Sulfonic acid group, effect on fluorescence, 376
Sulfoxides, absorption spectra, 251, 252
Symmetry, center of, 139, 148, 158, 216
  elements, 142, 153, 154
  of rotational states, 136
Symmetry operations, 142, 145, 156, 216
Symmetry orbitals, 173, 218

T

Terbium ion, fluorescence, 384
Terbium ion complexes, fluorescence, 388
Terphenyl, fluorescence, 361
Term (spectral), 107, 129
  rotational, 134
  vibrational, 133
Terpenoids, absorption spectra, 63
Tetradecaheptaene, absorption spectrum, 64
Tetrahedral orbital, 209
Tetrazine, absorption spectrum, 95, 96, 297
  fluorescence, 369
Thiacyclobutane, absorption spectrum, 291
Thiacyclohexane, absorption spectrum, 291
Thiacyclopentene, absorption spectrum, 291
Thianaphthene, absorption spectrum, 294
  phosphorescence, 419
Thiazole, absorption spectrum, 292
Thioacetamide, absorption spectrum, 251
Thioacetic acid, absorption spectrum, 247
  ionization energy, 247
Thiobenzophenone, absorption spectrum, 251
Thiocyclohexanone, absorption spectrum, 251
Thioethers, absorption spectrum, 60
Thioketones, absorption spectrum, 73
Thiophene, absorption spectrum, 292, 293
Thiosemicarbazones, absorption spectrum, 82
Thiourea, absorption spectrum, 251
Tiglic aldehyde, absorption spectrum, 76
Toluene, absorption spectrum, 86, 260, 269
  fluorescence, 365
  ionization energy, 269
  phosphorescence, 410
Transition, allowed, 9, 50, 347
  classification by solvent effects, 326
  electronic, 21
  fluorescence, 343
  forbidden, 9, 23, 30, 164, 215, 259, 264, 313, 346

  n-π^*, 59, 194, 226, 245, 247, 251, 252, 276, 297
    solvent effect on, 59, 72, 76, 242, 326, 356 *et seq.*
  N-Q, 226, 306, 329 (see also *Transition, n-π^**)
  N-R, see *Transition, Rydberg*
  n-σ^*, 59, 226, 245, 291
  N-V, 193, 226, 306, 325, 329
  phosphorescence, 343
  π-π^*, 59, 226, 252
  radiationless, 346
  Rydberg, 57, 70, 218, 226, 228, 231, 240, 242, 329
  σ-σ^*, 59, 226
  singlet-triplet, 123, 340
    effect of oxygen on, 431, 433
    transition moment of, 397
  triplet-triplet, 433 *et seq.*
Transition moment, 9, 37, 38, 49, 51, 53, 189, 202, 213, 239, 245, 269, 322, 347, 395, 397
  for substituted benzenes, 269 *et seq.*
Triazines, absorption spectrum, 96, 297
  phosphorescence, 419
Trigonal orbitals, 209
Trimethylamine, absorption spectrum, 61
Triphenylene, absorption spectrum, 92
  fluorescence, 360, 362, 400
  phosphorescence, 400
  triplet states of, 437
Triplet state, 54, 70, 118, 207, 339 (see also individual compounds)
  acid-base properties of, 449, 450
  lifetime, 398 (see also *Phosphorescence lifetime*)
    effect of metal ions on, 439
    by flash excitation, 439
  of rare earth complexes, 426, 427
Triplet-triplet absorption, 433 *et seq.*
Tryptophane, fluorescence, 374
Tunnel effect, 43
Tyrosine, fluorescence, 374

U

Ungerade (odd) state, 145, 148, 202, 203, 239
United atom, 126, 244

V

Vertical transition, 31
Vibrational energy, 132
Vibrational quantum number, 133
Vibrational spectrum, 11, 19, 21
Vibrational states, 134, 348
Vibrational structure (in spectra), 24, 68, 75, 78, 84, 265, 358, 407
Vibronic spectrum, see under *Spectrum*
Vibronic states, symmetry, 163
Vinyl chloride, absorption spectrum, 62
Vitamin A, fluorescence, 376

W

Water, absorption spectrum, 243, 244
Water molecule, ionization energy, 232, 243
  molecular orbitals, 173
  polarization of transitions, 347
Wave function, see *Eigenfunction*
Wave number, see *Radiation, wave number of*
Woodward's rules, 66, 67, 76–81, 250

X

Xanthophyll, absorption spectrum, 318

Z

Zero point energy, 12, 36, 41, 133, 137

8455
28/2/69

3/8/89

16-4-97

CHECKED
2008

VERIFIED
2013

C. F. T. R. I. LIBRARY, MYSORE.

Acc No. 8455

Call No. E1,5:f"n;1,N49 N48·9B

Please return this publication on or before the last DUE DATE stamped below to avoid incurring overdue charges.

19/5/80

To be issued from 4th June 1969.

~~T.S. Venugopal 14/6~~

A. Lalitha 19/6

~~[illegible] SFT.~~

4 ~~K. [illegible] TCBP.~~

~~Miss. K. Lalitha~~

~~17-6-69~~

Due Date	Return Date	Due Date	Return Date	Due Date	Return Date
17.6.69	18/6/69			14.4.71	16/4
4.7.69	3/7			1.5.71	4/5/71
18/7/69	18/7			19-5-71	17.5.'71
21.2.71	25/2			6-6-72	26 MAY 19
12.3.71	15-3-71			19-12.72	12.12.72
30.3.71	30-3-71			26/6/80	13.6.80
				16.2.83	15/2/84

CFTRI-MYSORE
8455
Chemical applica.

✓

93160